frontiers | Research Topics

Latest advances in neuroscience at the 9th Croatian Neuroscience Congress

Edited by
Kristina Mlinac-Jerković, Marija Heffer, Svjetlana Kalanj Bognar and Senka Blažetić

Published in
Frontiers in Molecular Neuroscience

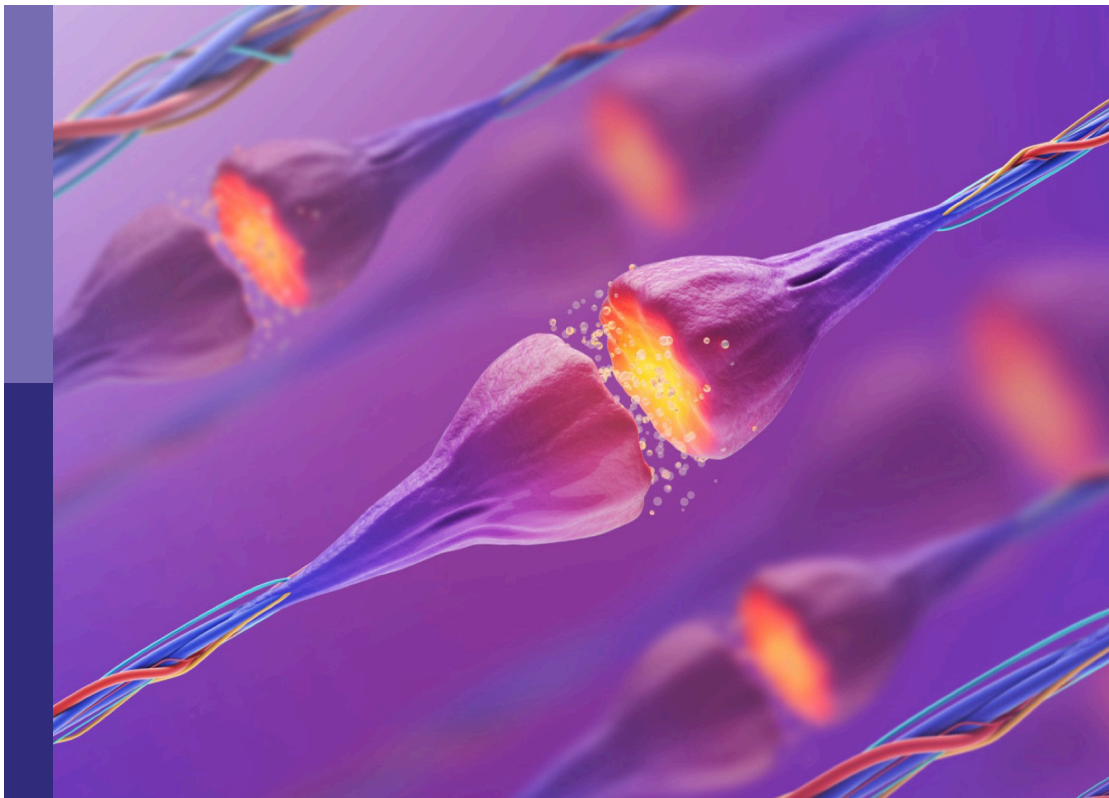

ISSN 1664-8714
ISBN 978-2-8325-6018-1
DOI 10.3389/978-2-8325-6018-1

About Frontiers

Frontiers is more than just an open access publisher of scholarly articles: it is a pioneering approach to the world of academia, radically improving the way scholarly research is managed. The grand vision of Frontiers is a world where all people have an equal opportunity to seek, share and generate knowledge. Frontiers provides immediate and permanent online open access to all its publications, but this alone is not enough to realize our grand goals.

Frontiers journal series

The Frontiers journal series is a multi-tier and interdisciplinary set of open-access, online journals, promising a paradigm shift from the current review, selection and dissemination processes in academic publishing. All Frontiers journals are driven by researchers for researchers; therefore, they constitute a service to the scholarly community. At the same time, the *Frontiers journal series* operates on a revolutionary invention, the tiered publishing system, initially addressing specific communities of scholars, and gradually climbing up to broader public understanding, thus serving the interests of the lay society, too.

Dedication to quality

Each Frontiers article is a landmark of the highest quality, thanks to genuinely collaborative interactions between authors and review editors, who include some of the world's best academicians. Research must be certified by peers before entering a stream of knowledge that may eventually reach the public - and shape society; therefore, Frontiers only applies the most rigorous and unbiased reviews. Frontiers revolutionizes research publishing by freely delivering the most outstanding research, evaluated with no bias from both the academic and social point of view. By applying the most advanced information technologies, Frontiers is catapulting scholarly publishing into a new generation.

What are Frontiers Research Topics?

Frontiers Research Topics are very popular trademarks of the *Frontiers journals series*: they are collections of at least ten articles, all centered on a particular subject. With their unique mix of varied contributions from Original Research to Review Articles, Frontiers Research Topics unify the most influential researchers, the latest key findings and historical advances in a hot research area.

Find out more on how to host your own Frontiers Research Topic or contribute to one as an author by contacting the Frontiers editorial office: frontiersin.org/about/contact

Latest advances in neuroscience at the 9th Croatian Neuroscience Congress

Topic editors

Kristina Mlinac-Jerković — University of Zagreb, Croatia
Marija Heffer — Josip Juraj Strossmayer University of Osijek, Croatia
Svjetlana Kalanj Bognar — University of Zagreb, Croatia
Senka Blažetić — Josip Juraj Strossmayer University of Osijek, Croatia

Citation

Mlinac-Jerković, K., Heffer, M., Kalanj Bognar, S., Blažetić, S., eds. (2025). *Latest advances in neuroscience at the 9th Croatian Neuroscience Congress*. Lausanne: Frontiers Media SA. doi: 10.3389/978-2-8325-6018-1

Table of contents

frontiers | Frontiers in Molecular Neuroscience

TYPE Editorial
PUBLISHED 06 February 2025
DOI 10.3389/fnmol.2025.1563899

OPEN ACCESS

EDITED AND REVIEWED BY
Clive R. Bramham,
University of Bergen, Norway

*CORRESPONDENCE
Kristina Mlinac-Jerkovic
✉ kristina.mlinac.jerkovic@mef.hr

RECEIVED 20 January 2025
ACCEPTED 27 January 2025
PUBLISHED 06 February 2025

CITATION
Mlinac-Jerkovic K, Heffer M, Kalanj-Bognar S and Blažetić S (2025) Editorial: Latest advances in neuroscience at the 9th Croatian Neuroscience Congress.
Front. Mol. Neurosci. 18:1563899.
doi: 10.3389/fnmol.2025.1563899

Editorial: Latest advances in neuroscience at the 9th Croatian Neuroscience Congress

Kristina Mlinac-Jerkovic[1,2]*, Marija Heffer[3], Svjetlana Kalanj-Bognar[1,2] and Senka Blažetić[4]

[1]School of Medicine, Croatian Institute for Brain Research, University of Zagreb, Zagreb, Croatia, [2]Department of Chemistry and Biochemistry, School of Medicine, University of Zagreb, Zagreb, Croatia, [3]Department of Medical Biology and Genetics, Faculty of Medicine, Josip Juraj Strossmayer University of Osijek, Osijek, Croatia, [4]Department of Biology, Josip Juraj Strossmayer University of Osijek, Osijek, Croatia

KEYWORDS

neurodevelopment, neurodegeneration, sphingolipids, glioma, CSF, oxytocin, neural stem cells (NSCs), brain injury

Editorial on the Research Topic
Latest advances in neuroscience at the 9th Croatian Neuroscience Congress

Like never before, neuroscience is simultaneously captivating minds as well as decoding them in a thrilling new research era. We are witnesses to sophisticated experimental research tools, augmented by tremendous potentials of artificial intelligence (AI)-assisted technologies and have a pool of knowledge that will hopefully set us on a path to unravel the mysteries of brain function, as well as elucidate complex brain disorders with the aim of improving diagnosis and therapy. With that in mind we held the 9th Croatian Neuroscience Congress. Our aim was to highlight the heterogeneity of our current research, covering diverse fields in neuroscience, so far contributed by some of the pivotal discoveries made by researchers from Croatia or of Croatian origin (Kaur et al., 2025; Kostovic and Rakic, 1990; Rakic, 1971).

This Research Topic includes papers which feature exciting findings and state-of-the art methodologies applied in brain research. Two original research papers address the intricacies of CSF pressure and volume redistribution. Jurjević et al. present data on experimentally caused CSF system impairment in animal model, which indicate that cervical stenosis in a head-up vertical position reduces blood perfusion of the whole brain, while aqueductal obstruction impairs only the perfusion of the local periventricular brain tissue. The reported phenomena give an important **insight into hydrocephalus development**. Strbačko et al. evaluate how body position influences CSF volume redistribution inside the cranial and spinal CSF compartments. The authors performed MRI volumetry in healthy volunteers in three different body positions and report significant CSF volume changes inside the spinal space in the tested body positions, with no significant CSF volume changes inside the cranium in two tested positions. Both papers significantly contribute to the understanding of fundamental physiological processes involved in **CSF dynamics**.

A study examining **regional cerebral oxygen saturation variability in preterm infants** reports a potential predictor or a **marker for increased likelihood of brain injury**. As shown by Caleta et al., preterm infants have an increased aberration of regional cerebral

oxygen saturation in early postdelivery period. This was found to be associated with an increased likelihood of brain injury (intraventricular/cerebellar hemorrhage or white matter injury) diagnosis at term-equivalent age. Since timely diagnosis is crucial for treating brain injuries, the results of this study may be used in future management strategies designed to improve neonatal outcomes.

A different study tackles specific aspects of neurodevelopment in young children. Križalkovičová et al. investigate the benefits of judo training in preschool children, 4–7 years old. The authors determined **significant improvements in cognitive and motor performance** in judo-practicing children compared to their non-judo counterparts. Since developmental kinesiology is an emerging field of study, particularly considering the sedentary lifestyle we embraced in the modern age, this finding is especially compelling. Sports encouraging natural movement patterns and proper body control, which is crucial for effective motor performance, will show to be exceptionally important for overall life-long health. Aligned in that direction, a Systematic Review by Szabó et al. sheds light on one particular benefit from sports: **exercise-induced oxytocin**. The authors explored the interplay between oxytocin and exercise. By detailed analysis of a staggering 175 studies, the authors highlight that exercise-induced oxytocin could promote tissue regeneration and has analgesic and anti-inflammatory effects. In addition, it can affect the amount of stress experienced by athletes, and their response to it. Therefore, examining oxytocin's complex interactions with exercise paves the way for future research and application in sports science, psychology, and biomedicine.

This Research Topic is also comprised of articles reporting methodological advances and breakthroughs. A research paper by Prkačin et al. describes a **novel approach to cytoarchitectonics through the use of a supervised neural network prediction algorithm**. The authors defined cortical regions and layers based on clear quantitative criteria and they reveal that the cytoarchitectonic descriptions were reflected in the morphometric measures and cell classifications obtained by the used prediction algorithm. The results of this study suggest that supervised machine learning could aid in defining the morphological characteristics of the cerebral cortex. A study by Lisjak et al. addresses the **treatment for stroke by transplantation of neural stem cells** (NSCs). The authors stereotaxically transplanted NSCs into the stroke affected mouse brains, assessed recovery by MRI and neurological scoring, and evaluated pyroptosis and necroptosis markers. The study shows that NSC transplantation significantly improved neurological recovery compared to control groups, and holds therapeutic potential in stroke recovery by targeting pyroptosis and necroptosis pathways.

Brain cancer is also in focus of this Research Topic, specifically diffuse gliomas. A study by Kafka et al., by using immunohistochemistry and methylation specific-PC, reports that **Secreted frizzled-related protein 4 (SFRP4)** expression is reduced in high grade astrocytomas which is not caused by the methylation of its promoter. The study contributes to the recognition of the significance of epigenetic changes in diffuse glioma indicating that restoring SFRP4 protein to its normal expression holds potential as therapeutic avenue. A Mini Review by Karmelić et al. examines the role of sphingolipids in the pathogenesis of highly aggressive adult-type diffuse gliomas. The authors summarize findings on the balance of the pro-apoptotic ceramide and pro-survival sphingosine-1-phosphate (S1P), the so-called **sphingolipid rheostat**. In gliomas, that balance is shifted toward cell survival and proliferation. The authors therefore discuss how targeting the sphingolipid rheostat, through reducing S1P levels or modulating S1P receptors to reduce cell proliferation, as well as through increasing ceramide levels to induce apoptosis, offers a potential therapeutic pathway for glioma treatment. A Perspective paper by Puljko et al. also discusses the link between brain tumors and (glycol)sphingolipids, but from a different aspect. The authors explore the physiological consequences of decreased **GD3 synthase** (GD3S) expression, an enzyme involved in ganglioside biosynthesis. Since GD3S overexpression enhances tumor growth, inhibiting GD3S activity has potential therapeutic effects across different cancer types. However, negative consequences of the inhibition of this enzyme have been underexplored, and the authors highlight them and show original data indicating that inactivated GD3S can generally negatively affect energy metabolism, regulatory pathways, and mitigation of oxidative stress.

A paper by Babić Leko et al. addresses **neurodegeneration**, specifically Alzheimer's disease (AD). The authors analyzed microtubule-associated protein tau (*MAPT*) gene haplotypes and specific *MAPT* haplotype-tagging polymorphisms in more than 900 individuals. Certain polymorphisms were found to be more represented among patients with dementia and apolipoprotein E (APOE) $\varepsilon 4$ carriers. Carriers of other specific *MAPT* haplotypes had worse performance on various neuropsychological tests. Hence, these results reveal another **intricate level of interaction between *MAPT* haplotypes**, *MAPT* haplotype-tagging polymorphisms, CSF biomarkers, *APOE* genotypes and the development of AD.

An intriguing study from Ratko et al. reports that **guanylate cyclase C (GC-C) expression in human prefrontal cortex depends on sex and feeding status**. The authors determined GC-C protein expression in specific areas of human prefrontal cortex involved in regulation of feeding behavior, as well as in the cerebellar cortex, arcuate nucleus of hypothalamus and substantia nigra in more than 30 brains. This is the first study of GC-C regulation and its possible function in human prefrontal cortex, providing a strong basis for future GC-C studies in human brain, as well as opening new riveting research questions.

Finally, an innovative Hypothesis and Theory article by Stojanovic and Kalanj-Bognar proposes that Toll-like receptors are a **missing link in Notch signaling cascade during neurodevelopment**. Based on data demonstrating Notch and TLR structural engagement and functions during neurodevelopment, along with the authors' description of novel molecular binding models, the authors advocate for the hypothesized role of TLRs in Notch signaling. A truly fresh theory!

In summary, this Research Topic, stemmed from the work presented at the 9th Croatian Neuroscience Congress, is a compendium of various article types, thus providing original findings, fresh perspectives on known topics, systematization of vast data on particular subjects, as well as intriguing and thought-provoking concepts. We hope this will serve as a go-to article collection in the diverse field of neuroscience.

Author contributions

KM-J: Conceptualization, Writing – original draft, Writing – review & editing. MH: Conceptualization, Writing – original draft, Writing – review & editing. SK-B: Conceptualization, Writing – original draft, Writing – review & editing. SB: Conceptualization, Writing – original draft, Writing – review & editing.

Conflict of interest

The authors declare that the research was conducted in the absence of any commercial or financial relationships that could be construed as a potential conflict of interest.

Publisher's note

References

Kaur, N., Kovner, R., Gulden, F. O., Pletikos, M., Andrijevic, D., Zhu, T., et al. (2025). Specification of claustro-amygdalar and palaeocortical neurons and circuits. *Nature*. doi: 10.1038/s41586-024-08361-5

Kostovic, I., and Rakic, P. (1990). Developmental history of the transient subplate zone in the visual and somatosensory cortex of the macaque monkey and human brain. *J. Comp. Neurol.* 178, 441–470. doi: 10.1002/cne.902970309

Rakic, P. (1971). Guidance of neurons migrating to the fetal monkey neocortex. *Brain Res.* 133, 471–476. doi: 10.1016/0006-8993(71)90119-3

frontiers | Frontiers in Molecular Neuroscience

TYPE Original Research
PUBLISHED 22 May 2024
DOI 10.3389/fnmol.2024.1361089

OPEN ACCESS

EDITED BY
Marija Heffer,
Josip Juraj Strossmayer University of Osijek, Croatia

REVIEWED BY
Anna Kozłowska,
University of Warmia and Mazury in Olsztyn, Poland
Branka Hrvoj Mihic,
University of California, San Diego, United States

*CORRESPONDENCE
Aleksandra Dugandžić
✉ aleksandra.dugandzic@mef.hr

RECEIVED 24 December 2023
ACCEPTED 30 April 2024
PUBLISHED 22 May 2024

CITATION
Ratko M, Crljen V, Tkalčić M, Mažuranić A, Bubalo P, Škavić P, Banovac I and Dugandžić A (2024) Expression of guanylate cyclase C in human prefrontal cortex depends on sex and feeding status.
Front. Mol. Neurosci. 17:1361089.
doi: 10.3389/fnmol.2024.1361089

Expression of guanylate cyclase C in human prefrontal cortex depends on sex and feeding status

Martina Ratko[1,2], Vladiana Crljen[1,2,3], Martina Tkalčić[4], Anton Mažuranić[4], Pero Bubalo[4], Petar Škavić[4], Ivan Banovac[5] and Aleksandra Dugandžić[1,2,3]*

[1]Laboratory for Cellular Neurophysiology, Croatian Institute for Brain Research, School of Medicine, University of Zagreb, Zagreb, Croatia, [2]Centre of Excellence for Basic, Clinical and Translational Neuroscience, School of Medicine, University of Zagreb, Zagreb, Croatia, [3]Department of Physiology, School of Medicine, University of Zagreb, Zagreb, Croatia, [4]Institute for Forensic Medicine, School of Medicine, University of Zagreb, Zagreb, Croatia, [5]Department of Anatomy and Clinical Anatomy, School of Medicine, University of Zagreb, Zagreb, Croatia

Introduction: Guanylate cyclase C (GC-C) has been detected in the rodent brain in neurons of the cerebral cortex, amygdala, midbrain, hypothalamus, and cerebellum.

Methods: In this study we determined GC-C protein expression in Brodmann areas (BA) 9, BA10, BA11, and BA32 of the human prefrontal cortex involved in regulation of feeding behavior, as well as in the cerebellar cortex, arcuate nucleus of hypothalamus and substantia nigra in brain samples of human 21 male and 13 female brains by ELISA with postmortem delay <24 h.

Results: GC-C was found in all tested brain areas and it was expressed in neurons of the third cortical layer of BA9. The regulation of GC-C expression by feeding was found in male BA11 and BA10-M, where GC-C expression was in negative correlation to the volume of stomach content during autopsy. In female BA11 there was no correlation detected, while in BA10-M there was even positive correlation. This suggests sex differences in GC-C expression regulation in BA11 and BA10-M. The amount of GC-C was higher in female BA9 only when the death occurred shortly after a meal, while expression of GC-C was higher in BA10-O only when the stomach was empty. The expression of GC-C in female hypothalamus was lower when compared to male hypothalamus only when the stomach was full, suggesting possibly lower satiety effects of GC-C agonists in women.

Discussion: These results point toward the possible role of GC-C in regulation of feeding behavior. Since, this is first study of GC-C regulation and its possible function in prefrontal cortex, to determine exact role of GC-C in different region of prefrontal cortex, especially in humans, need further studies.

KEYWORDS

human prefrontal cortex, cerebellum, hypothalamus, substantia nigra, feeding

Introduction

According to the World Health Organization (WHO), each year 4 million people die due to obesity. The prefrontal cortex (PFC) is involved in the regulation of human feeding behavior (Lowe et al., 2019). The areas of the PFC that play a role in feeding regulation are the dorsolateral, ventromedial and orbitofrontal cortex (Lowe et al., 2019; Rolls, 2023). Determined by fMRI, the dorsolateral prefrontal cortex (DLPFC)

is less active in obese patients which leads to overeating. In the case of a higher activity of the DLPFC, weight-loss and maintaining healthy weight in obese patients are more likely (Ester and Kullmann, 2022). The orbitofrontal cortex (OFC) is involved in the assessment of nutritive qualities of the food and it is suggested that decreased function of the OFC in patients with obesity could be responsible for addictive eating behavior (Saruco and Pleger, 2021). Furthermore, if the anterior cingulate cortex (ACC) is more active during a food-related inhibition task, the participants are leaner (Saruco and Pleger, 2021). Therefore, in this study we examined guanylate cyclase C (GC-C) expression in: BA9 (DLPFC), 11 (orbitofrontal cortex), 10 (anterior prefrontal cortex), and 32 (dorsal anterior cingulate area).

In the brain, the agonists of particulate (cell membrane) guanylate cyclase (GC-A, -B or -C) play a role in neuronal development, synaptic transmission and neuroprotection (Markerink-Van Ittersum et al., 1997). Plasma concentrations of brain natriuretic peptide (BNP), an agonist of GC-A, are in correlation to cognitive function in demented patients and are associated with increased risk of developing cognitive disorders (Naito et al., 2009). Activation of brain GC-C by systemic or locally applied (intracerebroventricular) guanylin peptides leads to satiety in laboratory animals (Valentino et al., 2011; Folgueira et al., 2016). The concentrations of pro-uroguanylin (pro-UGN) in plasma [precursor of GC-C agonist, uroguanylin (UGN)] are decreased in obesity (Rodríguez et al., 2016).

More recent research has shown a rapidly expanding family of hormones expressed and active in both the gastro-intestinal (GI) tract and the brain (Ferrini et al., 2009; Whissell et al., 2019). Apart from its function in the GI tract, ghrelin regulates satiety and energy homeostasis (Ferrini et al., 2009), cholecystokinin is involved in memory and cognition as well as in the development of anxiety disorders (Zwanzger et al., 2012; Whissell et al., 2019) and secretin, which regulates water and food homeostasis, motor learning, spatial memory, fear, and anxiety (Wang et al., 2019). Due to the blood-brain barrier, it is still not clear which of the effects could be attributed to the hormones delivered from the GI and which to locally produced hormones in the brain. A new member of this family is UGN, a 16-amino-acid polypeptide secreted after a meal from the enterochromaffin cells into the gut lumen, but also into the blood (Fan et al., 1996; Li et al., 1997). UGN exerts physiological function in intestine, kidney, and brain. Concertation of pro-UGN is decreased in plasma of obese people (Rodríguez et al., 2016) which might correspond to results obtained from obese mice which secret less UGN after a meal (Simões-Silva et al., 2013). However, the pro-UGN concentrations in blood did not differ in human subjects with obesity when compared to not obese subjects suggesting importance of possible difference in GC-C expression. Changing the food content does not change the postprandial increase in pro-UGN blood concertation (Patterson et al., 2020).

Even though UGN is an agonist of GC-C, its expression in the brain [cerebellum (Cb), hypothalamus (Hy), cerebral cortex, and midbrain (MB)] (Fan et al., 1997; Habek et al., 2023) is often contested and ignored (Kim et al., 2016).

GC-C is detected in the mouse cerebral cortex, amygdala (Amyg), MB, Hy, and cerebellar Purkinje cells (Gong et al., 2011; Valentino et al., 2011; Begg et al., 2014; Dugandzic et al., 2020; Habek et al., 2020, 2021). All these brain areas are, in one way or another, involved in feeding regulation (de Vrind et al., 2021; Low et al., 2021; Iosif et al., 2023). GC-C is expressed in dopaminergic neurons of the ventral tegmental area and substantia nigra (SN) where GC-C activation increases neuronal activity via potentiation of glutamate and acetylcholine effects suggesting that GC-C regulates dopamine release (Gong et al., 2011). Those GC-C positive neurons project to the nucleus caudatus and putamen, nucleus accumbens, olfactory tubercle, lateral hypothalamic area, and central nucleus of Amyg (Merlino et al., 2019).

GC-C is expressed in the neurons of the basolateral and cortical nucleus of Amyg, where it is involved in the regulation of anxiety-like behavior. In the Amyg, expression of GC-C mRNA increases 2 h after feeding in female mice, but not in male mice (Dugandzic et al., 2020). In addition to neurons expressing GC-C, the Amyg gets projections from GC-C positive neurons located in the Hy and MB (Merlino et al., 2019).

As we know so far, the main site of UGN metabolic effects is the Hy. GC-C is located in pro-opiomelanocortin (POMC) expressing neurons of the arcuate nucleus (Arc) of mice and humans (Habek et al., 2020). In addition, it is expressed in the ventral premammillary nucleus (PMV). The GC-C-positive neurons from the PMV project to the nucleus posterior of Amyg, ventral part of the lateral septal nucleus, nucleus of the stria terminalis, medial preoptic nucleus, Arc, and ventromedial nucleus (Merlino et al., 2019). Two hours after a meal, there is a lower expression of GC-C in Arc of the Hy in female mice compared to males, while the expression of GC-C is the same at fasting conditions (Habek et al., 2020).

The expression of GC-C in the human brain is confirmed in the hypothalamic Arc and PFC (Colantuoni et al., 2011; Habek et al., 2020). Since the expression in the female DLPFC (BA46 and BA9) decreases by age (Colantuoni et al., 2011) and the function of GC-C is dependent on sex and feeding status, aims of the study are to determine possible age and sex differences of GC-C expression in regions involved in feeding regulation: Brodmann areas (BA) 9 (DLPFC), BA11 (orbitofrontal cortex), BA10 (anterior prefrontal cortex), and BA32 (dorsal anterior cingulate area) in 21 male and 13 female brain samples with a postmortem delay less of 24 h (Brodmann, 1909; Banovac et al., 2020). Special attention is paid to the time passed between the subject's last meal and their time of death. Since previous research suggested differences in the regulation of eating behavior in the left and right hemispheres (Lowe et al., 2019), we also determined possible difference in GC-C expression in areas of interest in the left and right hemispheres. GC-C expression was confirmed in the Arc of the Hy, and, for the first time, it was detected in the human SN and the cerebellar cortex, which are areas known to be involved in feeding regulation.

Abbreviations: ACC, anterior cingulate cortex; Amyg, amygdala; Arc, arcuate nucleus; BNP, brain natriuretic peptide; BA, Brodmann area; Cb, cerebellum; DLPFC, Dorsolateral prefrontal cortex; ELISA, Enzyme-linked immunosorbent assay; GC-C, Guanylate cyclase C; GI, gastro-intestinal tract; HRP, horseradish peroxidase; Hy, hypothalamus; MB, midbrain; OFC, orbitofrontal cortex; PBS, phosphate-buffered saline; PFA, paraformaldehyde; PFC, prefrontal cortex; POMC, pro-opiomelanocortin; pro-UGN, pro-uroguanylin; SN, *substantia nigra*; UGN, uroguanylin; PMV, ventral premammillary nucleus.

Materials and methods

Tissue sampling

Human brain tissue was collected from 35 deceased persons (22 men and 13 women). The average age was 53 ± 3 years for men and of 64 ± 6 years for women ($p = 0.08$, difference not statistically significant). Brain tissue samples (Hy, MB, Cb, and PFC) from both hemispheres were collected during standard autopsy after obtaining a signed informed consent form from the deceased's next of kin. All personal data were stored under a generated code and processed electronically. The principal investigator and team members respected all regulations and standards for protection of personal information and the identity of the participants was not revealed to third persons. Differences in GC-C expression due to sex, age, and feeding status were determined in brain samples collected from 34 deceased subjects (Supplementary Table 1). The obesity was estimated by physician coroner during regular autopsies and equally distributed in both sexes (6 of 13 women and 10 of 21 men). Less than 100 mL of the stomach content was classified as an empty stomach (person died long after eating a last meal), and 100 mL or more of content found during autopsy was classified as a full stomach. Postmortem delay for all collected samples was under 24 h. After collection, half of the tissue for further protein isolation was frozen and stored at −80°C until further use.

The brain sample used for immunostaining was obtained from 40 years old men with no medical history of neurological or psychiatric disorders and no neuropathological deviations in the brain on autopsy. Relevant medical history was obtained from both autopsy reports and medical records. The analyzed subject died without a preagonal state, and the postmortem delay (6.5 h) represents the actual interval of neuron death. The brain tissue is a part of the Zagreb Neuroembryological Collection. It was obtained with the approval of the Ethics Committee of University of Zagreb School of Medicine (380–59-10106–14-55/152; Banovac et al., 2022).

Protein isolation

Frozen tissue samples were thawed on ice and washed in ice-cold phosphate-buffered saline (PBS) solution. The desired areas of the PFC were sampled [BA: 9 ($n = 28$), 10-orbital (O, $n = 29$), 10-medial (M, $n = 32$), 11 ($n = 30$) and 32 ($n = 28$)], as well as SN ($n = 22$), Arc of Hy ($n = 30$) and cerebellar cortex ($n = 33$). BA9 was sampled from the dorsal part of the superior frontal gyrus, BA10-O was sampled from the ventral (orbital) aspect of the frontal pole, BA10-M was sampled from the ventro-medial part of the superior frontal gyrus, BA11 was sampled from the rostral part of the straight gyrus (gyrus rectus) and BA32 was sampled from the paralimbic cortex situated between the paracingulate sulcus and the cingulate gyrus. The samples were not taken if it was not possible to sample the brain region of interest with a great degree of certainty. The number of samples for SN is the smallest because the sample was only taken when the structure was clearly visible which was not the case in some elderly subjects. Approximately 100 mg of tissue was excised per region, placed in a labeled microcentrifuge tube (Thermo Fisher Scientific, Waltham, MA, USA) and ice-cold PBS was added (1 g tissue = 9 mL PBS). The tissue was thoroughly homogenized with an ultrasonic processor (Q55 Sonicator®, QSonica Sonicators, Newton, CT, USA). Samples were centrifuged (5 min, 5,000 *g*, +4°C; Eppendorf Centrifuge 5415 R, Hamburg, Germany). The supernatant was transferred into a new microcentrifuge tube (Thermo Fisher Scientific) and stored at −80°C until use.

ELISA

GC-C expression was determined with a commercially available Enzyme-Linked Immunosorbent Assay kit (E5383Hu ELISA; Bioassay Technology Laboratory, Birmingham, UK) following the manufacturer's instructions. Briefly, all reagents and samples were brought to room temperature before use and standard solutions were prepared shortly before commencement. Standard solutions and samples (40 µl) were loaded into the provided 96-well plate pre-coated with the Human anti-GC-C antibody. Sample wells were then loaded with the biotinylated anti-GC-C antibody after which streptavidin-HRP (horseradish peroxidase) was added to all sample wells. The plate was incubated for 60 min at 37°C (Heratherm™ Compact Microbiological Incubator, Thermo Fisher Scientific). Excess streptavidin-HRP was then washed away (5 × 1 min) and substrate solutions were added to each well. Following a brief incubation (10 min, 37°C, dark environment) a stop solution was added and optical density was read using a microplate reader (GloMax® Explorer Multimode Microplate Reader, Promega Corporation, Madison, WI, USA) set at 450 nm. A standard curve was generated from the results and used to determine GC-C expression in each sample.

Tissue fixation

The brain tissue was cut into blocks following Talairach's coordinates (Talairach and Szikla, 1980). Tissue blocks of the DLPFC containing the superior frontal gyrus (BA9) were selected (Brodmann, 1909; Banovac et al., 2020). The tissue was first fixed by immersion in 4% paraformaldehyde (PFA; Biognost, Zagreb, Croatia) for 24 h, then dehydrated in an ethanol cascade (70, 96, and 100%; Biognost). Where needed, surface vessels were removed with tweezers to avoid tissue rupture during sectioning. Tissue was then incubated in toluene (2 × 4 h; Kemika d.d., Zagreb, Croatia) and lastly in paraffin (2 × 24 h; Biognost) before being embedded in paraffin blocks and stored at room temperature until use (Sadeghipour and Babaheidarian, 2019). Brain sample was cut on a microtome into 20-µm-thick coronal slices (Sy and Ang, 2019) and mounted on VitroGnost Plus Ultra adhesive microscope slides (BioGnost, Zagreb, Croatia).

TABLE 1 Primary and secondary antibodies used for immunofluorescence.

Antibody	Species and clonality	Manufacturer, catalog number (CN), lot	Working dilution
Primary antibodies			
Anti-NeuN	Rabbit; polyclonal	Abcam: CN: ab104225; lot: GR3370892-1	1:1000
Anti-GC-C (GUCY2C)	Mouse; monoclonal	US Biological Life Sciences: CN: 207689; lot: L21102855	1: 200
Secondary antibodies			
Conjugated anti-mouse Alexa 488	Donkey	ThermoFisher (Invitrogen): CN: A-21202; lot: 1915874	1:1000
Conjugated anti-rabbit Alexa 546	Donkey	ThermoFisher (Invitrogen): CN: A10040; lot: 1833519	1:1000

Immunohistochemistry

This part of the study was performed according to protocols for paraffin-embedded tissue (Zaqout et al., 2020). Histological sections were first photobleached for 48 h using a LED light source (Neumann and Gabel, 2002; Sun et al., 2017) in order to reduce autofluorescence. The sections were deparaffinized and heat antigen retrieval was performed in citrate-based (pH 6.0) unmasking solution (Boenisch, 2005) followed by protein blocking [1 h at room temperature (RT) in normal donkey serum (NDS; Chemicon, USA) diluted 1:30 in permeabilization solution (0.3% Triton X-100 in 1x PBS; Sigma-Aldrich, USA)]. The sections were then incubated overnight in primary antibodies at 4°C. After washing (3 times per 10 min in PBS), the sections were incubated with secondary antibodies for 1 h at room temperature. Primary and secondary antibodies used for immunofluorescence are shown in Table 1. To further reduce autofluorescence, brain sample was treated with TrueBlack® Lipofuscin Autofluorescence Quencher (Biotium, USA; Banovac et al., 2019, 2022) and coverslipped with VECTASHIELD® Antifade Mounting Medium (Vector Laboratories, USA). Histological sections were imaged using a laser confocal microscope (Olympus FLUOVIEW FV3000RS, Japan) on high-power magnification and using *Z*-stack in order to visualize the entire section thickness.

Statistical analyses

To test the normal distribution of the results we used the Kolmogorov-Smirnov test. When expression of GC-C is compared we used unpaired Student's *t*-tests. To determine possible correlations between age and GC-C expression or between different brain regions we used Pearson's correlation test. The data was presented as mean ± standard error mean (SEM) and $p < 0.05$ was considered statistically significant. For statistical analyses the GraphPad Instat statistical software (Graph-Pad Software, Boston, MA, USA) was used.

Results

In this study we determined the expression of GC-C in male and female Brodmann areas (BA) 9, 10 (O—orbital and M—medial), 11, 32, the Arc of the Hy, the SN and the cerebellar cortex. In his study we determine the expression of GC-C in correlation to feeding status determined as a volume of stomach content during autopsy, sex differences in GC-C expression and differences in GC-C expression in left compared to right hemisphere.

Expression of GC-C depends on feeding status

The expression of GC-C in BA9 was confirmed by immunohistochemical staining. GC-C was located in neurons of the layer III of man's BA9 prefrontal cortical area. The neuronal localization was confirmed by co-localizing with the neuronal marker Neu-N (Figure 1A). Statistically significant correlation between stomach volume determined during autopsy and expression of GC-C was found in BA11 and BA10-M. A volume of stomach content was negatively associated with GC-C expression in male BA11 and BA10-M ($r = -0.61$, $p = 0.015$ and $r = -0.52$, $p = 0.038$, respectively), while there was no significant correlation in female BA11 ($r = -0.03$, $p = 0.941$). Interestingly, in female 10-M there was a significant positive correlation between stomach content volume and GC-C expression ($r = 0.80$, $p = 0.010$) (Table 2).

Expression of GC-C is higher in female than male BA9

The sex difference was found in BA9 (Figure 1B). Even though, previous study showed negative correlation between expression of mRNA for GC-C in dorsolateral prefrontal cortex (BA46/9) with age in the female brain (Colantuoni et al., 2011), at the protein level there was no statistically significant correlation between age and GC-C expression for all tested cortical regions (Figure 1C).

To determine if feeding status can affect sex differences of GC-C expression in human prefrontal cortex, we compared GC-C expression in cortical regions when the stomach was empty or full during autopsy. Surprisingly, in fasting conditions there was no difference in GC-C expression between male and female BA9 (Figure 2A). Sex difference in GC-C expression in BA10-O existed only if the stomach was empty (Figure 2B).

Expression of GC-C in right and left hemisphere differs only in female brains

There was no statistically significant difference in GC-C expression between male left and right hemispheres in any of the examined cortical regions (Figure 3A). However, when the stomach was empty there was more than a two times higher expression of GC-C in the left than the right BA9 (right: 172 ± 11, $n = 3$; left: 381 ± 1 ng/L, $n = 2$; $p = 0.0007$). After

10.3389/fnmol.2024.1361089

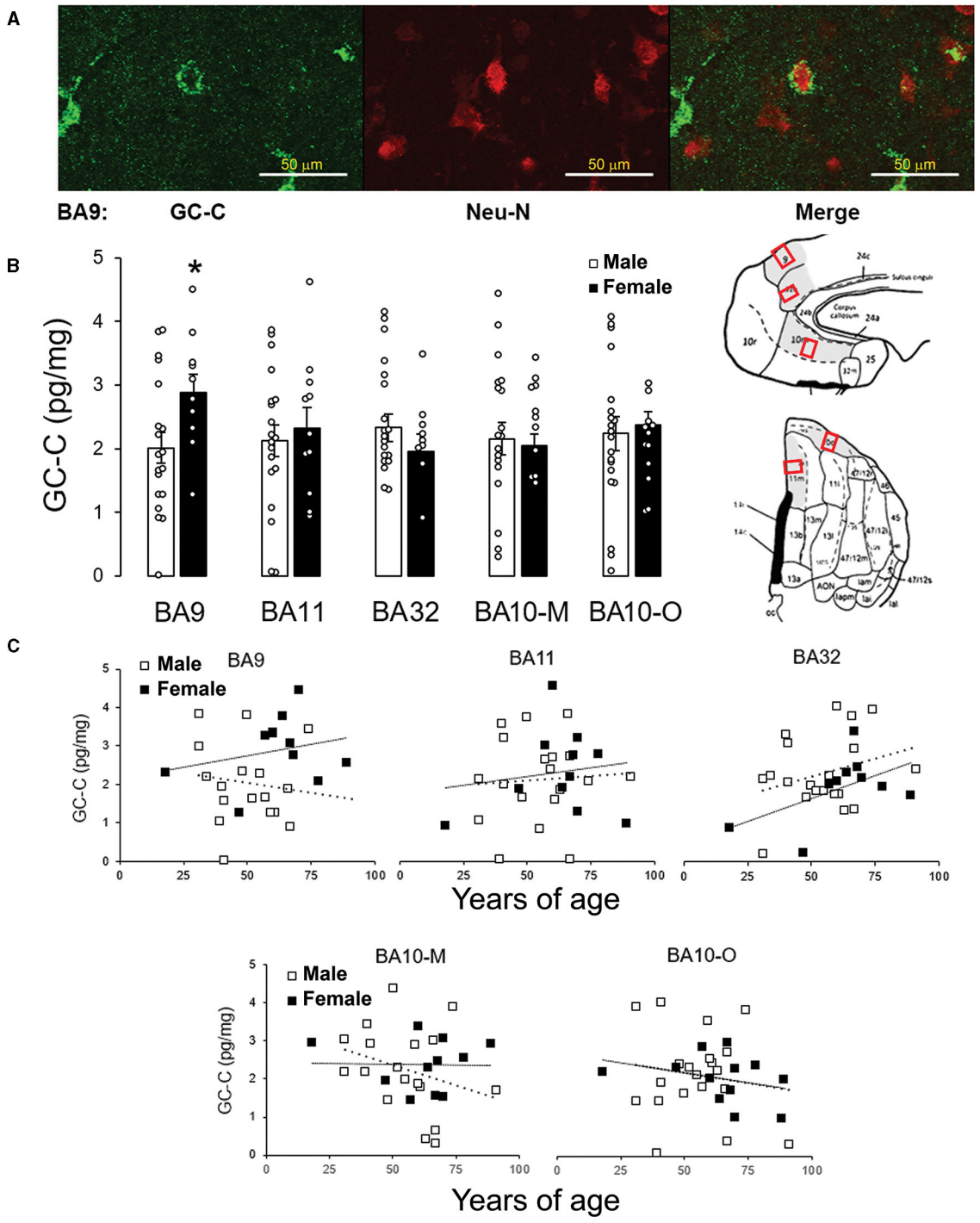

FIGURE 1
GC-C is more expressed in female than male BA9. GC-C is present in neurons in layer III of BA9. GC-C is presented as green and Neu-N (neuronal marker) as red. Bar represents 50 µm **(A)**. When the expression of GC-C was compared, of all tested areas the difference between male and female brains is found in BA9. Results are presented as mean ± SEM (pg/mg of tissue; $*p < 0.05$ statistically significant) **(B)**. Regions of interest are gray on the BA Maps (Ongür and Price, 2000; Ongür et al., 2003) and exact sampling location was presented by red squares. The expression of GC-C is not age dependent in men's and women's cortical regions. Results are presented as pg/mg of tissue. - - - line represents trendline for men. ..... line represents trendline for women **(C)**. BA, Brodmann area; GC-C, guanylate cyclase C.

a meal, the expression in the left BA9 decreased (192 ± 32 ng/L, $n = 8$; $p = 0.02$) compared to the left BA9 before meal. Furthermore, differences in GC-C expression between the left and right hemisphere were determined in female BA11 and BA10-O where GC-C had a higher expression in the right than in the left hemisphere (Figure 3B).

10.3389/fnmol.2024.1361089

TABLE 2 Correlation between GC-C expression and volume of stomach content.

GC-C/stomach content	Hy	MB	Cb	BA9	BA11	BA32	BA10-M	BA10-O
Male								
r	**−0.503**	−0.209	−0.039	−0.374	**−0.614**	0.200	**−0.523**	0.207
p	**0.040**	0.493	0.878	0.187	**0.015**	0.442	**0.038**	0.425
Female								
r	−0.555	−0.402	−0.011	0.316	0.029	0.001	**0.796**	−0.299
p	0.153	0.423	0.976	0.407	0.941	0.998	**0.010**	0.434

BA, Brodmann area; Cb, cerebellar cortex; Hy, hypothalamic Arcuate nucleus; O, orbital; M, medial. Bold values indicate statistically significant correlation when $p < 0.05$.

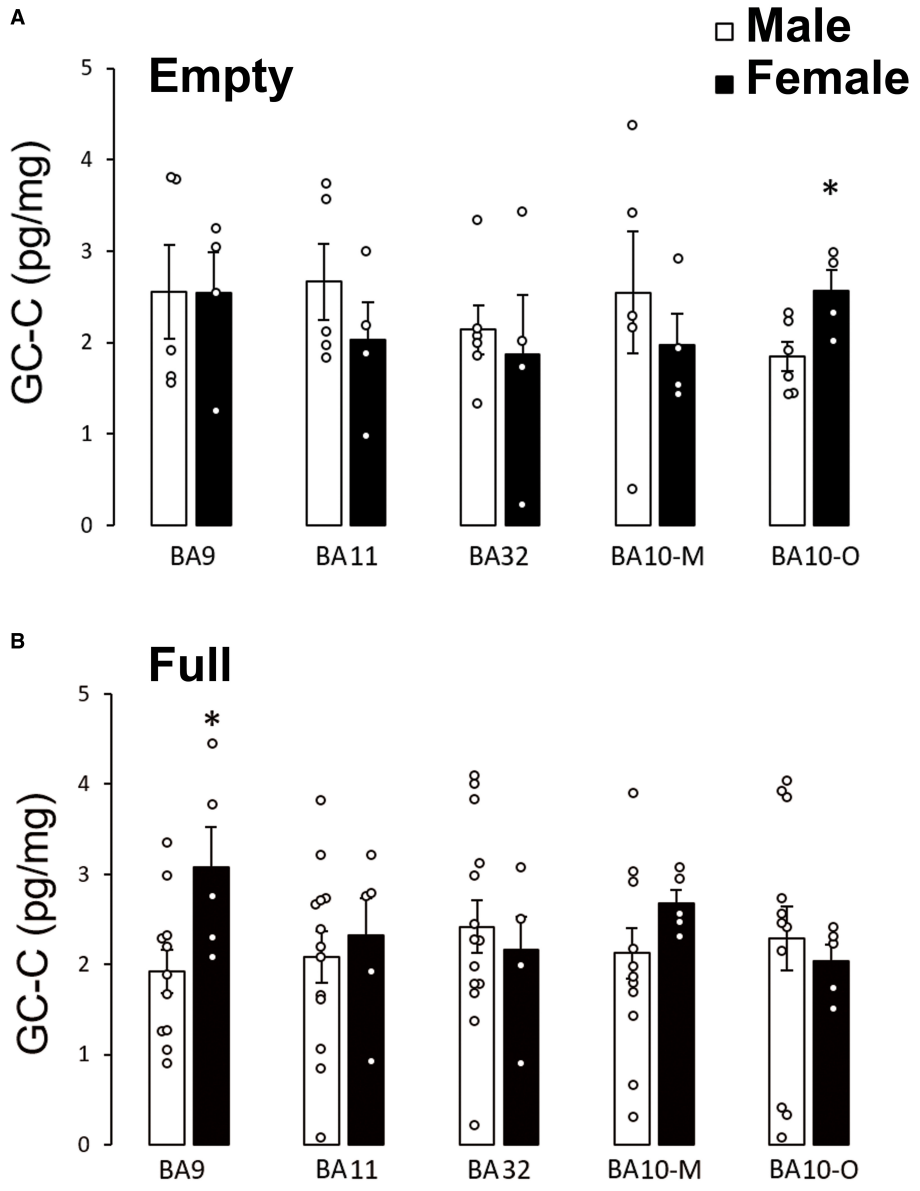

FIGURE 2
Sex differences of GC-C expression in the prefrontal cortex depended on feeding status. Sex differences in GC-C expression existed in BA10-O only if the stomach was empty (fasting conditions) in which case more GC-C is expressed in female participants **(A)**. Sex difference in BA9 exists if the stomach was full **(B)**. *$p < 0.05$ statistically significant. The results are presented as mean ± SEM (pg/mg of tissue). BA, Brodmann area; GC-C, guanylate cyclase C.

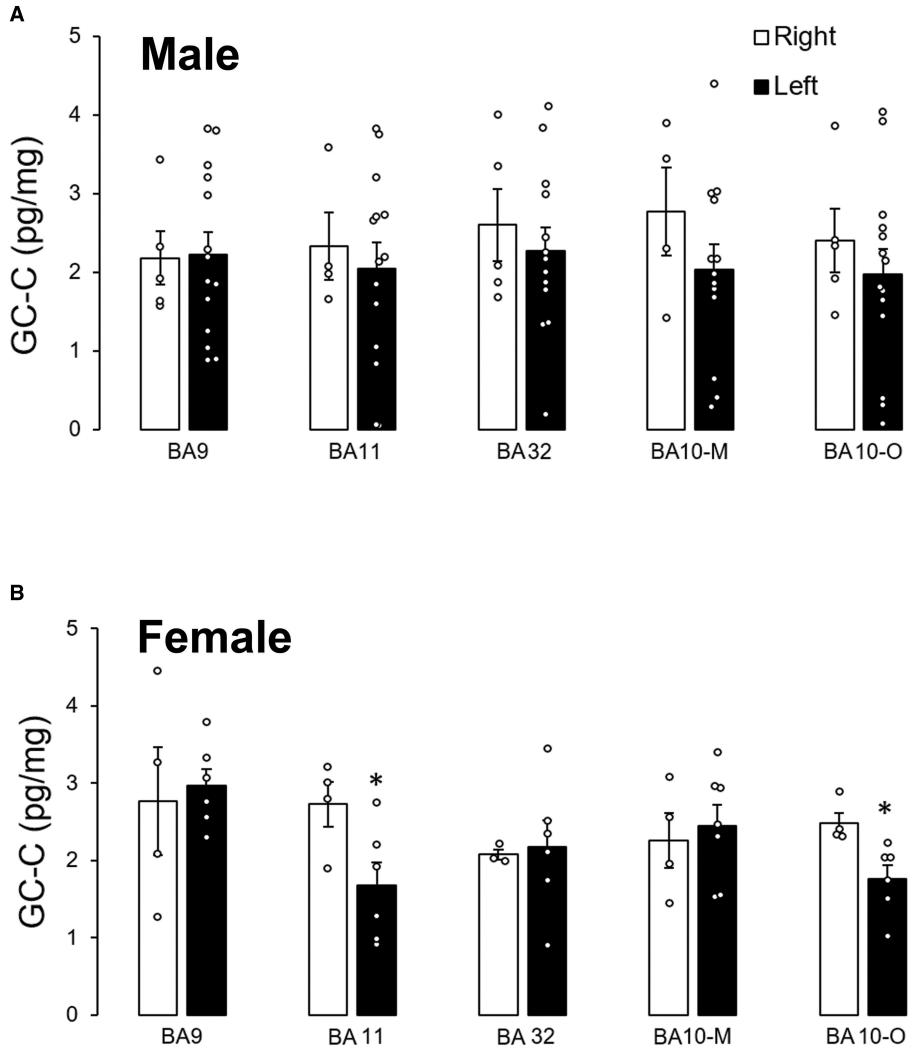

FIGURE 3
Expression of GC-C in right and left hemisphere was different only in female participants. There is no difference in GC-C expression between left and right male cortical regions **(A)**. Expression of GC-C in female BA11 and BA10-O is smaller in left hemisphere (*$p < 0.05$) **(B)**. The results are presented as mean ± SEM (pg/mg of tissue). BA, Brodmann area; GC-C, guanylate cyclase C.

GC-C expression in arcuate nucleus of hypothalamus is lower in female than male

To determine further sex difference in the human brain, we determined GC-C expression in the Arc of the Hy, the SN and the cerebellar cortex. Statistically significant negative correlation between the volume of stomach content and GC-C expression in the Arc of the Hy was found in male subjects ($r = -0.503$, $p = 0.040$), while this correlation was not statistically significant in female subjects ($r = -0.555$, $p = 0.153$, Table 2).

GC-C was less expressed in female Arc than in male. There was no statistically significant sex difference in GC-C expression in the SN (MB) or the cerebellar cortex (Figure 4A). Sex difference in GC-C expression was not present when the stomach was empty (Figure 4B), but was present when the stomach was full (Figure 4C).

The GC-C expression did not depend on age. Even though there was a possible negative correlation between age and GC-C expression in the female MB, this correlation was not statistically significant (Figure 5, $r = -0.51$, $p = 0.19$). GC-C was statistically significantly expressed more in female MB when compared to male but only until the age of 60 (expression in male SN is only 55% of female SN, $p = 0.009$). In older age this difference was not observed.

Furthermore, the expression of GC-C in the Cb was in positive correlation to the expression in the male Hy ($r = 0.67$, $p = 0.001$) but in negative correlation in female Hy ($r = -0.76$, $p = 0.01$, Figure 5B), which also suggested a difference in the expression and regulation of GC-C in the male and female brain.

In this study we did not find statistically significant correlation in GC-C expression between BA9, BA10, BA11, and BA32 and Hy, MB, or Cb (Supplementary Figure 1). When the results were analyzed by including feeding status, there was a negative correlation between expression of GC-C in the Cb compared to the expression in male BA11 when the stomach was empty ($r = -0.94$, $p = 0.016$). The negative correlation was also determined for female

10.3389/fnmol.2024.1361089

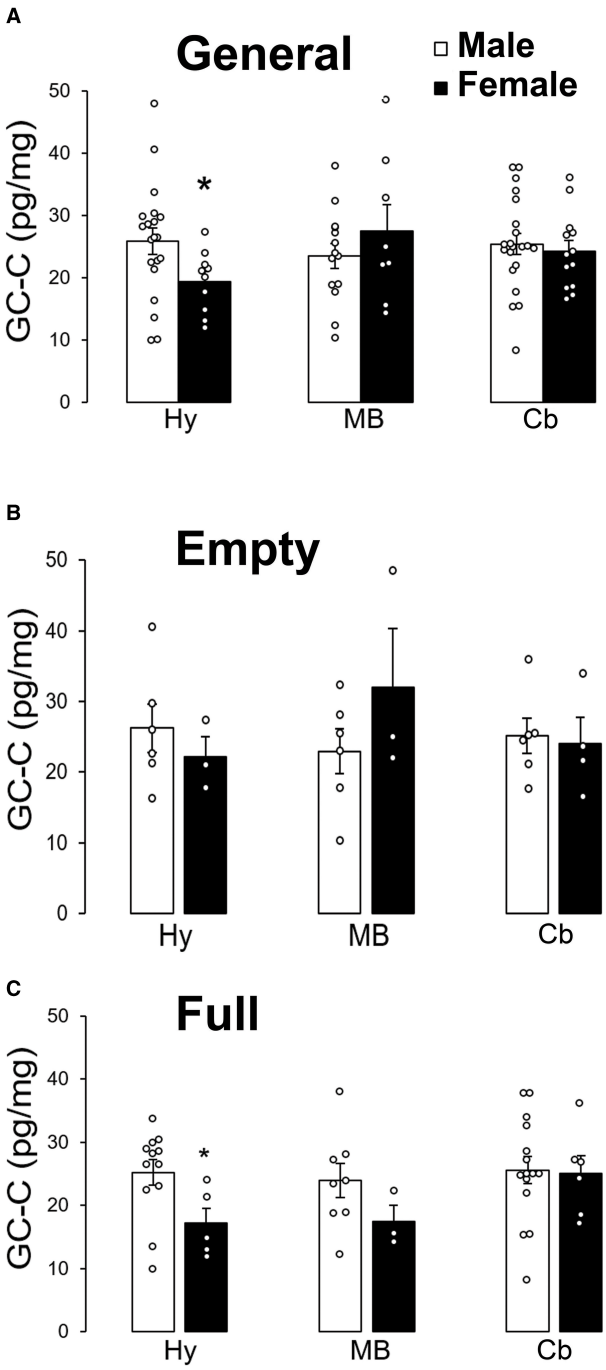

FIGURE 4
GC-C is less expressed in the female arcuate nucleus of the hypothalamus after a meal. GC-C is less expressed in female arcuate nucleus (Hy) than in male. Expression of GC-C in midbrain (MB, substantia nigra) and cerebellar cortex (Cb) did not statistically significantly differ between male and female participants **(A)**. There is no statistically significant difference in the GC-C expression in all tested regions of the brain when the stomach was empty **(B)**. Sex difference of GC-C expression in the hypothalamus only exists when the stomach was full **(C)**. *$p < 0.05$ statistically significant. The results are presented as mean ± SEM (pg/mg of tissue).

BA9 and Hy when the stomach was full. On the other hand, positive correlation was determined in GC-C expression in male BA9 and the Cb when the stomach was full (Supplementary Table 2). Those results suggest the importance of feeding status and sex in regulation of GC-C expression in different brain regions.

Discussion

Recent research points out the biological basis of sex differences in eating disorders (Culbert et al., 2021). Brian functions of estrogens on feeding regulation may be, at last partially, responsible for differences in food intake between men and women and higher occurrence of eating disorders in young women (Sodersten and Bergh, 2003). Additionally, to hunger and satiety regulation by the Hy, eating behavior is emotionally and motivationally regulated by the limbic system, Amyg and PFC. GC-C positive neurons are not found only in subcortical structures (MB, Amyg, Arc of Hy) but also, as we showed in this study, in the PFC. In humans such neurons are present especially in part of the cortex involved in regulation of feeding behavior. In this study we examined age, sex, and feeding status differences of GC-C expression in: BA9 (DLPFC), 11 (orbitofrontal cortex), 10 (anterior prefrontal cortex), 32 (dorsal anterior cingulate area), Arc of Hy, SN (MB), and cerebellar cortex. Since GC-C regulates feeding behavior in laboratory animals (Valentino et al., 2011; Folgueira et al., 2016), the differences in GC-C expression after a meal in comparison to fasting condition is not surprising. Sex differences in GC-C function is known in satiety and feeding regulation, brown adipose tissue activity and kidney function in laboratory animals (Dugandzic et al., 2020; Habek et al., 2020), therefore it is not surprising that the sex difference in GC-C expression exists as well in the human PFC.

Colantuoni et al. (2011) showed decreasing the expression of mRNA for GC-C with age in female DLPFC (BA46/9), but at the protein level there was no statistically significant correlation between age and GC-C expression for all tested cortical regions. In addition to differences in levels of expression of mRNA or protein, possible difference might be in the age span of our participants (18–96 years of age), since this study included only adults.

The regulation of GC-C expression by feeding status was found in male BA11 and BA10-M where GC-C expression was in negative correlation to volume of stomach content during autopsy. In female BA11 there was no detected correlation. On the other hand, in BA10-M the correlation was positive, which indicates sex differences in the regulation of GC-C, which in turn points to the regulation of BA11 and BA10-M function by feeding. The lack of GC-C regulation by feeding in female BA11 may contribute to the higher prevalence of eating disorders (Suda et al., 2010). To the best of our knowledge, this is the first study which compares the expression of proteins in the brain in relation to the feeding status during death by measuring the stomach content at autopsies. This can be a useful tool of determining the importance of proteins of interest in feeding regulation especially in the human PFC.

The expression of GC-C is regulated differently in male and female BA9. When the stomach is full, there is a higher expression of GC-C in women compared to men. These results are in accordance with a previously published study which shows that after showing images of hedonic foods to male and female participants, there is a greater activation of DLPFC in women when compared to men. Difference in activity was not shown

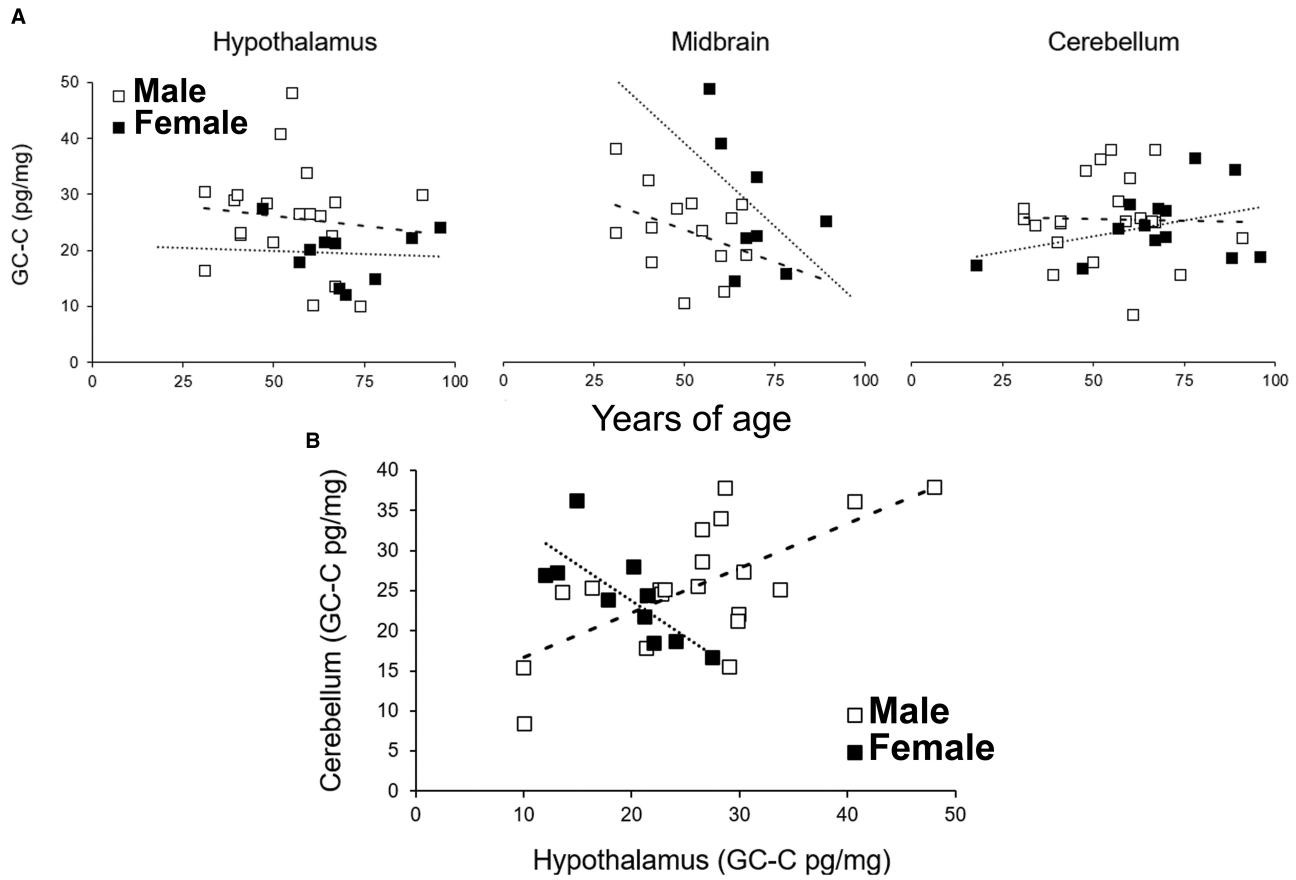

FIGURE 5
The expression of GC-C in the hypothalamus, midbrain and cerebellum is not correlated with age **(A)**. The expression of GC-C in the hypothalamus was in positive correlation to expression in cerebellar cortex in men, while it was in negative correlation in female participants **(B)**. Results are presented as pg/mg of tissue. - - - line represents trendline for male participants. ..... line represents trendline for female participants. GC-C, guanylate cyclase C.

when participants were hungry (Cornier et al., 2010). Higher expression of GC-C in female BA9 after a meal might be involved in greater activation of PFC which regulates executive functioning and inhibitory control after consumption of palatable food (Del Parigi et al., 2002; Cornier et al., 2010; Geliebter et al., 2013).

When the stomach is empty there is higher expression of GC-C in left then right male BA9 which decreased after a meal. This regulation was not observed in female BA9. Changing the eating behavior toward healthy food choices increased left DLPFC activity. The capability of left DLPFC activation seems to be a predictor for successful weight loss in women (Le et al., 2006; Ester and Kullmann, 2022). The regulation of GC-C expression in the left DLPFC could be involved in left DLPFC activation as response to a meal. The right PFC is also responsible for the regulation of feeding behavior (Ester and Kullmann, 2022), however, further research is needed to determine the possible regulation of GC-C expression in right hemisphere.

If the orbitofrontal cortex is more active when eating fats that person will consume more fats (Khorisantono et al., 2023) which might contribute to the obesity development. This brain region is a part of the brain reward system and it receives dopaminergic afferents from the MB where it is affected by GC-C (Schultz et al., 2000; Saper et al., 2002; Knutson et al., 2003; Heekeren et al., 2004; Cox et al., 2005; Gong et al., 2011). Eating behavior in persons with eating disorders is connected to the function of the left orbitofrontal cortex (Suda et al., 2010). Difference in GC-C expression between the left and right hemispheres was determined in female BA11, whereas GC-C is more expressed in the right than in the left hemisphere.

BA10 is involved in food evaluation process (Hollmann et al., 2013). Using fMRI, after looking a food pictures activities of left male BA10 decreased (Yoshikawa et al., 2016). In female left BA10 chronic stress reduced activity upon looking the picture of high calorie foods which might lead to obesity (Tryon et al., 2013). To determine the possible differences in regulation of GC-C expression in BA10, we separated this region into BA10-O and BA10-M. As shown for BA9, when the stomach is full, the higher expression of GC-C is found in female BA10-O, but only when the stomach is empty. Differences in GC-C expression between left and right hemisphere was determined in female BA10-O whereas GC-C is more expressed in men's the right than the left hemisphere, while there is no difference in men's either part of BA10.

BA32 (dorsal anterior cingulate area) is an integral part of the limbic system and is involved in the regulation of eating behavior (Zhang et al., 2023). In this study we found no statistically significant difference between male vs. female, left vs. right or feeding status regulation of GC-C expression in BA32.

The sex differences and feeding status are important for the regulation of GC-C expression in subcortical structures as well. As shown for the mouse Hy (Habek et al., 2020), sex difference in GC-C expression exist when the stomach is full, suggesting possibly lower satiety effects of GC-C agonists in women. The negative correlation exists in GC-C expression in female but not male BA9 and Hy when the stomach is full suggesting a different regulation of GC-C by feeding in the Hy and PFC with possibility that this regulation is sex dependent.

After activation either by glucose via glucose-sensitive neurons or via vagus from the intestine, VTA releases dopamine—the pleasure hormone. Dopamine release from dopaminergic neurons in the MB is potentiated by the activation of GC-C (Gong et al., 2011). Mice missing GC-C (GC-C KO) develop attention deficit hyperactivity disorder (ADHD; Gong et al., 2011). GC-C is expressed more in female MB in relation to male but only until the age of 60. These findings could potentially contribute in clarification of the higher prevalence of ADHD in younger men. Dopamine in the nucleus accumbens leads to the creation of feelings of happiness and satisfaction. The nucleus accumbens sends information to the Amyg that attributes to the experienced reward. Furthermore, by prediction of feeding, search for a food, and eating more dopamine is released in prefrontal cortex (Horvitz, 2000; Phillips et al., 2004). It is not surprising that GC-C is expressed in MB, PFC, and Amyg and its expression is higher in those regions of female brain (Dugandzic et al., 2020) which might contribute to their activation (executive functioning, inhibitory control and reward) after a meal.

To conclude, the regulation of PFC function by feeding includes sex dependent regulation of GC-C expression (BA9, BA11, BA10-O, and BA10-M). GC-C expression differs in the left and right hemispheres but only in female BA11 and BA10-O. For tested subcortical structures, the expression of GC-C in the female Hy was lower in relation to male, but only when the stomach was full. These results suggest possible role of GC-C in the regulation of feeding behavior and existing sex differences in this regulation. Further research is needed to reveal the connection between GC-C positive neurons in subcortical structures (Hy, Amyg, and SN) and PFC, and the importance of GC-C regulation of dopamine release, as well as its possible importance in eating disorders. Comparing the expression of proteins in relation to feeding status by measuring the stomach content at autopsies will give us better understanding how the PFC is involved in regulation of feeding behavior. Since the majority of the studies have been performed at men or even in mixed population, we have to pay more attention to sex differences for determining the specific role of PFC in regulation of eating and eating disorders.

Data availability statement

The raw data supporting the conclusions of this article will be made available by the authors, without undue reservation.

Ethics statement

The studies involving humans were approved by Ethical Committee of the University of Zagreb School of Medicine (641-01/18-02/01). The studies were conducted in accordance with the local legislation and institutional requirements. The human samples used in this study were acquired during standard autopsy after obtaining a signed informed consent form from the deceased's next of kin.

Author contributions

MR: Formal analysis, Methodology, Validation, Writing—review & editing, Data curation. VC: Data curation, Formal analysis, Methodology, Writing—review & editing. MT: Data curation, Formal analysis, Methodology, Writing—review & editing. AM: Data curation, Formal analysis, Methodology, Writing—review & editing. PB: Conceptualization, Data curation, Formal analysis, Methodology, Writing—review & editing. PŠ: Conceptualization, Data curation, Formal analysis, Methodology, Supervision, Writing—review & editing. IB: Conceptualization, Data curation, Formal analysis, Investigation, Methodology, Supervision, Writing—review & editing. AD: Conceptualization, Formal analysis, Funding acquisition, Investigation, Methodology, Project administration, Resources, Supervision, Validation, Visualization, Writing—original draft, Writing—review & editing.

Funding

The author(s) declare financial support was received for the research, authorship, and/or publication of this article. This publication was co-financed by the European Union through the European Regional Development Fund, Operational Programme Competitiveness and Cohesion, Grant Agreement No. KK.01.1.1.01.0007, CoRENeuro, and by the Croatian Science Foundation Research Grant (IP-2018-01- 7416).

Conflict of interest

The authors declare that the research was conducted in the absence of any commercial or financial relationships that could be construed as a potential conflict of interest.

Publisher's note

All claims expressed in this article are solely those of the authors and do not necessarily represent those of their affiliated organizations, or those of the publisher, the editors and the reviewers. Any product that may be evaluated in this article, or claim that may be made by its manufacturer, is not guaranteed or endorsed by the publisher.

Supplementary material

The Supplementary Material for this article can be found online at: https://www.frontiersin.org/articles/10.3389/fnmol.2024.1361089/full#supplementary-material

References

Banovac, I., Sedmak, D., Džaja, D., Jalšovec, D., Jovanov Milošević, N., Rašin, M. R., et al. (2019). Somato-dendritic morphology and axon origin site specify von Economo neurons as a subclass of modified pyramidal neurons in the human anterior cingulate cortex. *J. Anat.* 235, 651–669. doi: 10.1111/joa.13068

Banovac, I., Sedmak, D., Esclapez, M., and Petanjek, Z. (2022). The distinct characteristics of somatostatin neurons in the human brain. *Mol. Neurobiol.* 59, 4952–4965. doi: 10.1007/s12035-022-02892-6

Banovac, I., Sedmak, D., Rojnić Kuzman, M., Hladnik, A., and Petanjek, Z. (2020). Axon morphology of rapid Golgi-stained pyramidal neurons in the prefrontal cortex in schizophrenia. *Croat. Med. J.* 61, 354–365. doi: 10.3325/cmj.2020.61.354

Begg, D. P., Steinbrecher, K. A., Mul, J. D., Chambers, A. P., Kohli, R., Haller, A., et al. (2014). Effect of guanylate cyclase-C activity on energy and glucose homeostasis. *Diabetes* 63, 3798–3804. doi: 10.2337/db14-0160

Boenisch, T. (2005). Effect of heat-induced antigen retrieval following inconsistent formalin fixation. *Appl. Immunohistochem. Mol. Morphol.* 13, 283–286. doi: 10.1097/01.0000146524.74402.a4

Brodmann, K. (1909). *Vergleichende Lokalisationslehre der Grosshirnrinde in ihren Prinzipien dargestellt auf Grund des Zellenbaues*. Leipzig: Barth.

Colantuoni, C., Lipska, B. K., Ye, T., Hyde, T. M., Tao, R., Leek, J. T., et al. (2011). Temporal dynamics and genetic control of transcription in the human prefrontal cortex. *Nature* 478, 519–523. doi: 10.1038/nature10524

Cornier, M. A., Salzberg, A. K., Endly, D. C., Bessesen, D. H., and Tregellas, J. R. (2010). Sex-based differences in the behavioral and neuronal responses to food. *Physiol. Behav.* 99, 538–543. doi: 10.1016/j.physbeh.2010.01.008

Cox, S. M., Andrade, A., and Johnsrude, I. S. (2005). Learning to like: a role for human orbitofrontal cortex in conditioned reward. *J. Neurosci.* 25:273340. doi: 10.1523/JNEUROSCI.3360-04.2005

Culbert, K. M., Sisk, C. L., and Klump, K. L. (2021). A narrative review of sex differences in eating disorders: is there a biological basis? *Clin. Ther.* 43, 95–111. doi: 10.1016/j.clinthera.2020.12.003

de Vrind, V. A. J., van 't Sant, L. J., Rozeboom, A., Luijendijk-Berg, M. C. M., Omrani, A., and Adan, R. A. H. (2021). Leptin receptor expressing neurons in the substantia Nigra regulate locomotion, and in the ventral tegmental area motivation and feeding. *Front. Endocrinol.* 12:680494. doi: 10.3389/fendo.2021.680494

Del Parigi, A., Chen, K., Gautier, J. F., Salbe, A. D., Pratley, R. E., Ravussin, E., et al. (2002). Sex differences in the human brain's response to hunger and satiation. *Am. J. Clin. Nutr.* 75, 1017–1022. doi: 10.1093/ajcn/75.6.1017

Dugandzic, A., Ratko, M., and Habek, N. (2020). Anxiety-like behavior in female mice changes by feeding, possible effect of guanylate cyclase C. *Eur. J. Neurosci.* 2, 2781–2790. doi: 10.1111/ejn.14607

Ester, T., and Kullmann, S. (2022). Neurobiological regulation of eating behavior: evidence based on non-invasive brain stimulation. *Rev. Endocr. Metab. Disord.* 23, 753–772. doi: 10.1007/s11154-021-09697-3

Fan, X., Hamra, F. K., Freeman, R. H., Eber, S. L., Krause, W. J., Lim, R. W., et al. (1996). Uroguanylin: cloning of preprouroguanylin cDNA, mRNA expression in the intestine and heart and isolation of uroguanylin and prouroguanylin from plasma. *Biochem. Biophys. Res. Commun.* 219, 457–462. doi: 10.1006/bbrc.1996.0255

Fan, X., Wang, Y., London, R. M., Eber, S. L., Krause, W. J., Freeman, R. H., et al. (1997). Signaling pathways for guanylin and uroguanylin in the digestive, renal, central nervous, reproductive, and lymphoid Systems. *Endocrinology* 138, 4636–4648. doi: 10.1210/endo.138.11.5539

Ferrini, F., Salio, C., Lossi, L., and Merighi, A. (2009). Ghrelin in central neurons. *Curr. Neuropharmacol.* 7, 37–49. doi: 10.2174/157015909787602779

Folgueira, C., Beiroa, D., Callon, A., Al-Massadi, O., Barja-Fernandez, S., Senra, A., et al. (2016). Uroguanylin action in the brain reduces weight gain in obese mice via different efferent autonomic pathways. *Diabetes* 65, 421–432. doi: 10.2337/db15-0889

Geliebter, A., Pantazatos, S. P., McOuatt, H., Puma, L., Gibson, C. D., and Atalayer, D. (2013). Sex-based fMRI differences in obese humans in response to high vs. low energy food cues. *Behav. Brain. Res.* 243, 91–96. doi: 10.1016/j.bbr.2012.12.023

Gong, R., Ding, C., Hu, J., Lu, Y., Liu, F., Mann, E., et al. (2011). Role for the membrane receptor guanylyl cyclase-C in attention deficiency and hyperactive behavior. *Science* 333, 1642–1646. doi: 10.1126/science.1207675

Habek, N., Dobrivojević Radmilović, M., Kordić, M., Ilić, K., Grgić, S., Farkaš, V., et al. (2020). Activation of brown adipose tissue in diet-induced thermogenesis is GC-C dependent. *Pflugers. Arch.* 472, 405–417. doi: 10.1007/s00424-020-02347-8

Habek, N., Ratko, M., and Dugandžić, A. (2021). Uroguanylin increases Ca^{2+} concentration in astrocytes via guanylate cyclase C-independent signaling pathway. *Croat. Med. J.* 62, 250–263. doi: 10.3325/cmj.2021.62.250

Habek, N., Ratko, M., Kordić, M., and Dugandžić, A. (2023). Uroguanylin activation of brown adipose tissue is age, gender, and phase of the estrous cycle dependent. *J. Transl. Med.* 21:35. doi: 10.1186/s12967-022-03800-1

Heekeren, H. R., Marrett, S., Bandettini, P. A., and Ungerleider, L. G. (2004). A general mechanism for perceptual decision-making in the human brain. *Nature* 431, 859–862. doi: 10.1038/nature02966

Hollmann, M., Pleger, B., Villringer, A., and Horstmann, A. (2013). Brain imaging in the context of food perception and eating. *Curr. Opin. Lipidol.* 24, 18–24. doi: 10.1097/MOL.0b013e32835b61a4

Horvitz, J. C. (2000). Mesolimbocortical and nigrostriatal dopamine responses to salient non-reward events. *Neuroscience* 96, 651–656. doi: 10.1016/S0306-4522(00)00019-1

Iosif, C. I., Bashir, Z. I., Apps, R., and Pickford, J. (2023). Cerebellar prediction and feeding behaviour. *Cerebellum* 22, 1002–1019. doi: 10.1007/s12311-022-01476-3

Khorisantono, P. A., Huang, F. Y., Sutcliffe, M. P. F., Fletcher, P. C., Farooqi, I. S., and Grabenhorst, F. (2023). A neural mechanism in the human orbitofrontal cortex for preferring high-fat foods based on oral texture. *J. Neurosci.* 43, 8000–8017. doi: 10.1523/JNEUROSCI.1473-23.2023

Kim, G. W., Lin, J. E., Snook, A. E., Aing, A. S., Merlino, D. J., Li, P., et al. (2016). Calorie-induced ER stress suppresses uroguanylin satiety signaling in diet-induced obesity. *Nutr. Diabet.* 6:e211. doi: 10.1038/nutd.2016.18

Knutson, B., Fong, G. W., Bennett, S. M., Adams, C. M., and Hommer, D. (2003). A region of mesial prefrontal cortex tracks monetarily rewarding out comes: characterization with rapid event-related fMRI. *Neuroimage* 18:26372. doi: 10.1016/S1053-8119(02)00057-5

Le, D. S., Pannacciulli, N., Chen, K., Del Parigi, A., Salbe, A. D., Reiman, E. M., et al. (2006). Less activation of the left dorsolateral prefrontal cortex in response to a meal: a feature of obesity. *Am. J. Clin. Nutr.* 84, 725–731. doi: 10.1093/ajcn/84.4.725

Li, Z., Perkins, A. G., Peters, M. F., Campa, M. J., and Goy, M. F. (1997). Purification, cDNA sequence, and tissue distribution of rat uroguanylin. *Regul. Pept.* 68, 45–56. doi: 10.1016/S0167-0115(96)02103-9

Low, A. Y. T., Goldstein, N., Gaunt, J. R., Huang, K. P., Zainolabidin, N., Yip, A. K. K., et al. (2021). Reverse-translational identification of a cerebellar satiation network. *Nature* 600, 269–273. doi: 10.1038/s41586-021-04143-5

Lowe, C. J., Reichelt, A. C., and Hall, P. A. (2019). The prefrontal cortex and obesity: a health neuroscience perspective. *Trends. Cogn. Sci.* 23, 349–361. doi: 10.1016/j.tics.2019.01.005

Markerink-Van Ittersum, M., Steinbusch, H. W., and De Vente, J. (1997). Region-specific developmental patterns of atrial natriuretic factor- and nitric oxide-activated guanylyl cyclases in the postnatal frontal rat brain. *Neuroscience* 78, 571–587. doi: 10.1016/S0306-4522(96)00622-7

Merlino, D. J., Barton, J. R., Charsar, B. A., Byrne, M. D., Rappaport, J. A., Smeyne, R. J., et al. (2019). Two distinct GUCY2C circuits with PMV (hypothalamic) and SN/VTA (MB) origin. *Brain. Struct. Funct.* 224, 2983–2999. doi: 10.1007/s00429-019-01949-y

Naito, J., Naka, Y., and Watanabe, H. (2009). Clinical impression of brain natriuretic peptide levels in demented patients without cardiovascular disease. *Geriatr. Gerontol. Int.* 9, 242–245. doi: 10.1111/j.1447-0594.2009.00526.x

Neumann, M., and Gabel, D. (2002). Simple method for reduction of autofluorescence in fluorescence microscopy. *J. Histochem. Cytochem.* 50, 437–439. doi: 10.1177/002215540205000315

Ongür, D., Ferry, A. T., and Price, J. L. (2003). Architectonic subdivision of the human orbital and medial prefrontal cortex. *J. Comp. Neurol.* 460, 425–449. doi: 10.1002/cne.10609

Ongür, D., and Price, J. L. (2000). The organization of networks within the orbital and medial prefrontal cortex of rats, monkeys and humans. *Cereb. Cortex.* 10, 206–219. doi: 10.1093/cercor/10.3.206

Patterson, M., Ward, H., Halvai, D., Holm Nilsen, H. A., and Reeves, S. (2020). Postprandial regulation of prouroguanylin in humans of a healthy weight and those who are overweight or with obesity. *Peptides* 123:170179. doi: 10.1016/j.peptides.2019.170179

Phillips, A. G., Ahn, S., and Floresco, S. B. (2004). Magnitude of dopamine release in medial prefrontal cortex predicts accuracy of memory on a delayed response task. *J. Neurosci.* 24, 547–553. doi: 10.1523/JNEUROSCI.4653-03.2004

Rodríguez, A., Gómez-Ambrosi, J., Catalán, V., Ezquerro, S., Méndez-Giménez, L., Becerril, S., et al. (2016). Guanylin and uroguanylin stimulate lipolysis in human visceral adipocytes. *Int. J. Obes.* 40, 1405–1415. doi: 10.1038/ijo.2016.66

Rolls, E. T. (2023). The orbitofrontal cortex, food reward, body weight and obesity. *Soc. Cogn. Affect. Neurosci.* 18:nsab044. doi: 10.1093/scan/nsab044

Sadeghipour, A., and Babaheidarian, P. (2019). Making formalin-fixed, paraffin embedded blocks. *Methods. Mol. Biol.* 1897, 253–268. doi: 10.1007/978-1-4939-8935-5_22

Saper, C. B., Chou, T. C., and Elmquist, J. K. (2002). The need to feed:homeostatic and hedonic control of eating. *Neuron* 36, 199–211. doi: 10.1016/S0896-6273(02)00969-8

Saruco, E., and Pleger, B. (2021). A systematic review of obesity and binge eating associated impairment of the cognitive inhibition system. *Front. Nutr.* 8:609012. doi: 10.3389/fnut.2021.609012

Schultz, W., Tremblay, L., and Hollerman, J. R. (2000). Reward processing in primate orbitofrontal cortex and basal ganglia. *Cereb. Cortex.* 10, 272–284. doi: 10.1093/cercor/10.3.272

Simões-Silva, L., Moreira-Rodrigues, M., Quelhas-Santos, J., Fernandes-Cerqueira, C., Pestana, M., Soares-Silva, I., et al. (2013). Intestinal and renal guanylin peptides system in hypertensive obese mice. *Exp. Biol. Med.* 238, 90–97. doi: 10.1258/ebm.2012.012232

Sodersten, P., and Bergh, C. (2003). Anorexia nervosa: towards a neurobiologically based therapy. *Eur. J. Pharmacol.* 480, 67–74. doi: 10.1016/j.ejphar.2003.08.093

Suda, M., Uehara, T., Fukuda, M., Sato, T., Kameyama, M., and Mikuni, M. (2010). Dieting tendency and eating behavior problems in eating disorder correlate with right frontotemporal and left orbitofrontal cortex: a near-infrared spectroscopy study. *J. Psychiatr. Res.* 44, 547–555. doi: 10.1016/j.jpsychires.2009.11.005

Sun, Y., Ip, P., and Chakrabartty, A. (2017). Simple elimination of background fluorescence in formalin-fixed human brain tissue for immunofluorescence microscopy. *J. Vis. Exp.* 2017:56188. doi: 10.3791/56188

Sy, J., and Ang, L.-C. (2019). Microtomy: cutting formalin-fixed, paraffin-embedded sections. *Methods. Mol. Biol.* 1897, 269–278. doi: 10.1007/978-1-4939-8935-5_23

Talairach, J., and Szikla, G. (1980). Application of stereotactic concepts to the surgery of epilepsy. *Acta. Neurochir. Suppl.* 30, 35–54. doi: 10.1007/978-3-7091-8592-6_5

Tryon, M. S., Carter, C. S., Decant, R., and Laugero, K. D. (2013). Chronic stress exposure may affect the brain's response to high calorie food cues and predispose to obesogenic eating habits. *Physiol. Behav.* 120, 233–242. doi: 10.1016/j.physbeh.2013.08.010

Valentino, M. A., Lin, J. E., Snook, A. E., Li, P., Kim, G. W., Marszalowicz, G., et al. (2011). A uroguanylin-GUCY2C endocrine axis regulates feeding in mice. *J. Clin. Invest.* 121, 3578–3588. doi: 10.1172/JCI57925

Wang, R., Chow, B. K. C., and Zhang, L. (2019). Distribution and functional implication of secretin in multiple brain regions. *J. Mol. Neurosci.* 68, 485–493. doi: 10.1007/s12031-018-1089-z

Whissell, P. D., Bang, J. Y., Khan, I., Xie, Y.-F., Parfitt, G. M., Grenon, M., et al. (2019). Selective activation of cholecystokinin-expressing GABA (CCK-GABA) neurons enhances memory and cognition. *eNeuro* 6:360. doi: 10.1523/ENEURO.0360-18.2019

Yoshikawa, T., Tanaka, M., Ishii, A., Yamano, Y., and Watanabe, Y. (2016). Visual food stimulus changes resting oscillatory brain activities related to appetitive motive. *Behav. Brain. Funct.* 12:26. doi: 10.1186/s12993-016-0110-3

Zaqout, S., Becker, L. L., and Kaindl, A. M. (2020). Immunofluorescence staining of paraffin sections step by step. *Front. Neuroanat.* 14:582218. doi: 10.3389/fnana.2020.582218

Zhang, X., Wen, K., Han, J., and Chen, H. (2023). The neural processes in food decision-making and their effect on daily diet management in successful and unsuccessful restrained eaters. *Neuroscience* 517, 1–17. doi: 10.1016/j.neuroscience.2023.01.023

Zwanzger, P., Domschke, K., and Bradwejn, J. (2012). Neuronal network of panic disorder: the role of the neuropeptide cholecystokinin. *Depr. Anxiety* 29, 762–774. doi: 10.1002/da.21919

frontiers | Frontiers in Physiology

TYPE Systematic Review
PUBLISHED 10 June 2024
DOI 10.3389/fphys.2024.1393497

OPEN ACCESS

EDITED BY
Kristina Mlinac-Jerković,
University of Zagreb, Croatia

REVIEWED BY
Yuki Uchida,
Showa University, Japan
Angela J. Grippo,
Northern Illinois University, United States

*CORRESPONDENCE
Péter Szabó,
szabo.peter3@pte.hu

RECEIVED 01 March 2024
ACCEPTED 13 May 2024
PUBLISHED 10 June 2024

CITATION
Szabó P, Bonet S, Hetényi R, Hanna D, Kovács Z, Prisztóka G, Križalkovičová Z and Szentpéteri J (2024), Systematic review: pain, cognition, and cardioprotection—unpacking oxytocin's contributions in a sport context.
Front. Physiol. 15:1393497.
doi: 10.3389/fphys.2024.1393497

Systematic review: pain, cognition, and cardioprotection—unpacking oxytocin's contributions in a sport context

Péter Szabó[1,2,3]*, Sara Bonet[4], Roland Hetényi[5,6,7,8], Dániel Hanna[5,6,7,8], Zsófia Kovács[1], Gyöngyvér Prisztóka[1], Zuzana Križalkovičová[9] and József Szentpéteri[3]

[1]Faculty of Sciences, Institute of Sports Science and Physical Education, University of Pécs, Pécs, Hungary, [2]Faculty of Humanities, University of Pécs, Pécs, Hungary, [3]Medical School, Institute of Transdisciplinary Discoveries, University of Pécs, Pécs, Hungary, [4]Faculty of Medicine Osijek, Josip Juraj Strossmayer University of Osijek, Osijek, Croatia, [5]RoLink Biotechnology Kft., Pécs, Hungary, [6]Hungarian National Blood Transfusion Service, Budapest, Hungary, [7]Szentágothai Research Centre, University of Pécs, Pécs, Hungary, [8]National Virology Laboratory, University of Pécs, Pécs, Hungary, [9]Faculty of Health Sciences, Institute of Physiotherapy and Sport Science, Department of Sport Science, Pécs, Hungary

Introduction: This systematic review investigates the interplay between oxytocin and exercise; in terms of analgesic, anti-inflammatory, pro-regenerative, and cardioprotective effects. Furthermore, by analyzing measurement methods, we aim to improve measurement validity and reliability.

Methods: Utilizing PRISMA, GRADE, and MECIR protocols, we examined five databases with a modified SPIDER search. Including studies on healthy participants, published within the last 20 years, based on keywords "oxytocin," "exercise" and "measurement," 690 studies were retrieved initially (455 unique records). After excluding studies of clinically identifiable diseases, and unpublished and reproduction-focused studies, 175 studies qualified for the narrative cross-thematic and structural analysis.

Results: The analysis resulted in five categories showing the reciprocal impact of oxytocin and exercise: Exercise (50), Physiology (63), Environment (27), Social Context (65), and Stress (49). Exercise-induced oxytocin could promote tissue regeneration, with 32 studies showing its analgesic and anti-inflammatory effects, while 14 studies discussed memory and cognition. Furthermore, empathy-associated *OXTR* rs53576 polymorphism might influence team sports performance. Since dietary habits and substance abuse can impact oxytocin secretion too, combining self-report tests and repeated salivary measurements may help achieve precision.

Discussion: Oxytocin's effect on fear extinction and social cognition might generate strategies for mental training, and technical, and tactical development in sports. Exercise-induced oxytocin can affect the amount of stress experienced by athletes, and their response to it. However, oxytocin levels

Abbreviations: AVP, Arginine vasopressin; KO mice, knockout mice; LE rat, long-evans rat; mPFC, medial prefrontal cortex; MWM, morris water maze; OXTR, oxytocin receptor gene; SD rat, sprague dawley rat; SHR rat, spontaneously hypertensive rat; WKY rat, Wistar Kyoto rat; W rat, wistar rat; ZF rat, zucker fatty rat.

could depend on the type of sport in means of contact level, exercise intensity, and duration. The influence of oxytocin on athletes' performance and recovery could have been exploited due to its short half-life. Examining oxytocin's complex interactions with exercise paves the way for future research and application in sports science, psychology, and medical disciplines.

Systematic Review Registration: https://www.crd.york.ac.uk/prospero/display_record.php?RecordID=512184, identifier CRD42024512184

KEYWORDS

cardioprotection, cognition, exercise, measurement, oxytocin, pain

1 Introduction

Technology has made it increasingly difficult for children to interact and physically play with their peers. Movement and time spent together, when they gather in physical education classrooms, are clearly of paramount importance (Knaus et al., 2020). Through oxytocin secretion, sports might present opportunity to combat diseases, aggression, and bullying at school. Empathy and social care, related to oxytocin, may help this process (Jolliffe and Farrington, 2011). Finding the most appropriate sport is therefore key.

A brief overview of the relationship between oxytocin and exercise further warrants this review, as not much is explicitly known about the interplay between them. We do not know what the best sport is to aid the secretion of this hormone. This could be answered if a precise, stable, and robust measuring methodology, that could be followed in sports context, was available. The cardioprotective effect provided by exercise is already well established in sports and medical literature (Sakamoto et al., 2011). However, a deeper understanding of this relationship could provide a great benefit for sports science.

Oxytocin is a nonapeptide produced by neurohypophysis, most well-known for its role in social bonding, trust, love and intimacy, empathy, childbirth, and lactation. First identified in 1906 by Sir Henry Dale, who observed its ability to cause uterine contractions, it was later found to have much more complex functions and effects on both autonomic and cognitive processes. It is known today that oxytocin receptors are not only present in the central nervous system (amygdala, hippocampus, prefrontal cortex, and ventral tegmental area) but in other tissues as well—the uterus, heart, gastrointestinal tract, etc., Still, oxytocin's role might be underestimated in the sports science field. Strikingly, this gap in the literature has neither been emphasized nor explored at the time of writing this review. In humans, oxytocin increases both sympathetic and parasympathetic cardiac activity (Brailoiu et al., 2013), the understanding of which would yield valuable insight for health sciences. Even though progressive efforts are made (Michelini, 2007a; Michelini, 2007b) animal studies document a more detailed description of the relationship between oxytocin, cardioprotection, hypertension, and exercise than current research on humans. For the afore mentioned reasons we believe that there is a strong need for the investigation of oxytocin's exercise-related benefits.

In Wistar Kyoto (WKY) and Spontaneously Hypertensive (SHR) rats, walking and running on a treadmill decreased resting heart rate due to oxytocin (Michelini, 2007a; Michelini, 2007b; Ceroni et al., 2009; Higa-Taniguchi et al., 2009; Cavalleri et al., 2011). Exercise increases oxytocin, consequently boosting neuroplasticity, aiding its role in cardiac functions, and resting heart rate even in aging Wistar (W) rats using treadmills (Michelini, 2007a; Michelini, 2007b; Santos et al., 2018; Rocha-Santos et al., 2020). For cardioprotection, pre-treating, healing cardiac tissue, and hypertension-related issues oxytocin also shows positive and promising results in WKY, SHR, Sprague Dawley (SD), and W rats after either exercise-related or exogenous oxytocin adage (Martins et al., 2005; Moghimian et al., 2012; Gutkowska et al., 2016; Wang et al., 2020).

Looking at stress responses and recovery times, oxytocin might be a useful asset in both animals and humans (Stanić et al., 2017; Gümüs et al., 2015). Oxytocin's role in muscle mass and metabolic health is not yet fully understood (Stanić et al., 2017). However, even intranasal oxytocin may enhance muscle mass and improve metabolic profiles (Espinoza et al., 2021). This could be crucial for sports and exercise programs aimed at older or sedentary individuals. In addition, moderate-intensity exercise and oxytocin displayed hepatoprotection in comparison with other treatments, believed to be attached to its antioxidant and anti-inflammatory effects (ELKady et al., 2021).

Aerobic involuntary exercise was able to induce significant oxytocin changes in rodents. Swimming training seems to be a powerful tool to elicit exercise-induced oxytocin change usually applied through the Morris Water Maze (MWM). However, the result of such stimuli connected to physical stress seems to be outcome-dependent and possibly connected to behavioral despair which is important data for treating depression (Porsolt et al., 2001; Peijie et al., 2003; Engelmann et al., 2006). Exercise-induced oxytocin may also help to avoid drug self-administration behaviors in W and SD rats (Farzinpour et al., 2019; Carson et al., 2010). This phenomenon may be explained by the anti-stress and anti-depressant effect of oxytocin, which is not yet fully understood (Crestani et al., 2013). Unsurprisingly, oxytocin release can be induced by vigorous aerobic exercise like swimming training in C57BL6 mice and likely also in humans (Kim and Han, 2016; Azari et al., 2023). The interaction of hope, positive and negative reinforcement, and oxytocin could possibly hold staggering discoveries in the future as previously tested in a well-known study on rats where hope meant survival and increased mobility (Castagné et al., 2011). Furthermore, exogenous or administered oxytocin is capable of increasing exercise performance in SHR and W rats, which, if tested in humans, could lead to improved sports performance and recovery (Cruz et al., 2013; Juif and Poisbeau, 2013; Liu and Xue, 2017; Shima et al., 2022). It is also possible that higher oxytocin levels can be associated with better trainability in horses (Kim et al., 2021; Kim et al., 2023) and dogs (Mitsui et al., 2011), changing their proclivity to react preferably to ambiguous stimuli. Plasma oxytocin was also slightly elevated by aerobic running exercises in dogs, pulling a sled together (Leggieri et al., 2019). Of

course, for now, the meaning of these findings is unclear for human physiology.

Voluntary exercise, however, was not always able to stimulate oxytocin enough to elicit significant change. In male W, Lewis, SHR, and SD rats voluntary wheel running did not alter oxytocin significantly, moreover, the response again seemed stress-dependent (Bakos et al., 2007; Bakos et al., 2008; Takahashi et al., 2022). Elevated oxytocin levels offer cardioprotection through vasodilation and regulation of the resting heart rate originating from exercise. Aerobic endurance exercise in animal studies shows that there might be a threshold of exercise-induced oxytocin which may strengthen these cardioprotective effects (Hada et al., 2003; Lesimple et al., 2020; Tolentino Bento da Silva et al., 2021).

Cross-reading on the potential yields of exercise from animal studies is difficult, humans may perceive even an ultramarathon as voluntary and prolonged exercise. Interestingly, during prolonged exercise, the correlation of the antidiuretic hormone-arginine vasopressin (AVP) and oxytocin plays a role in social recognition which is crucial for human and animal relationships and mating (Hew-Butler et al., 2008a; Hew-Butler et al., 2008b; Zeng et al., 2012). Subsequently, being healthy carries mating benefits in humans and animals but this relationship warrants further studies (Zeng et al., 2012; Kenkel and Carter, 2016).

Another study found that martial arts may increase oxytocin. The research particularly examined different forms of martial arts, like ground grappling and "punch-kick" sparring. Insight into how intense physical and interactive exercises like martial arts impact oxytocin levels is crucial, as touch is a complicated phenomenon in sports science since the type, frequency, and valence of touch can alter oxytocin responses (Rassovsky et al., 2019). Although "Dennis Jiu Jitsu" as such, is a non-traditional and questionable martial art activity because of its belt system and utilization of various martial arts, the study's findings on oxytocin are of high value.

Sport types, however, can differ widely. As an example, dance and rhythm might be able to affect humans through the mirror neuron system and physical touch, which has an established connection with empathy and oxytocin (Heinskou and Liebst, 2016). Unfortunately, interaction with auditory stimuli might make it challenging to explore sports connected to music (Jezova et al., 2013). Oxytocin plays a role in how athletes perceive and respond to competitive stress, linking psychological states with physiological responses (Meijen et al., 2020). Furthermore, higher oxytocin levels, influenced by perceived social support, may lead to a "challenge state", enhancing athletes' self-esteem and improving performance.

Team sports therefore open many possibilities for investigation, as a single dose of intranasal oxytocin can change how people perceive each other, even from their body language (Bernaerts et al., 2016). Traditional hunting can be considered as aerobic exercise in humans, which also has shown a significant influence on oxytocin (Jaeggi et al., 2015).

Rugby, which involves high physical contact, and handball, which besides slightly different contact valence requires specialized team coordination, have already been investigated in connection with competitions (Kociuba et al., 2023), however, the half-life of oxytocin was not considered properly when measuring urinary samples days away from the competition itself. A study also recorded that acute hypoxia stimulates oxytocin release from the rat hypothalamus whereas thyrotropin-releasing hormone has an inhibitory action during a stress response. Acute hypoxia can be caused by anemia, asthma, or swimming exercise and training in SD rats (Xu et al., 2006).

In sports, this can occur in activities at high altitudes, such as mountain climbing, skiing, or high-altitude training for endurance athletes, but also in endurance sports like marathon running or cycling, where intense exertion may lead to temporary oxygen deficiency in muscles.

A study of well-established and defined sports on oxytocin levels could yield valuable insights into the relationship between oxytocin and exercise. Consequently, the type of sport may be a crucial factor in determining whether exercise will be sufficient to elicit change in oxytocin. Measurements therefore in sports science, concerning oxytocin, should account for the time, intensity, and environment of exercise so that the threshold of exercise can be documented, and the benefits of oxytocin can be further explored and utilized.

2 Methods

PICO key term and research question translated to SPIDER.

Population (P) = Sample (S): Inclusion: healthy adult male population (both animal and human). Exclusion: subjects under the age of 18 or with pre-existing medical conditions, females
Intervention/exposure (I) = The phenomenon of Interest (I): Oxytocin research and methodology particularly focusing on exercise
Comparison (C) = Design (D): Is oxytocin measured? If yes, did it increase or decrease? Did exercise performance increase or decrease due to said release?
Outcomes (O) = Evaluation (E): Involves information on oxytocin that may be connected to exercise. What is their causal relationship?
Research type (R) = English studies published in the last 20 years, randomized controlled trials (RCTs), non-randomized studies: randomized controlled trials, interrupted time series, systematic reviews, controlled before and after studies, and cohort studies were included in the study.

2.1 Eligibility criteria

2.1.1 Inclusion criteria

Randomized controlled trials (RCTs), non-randomized studies: interrupted time series, systematic reviews, controlled before and after studies, and cohort studies were included in our investigation. We confined our scope to the English language and studies published over the last 20 years, thus remaining contemporary. Studies were required to have information on oxytocin, measurements, and exercise. Included articles must be directly related to oxytocin, its measurement, sport theory, sports practice, and sport physiology and should provide insights applicable to these areas, while focusing on healthy populations. Through such an explicit approach we will filter out the works that are irrelevant to our research purposes and focus on the ones covering physiological, theoretical, and practical issues in exercise science both in humans and animals.

2.1.2 Exclusion criteria

We have set the exclusion criteria so that the review focuses on the most relevant, reliable, and the most up to date research. Conference abstracts and study protocols usually lack the rigorous peer review process needed for reliability. We did not include study reports that did not fulfill the CONSORT requirements, i.e., conference abstracts. Studies without published results (e.g., published protocols) were excluded too. Also, studies published in languages other than English were excluded since their results could be misinterpreted due to the potential linguistic barriers. A time cut-off was set for the studies published before 2003 to accommodate the review in drawing on recent methodological developments and understanding in the field. The reliability of the measurement strategies utilized in the studies was a crucial factor; hence, to preserve the validity of the review outcomes, any studies that applied unreliable measurement methods were taken out. Also, reviews concentrating on clinically diagnosed diseases were taken out of the review, as the aim was to study the association between oxytocin levels and exercise in otherwise healthy populations. Considering the scope of this review, we excluded studies that were carried out having female subjects only, with a focus on reproduction or on aspects of sexual function. The choice was made for this framework to achieve applicability to a wider demographic subset recognizing their needs separate a detailed investigation due to the complexities of these areas and the effect of states or conditions like menstrual cycle, pregnancy, birth control, and sex on oxytocin levels. In the end, studies that were not immediately applicable to exercise or did not have a direct impact on it were excluded, and the aim was to specifically identify the relationship between physical activity and oxytocin levels, the results thus obtained may be directly applied in the human performance and wellbeing improvement. This targeted approach to selecting studies aims to investigate the relationship between oxytocin and exercise, providing a comprehensive and accurate basis for future studies and applications in this field. The exclusion criteria were attentively made to warrant that the resulting framework is based on the most trustworthy, applicable, and contemporary scientific data.

Studies grouped for the syntheses (outlines the chapters of the review):

1. Exercise (Cognitive Functions and Gene Polymorphism)
2. Physiology (Pain, Analgesia, Injury, and Nutrition)
3. Environment (visual, auditory, and olfactory stimuli)
4. Social Context (physical contact, psychological interventions, and play)
5. Stress (acute, chronic, and restraint)
6. Measurements.

2.2 Information sources

These databases were last accessed on 2023-08-01. We searched Scopus, PubMed, Embase, Web of Science, and Ovid Medline. When applicable, MeSH was applied to boost accuracy. All databases were simultaneously accessed, with the results stored in Excel spreadsheets, for both reviewers to work alongside each other, and discuss the downloaded literature and documentation, to take readily available notes. PRISMA guidelines were followed and consulted throughout the study. To systematically generate our questions and keywords, we employed the "SPIDER" methodology. The query strings for Boolean operators were built on each side based on Pubmed's Query Builder and MeSH database integrated into the advanced search.

2.3 Search strategy

Filters applied: (2003–2023) English Only-last 20 years. MeSH was embedded into the keywords to increase search precision (DeMars and Perruso, 2022).

Scopus (68) (No MeSH available): TITLE-ABS-KEY-AUTH ((((("oxytocin") AND (((((("exercise") OR ("sport*")) OR ("physical activity")) OR ("train*")) OR ("workout*"))) AND ((("measur*") OR ("assess*")) OR ("evaluat*"))) AND NOT ((((((((((((((((("female") OR ("mother")) OR ("maternal*")) OR ("wom?n")) OR ("birth")) OR ("labor")) OR ("deliver*")) OR ("childbirth")) OR ("cancer")) OR ("disease")) OR ("disorder")) OR ("defect")) OR ("malad*")) OR ("ill")) OR ("sick*")) OR ("infect*")) OR ("syndrom*")))).

PubMed (68) (MeSH applied): ((("oxytocin") AND (((((("exercise") OR ("sport*")) OR ("physical activity")) OR ("train*")) OR ("workout*"))) AND ((("measur*") OR ("assess*")) OR ("evaluat*"))) NOT ((((((((((((((((("female") OR ("mother")) OR ("maternal*")) OR ("wom?n")) OR ("birth")) OR ("labor")) OR ("deliver*")) OR ("childbirth")) OR ("cancer")) OR ("disease")) OR ("disorder")) OR ("defect")) OR ("malad*")) OR ("ill")) OR ("sick*")) OR ("infect*")) OR ("syndrom*")))).

Embase (57) (MeSH applied): ("oxytocin"/exp OR "oxytocin") AND ("exercise"/exp OR "exercise" OR "sport*" OR "physical activity"/exp OR "physical activity" OR "train*" OR "workout*") AND ("measur*" OR "assess*" OR "evaluat*") NOT ("female"/exp OR "female" OR "mother"/exp OR "mother" OR "maternal*" OR "wom?n" OR "birth"/exp OR "birth" OR "labor"/exp OR "labor" OR "deliver*" OR "childbirth"/exp OR "childbirth" OR "cancer"/exp OR "cancer" OR "disease"/exp OR "disease" OR "disorder"/exp OR "disorder" OR "defect" OR "malad*" OR "ill" OR "sick*" OR "infect*" OR "syndrom*").

Web of Science (258) (No MeSH available): ((("oxytocin") AND (((((("exercise") OR ("sport*")) OR ("physical activity")) OR ("train*")) OR ("workout*"))) AND ((("measur*") OR ("assess*")) OR ("evaluat*"))) NOT ((((((((((((((((("female") OR ("mother")) OR ("maternal*")) OR ("wom?n")) OR ("birth")) OR ("labor")) OR ("deliver*")) OR ("childbirth")) OR ("cancer")) OR ("disease")) OR ("disorder")) OR ("defect")) OR ("malad*")) OR ("ill")) OR ("sick*")) OR ("infect*")) OR ("syndrom*")))).

Ovid (239) (MeSH applied): (("oxytocin" and ("exercise" or "sport*" or "physical activity" or "train*" or "workout*") and ("measur*" or "assess*" or "evaluat*")) not ("female" or "mother" or "maternal*" or "wom?n" or "birth" or "labor" or "deliver*" or "childbirth" or "cancer" or "disease" or "disorder" or "defect" or "malad*" or "ill" or "sick*" or "infect*" or "syndrom*")).mp. [mp=ab, bo, bt, ti, hw, tx, mc, st, or, tn, ps, ds, cb, rn, sq, mq, ge, tm, mi, ct, sh, ot, nm, fx, kf, ox, px, rx, an, ui, on, sy, ux, mx].

2.4 Selection process

After screening the titles and abstract for applicability, studies had to contain information about oxytocin, and/or exercise-related information that was directly relatable and applicable. Color-coding and categorizing the papers was independently done by two reviewers, and subsequent discussions were before our chosen mediator. We found 455 pieces of literature in total, out of which 39 were debated for inclusion. We ended up with 175 papers as full-text reviews. In addition, all decisions were documented with data validation to avoid manual mistakes and to enhance clarity.

2.5 Data collection process

Microsoft Power BI (Becker and Gould, 2019) was used to gather all additional and missing abstracts, and information based on DOI numbers and PubMed IDs, to have a comprehensive dataset in Excel, through the utilization of the site's respective APIs and in the case of open-access manual web scraping. The coding and the process are documented and can be made available if necessary. Two reviewers worked simultaneously, if possible, sometimes independently, with tracked changes and notes on a cloud-based Microsoft Excel dataset. The Power BI procedure, which was strengthened by a script-skipping mechanism, ensured that accurate data was retrieved on the abstracts. However, we recognized the inherent constraints of automated data collecting and performed manual checks to ensure thorough analysis.

Through structural and cross-thematic analysis we investigated 175 pieces of literature after applying our inclusion-exclusion criteria. Oxytocin measurement methodologies and psychological tests were screened in each text. Time points, analyses, and measurements were meticulously recorded in the "Measurement" section, compiling a comprehensive dataset, based on which we collected and evaluated the findings.

Our aim was to be as precise as possible in building a framework for measuring oxytocin and understanding the relation with exercise. The relevance of the results and potential applicability to females, necessitate additional investigation, and critical evaluation. While animal studies predominated due to the existing research gap in oxytocin, this fact was duly noted.

2.6 Study risk of bias assessment

The risk of bias assessment was crucial for us in determining the internal validity of the included studies; this is of paramount importance in our analysis. We evaluated numerous aspects of the research papers, such as the sample, protocols, and study types to determine whether the investigated articles had any methodological problems or biases. Generally, to "lower" the risk of bias means that the evidence is more trustworthy. The risk of bias was evaluated using standardized tools. RoB 2 (The Risk of Bias 2) for randomized controlled trials, ROBINS-I (Risk of Bias in Non-randomized Studies—of Interventions) for comparative studies, and ROBINS-E (Risk of Bias in Non-randomized Studies—of Exposures) for cross-sectional and cohort studies. Depending on the type of observations, case-control studies were assessed with either ROBINS-E or ROBINS-I. Assessment of reviews was performed using ROBIS (Risk of Bias in Systematic Reviews assessment tool) tool, and all the animal studies were assessed according to SYRCLE's (Systematic Review Centre for Laboratory Animal Experimentation) tool. Two reviewers performed the risk of bias assessment jointly, and in case of disagreement, a third reviewer was consulted. Where available, predefined automatization tools were used (through Microsoft Access for ROBIS, and Microsoft Excel for RoB 2 and ROBINS-E). ROBINS-I and SYRCLE were also prepared in Microsoft Excel to enable proper analysis of results (Higgins et al., 2024; Sterne et al., 2019; Hooijmans et al., 2014; Whiting et al., 2016; Sterne et al., 2016).

We performed a narrative, cross-thematic, and structural analysis of the included research papers (Campbell et al., 2020). The analysis of these factors is detailed in the discussion chapter. We conducted the narrative synthesis by searching for oxytocin in each study for the initial coding while noting what parts of the text might contain appropriate data and copying it to the shared Excel dataset. Later we automated the coding process using Power BI for a reliable frequency analysis with data validation via Power Query (Becker and Gould, 2019).

Due to the heterogeneity of the included studies, multiple tools were needed to perform an adequate risk of bias assessments. For the synthesis of the risk of bias assessment, studies were grouped based on the type of the study to produce comparable results. However, outcomes and results of the included studies were presented in a narrative form as this was decided as the most suitable and comprehensible way for synthesis.

Results of the risk of bias assessments were visually presented using Microsoft Excel, and grouped by tools (study types), to ensure comparability of the results (see Figures 1-6). No meta-analysis has been conducted. Power BI was adopted to further analyze the mass of the screened studies. Moreover, descriptive statistics were used due to having number of years and frequency of each type of study. Average year of publication is around 2015.73 there being an average of studies being published in the middle of 2010. The median year of publication: 2017, which implies that there are as many studies published within the 2017 and after 2017 years and thus, put the median year of publication at the end of the 2010s. Summarizing these statistics, most of the works on oxytocin in the sporting sphere are relatively current with a peak of studies in late 2010-ies. This reveals that as the studies continue to evolve, in general, the last two decades show that understanding of the relationship between oxytocin and exercise has deepened. With regards to oxytocin outcomes, (53) 55.79% of studies indicated that oxytocin increased due to exercise, while (7) 7.37% of studies indicated a decrease in oxytocin (mostly due to chronic physiological conditions); (13) 13.68% of studies indicated that oxytocin improved exercise performance, while (1) 1.05% indicated that oxytocin decreased exercise performance (exercise was assigned as novel a stressor); (21) 22.11% of studies indicated that oxytocin was administered either intranasally or with injection. (see interactive Supplementary Material for cross-filtering).

As for study types: (93) 53.14% of the studies were SYRCLE, (36) 20.57% were ROBIS, (20) 11.43% were ROBINS-E, (11) 6.29% ROB2, (9)5.14% ROBINS-I, (6) 3.43% In-Vitro. Regarding exercise types 63 studies contained no contact exercise, 9 contained contact; 60 were aerobic exercise, 9 anaerobic;

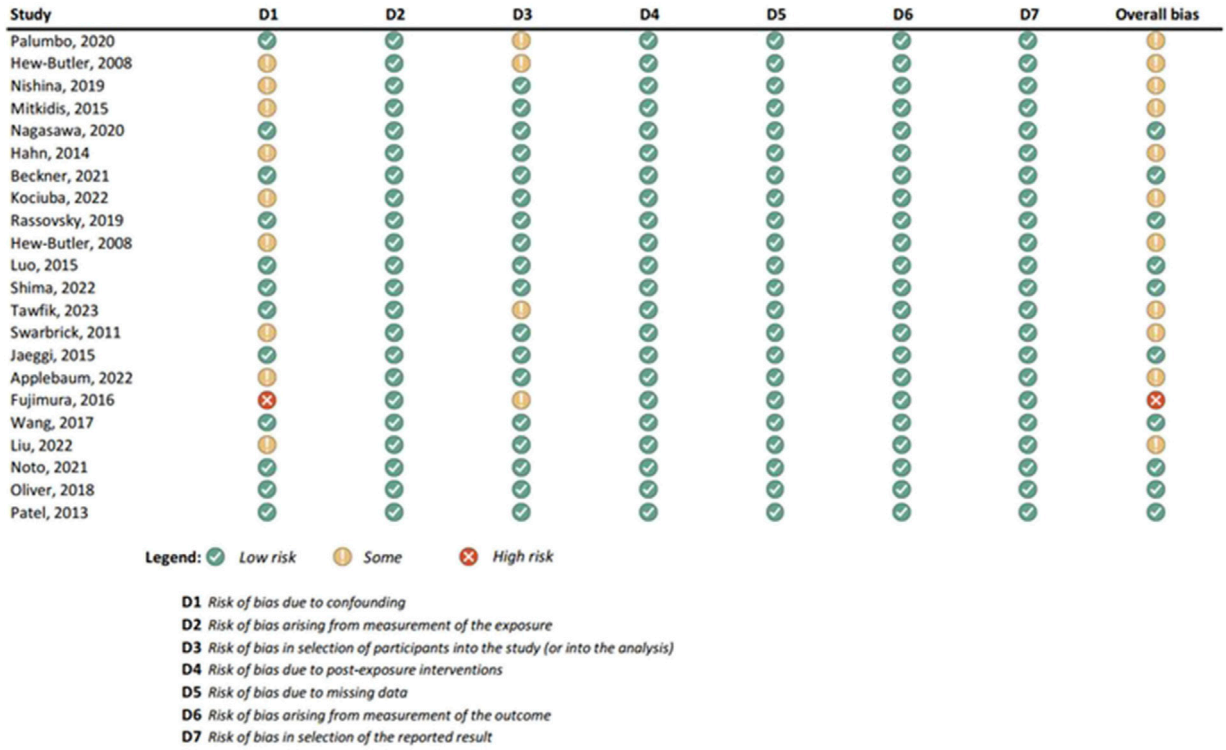

FIGURE 1
Results of individual study assessments done with ROBINS-E.

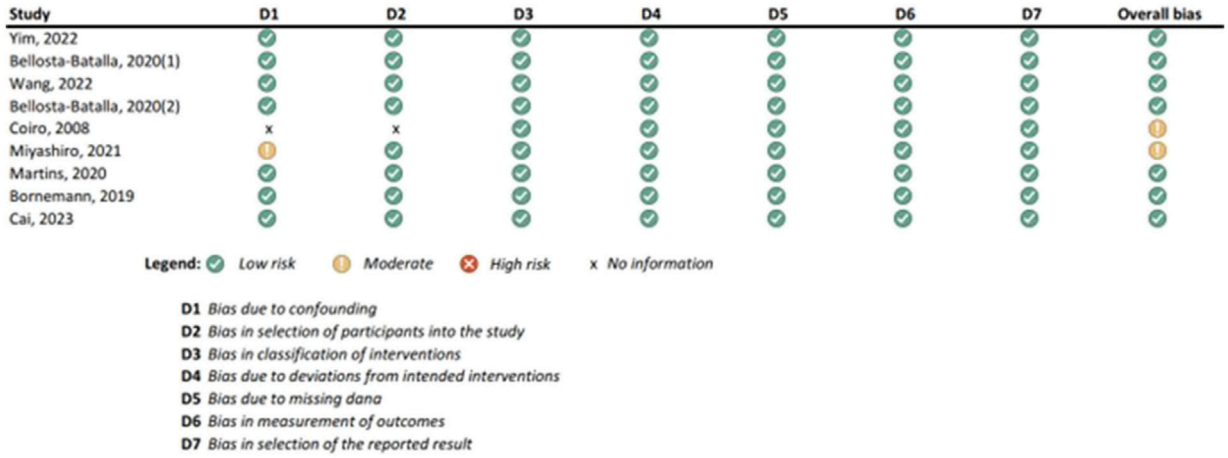

FIGURE 2
Results of individual study assessments done with ROBINS-I.

8 contained explicit exploratory behavior; 4 restraint stress or restricted movement; 3 exercise programs. To determine the quality of the included studies, a risk of bias assessment was performed for each study with a tool suitable for the study type. Considering the variety of studies included in the review, RoB 2, ROBINS-I, and ROBINS-E were used for evaluating human studies; SYRCLE's tool for animal studies and ROBIS tool included reviews and meta-analyses. To present the results of the risk of bias assessment, studies were divided into subgroups (one for each tool). *In vitro* studies were from 2009, 2018, 2020, 2022, and 2023. ROB2 studies were from 2008, with a notable presence in more recent years such as 2020, 2021, 2022, and 2023. ROBINS-E ranges from 2008 to 2023, with a peak in recent years, indicating continued relevance. ROBINS-I appeared in specific years such as 2008, 2019, 2020, 2021, 2022, and 2023. ROBIS has a broad range from 2003 through 2023, consistently, particularly in more recent

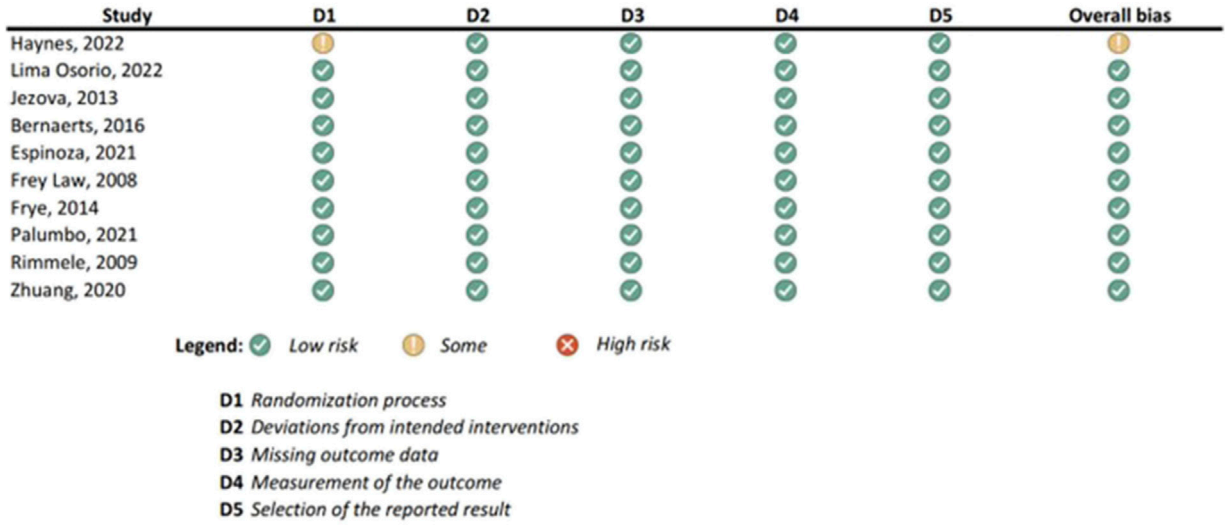

FIGURE 3
Results of individual study assessments done with RoB 2.

years. SYRCLE extensively showed up from the earliest years in the dataset (2003) up to 2023, with a peak in usage in 2020.

Attrition bias was appraised by assessing the completeness of data reporting and the handling of missing data. Studies with a low risk of attrition bias provided clear explanations for participant withdrawals and employed appropriate statistical methods to address missing data. The risk of reporting bias was considered low for studies with pre-specified outcomes and adherence to reporting guidelines. Summary statistical information and assessments of certainty are presented in a GRADE evidence manner (Zhang et al., 2019; Guyatt et al., 2011). To ensure the quality of included studies, a risk of bias assessment was performed using the tools mentioned above. All tools aimed to assess several aspects of the study. All studies were scrutinized for any indications of selection bias, such as inadequate randomization procedures or insufficient allocation concealment.

The risk of performance bias was assessed by examining the blinding procedures implemented in each study. To evaluate the potential for detection bias, the clarity and adequacy of outcome assessments were carefully examined. Clearly defined domains examined by each tool are listed in the tables with the results of the risk of bias assessments. Most of the studies were assessed as low risk of bias, still, it was not possible to make a clear judgment in the case when the study authors did not provide enough details, and these studies were marked as unclear. Although part of the reviews and animal studies were rated as high risk of bias, it was decided to include these studies in the review, to gather all potential data for careful evaluation. Several reasons influenced this decision. Sometimes due to the nature of their design, in the case of observation of wild animals and free groups, animal studies could not have clearly defined control groups. Such studies exhibited a higher risk of bias, but we still believe that they provide important insights into the dynamics of oxytocin and the factors that influence it, therefore their results are also included in this review, with the emphasis that they cannot be as reliable as the results obtained by RCTs (randomized-controlled trials) carried out on laboratory animals. Reviews assessed as high risk of bias, sometimes due to earlier publication, were insufficient in terms of defining the protocol, but they provided basic knowledge on this topic. Thus, we deemed it important to include them and consider their contribution to our overall understanding of oxytocin. A detailed risk of bias assessment for each included study, as well as an overview of the risk of bias for each of the study groups, are presented graphically.

3 Results

3.1 Search and selection process findings

175 studies met our inclusion criteria (see Figure 7). During our structural analysis of the study's "*Methods*" sections, we observed the following:

3.1.1 Psychological measurements

In our structural analysis, we found 63 psychological and or behavioral tests. After the assessment, 4 self-report tests accounted for the chapters we discussed in our review, potentially enhancing data filtering precision. Given that these tests are taken, not only does the data filtering become more reliable, but the emerging correlations may yield important data for researchers.

1. Perceived Stress Scale (PSS) (Nielsen et al., 2016) to account for stress (aiding in understanding the potential impact of stress on oxytocin levels, or how oxytocin may influence stress levels following an exercise intervention).
2. Multidimensional Scale of Perceived Social Context (MSPSS) (Zimet et al., 1988) for social context, shedding light on potential associations between oxytocin levels and social environments or their absence.
3. Numerical Rating Scale (NRS) (Karcioglu et al., 2018) for pain, investigating the impact of pain experienced by athletes before,

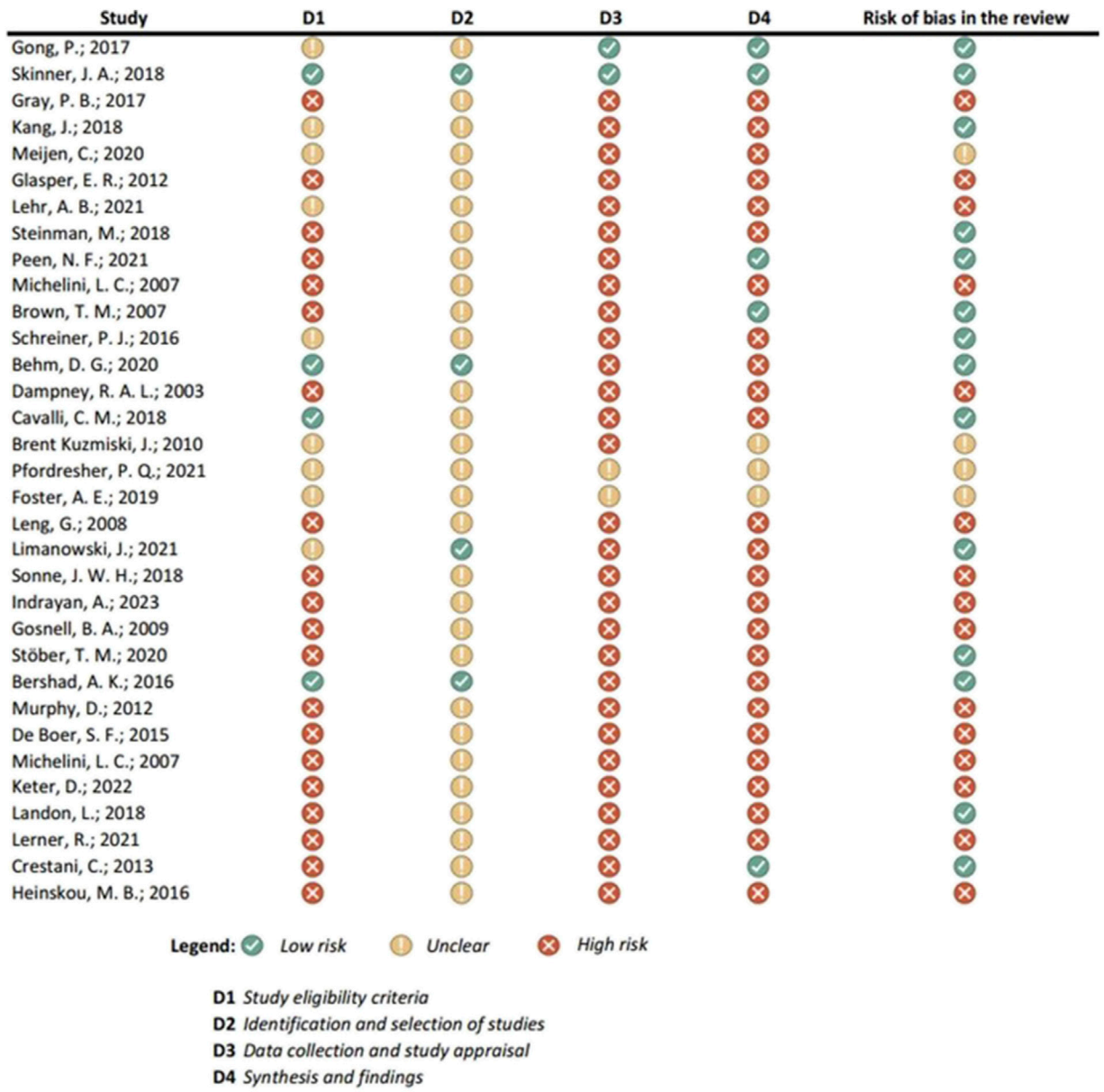

FIGURE 4
Results of individual study assessments done with ROBIS.

during, and after exercise on oxytocin levels and their fluctuations.

4. Council of Nutrition Appetite Questionnaire (CNAQ) (Hanisah et al., 2012) or Food Frequency Questionnaire (FFQ) (Shahar et al., 2003) as an alternative, for nutrition-related data.

3.1.2 Physiological measurements

In the following, we documented the layout of studies that dealt with physiological measurements and observed their occurrence from the total number of included studies (175) alongside oxytocin's sport related outcomes, so we could observe how measuring methods have been applied throughout the scientific realm.

Wefound thirty-three (32.67%) studies analyzing physiological measurement techniques likeanimal testing with surgery (immunochemistry or fluorescence).

Five (4.95%) studies examined urinary oxytocin, and two (0.99%–0.99%) studies examined utilized fMRI and oxytocin from hair samples respectively.

As for interventions, thirteen (12.87%) of studies utilized oxytocin injections, and six (5.94%) of studies introduced oxytocin intranasally.

Corresponding with the literature we conclude that plasma oxytocin is the most reliable sample when analyzed with radioimmunoassay (Oliver et al., 2018), which is also backed up by the frequency of its occurrence as we found thirty-two (31.68%) of them in the number of analyzed studies.

We found salivary oxytocin in ten (9.9%) studies as a replacement might solve the problems of plasma oxytocin measurements. Admittedly, needles may induce fear and anxiety (Olatunji et al., 2010) which may affect oxytocin in athletes. In

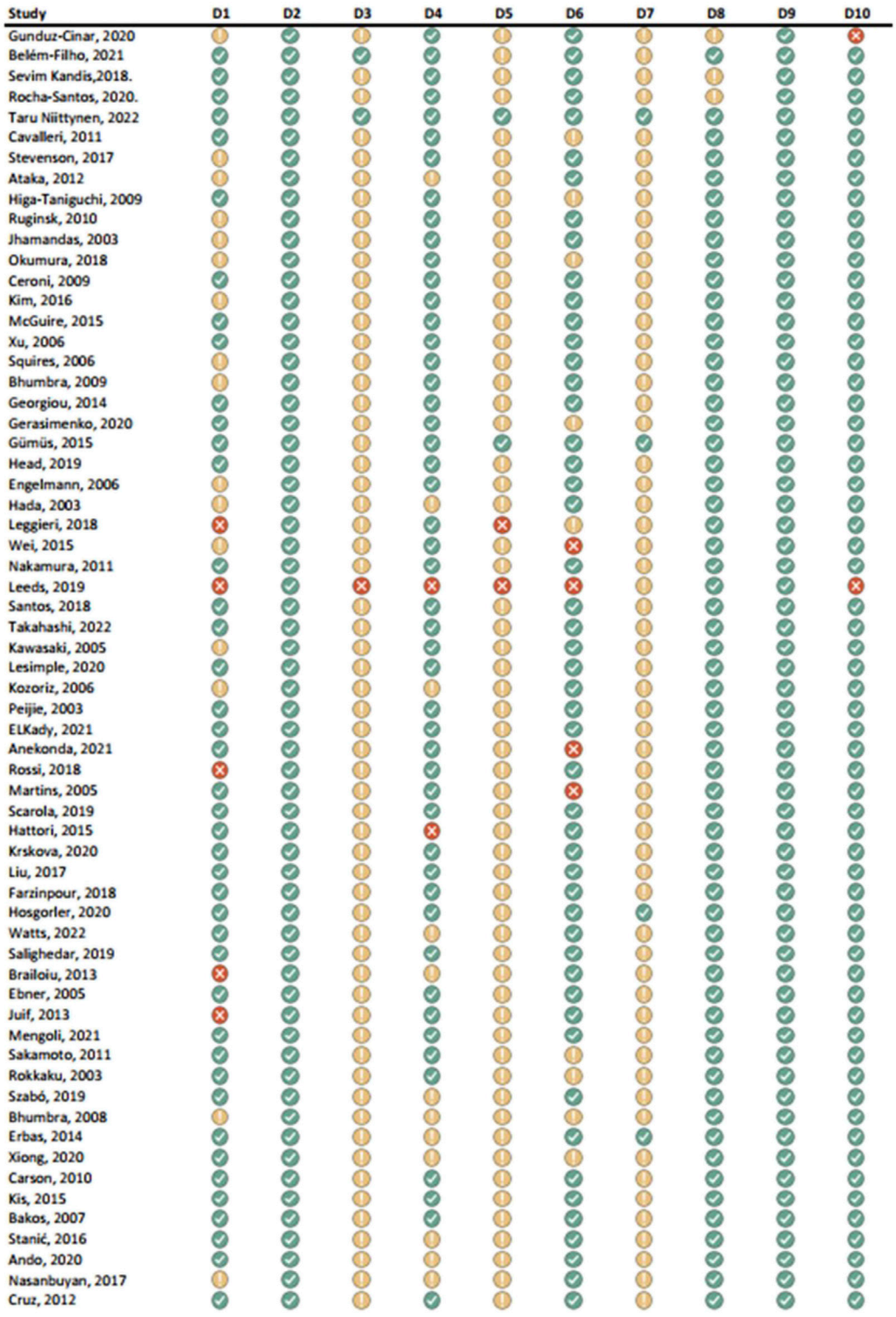

FIGURE 5
Results of individual study assessments done with SYRCLE (1).

addition, salivary testing is also non-invasive and has been done in a sports context (Rassovsky et al., 2019). At the same time, salivary oxytocin analyzed with ELISA kits if internally validated, sampled, and analyzed repeatedly has been a basis for reliable and trustworthy studies as a source of information published in reputable journals (Hew-Butler et al., 2008b; Coiro et al., 2008; Keenan Gerred and Kapoor, 2023; Leng and Ludwig, 2008; Mabrouk and Kennedy, 2012). Keeping up with the test manufacturer's instructions remains

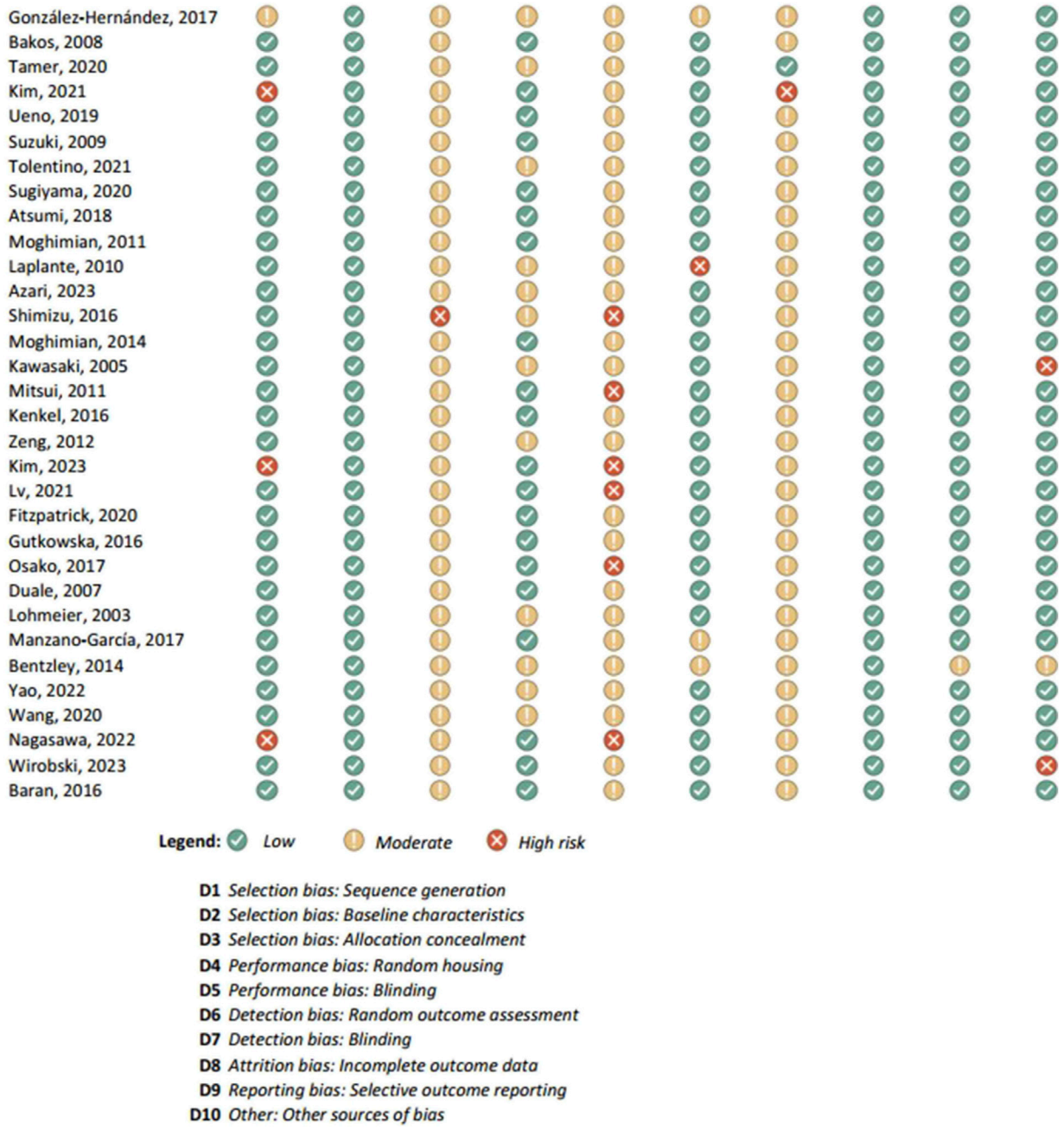

FIGURE 6
Results of individual study assessments done with SYRCLE (2).

a crucial part of measurements and testing and may prevent possible inaccuracies in measurement procedures (Hew-Butler et al., 2008a; Asano et al., 2018; Gan et al., 2023; Niittynen et al., 2022).

Regarding oxytocin outcomes associated with exercise, fifty-three (55.79%) studies indicated that oxytocin increased due to exercise, while eight (8.42%) studies indicated a decrease in oxytocin (exercise was assigned as a novel stressor); thirteen (13.68%) studies indicated that oxytocin improved exercise performance andtwenty-one (22.11%) studies indicated that oxytocin was administered either intranasally or with injection. (see interactive Supplementary Material for cross-filtering).

3.2 Studies that might appear to meet the inclusion criteria, but which were excluded, and explanation of their exclusion

Massage therapy in its essence is widely considered one of the most effective methods for post-exercise recovery. In contrast, there is limited literature on the effects of spinal manipulation and pose greater risks especially in hands of inexperienced practitioners. Regarding spinal manipulation's standard practices to this day if not done by a doctor are disputed, and the beliefs of athletes seem to matter a lot considering outcomes. It is more commonly used for more severe injuries or

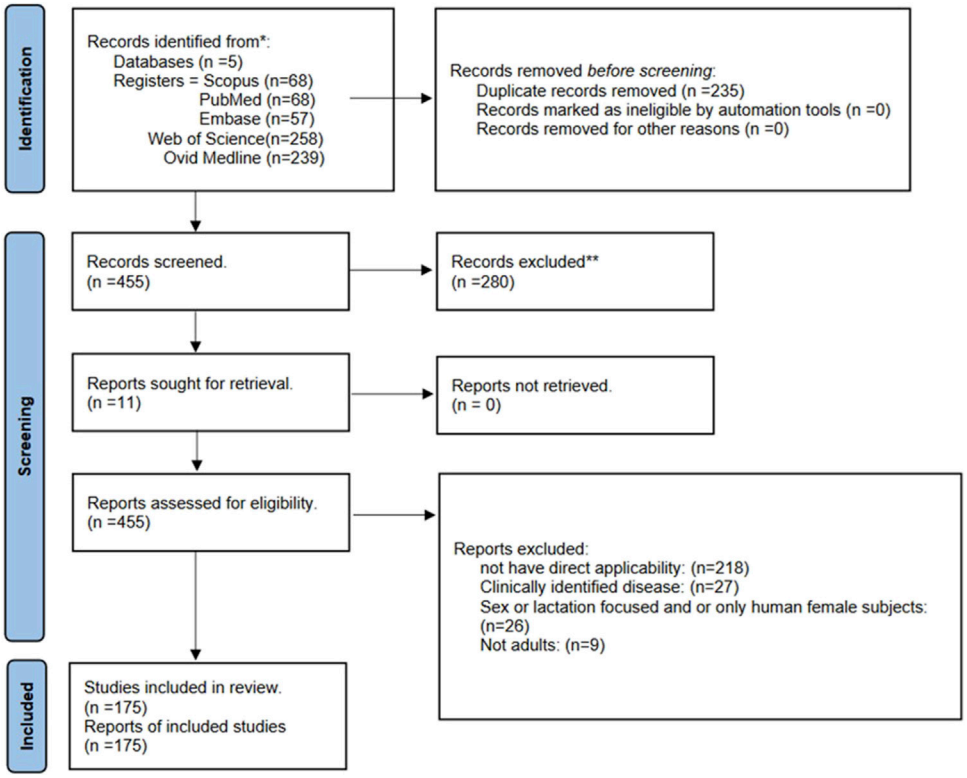

FIGURE 7
Flow diagram (based on Page et al., 2021).

illnesses, rather than otherwise healthy athletes; unlike some other aspects of physiotherapy, this is more limited as it can be done only on specific joints—which makes it challenging to point out the exact effect on athletes. Since spinal manipulation is often a treatment of some disorders, it's even harder to find relevant literature that will help decide whether to include such papers or not—possibly even how to interpret them (Kovanur-Sampath et al., 2017; Plaza-Manzano et al., 2014).

3.3 Study characteristics (see also references)

Characteristics of the included studies may be found in the Supplementary Material, containing doi numbers and details named "Database_OT_Review" Excel database, along with conclusions and reviewer information and inputs.

3.4 Risk of bias in studies: present assessments of risk of bias for each included study

Out of a total of 175 selected studies, 10 studies were evaluated with the RoB 2 tool, ROBINS-E was suitable for 22 studies, and ROBINS-I for 9 studies. A total of 33 reviews were analyzed using the ROBIS tool, and the SYRCLE tool was used for 95 animal studies. The remaining 6 *in vitro* studies were not assessed for risk of bias since this type of study is not subject to the standard errors that are tested by the risk of bias assessment tools. With the aim of comparability of the results obtained using individual tools, and to ensure sufficient precision and accuracy, the results of individual assessments are presented in groups where the studies are grouped according to the tool used for assessment, i.e., according to the type of study. All results are presented graphically in the manner of a traffic-light plot, and according to groups, they are combined into line graphs (both made using Microsoft Excel). A detailed risk of bias assessment for each included study, as well as an overview of the risk of bias for each of the study groups, are presented graphically.

3.5 Results of syntheses

Synthesis of risk of bias assessments is presented graphically (see Figures 8-12). Animal studies (assessed with SYRCE's tool) and RCTs (assessed with RoB 2) showed the lowest risk of bias. This is due to the controlled environment in which these outcomes were observed and adequately generated control groups. All the used tools were up to date, and all programs that we used showed no signs of improper functioning. The sensitivity of the involved tools is high all following MECIR (Hoffmann et al., 2014) guidelines.

3.6 Reporting biases

Fortunately, we had access to all of the studies during the assessment. In cases of missing data or articles, we contacted our

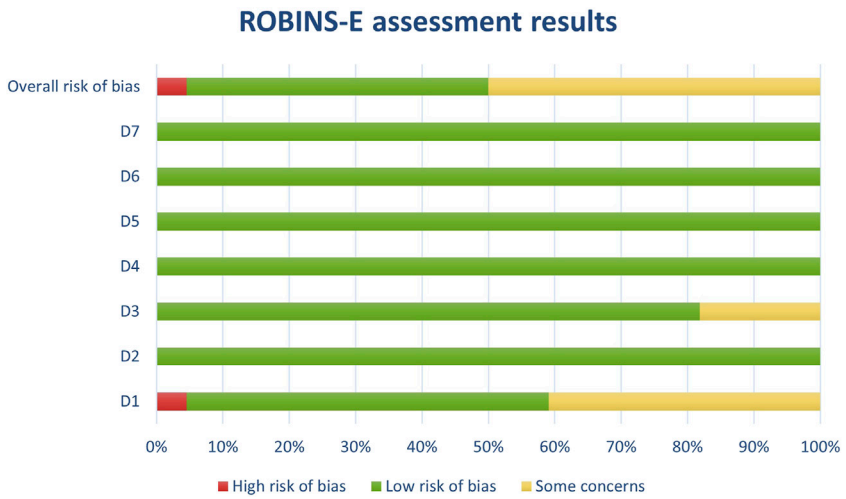

FIGURE 8
Results of overall risk of bias assessments for studies assessed with ROBINS-E.

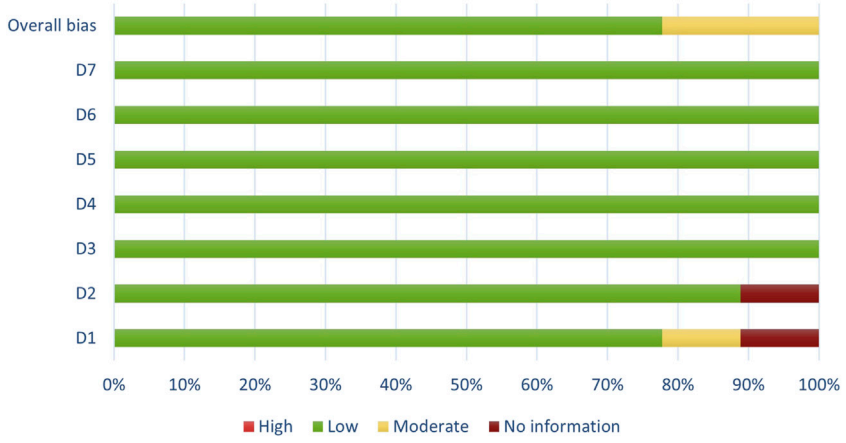

FIGURE 9
Results of overall risk of bias assessments for studies assessed with ROBINS-I.

colleagues and co-authors who had access to the appropriate databases to retrieve the full texts of articles and or Supplementary Material for a comprehensive analysis, after double-checking whether the doi and paid identifiers matched with our database we assessed the papers in accordance to the above-discussed protocols.

4 Discussion

4.1 Pain and analgesia

In our analysis, we reviewed 32 studies that provided information on injury, pain, and inflammation related to oxytocin. Oxytocin also plays a role in rehabilitation, which is supported by animal studies investigating face/mouth and liver damage (Michelini, 2007a; Michelini, 2007b; Moghimian et al., 2012; ELKady et al., 2021; Jhamandas and MacTavish, 2003; Yokoyama et al., 2009; Moghlmian et al., 2014; Okumura et al., 2019; Xiong et al., 2020; Anekonda et al., 2021). Additionally, oxytocin's recognized anti-inflammatory properties and its ability to facilitate tissue regeneration against oxidative stress have been recognized in rat studies (Wang et al., 2020; Frey Law et al., 2008; González-Hernández et al., 2017; Arabacı Tamer et al., 2020). Furthermore, the degree of inflammation seems to be linked directly to oxytocin in a dose-dependent manner in rats (Juif and Poisbeau, 2013; Bhumbra et al., 2009; Erbas et al., 2014; Indrayan et al., 2023). Exogenous oxytocin may have the ability to lower

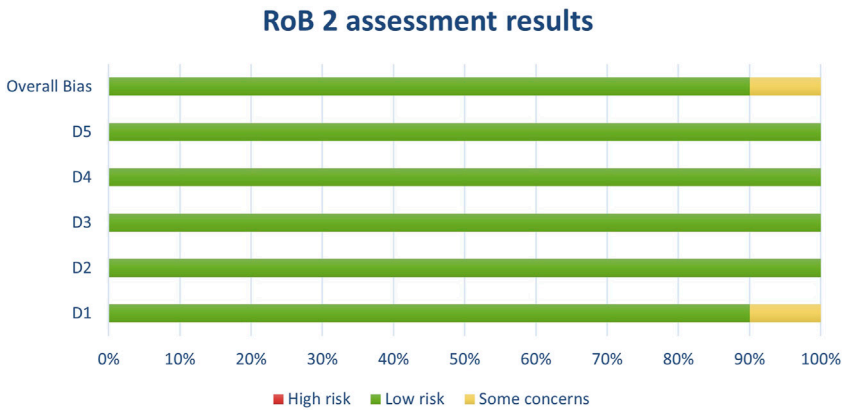

FIGURE 10
Results of overall risk of bias assessments for studies assessed with RoB 2.

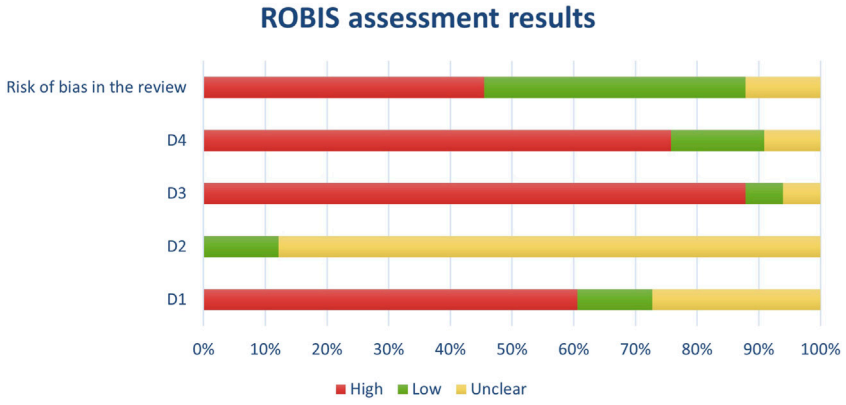

FIGURE 11
Results of overall risk of bias assessments for studies assessed with ROBIS.

muscle temperature in mice and rats (Watts et al., 2022), inevitably highlighting the importance of temperature and other variables. Based on this data, it might be possible that oxytocin later could serve as a complementary therapy for sports injuries.

The level of physical contact in sports may influence the social context, subsequently impacting the amount of oxytocin released, indirectly influencing results in both SD rats and humans (Pressman et al., 2013; Luo et al., 2015; Osako et al., 2018; Damian et al., 2022). Therefore, variations in individual differences and social contexts, e.g., loss of partner among humans, and prairie voles may also affect perceived pain and pain thresholds (Kenkel and Carter, 2016; Osako et al., 2018).

Meditation, often practiced before or as part of exercise routines, can likely contribute to increased oxytocin levels. Additionally, oxytocin might be "consumed" for pain reduction resulting in varied individual values (Miyashiro et al., 2021). The presence of meditation and mindfulness is crucial to precision in measurements, as they can potentially alter the perception of pain induced by sports-related oxytocin based on salivary measurements.

Examining correlations between exercise-induced oxytocin and pain could provide insights into the role of oxytocin in nociceptive mechanisms. To address the variability in pain, it is essential to consider individual pain perception, perceived social context, and the level of physical contact. External variables such as obesity in rats (Krskova et al., 2020) and drugs like paracetamol and benzodiazepines, which may be able to mimic oxytocin functions by alleviating anxiety and pain, therefore decreasing oxytocin because of its function being fulfilled, may also impact pain perception in prairie voles and SD rats (Ruginsk et al., 2010; Stevenson et al., 2017; Kandis et al., 2018).

Oxytocin may help athletes in the recovery process, after training or injury by reducing inflammation and promoting tissue regeneration, although this has not been thoroughly tested yet on humans. External factors including meditation and the use or abuse of certain substances, potentially altering oxytocin levels or mimicking its effects by decreased anxiety, inflammation, or pain, sports-related social interactions and physical contact may influence oxytocin release. Subsequently, this influences the psychophysiological state of athletes, which needs to be addressed to make measurements more precise. With self-report tests such as the Numerical Rating Scale (NRS) and the Multidimensional Scale of Perceived Social Context (MSPSS), we were able to consider these variables alongside the possibility of reporting the loss of a partner

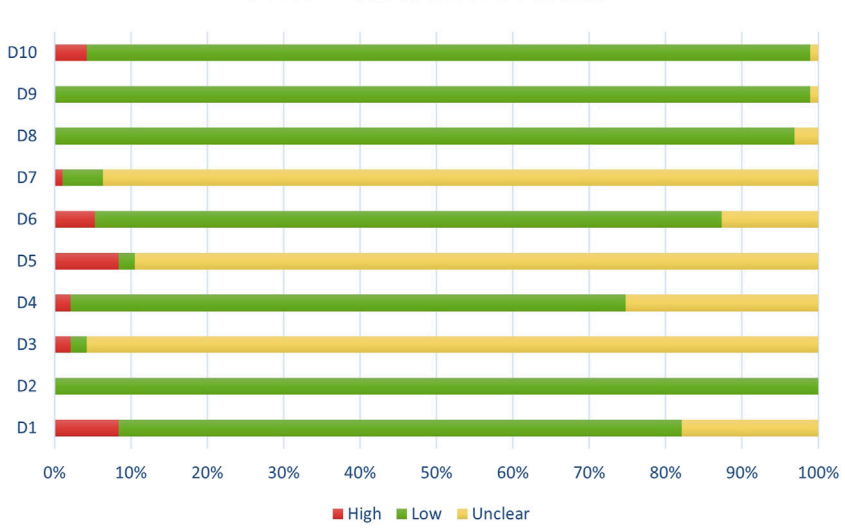

FIGURE 12
Results of overall risk of bias assessments for studies assessed with SYRCLE.

and commonly used substances (caffeine, tobacco, marijuana, painkillers, etc.) and examine the correlations. Admittedly, this may yield invaluable insights into the relationship of this neuropeptide to pain. In summary, understanding the depth of this relationship could help recovery protocols, training, and conditioning strategies for athletes.

4.2 Environment

Changes in environmental conditions such as temperature, olfactory, visual, and auditory stimuli, could influence oxytocin levels. Clarifying the relationships of these variables and then later optimizing for the secretion of oxytocin may be useful data for medicine, sports science, and education. Although there is not much data on visual stimuli, and accommodation periods connected to oxytocin with exercise; studies mention these variables as parts of other protocols (Cavalleri et al., 2011; Farzinpour et al., 2019; Bhumbra et al., 2009; Ataka et al., 2012; Ueno et al., 2019; Liu et al., 2022) warranting further exploration on the subject. The controlled environments in animal studies offer valuable insight into how the behavior of oxytocin may be changed in Long-Evans (LE), SD, W rats, and mice that carry a knock-out allele for the Nms gene. The majority of animal experiments involved in this chapter note all the standard settings in an environment which is also a marker of their reliability (Sakamoto et al., 2011; Cavalleri et al., 2011; Farzinpour et al., 2019; Takahashi et al., 2022; Jhamandas and MacTavish, 2003; Okumura et al., 2019; Arabacı Tamer et al., 2020; Bhumbra et al., 2009; Ataka et al., 2012; Ueno et al., 2019; Dampney and Horiuchi, 2003; Wei et al., 2015; Manzano-García et al., 2018; Head et al., 2019; Salighedar et al., 2019). Consistent cold storage for oxytocin, impacting its effectiveness, and keeping the samples we collect from athletes, will be crucial during the measurement (Oliver et al., 2018).

Exercise intensity can differentially affect oxytocin pathways in the brain, indicating a complex relationship between physical activity and oxytocin levels. In controlled environments, prairie voles (Kenkel and Carter, 2016) and W rats were subject to structured exercise programs, both affecting markers of oxytocin (Tolentino Bento da Silva et al., 2021). These studies show that differences in exercise intensity in both animals and humans may result in distinctive oxytocin responses. Admittedly, this could be invaluable in designing sports programs. The differential effects observed in WKY and SHR rats also point to the need for a punctual analysis of individual health statuses in sports-related oxytocin research (Martins et al., 2005). Furthermore, hard endurance training in SD rats, involving increased swimming durations and intensities, leads to significant rises in stress hormones and neuropeptides, including oxytocin, in the blood and central nervous system regions. Admittedly, changes suggest that physical exercise can modulate the immune system and stress response, however, careful examination of such phenomena is still required in human subjects who are much more complicated and frequently exposed to other sports-related supplementary therapies (Glasper et al., 2012; Behm et al., 2020). Consequently, the connection of exercise intensity's impact on health and performance remains crucial, attaching aerobic physical activity to potential immune benefits through hormonal pathways via oxytocin (Peijie et al., 2003).

In uncontrolled environments, a study on sled dogs showed a mild increase in oxytocin due to an exercise routine such as mushing (an aerobic endurance exercise) (Leggieri et al., 2019), however, it's unclear how much the environment influenced the secretion. Releasing horses from their paddock improved welfare, evidently, reduced stereotypic behaviors, and increased oxytocin levels, suggesting enhanced positive emotions. Whereas later, the values of the horse's markers (emotional and biological) worsened shortly after. Horses experiencing daily free movement in paddocks showed

increased oxytocin levels. This increase indicates that free movement positively affects horses' welfare (Lesimple et al., 2020). Nonetheless, another study found that it is physical exercise that produced changes in oxytocin (Hada et al., 2003). Still, this will require further exploration because even the person interacting with the horses can elicit change in their physiology. On the other hand, environmental enrichment in LE rats may decrease the consequences of chronic stress. Results showed that chronic stress negatively impacted immune response, but environmental enrichment could mitigate these effects. Acute stress combined with enrichment led to healthier immune and stress regulation profiles. These findings suggest that in human athletes, both the type and context of stress, along with environmental factors, might influence immune responses, underlining the complexity of stress-immune interactions in sports contexts. It remains unclear how visual stimuli would affect oxytocin in humans, (Scarola et al., 2019), calling for future studies.

4.2.1 Auditory

During our analysis, we found 12 papers dealing with auditory, and 5 with olfactory stimuli detailing environment. Most of the time animal studies control for auditory input in relation to oxytocin. At the time of writing this review, there is not enough information about the changes due to said input considering this neuropeptide, but it seems that the relationship between oxytocin and auditory input is species-dependent, namely, SD rats, wolves (a strong hierarchical order), cats (somewhat owner-dependent response), and zebra finch (mesotocin-spatial location of birds among each other) behaved differently (Watts et al., 2022; Baran et al., 2016; Fitzpatrick and Morrow, 2020; Hosgorler et al., 2020; Nagasawa et al., 2022; Wirobski et al., 2023). Humans commonly use singing in many rituals, and it is part of every culture throughout the world. Singing together as a social activity may be able to enhance oxytocin and therefore decrease anxiety (Heinskou and Liebst, 2016; Kang et al., 2018; Pfordresher, 2021). The introduction of oxytocin can help singers enhance performance and decrease anxiety (Osório et al., 2022). The social context belonging to the auditory input can lead to an increase in oxytocin through the mirror-neuron system and rhythmic entertainment when experienced by a group, as these systems are connected to our neurophysiology on an evolutionary basis. Two studies deal with a relationship between physical activity, and music as an intervention in humans, suggesting that massage, skin-to-skin contact, "warm touch," and music can together help recovery and decrease stress (Bellosta-Batalla et al., 2020; Palumbo et al., 2022) Unfamiliar and unpleasant sounds can lead to decreased oxytocin in humans. Exercise and mental challenge together had no effect on state anxiety when pleasant music was also played simultaneously. On the other hand, state anxiety rose when sounds from the same song were played backward. When state anxiety was higher, adrenocorticotropic hormone concentrations in response to mental challenges were lower, and systolic blood pressure measured alongside a handgrip exercise also decreased (Jezova et al., 2013). Personal preferences, cultural backgrounds, and individual differences in auditory processing might influence oxytocin responses, needing further exploration.

4.2.2 Olfactory

Modulating social behaviors and emotional states, oxytocin is present in key brain areas including the hippocampus and amygdala (Lv et al., 2022). While animal studies show oxytocin's behavior-modulating effects via olfactory mechanisms, such as inducing aggression or group protection in mice through urinary proteins and a way for individual recognition (Hattori et al., 2015), translating these findings to humans remains complicated because human social interactions and olfactory experiences are far more complex due to the somewhat different brain structure, social norms, and sensory processing. After all, smells and scents can both induce disgust or serve as the basis for a personal approach which are two widely different ways of behavior. Still, mice can discern between stress and relief odors, probing that humans might also detect emotional states through smell, potentially influencing social dynamics (Peen et al., 2021) In humans, oxytocin is known to decrease stress indicators like cortisol, relevant in scenarios combining physical effort with emotional experiences (Mitsui et al., 2011), suggesting that in activities involving both elements, oxytocin levels might rise. Measuring oxytocin levels, for instance, through saliva, can be impacted by various factors from the olfactory environment, and admittedly may be under the influence of circadian rhythms or dietary factors. To control this in animal studies, single housing arrangements and thorough cleaning of apparatuses are used to minimize the diffusion of oxytocin via olfactory mechanisms, and measurements usually take place at the same time (McGuire et al., 2015). Consequently, while animal research offers foundational insights, comprehensive human-specific studies are crucial for understanding oxytocin's role in social dynamics and its interaction with olfactory cues. Exploring how pleasant/unpleasant olfactory cues and the time of measurement affect oxytocin levels and social interactions may provide valuable insights in the future.

Pavlovian Conditioned Approach (PCA) may not have elicited changes in oxytocin levels in SD rats, possibly due to species-specific differences in cognitive and emotional processing, leaving the possibility open for similar research in humans. Exploring oxytocin levels in team sports or among singers may show how auditory stimuli, such as synchronized and rhythmic cheering or team chants, might influence team cohesion and performance. Considering individual sports, measurement of oxytocin may reveal the impact of the olfactory stimuli, as an example the distinct scents of a gym on an athlete's stress levels and/or performance. Whereas in rhythmic group exercises such as dance or synchronized swimming, monitoring oxytocin could show the intricacies of collective motion and music improving group cohesion and reducing anxiety. Apparently, we might be able to show and underline the role of the mirror neuron system in activities like dance, in which facial expressions and posture vary depending on styles. Sports psychology and trainers, training facilities could potentially benefit from understanding and manipulating auditory and olfactory stimuli around athletes similarly to how the sound, light, and scents are optimized in-store atmospherics (Spence et al., 2014). In the process of measuring oxytocin, careful consideration should be given to exclude potentially unpleasant stimuli unfamiliar to athletes, as this might lead to more precise measurement outcomes. This approach could open new avenues in optimizing athletic performance and team dynamics. Accounting

for environmental changes impacting oxytocin levels is crucial. The temperature, time of measurement, and presence of supplemental therapy (olfactory, auditory), including other instruments (object density), might serve as useful additional information. We understand that athletes may not be placed in a controlled setting just for the purpose of oxytocin measures. However, athletes having their own usual exercise setting might be advantageous to the validity of the scores wherever possible, so that they are accommodated in the same settings.

4.3 Cognitive functions

We found 14 studies connected to cognitive functions. Learning and memory are crucial depending on the type and purpose of exercise we engage in. Oxytocin has the potential ability to improve learning and adaptability in humans influencing both positive and negative feedback. This might aid athletes to focus better by reducing distraction from errors and increasing awareness and motivation to correct potential mistakes (Zhuang et al., 2021). Still, individual variations may influence how this will play out in athletes. In the medial prefrontal cortex (mPFC) region of rats' and mice's brains, oxytocin can improve memory and counter memory impairment caused by morphine (Salighedar et al., 2019), demonstrating that oxytocin in the prelimbic cortex of the mPFC improves memory performance. In addition, oxytocin pretreatment prevented impaired memory functions induced by morphine in this brain region which was tested in a MWM. As of yet, the applicability of the theory on exercise-induced oxytocin to humans remains to be determined. Nevertheless, considering the action mechanisms of oxytocin on memory processing may lead to therapeutic approaches (Salighedar et al., 2019). At the same time, however, this highlights the need for athletes' self-reporting of whether they consumed drugs or not during a measurement which is addressed in the pain and analgesia, inflammation chapter too. We also found a theoretical study that delved into the role of oxytocin in prioritizing memory sequences in the hippocampus, highlighting its importance in social recognition memory and suggesting a complex interplay between different brain regions and neuromodulators (Stöber et al., 2020) The CA2 and CA3 areas of the hippocampus play a role in deciding what memories to focus on and what to execute. Understanding how oxytocin might affect these areas could lead to better performance in exercise with a focus on technical and tactical development, to facilitate training connected to memory in sports. Social cognition is a crucial part of development in team sports and an essential part of life and learning for humans. In people, oxytocin increased trust in strangers but did not affect the willingness to take non-social risks. This suggests that oxytocin may work by reducing fear responses in the brain (Wang et al., 2017), which inevitably plays a role in any type of sports game and prolonged exercise. We found a study hinting at oxytocin's link to social bonding in pet owners, which might protect cognitive function in humans, though the exact biological pathways remain unclear (Applebaum et al., 2023). Connected to exercise, the involvement of pets and dogs is more and more common in leisure activities, the presence of which could influence oxytocin secretion. Research on dogs and mice showed that oxytocin enhances social cognition, affecting behaviors like gazing and shoaling. We also found a study indicating oxytocin's role in processing social cues across different species (Atsumi et al., 2018). A more in-depth look at this paper shows how mice distinguish between biological motion and scrambled motion in the presence of oxytocin. Despite humans being more complex, spatial coordination, strategy, and team interactions may be likewise influenced by oxytocin. In rats, spatial learning in a MWM improved social recognition, potentially due to increased oxytocin and AVP levels. The study suggests that these neuropeptides enhance social behavior following certain learning experiences (Zeng et al., 2012). Through oxytocin pathways, spatial learning activities may affect the performance and social cognition of athletes.

The fear extinction process could be connected to a sports injury or situation where a person or animal gradually loses their fear response to something that used to scare them. Previous studies have investigated the notion that oxytocin helped reduce fear responses in mice and humans, suggesting its potential use in treating trauma-related disorders. Intranasal oxytocin and direct brain infusions in animals showed reduced fear, with a focus on a specific mouse strain (S1) known for poor fear extinction (Gunduz-Cinar et al., 2020). Investigating this further would in all probability provide crucial insights into managing sport-related anxiety, which may help with performance. In mice, oxytocin aids in overcoming fear memories. Furthermore, higher oxytocin and AVP levels can lead to prolonged social memory and excessive grooming, which may serve as a potential distraction from fear responses (Squires et al., 2006). This could occur in humans too when they are under pressure before partaking in a competition, although oxytocin's interplay here is not clear. In mice, these effects depend on brain region and dosage. Unfortunately, for now, it would be far-fetched to assume a direct translation to humans, but accounting for body language signs also could be a possibility in measuring fear-related oxytocin and social cognition. Oxytocin did not significantly alter cognitive biases or preferences in a modified conditioned place preference test in rats. Oxytocin's anxiolytic effects may not directly influence cognitive bias, therefore further research is needed on this front (McGuire et al., 2015). Quick decision-making under pressure is an essential part of team sports, and oxytocin's role in shaping cognitive biases and responses to uncertainty could be relevant.

Oxytocin influences how athletes may process both positive and negative feedback. A more in-depth understanding of oxytocin's effects on memory and cognitive functions of rats and mice translated to humans could potentially aid mental training and recovery in sports, particularly in technical, tactical development, and mental training. The role of oxytocin in fear extinction and its impact on social cognition is crucial. Managing sports-related anxiety and enhancing team dynamics can be associated with oxytocin's relation to cognitive functions.

4.4 Genes and gene polymorphism

In animals, oxytocin, stress, gene expression, and metabolism show a complex network of relations. In horse breeds, genetic variations may reveal the interplay between oxytocin on trainability, where a correlation is found between trainability, oxytocin, and serotonin (Kim et al., 2023). The neurohormonal and genetic profiles in dogs could reveal roles that they play in humans, as oxytocin is part of dogs' bonding process related to their

gazing behavior (Cavalli et al., 2018; Mengoli et al., 2021), or helped dogs react more positively to ambiguous stimuli (Kis et al., 2015). Oxytocin receptor-null mice exhibited abnormal aggression patterns, suggesting a key role of the oxytocin receptor gene (*OXTR*) in modulating social and competitive behaviors (Hattori et al., 2015). Research on C57BL/6J mice demonstrates that social defeat stress activates oxytocin neurons in key brain regions (Gerasimenko et al., 2020), suggesting a genetic predisposition influencing athletes' responses to stress and defeat, potentially affecting their resilience and recovery. (Nasanbuyan et al., 2018). This could imply that variations in the human *OXTR* might influence athletes' responses to competitive situations and aggression, impacting their performance and team dynamics. On a metabolic note, the P2Y1 receptor's role in hormone secretion, particularly leptin in adipocytes, offers insights into how exercise and oxytocin might interact with metabolic processes in WT and P2Y1 KO mice (Laplante et al., 2010).

WK and SHR rats showed that exercise activates oxytocinergic projections in their nucleus tractus solitarii, influencing oxytocin mRNA expression in the brain (Martins et al., 2005). The interplay between exercise metabolism and hormonal regulation, including the relationship between GLUT4 mRNA (Bakos et al., 2007) and oxytocin mRNA, suggests a potential indirect interaction between exercise-induced metabolic changes and oxytocin regulation in SD rats, the exploration of which could be useful in optimizing athletes' training and recovery. Another study on W rats demonstrated acute exercise's impact on oxytocin and cholecystokinin levels, along with their role in modulating gastric functions, highlighting the intricate neurohumoral mechanisms that are influenced by physical activity (Tolentino Bento da Silva et al., 2021). Similarly, another study examined stress induction and oxytocin administration in W rats connected to metabolism. Heat Shock Protein, the Hsp27 gene was significantly upregulated (Moghlmian et al., 2014), suggesting a link between oxytocin signaling and stress-related gene activation. W and SHR rats have been shown to increase oxytocin mRNA and immunoreactivity within key brain areas impacting autonomic control (Cruz et al., 2013), which might lead in principle to performance increase for human athletes later. Research on the effect of exercise on cardiovascular regulation in rats, focusing on phenylethanolamine N-methyltransferase (PNMT) gene expression and oxytocin's cardiovascular response, has revealed significant exercise-induced changes in gene expression. In rats, voluntary wheel running failed to modify sensitivity to the cardiovascular action of oxytocin but resulted in increased gene expression of the PNMT gene in the left, but not right, heart atrium in a running activity-dependent manner (Bakos et al., 2008). In conclusion, the relationship between oxytocin, exercise, and genetics in animals appears to vary depending on the species. Nevertheless, the social aspect surrounding animals and their dietary attributes may be influenced by genetic underpinnings related to oxytocin. Further investigations could explore the presence and mechanisms of such changes in humans.

In humans, similar patterns can be perceived. A study linked the *SIM*1 gene to obesity, announcing that genetic factors influence body weight regulation (Swarbrick et al., 2011), which is parallel to animal studies also mentioning dietary variables (see chapter on nutrition). *AVPR1a* (central AVP receptor 1A) alongside oxytocin and higher cognitive levels can affect social variables of trust, and reciprocity (Nishina et al., 2019), which might contribute to understanding performance in team sports.

The most well-researched oxytocin receptor variant is *OXTR* rs53576 on human chromosome 3p.25.3. A meta-analysis on *OXTR* rs53576 polymorphism found a significant association with empathy, particularly in individuals with the GG genotype (Gong et al., 2017). Variations in *OXTR* rs53576 are associated with differences in trust behavior alongside AVPR1a. This finding indicates that oxytocin acts on trust-related elements whereas AVP acts on aspects linked to wider pro-social behavior and may address many forms of anxiety (Nishina et al., 2019). Genetic variation in *OXTR* rs53576 between cultures, linking it to differences in altruistic, empathic, and compassionate behaviors. In European Americans, the guanine variant (G) is more prevalent, but in collectivist East Asians, adenine (A) is more common. Carriers of *OXTR* rs53576 and *AVPR1a* are more likely to engage in prosocial behaviors, such as trust in strangers and participation in charitable activities, but an introduction of intranasal oxytocin showed varied results (Sonne and Gash, 2018). Interestingly, a study done in Japan showed that physical activity levels might interact with genetic predispositions to influence emotional and cognitive processes relevant to sports performance, particularly in individuals carrying the G variant of the *OXTR* rs53576 and *AVP V1b* (Shima et al., 2022). Lastly, *OXTR* rs53576 can even influence how empathetically one reacts to the pain of others outside or inside their racial group suggesting that there might be individual differences in oxytocin receptor functioning that can affect social and emotional processing (Luo et al., 2015).

In individual sports, the presence of *OXTR* rs53576 might not be as crucial as in team sports. Enhanced attention to empathy and trust, however, is crucial in the latter. It might be possible to test for these genes in the future so that people could choose appropriate sports, or sports and teams may choose optimal athletes (Sezen-Balçikanli and Sezen, 2017; Kavussanu and Stanger, 2017). A comparative study on the composition of humans participating in individual and team sports associated with their oxytocin levels would in all probability shed light on the interplay of genes in sports connected to oxytocin.

4.5 Social context

4.5.1 Oxytocin as a reward related to sports in social context

Oxytocin and social context are closely related, the former being released as a reward connected to prosocial behavior in most vertebrate species (Wei et al., 2015; Glasper et al., 2012; Baran et al., 2016). Oxytocin is significantly correlated with perceived social support, playing a role in stress regulation, and promoting faster recovery (Pressman et al., 2013; Heinrichs et al., 2003). Positive verbal and tactile interactions facilitated the secretion of oxytocin in both humans and animals (Rassovsky et al., 2019; Nagasawa et al., 2022). The absence of social peers in rats increases the chances of cocaine addiction. Oxytocin lowered both the desired quantity of cocaine and the motivation to obtain it while reducing relapse behavior (Bentzley et al., 2014). Consequently, oxytocin might be instrumental in sports, to help athletes with motivation and potentially mitigate the

risk of developing unhealthy or addictive behaviors. Stress-induced cortisol release can be buffered by positive social experiences and at least partially mediated by oxytocin release (Tawfik et al., 2023). In Tsimane' hunters' salivary oxytocin levels were significantly higher upon returning home compared to baseline, suggesting that oxytocin responds to social reunions and is likely involved in reinforcing social bonds and positive social interactions. Correlation between oxytocin levels and factors like meat sharing, cooperative hunting, family size, and physical activity indicate that oxytocin's increase was specifically related to the social aspect of returning home (Jaeggi et al., 2015). A study on dogs and wolves found that synchronized movement was positively related to oxytocin concentrations. Strikingly, synchronized movements and singing (akin to howling perhaps) are present in humans, connected to oxytocin (Pfordresher, 2021). Territorial behavior was positively related to oxytocin and glucocorticoid release, and separation from the pack increased glucocorticoid concentrations, indicating that social and environmental factors, such as returning home or social reunions, can differently affect oxytocin levels in animals too (Wirobski et al., 2023). Consequently, it is suggested that the level of oxytocin should be measured at different time points (Fitzpatrick and Morrow, 2020).

4.5.2 Fear connected to oxytocin and sports

The mechanism by which oxytocin promotes trust and alleviates social stress appears to involve deactivating brain circuits in the amygdala in both humans and rodents. The amygdala is involved in fear processing as a reaction to a fearful face in humans (Lv et al., 2022; Wang et al., 2017; Nishina et al., 2019; Frye et al., 2014; Murphy et al., 2012; Hahn et al., 2015) which is related to the mirror neuron system and empathy. On the other hand, in C57BL/6N mice oxytocin may enhance curiosity or interest in the environmental elements rather than directly promoting empathetic behavior, related to the transmission of fear (Ueno et al., 2019). In 129S1/SvImJ mice, this connection seems to be dose-dependent with even relatively low doses being sufficient to elicit positive behavior change and fear extinction memory (Gunduz-Cinar et al., 2020). Admittedly, further investigation is needed to interpret the last two findings for humans. In addition, music could be particularly effective in stimulating oxytocin release, thereby enhancing team cohesion and performance. It is relatively well-known that singing increases social bonding. This aligns with the idea that group activities, be they musical or athletic, serve an important role in social bonding facilitated by oxytocin (Pfordresher, 2021). Oxytocin can reduce social stress, and performance anxiety in musicians, further reducing negative or even catastrophic thoughts on professional activities. In a related study, oxytocin improved self-perception and helped to manage negative thoughts associated with music performance anxiety (Osório et al., 2022). This is in line with the finding that athletes who perceive high social support, such as from coaches, teammates, or fans, might have higher oxytocin levels, facilitating a challenge state and enabling them to utilize favorable conditions effectively, thereby maximizing their performance potential (Meijen et al., 2020). Oxytocin may be increased by stress such as pain, fear, and intense exercise in rats, humans, and horses. A study found it was exercise that facilitated meaningful oxytocin-level change in horses (Kim et al., 2023; Hada et al., 2003). Furthermore, horses with a high concentration of oxytocin show lower levels of fearfulness and dominant behavior, which are associated with better trainability (Kim et al., 2021).

4.5.3 Oxytocin as the trust hormone in sports

A crucial function of oxytocin is the early processing of the most basic class of social stimuli which is most often the face (Fujimura and Okanoya, 2016; Rimmele et al., 2009). Social cognition, recognition, and memory are essential prerequisites of more complex social behaviors both of which are enhanced and partly regulated by oxytocin (Zeng et al., 2012; Applebaum et al., 2023; Atsumi et al., 2018; Squires et al., 2006; Kis et al., 2015; Rimmele et al., 2009). Athletes' ability to remember and learn from social interactions and team experiences also could be shaped by hippocampal mechanisms connected to oxytocin (Stöber et al., 2020; Lehr et al., 2021). Subsequently, locomotive activity and oxytocin may be connected. Compared to healthy controls, CD157 and CD38 KO mice (oxytocin release is disturbed) showed decreased locomotor activity and increased immobility, along with an inability to differentiate between familiar and novel social stimuli (Gerasimenko et al., 2020). Oxytocin can be looked at as a double-edged sword in relation to sports teams. While it promotes selective trust inside groups, on some level it facilitates negative attitudes towards others outside the given group (Hattori et al., 2015; Bershad et al., 2016; Landon et al., 2018). Oxytocin is capable of amplifying both positive and negative social interactions (Bernaerts et al., 2016; Bellosta-Batalla et al., 2020; Peen et al., 2021; Leeds et al., 2020; Steinman et al., 2019). The dynamic nature of trust, as indicated by changes in trust levels during trust games, could also parallel how exercise-induced physiological changes (like fluctuations in oxytocin levels) may influence social behaviors and trust in a sports setting, even synchronize heart rates and arousal (Hahn et al., 2015; Mitkidis et al., 2015). Oxytocin was found to lower the moral acceptability of outcome-maximizing choices, which might take part in moral decision-making (Palumbo et al., 2020) of athletes indirectly, leading to a more humanistic behavior in sports through empathy. As of yet, the aforementioned findings are genetic profile-related (Gong et al., 2017; Sonne and Gash, 2018). Interestingly, excess exogenous oxytocin might have other effects on outsiders from the group. Oxytocin even increased participants' willingness to trust strangers but did not change their willingness to take non-social risks (Wang et al., 2017) which might be meaningful in eliciting team cohesion. By the same token, individuals who received oxytocin did not decrease their trust in response to a partner's breach of trust, while those participants who had received a placebo adjusted their behavior naturally.

4.5.4 Play, physical touch, and oxytocin in sports

Play and eliciting playful behavior in both animals and humans show a significant link to oxytocin levels, particularly in social contexts. This is evident in studies examining interactions between pets and their owners, as well as father-infant dynamics, highlighting oxytocin's role in enhancing social bonding and trust, potentially influencing sports performance (Mitkidis et al., 2015; Gray et al., 2017; Nagasawa et al., 2020; Rossi et al., 2018; Schreiner, 2016). Oxytocin's role in sports-related physical contact underlines its significance in enhancing team cohesion, trust, and overall wellbeing in athletes (Mitsui et al., 2011; Kociuba et al., 2023; Frey Law et al., 2008; Bellosta-Batalla et al., 2020; McGuire et al., 2015; Rossi et al., 2018). Physical touch in sports, such as grappling, instead of kicking and punching can lead to increased oxytocin levels, enhancing social bonding and reducing stress (Rassovsky et al., 2019; Haynes et al., 2022) hinting at the idea, that

the intensity and salience of the touch might matter. Both human and animal studies support that, oxytocin release during exercise, depending on physical contact may contribute to positive emotional responses and improved social interactions among athletes (Leggieri et al., 2019; Niittynen et al., 2022; Damian et al., 2022; Baran et al., 2016; Cavalli et al., 2018; Mengoli et al., 2021; Nagasawa et al., 2020). Furthermore, these positive effects of oxytocin, released during physical contact in sports, can extend beyond the activity itself, influencing mood and social behaviors (Behm et al., 2020; Haynes et al., 2022; Limanowski, 2022).

Oxytocin is influenced by social interactions, and *vice versa*. Team bonding and physical contact, alongside playful behaviors, are common in sports settings. The type of sport therefore seems a determining factor regarding the aforementioned variables. Consequently, oxytocin's influence on athletes' social behavior and its performance-enhancing effect proposes interesting moral dilemmas about this neuropeptide as it might have potential uses for pro-athletes both increasing performance and recovery. Future studies could delve into dose-response reactions in humans regarding fear, performance, and trust. Regarding psychometric testing with the Multidimensional Scale of Perceived Social Context (MSPSS) individuals reporting very low levels could potentially be excluded from the samples.

4.6 Substances and nutrition

The relationship between AVP and oxytocin is complex, and the exact mechanisms aren't fully understood yet. Factors like individual variability, overall health, and hormonal feedback loops can all influence this interaction. Even still, both animal and human studies prove that water and salt intake may influence blood pressure, AVP, and consequently oxytocin (Michelini, 2007a; Michelini, 2007b; Yokoyama et al., 2009; Duale et al., 2007; Kawasaki A. et al., 2005; Kawasaki M. et al., 2005; Kozoriz et al., 2006). When AVP levels rise, it can affect the release of oxytocin because they share common pathways and receptors (Kawasaki A. et al., 2005; Bhumbra et al., 2008; Nakamura et al., 2011). This is possible as an example, through the endocannabinoid system (Ruginsk et al., 2010) Improved hydration strategies for athletes with water-salt intake connected to oxytocin may lead to meaningful results in recovery, through cardioprotection and pain management.

Food intake behavior is affected by oxytocin, lowering appetite. Oxytocin could offer heart protection from dietary problems, help the regeneration of multiple tissues, and both directly and indirectly reduce obesity, through portion control both in humans [in the hedonic (pleasure-related) and homeostatic (energy balance-related) aspects of feeding] and animals (Espinoza et al., 2021; Mitsui et al., 2011; Yokoyama et al., 2009; Anekonda et al., 2021; Head et al., 2019; Nakamura et al., 2011; Gosnell and Levine, 2009; Lohmeier et al., 2003; Shimizu et al., 2016; Skinner et al., 2019; Yao et al., 2022). Admittedly, this needs additional research on humans, particularly dose-response studies, and an understanding of related genetics (Swarbrick et al., 2011).

In Zucker fatty (ZF) rats, circulating oxytocin levels were accompanied by significantly improved glucose utilization, highlighting the potential role of oxytocin in metabolic regulation, which could be influenced by nutritional status (Krskova et al., 2020). A study examined neuromedin U, which facilitates oxytocin release, at least in part, via activation of beta-adrenoceptors in W rats (Rokkaku et al., 2003), acting similarly on dietary intake related to oxytocin. Ghrelin has been used as an antagonist for inducing hunger by reducing oxytocin (Yokoyama et al., 2009; Szabó et al., 2019). At the same time, oxytocin was found to inhibit the increase in neuropeptide Y levels induced by ghrelin in humans (Coiro et al., 2008), leading to inconclusive evidence in light of the aforementioned studies for now. Aromatherapy through essential oils may hold promise for assisting athletes' dietary changes through increased oxytocin release (Cai et al., 2023). Alcohol and painkillers may decrease oxytocin, potentially slowing recovery processes (Jhamandas and MacTavish, 2003; Stevenson et al., 2017; Kandis et al., 2018; McGuire et al., 2015; Skinner et al., 2019). Centrally administered oxytocin can reduce the feeling of visceral gastrointestinal sensations in SD rats, pointing out its possible involvement in pain relief. If this is confirmed in humans, dietary components might influence central oxytocin levels and, consequently, pain perception and stress responses (Okumura et al., 2019). In addition to this, circadian rhythms may influence the measurements through dietary and hormonal, neural pathways, possibly influencing exercise performance (Bhumbra et al., 2009; Sugiyama et al., 2020). Oxytocin's role in nutrition concerning sports science is a developing area of research, that holds promising potential for increased performance and lowered recovery times through several biomarkers being influenced in both humans and animals (Lesimple et al., 2020; Zhuang et al., 2021; Laplante et al., 2010; Beckner et al., 2021). Attention is needed for proper pharmaceutical solutions to explore and utilize these findings, which could mean psychophysiological improvements for all humans (Ohno et al., 2009).

It is crucial to consider the fluid, salt intake, and diets athletes consume as this may be a determining factor in oxytocin release. Examining the correlation between pain and cognitive functions alongside other factors mentioned in this review might provide insight into how this hormone works exactly. The Council of Nutrition Appetite Questionnaire (CNAQ) (Hanisah et al., 2012) or Food Frequency Questionnaire (FFQ) (Shahar et al., 2003) as an alternative, for nutrition encompasses a great variety of nutritional variables for this purpose. Furthermore, the ethical considerations here are crucial, meaning the development of drugs and therapies must be carefully undertaken. It is possible that athletes have used oxytocin to boost performance and recovery for a time, and because of the half-life of this neuropeptide in the body, this must have been difficult to test for, if not impossible.

4.7 Stress

4.7.1 Oxytocin's role in stress reduction

Oxytocin is often used in both human and animal studies as a biomarker of positive health status (Indrayan et al., 2023; Lerner et al., 2022). When under stress caused by exercise, W rats produce the adrenocorticotropic hormone, in response to which oxytocin is also secreted as a buffer in the stress response. However, in humans, this might be dependent on the stress scenario, the environment, genetic profiles, early life experiences, and nutrition (Takahashi et al., 2022; Liu et al., 2022; Scarola et al., 2019; Skinner et al., 2019; Cai et al., 2023; Ebner et al., 2005; Noto et al., 2021; Weisman et al., 2013). At the same time, individual variations will contribute to how much stress gets reduced by oxytocin (Fitzpatrick and

Morrow, 2020; Sonne and Gash, 2018). Prolonged endurance exercise, a form of physical stress, triggers significant hormonal changes, including increases in oxytocin levels significantly correlating with AVP, suggesting that exercise can modulate stress responses through hormonal pathways (Hew-Butler et al., 2008a; Hew-Butler et al., 2008b). Oxytocin seems to inhibit social stress and attenuate activation of the amygdala response to a fearful face, making faces, more familiar" (Rimmele et al., 2009). Oxytocin and AVP may have opposite effects on the brain in response to social stress and cardiovascular control (Gutkowska et al., 2016; Crestani et al., 2013; Nishina et al., 2019), which might not be a coincidence. Acute osmotic change as physiological stress may alter a response in oxytocin because of the relationship between the two hormones (Kawasaki A. et al., 2005; Kawasaki M. et al., 2005). Both chronic and acute stress experiences can significantly alter neuroendocrine responses, specifically involving oxytocin and corticotropin-releasing hormone and their interaction (Peen et al., 2021), suggesting that social interactions play a crucial role in modulating these stress responses both in animals and humans (Pressman et al., 2013; Lv et al., 2022; Gerasimenko et al., 2020; Frye et al., 2014; Leeds et al., 2020; Trieu et al., 2019). In addition, the endocannabinoid system takes part in the regulation of social reward by oxytocin reinforcing the connection with social context further (Wei et al., 2015). In sports contexts where team dynamics and social support are key factors, both the variables are important.

4.7.2 Acute stress

In humans, acute stress impacts cognitive functions and the potential buffering effects of oxytocin. Interestingly, oxytocin which is related to resilience and fitness, remained stable during simulated military operational stress, although the study notes problems with oxytocin measurement unreliability (Beckner et al., 2021), which this current review aims to address directly. With regards to acute stress, the immediate connection between heart rate and cardioprotection, with hormonal changes may contain valuable information about oxytocin's role in the stress response (Moghimian et al., 2012; Moghlmian et al., 2014; Dampney and Horiuchi, 2003; Yao et al., 2022) offers promising research areas for the future.

Athletes, with varying levels of social risk-taking tendencies, might respond to acute stressors in competitive sports differently (Wang et al., 2017). Individuals' propensity for social risk-taking influences their trust decisions in uncertain social interactions (Bershad et al., 2016).

Exercise, by affecting oxytocin levels, might be a valuable component in managing stress and improving mental health in various populations, including those with addiction issues (Wang and Zou, 2022). Likely through the opioid receptors in the mPFC, forced swimming as acute stress and its impact on meth and morphine-seeking behavior in humans and W rats suggests that stress can significantly influence neurochemical activity related to reward and motivation (Farzinpour et al., 2019; Carson et al., 2010; Kim and Han, 2016; Salighedar et al., 2019). Similarly, the MWM test exposure also triggered a transient release of oxytocin (Engelmann et al., 2006). Interestingly, even with music playing backward as an acute stressor, concentrations of testosterone, oxytocin, AVP, and aldosterone were slightly increased accompanied by increased anxiety (Jezova et al., 2013).

The amygdala's role in fear extinction, as observed in male S1 mice, provides insights into how stress affects athletes' neurochemical pathways during competition. This is similar to studies on C57BL/6J mice and oxytocin receptor-deficient mice, where oxytocin receptors are linked to behavioral responses to social stress. In human athletes facing competitive stress, the modulation of emotional and stress responses by oxytocin suggests a parallel mechanism. Oxytocin may influence stress and fear-related processes in athletes, mirroring the neurochemical pathways activated in these mice models during stress.

Furthermore, oxytocin predicts behavioral responses to foundation training in horses as an acute stress scenario, where cortisol is continually reduced for 9 months likely due to oxytocin. Training in horses can lead to measurable changes in oxytocin levels, which are associated with different behavioral responses (Niittynen et al., 2022). This suggests that in sports contexts, acute stress situations might similarly influence oxytocin levels, helping with acclimatization periods to training.

4.7.3 Chronic stress

Oxytocin has been shown to play an important role in wound healing via modulating stress responses by activating the processes of neovascularization, and proliferation of endotheliocytes and histiocytes (Gümüs et al., 2015). This may result in effective clearance of the wound, and optimal granulation tissue formation, which may also help athletes if tested on humans later in their recovery processes. Furthermore, chronic exercise training can modulate oxytocinergic and vasopressinergic pathways, affecting cardiovascular control. The long-term impact of regular exercise on these neuroendocrine systems may influence stress responses in athletes (Michelini, 2007a; Michelini, 2007b). Chronic stress boosts the levels of certain hormones like orexin, melanin-concentrating hormone, oxytocin, AVP, and thyrotropin-releasing hormone in the basolateral amygdala. On the other hand, exercise has an antidepressant effect by reducing the expression of these hormones in the basolateral amygdala, further strengthening oxytocin's critical role in mood regulation (Kim and Han, 2016). A study examined the effects of continual hypoxia, which is a form of chronic stress, on hormone regulation. C57BL/6 mice were subjected to chronic stress (restraint treatment) and moderate physical exercise (running wheel). Acute continual hypoxia-affected prolactin levels, mediated through corticotropin-releasing hormone receptor 1, may affect oxytocin levels in SD rats (Dampney and Horiuchi, 2003). Acute hypoxia can be caused by anemia or asthma, training swimming, or chronic stress in athletes.

Vasopressin's response to chronic stress could imply that similar mechanisms may influence oxytocin levels under chronic stress in athletes. Understanding how chronic stressors, like intensive training or injury, might impact athletes' neuroendocrine responses and, subsequently, their performance and recovery processes are likely connected to the regulation of AVP (Suzuki et al., 2009). Sustained inflammatory stress on AVP-eGFP Wistar transgenic rats, was used to analyze the expression of an AVP-enhanced green fluorescent protein fusion gene in response to chronic inflammatory stress. Furthermore, chronic corticosterone administration as a model of chronic stress in W rats suggests, that oxytocin may have protective effects against stress-induced changes in the adrenal gland (Stanić et al., 2017) as one potential theory of how exercise may promote stress reduction through oxytocin. In prairie voles, the influence of social bonds and their disruption on both physical (pain perception) and psychological (anxiety) aspects of social stress due to partner loss could significantly impact how individuals respond to stressors connected to oxytocin

(Osako et al., 2018), which needs to be accounted for in the measurements for humans.

The type of stress may be a determining factor in the secretion of oxytocin due to exercise. Stress management for athletes is a crucial step for sports science and psychology. To know more about what kind of stress affects oxytocin, and how this interacts with other psychological and physiological systems documenting individual results with the Perceived Stress Scale (PSS) alongside the Numerical Rating Scale (NRS) may be informative to notice important correlations. The type of exercise will definitely play a role in the amount of stress experienced by athletes, and their response to said stress, because of the endogenous oxytocin released.

4.8 Limitations of the evidence included in the review

While this review incorporates frequent animal studies, they do not always have direct applicability to humans. However, it was deemed necessary for maintaining the stability of the measurement framework. The English language restriction could also limit the review's scope. Furthermore, the reviewer processes, involving independent work and subsequent online debates, may introduce potential biases. Despite these limitations, this review aims to establish a robust methodology framework for measuring a neuropeptide and exploring correlation studies, contributing to the understanding of the complex interplay between exercise and oxytocin. Utilization of a business intelligence tool with automation, like Power BI for thematic analysis and statistical validation may also offer insights for future methodological studies.

4.8.1 Limitations of the review processes used

At some points, the two reviewers worked independently, and the debates were held later online in meetings, the results of which were documented in the Excel sheets, with reviewer notes and data validation following each decision.

4.8.2 Implications of the results for practice, policy, and future research

Our review aims to build a methodology framework for measuring a neuropeptide and finding possible tests for important correlation studies. Furthermore, it builds an understanding of exercise and oxytocin's interplay. Utilizing Power BI for thematical analysis through data validation and statistics may lead to new methodological studies and frameworks. Our findings may be directly and indirectly applicable to sports and medical science.

Data availability statement

The original contributions presented in the study are included in the article/Supplementary Material, further inquiries can be directed to the corresponding author.

Author contributions

PS: Conceptualization, Data curation, Formal Analysis, Funding acquisition, Investigation, Methodology, Project administration, Resources, Software, Supervision, Validation, Visualization, Writing–original draft, Writing–review and editing. SB: Conceptualization, Formal Analysis, Investigation, Methodology, Resources, Writing–review and editing. RH: Data curation, Software, Supervision, Validation, Visualization, Writing–review and editing. DH: Data curation, Investigation, Supervision, Visualization, Writing–review and editing. ZKo: Supervision, Writing–review and editing, Conceptualization. GP: Conceptualization, Supervision, Writing–review and editing, Project administration. ZKr: Conceptualization, Writing–review and editing, Investigation. JS: Conceptualization, Investigation, Writing–review and editing, Data curation, Funding acquisition, Project administration, Resources, Supervision, Validation, Visualization.

Funding

The author(s) declare that financial support was received for the research, authorship, and/or publication of this article. This research was primarily supported by ÚNKP (2023-24), Grant identifier: ÚNKP-23-2-I-PTE-1970. New National Excellence Program of the Ministry for Culture and Innovation from the source of the National Research, Development and Innovation Fund. This work was also supported by Project No. TKP2021-NVA-06 with the support provided by the National Research, Development, and Innovation Fund of Hungary, financed under the TKP2021-NVA funding scheme.

Acknowledgments

The authors express their special thanks to: Kata Kumli: Outstanding consultant on psychometric scales. Kinga Dávid, Dávid Fellenbeck, and Andreas Bergheim Graff: Critique of scientific writing and communication. Alexandra Sámóczi: Aiding the documentation of scholarships and research. Monika Berecki: Initial guidance and suggestions on SYRCLE's RoB assessments.

Conflict of interest

Authors RH and DH were employed by RoLink Biotechnology Kft.

The remaining authors declare that the research was conducted in the absence of any commercial or financial relationships that could be construed as a potential conflict of interest.

Publisher's note

Supplementary material

The Supplementary Material for this article can be found online at: https://www.frontiersin.org/articles/10.3389/fphys.2024.1393497/full#supplementary-material

References

Anekonda, V. T., Thompson, B. W., Ho, J. M., Roberts, Z. S., Edwards, M. M., Nguyen, H. K., et al. (2021). Hindbrain administration of oxytocin reduces food intake, weight gain and activates catecholamine neurons in the hindbrain nucleus of the solitary tract in rats. *J. Clin. Med.* 10 (21), 5078. doi:10.3390/jcm10215078

Applebaum, J. W., Shieu, M. M., McDonald, S. E., Dunietz, G. L., and Braley, T. J. (2023). The impact of sustained ownership of a pet on cognitive health: a population-based study. *J. Aging Health* 35 (3–4), 230–241. doi:10.1177/08982643221122641

Arabacı Tamer, S., Üçem, S., Büke, B., Güner, M., Karaküçük, A. G., Yiğit, N., et al. (2020). Regular moderate exercise alleviates gastric oxidative damage in rats via the contribution of oxytocin receptors. *J. Physiol.* 598 (12), 2355–2370. doi:10.1113/JP279577

Asano, A., Shiibashi, M., and Kudo, H. (2018). "Development of an electrochemical immunosensor for salivary oxytocin determination," in *2018 11th biomedical engineering international conference (BMEiCON)* (IEEE), 1–5. doi:10.1109/BMEiCON.2018.8609952

Ataka, K., Nagaishi, K., Asakawa, A., Inui, A., and Fujimiya, M. (2012). Alteration of antral and proximal colonic motility induced by chronic psychological stress involves central urocortin 3 and vasopressin in rats. *Am. J. Physiology-Gastrointestinal Liver Physiology* 303 (4), G519–G528. doi:10.1152/ajpgi.00390.2011

Atsumi, T., Ide, M., and Wada, M. (2018). Spontaneous discriminative response to the biological motion displays involving a walking conspecific in mice. *Front. Behav. Neurosci.* 12, 263. doi:10.3389/fnbeh.2018.00263

Azari, A. E., Peeri, M., and Masrour, F. F. (2023). The role of the oxytocinergic system in the antidepressant-like effect of swimming training in male mice. *Behav. Brain Res.* 449, 114474. doi:10.1016/j.bbr.2023.114474

Bakos, J., Bobryshev, P., Tillinger, A., Kvetňanský, R., and Jezova, D. (2008). Phenylethanolamine *N* -methyltransferase gene expression in the heart and blood pressure response to oxytocin treatment in rats exposed to voluntary wheel running. *Ann. N. Y. Acad. Sci.* 1148 (1), 302–307. doi:10.1196/annals.1410.031

Bakos, J., Hlavacova, N., Makatsori, A., Tybitanclova, K., Zorad, S., Hinghofer-Szalkay, H., et al. (2007). Oxytocin levels in the posterior pituitary and in the heart are modified by voluntary wheel running. *Regul. Pept.* 139 (1–3), 96–101. doi:10.1016/j.regpep.2006.10.011

Baran, N. M., Sklar, N. C., and Adkins-Regan, E. (2016). Developmental effects of vasotocin and nonapeptide receptors on early social attachment and affiliative behavior in the zebra finch. *Horm. Behav.* 78, 20–31. doi:10.1016/j.yhbeh.2015.10.005

Becker, L. T., and Gould, E. M. (2019). Microsoft power BI: extending Excel to manipulate, analyze, and visualize diverse data. *Ser. Rev.* 45 (3), 184–188. doi:10.1080/00987913.2019.1644891

Beckner, M. E., Conkright, W. R., Eagle, S. R., Martin, B. J., Sinnott, A. M., LaGoy, A. D., et al. (2021). Impact of simulated military operational stress on executive function relative to trait resilience, aerobic fitness, and neuroendocrine biomarkers. *Physiol. Behav.* 236, 113413. doi:10.1016/j.physbeh.2021.113413

Behm, D. G., Alizadeh, S., Hadjizadeh Anvar, S., Mahmoud, M. M. I., Ramsay, E., Hanlon, C., et al. (2020). Foam rolling prescription: a clinical commentary. *J. Strength Cond. Res.* 34 (11), 3301–3308. doi:10.1519/JSC.0000000000003765

Bellosta-Batalla, M., Blanco-Gandía, M. C., Rodríguez-Arias, M., Cebolla, A., Pérez-Blasco, J., and Moya-Albiol, L. (2020). Increased salivary oxytocin and empathy in students of clinical and health psychology after a mindfulness and compassion-based intervention. *Mindfulness (N Y)* 11 (4), 1006–1017. doi:10.1007/s12671-020-01316-7

Bentzley, B. S., Jhou, T. C., and Aston-Jones, G. (2014). Economic demand predicts addiction-like behavior and therapeutic efficacy of oxytocin in the rat. *Proc. Natl. Acad. Sci.* 111 (32), 11822–11827. doi:10.1073/pnas.1406324111

Bernaerts, S., Berra, E., Wenderoth, N., and Alaerts, K. (2016). Influence of oxytocin on emotion recognition from body language: a randomized placebo-controlled trial. *Psychoneuroendocrinology* 72, 182–189. doi:10.1016/j.psyneuen.2016.07.002

Bershad, A. K., Miller, M. A., Baggott, M. J., and de Wit, H. (2016). The effects of MDMA on socio-emotional processing: does MDMA differ from other stimulants? *J. Psychopharmacol.* 30 (12), 1248–1258. doi:10.1177/0269881116663120

Bhumbra, G. S., Lombardelli, S., Gonzalez, J. A., Parsy, K. S., and Dyball, R. E. J. (2009). Daily rhythms of spike coding in the rat supraoptic nucleus. *J. Neuroendocrinol.* 21 (11), 935–945. doi:10.1111/j.1365-2826.2009.01918.x

Bhumbra, G. S., Orlans, H. O., and Dyball, R. E. J. (2008). Osmotic modulation of stimulus-evoked responses in the rat supraoptic nucleus. *Eur. J. Neurosci.* 27 (8), 1989–1998. doi:10.1111/j.1460-9568.2008.06163.x

Brailoiu, G. C., Deliu, E., Tica, A. A., Rabinowitz, J. E., Tilley, D. G., Benamar, K., et al. (2013). Nesfatin-1 activates cardiac vagal neurons of nucleus ambiguus and elicits bradycardia in conscious rats. *J. Neurochem.* 126 (6), 739–748. doi:10.1111/jnc.12355

Cai, Z., Tang, S., Wang, L., Feng, Q., Teng, J., Chen, Y., et al. (2023). The effect of inhaling an essential oil compound containing *Eupatorium fortunei* turcz: a pilot study. *IEEJ Trans. Electr. Electron. Eng.* 18 (3), 325–331. doi:10.1002/tee.23730

Campbell, M., McKenzie, J. E., Sowden, A., Katikireddi, S. V., Brennan, S. E., Ellis, S., et al. (2020). Synthesis without meta-analysis (SWiM) in systematic reviews: reporting guideline. *BMJ* 368, l6890. doi:10.1136/bmj.l6890

Carson, D. S., Cornish, J. L., Guastella, A. J., Hunt, G. E., and McGregor, I. S. (2010). Oxytocin decreases methamphetamine self-administration, methamphetamine hyperactivity, and relapse to methamphetamine-seeking behaviour in rats. *Neuropharmacology* 58 (1), 38–43. doi:10.1016/j.neuropharm.2009.06.018

Castagné, V., Moser, P., Roux, S., and Porsolt, R. D. (2011). Rodent models of depression: forced swim and tail suspension behavioral despair tests in rats and mice. *Curr. Protoc. Neurosci.* 55 (1), Unit 8.10A. doi:10.1002/0471142301.ns0810as55

Cavalleri, M. T., Burgi, K., Cruz, J. C., Jordão, M. T., Ceroni, A., and Michelini, L. C. (2011). Afferent signaling drives oxytocinergic preautonomic neurons and mediates training-induced plasticity. *Am. J. Physiology-Regulatory, Integr. Comp. Physiology* 301 (4), R958–R966. doi:10.1152/ajpregu.00104.2011

Cavalli, C. M., Carballo, F., and Bentosela, M. (2018). Gazing behavior during problem solving tasks in domestic dogs. *A Crit. Rev. Dog Behav.* 4 (3). doi:10.4454/db.v4i3.68

Ceroni, A., Chaar, L. J., Bombein, R. L., and Michelini, L. C. (2009). Chronic absence of baroreceptor inputs prevents training-induced cardiovascular adjustments in normotensive and spontaneously hypertensive rats. *Exp. Physiol.* 94 (6), 630–640. doi:10.1113/expphysiol.2008.046128

Coiro, V., Saccani-Jotti, G., Rubino, P., Manfredi, G., Vacca, P., Volta, E., et al. (2008). Oxytocin inhibits the stimulatory effect of ghrelin on circulating neuropeptide Y levels in humans. *J. Neural Transm.* 115 (9), 1265–1267. doi:10.1007/s00702-008-0057-0

Crestani, C., Alves, F., Gomes, F., Resstel, L., Correa, F., and Herman, J. (2013). Mechanisms in the bed nucleus of the stria terminalis involved in control of autonomic and neuroendocrine functions: a review. *Curr. Neuropharmacol.* 11 (2), 141–159. doi:10.2174/1570159X11311020002

Cruz, J. C., Cavalleri, M. T., Ceroni, A., and Michelini, L. C. (2013). Peripheral chemoreceptors mediate training-induced plasticity in paraventricular nucleus pre-autonomic oxytocinergic neurons. *Exp. Physiol.* 98 (2), 386–396. doi:10.1113/expphysiol.2012.065888

Damian, K., Chad, C., Kenneth, L., and David, G. (2022). Time to evolve: the applicability of pain phenotyping in manual therapy. *J. Man. Manip. Ther.* 30 (2), 61–67. doi:10.1080/10669817.2022.2052560

Dampney, R. A. L., and Horiuchi, J. (2003). Functional organisation of central cardiovascular pathways: studies using c-fos gene expression. *Prog. Neurobiol.* 71 (5), 359–384. doi:10.1016/j.pneurobio.2003.11.001

DeMars, M. M., and Perruso, C. (2022). MeSH and text-word search strategies: precision, recall, and their implications for library instruction. *J. Med. Libr. Assoc.* 110 (1), 23–33. doi:10.5195/jmla.2022.1283

Duale, H., Waki, H., Howorth, P., Kasparov, S., Teschemacher, A., and Paton, J. (2007). Restraining influence of A2 neurons in chronic control of arterial pressure in spontaneously hypertensive rats. *Cardiovasc Res.* 76 (1), 184–193. doi:10.1016/j.cardiores.2007.06.018

Ebner, K., Wotjak, C. T., Landgraf, R., and Engelmann, M. (2005). Neuroendocrine and behavioral response to social confrontation: residents versus intruders, active versus passive coping styles. *Horm. Behav.* 47 (1), 14–21. doi:10.1016/j.yhbeh.2004.08.002

Elkady, A. H., Elkafoury, B. M., Saad, D. A., Abd el-Wahed, D. M., Baher, W., and Ahmed, M. A. (2021). Hepatic ischemia reperfusion injury: effect of moderate intensity exercise and oxytocin compared to l-arginine in a rat model. *Egypt. Liver J.* 11 (1), 45. doi:10.1186/s43066-021-00111-w

Engelmann, M., Ebner, K., Landgraf, R., and Wotjak, C. T. (2006). Effects of Morris water maze testing on the neuroendocrine stress response and intrahypothalamic release of vasopressin and oxytocin in the rat. *Horm. Behav.* 50 (3), 496–501. doi:10.1016/j.yhbeh.2006.04.009

Erbas, O., Anil Korkmaz, H., Oltulu, F., Aktug, H., Yavasoglu, A., Akman, L., et al. (2014). Oxytocin alleviates cisplatin-induced renal damage in rats. *Iran. J. Basic Med. Sci.* 17, 747–752.

Espinoza, S. E., Lee, J. L., Wang, C. P., Ganapathy, V., MacCarthy, D., Pascucci, C., et al. (2021). Intranasal oxytocin improves lean muscle mass and lowers ldl cholesterol in older adults with sarcopenic obesity: a pilot randomized controlled trial. *J. Am. Med. Dir. Assoc.* 22 (9), 1877–1882.e2. doi:10.1016/j.jamda.2021.04.015

Farzinpour, Z., Taslimi, Z., Azizbeigi, R., Karimi-Haghighi, S., and Haghparast, A. (2019). Involvement of orexinergic receptors in the nucleus accumbens, in the effect of forced swim stress on the reinstatement of morphine seeking behaviors. *Behav. Brain Res.* 356, 279–287. doi:10.1016/j.bbr.2018.08.021

Fitzpatrick, C. J., and Morrow, J. D. (2020). Individual variation in the attribution of incentive salience to social cues. *Sci. Rep.* 10 (1), 2583. doi:10.1038/s41598-020-59378-5

Frey Law, L. A., Evans, S., Knudtson, J., Nus, S., Scholl, K., and Sluka, K. A. (2008). Massage reduces pain perception and hyperalgesia in experimental muscle pain: a randomized, controlled trial. *J. Pain* 9 (8), 714–721. doi:10.1016/j.jpain.2008.03.009

Frye, C. G., Wardle, M. C., Norman, G. J., and de Wit, H. (2014). MDMA decreases the effects of simulated social rejection. *Pharmacol. Biochem. Behav.* 117, 1–6. doi:10.1016/j.pbb.2013.11.030

Fujimura, T., and Okanoya, K. (2016). Untrustworthiness inhibits congruent facial reactions to happy faces. *Biol. Psychol.* 121, 30–38. doi:10.1016/j.biopsycho.2016.09.005

Gan, H.-W., Leeson, C., Aitkenhead, H., and Dattani, M. (2023). Inaccuracies in plasma oxytocin extraction and enzyme immunoassay techniques. *Compr. Psychoneuroendocrinol* 15, 100188. doi:10.1016/j.cpnec.2023.100188

Gerasimenko, M., Lopatina, O., Shabalova, A. A., Cherepanov, S. M., Salmina, A. B., Yokoyama, S., et al. (2020). Distinct physical condition and social behavior phenotypes of CD157 and CD38 knockout mice during aging. *PLoS One* 15 (12), e0244022. doi:10.1371/journal.pone.0244022

Glasper, E. R., Schoenfeld, T. J., and Gould, E. (2012). Adult neurogenesis: optimizing hippocampal function to suit the environment. *Behav. Brain Res.* 227 (2), 380–383. doi:10.1016/j.bbr.2011.05.013

Gong, P., Fan, H., Liu, J., Yang, X., Zhang, K., and Zhou, X. (2017). Revisiting the impact of OXTR rs53576 on empathy: a population-based study and a meta-analysis. *Psychoneuroendocrinology* 80, 131–136. doi:10.1016/j.psyneuen.2017.03.005

González-Hernández, A., Manzano-García, A., Martínez-Lorenzana, G., Tello-García, I. A., Carranza, M., Arámburo, C., et al. (2017). Peripheral oxytocin receptors inhibit the nociceptive input signal to spinal dorsal horn wide-dynamic-range neurons. *Pain* 158 (11), 2117–2128. doi:10.1097/j.pain.0000000000001024

Gosnell, B. A., and Levine, A. S. (2009). Reward systems and food intake: role of opioids. *Int. J. Obes.* 33 (S2), S54–S58. doi:10.1038/ijo.2009.73

Gray, P. B., McHale, T. S., and Carré, J. M. (2017). A review of human male field studies of hormones and behavioral reproductive effort. *Horm. Behav.* 91, 52–67. doi:10.1016/j.yhbeh.2016.07.004

Gümüs, B., Kuyucu, E., Erbas, O., Kazimoglu, C., Oltulu, F., and Bora, O. A. (2015). Effect of oxytocin administration on nerve recovery in the rat sciatic nerve damage model. *J. Orthop. Surg. Res.* 10 (1), 161. doi:10.1186/s13018-015-0301-x

Gunduz-Cinar, O., Brockway, E. T., Castillo, L. I., Pollack, G. A., Erguven, T., and Holmes, A. (2020). Selective sub-nucleus effects of intra-amygdala oxytocin on fear extinction. *Behav. Brain Res.* 393, 112798. doi:10.1016/j.bbr.2020.112798

Gutkowska, J., Aliou, Y., Lavoie, J. L., Gaab, K., Jankowski, M., and Broderick, T. L. (2016). Oxytocin decreases diurnal and nocturnal arterial blood pressure in the conscious unrestrained spontaneously hypertensive rat. *Pathophysiology* 23 (2), 111–121. doi:10.1016/j.pathophys.2016.03.003

Guyatt, G., Oxman, A. D., Akl, E. A., Kunz, R., Vist, G., Brozek, J., et al. (2011). GRADE guidelines: 1. Introduction—GRADE evidence profiles and summary of findings tables. *J. Clin. Epidemiol.* 64 (4), 383–394. doi:10.1016/j.jclinepi.2010.04.026

Hada, T., Onaka, T., Takahashi, T., Hiraga, A., and Yagi, K. (2003). Effects of novelty stress on neuroendocrine activities and running performance in thoroughbred horses. *J. Neuroendocrinol.* 15 (7), 638–648. doi:10.1046/j.1365-2826.2003.01042.x

Hahn, T., Notebaert, K., Anderl, C., Teckentrup, V., Kaßecker, A., and Windmann, S. (2015). How to trust a perfect stranger: predicting initial trust behavior from resting-state brain-electrical connectivity. *Soc. Cogn. Affect Neurosci.* 10 (6), 809–813. doi:10.1093/scan/nsu122

Hanisah, R., Shahar, S., and Lee, F. S. (2012). Validation of screening tools to assess appetite among geriatric patients. *J. Nutr. Health Aging* 16 (7), 660–665. doi:10.1007/s12603-012-0056-6

Hattori, T., Kanno, K., Nagasawa, M., Nishimori, K., Mogi, K., and Kikusui, T. (2015). Impairment of interstrain social recognition during territorial aggressive behavior in oxytocin receptor-null mice. *Neurosci. Res.* 90, 90–94. doi:10.1016/j.neures.2014.05.003

Haynes, A. C., Lywood, A., Crowe, E. M., Fielding, J. L., Rossiter, J. M., and Kent, C. (2022). A calming hug: design and validation of a tactile aid to ease anxiety. *PLoS One* 17 (3), e0259838. doi:10.1371/journal.pone.0259838

Head, M. A., Jewett, D. C., Gartner, S. N., Klockars, A., Levine, A. S., and Olszewski, P. K. (2019). Effect of oxytocin on hunger discrimination. *Front. Endocrinol. (Lausanne)* 10, 297. doi:10.3389/fendo.2019.00297

Heinrichs, M., Baumgartner, T., Kirschbaum, C., and Ehlert, U. (2003). Social support and oxytocin interact to suppress cortisol and subjective responses to psychosocial stress. *Biol. Psychiatry* 54 (12), 1389–1398. doi:10.1016/s0006-3223(03)00465-7

Heinskou, M. B., and Liebst, L. S. (2016). On the elementary neural forms of micro-interactional rituals: integrating autonomic nervous system functioning into interaction ritual theory. *Sociol. Forum* 31 (2), 354–376. doi:10.1111/socf.12248

Hew-Butler, T., Jordaan, E., Stuempfle, K. J., Speedy, D. B., Siegel, A. J., Noakes, T. D., et al. (2008b). Osmotic and nonosmotic regulation of arginine vasopressin during prolonged endurance exercise. *J. Clin. Endocrinol. Metab.* 93 (6), 2072–2078. doi:10.1210/jc.2007-2336

Hew-Butler, T., Noakes, T. D., Soldin, S. J., and Verbalis, J. G. (2008a). Acute changes in endocrine and fluid balance markers during high-intensity, steady-state, and prolonged endurance running: unexpected increases in oxytocin and brain natriuretic peptide during exercise. *Eur. J. Endocrinol.* 159 (6), 729–737. doi:10.1530/EJE-08-0064

Higa-Taniguchi, K. T., Felix, J. V. C., and Michelini, L. C. (2009). Brainstem oxytocinergic modulation of heart rate control in rats: effects of hypertension and exercise training. *Exp. Physiol.* 94 (11), 1103–1113. doi:10.1113/expphysiol.2009.049262

Higgins, J. P. T, Morgan, R. L., Rooney, A. A., Taylor, K. W., Thayer, K. A., and Silva, R. A. (2024) *ROBINS-E- risk of bias in non-randomized studies - of exposures*. Bristol, UK: ROBINS-E Development Group. Available at: https://www.riskofbias.info/welcome/robins-e-tool (Accessed March 09, 2024). doi:10.1016/j.envint.2024.108602

Hoffmann, T. C., Glasziou, P. P., Boutron, I., Milne, R., Perera, R., Moher, D., et al. (2014). Better reporting of interventions: template for intervention description and replication (TIDieR) checklist and guide. *BMJ* 348, g1687. doi:10.1136/bmj.g1687

Hooijmans, C. R., Rovers, M. M., de Vries, R. B., Leenaars, M., Ritskes-Hoitinga, M., and Langendam, M. W. (2014). SYRCLE's risk of bias tool for animal studies. *BMC Med. Res. Methodol.* 14 (1), 43. doi:10.1186/1471-2288-14-43

Hosgorler, F., Koc, B., Kizildag, S., Canpolat, S., Argon, A., Karakilic, A., et al. (2020). Magnesium acetyl taurate prevents tissue damage and deterioration of prosocial behavior related with vasopressin levels in traumatic brain injured rats. *Turk Neurosurg.* 30, 723–733. doi:10.5137/1019-5149.JTN.29272-20.1

Indrayan, A., Vishwakarma, G., Verma, S., Sarmukaddam, S., and Tyagi, A. (2023). Quest for biomarkers of positive health: a review. *Indian J. Community Med.* 48 (3), 382–389. doi:10.4103/ijcm.ijcm_480_22

Jaeggi, A. V., Trumble, B. C., Kaplan, H. S., and Gurven, M. (2015). Salivary oxytocin increases concurrently with testosterone and time away from home among returning Tsimane' hunters. *Biol. Lett.* 11 (3), 20150058. doi:10.1098/rsbl.2015.0058

Jezova, D., Hlavacova, N., Makatsori, A., Duncko, R., Loder, I., and Hinghofer-Szalkay, H. (2013). Increased anxiety induced by listening to unpleasant music during stress exposure is associated with reduced blood pressure and ACTH responses in healthy men. *Neuroendocrinology* 98 (2), 144–150. doi:10.1159/000354202

Jhamandas, J. H., and MacTavish, D. (2003). Central administration of neuropeptide FF causes activation of oxytocin paraventricular hypothalamic neurones that Project to the brainstem. *J. Neuroendocrinol.* 15 (1), 24–32. doi:10.1046/j.1365-2826.2003.00869.x

Jolliffe, D., and Farrington, D. P. (2011). Is low empathy related to bullying after controlling for individual and social background variables? *J. Adolesc.* 34 (1), 59–71. doi:10.1016/j.adolescence.2010.02.001

Juif, P.-E., and Poisbeau, P. (2013). Neurohormonal effects of oxytocin and vasopressin receptor agonists on spinal pain processing in male rats. *Pain* 154 (8), 1449–1456. doi:10.1016/j.pain.2013.05.003

Kandis, S., Ates, M., Kizildag, S., Camsari, G. B., Yuce, Z., Guvendi, G., et al. (2018). Acetaminophen (paracetamol) affects empathy-like behavior in rats: dose-response relationship. *Pharmacol. Biochem. Behav.* 175, 146–151. doi:10.1016/j.pbb.2018.10.004

Kang, J., Scholp, A., and Jiang, J. J. (2018). A review of the physiological effects and mechanisms of singing. *J. Voice* 32 (4), 390–395. doi:10.1016/j.jvoice.2017.07.008

Karcioglu, O., Topacoglu, H., Dikme, O., and Dikme, O. (2018). A systematic review of the pain scales in adults: which to use? *Am. J. Emerg. Med.* 36 (4), 707–714. doi:10.1016/j.ajem.2018.01.008

Kavussanu, M., and Stanger, N. (2017). Moral behavior in sport. *Curr. Opin. Psychol.* 16, 185–192. doi:10.1016/j.copsyc.2017.05.010

Kawasaki, A., Hoshi, K., Kawano, M., Nogami, H., Yoshikawa, H., and Hisano, S. (2005a). Up-regulation of VGLUT2 expression in hypothalamic-neurohypophysial neurons of the rat following osmotic challenge. *Eur. J. Neurosci.* 22 (3), 672–680. doi:10.1111/j.1460-9568.2005.04240.x

Kawasaki, M., Yamaguchi, K., Saito, J., Ozaki, Y., Mera, T., Hashimoto, H., et al. (2005b). Expression of immediate early genes and vasopressin heteronuclear RNA in the paraventricular and supraoptic nuclei of rats after acute osmotic stimulus. *J. Neuroendocrinol.* 17 (4), 227–237. doi:10.1111/j.1365-2826.2005.01297.x

Keenan Gerred, A. K., and Kapoor, A. (2023). Validation of a commercial radioimmunoassay for measurement of human peripheral oxytocin. *bioRxiv*. doi:10.1101/2023.03.22.533823

Kenkel, W. M., and Carter, C. S. (2016). Voluntary exercise facilitates pair-bonding in male prairie voles. *Behav. Brain Res.* 296, 326–330. doi:10.1016/j.bbr.2015.09.028

Kim, J., Jung, H., and Yoon, M. (2023). Relationship between plasma dopamine concentration and temperament in horses. *Domest. Anim. Endocrinol.* 83, 106788. doi:10.1016/j.domaniend.2023.106788

Kim, J., Park, Y., Kim, E. J., Jung, H., and Yoon, M. (2021). Relationship between oxytocin and serotonin and the fearfulness, dominance, and trainability of horses. *J. Anim. Sci. Technol.* 63 (2), 453–460. doi:10.5187/jast.2021.e29

Kim, T.-K., and Han, P.-L. (2016). Chronic stress and moderate physical exercise prompt widespread common activation and limited differential activation in specific brain regions. *Neurochem. Int.* 99, 252–261. doi:10.1016/j.neuint.2016.08.007

Kis, A., Hernádi, A., Kanizsár, O., Gácsi, M., and Topál, J. (2015). Oxytocin induces positive expectations about ambivalent stimuli (cognitive bias) in dogs. *Horm. Behav.* 69, 1–7. doi:10.1016/j.yhbeh.2014.12.004

Knaus, M. C., Lechner, M., and Reimers, A. K. (2020). For better or worse? – The effects of physical education on child development. *Labour Econ.* 67, 101904. doi:10.1016/j.labeco.2020.101904

Kociuba, M., Ignasiak, Z., Rokita, A., Cichy, I., Dudkowski, A., Ściślak, M., et al. (2023). Level of oxytocin prior to rugby and handball matches: an exploratory study among groups of Polish players. *Anthropol. Rev.* 85 (4), 83–94. doi:10.18778/1898-6773.85.4.06

Kovanur-Sampath, K., Mani, R., Cotter, J., Gisselman, A. S., and Tumilty, S. (2017). Changes in biochemical markers following spinal manipulation-a systematic review and meta-analysis. *Musculoskelet. Sci. Pract.* 29, 120–131. doi:10.1016/j.msksp.2017.04.004

Kozoriz, M. G., Kuzmiski, J. B., Hirasawa, M., and Pittman, Q. J. (2006). Galanin modulates neuronal and synaptic properties in the rat supraoptic nucleus in a use and state dependent manner. *J. Neurophysiol.* 96 (1), 154–164. doi:10.1152/jn.01028.2005

Krskova, K., Balazova, L., Dobrocsyova, V., Olszanecki, R., Suski, M., Chai, S. Y., et al. (2020). Insulin-regulated aminopeptidase inhibition ameliorates metabolism in obese zucker rats. *Front. Mol. Biosci.* 7, 586225. doi:10.3389/fmolb.2020.586225

Landon, L. B., Slack, K. J., and Barrett, J. D. (2018). Teamwork and collaboration in long-duration space missions: going to extremes. *Am. Psychol.* 73 (4), 563–575. doi:10.1037/amp0000260

Laplante, M.-A., Monassier, L., Freund, M., Bousquet, P., and Gachet, C. (2010). The purinergic P2Y1 receptor supports leptin secretion in adipose tissue. *Endocrinology* 151 (5), 2060–2070. doi:10.1210/en.2009-1134

Leeds, A., Good, J., Schook, M. W., Dennis, P. M., Stoinski, T. S., Willis, M. A., et al. (2020). Evaluating changes in salivary oxytocin and cortisol following positive reinforcement training in two adult male western lowland gorillas (*Gorilla gorilla gorilla*). *Zoo. Biol.* 39 (1), 51–55. doi:10.1002/zoo.21524

Leggieri, L. R., Marozzi, A., Panebianco, A., Gregorio, P., and Carmanchahi, P. (2019). Effects of short-distance recreational mushing on oxytocin, gastrin, and creatinine kinase in sled dogs. *J. Appl. Animal Welf. Sci.* 22 (4), 320–328. doi:10.1080/10888705.2018.1500287

Lehr, A. B., Kumar, A., Tetzlaff, C., Hafting, T., Fyhn, M., and Stöber, T. M. (2021). CA2 beyond social memory: evidence for a fundamental role in hippocampal information processing. *Neurosci. Biobehav Rev.* 126, 398–412. doi:10.1016/j.neubiorev.2021.03.020

Leng, G., and Ludwig, M. (2008). Neurotransmitters and peptides: whispered secrets and public announcements. *J. Physiol.* 586 (23), 5625–5632. doi:10.1113/jphysiol.2008.159103

Lerner, R. M., Bornstein, M. H., and Jervis, P. (2022). The development of positive attributes of character: on the embodiment of specificity, holism, and self-system processes. *Hum. Dev.* 66 (1), 34–47. doi:10.1159/000521583

Lesimple, C., Reverchon-Billot, L., Galloux, P., Stomp, M., Boichot, L., Coste, C., et al. (2020). Free movement: a key for welfare improvement in sport horses? *Appl. Anim. Behav. Sci.* 225, 104972. doi:10.1016/j.applanim.2020.104972

Limanowski, J. (2022). Precision control for a flexible body representation. *Neurosci. Biobehav Rev.* 134, 104401. doi:10.1016/j.neubiorev.2021.10.023

Liu, H., and Xue, J. (2017). Involvement of hypothalamic nitric oxide signaling in the modulation of a rat's exercise capacity. *Neuroreport* 28 (7), 408–413. doi:10.1097/WNR.0000000000000763

Liu, S., Wang, H., Liu, W., Lai, S., Zhao, X., He, X., et al. (2022). The influence of physical burden on the esthetic preference for green natural environment. *Environ. Behav.* 54 (5), 867–892. doi:10.1177/00139165221093881

Lohmeier, T. E., Warren, S., and Cunningham, J. T. (2003). Sustained activation of the central baroreceptor pathway in obesity hypertension. *Hypertension* 42 (1), 96–102. doi:10.1161/01.HYP.0000076092.10923.FD

Luo, S., Li, B., Ma, Y., Zhang, W., Rao, Y., and Han, S. (2015). Oxytocin receptor gene and racial ingroup bias in empathy-related brain activity. *Neuroimage* 110, 22–31. doi:10.1016/j.neuroimage.2015.01.042

Lv, Y., Fan, Y., Tian, X., Yu, B., Song, C., Feng, C., et al. (2022). The anti-depressive effects of ultra-high static magnetic field. *J. Magnetic Reson. Imaging* 56 (2), 354–365. doi:10.1002/jmri.28035

Mabrouk, O. S., and Kennedy, R. T. (2012). Simultaneous oxytocin and arg-vasopressin measurements in microdialysates using capillary liquid chromatography–mass spectrometry. *J. Neurosci. Methods* 209 (1), 127–133. doi:10.1016/j.jneumeth.2012.06.006

Manzano-García, A., González-Hernández, A., Tello-García, I. A., Martínez-Lorenzana, G., and Condés-Lara, M. (2018). The role of peripheral vasopressin 1A and oxytocin receptors on the subcutaneous vasopressin antinociceptive effects. *Eur. J. Pain* 22 (3), 511–526. doi:10.1002/ejp.1134

Martins, A. S., Crescenzi, A., Stern, J. E., Bordin, S., and Michelini, L. C. (2005). Hypertension and exercise training differentially affect oxytocin and oxytocin receptor expression in the brain. *Hypertension* 46 (4), 1004–1009. doi:10.1161/01.HYP.0000175812.03322.59

McGuire, M. C., Williams, K. L., Welling, L. L. M., and Vonk, J. (2015). Cognitive bias in rats is not influenced by oxytocin. *Front. Psychol.* 6, 1306. doi:10.3389/fpsyg.2015.01306

Meijen, C., Turner, M., Jones, M. V., Sheffield, D., and McCarthy, P. (2020). A theory of challenge and threat states in athletes: a revised conceptualization. *Front. Psychol.* 11, 126. doi:10.3389/fpsyg.2020.00126

Mengoli, M., Oliva, J. L., Mendonça, T., Chabaud, C., Arroub, S., Lafont-Lecuelle, C., et al. (2021). Neurohormonal profiles of assistance dogs compared to pet dogs: what is the impact of different lifestyles? *Animals* 11 (9), 2594. doi:10.3390/ani11092594

Michelini, L. C. (2007a). Differential effects of vasopressinergic and oxytocinergic pre-autonomic neurons on circulatory control: reflex mechanisms and changes during exercise. *Clin. Exp. Pharmacol. Physiol.* 34 (4), 369–376. doi:10.1111/j.1440-1681.2007.04589.x

Michelini, L. C. (2007b). The NTS and integration of cardiovascular control during exercise in normotensive and hypertensive individuals. *Curr. Hypertens. Rep.* 9 (3), 214–221. doi:10.1007/s11906-007-0039-x

Mitkidis, P., McGraw, J. J., Roepstorff, A., and Wallot, S. (2015). Building trust: heart rate synchrony and arousal during joint action increased by public goods game. *Physiol. Behav.* 149, 101–106. doi:10.1016/j.physbeh.2015.05.033

Mitsui, S., Yamamoto, M., Nagasawa, M., Mogi, K., Kikusui, T., Ohtani, N., et al. (2011). Urinary oxytocin as a noninvasive biomarker of positive emotion in dogs. *Horm. Behav.* 60 (3), 239–243. doi:10.1016/j.yhbeh.2011.05.012

Miyashiro, S., Yamada, Y., Nagaoka, M., Shima, R., Muta, T., Ishikawa, H., et al. (2021). Pain relief associated with decreased oxyhemoglobin level in left dorsolateral prefrontal cortex. *PLoS One* 16 (8), e0256626. doi:10.1371/journal.pone.0256626

Moghimian, M., Faghihi, M., Karimian, S. M., and Imani, A. (2012). The effect of acute stress exposure on ischemia and reperfusion injury in rat heart: role of oxytocin. *Stress* 15 (4), 385–392. doi:10.3109/10253890.2011.630436

Moghlmian, M., Faghihi, M., Karimian, S. M., Imani, A., and Mobasheri, M. B. (2014). Upregulated Hsp27 expression in the cardioprotection induced by acute stress and oxytocin in ischemic reperfused hearts of the rat. *Chin. J. Physiol.* 57 (6), 329–334. doi:10.4077/CJP.2014.BAC257

Murphy, D., Konopacka, A., Hindmarch, C., Paton, J. F. R., Sweedler, J. V., Gillette, M. U., et al. (2012). The hypothalamic-neurohypophyseal system: from genome to physiology. *J. Neuroendocrinol.* 24 (4), 539–553. doi:10.1111/j.1365-2826.2011.02241.x

Nagasawa, T., Kimura, Y., Masuda, K., and Uchiyama, H. (2022). Physiological assessment of the health and welfare of domestic cats—an exploration of factors affecting urinary cortisol and oxytocin. *Animals* 12 (23), 3330. doi:10.3390/ani12233330

Nagasawa, T., Ohta, M., and Uchiyama, H. (2020). Effects of the characteristic temperament of cats on the emotions and hemodynamic responses of humans. *PLoS One* 15 (6), e0235188. doi:10.1371/journal.pone.0235188

Nakamura, K., Yamashita, T., Fujiki, H., Aoyagi, T., Yamauchi, J., Mori, T., et al. (2011). Enhanced glucose tolerance in the Brattleboro rat. *Biochem. Biophys. Res. Commun.* 405 (1), 64–67. doi:10.1016/j.bbrc.2010.12.126

Nasanbuyan, N., Yoshida, M., Takayanagi, Y., Inutsuka, A., Nishimori, K., Yamanaka, A., et al. (2018). Oxytocin–oxytocin receptor systems facilitate social defeat posture in male mice. *Endocrinology* 159 (2), 763–775. doi:10.1210/en.2017-00606

Nielsen, M. G., Ørnbøl, E., Vestergaard, M., Bech, P., Larsen, F. B., Lasgaard, M., et al. (2016). The construct validity of the perceived stress scale. *J. Psychosom. Res.* 84, 22–30. doi:10.1016/j.jpsychores.2016.03.009

Niittynen, T., Riihonen, V., Moscovice, L. R., and Koski, S. E. (2022). Acute changes in oxytocin predict behavioral responses to foundation training in horses. *Appl. Anim. Behav. Sci.* 254, 105707. doi:10.1016/j.applanim.2022.105707

Nishina, K., Takagishi, H., Takahashi, H., Sakagami, M., and Inoue-Murayama, M. (2019). Association of polymorphism of arginine-vasopressin receptor 1A (AVPR1a) gene with trust and reciprocity. *Front. Hum. Neurosci.* 13, 230. doi:10.3389/fnhum.2019.00230

Noto, K., Suzuki, A., Shirata, T., Matsumoto, Y., Muraosa, H., Goto, K., et al. (2021). Oxytocin receptor polymorphism influences characterization of harm avoidance by moderating susceptibility to affectionless control parenting. *Brain Behav.* 11 (11), e2393. doi:10.1002/brb3.2393

Ohno, A., Kawasaki, N., Fukuhara, K., Okuda, H., and Yamaguchi, T. (2009). Time-dependent changes of oxytocin using 1H-nmr coupled with multivariate analysis: a new approach for quality evaluation of protein/peptide biologic drugs. *Chem. Pharm. Bull. (Tokyo)* 57 (12), 1396–1399. doi:10.1248/cpb.57.1396

Okumura, T., Nozu, T., Kumei, S., and Ohhira, M. (2019). Central oxytocin signaling mediates the central orexin-induced visceral antinociception through the opioid system in conscious rats. *Physiol. Behav.* 198, 96–101. doi:10.1016/j.physbeh.2018.10.007

Olatunji, B. O., Sawchuk, C. N., Moretz, M. W., David, B., Armstrong, T., and Ciesielski, B. G. (2010). Factor structure and psychometric properties of the injection phobia scale–anxiety. *Psychol. Assess.* 22 (1), 167–179. doi:10.1037/a0018125

Oliver, V. L., Lambert, P. A., Than, K. K., Mohamed, Y., Luchters, S., Verma, S., et al. (2018). Knowledge, perception and practice towards oxytocin stability and quality: a qualitative study of stakeholders in three resource-limited countries. *PLoS One* 13 (9), e0203810. doi:10.1371/journal.pone.0203810

Osako, Y., Nobuhara, R., Arai, Y. C. P., Tanaka, K., Young, L. J., Nishihara, M., et al. (2018). Partner loss in monogamous rodents: modulation of pain and emotional behavior in male prairie voles. *Psychosom. Med.* 80 (1), 62–68. doi:10.1097/PSY.0000000000000524

Osório, F. de L., Espitia-Rojas, G. V., and Aguiar-Ricz, L. N. (2022). Effects of intranasal oxytocin on the self-perception and anxiety of singers during a simulated public singing performance: a randomized, placebo-controlled trial. *Front. Neurosci.* 16, 943578. doi:10.3389/fnins.2022.943578

Page, M. J., McKenzie, J. E., Bossuyt, P. M., Boutron, I., Hoffmann, T. C., Mulrow, C. D., et al. (2021). The PRISMA 2020 statement: an updated guideline for reporting systematic reviews. *BMJ* 372, 71. doi:10.1136/bmj.n71

Palumbo, A., Aluru, V., Battaglia, J., Geller, D., Turry, A., Ross, M., et al. (2022). Music upper limb therapy-integrated provides a feasible enriched environment and reduces post-stroke depression: a pilot randomized controlled trial. *Am. J. Phys. Med. Rehabil.* 101 (10), 937–946. doi:10.1097/PHM.0000000000001938

Palumbo, S., Mariotti, V., Anastasio, T., Rota, G., Lucchi, L., Manfrinati, A., et al. (2020). A genetic profile of oxytocin receptor improves moral acceptability of outcome-maximizing harm in male insurance brokers. *Behav. Brain Res.* 392, 112681. doi:10.1016/j.bbr.2020.112681

Peen, N. F., Duque-Wilckens, N., and Trainor, B. C. (2021). Convergent neuroendocrine mechanisms of social buffering and stress contagion. *Horm. Behav.* 129, 104933. doi:10.1016/j.yhbeh.2021.104933

Peijie, C., Hongwu, L., Fengpeng, X., Jie, R., and Jie, Z. (2003). Heavy load exercise induced dysfunction of immunity and neuroendocrine responses in rats. *Life Sci.* 72 (20), 2255–2262. doi:10.1016/S0024-3205(03)00115-2

Pfordresher, P. Q. (2021). Music production deficits and social bonding: the case of poor-pitch singing. *Behav. Brain Sci.* 44, e86. doi:10.1017/S0140525X20001247

Plaza-Manzano, G., Molina-Ortega, F., Lomas-Vega, R., Martínez-Amat, A., Achalandabaso, A., and Hita-Contreras, F. (2014). Changes in biochemical markers of pain perception and stress response after spinal manipulation. *J. Orthop. Sports Phys. Ther.* 44 (4), 231–239. doi:10.2519/jospt.2014.4996

Porsolt, R. D., Brossard, G., Hautbois, C., and Roux, S. (2001). Rodent models of depression: forced swimming and tail suspension behavioral despair tests in rats and mice. *Curr. Protoc. Neurosci.* 14 (1), Unit 8.10A. doi:10.1002/0471142301.ns0810as14

Pressman, S. D., Freche, R. E., and Patel, J. S. (2013). The interaction between perceived social support and salivary oxytocin in the cortisol stress response. *Psychosom. Med.* 75 (3). doi:10.1097/01.psy.0000429452.16135.1b

Rassovsky, Y., Harwood, A., Zagoory-Sharon, O., and Feldman, R. (2019). Martial arts increase oxytocin production. *Sci. Rep.* 9 (1), 12980. doi:10.1038/s41598-019-49620-0

Rimmele, U., Hediger, K., Heinrichs, M., and Klaver, P. (2009). Oxytocin makes a face in memory familiar. *J. Neurosci.* 29 (1), 38–42. doi:10.1523/JNEUROSCI.4260-08.2009

Rocha-Santos, C., Braga, D. C., Ceroni, A., and Michelini, L. C. (2020). Activity-dependent neuroplastic changes in autonomic circuitry modulating cardiovascular control: the essential role of baroreceptors and chemoreceptors signaling. *Front. Physiol.* 11, 309. doi:10.3389/fphys.2020.00309

Rokkaku, K., Onaka, T., Okada, N., Ideno, J., Kawakami, A., Honda, K., et al. (2003). Neuromedin U facilitates oxytocin release from the pituitary via beta adrenoceptors. *Neuroreport* 14 (15), 1997–2000. doi:10.1097/00001756-200310270-00024

Rossi, A., Parada, F. J., Stewart, R., Barwell, C., Demas, G., and Allen, C. (2018). Hormonal correlates of exploratory and play-soliciting behavior in domestic dogs. *Front. Psychol.* 9, 1559. doi:10.3389/fpsyg.2018.01559

Ruginsk, S. G., Uchoa, E. T., Elias, L. L. K., and Antunes-Rodrigues, J. (2010). CB1 modulation of hormone secretion, neuronal activation and mRNA expression following extracellular volume expansion. *Exp. Neurol.* 224 (1), 114–122. doi:10.1016/j.expneurol.2010.03.001

Sakamoto, T., Nakahara, K., Maruyama, K., Katayama, T., Mori, K., Miyazato, M., et al. (2011). Neuromedin S regulates cardiovascular function through the sympathetic nervous system in mice. *Pept. (N.Y.)* 32 (5), 1020–1026. doi:10.1016/j.peptides.2011.02.015

Salighedar, R., Erfanparast, A., Tamaddonfard, E., and Soltanalinejad, F. (2019). Medial prefrontal cortex oxytocin-opioid receptors interaction in spatial memory processing in rats. *Physiol. Behav.* 209, 112599. doi:10.1016/j.physbeh.2019.112599

Santos, C. R., Ruggeri, A., Ceroni, A., and Michelini, L. C. (2018). Exercise training abrogates age-dependent loss of hypothalamic oxytocinergic circuitry and maintains high parasympathetic activity. *J. Neuroendocrinol.* 30 (8), e12601. doi:10.1111/jne.12601

Scarola, S. J., Perdomo Trejo, J. R., Granger, M. E., Gerecke, K. M., and Bardi, M. (2019). Immunomodulatory effects of stress and environmental enrichment in long–evans rats (*Rattus norvegicus*). *Comp. Med.* 69 (1), 35–47. doi:10.30802/AALAS-CM-18-000025

Schreiner, P. J. (2016). Emerging cardiovascular risk research: impact of pets on cardiovascular risk prevention. *Curr. Cardiovasc Risk Rep.* 10 (2), 8. doi:10.1007/s12170-016-0489-2

Sezen-Balçikanli, G., and Sezen, M. (2017). Professional sports and empathy: relationship between professional futsal players' tendency toward empathy and fouls. *Phys. Cult. Sport. Stud. Res.* 73 (1), 27–35. doi:10.1515/pcssr-2017-0003

Shahar, D., Shai, I., Vardi, H., Brener-Azrad, A., and Fraser, D. (2003). Development of a semi-quantitative Food Frequency Questionnaire (FFQ) to assess dietary intake of multiethnic populations. *Eur. J. Epidemiol.* 18 (9), 855–861. doi:10.1023/A:1025634020718

Shima, T., Jesmin, S., Onishi, H., Yoshikawa, T., and Saitoh, R. (2022). Physical activity associates empathy in Japanese young adults with specific gene variations of oxytocin receptor and vasopressin V1B receptor. *Physiol. Behav.* 255, 113930. doi:10.1016/j.physbeh.2022.113930

Shimizu, H., Tanaka, M., and Osaki, A. (2016). Transgenic mice overexpressing nesfatin/nucleobindin-2 are susceptible to high-fat diet-induced obesity. *Nutr. Diabetes* 6 (3), e201. doi:10.1038/nutd.2015.42

Skinner, J. A., Campbell, E. J., Dayas, C. V., Garg, M. L., and Burrows, T. L. (2019). The relationship between oxytocin, dietary intake and feeding: a systematic review and meta-analysis of studies in mice and rats. *Front. Neuroendocrinol.* 52, 65–78. doi:10.1016/j.yfrne.2018.09.002

Sonne, J. W. H., and Gash, D. M. (2018). Psychopathy to altruism: neurobiology of the selfish–selfless spectrum. *Front. Psychol.* 9, 575. doi:10.3389/fpsyg.2018.00575

Spence, C., Puccinelli, N. M., Grewal, D., and Roggeveen, A. L. (2014). Store atmospherics: a multisensory perspective. *Psychol. Mark.* 31 (7), 472–488. doi:10.1002/mar.20709

Squires, A. S., Peddle, R., Milway, S. J., and Harley, C. W. (2006). Cytotoxic lesions of the hippocampus do not impair social recognition memory in socially housed rats. *Neurobiol. Learn Mem.* 85 (1), 95–101. doi:10.1016/j.nlm.2005.08.012

Stanić, D., Plećaš-Solarović, B., Mirković, D., Jovanović, P., Dronjak, S., Marković, B., et al. (2017). Oxytocin in corticosterone-induced chronic stress model: focus on adrenal gland function. *Psychoneuroendocrinology* 80, 137–146. doi:10.1016/j.psyneuen.2017.03.011

Steinman, M. Q., Duque-Wilckens, N., and Trainor, B. C. (2019). Complementary neural circuits for divergent effects of oxytocin: social approach versus social anxiety. *Biol. Psychiatry* 85 (10), 792–801. doi:10.1016/j.biopsych.2018.10.008

Sterne, J. A., Hernán, M. A., Reeves, B. C., Savović, J., Berkman, N. D., Viswanathan, M., et al. (2016). ROBINS-I: a tool for assessing risk of bias in non-randomised studies of interventions. *BMJ* 355, i4919. doi:10.1136/bmj.i4919

Sterne, J. A. C., Savović, J., Page, M. J., Elbers, R. G., Blencowe, N. S., Boutron, I., et al. (2019). RoB 2: a revised tool for assessing risk of bias in randomised trials. *BMJ* 366, l4898. doi:10.1136/bmj.l4898

Stevenson, J. R., Young, K. A., Bohidar, A. E., Francomacaro, L. M., Fasold, T. R., Buirkle, J. M., et al. (2017). Alcohol consumption decreases oxytocin neurons in the anterior paraventricular nucleus of the hypothalamus in prairie voles. *Alcohol Clin. Exp. Res.* 41 (8), 1444–1451. doi:10.1111/acer.13430

Stöber, T. M., Lehr, A. B., Hafting, T., Kumar, A., and Fyhn, M. (2020). Selective neuromodulation and mutual inhibition within the CA3–CA2 system can prioritize sequences for replay. *Hippocampus* 30 (11), 1228–1238. doi:10.1002/hipo.23256

Sugiyama, M., Nishijima, I., Miyazaki, S., and Nakamura, T. J. (2020). Secretin receptor-deficient mice exhibit altered circadian rhythm in wheel-running activity. *Neurosci. Lett.* 722, 134814. doi:10.1016/j.neulet.2020.134814

Suzuki, H., Onaka, T., Kasai, M., Kawasaki, M., Ohnishi, H., Otsubo, H., et al. (2009). Response of arginine vasopressin-enhanced green fluorescent protein fusion gene in the hypothalamus of adjuvant-induced arthritic rats. *J. Neuroendocrinol.* 21 (3), 183–190. doi:10.1111/j.1365-2826.2009.01841.x

Swarbrick, M. M., Evans, D. S., Valle, M. I., Favre, H., Wu, S. H., Njajou, O. T., et al. (2011). Replication and extension of association between common genetic variants in *SIM1* and human adiposity. *Obesity* 19 (12), 2394–2403. doi:10.1038/oby.2011.79

Szabó, R., Ménesi, R., H Molnár, A., Szalai, Z., Daruka, L., Tóth, G., et al. (2019). New metabolic influencer on oxytocin release: the ghrelin. *Molecules* 24 (4), 735. doi:10.3390/molecules24040735

Takahashi, K., Shima, T., Soya, M., Yook, J. S., Koizumi, H., Jesmin, S., et al. (2022). Exercise-induced adrenocorticotropic hormone response is cooperatively regulated by hypothalamic arginine vasopressin and corticotrophin-releasing hormone. *Neuroendocrinology* 112 (9), 894–903. doi:10.1159/000521237

Tawfik, D. S., Rovnaghi, C., Profit, J., Cornell, T. T., and Anand, K. J. S. (2023). Prevalence of burnout and its relation to the neuroendocrine system among pediatric residents during the early Covid-19 pandemic: a pilot feasibility study. *Compr. Psychoneuroendocrinol* 14, 100174. doi:10.1016/j.cpnec.2023.100174

Tolentino Bento da Silva, M., Palheta-Junior, R. C., Silva, C. M. S., Cavalcante, A. K. M., Quetz, J. d. S., Havt, A., et al. (2021). Role of cholecystokinin and oxytocin in slower gastric emptying induced by physical exercise in rats. *Physiol. Behav.* 233, 113355. doi:10.1016/j.physbeh.2021.113355

Trieu, M., Foster, A. E., Yaseen, Z. S., Beaubian, C., and Calati, R. (2019). "Neurobiology of empathy," in *Teaching empathy in healthcare* (Cham: Springer International Publishing), 17–39. doi:10.1007/978-3-030-29876-0_2

Ueno, H., Suemitsu, S., Murakami, S., Kitamura, N., Wani, K., Takahashi, Y., et al. (2019). Rescue-like behaviour in mice is mediated by their interest in the restraint tool. *Sci. Rep.* 9 (1), 10648. doi:10.1038/s41598-019-46128-5

Wang, J., and Zou, Z. (2022). Establishment of a biomarker of peripheral stress in opioid addicts based on the hypothalamic-pituitary-adrenal axis—the improvement effect of exercise. *Front. Psychiatry* 13, 1072896. doi:10.3389/fpsyt.2022.1072896

Wang, M., Zhou, R., Xiong, W., Wang, Z., Wang, J., He, L., et al. (2020). Oxytocin mediated cardioprotection is independent of coronary endothelial function in rats. *Pept. (N.Y.)* 130, 170333. doi:10.1016/j.peptides.2020.170333

Wang, Y., Jing, Y., Zhang, Z., Lin, C., and Valadez, E. A. (2017). How dispositional social risk-seeking promotes trusting strangers: evidence based on

brain potentials and neural oscillations. *J. Exp. Psychol. Gen.* 146 (8), 1150–1163. doi:10.1037/xge0000328

Watts, C. A., Haupt, A., Smith, J., Welch, E., Malik, A., Giacomino, R., et al. (2022). Measuring skeletal muscle thermogenesis in mice and rats. *J. Vis. Exp.* 185. doi:10.3791/64264

Wei, D., Lee, D., Cox, C. D., Karsten, C. A., Peñagarikano, O., Geschwind, D. H., et al. (2015). Endocannabinoid signaling mediates oxytocin-driven social reward. *Proc. Natl. Acad. Sci.* 112 (45), 14084–14089. doi:10.1073/pnas.1509795112

Weisman, O., Zagoory-Sharon, O., and Feldman, R. (2013). Oxytocin administration alters HPA reactivity in the context of parent–infant interaction. *Eur. Neuropsychopharmacol.* 23 (12), 1724–1731. doi:10.1016/j.euroneuro.2013.06.006

Whiting, P., Savović, J., Higgins, J. P. T., Caldwell, D. M., Reeves, B. C., Shea, B., et al. (2016). ROBIS: a new tool to assess risk of bias in systematic reviews was developed. *J. Clin. Epidemiol.* 69, 225–234. doi:10.1016/j.jclinepi.2015.06.005

Wirobski, G., Range, F., Graat, E. A. M., Palme, R., Deschner, T., and Marshall-Pescini, S. (2023). Similar behavioral but different endocrine responses to conspecific interactions in hand-raised wolves and dogs. *iScience* 26 (2), 105978. doi:10.1016/j.isci.2023.105978

Xiong, W., Yao, M., Zhou, R., Qu, Y., Yang, Y., Wang, Z., et al. (2020). Oxytocin ameliorates ischemia/reperfusion-induced injury by inhibiting mast cell degranulation and inflammation in the rat heart. *Biomed. Pharmacother.* 128, 110358. doi:10.1016/j.biopha.2020.110358

Xu, J.-F., Chen, X.-Q., and Du, J.-Z. (2006). CRH receptor type 1 mediates continual hypoxia-induced changes of immunoreactive prolactin and prolactin mRNA expression in rat pituitary. *Horm. Behav.* 49 (2), 181–189. doi:10.1016/j.yhbeh.2005.06.004

Yao, M., Wang, Z., Jiang, L., Wang, L., Yang, Y., Wang, Q., et al. (2022). Oxytocin ameliorates high glucose- and ischemia/reperfusion-induced myocardial injury by suppressing pyroptosis via AMPK signaling pathway. *Biomed. Pharmacother.* 153, 113498. doi:10.1016/j.biopha.2022.113498

Yokoyama, T., Saito, T., Ohbuchi, T., Suzuki, H., Otsubo, H., Okamoto, T., et al. (2009). Ghrelin potentiates miniature excitatory postsynaptic currents in supraoptic magnocellular neurones. *J. Neuroendocrinol.* 21 (11), 910–920. doi:10.1111/j.1365-2826.2009.01911.x

Zeng, Q., Han, J., Wang, B., An, S., Duan, Y., Dong, S., et al. (2012). Water maze spatial learning enhances social recognition ability in aged rats. *Neurophysiology* 44 (6), 464–469. doi:10.1007/s11062-012-9319-4

Zhang, Y., Akl, E. A., and Schünemann, H. J. (2019). Using systematic reviews in guideline development: the GRADE approach. *Res. Synth. Methods* 10 (3), 312–329. doi:10.1002/jrsm.1313

Zhuang, Q., Zhu, S., Yang, X., Zhou, X., Xu, X., Chen, Z., et al. (2021). Oxytocin-induced facilitation of learning in a probabilistic task is associated with reduced feedback- and error-related negativity potentials. *J. Psychopharmacol.* 35 (1), 269881120972347–269881120972349. doi:10.1177/0269881120972347

Zimet, G. D., Dahlem, N. W., Zimet, S. G., and Farley, G. K. (1988). The multidimensional scale of perceived social support. *J. Pers. Assess.* 52 (1), 30–41. doi:10.1207/s15327752jpa5201_2

frontiers | Frontiers in Molecular Neuroscience

TYPE Original Research
PUBLISHED 14 June 2024
DOI 10.3389/fnmol.2024.1397808

OPEN ACCESS

EDITED BY
Marija Heffer,
Josip Juraj Strossmayer University of Osijek, Croatia

REVIEWED BY
Roberto Henzi,
Temuco Catholic University, Chile
Olivier Baledent,
University of Picardie Jules Verne, France

*CORRESPONDENCE
Marijan Klarica
✉ mklarica@mef.hr

RECEIVED 08 March 2024
ACCEPTED 24 May 2024
PUBLISHED 14 June 2024

CITATION
Jurjević I, Orešković D, Radoš M, Brgić K and Klarica M (2024) Changes of cerebrospinal fluid pressure gradient in different body positions under experimental impairment of cerebrospinal fluid pathway: new insight into hydrocephalus development.
Front. Mol. Neurosci. 17:1397808.
doi: 10.3389/fnmol.2024.1397808

Changes of cerebrospinal fluid pressure gradient in different body positions under experimental impairment of cerebrospinal fluid pathway: new insight into hydrocephalus development

Ivana Jurjević[1,2], Darko Orešković[3], Milan Radoš[1], Klara Brgić[4] and Marijan Klarica[1]*

[1]Department of Pharmacology and Croatian Institute for Brain Research, School of Medicine, University of Zagreb, Zagreb, Croatia, [2]Department of Neurology, University Hospital Centre Zagreb, Zagreb, Croatia, [3]Department of Molecular Biology, Ruđer Bošković Institute, Zagreb, Croatia, [4]Department of Neurosurgery, Univesity Hospital Centre Zagreb, Zagreb, Croatia

It is generally accepted that hydrocephalus is a consequence of the disbalance between cerebrospinal fluid (CSF) secretion and absorption which should in turn lead to CSF pressure gradient development and ventricular enlargement. To test CSF pressure gradient role in hydrocephalus development, we experimentally caused CSF system impairment at two sites in cats. In the first group of animals, we caused Sylvian aqueduct obstruction and recorded CSF pressure changes pre and post obstruction at three measuring sites (lateral ventricle -LV, cortical-CSS and lumbar subarachnoid space -LSS) during 15 min periods and in different body positions over 360 degrees. In the second group of experiments, we caused cervical stenosis by epidural plastic semiring implantation and monitored CSF pressure changes pre and post stenosis implantation at two measuring sites (lateral ventricle and lumbar subarachnoid space) during 15 min periods in different body positions over 360 degrees. Both groups of experimental animals had similar CSF pressures before stenosis or obstruction at all measuring points in the horizontal position. During head-up verticalization, CSF pressures inside the cranium gradually became more subatmospheric with no significant difference between LV and CSS, as they are measured at the same hydrostatic level, while CSF pressure inside LSS became more positive, causing the development of a large hydrostatic gradient between the cranial and the spinal space. With cervical stenosis, CSF pressure inside the cranium is positive during head-up verticalization, while in cats with aqueductal obstruction CSF pressure inside the CSS remains negative, as it was during control period. Concomitantly, CSF pressure inside LV becomes less negative, thus creating a small hydrostatic gradient between LV and CSS. Since CSF pressure and gradient changes occur only by shifting body position from the horizontal plane, our results indicate that cervical stenosis in a head-up vertical position reduces blood perfusion of the whole brain, while aqueductal obstruction impairs only the perfusion of the local periventricular brain tissue. It seems that, for evolutionary important bipedal activity, free craniospinal communication and good spinal space compliance represent crucial biophysical parameters for adequate cerebral blood perfusion

and prevention of pathophysiological changes leading to the development of hydrocephalus.

KEYWORDS

CSF pressure gradient, body position, aqueductal obstruction, cervical stenosis, hydrocephalus

1 Introduction

In accordance to the classical hypothesis of cerebrospinal fluid (CSF) hydrodinamics (Davson et al., 1987; Pollay, 2010; Sakka et al., 2011; Brinker et al., 2014) hydrocephalus may develop as a result of an obstruction of the circulating pathways, a reduction in the ability to absorb the CSF, or by an overproduction of CSF. Hence, it is believed that the general mechanism of hydrocephalus development is an imbalance between the CSF formation and absorption where more CSF is formed than absorbed, which results in an abnormal increase of CSF volume and pressure inside the cranial CSF space. Obstruction of the CSF pathways somewhere between the hypothetical site of CSF formation and the site of its absorption is deemed as the main cause of the mentioned imbalance, diminishing or preventing CSF outflow from the cranial space (Milhorat, 1972; Hochwald, 1984; Pollay, 1984; Davson et al., 1987; McComb, 1989; Milhorat, 1989). In the case of CSF circulation obstruction, hydrostatic CSF pressure gradient develops between the ventricles and the subarachnoid space due to supposed accumulation of the newly formed CSF, which is instrumental for the rapid hydrocephalus development (so-called acute hydrocephalus) (Dandy, 1919; Milhorat, 1972; Hochwald, 1984; Pollay, 1984; Davson et al., 1987; McComb, 1989; Milhorat, 1989).

Thus, according to the classical concept, the mechanism of hydrocephalus development primarily involves active CSF production or overproduction by choroid plexuses, impaired circulation, decreased absorption and increased hydrostatic CSF pressure (Dandy, 1919; Di Chiro, 1964; Milhorat, 1972; Welch, 1975; Hochwald, 1984; Pollay, 1984; Davson et al., 1987; McComb, 1989; Milhorat, 1989; Pollay, 2010; Sakka et al., 2011; Brinker et al., 2014). However, many forms of hydrocephalus cannot be explained by this concept, mostly emphasising the specific forms of communicating hydrocephalus such as unilateral communicating hydrocephalus, transitory hydrocephalus and arrested or slow-progressing forms with normal pressure such as iNPH (Foltz and Shurtleff, 1966; Holtzer and de Lange, 1973; Di Rocco et al., 1978; Davis, 1981; Griffith and Jamjoom, 1990; Klarica et al., 2009, 2013, 2014; Krishnamurthy et al., 2009; Radoš et al., 2014a,b; Xi et al., 2014; Orešković et al., 2017; Jovanović et al., 2021). The concept also does not provide an adequate explanation of some forms of hydrocephalus which develop concomitantly with tumors or other pathological conditions situated inside the spinal space (Arseni and Maretsis, 1967; Raynor, 1969; Borgesen et al., 1977; Rifkinson-Mann et al., 1990; Cinalli et al., 1995; Morandi et al., 2006; Mirone et al., 2011; Wilson et al., 2013; Mukherjee et al., 2019; Mathkour et al., 2020), since these conditions do not physically interrupt free CSF movement from the hypothetical site of its secretion to the hypothetically dominant site of its absorption (dural sinuses arachnoid granulations) inside the cranium.

Additionally, it is not possible to explain the existence and even aggravation of hydrocephalus post plexectomy (Orešković and Klarica, 2011; Orešković, 2015). Many results of experimental studies on animals, as well as the results from clinical studies imply that there is also a substantial CSF absorption inside the brain ventricles (in both free communicating ventricles and those under obstruction or stenosis) and that significant CSF absorption from the spinal subarachnoid space also takes place (Orešković and Klarica, 2010; Bulat and Klarica, 2011; Orešković and Klarica, 2011; Klarica and Orešković, 2014). Some literature data imply that choroid plexuses and brain ventricles are not the main and exclusive sources of CSF (Bering, 1952; Orešković et al., 1991; Oreškovic et al., 2001; Orešković et al., 2002; Maraković et al., 2010; Klarica et al., 2013; Igarashi et al., 2014; Mehemed et al., 2014; Nakada, 2014; Orešković, 2015), i.e., that CSF can be formed and absorbed anywhere across the CNS capillary network under the gradient of hydrostatic and osmotic forces (Orešković et al., 1991; Bulat et al., 2008; Klarica and Orešković, 2014; Orešković and Klarica, 2014). It was also demonstrated that, in the case of completely patent CSF pathways, an experimental increase of osmolarity can result in hydrocephalus development (Krishnamurthy et al., 2012; Klarica et al., 2013). Ventriculomegaly formation was also observed during experimental subchronic cervical stenosis (Klarica et al., 2016). All of the aforementioned implies that it is necessary to reconsider former concepts of hydrocephalus development, especially those connected to CSF circulation obstruction within the entire craniospinal system and development of CSF pressure gradient. For this purpose, we have experimentally induced an obstruction inside the cranium and spinal stenosis of the CSF system in cats in order to investigate biophysical conditions of either hydrostatic CSF pressure increase or gradient formation by monitoring the changes of CSF pressure at various measuring sites and in different body positions.

2 Materials and methods

2.1 Experimental animals

The study was performed on a total of 9 adult cats (both sex; 2.2–3.4 kg body weight). The animals were obtained from private owners according to the old Croatian Animal Welfare Act which allowed us to obtain experimental animals from domestic breeding. However, today in Croatia we have a new Animal Welfare Act by which it is possible to obtain experimental animals only from official suppliers (and we are currently doing so). The owners were verbally informed about the experimental protocol which was previously approved by official Ethical committee (written consent form was not needed in that time). The animals were kept in cages with natural light–dark cycles and had access to water and food (SP215 Feline,

Hill's Pet Nutrition Inc., Topeka, KS, United States). They were in quarantine for 30 days prior to the experiments, and the procedures were performed in accordance with the Croatian Animal Welfare Act. The protocol was approved by the Ethics Committee of the University of Zagreb Medical School (Approval No. 04–76/2009–761). All efforts were made to minimize suffering, and all surgery according to protocol was performed under anesthesia. The cats were anaesthetized with a-chloralose (Fluka; 100 mg/ kg i.p.) and fixed in a stereotaxic head holder (David Kopf, Tununga, CA, United States) in the sphinx position. The femoral artery was cannulated, the blood pressure was recorded via a T-connector, and samples of blood were taken for analysis of the blood gases. No significant changes, either in blood pressure or blood gases, were observed during these experiments on cats, which continued breathing spontaneously under the chloralose anesthesia. At the end of experiment the animals were sacrified with an excessive dose of anesthesia (thiopental).

2.2 Surgical procedure

Surgical procedure and position of animal during recording CSF pressure are previously described in detail (Klarica et al., 2014, 2016). In short, the anesthetized cats were set into the stereotaxic device in a sphynx position. A stainless steel cannula (0.9 mm ID) was introduced into the left lateral ventricle (LV; cannula with siringe in Figure 1A) at 2 mm lateral and 15 mm anterior to the stereotaxic zero point, and 10–12 mm below the dural surface. A second cannula was placed in the right lateral ventricle (LV) (at same position as the cannula in the left LV). A third cannula was then placed into the cortical subarachnoid space (CSS) at the same hydrostatic level as the cannula placed in the LV when the body is in vertical position. In horizontal body position cannula in CSS is about 0.5 cm above the cannula in LV. The cannulas in the right LV and the CSS were used for the measurement of intracranial CSF pressures. In order to measure the spinal CSF pressure in the lumbar region, a laminectomy (5.0 × 10.0 mm) of the L3 vertebra was performed. After incision of the spinal dura and arachnoidea, a fourth plastic cannula (0.9 mm ID) was introduced into the lumbar subarachnoid space (LSS). Leakage of CSF was prevented by applying cyanoacrylate glue to the dura around the cannula. Bone openings in the cranium and vertebra were hermetically closed by the application of a dental acrylate. After setting the measuring cannulas, the cat was removed from the stereotaxic device and then fixed in a prone position on a board (Figure 1A). CSF pressures were recorded using pressure transducers (Gould P23 ID, Gould Instruments, Cleveland, OH, United States) which were connected to a system that transformed analogous to digital data (Quand Bridge and PowerLab/800, ADInstruments, Castle Hill, NSW, Australia), and then entered into a computer (IBM, White Plains, NY, United States). Pressure transducers were calibrated by use of a water column; the interaural line was taken as zero pressure. Instruments for pressure measurement were fixed on the board in such a way that the membrane of each transducer was at the same hydrostatic level as the corresponding measuring cannula, so there was no need to additionally adjust the transducers during the body position changes. The cats were also fixed onto the measuring board by their extremities and their head to avoid any movement during body position changes. This enabled us to maintain the same

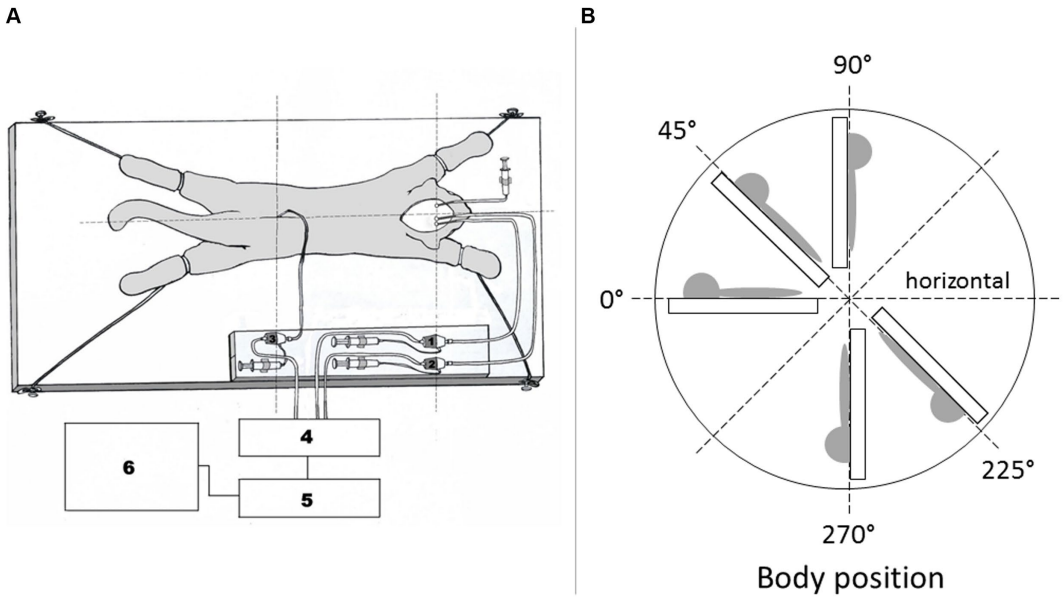

FIGURE 1
(A) Scheme of a cat experimental model. The animal is fixed onto the flat board, together with pressure tranducers and measuring cannulas. 1 – pressure transducer connected to the measuring cannula inside the right lateral ventricle, 2 – pressure transducer connected to the measuring cannula inside the cortical subarachnoid space, 3 – pressure transducer connected to the measuring cannula inside the lumbar subarachnoid space. 4 – Quad Bridge, 5 – PowerLab/800, AD Instruments, Castle Hill, NSW, Australia, 6 – computer. Syringe is connected to cannula in left lateral ventricle. **(B)** Schematic display of the body position changes in which CSF pressure measurements were performed. CSF pressure was measured inside the lumbar and cortical subarachnoid space, as well as in the lateral ventricle of experimental animals in horizontal position 0°, head- up position 45°, head-up position 90°, head-down position 225°, and head-down position 270°.

distance of the measuring cannulas and the pressure tranducers according to their real hydrostatic level in any body position, thus giving us an opportunity to examine how the CSF pressure changes in relation to the distance of the measuring cannulas from cisterna magna.

2.3 Basic measurements during control period (normal CSF pathway)

According to RRR principals each experimental animal ($n = 9$) also served for control measurements of CSF pressure. During that control period we measured CSF pressures inside the LV, CSS and LSS in different body positions without any CSF pathway impairment (horizontal 0°, head-up 45°, vertical head-up 90°, head-down 225°, and vertical head-down 270°) (Figure 1B). CSF pressure changes were recorded at 15 min intervals.

2.4 Blockade of the Sylvian aqueduct

In the first group of experiments on anesthetized cats ($n = 4$) after control period of CSF pressure measurement we performed occipital craniectomy followed by tunneling of the cerebellar vermis right up to the entrance into the Sylvian aqueduct. A plastic cannula with the diametar corresponding to the aqueductal width was carefully manually inserted through the tunnel in order to avoid the damage of the surrounding tissue. A drop of cyanoacrylate glue (Super Attack glue) was used to fix the cannula to the brain tissue to completely block the aqueduct. After reconstructing the bone and hermetically closing the surgical wound we proceeded to introduce the measuring cannulas into the LV and CSS as was previously described, followed by measurments of CSF pressures in different body positions, as mentioned above (Figure 2B).

2.5 Cervical stenosis

In the second group of experiments ($n = 5$) on anesthetized cats after control period of CSF pressure recording we performed additional laminectomy of the cervical C2 vertebrae (5.0 ×10.0 mm) exposing the dura. Immediately after opening, a plastic semiring (width 2.0 mm; length 10.0 mm; thickness 1.0 mm) covering the dorsal and lateral parts of the dura and gently pressing on the cord was positioned in order to disable the communication between the cranial and the spinal subarachnoid space [details previously described in Klarica et al. (2014, 2016)]. We swiftly covered the opening with dental acrylate, that way hermetically isolating the system from the atmospheric pressure influence. The CSF pressures were then measured in the ventricles and in the lumbar subarachnoid space in different body positions, as described before (Figure 3B).

2.6 Statistical analysis

Data are shown as a mean value ± standard error of the mean (SEM). A statistical analysis of all of the results was performed using the Paired Student's *t*-test and ANOVA for repeated measures. All statistical analysis was performed using the Statistica 7.1 (StatSoft Inc., Tulsa, OK, United States). $p < 0.05$ was considered as statistically significant.

3 Results

In the first group of experiments control results were obtained on 4 cats in which CSF pressure changes were observed inside the lateral ventricle (LV), cortical (CSS) and lumbar subarachnoid space (LSS) before surgical impairment of the Sylvian aqueduct. CSF pressures were measured during body position changes, as described above.

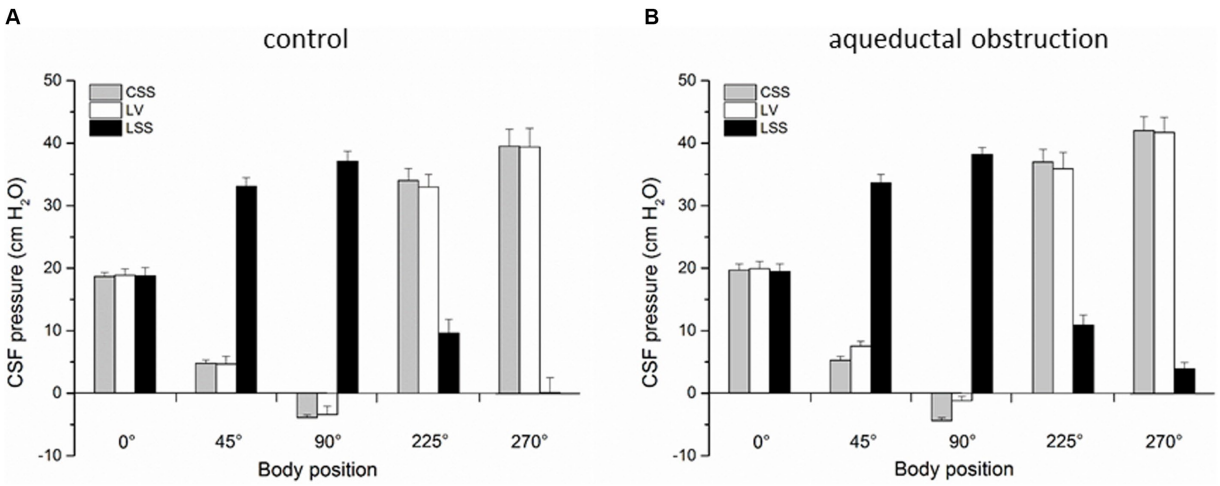

FIGURE 2
(A) Changes of CSF pressure (cm H_2O) inside the lateral ventricle (LV, □), cortical (CSS, ▨) and lumbar (LSS, ■) subarachnoid space in horizontal position (0°), head-up position (45°), head-up position (90°), head-down position (225°), and head-down position (270°) in cats ($n = 4$) with open CSF pathway (control). **(B)** Changes of CSF pressure inside the lateral ventricle (LV, □), cortical (CSS, ▨) and lumbar (LSS, ■) subarachnoid space in horizontal position (0°), head-up position (45°), head-up position (90°), head-down position (225°), and head-down position (270°) in cats ($n = 4$) with aqueductal obstruction. The columnes represent the mean values, and the vertical marks are standard errors of the mean.

10.3389/fnmol.2024.1397808

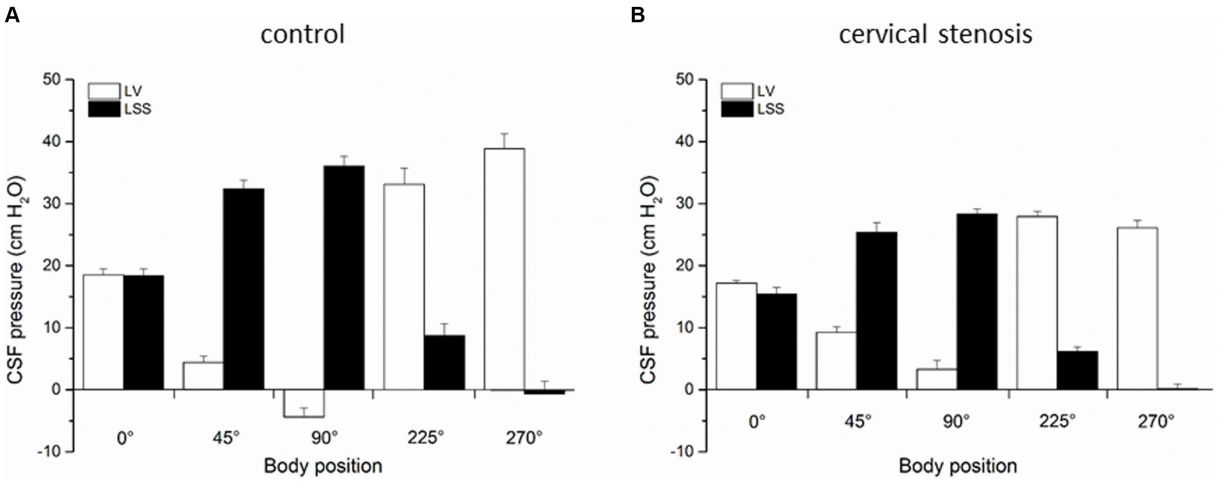

FIGURE 3
(A) Changes of CSF pressure (cm H_2O) inside the lateral ventricle (LV, □), and lumbar (LSS, ■) subarachnoid space in horizontal position (0°), head-up position (45°), head-up position (90°), head-down position (225°), and head-down position (270°) in cats ($n = 5$) with normal CSF pathway communication (control). **(B)** Changes of CSF pressure inside the lateral ventricle (LV, □), and lumbar (LSS, ■) subarachnoid space in horizontal position (0°), head-up position (45°), head-up position (90°), head-down position (225°), and head-down position (270°) in cats ($n = 5$) with cervical stenosis. The columnes represent the mean values, and the vertical marks are standard errors of the mean.

Figure 2A shows that in horizontal position there is no statistical difference between the pressures measured inside the LV (18.9 ± 1.0 cm H_2O), CSS (18.7 ± 0.6 cm H_2O) and LSS (18.8 ± 1.3 cm H_2O). During head-up position 45°, CSF pressure inside the lumbar space gradually increases to 33.1 ± 1.4 cm H_2O and in vertical head-up position 90° it reaches 37.1 ± 1.6 cm H_2O, while the cranial CSF pressure gradually decreases and amounts to 4.7 ± 1.2 cm H_2O inside LV and 4.8 ± 0.5 cm H_2O inside CSS during head-up position 45°, decreasing further to negative values in vertical head-up position 90° (−3.4 ± 1.3 cm H_2O inside LV and −3.9 ± 0.4 cm H_2O inside CSS). CSF pressures inside the cranium do not significantly differ and they are measured at the same hydrostatic level. In head-down position 225° CSF pressure inside LSS decreases to 9.6 ± 2.2 cm H_2O and in head-down position 270° it was 0.1 ± 2.4 cm H_2O, while the cranial CSF pressure gradually increases in head-down position 225° to 33.0 ± 2.2 cm H_2O inside the LV and 34.0 ± 1.9 cm H_2O inside CSS, further increasing in head-down position 270° to 39.4 ± 3.0 cm H_2O inside the LV and 39.5 ± 2.7 cm H_2O inside CSS. Again, there is no statistical difference between cranial pressures in these positions (Figure 2A).

In the second group of experiments done on the same cats ($n = 4$) described above, corresponding measurements of CSF pressures were performed inside the LV, CSS and LSS after blockade of the Sylvian aqueduct by insertion of a plastic tube matching in diametar to the width of the aqueduct. Figure 2B shows once more that the LV, CSS and LSS pressures are approximately the same (LV = 19.9 ± 1.2 cm H_2O; CSS = 19.7 ± 1.0 cm H_2O; LSS = 19.5 ± 1.2 cm H_2O) and without statistically significant difference ($p = 0.91$). However, in an upright position LV and CSS pressures are not equally negative any more, i.e., CSF pressure inside the LV is now more positive than the one inside the CSS, measuring 7.5 ± 0.8 cm H_2O in the head-up position 45° and −1.2 ± 0.7 cm H_2O in the head-up position 90°, while the CSF pressure inside the CSS remains equally low as in the case of open aqueduct, amounting to 5.3 ± 0.6 cm H_2O in head-up position 45°, while it is −4.4 ± 0.5 cm H_2O in head-up position 90°. Thus, during animal verticalization to head-up position 90° a statistically significant difference between the CSF pressure inside LV and CSS can be observed ($p = 0.01$). At the same time, CSF pressure inside the LSS increases again to positive values and measures 33.6 ± 1.4 cm H_2O in head-up position 45° and 38.2 ± 1.1 cm H_2O in head-up position 90°. In the head-down position 225° CSF pressure lumbally decreases to 10.9 ± 1.6 cm H_2O, and to 3.9 ± 1.0 cm H_2O in head-down position 270°, while the CSF pressures inside the LV and CSS rise again to equally positive values, amounting to 35.9 ± 2.6 cm H_2O in head-down position 225° and to 41.7 ± 2.4 cm H_2O in head-down position 270° in LV, while it was 37.0 ± 2.0 cm H_2O in head-down position 225° and 42.0 ± 2.2 cm H_2O in head-down position 270° in CSS (Figure 2B).

The third group of experiments was done as control measurements on cats ($n = 5$) before insertion of cervical stenosis. CSF pressure changes were measured inside the lateral ventricle LV, CSS and LSS in different body positions, as described before. Figure 3A shows again that the pressures inside the LV and LSS do not differ in horizontal position (LV = 18.5 ± 1.0 cm H_2O, LSS = 18.4 ± 1.1 cm H_2O) and are not statistically significantly different, while in the head-up position lumbar pressure gradually increases, amounting to 32.4 ± 1.3 cm H_2O in head-up position 45° and 36.0 ± 1.6 cm H_2O in head-up position 90°. The pressure inside the cranial LV simultaneously drops to negative values, and measures 4.4 ± 1.0 cm H_2O in head-up position 45° and −4.4 ± 1.4 cm H_2O in head-up position 90°. During the cat head-down position, LSS pressure gradually becomes negative and in the head-down position 225° it is 8.7 ± 1.9 cm H_2O, while in the head-down position 270° it is −0.7 ± 2.0 cm H_2O. At the same time, pressure inside LV increases to 33.1 ± 1.6 cm H_2O in the head-down position 225° and to 38.9 ± 2.9 cm H_2O in the head-down position 270° (Figure 3A).

In the last experimental series, an insertion of cervical stenosis was performed in cats ($n = 5$), as described in Materials and methods. We then performed measurements of CSF pressures inside the LV and LSS in aforementioned various body positions. Figure 3B shows that

in horizontal position pressures inside the LV and LSS are still equal (LV = 17.2 ± 0.4 cm H_2O; LSS = 15.5 ± 1.0 cm H_2O) and without significant statistical difference ($p = 0.239$). However, LV pressure now remains positive in both head-up position 45° (9.2 ± 0.9 cm H_2O) and in head-up position 90° (3.3 ± 1.4 cm H_2O), while LSS pressure increases again to even more positive values in both head-up position 45° (25.4 ± 1.6 cm H_2O) and in head-up position 90° (28.3 ± 0.8 cm H_2O). Thus, compared with the control measurements done on the same animals before insertion of cervical stenosis in the same body positions, LV pressure differs significantly post cervical stenosis (in the head-up position 45° $p = 0.0075$, in the head-up position 90° $p = 0.0054$). During the cat head-down position, CSF pressure inside the LV increases, and amounts to 27.9 ± 1.8 cm H_2O at 225° and to 26.1 ± 1.2 cm H_2O at 270°, while LSS pressure decreases, measuring 6.1 ± 0.8 cm at 225° and 0.1 ± 0.8 cm H_2O at 270° (Figure 3B).

4 Discussion

4.1 CSF pressure changes inside the cranium during head-up verticalization

Results of CSF pressure measurement inside the LV, CSS and LS of control animals (no obstruction or stenosis) during the changes of body position were in accordance with previously published results (Kuzman et al., 2012; Klarica et al., 2014, 2022). Namely, during gradual head-up verticalization CSF pressure inside the cranium progresivelly dropped to subatmospheric (negative) values in the vertical head-up position 90° (Figures 2A, 3A). CSF pressures inside the LV and CSS were around −4 cm H_2O, which corresponded to the hydrostatic distance from the measuring cannulas inside the LV and CSS to foramen magnum (Figure 2A). In accordance with the law of fluid mechanics, hydrostatic pressure can be calculated anywhere within the system if the distance from the reference point is known ($P = \rho \times g \times h$, where P is the pressure, ρ is the fluid density, g is the gravitational force, and h is the height of fluid column), and by that it is possible to explain the changes in pressure at different body positions. All of this suggests that CSF pressure changes during the changes of body position do not depend on CSF secretion, circulation and absorption, as was explained in detail in previous publications (Klarica et al., 2014, 2022).

In addition, Sylvian aqueduct obstruction during head-up verticalization caused CSF pressure inside the LV to decrease more slowly, so in vertical head-up position 90° pressure inside the LV was less negative and amounted to −1 cm H_2O (Figure 2B). At the same time, CSF pressure inside the CSS gradually decreased as in control conditions (there was normal CSF communication between CSS and LSS), and in vertical head-up position 90° it was about −4 cm H_2O, which led to development of a slight gradient between LV and CSS (Figure 2B). With aqueductal obstruction, CSF pressures inside the LV, CSS and LSS are equal in horizontal position 0° (Figure 2B) and pressure gradient between LV and CSS only starts forming after the change of body position. According to the classical concept of CSF secretion inside the ventricles, it would be expected that ventricular obstrucion resulted in an increased CSF pressure inside the ventricles, regardless of the position of the head toward the rest of the body. Thus, it is only during bipedal walking that aqueductal obstruction would be able to cause a lesser change of the CSF pressure inside the ventricles compared to the pressure change that occurs inside the subarachnoid space, which would potentially create a pressure gradient that inhibits blood perfusion of the brain tissue surrounding the ventrilces (compared to the more adequate perfusion of the cortical gray matter), further enabling the right biopyhsical conditions for the beginning of hydrcoephalus development.

Contrary to that, cervical stenosis during head-up verticalization caused even greater delay in CSF pressure decrease inside the LV compared to Sylvian aqueduct obstruction, and it finally remained on the positive level of +4 cm H_2O which represents the hydrostatic distance between the measuring cannula inside the LV and foramen magnum (Figure 3B). In the horizontal position, cervical stenosis caused a slight difference between CSF pressures inside the LV and LSS, however, that difference significantly increased during head-up verticalization. Thus, in this case verticalization changed CSF pressure inside the LV by 8 cm H_2O (from −4 cm H_2O to +4 cm H_2O) which also led to significantly decreased cerebral perfusion pressure (CPP). These results clearly indicate that during bipedal walking with normal CSF space communication CPP is much higher than it was previously believed (CSF pressure values are subatmospheric), and that different pathological processes which impair cranio-spinal communication (e.g., Arnold-Chiari malformation, tumours and other conditions that produce mass-effect inside the spinal space) significantly reduce CPP. It was previously believed that appearance of low or negative CSF pressure during head-up body verticalization is a transitory phenomenon caused by a slight and brief shift of CSF and blood from hydrostatically higher to hydrostatically lower compartments under the influence of gravity (Davson, 1967; Magnaes, 1976a,b; Davson et al., 1987). Shortly after (in a few minutes) it should go back to positive values due to hypothetical continuous CSF formation (Davson, 1967; Magnaes, 1976a,b; Davson et al., 1987). However, many clinical and animal research data imply that CSF pressure values are stabile as long as the body remains in a certain position, whether horizontal or head-up. Namely, in patients whose CSF pressure was measured for 60 min sitting up, it was constantly at the atmospheric level (zero CSF pressure) in the upper cervical region and at the same time positive inside the lumbar region, while the pressure values corresponded to the distance in cm from cisterna magna to the site of measurement in the lumbar part (Magnaes, 1976a,b). Similar results were obtained during intracranial pressure measurements in patients whose bodies were gradually verticalized (Chapman et al., 1990).

In our previous research, we kept experimental animals in a head-up position from 75 to 150 min and during that entire measuring period CSF pressure recorded inside the LV in those animals remained steadily negative (Klarica et al., 2014). It seems that appearance of negative CSF pressure is not a transitory phenomenon. Thus, although in this research we measured CSF pressure for a period of 15 min in one position before and after obstruction, we would expect for CSF pressure to remain equal and stabile even if we measured it for a longer period of time. Even in the case of aqueductal obstruction lasting 120 min (Klarica et al., 2009) or cervical stenosis over a period of 60 min (Klarica et al., 2016) in our previous work CSF pressure values inside the cranium measured in the spynx position were unchanged.

4.2 Changes of cranial and spinal CSF pressure during head-up verticalization

With normal CSF pathway communication (control animals), head-up verticalization 90° creates a large hydrostatic gradient (about

40 cm H_2O) between the cranial (LV, CSS) and spinal (LSS) CSF space, preventing existence of a hypothetical unilateral CSF circulation from the ventricles to the cisterna magna (CM) and from there to LSS (Figure 2). In the case of aqueductal obstruction, that pressure gradient between the cranial and spinal space is maintained (Figure 2B). Following cervical stenosis, which interrupts hydrostatic CSF column, gradient becomes decreased (Figure 3) as it drops from 40 cm H_2O (+36 cm H_2O in LSS plus −4 cm H_2O in LV) to 24 cm H_2O (+28 cm H_2O in LSS minus +4 cm H_2O in LV). Thus, in neither of those cases do pressure gradients support the presumed unidirectional CSF circulation from the ventricles to the CM and to LSS.

Compliance is a ratio between the changes in CSF volume and CSF pressure expressed in mL/cm H_2O. Distribution of craniospinal compliance is a fundamental question. A large number of studies were performed on animals and in humans in order to determine the contribution of individual cranial and spinal compliance to the total craniospinal compliance (Lofgren et al., 1973; Marmarou et al., 1975; Magnaes, 1989; Wahlin et al., 2010; Gehlen et al., 2017; Burman et al., 2018; Caton et al., 2021; Klarica et al., 2022).

It would be possible to determine the contribution of each individual compartment only if we separated the cranial from the spinal space (as ideally as possible) and then tested volume load-induced pressure changes inside each compartment. Thus, Marmarou has determined the cranial space contribution to be around 2/3 of the total compliance in his experiments on cats in which he separated the cranial from the spinal part of the CSF system at the cervical and the thoracic junction (Marmarou et al., 1975). Contrary to that, Lofgren et al. (1973) separated the cranial from the spinal space at the C_1 level in dogs, and determined that the spinal compartment contribution is around 70%. Their results were more in line with the research from Magnaes who applied separate infusion boluses into the cranial and the spinal part of the CSF system in patients with cervical blockage (Magnaes, 1989). In our previous study, compliance was calculated in animals and in phantom after the addition/removal of a fluid volume from the spinal part of the system (Klarica et al., 2022). The calculation has been done for both horizontal and vertical positions. There was an exponential relationship between pressure changes and compliance. According to a well-known phenomenon, the value of compliance decreases with increasing CSF pressure, so this can be seen in our research. A similar phenomenon was also observed in patients during gravity-induced CSF pressure changes (Gehlen et al., 2017).

In this study, we have not performed volume changes by addition or substracion of fluid post surgically placed impairments inside the CSF system, so we cannot determine which compliance changes have been induced. However, based on the observed CSF pressure changes inside each individual CSF compartment, according to the well-known phenomenon, we can point to the direction of compliance changes. Therefore, if the pressure has increased, the compliance will decrease, and if the pressure has decreased, compliance will increase (Klarica et al., 2022).

4.3 Changes of cranial and spinal CSF pressure during head-down verticalization

In the head-down position at 270°, measurements of CSF pressures inside the LV, CSS and LSS in control animals with no CSF system impairment showed positive and similar pressure values inside the LV and CSS (around 40 cm H_2O), which also corresponded to the hight of the total fluid column, i.e., to the distance between the lumbar space and cisterna magna (35–37 cm) with addition of the distance between cisterna magna and the cranial measuring cannulas (around 4 cm). In the case of Sylvian aqueduct obstruction, CSF pressures inside the LV, CSS and LSS remained similar to those obtained in animals without impairment (all of the measured values were somewhat higher than dose before aqueduct obstruction in the same position), which shows once again that there is no net CSF formation inside the isolated ventricles and no pressure gradient formation. It appears that in the head-down position there is a simultaneous transmission of pressure from the CSS in all directions across the larger surface of brain tissue to the smaller surface of isolated LV in the middle part of the brain, explaining gradient nonexistence. Similar effect was observed during mock CSF infusions into the CM at various rates in animals with aqueductal occlusion (Klarica et al., 2009). Infusions induced an increase of CSF pressure inside the subarachnoid space, which was instantly trasmitted across the brain tissue into the isolated ventricles, not resulting in gradient formation (Klarica et al., 2009). In fact, pressure gradient in those experiments developed only following infusions into isolated ventricles.

After insertion of cervical stenosis, CSF pressure inside the LV during head-down verticalization once again becomes positive. It appears that under higher pressure, a partial breach of stenosis occurs, causing hydrostatic pressure column to transfer partially from spinal subarachnoid space to cranial space (CSF pressure inside the LV in the head-down position at 270 ° was +38.9 cm H_2O without stenosis and + 26.1 cm H_2O with stenosis).

4.4 Clinical implications of our results

Since it is believed that CSF physiology in different animal species does not differ from that in humans, results of our research could provide an elucidation for many cases of various pathological conditions such as Arnold-Chiari malformations, spinal tumors, spinal haematomas, AV malformations or spinal oedema described in the literature related to concomitant hydrocephalus development in which the mechanism was described as unknown or unclear (Arseni and Maretsis, 1967; Raynor, 1969; Borgesen et al., 1977; Rifkinson-Mann et al., 1990; Cinalli et al., 1995; Morandi et al., 2006; Mirone et al., 2011; Wilson et al., 2013; Mukherjee et al., 2019; Mathkour et al., 2020). In the case of Arnold-Chiari type I malformation, the exact pathological mechanism for conjoined hydrocephalus development is still not clear. It is usually explained by primarily enlarged ventricles causing tonsilar prolaps through foramen magnum, or the prolaps causing an interruption of presumed unidirectional CSF circulation on the cranial basis level (Mukherjee et al., 2019; Mathkour et al., 2020). However, according to our results it seems that the process actually develops the other way around, i.e., that Arnold Chiari malformation primarily leads to impaired craniospinal CSF communication which in turn enables hydrocephalus development. This could also be corroborated by a number of literature data that shows variable results of surgical treatment (Mukherjee et al., 2019; Mathkour et al., 2020). Most often this implies foramen magnum decompression, however, not always succesful, and sometimes even causing the development of hydrocephalus that was not present prior to the procedure (Mukherjee et al., 2019). Thus, our results show major significance of the CSF system spinal compartment for the

compensation of pressure and volume changes that occur inside the cranial space and how its stenosis for a number of possible reasons contributes to hydrocephalus development, particularly in an upright position in which we spend most of the time.

We also provide an explanation for the changes of CPP in different body positions during CSF pathway obstruction or stenosis on two different levels, with high and stable CPP in an upright position without any impairment that only slightly decreased in that same position after aqueductal blockade, but significantly decreases during cervical stenosis, which could, together with gradient development, also contribute to hydrocephalus development leading to tissue ischaemia. However, our results also show that aqueductal blockade by itself is insufficient to cause acute hydrocephalus development, especially in horizontal position, while in the vertical position only a slight gradient develops which is also unlikely to cause acute ventricular enlargement without any additional intracranial pathology. It is actually evident from this research that spinal pathological processes have much higher potential for acute hydrocephalus development than intracranial processes that block the aqueduct, primarily during the time we spend in an upright position. Thus, it would seem clinically important to perform a neuroradiological examination of the entire CNS system in the case of either spinal pathology or enlarged ventricles without other known intracranial causes.

5 Conclusion

In this research performed on cats as experimental animals, we have shown that CSF pressures measured inside the cranium gradually decrease below atmospheric level during animal head-up verticalization, and that there is no significant difference in the pressure values measured at the same hydrostatic level inside the LV and CSS. Additionally, we have found that experimentally caused aqueductal obstruction and subarachnoid space cervical stenosis do not induce CSF pressure gradient development during the horizontal plane measuring period. CSF pressure gradient develops only if the body position changes from horizontal to any other plane. These results suggest that cervical stenosis during the head-up vertical position can cause reduction of blood perfusion through the entire brain, and that aqueductal obstruction will only diminish the perfusion of the brain tissue surrounding the ventricles. Thus, observed phenomena imply that unimpaired cerebrospinal communication and preserved spinal space compliance could be evolutionary crucial for the development of bipedal walking as they enable optimal cerebral blood perfusion in any body position and prevent the development of pathophysiological changes which could in turn lead to hydrocephalus development.

6 Limitations

In this research, we have measured the changes of CSF pressure and observed the potential hydrocephalus development after experimentally induced impairment of CSF movement only during 15 min time periods following each change of the body position. We have not perfomed control phase measurements in the form of sham experiments since this would mean exposing cranial contets to atmospheric pressure. In order to avoid atmospheric pressure influence, we would have to hermetically close occipital craniectomy, than perform the control measurements, followed by reopening of occipital bone or cervical vertebrae in order to install stenosis or opstruction, than close the surgical field again. All of this would additionally damage the tissue (possible haemorrhage etc.) which could lead to experimental failure. Thus, we would have to additionally increase the number of experimental animals which goes against the RRR rules. Since during the experiments animals were not connected to ECG (it is techically challenging to record ECG during the changes of board and animal body positions), we were not able to measure heart frequency or amplitude of CSF pressure during cardiac cycle. However, the results are comparable to our previously published results obtained after similar experimentally caused CSF system stenosis or obstruction measured for longer periods of time, but mainly in one (mostly horizontal) body position. Since hydrocephalus development is usually a long-lasting (chronic) process, future investigations should strive to follow CSF pressure gradient changes in various pathological processes impairing normal CSF movement over much longer time periods.

Data availability statement

The raw data supporting the conclusions of this article will be made available by the authors, without undue reservation.

Ethics statement

The animal studies were approved by Ethics Committee of the University of Zagreb Medical School (Approval No. 04-76/2009-761). The studies were conducted in accordance with the local legislation and institutional requirements. Written informed consent was not obtained from the owners for the participation of their animals in this study because The owners were verbally informed about the experimental protocol which was previously approved by official Ethical committee (written consent form was not needed in that time).

Author contributions

IJ: Data curation, Formal analysis, Investigation, Methodology, Writing – original draft, Writing – review & editing. DO: Conceptualization, Formal analysis, Funding acquisition, Project administration, Writing – original draft, Writing – review & editing. MR: Data curation, Formal analysis, Investigation, Writing – original draft, Writing – review & editing. KB: Formal analysis, Investigation, Methodology, Writing – original draft, Writing – review & editing. MK: Conceptualization, Data curation, Formal analysis, Funding acquisition, Investigation, Methodology, Project administration, Resources, Supervision, Validation, Writing – original draft, Writing – review & editing.

Funding

The author(s) declare that financial support was received for the research, authorship, and/or publication of this article. This work has been supported by the Croatian Science Foundation and the Ministry of Science and Education of the Republic of Croatia (Projects: 1.

Pathophysiology of cerebrospinal fluid and intracranial pressure. No. 108–1080231-0023; and 2. Serotonergic modulation of obesity: cross-talk between regulatory molecules and pathways. No. IP-2014-09-7827). The research was co-financed by the Scientific Centre of Excellence for Basic, Clinical and Translational Neuroscience (project "Experimental and clinical research of hypoxic–ischemic damage in perinatal and adult brain"; GA KK01.1.1.01.0007 funded by the European Union through Europe).

Acknowledgments

We would like to thank Mrs. Ljiljana Krznar for technical assistance in performing the experiments.

Conflict of interest

The authors declare that the research was conducted in the absence of any commercial or financial relationships that could be construed as a potential conflict of interest.

Publisher's note

References

Arseni, C., and Maretsis, M. (1967). Tumors of the lower spinal cord associated with increased intracranial pressure and papilledema. *J. Neurosurg.* 27, 105–110. doi: 10.3171/jns.1967.27.2.0105

Bering, E. A. (1952). Water exchange of central nervous system and cerebrospinal fluid. *J. Neurosurg.* 9, 275–287. doi: 10.3171/jns.1952.9.3.0275

Borgesen, S. E., Sorensen, S. C., Olesen, J., and Gjerris, F. (1977). Spinal tumours associated with increased intracranial pressure. Report of two cases and a discussion on the pathophysiology. *Acta Neurol. Scand.* 56, 263–268. doi: 10.1111/j.1600-0404.1977.tb01432.x

Brinker, T., Stopa, E., Morrison, J., and Klinge, P. (2014). A new look at cerebrospinal fluid circulation. *Fluids Barriers CNS* 11:10. doi: 10.1186/2045-8118-11-10

Bulat, M., and Klarica, M. (2011). Recent insights into a new hydrodynamics of the cerebrospinal fluid. *Brain Res. Rev.* 65, 99–112. doi: 10.1016/j.brainresrev.2010.08.002

Bulat, M., Lupret, V., Orešković, D., and Klarica, M. (2008). Transventricular and transpial absorption of cerebrospinal fluid into cerebral microvessels. *Coll. Antropol.* 32, 43–50.

Burman, R., Alperin, N., Lee, S. H., and Ertl-Wagner, B. (2018). Patient-specific cranio-spinal compliance distribution using lumbed-parameter model.Its relation with ICP over a wide age range. *Fluids Barriers CNS* 15:29. doi: 10.1186/s12987-018-0115-4

Caton, M. T., Laguna, B., Soderlund, K. A., Dillon, W. P., and Shah, V. N. (2021). Spinal comliance curves: preliminary experience with a new tool for evaluating suspected CSF venous fistulas on CSF myelography in patients with spontaneous intracranial hypotension. *Am. J. Neuroradiol.* 42, 986–992. doi: 10.3174/ajnr.A7018

Chapman, P. H., Cosman, E. R., and Arnold, M. A. (1990). The relationship between ventricular fluid pressure and body position in normal subjects and subjects with shunts: a telemetric study. *Neurosurgery* 26, 181–189. doi: 10.1227/00006123-199002000-00001

Cinalli, G., Sainte-Rose, C., Lellouch-Tubiana, A., Sebag, G., Renier, D., and Pierre-Kahn, A. (1995). Hydrocephalus associated with intramedullary low-grade glioma. Illustrative cases and review of the literature. *J. Neurosurg.* 83, 480–485. doi: 10.3171/jns.1995.83.3.0480

Dandy, W. E. (1919). Experimental hydrocephalus. *Ann. Surg.* 70, 129–142. doi: 10.1097/00000658-191908000-00001

Davis, L. E. (1981). Communicating hydrocephalus in newborn hamsters and cats following vaccinia virus infection. *J. Neurosurg.* 54, 767–772. doi: 10.3171/jns.1981.54.6.0767

Davson, H. (1967). *Physiology of the cerebrospinal fluid*. London: Churchill Livingstone.

Davson, H., Welch, K., and Segal, M. B. (1987). *Physiology and pathophysiology of the cerebrospinal fluid*. Edinburgh: Churchill Livingstone.

Di Chiro, G. (1964). Movement of the cerebrospinal fluid in human beings. *Nature* 204, 290–291. doi: 10.1038/204290a0

Di Rocco, C., Pettorossi, V. E., Caldarelli, M., Mancinelli, R., and Velardi, F. (1978). Communicating hydrocephalus induced by mechanically increased amplitude of the intraventricular cerebrospinal fluid pressure: experimental studies. *Exp. Neurol.* 59, 40–52. doi: 10.1016/0014-4886(78)90199-1

Foltz, E. L., and Shurtleff, D. B. (1966). Conversion of communicating hydrocephalus to stenosis or occlusion of the aqueduct during ventricular shunt. *J. Neurosurg.* 24, 520–529. doi: 10.3171/jns.1966.24.2.0520

Gehlen, M., Kurtucuoglu, V., and Schmid Daners, M. (2017). Is posture-related craniospinal compliance shift caused by jugular venous collapse? Theoretical analysis. *Fluids Barriers CNS* 14:5. doi: 10.1186/s12987-017-0053-6

Griffith, H. B., and Jamjoom, A. B. (1990). The treatment of childhood hydrocephalus by choroid plexus coagulation and artificial cerebrospinal fluid perfusion. *Br. J. Neurosurg.* 4, 95–100. doi: 10.3109/02688699008992706

Hochwald, G. (1984). "Animal model in hydrocephalus" in *Hydrocephalus*. eds. K. Shapiro, A. Marmarou and H. Portnoy (New York: Raven Press Books), 199–213.

Holtzer, G. J., and de Lange, S. A. (1973). Shunt-independent arrest of hydrocephalus. *J. Neurosurg.* 39, 698–701. doi: 10.3171/jns.1973.39.6.0698

Igarashi, H., Tsujita, M., Kwee, I. L., and Nakada, T. (2014). Water influx into cerebrospinal fluid is primarily controlled by aquaporin-4, not by aquaporin-1: 17O JJVCPE MRI study in knockout mice. *Neuroreport* 25, 39–43. doi: 10.1097/WNR.0000000000000042

Jovanović, I., Nemir, J., Gardijan, D., Milošević, M., Poljaković, Z., Klarica, M., et al. (2021). Transient acute hydrocephalus after aneurysmal subarachnoid hemorrhage and aneurysm embolization: a single-center experience. *Neuroradiology* 63, 2111–2119. doi: 10.1007/s00234-021-02747-2

Klarica, M., Jukić, T., Miše, B., Kudelić, N., Radoš, M., and Orešković, D. (2016). Experimental spinal stenosis in cats: new insight in mechanisms of hydrocephalus development. *Brain Pathol.* 26, 701–712. doi: 10.1111/bpa.12337

Klarica, M., Miše, B., Vladić, A., Radoš, M., and Orešković, D. (2013). "Compensated hyperosmolarity" of cerebrospinal fluid and the development of hydrocephalus. *Neuroscience* 248, 278–289. doi: 10.1016/j.neuroscience.2013.06.022

Klarica, M., and Orešković, D. (2014). Enigma of cerebrospinal fluid dynamics. *Croat. Med. J.* 55, 287–298. doi: 10.3325/cmj.2014.55.287

Klarica, M., Oresković, D., Bozić, B., Vukić, M., Butković, V., and Bulat, M. (2009). New experimental model of acute aqueductal blockage in cats: effects on cerebrospinal fluid pressure and the size of brain ventricles. *Neuroscience* 158, 1397–1405. doi: 10.1016/j.neuroscience.2008.11.041

Klarica, M., Radoš, M., Erceg, G., Jurjević, I., Petošić, A., Virag, Z., et al. (2022). Cerebrospinal fluid micro-volume changes inside the spinal space affect intracranial pressure in different body positions of animals and phantom. *Front. Mol. Neurosci.* 15:e931091. doi: 10.3389/fnmol.2022.931091

Klarica, M., Radoš, M., Erceg, G., Petošić, A., Jurjević, I., and Orešković, D. (2014). The influence of body position on cerebrospinal fluid pressure gradient and movement in cats with normal and impaired craniospinal communication. *PLoS One* 9:e95229. doi: 10.1371/journal.pone.0095229

Krishnamurthy, S., Li, J., Schultz, L., and Jenrow, K. A. (2012). Increased CSF osmolarity reversibly induces hydrocephalus in the normal rat brain. *Fluids Barriers CNS* 9:13. doi: 10.1186/2045-8118-9-13

Krishnamurthy, S., Li, J., Schultz, L., and McAllister, J. P. (2009). Intraventricular infusion of hyperosmolar dextran induces hydrocephalus: a novel animal model of hydrocephalus. *Cerebrospinal Fluid Res.* 6:16. doi: 10.1186/1743-8454-6-16

Kuzman, T., Jurjević, I., Mandac, I., Radoš, M., Orešković, D., Jednačak, H., et al. (2012). The effect of body position on intraocular and CSF pressures in the lateral ventricle, and in cortical and lumbar subarachnoid spaces in cats. *Acta Neurochir. Suppl.* 114, 357–361. doi: 10.1007/978-3-7091-0956-4_69

Lofgren, J., von Essen, C., and Zwetnow, N. N. (1973). The pressure-volume curve of the cerebrospinal fluid space in dogs. *Acta Neurol. Scand.* 49, 557–574. doi: 10.1111/j.1600-0404.1973.tb01330.x

Magnaes, B. (1976a). Body position and cerebrospinal fluid pressure. Part 1: clinical studies on the effect of rapid postural changes. *J. Neurosurg.* 44, 687–697. doi: 10.3171/jns.1976.44.6.0687

Magnaes, B. (1976b). Body position and cerebrospinal fluid pressure. Part 2: clinical studies on orthostatic pressure and the hydrostatic indifferent point. *J. Neurosurg.* 44, 698–705. doi: 10.3171/jns.1976.44.6.0698

Magnaes, B. (1989). Clinical studies of cranial and spinal compliance and the craniospinal flow of cerebrospinal fluid. *Br. J. Neurosurg.* 3, 659–668. doi: 10.3109/02688698908992689

Maraković, J., Oresković, D., Rados, M., Vukić, M., Jurjević, I., Chudy, D., et al. (2010). Effect of osmolarity on CSF volume during ventriculo-aqueductal and ventriculo-cisternal perfusions in cats. *Neurosci. Lett.* 484, 93–97. doi: 10.1016/j.neulet.2010.07.058

Marmarou, A., Shulman, K., and LaMorgese, J. (1975). Compartmental analysis of copliance and outflow resistance of the cerebrospinal fluid system. *J. Neurosurg.* 43, 523–534. doi: 10.3171/jns.1975.43.5.0523

Mathkour, M., Keen, J. R., Huang, B., Werner, C., Scullen, T., Garces, J., et al. (2020). "two-birds-one-stone" approach for treating an infant with Chiari I malformation and hydrocephalus: is cerebrospinal fluid diversion as sole treatment enough? *World Neurosurg.* 137, 174–177. doi: 10.1016/j.wneu.2020.01.188

McComb, J. G. (1989). "Cerebrospinal fluid formation and absorption" in *Pediatric neurosurgery*. eds. R. L. McLaurin, L. Schult, J. L. Venes and F. Epstein. *2nd* ed (Philadelphia: Saunders), 159–169.

Mehemed, T. M., Fushimi, Y., Okada, T., Yamamoto, A., Kanagaki, M., Kido, A., et al. (2014). Dynamic oxygen-enhanced MRI of cerebrospinal fluid. *PLoS One* 9:e100723. doi: 10.1371/journal.pone.0100723

Milhorat, T. H. (1972). *Hydrocephalus and the cerebrospinal fluid*. Baltimore: Williams and Wilkins.

Milhorat, T. H. (1989). "Circulation of the cerebrospinal fluid" in *Pediatric neurosurgery*. eds. R. L. McLaurin, L. Schult, J. L. Venes and F. Epstein. *2nd* ed (Philadelphia: Saunders), 170–179.

Mirone, G., Cinalli, G., Spennato, P., Ruggiero, C., and Aliberti, F. (2011). Hydrocephalus and spinal cord tumors: a review. *Childs Nerv. Syst.* 27, 1741–1749. doi: 10.1007/s00381-011-1543-5

Morandi, X., Amlashi, S. F., and Riffaud, L. (2006). A dynamic theory for hydrocephalus revealing benign intraspinal tumours: tumoural obstruction of the spinal subarachnoid space reduces total CSF compartment compliance. *Med. Hypotheses* 67, 79–81. doi: 10.1016/j.mehy.2006.01.005

Mukherjee, S., Kalra, N., Warren, D., Sivakumar, G., Goodden, J. R., Tyagi, A. K., et al. (2019). Chiari I malformation and altered cerebrospinal fluid dynamics-the highs and the lows. *Childs Nerv. Syst.* 35, 1711–1717. doi: 10.1007/s00381-019-04233-w

Nakada, T. (2014). Virchow-Robin space and aquaporin-4: new insights on an old friend. *Croat. Med. J.* 55, 328–336. doi: 10.3325/cmj.2014.55.328

Orešković, D. (2015). The controversy on choroid plexus function in cerebrospinal fluid production in humans: how long different views could be neglected? *Croat. Med. J.* 56, 306–310. doi: 10.3325/cmj.2015.56.306

Orešković, D., and Klarica, M. (2010). The formation of cerebrospinal fluid: nearly a hundred years of interpretations and misinterpretations. *Brain Res. Rev.* 64, 241–262. doi: 10.1016/j.brainresrev.2010.04.006

Orešković, D., and Klarica, M. (2011). Development of hydrocephalus and classical hypothesis of cerebrospinal fluid hydrodynamics: facts and illusions. *Prog. Neurobiol.* 94, 238–258. doi: 10.1016/j.pneurobio.2011.05.005

Orešković, D., and Klarica, M. (2014). Measurement of cerebrospinal fluid formation and absorption by ventriculo-cisternal perfusion: what is really measured? *Croat. Med. J.* 55, 317–327. doi: 10.3325/cmj.2014.55.317

Oreškovic, D., Klarica, M., and Vukić, M. (2001). Does the secretion and circulation of the cerebrospinal fluid really exist? *Med. Hypotheses* 56, 622–624. doi: 10.1054/mehy.2000.1178

Orešković, D., Klarica, M., and Vukić, M. (2002). The formation and circulation of cerebrospinal fluid inside the cat brain ventricles: a fact or an illusion? *Neurosci. Lett.* 327, 103–106. doi: 10.1016/s0304-3940(02)00395-6

Orešković, D., Radoš, M., and Klarica, M. (2017). New concepts of cerebrospinal fluid physiology and development of hydrocephalus. *Pediatr. Neurosurg.* 52, 417–425. doi: 10.1159/000452169

Orešković, D., Whitton, P. S., and Lupret, V. (1991). Effect of intracranial pressure on cerebrospinal fluid formation in isolated brain ventricles. *Neuroscience* 41, 773–777. doi: 10.1016/0306-4522(91)90367-w

Pollay, M. (1984). "Research into human hydrocephalus: a review" in *Hydrocephalus*. eds. K. Shapiro, A. Marmarou and H. Portnoy (New York: Raven Press Books), 301–314.

Pollay, M. (2010). The function and structure of the cerebrospinal fluid outflow system. *Cerebrospinal Fluid Res.* 7:9. doi: 10.1186/1743-8454-7-9

Radoš, M., Klarica, M., Mučić-Pucić, B., Nikić, I., Raguž, M., Galkowski, V., et al. (2014a). Volumetric analysis of cerebrospinal fluid and brain parenchyma in a patient with hydranencephaly and macrocephaly--case report. *Croat. Med. J.* 55, 388–393. doi: 10.3325/cmj.2014.55.388

Radoš, M., Orešković, D., Radoš, M., Jurjević, I., and Klarica, M. (2014b). Long lasting near-obstruction stenosis of mesencephalic aqueduct without development of hydrocephalus--case report. *Croat. Med. J.* 55, 394–398. doi: 10.3325/cmj.2014.55.394

Raynor, R. B. (1969). Papilledema associated with tumors of the spinal cord. *Neurology* 19, 700–704. doi: 10.1212/wnl.19.7.700

Rifkinson-Mann, S., Wisoff, J. H., and Epstein, F. (1990). The association of hydrocephalus with intramedullary spinal cord tumors: a series of 25 patients. *Neurosurgery* 27, 749–754. doi: 10.1227/00006123-199011000-00012

Sakka, L., Coll, G., and Chazal, J. (2011). Anatomy and physiology of cerebrospinal fluid. *Eur. Ann. Otorhinolaryngol. Head Neck Dis.* 128, 309–316. doi: 10.1016/j.anorl.2011.03.002

Wahlin, S., Ambarki, K., Birgander, R., Alperin, N., Malm, J., and Eklund, A. (2010). Assessment of craniospinal pressure-volume indices. *Am. J. Neuroradiol.* 31, 1645–1650. doi: 10.3174/ajnr.A2166

Welch, K. (1975). The principles of physiology of the cerebrospinal fluid in relation to hydrocephalus including normal pressure hydrocephalus. *Adv. Neurol.* 13, 247–332

Wilson, M. P., Aronyk, K. E., Yeo, T., Chow, M., and Pugh, J. A. (2013). Communicating hydrocephalus caused by an unruptured perimedullary arteriovenous fistula in the lumbar region of an infant. *J. Neurosurg. Pediatr.* 11, 346–349. doi: 10.3171/2012.11.PEDS12244

Xi, G., Strahle, J., Hua, Y., and Keep, R. F. (2014). Progress in translational research on intracerebral hemorrhage: is there an end in sight? *Prog. Neurobiol.* 115, 45–63. doi: 10.1016/j.pneurobio.2013.09.007

frontiers | Frontiers in Molecular Neuroscience

TYPE Original Research
PUBLISHED 27 June 2024
DOI 10.3389/fnmol.2024.1398872

OPEN ACCESS

EDITED BY
Marija Heffer,
Josip Juraj Strossmayer University of Osijek, Croatia

REVIEWED BY
Julio Plata Bello,
Hospital Universitario de Canarias, Spain
Alen Rončević,
Klinički bolnički centar Osijek, Croatia

*CORRESPONDENCE
Anja Kafka
✉ anja.kafka@mef.hr

†These authors have contributed equally to this work

RECEIVED 10 March 2024
ACCEPTED 31 May 2024
PUBLISHED 27 June 2024

CITATION
Kafka A, Pećina-Šlaus N, Drmić D, Bukovac A, Njirić N, Žarković K and Jakovčević A (2024) *SFRP4* protein expression is reduced in high grade astrocytomas which is not caused by the methylation of its promoter.
Front. Mol. Neurosci. 17:1398872.
doi: 10.3389/fnmol.2024.1398872

SFRP4 protein expression is reduced in high grade astrocytomas which is not caused by the methylation of its promoter

Anja Kafka[1,2*†], Nives Pećina-Šlaus[1,2†], Denis Drmić[1], Anja Bukovac[1,2], Niko Njirić[3], Kamelija Žarković[4,5] and Antonia Jakovčević[4,5]

[1]Laboratory of Neuro-oncology, Croatian Institute for Brain Research, School of Medicine, University of Zagreb, Zagreb, Croatia, [2]Department of Biology, School of Medicine, University of Zagreb, Zagreb, Croatia, [3]Department of Neurosurgery, University Hospital Center "Zagreb", School of Medicine, University of Zagreb, Zagreb, Croatia, [4]Department of Pathology, School of Medicine, University of Zagreb, Zagreb, Croatia, [5]Division of Pathology, University Hospital Center "Zagreb", Zagreb, Croatia

Introduction: Epigenetics play a vital role in stratifying CNS tumors and gliomas. The importance of studying Secreted frizzled-related protein 4 (SFRP4) in gliomas is to improve diffuse glioma methylation profiling. Here we examined the methylation status of *SFRP4* promoter and the level of its protein expression in diffuse gliomas WHO grades 2–4.

Methods: SFRP4 expression was detected by immunohistochemistry and evaluated semi-quantitatively. In the tumor hot-spot area, the intensity of protein expression in 200 cells was determined using ImageJ (National Institutes of Health, United States). The assessment of immunopositivity was based on the IRS score (Immunoreactivity Score). Promoter methylation was examined by methylation specific-PCR (MSP) in fifty-one diffuse glioma samples and appropriate controls. Isolated DNA was treated with bisulfite conversion and afterwards used for MSP. Public databases (cBioPortal, COSMIC and LOVD) were searched to corroborate the results.

Results and discussion: SFRP4 protein expression in glioblastomas was very weak or non-existent in 86.7% of samples, moderate in 13.3%, while strong expression was not observed. The increase in astrocytoma grade resulted in SFRP4 protein decrease ($p = 0.008$), indicating the loss of its antagonistic role in Wnt signaling. Promoter methylation of *SFRP4* gene was found in 16.3% of cases. Astrocytomas grade 2 had significantly more methylated cases compared to grade 3 astrocytomas ($p = 0.004$) and glioblastomas ($p < 0.001$), which may indicate temporal niche of methylation in grade 2. Furthermore, the expression levels of SFRP4 were high in samples with methylated *SFRP4* promoter and low or missing in unmethylated cases (Pearson's $R = -0.413$; $p = 0.003$). We also investigated the association of SFRP4 changes to key Wnt regulators *GSK3β* and *DKK3* and established a positive correlation between methylations of *SFRP4* and *GSK3β* (Pearson's $R = 0.323$; $p = 0.03$). Furthermore, SFRP4 expression was correlated to unmethylated *DKK3* (Chi square = 7.254; $p = 0.027$) indication that Wnt signaling antagonist is associated to negative regulator's demethylation.

Conclusion: The study contributes to the recognition of the significance of epigenetic changes in diffuse glioma indicating that restoring SFRP4 protein

holds potential as therapeutic avenue. Reduced expression of SFRP4 in glioblastomas, not following promoter methylation pattern, suggests another mechanism, possible global methylation, that turns off SFRP4 expression in higher grades.

KEYWORDS

astrocytoma, Wnt signaling pathway, SFRP4, promoter methylation, methylation specific PCR, IRS score

Introduction

Gliomas comprise about 30 percent of all brain tumors and about 80 percent of all malignant brain tumors. Currently histological and molecular features are strongly integrated in glioma classification (Louis et al., 2021). The most comprehensive changes were figured out for different glioma types and now four general groups of diffuse gliomas are recognized. Astrocytomas are the most common type characterized by diffuse infiltrative growth in the brain parenchyma. WHO tumor grading is essential in risk stratification. The inclusion of both phenotypic and molecular parameters has led to changes in the 2016 WHO (World Health Organization) classification (Louis et al., 2016) and improved the prognosis of gliomas (Louis et al., 2021). Now all diffuse gliomas, whether astrocytic or not, are grouped into one category based on mitotic activity, diffuse growth pattern, and the mutational status of the *IDH1* and *IDH2* genes, together with several other molecular biomarker testing. Tumors are graded within tumor types rather than across different types (Park et al., 2023). For example, patients with grade 3 gliomas carrying a 1p/19q co-deletion have a better prognosis than IDH wild-type grade 2 glioma. The prognosis of diffuse glioma depends on several factors including tumor grade. In general, grade 2 tumors have 8 year overall median survival while patients with grade 3 tumor are living 2–5 years after diagnosis. Despite recent advances in diagnosis and treatment of glioblastoma, the prognosis of the disease is poor. Glioblastoma have a very high mortality rate, with average survival time from 12 to 18 months (Barthel et al., 2018; Narayanan and Turcan, 2020; Barthel et al., 2022; Malta et al., 2024).

Previously, it has been demonstrated that specific family of WNT signaling antagonists - the Secreted Frizzled-Related Protein (SFRP) family, is responsible for the decrease in proliferation of glioma cells and for making them sensitive to chemotherapeutics (Warrier et al., 2013; Schiefer et al., 2014). The SFRPs have a far-reaching effect across Wnt pathways, being able to antagonize both canonical and noncanonical branches (Yu et al., 2019). The canonical pathway is regulated at multiple levels. A fine-tuned homeostatic balance between cytoplasmic and nuclear β-catenin determines the final outcome of the Wnt signalization. The balance is achieved by extracellular antagonists of Wnt signaling (Schiefer et al., 2014). They are expressed in various tissues and control a multitude of biological processes during embryonic development and adulthood (Nusse and Clevers, 2017; Rim et al., 2022). In the absence of the Wnt ligand, a β-catenin destruction complex is formed in the cytoplasm. Phosphokinases CK1 and GSK3β sequentially phosphorylate axin-bound β-catenin on a series of regularly spaced serine and threonine residues at its N-terminus. Phosphorylated motifs act as a dock for the E3 ubiquitin ligase subunit β-TrCP (β-Transducin Repeat Containing Protein), which induces ubiquitination and consequently proteasomal degradation of β-catenin. Thus, the level of β-catenin in the cell remains low (Hayat et al., 2022; Rim et al., 2022). Binding of Wnt ligand to membranous receptor Frizzled (Fz) and its co-receptor low density lipoprotein receptor related protein (LRP) initiates a cascade of events leading to the disassembly of the APC/Axin/GSK3β/CK1 destruction complex and the stabilization of cytoplasmic β-catenin. Accumulation of β-catenin in the cytoplasm leads to its translocation to the nucleus and activation of target genes mediated by transcription factors TCF/LEF (Hayat et al., 2022; Rim et al., 2022). In recent years, Wnt antagonists received a lot of attention due to their frequent inactivation in cancer (Pawar and Rao, 2018). *SFRP* genes (in human number 1–5) are frequently hypermethylated in a variety of human cancers and thereby transcriptionally silent (Schiefer et al., 2014). Silencing of *SFRP* genes via hypermethylation at the promoter region has been reported for glioblastoma, too (Götze et al., 2010; Schiefer et al., 2014; Bhuvanalakshmi et al., 2018). Suppression of Wnt signaling by SFRP proteins also contributes to normal astrocyte development (Sun et al., 2015).

Secreted frizzled-related protein 4 (SFRP4) is an extracellular modulator of the Wnt signaling that can bind both the Wnt ligand and frizzled receptor. Thus, it acts as an antagonist of Wnt ligands, preventing their binding to the receptor. With a molecular weight of 39.9 kDa and a length of 346 amino acids, SFRP4 is the largest member of the SFRP family (Pohl et al., 2015). Altered SFRP4 expression in different types of tumors indicates its essential role in maintaining tissue homeostasis (Bovolenta et al., 2008; Pawar and Rao, 2018). Also, silenced *SFRP4* gene or its decreased protein expression causes the activation of the Wnt pathway. *SFRP4* contains dense CpG islands flanking the first exon. Their hypermethylation is one of the mechanisms of gene silencing, which creates a predisposition for malignant changes (Müller and Győrffy, 2022; Ramazi et al., 2023).

Whilst the aforementioned studies have shown that SFRP4 could be involved in the molecular pathogenesis of diffuse gliomas, its specific role in astrocytoma subtypes has not been sufficiently investigated. Therefore, the present study aims to explore the *SFRP4* promoter methylation status and its consequence on protein levels in diffuse astrocytoma grade 2–4. In order to elucidate *SFRP4's* effect on Wnt cascade its correlation to GSK3β, DKK1, DKK3, LEF1 and β-catenin was also tested in our study.

Materials and methods

Tissue samples

Fifty-one diffuse astrocytoma sample graded from 2 to 4 together with paired blood and formalin-fixed paraffin-embedded (FFPE)

slides of tumor tissues were collected from the Department of Neurosurgery and Department of Pathology University Hospital Center "Zagreb." Certified neuropathologist (KŽ, AJ) reviewed chosen slides to set the accurate diagnosis (CNS WHO grade 2–4) in concordance with the most recent WHO classification (Louis et al., 2021). The patients included in the study had no family history of brain tumors and did not undergo any cancer treatment, prior to surgery, which could affect the results of molecular analyses. The sample consisted of 11 astrocytoma CNS WHO grade 2, 10 astrocytoma CNS WHO grade 3 and 30 astrocytoma CNS WHO grade 4. Twenty-nine patients were male and twenty-two were female. The age of patients varied from 6 to 83 (mean age = 50.31, median = 54 years, std. deviation = 18.099). The mean age of diagnosis for males was 47 years (median 49, std. deviation = 19.085) and for females 56 (median 63, std. deviation = 15.710) (Table 1).

The study was approved by the Ethical Committees, School of Medicine University of Zagreb (Case number: 380–59–10,106-14-55/147; Class: 641–01/14–02/01) and University Hospital Center "Zagreb" (number 02/21/JG, class: 8.1.-14/54–2). Patients gave their informed consent.

Immunohistochemistry (IHC)

IHC staining was performed on 4 µm thick FFPE sections mounted on silanized glass slides (DakoCytomation, Glostrup, Denmark). Tissue sections went through deparaffinization in xylene (3x, 5 min), rehydration in graded ethanol series, (100, 96 and 70% ethanol, 2x, 3 min), and water (30 s). Next, sections were heated in 6 M citrate buffer in the microwave oven two times for 10 min at 400 W and three times for 5 min at 350 W in order to recover antigen epitopes. Afterward, the endogenous peroxidase activity was blocked using 3% hydrogen peroxide for 10 min in dark. Non-specific binding was blocked by incubating samples with protein block serum-free ready-to-use (Agilent Technologies, United States) for 30 min at 4°C. Sections were incubated with primary antibody Anti-SFRP-4 [EPR9389] (rabbit monoclonal anti-human; ab154167, Abcam, United States; dilution 1:100) overnight at 4°C. Dako REAL Envision detection system Peroxidase/DAB, Rabbit/Mouse, HRP (Agilent Technologies, United States) was used for visualization following the manufacturer's instructions and the sections were afterwards counterstained with hematoxylin.

The level of SFRP4 expression in the healthy brain was determined by using the cerebral cortex of the human brain (Amsbio, Oxfordshire, UK). The level of immunoreactivity in the healthy brain tissue was moderate, and the signal was detected in the cytoplasm. Human ovarian carcinoma tissue that, according to the antibody datasheet, expresses SFRP4 was used as positive control. Negative controls underwent the same procedure with the omission of incubation with primary antibody.

Semiquantitative analysis by IRS score

Tissue sections were examined using Olympus BX52 microscope (Olympus Life Science). In the tumor hot-spot area, 200 cells were counted and the intensity of protein expression was determined using the computer program ImageJ (National Institutes of Health, United States). The assessment of immunopositivity in the membrane, cytoplasm and/or nuclei of tumor cells was based on the determination of the staining IRS score (Immunoreactivity Score). IRS is the number obtained by multiplying the percentage of cells with positive signal (PP, Positive Cells Proportion Score) with the intensity of the signal (SI, Staining Intensity Score). Five different categories of staining power (PP) were determined: (0) no immunopositivity in tumor cells, (1) immunopositivity in 1–25% of tumor cells, (2) immunopositivity in 26–50% of tumor cells, (3) immunopositivity in 51–85% of tumor cells, (4) immunopositivity in >85% of tumor cells. The staining intensity (SI) was assessed into three categories: (1) no/weak immunopositivity-yellowish staining, (2) moderate-brownish staining, (3) strong-dark brown staining. Due to the needs of statistical analysis, IRS values ranging from 0 to 12 were assessed: 1 (IRS = 0–4) no expression or weak expression, 2 (IRS = 5–8) moderate expression and 3 (IRS = 9–12) strong expression.

DNA extraction

The genomic DNA extraction from unfixed frozen tumor tissue was performed according to the protocol by Green and Sambrook (1989). Briefly, approximately 0.5 g of tumor tissue was homogenized with 1 mL extraction buffer (10 mM Tris–HCl, pH 8.0; 0.1 M EDTA, pH 8.0; 0.5% sodium dodecyl sulfate) and incubated with proteinase K (100 µg/mL; Sigma-Aldrich, St. Louis, MO, United States) overnight at 37°C. Organic (phenol–chloroform) extraction and ethanol precipitation followed. The extracted DNA was successfully used for epigenetic (MS-PCR) analysis.

Methylation-specific PCR (MSP)

Isolated DNA was treated with bisulfite using the MethylEdge Bisulfite Conversion System (Promega, Madison, Wisconsin, United States) following the manufacturer's instruction. Bisulfite-treated DNA was afterward used for methylation-specific PCR (MSP). Primer sequences for *SFRP4* promoter region for MSP were synthesized according to Schiefer et al. (2014): methylated primers, F: 5' GGGTGATGTTATCGTTTTTGTATCGAC 3′ and R: 5' CCTCCCCTAACGTAAACTCGAAACG 3′; unmethylated primers, F: GGGGGTGATGTTATTGTTTTTGTATTGAT and R: CACCTCCCCTAACATAAACTCAAAACA 3′. Expected product size for methylated reaction was 111 bp, and for unmethylated reaction 115 bp.

PCRs for bisulfite-treated DNA were performed using TaKaRa EpiTaq HS (TaKaRa Bio, Unites States): 1XEpiTaq PCR Buffer (Mg2+ free), 2.5 mM MgCl2, 0.3 mM dNTPs, 20 pmol of each primer (Sigma-Aldrich, USA), 50 ng of DNA, and 1.5 Units of TaKaRa EpiTaq HS DNA Polymerase in a 25 µL final reaction volume. PCR cycling conditions were as following: initial denaturation at 95°C for 5 min, followed by 35 cycles consisting of three steps: 95°C for 30 s, the respective annealing temperature for 30 s, 72°C for 30 s, followed by a final extension at 72°C for 7 min. For the amplification of methylated *SFRP4* promoter region the annealing temperature was 65°C, while for unmethylated *SFRP4* promoter region was 63°C.

10.3389/fnmol.2024.1398872

TABLE 1 Demographic and clinical data of astrocytoma patients.

Patient no	Grade	Age	Sex	Molecular features
1	2	31	M	IDH1 +, ATRX+
2	2	39	F	IDH1 +,1p19q codeletion positive, ATRX-, p53+
3	2	31	F	IDH1 +, ATRX+, p53+
4	2	36	F	IDH1 +
5	2	32	M	IDH1 +,1p19q codeletion positive, ATRX-, p53+
6	2	49	M	IDH1 +, ATRX+, p53+
7	2	27	M	IDH1 -, ATRX+, p53-
8	2	44	M	IDH1 +, ATRX+, p53+
9	2	56	M	IDH1 +
10	2	38	F	IDH1 +
11	2	48	M	IDH1 +
12	3	35	M	ND
13	3	66	F	IDH1 -, ATRX -, p53+
14	3	24	M	IDH1 -, NOS, p53+
15	3	34	M	IDH1 +, ATRX+, p53+
16	3	29	M	IDH1 +, ATRX-
17	3	51	M	IDH1 -
18	3	34	F	IDH1 +, ATRX+, p53+
19	3	55	F	IDH1 +
20	3	58	M	IDH1+
21	3	46	M	IDH1+
22	4	67	F	ND
23	4	68	M	IDH1 -
24	4	62	M	ND
25	4	77	F	IDH1 -
26	4	61	F	ND
27	4	40	F	IDH1 +
28	4	65	F	IDH1 -
29	4	30	M	IDH1 +
30	4	58	M	IDH1 -
31	4	77	F	P53+
32	4	42	M	IDH1 -, P53+
33	4	54	M	IDH1 -, ATRX-, P53+
34	4	65	F	IDH1 -, 1p19q codeletion negative, ATRX-, p53+
35	4	71	F	IDH1 -, 1p19q codeletion negative, ATRX-, p53+
36	4	83	M	IDH1 +
37	4	68	M	IDH1 -
38	4	55	F	ND
39	4	54	M	IDH1 -, 1p19q codeletion negative, ATRX-, p53+
40	4	39	F	IDH1 -, ATRX+, p53+
41	4	56	M	IDH1 -, 1p19q codeletion negative, ATRX+, p53+
42	4	70	F	ND
43	4	62	M	IDH1 -, p53+
44	4	53	F	IDH1 -
45	4	67	F	IDH1 -, p53+

(Continued)

TABLE 1 (Continued)

Patient no	Grade	Age	Sex	Molecular features
46	4	79	M	IDH1 -
47	4	72	F	IDH1 -
48	4	6	M	IDH1 -
49	4	6	M	IDH1 -
50	4	69	M	ND
51	4	65	F	IDH1 -, p53+

M, male; F, female; IDH1 +, IDH1 mutant; IDH1 -, IDH1 wild-type; ATRX +, strong nuclear postivity; ATRX -, loss of ATRX expression (mutated); p53 +, p53 mutation.

PCR products were separated on 2% agarose gel stained with Syber Safe nucleic acid stain (Invtrogen, Thermo Scientific, United States) and visualized on a UV transilluminator. Methylated Human Control (Promega, Madison, Wisconsin, United States) was used as a positive control for the methylated reaction, while unmethylated DNA EpiTect Control DNA (Qiagen, Hilden, Germany) served as a positive control for the unmethylated reaction. Nuclease-free water was used as a negative control.

Samples that displayed bands in methylated reactions were classified as methylated. In our experiment, all methylated samples also showed parallel unmethylated bands for specific patient denoting unmethylated promoters. However, due to the appearance of methylated promoters, we classified those samples as methylated since amplification of a band is observed in methylated reaction. The presence of both reactions, methylated and unmethylated, can be explained by glioma's intrinsic intra-tumor heterogeneity, so some tumor cells will have unmethylated promoters and others methylated. We should also consider point of time in this process where methylation or unmethylation can happen in specific time frame. The other possibility is that there might be DNA extracted from non-tumor origin from abundance of cells that form tumor mass that may be amplified to show parallel unmethylated bands. We can discuss the band intensities as possible cut-off point for methylation, but we decided to classify binary when band is present in the methylated reaction the promoter was classified as methylated.

Statistical analysis

Methylation status of *SFRP4* gene, data on its protein expression levels were analyzed together with grade, and other clinical and demographic features. Statistical analysis was performed using SPSS v.19.0.1 (SPSS, Chicago, IL, United States) statistical program. The significance level was set at $p < 0.05$.

The normality of the distribution of the obtained data was assessed with the Kolmogorov–Smirnov test. A p-value lower than $p < 0.05$ indicates that the distribution is significantly different from normal. In the case of normal distribution, differences in the values between astrocytoma grades were examined using one-way analysis of variance (ANOVA), and in case of deviation from normality, the Kruskal-Wallis test was used. Differences in values between the two groups were tested with Student's t-test in case of normal distribution, and in case of deviation from normality with Mann–Whitney test. Differences in the frequency of the analyzed features were tested with the Pearson $\chi 2$ test.

Pearson and Spearman's correlations were used to test the relationships between SFRP4 and GSK3β, DKK1, DKK3, LEF1 and β-catenin.

Analysis of public database cBioPortal and LOVD

In order to test the compatibility of our results we investigated data from publicly available databases. Genetic changes reported on *SFRP4* gene were assessed from cBioPortal (https://www.cbioportal.org/, accessed on 29th February 2024) (Cerami et al., 2012), COSMIC[1] and LOVD (Leiden Open Variation Database, https://databases.lovd.nl/shared/gene), a publicly available databases for tumor genomics and transcriptomics. The *in silico* analysis was performed on the combined study encompassing 3,735 samples. The analysis queried following studies: Brain Lower Grade Glioma (TCGA, Firehose Legacy); Diffuse Glioma (GLASS Consortium); Diffuse Glioma (GLASS Consortium, Nature 2019); Diffuse Glioma (MSK, Clin Cancer Res 2024); Glioma (MSK, Clin Cancer Res 2019); Glioma (MSK, Nature 2019); Low-Grade Gliomas (UCSF, Science 2014); Brain Tumor PDXs (Mayo Clinic, Clin Cancer Res 2020); Glioblastoma (Columbia, Nat Med. 2019); Glioblastoma Multiforme (TCGA, PanCancer Atlas); Glioblastoma (CPTAC, Cell 2021).

Results

Tumor tissue samples

Analysis of SFRP4 protein expression and *SFRP4* promoter methylation status was performed on a total of 51 patients. Regarding tumor grade, there were 11 samples of diffuse astrocytoma (21.6%), 10 samples of anaplastic astrocytoma (19.6%) and 30 samples of glioblastoma (58.8%). Results of the ANOVA test showed significant differences between patient age and astrocytoma grade ($p = 0.002$). Glioblastomas were found to occur later in life compared to grade 2 ($p = 0.003$) and grade 3 astrocytoma ($p = 0.027$).

1 https://cancer.sanger.ac.uk/cosmic

TABLE 2 SFRP4 protein expression in different astrocytoma grades.

IRS value		SFRP4		
		Grade 2	Grade 3	Grade 4
IRS 0–4	N	4/10	6/10	26/30
	%	40	60	86.7
IRS 6–8	N	4/10	3/10	4/30
	%	40	30	13.3
IRS 9–12	N	2/10	1/10	0/30
	%	20	10	0
In total	N	10	10	30
	%	100	100	100

N, number of samples; %, percentage of samples.

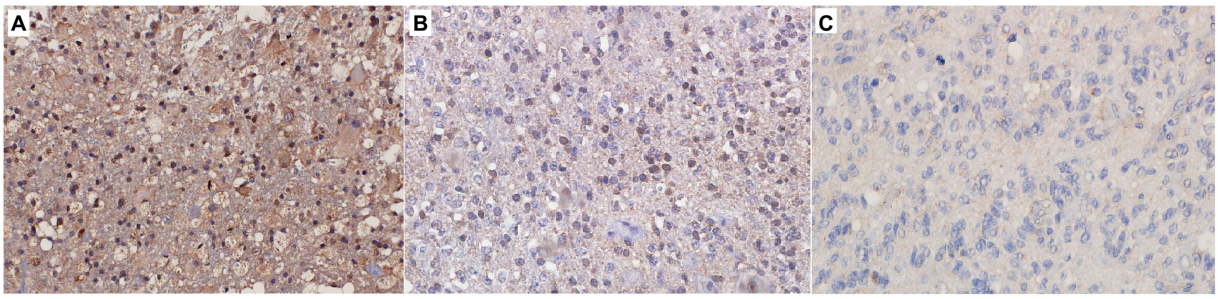

FIGURE 1
Immunohistochemical staining of **(A)** CNS WHO grade 2 astrocytoma, **(B)** CNS WHO grade 3 astrocytoma, **(C)** CNS WHO grade 4 astrocytoma. Figure shows strong **(A)**, moderate **(B)** and weak **(C)** expression of the SFRP4 protein (200x magnification).

SFRP4 protein expression in astrocytoma samples

The levels of SFRP4 protein were generally low in our total sample. SFRP4 expression in a total of 50 astrocytomas of different grades showed low or lack of expression in 72% (36/50), moderate in 22% (11/50) and strong in 6% (3/50) of cases. The Kruscal-Wallis test revealed a significant difference in the expression level of SFRP4 protein regarding tumor grade ($p = 0.008$), and the Spearman test also confirmed a moderate negative correlation between the analyzed variables ($rs = -0.442$, $p = 0.001$). A significantly higher number of samples with moderate and strong expression was present in the group of diffuse astrocytomas (CNS WHO grade 2), while samples with low protein expression predominated in higher astrocytoma grades (CNS WHO grades 3 and 4) ($p = 0.002$). Diffuse astrocytomas showed low or no expression in 40% of samples, moderate in 40%, while 20% of samples had strong expression. In the group of anaplastic astrocytomas, 60% of samples showed low or no expression, 30% had moderate, while 10% showed strong expression. SFRP4 protein expression in glioblastomas was very weak or non-existent in 86.7%, and moderate in 13.3% of samples, while strong expression was not observed in glioblastoma (Table 2; Figure 1). The signal was localized on the membrane, in the cytoplasm and in the nucleus (Figure 2). All the samples showed immunopositivity in the cytoplasm, 34.7% of samples has signal also in the nucleus and membrane in addition to the cytoplasm and 14.3% of samples has signal in the cytoplasm and membrane but not in the nucleus. However, we did not observe that localization of *SFRP4* was associated with an aggressive phenotype or survival. We also checked if *SFRP4* localization had any association with all other investigated variables but could not establish such connection (Table 3).

Methylation status of the *SFRP4* gene promoter

Promoter methylation of the *SFRP4* gene in astrocytoma samples was examined by the MS-PCR. The detected product was between 100 and 150 bp long. The MS-PCR reaction was considered optimized when the methylated control sample gave the product of the desired size only in the methylated reaction of the methylated control while the unmethylated control sample gave product in the unmethylated reaction of the unmethylated control. Nuclease-free water was used as a negative control and the absence of product formation in it was evidence that no contamination was present. In case the product was formed only in the unmethylated reaction, the sample was considered unmethylated. In case the product was formed in both, the methylated and the unmethylated reaction, the sample was considered methylated. Results of the reaction for each sample are shown in Figure 3.

Analysis of 49 astrocytoma samples showed that 16.3% (8/49) of cases had a methylated *SFRP4* promoter while 83.7% (41/49) had an unmethylated one (Figure 4). DNA promoter methylation

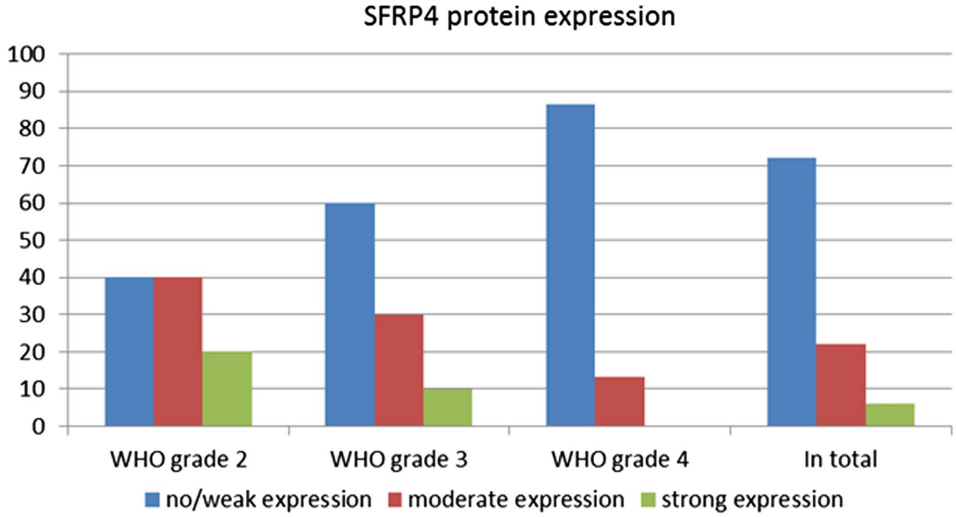

FIGURE 2
SFRP4 protein expression between different astrocytoma grades.

TABLE 3 Promoter methylation status, expression levels and localizations of Secreted Frizzled Related Protein 4 (SFRP4) protein in astrocytoma samples and patients' survival.

Patient no	*SFRP4* methylation	*SFRP4* expression	Localization	Survival (months)
1	U	2	C	103
2	M	2	C+M+N	61
3	M	1	C	71
4	U	1	C+M+N	105
5	U	1	C	129
6	M	3	C+M+N	42
7	M	3	C+M+N	20
8	M	ND	ND	79
9	M	2	C+M	ND
10	M	1	C+M+N	ND
11	M	2	C+M	ND
12	U	1	C	ND
13	ND	1	C+M+N	4
14	U	2	C+M+N	83
15	U	1	C+M+N	55
16	U	1	C+M+N	100
17	U	2	C+M+N	14
18	U	1	C	ND
19	U	2	C	ND
20	U	3	C+M	ND
21	U	1	C+M+N	ND
22	U	1	C+M	7
23	U	1	C	10
24	U	2	C	18
25	U	1	C+M+N	26
26	U	1	0	10

(Continued)

TABLE 3 (Continued)

Patient no	*SFRP4* methylation	*SFRP4* expression	Localization	Survival (months)
27	U	1	C	25
28	U	1	C	47
29	U	1	0	81
30	U	1	C	11
31	U	1	C	ND
32	U	1	C	48
33	U	1	C	19
34	U	1	C + M	5
35	U	2	C + M	13
36	U	1	C	33
37	U	1	C + M + N	6
38	U	2	C + M + N	97
39	U	1	C	10
40	U	1	C + M + N	41
41	U	1	C	25
42	U	1	C	ND
43	U	1	C	36
44	U	1	C + M	5
45	ND	1	C + M + N	ND
46	U	1	C	3
47	U	2	C	3
48	U	1	C	ND
49	U	1	C + N	10
50	U	1	C + M + N	8
51	U	1	C	14

M, methylated; U, unmethylated; 1, weak or lack of expression; 2, moderate expression; 3, strong expression; C, cytoplasmic; M, membranous; N, nuclear; ND, not determined.

of *SFRP4* was exclusively observed in diffuse astrocytoma (8/11 cases, 72.7%), while all anaplastic astrocytomas and glioblastomas samples were unmethylated (Figure 5). Pearson's $\chi 2$ - test showed statistically significant differences in methylation status of the *SFRP4* gene between astrocytoma malignancy grades ($p < 0.001$). *Post-hoc* analysis revealed that the promoter region of *SFRP4* gene in diffuse astrocytomas was significantly more frequently methylated than in glioblastomas ($p < 0.001$), consistently glioblastomas had a significantly higher number of unmethylated promoters compared to diffuse astrocytomas ($p < 0.001$). Kruskal - Wallis test also confirmed significant differences in the methylation pattern within different astrocytoma grades ($\lambda = 22.149$; $p < 0.001$). The Mann–Whitney U test found that diffuse astrocytomas had significantly more methylated samples compared to anaplastic astrocytomas ($p = 0.004$) and glioblastomas ($p < 0.001$).

In addition, student's *t*-test showed a significant connection between the age of tumor occurrence and the methylation of *SFRP4* gene promoters ($p = 0.011$). Younger patients were more likely to have a methylated promoter of the *SFRP4*. The mean age of patients with unmethylated promoters was higher (52.37 years) compared to age of patients with methylated promoters (41.5 years). A significant connection between the age of tumor occurrence and the methylation of SFRP4 gene promoters ($p = 0.011$) could also be influenced by the fact that in diffuse astrocytomas the age of onset is earlier than for glioblastomas.

Results of the MS-PCR reaction showed the presence of *SFRP4* promoter methylation in the majority of diffuse astrocytoma samples and the absence of methylation in higher astrocytoma grades (Table 3; Figure 5).

The results of the $\chi 2$-test showed that there is a statistically significant connection between *SFRP4* gene methylation and SFRP4 protein expression ($p = 0.007$). Weak expression of the SFRP4 protein was observed in 28.5% of astrocytoma samples with methylated promoters and 78% of unmethylated samples. Moderate and strong SFRP4 expression was present in 71.5% of methylated samples and 22% of unmethylated samples (Figure 6). Furthermore, our results show that the expression levels of SFRP4 are strongly correlated with methylation of the *SFRP4* gene (Pearson's $R = -0.413$; $p = 0.003$). In the sense that, when the gene was methylated, protein levels were high, and when the expression was low or missing the gene was unmethylated. This behavior is contrary to the expected and indicates

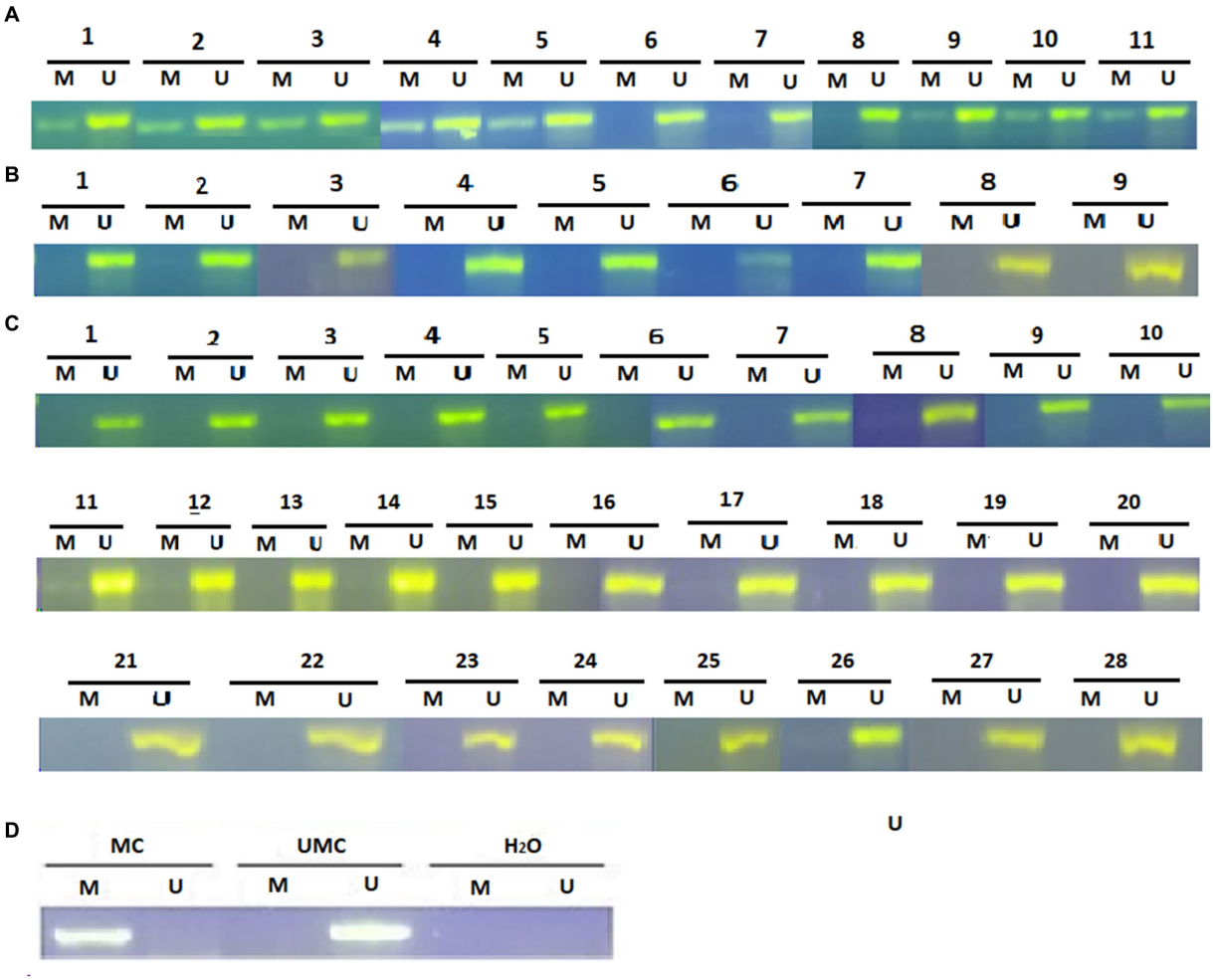

FIGURE 3
Methylation-specific PCR (MSP) analysis for *SFRP4* gene promoter in astrocytic brain tumors **(A)** grade 2, **(B)** grade 3 and **(C)** grade 4. The presence of a visible PCR product in lanes marked U indicates the presence of unmethylated promoters; the presence of a product in lanes marked M indicates the presence of methylated promoters. **(D)** Methylated human control (MC) was used as positive control for methylated reaction, unmethylated human control (UMC) was used as positive control for unmethylated reaction, and water served as negative control. M, methylated reaction; UM, unmethylated reaction.

another mechanism besides methylation that turns off gene expression in higher grades.

Survival analysis revealed no significant impact of *SFRP4* promoter methylation nor SFRP4 protein expression on patients' outcome.

The correlations of SFRP4's effect on GSK3β, DKK1, DKK3, LEF1 and β-catenin

We tested several players of Wnt signaling, namely GSK3β, DKK1, DKK3, LEF1 and β-catenin. We established a positive correlation between methylations of *SFRP4* and *GSK3β*. In samples where *SFRP4* was methylated, the same was observed for *GSK3β* (Pearson's $R = 0.323$; $p = 0.03$). Additionally, when SFRP4 protein is expressed then *DKK3* gene was unmethylated (Chi square = 7.254; $p = 0.027$). Wnt signaling antagonist is associated to negative regulator's demethylation. Correlations between SFRP4 and SFRP1, LEF1, DKK1, and β-catenin were not detected.

SFRP4 alterations from cBioPortal, COSMIC and LOVD

The variants listed in cBioPortal and LOVD were rather scarce and can be viewed at the following URLs: https://www.cbioportal.org/results/mutations?cancer_study_list=lgg_tcga%2Cdifg_glass%2Cdifg_glass_2019%2Cdifg_msk_2023%2Cglioma_mskcc_2019%2Cglioma_msk_2018%2Clgg_ucsf_2014%2Cgbm_mayo_pdx_sarkaria_2019%2Cgbm_columbia_2019%2Cgbm_tcga_pan_can_atlas_2018%2Cgbm_cptac_2021&Z_SCORE_THRESHOLD=2.0&RPPA_SCORE_THRESHOLD=2.0&profileFilter=mutations%2Cstructural_variants%2Cgistic%2Ccna&case_set_id=all&gene_list=SFRP4&geneset_list=%20&tab_index=tab_visualize&Action=Submit; https://databases.lovd.nl/shared/users/03344, respectively. cBioPortal reports only two mutations in TCGA Pancancer Atlas: mutations S242F and C97S. Both mutations were found in glioblastoma and represent missense which are of unknown significance. For C97S PolyPhen, CADD, REVEL, MetaLR all predict to be likely deleterious. On the other hand, cBioPortal also reports on amplification of this gene

(Figure 7). The percentage of changes in relation to other Wnt signaling components is shown in Figure 8. COSMIC reports on 6 coding regions mutations of SFRP4 in glioblastoma and one in anaplastic astrocytoma of which 5 are missense and two are silent ones and can be viewed on https://cancer.sanger.ac.uk/cosmic/gene/samples?all_data=&coords=AA%3AAA&dr=&end=347&gd=&id=373763&ln=SFRP4&seqlen=347&sn=central_nervous_system&src=gene&start=1#complete. The following mutations were reported: c.767 T > G, p.I256S, COSM9220797; c.737C > T, p.P246L, COSM9199206; c.677C > T, p.S226F, COSM9199207; c.532 T > C, p.C178R, COSM9199208; c.290G > C, p.C97S, COSM7481169; c.258C > T, p.T86=, COSM8264978; c.243C > T, p.Y81=, COSM8259479.

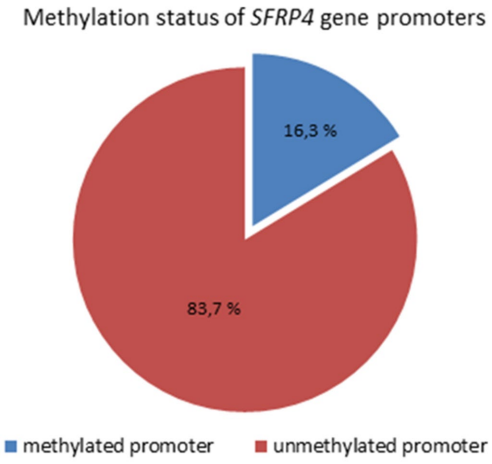

FIGURE 4
Methylation status of SFRP4 gene promoters in total astrocytoma samples of different grades.

We also checked cBioPortal for survival and it demonstrated that patients with changed *SFRP4* had shorter survival than those without gene alterations.

Discussion

Patterns of DNA methylation are changed in human malignant tumors. These pervasive changes encompass global hypomethylation of tumor genome but also the focal hypermethylation of numerous 5′-cytosine-phosphate-guanine-3′ (CpG) islands. The majority of CpG islands reside within or in close proximity to gene promoters. Their hypermethylation represents one of the mechanisms for gene silencing, which predisposes cells to malignant transformation (Bovolenta et al., 2008; Pawar and Rao, 2018). However, it has been challenging to associate specific DNA methylation changes in a cause-and-effect relationship for every step of tumorigenesis.

Functionally, Wnt antagonists can be divided into two classes. The first class binds the Wnt ligands and frizzled receptors directly and includes SFRP protein family, Cerberus and WIF-1 (Wnt inhibitory factor-1). The second class binds to LRP5/6 and includes the Dickkopf (DKK) family. In various tumors including gliomas, SFRP genes have been shown to be transcriptionally silenced by hypermethylation of the promoter region. Furthermore, SFRP proteins showed the ability to sensitize glioma cells to chemotherapeutic agents, cisplatin and doxorubicin, lower their proliferation rate, and induce apoptosis (Warrier et al., 2013). SFRP4 is a member of Wnt inhibitors that binds directly to Wnt and antagonizes Wnt pathways. Antiproliferative and proapoptotic roles for SFRP4 have been demonstrated during normal homeostasis in tissues such as ovary, corpus luteum, placenta, and mammary gland. Silencing of *SFRP4* gene in pathological states results in the activation of Wnt signaling which in addition to promoting tumor evolution also leads to the inhibition of apoptosis of tumor cells. Multiple different carcinoma cell lines that were transfected with recombinant SFRP4 demonstrated increased sensitivity to

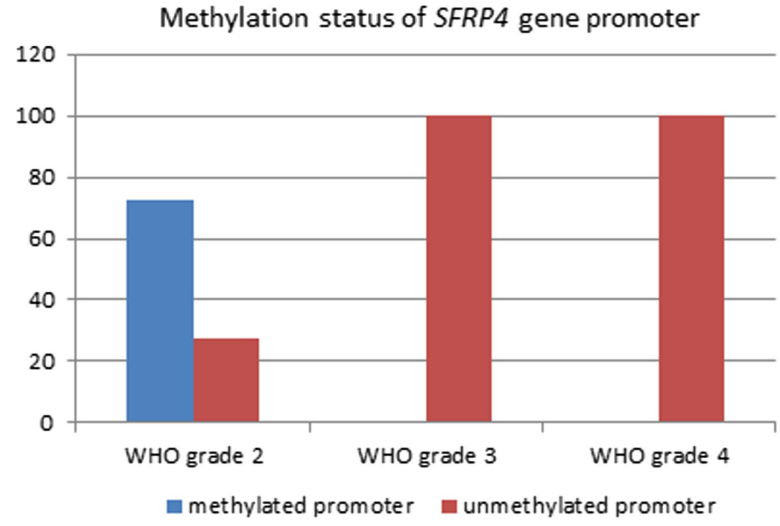

FIGURE 5
Percentage of SFRP4 promoter methylation across different astrocytoma grades.

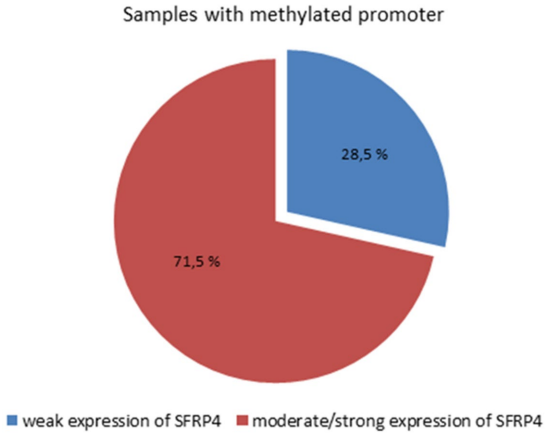

FIGURE 6
Connection between SFRP4 promoter methylation and protein expression.

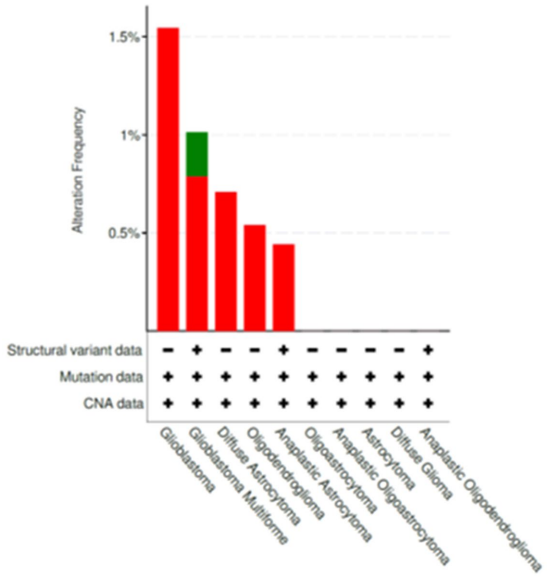

FIGURE 7
Changes publicly reported for SFRP4 gene from cBioPortal database (https://www.cbioportal.org/). Alterations that were listed for SFRP4 included amplifications and mutations.

chemotherapeutics, decreased aggressiveness and invasiveness (Warrier et al., 2013).

Our study demonstrated that the protein levels of this Wnt antagonist were generally low with only 6% of our total astrocytoma sample showing strong expression of SFRP4 protein. Low SFRP4 expression predominated in higher astrocytoma grades (3 and 4) ($p = 0.002$) where 60% of grade 3 astrocytomas and 86.7% of glioblastomas showed weak or lack of expression. In the group of diffuse astrocytomas (grade 2) a significantly higher number of cases with moderate and strong expression was observed, 40% with moderate and 20% with strong expression. A significant difference between expression levels of SFRP4 protein regarding tumor grade ($p = 0.008$) was established. The increase in astrocytoma grade leads to a decrease in SFRP4 protein expression suggesting that SFRP4 acts as a tumor suppressor and inhibits the activity of the Wnt signaling. Similarly, Hrzenjak et al. (2004) showed a reduced expression of SFRP4 protein in more aggressive forms of endometrial sarcomas compared to lower-grades. The association of loss or reduced expression of SFRP4 protein with tumor progression has been documented in esophageal adenocarcinoma (Zou et al., 2005), pancreatic cancer (Bu et al., 2008), mesothelioma (He et al., 2005) and pituitary adenoma (Wu et al., 2015). These findings are in accordance with the results of our research. Conversely, there are other studies that have yielded controversial results on positive correlation between SFRP4 protein expression and tumor malignancy (Abu-Jawdeh et al., 1999; Mii and Taira, 2011; Xavier et al., 2014). Liang et al. (2019) which showed that nuclear SFRP3 and SFRP4 enhance the recruitment of β-catenin to the transcription factor TCF4, promoting transcriptional activity which also contributes to the tumor stemness. This result points on SFRP4 potential pro-oncogenic effect in some tumors which supports the claim on its dual role in tumorigenesis.

High frequency of DNA methylation at the CpG islands of the promoter regions of tumor suppressor genes is a common feature in human tumors and may occur at different stages of tumor evolution (Bovolenta et al., 2008; Pawar and Rao, 2018). Our analysis of methylation status of *SFRP4* gene across astrocytoma grades showed that the majority of samples (83.7%) did not have methylated promoter. Interestingly, *SFRP4* promoter methylation was exclusively observed in 72.7% of grade 2 astrocytoma, while in higher tumor grades methylated promoters were not detected. Statistical analysis revealed significant differences in the methylation status of the *SFRP4* gene between malignancy grades ($p < 0.001$). Astrocytomas grade 2 were significantly more methylated compared to astrocytomas grade 3 ($p = 0.004$) and glioblastomas ($p < 0.001$). All samples in which methylated promoters were detected, also showed bands denoting unmethylated promoters. Possible explanation of our result on methylation that is confined only to lower grade 2 is that in higher astrocytoma grades demethylation processes may occur. It is necessary to keep in mind that astocytomas harbor great heterogeneity and the tumor can consist of heterogeneous cells - some harboring methylated and some unmethylated promoters of *SFRP4* gene. It is possible that astrocytoma samples which did not show SFRP4 promoter methylation are regulated by alternative epigenetic regulatory events. Downregulation of sFRP4 expression in breast, prostate, and ovary cancer stem cells can be attributed to aberrant promoter hypermethylation together with histone modification (Deshmukh et al., 2019). Furthermore, Belur Nagaraj et al. (2021) identified miR-181a as activator of Wnt/β-catenin signaling that drives stemness and chemoresistance in ovarian cancer via the inhibition of SFRP4. MicroRNA-96-5p facilitated the viability, migration, and invasion of cervical cancer cells by silencing SFRP4 (Zhang et al., 2020).

Novel findings report that specific types of tumors, such as low-grade gliomas, are characterized by a so-called CpG island methylator phenotype (CIMP) which could explain our results. CIMP phenotype is characterized by few thousand CpG islands that are methylated simultaneously in an individual cancer sample (Pfeifer, 2018; Malta et al., 2024) and need not to be confined to promoter region. We can speculate that methylation of *SFRP4* confined only to

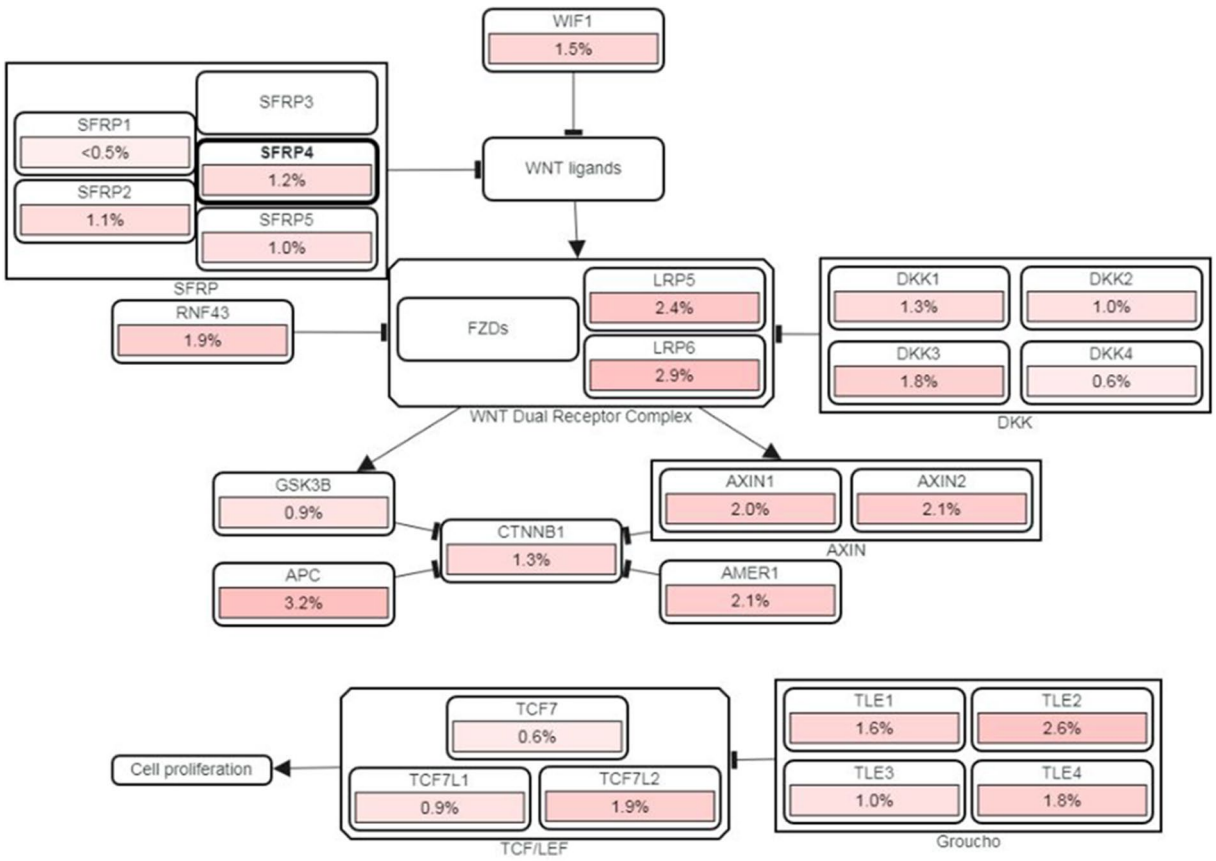

FIGURE 8
cBioPortal's PathwayMapper graph showing percentage of changes of SFRP4 (circled bold) and of other components of Wnt signaling. The intensity of pink shades corresponds to a higher percentage of alteration.

grade 2 astrocytomas may act as "driver methylation" that initially inactivates relevant suppressor gene (Pfeifer, 2018). CpG sites are dispersed throughout the genome and are usually methylated, called CpG islands (CGIs). CGIs located at promoter regions are generally unmethylated. Methylomes contain parts of DNA containing frequent CpG sites, CGIs usually overlap gene promoters and are located at the 5′ end of genes. However, they can be located in gene bodies and in other regions, too. So, we have CpG shores (2 kb regions flanking CGIs), CpG shelves (>2 kb regions flanking CpG shores), and also open sea regions (>4 kb to the nearest CGIs). It is obvious that methylomes are versatile in physiological circumstances. In cancer, DNA methylation becomes aberrant mostly by focally hypermethylating promoters of genes but also gene bodies (Pfeifer, 2018; Malta et al., 2024).

Several different studies reported hypermethylation of the *SFRP4* gene promoter and decreased expression of the SFRP4 protein in tumors of the endometrium, cervix, bladder, pancreas, kidney, esophagus, pituitary gland, and mesothelioma (Pohl et al., 2015). Meta-analysis by Yu et al. (2019) revealed an increased risk of colorectal, ovarian, cervical and kidney cancers associated with methylation of the *SFRP4* promoter, while no such risk was found for endometrial and stomach cancers. Nevertheless, a large heterogeneity within the groups was observed in this meta-analysis. Investigations on four different human glioblastoma cell lines by Schiefer et al. (2014) showed that *SFRP4* gene silencing induced by promoter methylation is one of the glioblastoma features. The four remaining SFRPs were also hypermethylated in all four glioblastoma cell lines. This is contrary to our results on 16.3% of methylated promoters confined only to the lower grade.

In our cohort of astrocytomas, glioblastomas were found to occur later in life compared to grade 2 ($p = 0.003$) and grade 3 cases ($p = 0.027$). It has been shown previously that epigenetic changes and mutation frequencies are distinct between primary and secondary glioblastomas (Barthel et al., 2018). GBM have traditionally been divided into primary (accounting for 90% of cases and arising *de novo*) and secondary (accounting for 10% of cases and developing from a pre-existing lower grade tumor) (Ohgaki and Kleihues, 2013). These historical terms now correlate closely to IDH-mutation status: primary or *de novo* GBMs are classified as IDH-wildtype GBMs. In contrast, IDH-mutant GBMs are defined as secondary GBMs and are currently included in astrocytoma WHO CNS grade 4 (Ohgaki and Kleihues, 2013; Louis et al., 2016). We have also demonstrated here that *SFRP4* promoter methylation was more frequent in younger patients ($p = 0.011$). One possible explanation is that CNS grade 2 and grade 3 astrocytomas coincide to younger age. Also, it has been demonstrated that the process of ageing contributes to the general loss of methyl groups (Unnikrishnan et al., 2019). Foltz et al. (2010) indicated that posttranslational modifications of histones are responsible for the modulation of Wnt pathway antagonists. Götze et al. (2010) investigated 70 astrocytic gliomas for promoter

hypermethylation of different Wnt pathway inhibitor genes including *SFRP4*. Results revealed that hypermethylation of *SFRP4* was rare in gliomas, in only 6% of tumors. The cutting-edge research proposes that DNA methylation profiling is indispensable for identification of specific tumor types (Malta et al., 2024). DNA methylation profiling continues to identify numerous tumor types with specific methylation patterns that have characteristic genetic alterations and clinical behavior. Glioma epigenome remains incompletely characterized especially its effect on progression and recurrence. Molecular changes at other levels and other genes in concert with epigenetics, especially methylation, are also not adequately characterized. Therefore, unique DNA methylation profiles could be very helpful in diagnosis of specific subtypes of diffuse gliomas. Glioma Longitudinal AnalySiS (GLASS) international consortium (Malta et al., 2024), analyzed an epigenetic cohort of glioma patients with matched initial and first recurrent tumors and showed that IDHwt gliomas have lower DNA methylation levels with aggressive cases having the lowest genome-wide levels of DNA methylation. Even within IDH-mutant gliomas, a subset of cases presented with a lower degree of DNA methylation had poorer outcome, while highly methylated ones had better prognosis (Malta et al., 2024).

Our finding on significant connection between *SFRP4* gene methylation and its protein expression ($p = 0.007$) backed up with strong negative correlation (Pearson's $R = -0.413$; $p = 0.003$) can be interpreted that when the gene was methylated, protein levels were high, and in turn when the levels were low or missing, the gene was unmethylated. This behavior is contrary to the expected and suggests that the expression of *SFRP4* gene in higher grades has been regulated by alternative mechanisms. It is possible that *SFRP4* is targeted by genetic alterations as it has been described for *SFRP1* in colon cancers. Other possible epigenetic mechanisms may also be involved. An equally important mechanism to silence genes, besides DNA methylation, are genetic alterations. Although our study did not examine alternative mechanisms of *SFRP4* silencing our search through the public databases revealed four missense mutations found in glioblastoma and one in anaplastic astrocytoma. Several mutations of SFRP4 gene are reported as part of Pyle disease etiology and altogether 105 mutations can be found in different cancers,[2] interestingly the ones that have been characterized as pathogenic all result in frameshift or nonsense indicating that the protein is lost. It is important to stress that the mutational profile availability was not very frequently reported. There are only few reported mutations of SFRP4 gene throughout the analyzed databases, cBioPortal, COSMIC and LOVD. A study by Liu et al. (2006) suggests that silencing of SFRPs by CpG island methylation is involved in chronic lymphocytic leukemia (CLL) as one possible mechanism contributing to aberrant activation of Wnt pathway. Marked differences in the levels of aberrant DNA methylation between *SFRP* genes was found, namely, *SFRP1* was methylated in 100% of cases, *SFRP2* in 55%, *SFRP4* in 30%, and *SFRP5* in 15%, suggesting that epigenetic silencing of these SFRPs and especially *SFRP1* could be important in the onset of CLL. However, *SFRP2* and *SFRP4* were also frequently silenced in CLL, although not through CpG island methylation. SFRP4 was downregulated or silenced in 9.1% of colorectal adenomas relative to the normal mucosa. The downregulation of SFRP 2, 4 and 5 was more frequent in colon carcinoma than in adenoma. However, the methylation and downregulation of SFRP4 were less common than SFRP1, 2 and 5 genes in colorectal tumor, though they were both high in mesothelioma and esophageal adenocarcinoma (Qi et al., 2006). Wallner et al. (2006) also showed that the frequency of methylated *SFRP4* gene in serum DNA of the metastasized colon cancer increased when compared to local disease.

Collective results of our previous work have shown that glioma proliferation and invasion are fueled by Wnt signaling activation (Pećina-Šlaus et al., 2014; Kafka et al., 2019). We have found that promoters of selected genes displayed different methylation frequencies (Pećina-Šlaus et al., 2011; Kafka et al., 2017, 2021). *DKK3* and *DKK1* displayed the highest methylation frequencies 43% and 38%, respectively. *SFRP1* followed with 32%, while *GSK3β* promoters were less methylated, in 18% of samples (Kafka et al., 2018). GSK3β (glycogen synthase kinase 3) is a key enzyme in Wnt signaling. Dickkopfs (DKK) act as inhibitors of the WNT pathway by binding to low-density lipoprotein receptor-related proteins (LRP) 5/6 and Kremen. DKK3 is omnipresent in normal human tissues, including the brain; however, it is significantly depleted in various cancer cell types. Additionally, we have demonstrated that the number of samples with hypermethylated promoter of *SFRP1* gene increased in glioblastomas (grade 4, $p = 0.042$) compared to lower grades, which is contrary to the present situation with *SFRP4*. Also contrary to the result of the present study, is the behavior of SFRP1. Samples with methylated promoter expressed significantly less protein than unmethylated ones ($p = 0.031$). Therefore, in the present investigation we decided to correlate SFRP4's effect with the findings on GSK3β, DKK1, DKK3, LEF1 and β-catenin. A positive correlation between methylations of *SFRP4* and *GSK3β* genes was shown. In samples where *SFRP4* was methylated, the same was observed for *GSK3β* gene (Pearson's $R = 0.323$; $p = 0.03$). Another positive correlation was observed between SFRP4 expression and *DKK3* methylation. When SFRP4 is expressed then *DKK3* gene was unmethylated (Chi square = 7.254; $p = 0.027$) indicating that Wnt signaling antagonist is associated to negative regulator's demethylation.

And finally, it is important to mention glioma stem cells (GSCs) and Wnt antagonists. A previous study reported that Wnt antagonists are epigenetically silenced in glioblastoma. Furthermore, it has been reported that the SFRP4 reduces the stemness of glioblastoma by its netrin-like domain. The authors hypothesized that the Wnt pathway could be important in maintaining glioma stemness (Schiefer et al., 2014). This suggests that SFRP4 may have destructive effect on GSCs and holds potential as epigenetic-based therapy with demethylation agents.

Wnt signaling is being extensively investigated together with therapeutic strategies to target pathway components. SFRP4 is an interesting molecular factor in the occurrence and development of astrocytomas. Reduced expression or silencing of *SFRP4* gene results in overactivation of Wnt pathway. The results of present investigation show reduced expression of SFRP4 in glioblastomas compared to lower grade diffuse gliomas, indicating its tumor suppressor character. SFRP family members were originally considered inhibitors of Wnt signaling, however, it has been reported that SFRP4 has the least homology with other family members. Our results may suggest that the Wnt signaling is regulated by different SFRP molecules in different

2 https://www.ncbi.nlm.nih.gov/clinvar

context. Additional research is indicated to determine the mechanism, genetic or epigenetic, that is behind SFRP4 lowered expression in higher astrocytoma grades. The limitation of this study is relatively small number of samples and the inability to reveal the whole methylation pattern of this gene. However, the study contributes to the recognition of the significance of epigenetic changes in diffuse glioma indicating that restoring SFRP4 protein holds potential as therapeutic avenue.

Data availability statement

The original contributions presented in the study are included in the article/supplementary material, further inquiries can be directed to the corresponding author.

Ethics statement

The studies involving humans were approved by Ethical Committees, School of Medicine University of Zagreb (Case number: 380-59-10106-14-55/147; Class: 641-01/14-02/01) and University Hospital Center "Zagreb" (number 02/21/JG, class: 8.1.-14/54-2). The studies were conducted in accordance with the local legislation and institutional requirements. The participants provided their written informed consent to participate in this study.

Author contributions

AK: Conceptualization, Data curation, Formal analysis, Investigation, Methodology, Supervision, Validation, Writing – original draft. NP-Š: Conceptualization, Data curation, Formal analysis, Funding acquisition, Investigation, Project administration, Resources, Supervision, Writing – original draft. DD: Investigation, Methodology, Writing – original draft. AB: Formal analysis, Methodology, Validation, Writing – review & editing. NN: Data curation, Formal analysis, Validation, Writing – review & editing. KŽ: Data curation, Formal analysis, Validation, Writing – review & editing. AJ: Data curation, Formal analysis, Validation, Writing – review & editing.

Funding

The author(s) declare that financial support was received for the research, authorship, and/or publication of this article. Scientific Centre of Excellence for Basic, Clinical and Translational Neuroscience (project "Experimental and clinical research of hypoxic-ischemic damage in perinatal and adult brain"; GA KK01.1.1.01.0007 funded by the European Union through the European Regional Development Fund. University of Zagreb Science Fund project Number: 10106-23-2393. Association of methylation status of MGMT transferase with malfunction of MMR post-replication repair in human glioblastoma).

Conflict of interest

The authors declare that the research was conducted in the absence of any commercial or financial relationships that could be construed as a potential conflict of interest.

Publisher's note

All claims expressed in this article are solely those of the authors and do not necessarily represent those of their affiliated organizations, or those of the publisher, the editors and the reviewers. Any product that may be evaluated in this article, or claim that may be made by its manufacturer, is not guaranteed or endorsed by the publisher.

References

Abu-Jawdeh, G., Comella, N., Tomita, Y., Brown, L. F., Tognazzi, K., Sokol, S. Y., et al. (1999). Differential expression of frpHE: a novel human stromal protein of the secreted frizzled gene family, during the endometrial cycle and malignancy. *Lab. Investig.* 79, 439–447

Barthel, L., Hadamitzky, M., Dammann, P., Schedlowski, M., Sure, U., Thakur, B. K., et al. (2022). Glioma: molecular signature and crossroads with tumor microenvironment. *Cancer Metastasis Rev.* 41, 53–75. doi: 10.1007/s10555-021-09997-9

Barthel, F. P., Wesseling, P., and Verhaak, R. G. W. (2018). Reconstructing the molecular life history of gliomas. *Acta Neuropathol.* 135, 649–670. doi: 10.1007/s00401-018-1842-y

Belur Nagaraj, A., Knarr, M., Sekhar, S., Connor, R. S., Joseph, P., Kovalenko, O., et al. (2021). The miR-181a-SFRP4 Axis regulates Wnt activation to drive Stemness and platinum resistance in ovarian Cancer. *Cancer Res.* 81, 2044–2055. doi: 10.1158/0008-5472.CAN-20-2041

Bhuvanalakshmi, G., Gamit, N., Patil, M., Arfuso, F., Sethi, G., Dharmarajan, A., et al. (2018). Stemness, Pluripotentiality, and Wnt antagonism: sFRP4, a Wnt antagonist mediates pluripotency and Stemness in glioblastoma. *Cancers* 11:25. doi: 10.3390/cancers11010025

Bovolenta, P., Esteve, P., Ruiz, J., Cisneros, E., and Lopez-Rios, J. (2008). Beyond Wnt inhibition: new functions of secreted frizzled-related proteins in development and disease. *J. Cell Sci.* 121, 737–746. doi: 10.1242/jcs.026096

Bu, X. M., Zhao, C. H., Zhang, N., Gao, F., Lin, S., and Dai, X. W. (2008). Hypermethylation and aberrant expression of secreted frizzled-related protein genes in pancreatic cancer. *World J. Gastroenterol.* 14, 3421–3424. doi: 10.3748/wjg.14.3421

Cerami, E., Gao, J., Dogrusoz, U., Gross, B. E., Sumer, S. O., Aksoy, B. A., et al. (2012). The cBio cancer genomics portal: an open platform for exploring multidimensional cancer genomics data. *Cancer Discov.* 2, 401–404. doi: 10.1158/2159-8290.CD-12-0095

Deshmukh, A., Arfuso, F., Newsholme, P., and Dharmarajan, A. (2019). Epigenetic demethylation of sFRPs, with emphasis on sFRP4 activation, leading to Wnt signalling suppression and histone modifications in breast, prostate, and ovary cancer stem cells. *Int. J. Biochem. Cell Biol.* 109, 23–32. doi: 10.1016/j.biocel.2019.01.016

Foltz, G., Yoon, J. G., Lee, H., Ma, L., Tian, Q., Hood, L., et al. (2010). Epigenetic regulation of Wnt pathway antagonists in human glioblastoma multiforme. *Genes Cancer* 1, 81–90. doi: 10.1177/1947601909356103

Götze, S., Wolter, M., Reifenberger, G., Müller, O., and Sievers, S. (2010). Frequent promoter hypermethylation of Wnt pathway inhibitor genes in malignant astrocytic gliomas. *Int. J. Cancer* 126, 2584–2593. doi: 10.1002/ijc.24981

Green, M. R., and Sambrook, J. (1989). *Molecular cloning: A laboratory manual. 4th* Edn. Cold Spring Harbor (NY): Cold Spring Harbor Laboratory Press.

Hayat, R., Manzoor, M., and Hussain, A. (2022). Wnt signaling pathway: a comprehensive review. *Cell Biol. Int.* 46, 863–877. doi: 10.1002/cbin.11797

He, B., Lee, A. Y., Dadfarmay, S., You, L., Xu, Z., Reguart, N., et al. (2005). Secreted frizzled-related protein 4 is silenced by hypermethylation and induces apoptosis in beta-catenin-deficient human mesothelioma cells. *Cancer Res.* 65, 743–748. doi: 10.1158/0008-5472.743.65.3

Hrzenjak, A., Tippl, M., Kremser, M. L., Strohmeier, B., Guelly, C., Neumeister, D., et al. (2004). Inverse correlation of secreted frizzled-related protein 4 and beta-catenin expression in endometrial stromal sarcomas. *J. Pathol.* 204, 19–27. doi: 10.1002/path.1616

Kafka, A., Bačić, M., Tomas, D., Žarković, K., Bukovac, A., Njirić, N., et al. (2019). Different behaviour of DVL1, DVL2, DVL3 in astrocytoma malignancy grades and their association to TCF1 and LEF1 upregulation. *J. Cell. Mol. Med.* 23, 641–655. doi: 10.1111/jcmm.13969

Kafka, A., Bukovac, A., Brglez, E., Jarmek, A. M., Poljak, K., Brlek, P., et al. (2021). Methylation patterns of DKK1, DKK3 and GSK3β are accompanied with different expression levels in human astrocytoma. *Cancers* 13:2530. doi: 10.3390/cancers13112530

Kafka, A., Karin-Kujundžić, V., Šerman, L., Bukovac, A., Njirić, N., Jakovčević, A., et al. (2018). Hypermethylation of secreted frizzled related protein 1 gene promoter in different astrocytoma grades. *Croat. Med. J.* 59, 213–223. doi: 10.3325/cmj.2018.59.213

Kafka, A., Tomas, D., Lechpammer, M., Gabud, T., Pažanin, L., and Pećina-Šlaus, N. (2017). Expression levels and localizations of DVL3 and sFRP3 in glioblastoma. *Dis. Markers* 2017, 9253495–9253410. doi: 10.1155/2017/9253495

Liang, C. J., Wang, Z. W., Chang, Y. W., Lee, K. C., Lin, W. H., and Lee, J. L. (2019). SFRPs are biphasic modulators of Wnt-signaling-elicited Cancer stem cell properties beyond extracellular control. *Cell Rep.* 28, 1511–1525.e5. doi: 10.1016/j.celrep.2019.07.023

Liu, T. H., Raval, A., Chen, S. S., Matkovic, J. J., Byrd, J. C., and Plass, C. (2006). CpG island methylation and expression of the secreted frizzled-related protein gene family in chronic lymphocytic leukemia. *Cancer Res.* 66, 653–658. doi: 10.1158/0008-5472.CAN-05-3712

Louis, D. N., Perry, A., Reifenberger, G., von Deimling, A., Figarella-Branger, D., Cavenee, W. K., et al. (2016). The 2016 World Health Organization classification of tumors of the central nervous system: a summary. *Acta Neuropathol.* 131, 803–820. doi: 10.1007/s00401-016-1545-1

Louis, D. N., Perry, A., Wesseling, P., Brat, D. J., Cree, I. A., Figarella-Branger, D., et al. (2021). The 2021 WHO classification of tumors of the central nervous system: a summary. *Neuro Oncol.* 23, 1231–1251. doi: 10.1093/neuonc/noab106

Malta, T. M., Sabedot, T. S., Morosini, N. S., Datta, I., Garofano, L., Vallentgoed, W., et al. (2024). Consortium the GLASS; Verhaak RGW, Iavarone a, Noushmehr H. The epigenetic evolution of glioma is determined by the IDH1 mutation status and treatment regimen. *Cancer Res.* 84, 741–756. doi: 10.1158/0008-5472.CAN-23-2093

Mii, Y., and Taira, M. (2011). Secreted Wnt "inhibitors" are not just inhibitors: regulation of extracellular Wnt by secreted frizzled-related proteins. *Develop. Growth Differ.* 53, 911–923. doi: 10.1111/j.1440-169X.2011.01299.x

Müller, D., and Győrffy, B. (2022). DNA methylation-based diagnostic, prognostic, and predictive biomarkers in colorectal cancer. *Biochim. Biophys. Acta Rev. Cancer* 1877:188722. doi: 10.1016/j.bbcan.2022.188722

Narayanan, A., and Turcan, S. (2020). The magnifying GLASS: longitudinal analysis of adult diffuse gliomas. *Cell* 180, 407–409. doi: 10.1016/j.cell.2020.01.016

Nusse, R., and Clevers, H. (2017). Wnt/β-catenin signaling, disease, and emerging therapeutic modalities. *Cell* 169, 985–999. doi: 10.1016/j.cell.2017.05.016

Ohgaki, H., and Kleihues, P. (2013). The definition of primary and secondary glioblastoma. *Clin. Cancer Res.* 19, 764–772. doi: 10.1158/1078-0432.CCR-12-3002

Park, Y. W., Vollmuth, P., Foltyn-Dumitru, M., Sahm, F., Ahn, S. S., Chang, J. H., et al. (2023). The 2021 WHO classification for gliomas and implications on imaging diagnosis: part 1-key points of the fifth edition and summary of imaging findings on adult-type diffuse gliomas. *J. Magn. Reson. Imaging* 58, 677–689. doi: 10.1002/jmri.28743

Pawar, N. M., and Rao, P. (2018). Secreted frizzled related protein 4 (sFRP4) update: a brief review. *Cell. Signal.* 45, 63–70. doi: 10.1016/j.cellsig.2018.01.019

Pećina-Šlaus, N., Kafka, A., Tomas, D., Marković, L., Okštajner, P. K., Sukser, V., et al. (2014). Wnt signaling transcription factors TCF-1 and LEF-1 are upregulated in malignant astrocytic brain tumors. *Histol. Histopathol.* 29, 1557–1564. doi: 10.14670/HH-29.1557

Pećina-Šlaus, N., Nikuševa Martić, T., Kokotović, T., Kušec, V., Tomas, D., and Hrašćan, R. (2011). AXIN-1 protein expression and localization in glioblastoma. *Coll. Antropol.* 35 Suppl. 1: 101–106.

Pfeifer, G. P. (2018). Defining driver DNA methylation changes in human Cancer. *Int. J. Mol. Sci.* 19:1166. doi: 10.3390/ijms19041166

Pohl, S., Scott, R., Arfuso, F., Perumal, V., and Dharmarajan, A. (2015). Secreted frizzled-related protein 4 and its implications in cancer and apoptosis. *Tumour Biol.* 36, 143–152. doi: 10.1007/s13277-014-2956-z

Qi, J., Zhu, Y. Q., Luo, J., and Tao, W. H. (2006). Hypermethylation and expression regulation of secreted frizzled-related protein genes in colorectal tumor. *World J. Gastroenterol.* 12, 7113–7117. doi: 10.3748/wjg.v12.i44.7113

Ramazi, S., Daddzadi, M., Sahafnejad, Z., and Allahverdi, A. (2023). Epigenetic regulation in lung cancer. *MedComm* 4:e401. doi: 10.1002/mco2.401

Rim, E. Y., Clevers, H., and Nusse, R. (2022). The Wnt pathway: from signaling mechanisms to synthetic modulators. *Annu. Rev. Biochem.* 91, 571–598. doi: 10.1146/annurev-biochem-040320-103615

Schiefer, L., Visweswaran, M., Perumal, V., Arfuso, F., Groth, D., Newsholme, P., et al. (2014). Epigenetic regulation of the secreted frizzled-related protein family in human glioblastoma multiforme. *Cancer Gene Ther.* 21, 297–303. doi: 10.1038/cgt.2014.30

Sun, J., Bonaguidi, M. A., Jun, H., Guo, J. U., Sun, G. J., Will, B., et al. (2015). A septo-temporal molecular gradient of sfrp3 in the dentate gyrus differentially regulates quiescent adult hippocampal neural stem cell activation. *Mol. Brain* 8:52. doi: 10.1186/s13041-015-0143-9

Unnikrishnan, A., Freeman, W. M., Jackson, J., Wren, J. D., Porter, H., and Richardson, A. (2019). The role of DNA methylation in epigenetics of aging. *Pharmacol. Ther.* 195, 172–185. doi: 10.1016/j.pharmthera.2018.11.001

Wallner, M., Herbst, A., Behrens, A., Crispin, A., Stieber, P., Göke, B., et al. (2006). Methylation of serum DNA is an independent prognostic marker in colorectal cancer. *Clin. Cancer Res.* 12, 7347–7352. doi: 10.1158/1078-0432.CCR-06-1264

Warrier, S., Balu, S. K., Kumar, A. P., Millward, M., and Dharmarajan, A. (2013). Wnt antagonist, secreted frizzled-related protein 4 (sFRP4), increases chemotherapeutic response of glioma stem-like cells. *Oncol. Res.* 21, 93–102. doi: 10.3727/096504013X13786659070154

Wu, Y., Bai, J., Li, Z., Wang, F., Cao, L., Liu, C., et al. (2015). Low expression of secreted frizzled-related protein 4 in aggressive pituitary adenoma. *Pituitary* 18, 335–342. doi: 10.1007/s11102-014-0579-4

Xavier, C. P., Melikovaa, M., Chumana, Y., Üren, A., Baljinnyam, B., and Rubin, J. S. (2014). Secreted frizzled-related protein potentiation versus inhibition of Wnt3a/β-catenin signaling. *Cell. Signal.* 26, 94–101. doi: 10.1016/j.cellsig.2013.09.016

Yu, J., Xie, Y., Li, M., Zhou, F., Zhong, Z., Liu, Y., et al. (2019). Association between SFRP promoter hypermethylation and different types of cancer: a systematic review and meta-analysis. *Oncol. Lett.* 18, 3481–3492. doi: 10.3892/ol.2019.10709

Zhang, H., Chen, R., and Shao, J. (2020). MicroRNA-96-5p facilitates the viability, migration, and invasion and suppresses the apoptosis of cervical Cancer cells by negatively modulating SFRP4. *Technol. Cancer Res. Treat.* 19:19. doi: 10.1177/1533033820934132

Zou, H., Molina, J. R., Harrington, J. J., Osborn, N. K., Klatt, K. K., Romero, Y., et al. (2005). Aberrant methylation of secreted frizzled-related protein genes in esophageal adenocarcinoma and Barrett's esophagus. *Int. J. Cancer* 116, 584–591. doi: 10.1002/ijc.21045

frontiers | Frontiers in Pediatrics

TYPE Original Research
PUBLISHED 22 July 2024
DOI 10.3389/fped.2024.1426874

OPEN ACCESS

EDITED BY
Graeme R. Polglase,
Monash University, Australia

REVIEWED BY
Mark Steven Scher,
Case Western Reserve University, United States
Frank Van Bel,
University Medical Center Utrecht, Netherlands

*CORRESPONDENCE
Ruža Grizelj
ruza.grizelj@kbc-zagreb.hr

†These authors have contributed equally to this work and share first authorship

RECEIVED 15 May 2024
ACCEPTED 09 July 2024
PUBLISHED 22 July 2024

CITATION
Ćaleta T, Ryll MJ, Bojanić K, Dessardo NS, Schroeder DR, Sprung J, Weingarten TN, Radoš M, Kostović I and Grizelj R (2024) Regional cerebral oxygen saturation variability and brain injury in preterm infants. Front. Pediatr. 12:1426874. doi: 10.3389/fped.2024.1426874

Regional cerebral oxygen saturation variability and brain injury in preterm infants

Tomislav Ćaleta[1†], Martin J. Ryll[2†], Katarina Bojanić[3], Nada Sindičić Dessardo[1], Darrell R. Schroeder[4], Juraj Sprung[2], Toby N. Weingarten[2], Milan Radoš[5], Ivica Kostović[5] and Ruža Grizelj[1,6*]

[1]Department of Pediatrics, School of Medicine University of Zagreb, University Hospital Centre Zagreb, Zagreb, Croatia, [2]Department of Anesthesiology and Perioperative Medicine, Mayo Clinic College of Medicine and Science, Rochester, MN, United States, [3]Division of Neonatology, Department of Obstetrics and Gynecology, University Hospital Merkur, Zagreb, Croatia, [4]Health Sciences Research, Division of Epidemiology, Mayo Clinic College of Medicine and Science, Rochester, MN, United States, [5]Croatian Institute for Brain Research, School of Medicine University of Zagreb, Zagreb, Croatia, [6]Center for Research on Perinatal Etiopathogenesis of Neurological and Cognitive Diseases, School of Medicine University of Zagreb, Zagreb, Croatia

Objective: To examine whether variation of regional cerebral oxygen saturation ($rScO_2$) within three days after delivery predicts development of brain injury (intraventricular/cerebellar hemorrhage or white matter injury) in preterm infants.
Study design: A prospective study of neonates <32 weeks gestational age with normal cranial ultrasound admitted between 2018 and 2022. All received $rScO_2$ monitoring with near-infrared spectroscopy at admission up to 72 h of life. To assess brain injury a magnetic resonance imaging was performed at term-equivalent age. We assessed the association between $rScO_2$ variability (short-term average real variability, $rScO_{2ARV}$, and standard deviation, $rScO_{2SD}$), mean $rScO_2$ ($rScO_{2MEAN}$), and percentage of time $rScO_2$ spent below 60% ($rScO_{2TIME<60\%}$) during the first 72 h of life and brain injury.
Results: The median [IQR] time from birth to brain imaging was 68 [59-79] days. Of 81 neonates, 49 had some form of brain injury. Compared to neonates without injury, in those with injury $rScO_{2ARV}$ was higher during the first 24 h ($P = 0.026$); $rScO_{2SD}$ was higher at 24 and 72 h ($P = 0.029$ and $P = 0.030$, respectively), $rScO_{2MEAN}$ was lower at 48 h ($P = 0.042$), and $rScO_{2TIME<60\%}$ was longer at 24, 48, and 72 h ($P = 0.050$, $P = 0.041$, and $P = 0.009$, respectively). Similar results were observed in multivariable logistic regression. Although not all results were statistically significant, increased $rScO_2$ variability ($rScO_{2ARV}$ and $rScO_{2SD}$) and lower mean values of rScO2 were associated with increased likelihood of brain injury.
Conclusions: In preterm infants increased aberration of $rScO_2$ in early postdelivery period was associated with an increased likelihood of brain injury diagnosis at term-equivalent age.

KEYWORDS

neonates, preterm infants, magnetic resonance imaging, intraventricular hemorrhage, white matter injury, near-infrared spectroscopy, regional cerebral oxygen saturation

Abbreviations

ARV, average real variability; cUS, cranial ultrasound; GA, gestational age; IQR, interquartile range; IVH, intraventricular hemorrhage; MRI, magnetic resonance imaging; NICU, Neonatal Intensive Care Unit; NIRS, near infrared spectroscopy; $rScO_2$, Regional cerebral oxygen saturation; $rScO_{2ARV}$, $rScO_2$ average real variability; $rScO_{2MEAN}$, Mean $rScO_2$; $rScO_{2SD}$, $rScO_2$ standard deviation; $rScO_{2TIME<60\%}$, percentage of time neonate had $rScO_2$ below 60%; SD, standard deviation; TEA, term-equivalent age; WMI, white matter injury.

1 Introduction

Brain injury in the preterm infant results from the combined developmental and destructive effects on the maturing nervous system due to multisystemic diseases and conditions from prenatal to postnatal life (1). Pre-conceptional maternal toxic stress and pregnancy-related illnesses affecting the maternal-placental-fetal triad can disrupt fetal brain development, contributing to preterm birth and/or increasing risks for peripartum brain injuries (1, 2). Various postnatal injurious triggers such as respiratory insufficiency and hemodynamic instability secondary to severe respiratory disease, recurrent apneic spells, hemodynamically significant ductus arteriosus, late-onset sepsis or conditions such as necrotizing enterocolitis further increase the risk and promote subsequent brain injury (3, 4).

Intracranial hemorrhage and white matter injury (WMI) are frequent pathologies (20%–30%) in preterm infants (5–8). Intraventricular hemorrhage (IVH) usually originates in the subependymal germinal matrix, a richly vascularized collection of neuronal-glial precursor cells in the developing brain (9). The risk of hemorrhage is inversely proportional to gestational age (GA), with most of IVH occurring in infants less than 32 weeks of gestation (10). Factors primarily related to dysregulation of cerebral blood flow and pressure in the microvascular bed of the germinal matrix play a major contributory pathogenic role (9, 11, 12). Most IVH events occur within the first week of delivery, and in the majority (90%) can be detected within the first 72 h of life (13). Cerebellar hemorrhage is also a common form of brain injury in preterm infants. Detection of these injuries by magnetic resonance imaging (MRI) has been reported in up to 37% of infants less than 33 weeks GA (14). WMI represents a spectrum of disease that ranges from focal necrotic lesions deep in the white matter, with or without subsequent cyst formation, to the more common, diffuse, and nondestructive WMI (15). The injury is believed to be induced by cerebral ischemia, infection and/or inflammation (16). Several fundamental physiological factors related to cerebral blood flow, including oxygenation, hypocarbia, levels of glucose and its metabolites, and a variety of inflammatory factors, likely influence the severity of WMI (17).

Considering that prevalent types of brain injury among preterm infants often coincide with hypoxic, ischemic, and reperfusion events in the early postdelivery period, it is of utmost importance to be able to assess adequacy of cerebral blood flow to improve managements designed to mitigate the risk for injury. Near-infrared spectroscopy (NIRS) monitors regional cerebral oxygen saturation ($rScO_2$), provides non-invasive information on hemodynamics, real time brain oxygen delivery (18), and is considered to be a surrogate marker for cerebral blood flow (19–21). NIRS uses multiple wavelengths of near-infrared light and relies on the absorption spectra of oxygenated and deoxygenated hemoglobin to calculate relative concentrations of each, which are then used to calculate $rScO_2$. Since NIRS makes no distinction between brain blood compartments, $rScO_2$ estimates hemoglobin oxygen saturation in a mixed arterial, capillary, and venous compartments (22). The association between $rScO_2$ measurements and development of brain injury is not well explored. In the current study we hypothesize that variability in $rScO_2$ recorded from NIRS in the early postdelivery period may predict brain injury assessed from MRI at term-equivalent age (TEA). We especially focus on short-term average real variability (ARV) of $rScO_2$ during early postdelivery period as a potential culprit for brain injury. This hypothesis was tested on preterm infants by $rScO_2$ monitoring with NIRS for the first 72 h after birth. An improved understanding of the relationship between altered $rScO_2$ and development of brain injury may be used in future management strategies designed to improve neonatal outcomes.

2 Methods

2.1 Settings

This study was conducted in the University Hospital Centre (UHC) and the Croatian Institute for Brain Research, Zagreb, Croatia as a part of a multidisciplinary, longitudinal research project. The UHC is the largest Croatian tertiary referral center for neonatal care and does not have a maternity ward. The hospital admits preterm infants from hospitals that do have maternity wards but do not have the capacity to manage high-risk neonates. Therefore, all neonates in the current study are outborns.

2.2 Patient population, inclusion/exclusion criteria

This is a prospective study of all consecutive newborn admissions to the Neonatal Intensive Care Unit (NICU) at the UHC Zagreb between May 1st, 2018, and June 31st, 2022. The infants were eligible for enrollment if they were less than 32 weeks' GA at birth and had a normal cranial ultrasound (cUS) on admission. Preterm infants with chromosomal or congenital anomalies, and those with delayed transfer (>12 h) from outside institutions were excluded.

2.3 Study design, NIRS monitoring and study aims

Upon NICU admission cUS was performed to exclude the presence of brain injury. All qualified infants (i.e., no brain injury on cUS) received $rScO_2$ monitoring using NIRS immediately on admission for up to 72 h of life. A 72-hour period has been accepted as a suitable time frame for NIRS monitoring in premature infants (23), as majority of IVH in premature infants happens within the first 3 days of life (24). In our study a two wavelength (730 and 810 nm) near-infrared spectrometer (INVOS 5100, Covidien, Mansfeld, MA) was used by firmly attaching a small neonatal sensor (Covidien, Mansfield, MA) on the left side of the infant's forehead. Four $rScO_2$ summary statistics were considered: (1) short-term $rScO_2$ average real variability ($rScO_{2ARV}$) using following equation:

$$rScO_{2AVR} = \frac{1}{N-1}\sum_{k=1}^{N-1}|rScO_{2k+1} - rScO_{2k}|$$

(2) $rScO_2$ standard deviation ($rScO_{2SD}$), (3) $rScO_2$ mean ($rScO_{2MEAN}$), and 4) the percentage of time neonate spent with $rScO_2$<60% ($rScO_{2TIME<60\%}$) all during 72 h after birth. The primary aim was to assess the association between variability of $rScO_2$ ($rScO_{2ARV}$ and $rScO_{2SD}$) and brain injury, and secondary aims were to assess the association between average $rScO_2$, ($rScO_{2MEAN}$) and percentage of time spent at oxygen saturation below 60% ($rScO_{2TIME<60\%}$) and brain injury.

2.4 Data collection

We reviewed obstetric, demographic and neonatal data from the hospital records: sex, GA, birth weight, type of delivery (natural delivery vs. Cesarean section), antenatal corticosteroid treatment, Apgar scores, age at hospital admission, Scores for Neonatal Acute Physiology Perinatal Extension II (SNAPPE-II); variables related to treatment: primary respiratory support, duration of mechanical ventilation, surfactant administration, transfusion of blood and blood products, use of inotropes; and prematurity related complications: pneumothorax, bronchopulmonary dysplasia, necrotizing enterocolitis, infection/sepsis, retinopathy of prematurity.

2.5 Grading of brain injuries

Brain imaging at TEA was done using a 3T MRI scanner (Magnetom, Prisma^{FIT}, Siemens). MRI scanning was performed after regular feeding, infants were wrapped with linen diapers and a blanket. A neuroradiologist blinded to clinical data evaluated the MRI findings. WMI grades considered are: Grade I—punctate lesions; Grade II—small periventricular cysts; Grade III—extensive periventricular cysts; Grade IV—extensive subcortical cysts—also called multicystic encephalomalacia (25–27). IVH was classified according to Papile classification: Grade I—hemorrhage limited to germinal matrix; Grade II—extension into normal-sized ventricles; Grade III—extensive hemorrhage with dilatation of the ventricles; Grade IV—parenchymal involvement (28, 29). Cerebellar hemorrhage was noted as present or absent.

2.6 Statistical analysis

Raw $rScO_2$ NIRS measurements were recorded every 5–15 s. To exclude outliers, we aggregated raw $rScO_2$ data as a mean over 5-minute intervals for the four features of interest. The aggregated $rScO_2$ measurements were analyzed for 24-, 48-, and 72-hour intervals following birth. We examined the association between four $rScO_2$ features (time-weighted $rScO_{2ARV}$, $rScO_{2SD}$, $rScO_{2MEAN}$, and $rScO_{2TIME<60\%}$) and brain injury at TEA. The $rScO_{2ARV}$ was calculated as the average of absolute differences between consecutive $rScO_2$ measurements during the observed time frame using a previously described equation (30, 31). $rScO_{2ARV}$ feature accounts for the order in which the respective $rScO_2$ measurements occurred and corrects for limitations of the commonly used measures of variability such as standard deviation, which accounts only for the dispersion of values around the mean, and not for the order of the respective readings (31). Patients with >50% missing $rScO_2$ values during the predetermined time intervals following admission were assigned a missing value for the respective feature. For calculating the $rScO_{2ARV}$ and $rScO_{2SD}$, the $rScO_2$ ceiling-value of 95% was handled by excluding any of the aggregated 95% measurements, that were flanked on both sides by 95% measurements. For calculating the $rScO_{2MEAN}$ and the $rScO_{2TIME<60\%}$ these 95%-measurements were not excluded.

For univariable analysis, $rScO_2$ features were compared between those with and without brain injury using the two-sample *t*-test or Mann Whitney *U*-test as appropriate. For the multivariable logistic regression analysis, our cohort size allows for two covariates aside from our feature of interest, for which we chose GA and birth weight. Results from the multivariable logistic regression model are summarized as odds ratio and 95% confidence interval for the given $rScO_2$ feature. There was no evidence of significant non-linearity of GA, birth weight, and all $rScO_2$ features, as tested by comparing a univariable linear and a univariable restricted cubic spline model (with knots at the 5th, 50th, and 95th or 15th, 50th, and 95th percentile) via the likelihood ratio test for each variable. A *P*-value <0.05 was determined statistically significant throughout. All statistical analyses were performed with Python v.3.9 (Python Software Foundation, Wilmington, Delaware, USA).

3 Results

3.1 Cohort characteristics

Between May 1st, 2018, and June 31st, 2022, 81 neonates met criteria and were included in the study. The median [IQR] time from birth to initiation of NIRS monitoring was 2.5 [1.4–3.6] hours, and from birth to MRI at TEA 68 [59–79] days. MRI at TEA ruled out the presence of brain injury in 32 neonates, while 49 were diagnosed with single or multiple brain injuries (all were mild, grades I or II): 33 (40.7%) neonates had IVH, 28 (34.6%) had WMI, and 8 (10%) had cerebellar hemorrhage (Figure 1). Table 1 shows neonatal characteristics, overall and according to the presence or absence of brain injury. There were no significant differences in characteristics between infants with and without injury: GA at delivery ($P = 0.555$), Apgar scores at 1 and 5 min ($P = 0.673$ and 0.899, respectively), and main comorbidities (sepsis, $P > 0.99$; need for respiratory support, $P = 0.155$; necrotizing enterocolitis, $P = 0.462$; bronchopulmonary dysplasia, $P = 0.590$; or retinopathy, $P = 0.511$).

3.2 Association of $rScO_2$ features with brain injury at TEA

Of the 81 neonates, 72, 77, and 80 had sufficient $rScO_2$ data (continuous NIRS monitoring for >50% of the timeframe) for the 24-, 48-, and 72-hours after birth, respectively. Compared to neonates without brain injury, $rScO_{2ARV}$ was higher during the first 24 h in those diagnosed with brain injury, $P = 0.026$

10.3389/fped.2024.1426874

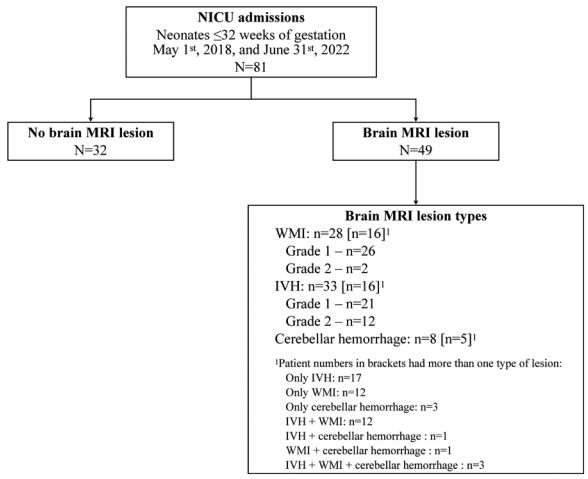

FIGURE 1
Summary of 81 preterm infants according to MRI results at term-equivalent age. IVH, intraventricular hemorrhage; WMI, white matter injury.

(Table 2, Figure 2). Similarly, $rScO_{2SD}$ was higher at 24 and 72 h ($P = 0.029$ and $P = 0.030$, respectively) in those with injury. The $rScO_{2MEAN}$ was lower at 48 h ($P = 0.042$) in those with injury, and the percentage of time neonates spent at $rScO_{2TIME<60\%}$ was higher in those with injury ($P = 0.050$, $P = 0.041$, and $P = 0.009$ at 24-, 48-, and 72-hours, respectively) (Table 2, Supplementary Figure S1). Similar results were observed from logistic regression analysis adjusted for GA and birth weight (Table 2). Although not all results were significant, increased $rScO_2$ variability ($rScO_{2ARV}$, $rScO_{2SD}$) was consistently associated with increased likelihood of brain injury at TEA. Also, lower values of $rScO_2$ ($rScO_{2MEAN}$ and $rScO_{2TIME<60\%}$) were associated with increased likelihood of brain injury (Table 2 and Figure 2).

4 Discussion

The most important findings of this study are that increased variability of regional cerebral oxygen saturation, lower mean saturation, and longer time neonates spent at saturation below 60% in the early postdelivery period were

TABLE 1 Demographic and clinical characteristics of preterm infants in our cohort.

Characteristics	All patients ($N = 81$)	Normal MRI ($n = 32$)	Abnormal MRI ($n = 49$)	P value
Sex (male)	39 (48.1%)	17 (53.1%)	22 (44.9%)	0.619
GA at delivery (weeks)	30.1 [28.6–31.6]	30.9 [29.1–31.6]	30.0 [28.0–31.6]	0.555
Delivery (C-section)	44 (54.3%)	18 (56.2%)	26 (53.1%)	0.957
Birth weight (grams)	1,345 [1,125–1,550]	1,315 [1,129–1,513]	1,355 [1,105–1,560]	0.768
Head circumference (cm)	28.0 [26.5–29.0]	28.0 [26.5–29.0]	27.5 [26.0–29.0]	0.454
Apgar score at 1 min	7.0 [3.0–8.0]	7.0 [3.0–8.0]	7.0 [4.0–8.0]	0.673
Apgar score at 5 min	8.0 [6.0–9.0]	7.5 [5.2–9.0]	8.0 [6.0–9.0]	0.899
SNAPPE II score	23.0 [9.0–38.0]	20.5 [5.0–38.8]	23.0 [13.0–34.0]	0.670
Full steroid course received	17 (21.0%)	6 (18.8%)	11 (22.4%)	0.904
Surfactant administered	43 (53.1%)	15 (46.9%)	28 (57.1%)	0.498
Inotropes during first 3 days	15 (18.5%)	4 (12.5%)	11 (22.4%)	0.382
RBC transfusion	11 (13.6%)	3 (9.4%)	8 (16.3%)	0.513
Sepsis	12 (14.8%)	5 (15.6%)	7 (14.3%)	> 0.99
Pneumothorax	8 (9.9%)	3 (9.4%)	5 (10.2%)	> 0.99
Primary respiratory support				0.155
Invasive ventilation	39 (48.1%)	12 (37.5%)	27 (55.1%)	
nCPAP	40 (49.4%)	19 (59.4%)	21 (42.9%)	
None	2 (2.5%)	1 (3.1%)	1 (2.1%)	
Necrotizing enterocolitis				0.462
No	77 (95.1%)	31 (96.9%)	46 (93.9%)	
1st grade	1 (1.2%)	0 (0%)	1 (2.0%)	
2nd grade	2 (2.5%)	0 (0%)	2 (4.1%)	
3rd grade	1 (1.2%)	1 (3.1%)	0 (0%)	
Bronchopulmonary dysplasia				0.590
No	57 (70.4%)	24 (75.0%)	33 (67.3%)	
Mild	22 (27.2%)	8 (25.0%)	14 (28.6%)	
Moderate	2 (2.5%)	0 (0%)	2 (4.1%)	
Retinopathy of prematurity				0.511
No	55 (67.9%)	25 (78.1%)	30 (61.2%)	
1st stage	5 (6.2%)	1 (3.1%)	4 (8.2%)	
2nd stage	17 (21.0%)	5 (15.6%)	12 (24.5%)	
3rd stage	4 (4.9%)	1 (3.1%)	3 (6.1%)	

Continuous variables are presented as median [IQR] and were compared by independent *t*-test or Mann-Whitney *U*-test (depending on whether they were normally distributed). Binary variables are presented as count (percentage) and were compared via Chi-Square or Fisher's Exact test, as appropriate. GA, gestational age; SNAPPE II, Score for Neonatal Acute Physiology with Perinatal Extension-II; nCPAP, nasal continuous positive airway pressure; RBC, red blood cells.

TABLE 2 Comparison of four $rScO_2$ features during the first 72 h of life in infants with and without brain injury as seen on magnetic resonance imaging at term-equivalent age.

$rScO_2$ features	Hours[a]	All infants[b] ($N = 81$)	Normal MRI[b] ($n = 32$)	Abnormal MRI[b] ($n = 49$)	P[c]	ORs [95% CI][d]	P[d]
$rScO_{2ARV}$	24	1.9 [1.7–2.3]	1.8 [1.6–2.0]	2.1 [1.7–2.6]	**0.026**	**3.1 [1.09–8.84]**	**0.034**
	48	2.0 [1.7–2.3]	2.0 [1.6–2.2]	2.0 [1.7–2.3]	0.411	1.69 [0.59–4.86]	0.328
	72	1.9 [1.7–2.3]	1.9 [1.7–2.2]	1.9 [1.8–2.3]	0.364	1.79 [0.61–5.29]	0.289
$rScO_{2SD}$	24	5.7 [4.4–6.8]	5.3 [3.9–6.5]	6.2 [4.5–7.9]	**0.029**	1.29 [1.0–1.68]	0.054
	48	6.1 [4.9–7.5]	6.1 [4.6–7.0]	6.1 [5.0–7.7]	0.201	1.16 [0.9–1.5]	0.252
	72	6.5 [5.4–7.7]	6.2 [5.3–6.9]	6.6 [5.4–8.0]	**0.030**	**1.34 [1.0–1.78]**	**0.046**
$rScO_{2MEAN}$	24	76.6 [73.1–80.0]	77.0 [73.5–82.6]	76.1 [72.2–77.8]	0.132	0.94 [0.86–1.02]	0.120
	48	78.9 [75.4–82.5]	79.9 [76.1–86.4]	78.6 [75.3–80.6]	**0.042**	**0.91 [0.83–1.0]**	**0.044**
	72	79.4 [77.1–83.1]	80.0 [77.4–86.8]	79.0 [76.4–82.0]	0.054	0.91 [0.83–1.0]	0.054
$rScO_{2TIME<60\%}$	24	0.5 [0.0–3.0]	0.0 [0.0–1.8]	0.8 [0.0–4.2]	**0.049**	1.17 [0.98–1.4]	0.088
	48	0.2 [0.0–1.8]	0.0 [0.0–0.7]	0.4 [0.0–2.4]	**0.041**	1.22 [0.97–1.54]	0.092
	72	0.3 [0.0–1.3]	0.0 [0.0–0.6]	0.5 [0.1–2.5]	**0.009**	1.29 [0.96–1.74]	0.090

All values for ARV, SD and mean are per 1% change in $rScO_2$; time <60% are per 1% of that timeframe below $rScO_2$ of 60%. $rScO_2$, Regional cerebral oxygen saturation; $rScO_{2ARV}$, $rScO_2$ average real variability; $rScO_{2SD}$, $rScO_2$ standard deviation; $rScO_{2MEAN}$, $rScO_2$ mean; $rScO_{2TIME<60\%}$, percentage of time $rScO_2$ was below 60%.

[a]The duration (hours) of monitoring after birth.

[b]Data presented as "median [25th percentile—75th percentile]".

[c]Univariable comparison via independent *t*-test or Mann-Whitney *U*-test as appropriate.

[d]Logistic regression model adjusted for both gestational age at delivery and birth weight. Significant values are bolded.

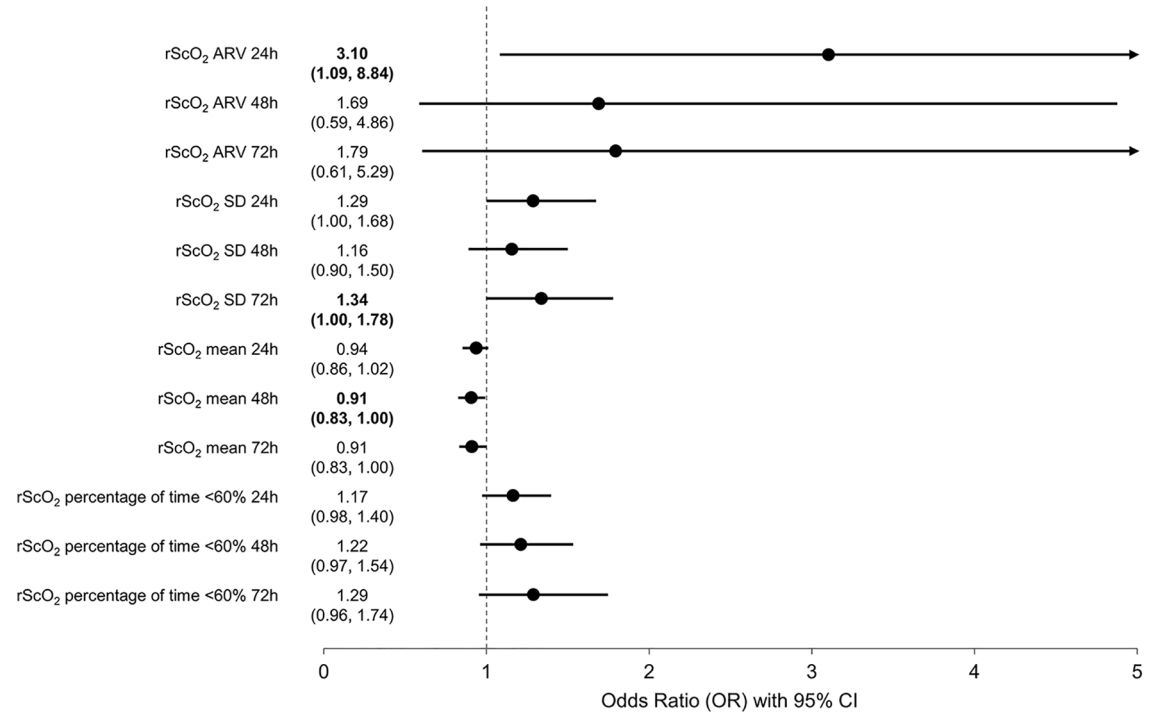

FIGURE 2
Results of logistic regression analysis showing the association between $rScO_2$ features (average real variability; $rScO_{2ARV}$; standard deviation, $rScO_{2SD}$; mean, $rScO_{2MEAN}$; and percentage of time below 60%, $rScO_{2TIME<60\%}$) and brain injury at term-equivalent age. Values >1 indicate increased likelihood for brain injury at term-equivalent age.

associated with an increased likelihood for being diagnosed with brain injury at TEA. Our results cannot distinguish if this association is consequential ($rScO_2$ pattern reflects presence of injury) or causative ($rScO_2$ pattern contributed to development of injury), therefore our study provides direction for future research.

Variations in cerebral perfusion and oxygenation are considered to be the key risk factors for brain injury in preterm infants (9, 11, 12). Continuous assessment of $rScO_2$ can identify infants with altered cerebral oxygenation (32). Although NIRS is increasingly used by neonatologists for $rScO_2$ monitoring, there are no reports that consistently establish the $rScO_2$ references or

cut-off values for adverse outcomes related to altered brain oxygenation (23, 33). Alderliesten et al. (23) published reference values of $rScO_2$ during the first three days of life in 999 preterm infants (GA <32 weeks) and found that at NICU admission the average $rScO_2$ was ~65% and continued to increase with GA at a mean rate of 1% per week, following a parabolic curve in relation to postnatal age with a peak at −36 h. It is important to note, Alderliesten et al. (23) references were obtained mostly from measurements using small adult sensors (983 small adult sensors and 16 neonatal sensors). In order to convert neonatal sensor readings to the small adult sensor equivalent, the obtained $rScO_2$ values were interpolated using statistical modelling tools (23). It is well established that $rScO_2$ values depend on the type of NIRS sensor used (e.g., adult, neonatal, pediatric) (23, 34). In comparison to adult sensors, neonatal $rScO_2$ sensor readings are consistently higher, but the difference is not fixed and is less at the threshold indicative of cerebral hypoxia; the neonatal sensor difference is approximately 10% when adult sensors read 85%, but nearly similar (58.8%) when adult sensors read 55% (35). The SafeBoosC-III study evaluating the benefit of an interventional strategy to reduce cerebral hypoxia using NIRS-derived $rScO_2$ monitoring demonstrate no significant difference between group in rates of death or severe brain injury at 36 weeks post-menstrual age (36). The study used at least 5 different device and sensor combinations with varying hypoxia thresholds based on linear transformations obtained in an *in vitro* model. Although the trial did not show evidence of decreased mortality or severe brain injury, concerns remain that the selected thresholds were not equivalent across devices due to proprietary algorithms and the nonlinear nature of human physiology (37). Therefore, in order to properly interpret $rScO_2$ cut-off values, it is of utmost importance to specify the type of sensor when comparing the data between studies.

Because low brain blood flow is associated with reduced oxygenation it poses a risk for development of brain injury. Specifically, Alderliesten et al. (34) found that a $rScO_2$<55% (using a small adult sensor) increased risk for grade III/IV IVH with an odds ratio of 1.017 per one percent (95%CI 1.007–1.026, GA corrected) of time spent below 55%, as well as in neonates who spent at least 20% of time below 55% in the first 72 h following delivery. Furthermore, Alderliesten et al. (34) found that a $rScO_2$<55% was associated with unfavorable cognitive outcomes at 24 months with an OR of 1.4 (CI 1.1–1.7) for neonates who spent at least 20% of time below that threshold during the first 3 days after delivery. Chock et al. (38) measured $rScO_2$ with neonatal sensors and reported that infants with adverse outcomes had significantly lower mean $rScO_2$ (67 ± 9%) compared with those without adverse outcomes (72 ± 7%), and that $rScO_2$ below 50% could be identified as a cut-off point for identifying infants with adverse outcome with an area under the curve of 0.76. Verhagen et al. (39), using pediatric sensors, demonstrated that preterm infants with IVH, compared to those without IVH, had lower median $rScO_2$ during the first two weeks following birth, suggesting that lower cerebral blood flow in those with injuries remains present for a longer period than just the first few hours after birth. However, it remains unknown whether this lower blood flow and oxygenation contributed to injury or rather reflects the presence of hemorrhage. In our cohort few infants had $rScO_2$ below 50%, therefore we examined the time spent with $rScO_2$ below 60% during 72 postdelivery hours. Using this cut-off point in unadjusted analysis we found a positive association between $rScO_{2TIME<60\%}$ and brain injury, however after adjusting for weight and GA the significance was lost, but the trend towards positive association remained.

A short-term ARV represents measurement-to-measurement, within-subject variability in the parameter (in our study parameter of interest was $rScO_2$) that accounts for the order in which measurements has occurred (31). In cardiovascular research short-term ARV was shown to be an independent risk factor for severity of organ damage (40, 41), cardiovascular morbidity and mortality (30, 42). The precision of estimates from ARV is dependent on frequency of sequential readings (measurements), and in the current study data were recorded every 5–15 s, and ARV was aggregated over 5-minute intervals during 72-hours after delivery. Therefore, our frequency of measurements provides a reliable assessment of $rScO_{2ARV}$ features in regard to the outcome sought. It is well known that inadequate or fluctuating cerebral perfusion and oxygenation contribute to IVH and WMI (10, 12, 38, 43–47). Preterm infants are at high risk for early hemodynamic instability and many factors may contribute to fluctuations in systemic blood pressure in the first few days of life. Moreover, cerebral autoregulation has limited capacity and is thought to be particularly fragile in the immature brain (48). A number of factors that influence vascular reactivity are likely to promote the pressure passive state (hypoxia, hypocarbia, hypercarbia), significantly perturb cerebral blood flow and increase the risk for WMI and intracranial hemorrhage (49–52). The proportion of infants with impaired cerebral autoregulation and increased periods of pressure-passive cerebral circulation appear to be substantial (53, 54). As the pressure-passive state can fluctuate over time and can occur without markedly low blood pressures, it could be readily overlooked with routine monitoring (54). On the other side, increases in systemic blood pressure, especially abrupt increases, could lead to cerebral hyperperfusion and hemorrhagic complications. Since oscillations of systemic blood pressure create variations in regional blood flow which can be assessed with NIRS (55), $rScO_2$ ARV emerges as an attractive approach to assess the adequacy of regional brain perfusion and oxygenation. To the best of our knowledge $rScO_{2ARV}$ using NIRS has never been examined in assessing the association between $rScO_2$ and brain injury. Our study suggests that increased short-term $rScO_{2ARV}$, early following delivery of preterm infants may be either a predictor or a marker for increased likelihood of brain injury.

4.1 Strengths and limitations

A strength of this study is prospective enrollment of consecutive neonates who fulfilled the research criteria. To examine more precisely the relationship between $rScO_2$ and brain injury only neonates with a normal cUS on admission were included. Another strength of our study is the use of MRI over cUS to detect the severity and extension of brain injury.

Compared with cUS, MRI is more sensitive for detection of low grade IVH, non-cystic WMI, especially punctate white matter lesions which correspond to small periventricular necroses of apparent ischemic or hemorrhagic nature, as well as cerebellar hemorrhage, particularly small punctate hemorrhages (56, 57).

Our study must be interpreted in the context of several limitations. First, we focused on $rScO_2$ monitoring in the first 3 days following birth. While most brain injuries (70%) are expected to occur within the first 72 h following birth (13), this monitoring window may not be adequate to capture injuries that occur later (of note, it is estimated that 95% of brain injuries occur by day 7, with a very small additional percentage between days 7 and 10) (24). Our study assumes that the majority of injuries occurred during 72-hour time frame after birth, as well that these injuries may be associated with altered $rScO_2$. Second, our study assumes that early occurring brain injuries remain detectable with MRI at TEA, and ignores the possibility that some may have resolved in interim. Third, there was a substantial variability in measured $rScO_2$ values which limits the statistical power of consistently detecting differences. Although we found evidence that $rScO_2$ in early postdelivery period is associated with brain injury at TEA, as well that the time spent below 60% saturation is associated with increased risk for brain injury, our study is not large enough to provide the exact cut-off point for critical $rScO_2$ levels. Therefore, future studies are needed to define critical $rScO_2$ values and examine whether interventions designed to optimize $rScO_2$ can prevent brain injury in infants.

5 Conclusion

In conclusion, our results suggest that features of increased $rScO_2$ variability in preterm infants, as well as lower $rScO_{2MEAN}$ and increased percentage of time spent <60% within the first three days following delivery may be associated with increased likelihood for brain injury at TEA. Our study design does not allow to discern whether the observed association between $rScO_2$ and brain injury is causative or is rather a marker of its presence. Therefore, our study opens an intriguing question and provides direction for future research.

Data availability statement

The raw data supporting the conclusions of this article will be made available by the authors, without undue reservation.

Ethics statement

The studies involving humans were approved by Institutional Ethics Committee of the University Hospital Centre Zagreb and Institutional Ethics Committee of the School of Medicine University of Zagreb. The studies were conducted in accordance with the local legislation and institutional requirements. Written informed consent for participation in this study was provided by the participants' legal guardians/next of kin.

Author contributions

TĆ: Investigation, Methodology, Writing – original draft. MR: Data curation, Writing – review & editing, Formal Analysis, Validation. KB: Writing – review & editing. ND: Writing – review & editing, Investigation. DS: Data curation, Writing – review & editing, Formal Analysis, Validation. JS: Writing – review & editing, Data curation, Methodology, Supervision. TW: Writing – review & editing. MR: Investigation, Writing – review & editing, Funding acquisition. IK: Investigation, Writing – review & editing. RG: Investigation, Methodology, Project administration, Supervision, Writing – review & editing.

Funding

The author(s) declare that financial support was received for the research, authorship, and/or publication of this article.

This publication was supported by Croatian Science Foundation projects IP-2020-02-7166; co-financed by the Scientific Centre of Excellence for Basic, Clinical and Translational Neuroscience project "Experimental and clinical research of hypoxic-ischemic damage in perinatal and adult brain"; GA KK01.1.1.01.0007 funded by the European Union through the European Regional Development Fund.

Conflict of interest

The authors declare that the research was conducted in the absence of any commercial or financial relationships that could be construed as a potential conflict of interest.

Publisher's note

Supplementary material

The Supplementary Material for this article can be found online at: https://www.frontiersin.org/articles/10.3389/fped.2024.1426874/full#supplementary-material

References

1. Scher MS. "The first thousand days" define a fetal/neonatal neurology program. *Front Pediatr.* (2021) 9:683138. doi: 10.3389/fped.2021.683138

2. Scher MS. Interdisciplinary fetal-neonatal neurology training applies neural exposome perspectives to neurology principles and practice. *Front Neurol.* (2024) 14:1321674. doi: 10.3389/fneur.2023.1321674

3. Kartam M, Embaireeg A, Albalool S, Almesafer A, Hammoud M, Al-Hathal M, et al. Late-onset sepsis in preterm neonates is associated with higher risks of cerebellar hemorrhage and lower motor scores at three years of age. *Oman Med J.* (2022) 37(2): e368. doi: 10.5001/omj.2022.41

4. Lu J, Martin CR, Claud EC. Neurodevelopmental outcome of infants who develop necrotizing enterocolitis: the gut-brain axis. *Semin. Perinatol.* (2023) 47(1):151694. doi: 10.1016/j.semperi.2022.151694

5. Kusters CD, Chen ML, Follett PL, Dammann O. "Intraventricular" hemorrhage and cystic periventricular leukomalacia in preterm infants: how are they related? *J Child Neurol.* (2009) 24(9):1158–70. doi: 10.1177/0883073809338064

6. Stoll BJ, Hansen NI, Bell EF, Shankaran S, Laptook AR, Walsh MC, et al. Neonatal outcomes of extremely preterm infants from the NICHD neonatal research network. *Pediatrics.* (2010) 126(3):443–56. doi: 10.1542/peds.2009-2959

7. Arulkumaran S, Tusor N, Chew A, Falconer S, Kennea N, Nongena P, et al. MRI findings at term-corrected age and neurodevelopmental outcomes in a large cohort of very preterm infants. *AJNR Am J Neuroradiol.* (2020) 41(8):1509–16. doi: 10.3174/ajnr.A6666

8. Kostović I, Kostović-Srzentić M, Benjak V, Jovanov-Milošević N, Radoš M. Developmental dynamics of radial vulnerability in the cerebral compartments in preterm infants and neonates. *Front Neurol.* (2014) 5:139. doi: 10.3389/fneur.2014.00139

9. Ballabh P, de Vries LS. White matter injury in infants with intraventricular haemorrhage: mechanisms and therapies. *Nat Rev Neurol.* (2021) 17(4):199–214. doi: 10.1038/s41582-020-00447-8

10. Lou HC, Lassen NA, Friis-Hansen B. Impaired autoregulation of cerebral blood flow in the distressed newborn infant. *J Pediatr.* (1979) 94(1):118–21. doi: 10.1016/s0022-3476(79)80373-x

11. Inder TE, Perlman JM, Volpe JJ. Preterm intraventricular hemorrhage/posthemorrhagic hydrocephalus. In: Volpe JJ, editor. *Neurology of the Newborn.* Philadelphia: Elsevier (2018). p. 637–98.

12. Lu H, Wang Q, Lu J, Zhang Q, Kumar P. Risk factors for intraventricular hemorrhage in preterm infants born at 34 weeks of gestation or less following preterm premature rupture of membranes. *J Stroke Cerebrovasc Dis.* (2016) 25 (4):807–12. doi: 10.1016/j.jstrokecerebrovasdis.2015.12.011

13. McCrea HJ, Ment LR. The diagnosis, management, and postnatal prevention of intraventricular hemorrhage in the preterm neonate. *Clin Perinatol.* (2008) 35 (4):777–92. doi: 10.1016/j.clp.2008.07.014

14. Gano D, Ho ML, Partridge JC, Glass HC, Xu D, Barkovich AJ, et al. Antenatal exposure to magnesium sulfate is associated with reduced cerebellar hemorrhage in preterm newborns. *J Pediatr.* (2016) 178:68–74. doi: 10.1016/j.jpeds.2016.06.053

15. Inder TE, Anderson NJ, Spencer C, Wells S, Volpe JJ. White matter injury in the premature infant: a comparison between serial cranial sonographic and MR findings at term. *AJNR Am J Neuroradiol.* (2003) 24(5):805–9. PMID: 12748075; PMCID: PMC7975772.

16. Back SA. White matter injury in the preterm infant: pathology and mechanisms. *Acta Neuropathol.* (2017) 134(3):331–49. doi: 10.1007/s00401-017-1718-6

17. Back SA, Volpe JJ. Encephalopathy of prematurity: pathophysiology. In: Volpe JJ, editor. *Neurology of the Newborn.* Philadelphia: Elsevier (2018). p. 405–24.

18. Zhang Y, Liu D, Mao Y, Gao Q, Xiong T. Cerebral near-infrared spectroscopy monitoring to predict periventricular-intraventricular haemorrhage and neurodevelopmental outcomes in preterm infants: a protocol for a systematic review and meta-analysis. *BMJ Paediatr Open.* (2023) 7(1):e001859. doi: 10.1136/bmjpo-2023-001859

19. Zweifel C, Castellani G, Czosnyka M, Helmy A, Manktelow A, Carrera E, et al. Noninvasive monitoring of cerebrovascular reactivity with near infrared spectroscopy in head-injured patients. *J Neurotrauma.* (2010) 27(11):1951–8. doi: 10.1089/neu.2010.1388

20. Brady K, Joshi B, Zweifel C, Smielewski P, Czosnyka M, Easley RB, et al. Real-time continuous monitoring of cerebral blood flow autoregulation using near-infrared spectroscopy in patients undergoing cardiopulmonary bypass. *Stroke.* (2010) 41 (9):1951–6. doi: 10.1161/STROKEAHA.109.575159

21. Caicedo A, De Smet D, Naulaers G, Ameye L, Vanderhaegen J, Lemmers P, et al. Cerebral tissue oxygenation and regional oxygen saturation can be used to study cerebral autoregulation in prematurely born infants. *Pediatr Res.* (2011) 69 (6):548–53. doi: 10.1203/PDR.0b013e3182176d85

22. Watzman HM, Kurth CD, Montenegro LM, Rome J, Steven JM, Nicolson SC. Arterial and venous contributions to near-infrared cerebral oximetry. *Anesthesiology.* (2000) 93(4):947–53. doi: 10.1097/00000542-200010000-00012

23. Alderliesten T, Dix L, Baerts W, Caicedo A, van Huffel S, Naulaers G, et al. Reference values of regional cerebral oxygen saturation during the first 3 days of life in preterm neonates. *Pediatr Res.* (2016) 79(1-1):55–64. doi: 10.1038/pr.2015.186

24. Hand IL, Shellhaas RA, Milla SS, Committee on Fetus and Newborn, , Section on Neurology, Section on Radiology. Routine neuroimaging of the preterm brain. *Pediatrics.* (2020) 146(5):e2020029082. doi: 10.1542/peds.2020-029082

25. de Vries LS, Eken P, Dubowitz LM. The spectrum of leukomalacia using cranial ultrasound. *Behav Brain Res.* (1992) 49(1):1–6. doi: 10.1016/s0166-4328(05)80189-5

26. Dorner RA, Burton VJ, Allen MC, Robinson S, Soares BP. Preterm neuroimaging and neurodevelopmental outcome: a focus on intraventricular hemorrhage, post-hemorrhagic hydrocephalus, and associated brain injury. *J Perinatol.* (2018) 38(11):1431–43. doi: 10.1038/s41372-018-0209-5

27. Agut T, Alarcon A, Cabañas F, Bartocci M, Martinez-Biarge M, Horsch S, et al. Preterm white matter injury: ultrasound diagnosis and classification. *Pediatr Res.* (2020) 87(Suppl 1):37–49. doi: 10.1038/s41390-020-0781-1

28. Papile LA, Burstein J, Burstein R, Koffler H. Incidence and evolution of subependymal and intraventricular hemorrhage: a study of infants with birth weights less than 1,500 gm. *J Pediatr.* (1978) 92(4):529–34. doi: 10.1016/s0022-3476(78)80282-0

29. Starr R, De Jesus O, Shah SD, Borger J. *Periventricular and Intraventricular Hemorrhage. in StatPearls.* Treasure Island, FL: StatPearls Publishing (2023). Available online at: https://www.ncbi.nlm.nih.gov/books/NBK538310/ (accessed April 21, 2024).

30. Mena L, Pintos S, Queipo NV, Aizpúrua JA, Maestre G, Sulbarán T. A reliable index for the prognostic significance of blood pressure variability. *J Hypertens.* (2005) 23(3):505–11. doi: 10.1097/01.hjh.0000160205.81652.5a

31. Mena LJ, Maestre GE, Hansen TW, Thijs L, Liu Y, Boggia J, et al. How many measurements are needed to estimate blood pressure variability without loss of prognostic information? *Am J Hypertens.* (2014) 27(1):46–55. doi: 10.1093/ajh/hpt142

32. Alderliesten T, Lemmers PM, Smarius JJ, van de Vosse RE, Baerts W, van Bel F. Cerebral oxygenation, extraction, and autoregulation in very preterm infants who develop peri-intraventricular hemorrhage. *J Pediatr.* (2013) 162(4):698–704.e2. doi: 10.1016/j.jpeds.2012.09.038

33. Hyttel-Sorensen S, Pellicer A, Alderliesten T, Austin T, van Bel F, Benders M, et al. Cerebral near infrared spectroscopy oximetry in extremely preterm infants: phase II randomised clinical trial. *Br Med J.* (2015) 350:g7635. doi: 10.1136/bmj.g7635

34. Alderliesten T, van Bel F, van der Aa NE, Steendijk P, van Haastert IC, de Vries LS, et al. Low cerebral oxygenation in preterm infants is associated with adverse neurodevelopmental outcome. *J Pediatr.* (2019) 207:109–116.e2. doi: 10.1016/j.jpeds.2018.11.038

35. Variane GFT, Dahlen A, Noh CY, Zeng J, Yan ES, Kaneko JS, et al. Cerebral oxygen saturation in neonates: a bedside comparison between neonatal and adult NIRS sensors. *Pediatr Res.* (2023) 94(5):1810–6. doi: 10.1038/s41390-023-02705-z

36. Hansen ML, Pellicer A, Hyttel-Sørensen S, Ergenekon E, Szczapa T, Hagmann C, et al. Cerebral oximetry monitoring in extremely preterm infants. *N Engl J Med.* (2023) 388(16):1501–11. doi: 10.1056/NEJMoa2207554

37. Chock VY, Vesoulis ZA, El-Dib M, Austin T, van Bel F. The future of neonatal cerebral oxygenation monitoring: directions after the SafeBoosC-III trial. *J Pediatr.* (2024) 270:114016. doi: 10.1016/j.jpeds.2024.114016

38. Chock VY, Kwon SH, Ambalavanan N, Batton B, Nelin LD, Chalak LF, et al. Cerebral oxygenation and autoregulation in preterm infants (early NIRS study). *J Pediatr.* (2020) 227:94–100.e1. doi: 10.1016/j.jpeds.2020.08.036

39. Verhagen EA, Ter Horst HJ, Keating P, Martijn A, Van Braeckel KN, Bos AF. Cerebral oxygenation in preterm infants with germinal matrix-intraventricular hemorrhages. *Stroke.* (2010) 41(12):2901–7. doi: 10.1161/STROKEAHA.110.597229

40. Sega R, Corrao G, Bombelli M, Beltrame L, Facchetti R, Grassi G, et al. Blood pressure variability and organ damage in a general population: results from the PAMELA study (pressioni arteriose monitorate E loro associazioni). *Hypertension.* (2002) 39(2 Pt 2):710–4. doi: 10.1161/hy0202.104376

41. Li CL, Liu R, Wang JR, Yang J. Relationship between blood pressure variability and target organ damage in elderly patients. *Eur Rev Med Pharmacol Sci.* (2017) 21 (23):5451–5. doi: 10.26355/eurrev_201712_13934

42. Del Giorno R, Balestra L, Heiniger PS, Gabutti L. Blood pressure variability with different measurement methods: reliability and predictors. A proof of concept cross sectional study in elderly hypertensive hospitalized patients. *Medicine (Baltimore).* (2019) 98(28):e16347. doi: 10.1097/MD.0000000000016347

43. Aspide R. Relationship between brain tissue oxygen and near-infrared spectroscopy in patients with nontraumatic subarachnoid hemorrhage: invited commentary. *Neurocrit Care.* (2022) 37(3):616–7. doi: 10.1007/s12028-022-01566-4

44. Ballabh P. Pathogenesis and prevention of intraventricular hemorrhage. *Clin Perinatol.* (2014) 41(1):47–67. doi: 10.1016/j.clp.2013.09.007

45. Noori S, McCoy M, Anderson MP, Ramji F, Seri I. Changes in cardiac function and cerebral blood flow in relation to peri/intraventricular hemorrhage in extremely preterm infants. *J Pediatr.* (2014) 164(2):264–70.e703. doi: 10.1016/j.jpeds.2013.09.045

46. Sorensen LC, Maroun LL, Borch K, Lou HC, Greisen G. Neonatal cerebral oxygenation is not linked to foetal vasculitis and predicts intraventricular haemorrhage in preterm infants. *Acta Paediatr*. (2008) 97(11):1529–34. doi: 10.1111/j.1651-2227.2008.00970.x

47. Vesoulis ZA, Whitehead HV, Liao SM, Mathur AM. The hidden consequence of intraventricular hemorrhage: persistent cerebral desaturation after IVH in preterm infants. *Pediatr. Res*. (2021) 89(4):869–77. doi: 10.1038/s41390-020-01189-5

48. Volpe JJ. Brain injury in the premature infant: neuropathology, clinical aspects, and pathogenesis. *Ment. Retard Dev Disabil Res Rev*. (1997) 5(3):3–12. doi: 10.1002/(SICI)1098-2779(1997)3:1%3C3::AID-MRDD2%3E3.0.CO;2-U

49. Fabres J, Carlo WA, Phillips V, Howard G, Ambalavanan N. Both extremes of arterial carbon dioxide pressure and the magnitude of fluctuations in arterial carbon dioxide pressure are associated with severe intraventricular hemorrhage in preterm infants. *Pediatrics*. (2007) 119(2):299–305. doi: 10.1542/peds.2006-2434

50. Erickson SJ, Grauaug A, Gurrin L, Swaminathan M. Hypocarbia in the ventilated preterm infant and its effect on intraventricular haemorrhage and bronchopulmonary dysplasia. *J Paediatr Child Health*. (2002) 38(6):560–2. doi: 10.1046/j.1440-1754.2002.00041.x

51. Greisen G, Vannucci RC. Is periventricular leucomalacia a result of hypoxic-ischaemic injury? Hypocapnia and the preterm brain. *Biol Neonate*. (2001) 79(3-4):194–200. doi: 10.1159/000047090

52. Pryds O. Control of cerebral circulation in the high-risk neonate. *Ann Neurol*. (1991) 30(3):321–9. doi: 10.1002/ana.410300302

53. Tsuji M, Saul JP, du Plessis A, Eichenwald E, Sobh J, Crocker R, et al. Cerebral intravascular oxygenation correlates with mean arterial pressure in critically ill premature infants. *Pediatrics*. (2000) 106(4):625–32. doi: 10.1542/peds.106.4.625

54. Soul JS, Hammer PE, Tsuji M, Saul JP, Bassan H, Limperopoulos C, et al. Fluctuating pressure-passivity is common in the cerebral circulation of sick premature infants. *Pediatr Res*. (2007) 61(4):467–73. doi: 10.1203/pdr.0b013e31803237f6

55. Alderliesten T, Lemmers PM, van Haastert IC, de Vries LS, Bonestroo HJ, Baerts W, et al. Hypotension in preterm neonates: low blood pressure alone does not affect neurodevelopmental outcome. *J Pediatr*. (2014) 164(5):986–91. doi: 10.1016/j.jpeds.2013.12.042

56. Woodward LJ, Anderson PJ, Austin NC, Howard K, Inder TE. Neonatal MRI to predict neurodevelopmental outcomes in preterm infants. *N Engl J Med*. (2006) 355(7):685–94. doi: 10.1056/NEJMoa053792

57. Inder TE, de Vries LS, Ferriero DM, Grant PE, Ment LR, Miller SP, et al. Neuroimaging of the preterm brain: review and recommendations. *J Pediatr*. (2021) 237:276–287.e4. doi: 10.1016/j.jpeds.2021.06.014

frontiers | Frontiers in Neuroanatomy

TYPE Original Research
PUBLISHED 12 August 2024
DOI 10.3389/fnana.2024.1441645

OPEN ACCESS

EDITED BY
Senka Blažetić,
Josip Juraj Strossmayer University of Osijek, Croatia

REVIEWED BY
Daniel Menezes Guimarães,
D'Or Institute for Research and Education (IDOR), Brazil
Yu Tang,
Gabaeron, Inc., United States

*CORRESPONDENCE
Ivan Banovac
✉ ivan.banovac@mef.hr

RECEIVED 06 June 2024
ACCEPTED 26 July 2024
PUBLISHED 12 August 2024

CITATION
Prkačin MV, Petanjek Z and Banovac I (2024) A novel approach to cytoarchitectonics: developing an objective framework for the morphological analysis of the cerebral cortex. *Front. Neuroanat.* 18:1441645. doi: 10.3389/fnana.2024.1441645

A novel approach to cytoarchitectonics: developing an objective framework for the morphological analysis of the cerebral cortex

Matija Vid Prkačin[1,2], Zdravko Petanjek[1,2] and Ivan Banovac[1,2]*

[1]Department of Anatomy and Clinical Anatomy, University of Zagreb School of Medicine, Zagreb, Croatia, [2]Croatian Institute for Brain Research, University of Zagreb School of Medicine, Zagreb, Croatia

Introduction: The cytoarchitectonic boundaries between cortical regions and layers are usually defined by the presence or absence of certain cell types. However, these cell types are often not clearly defined and determining the exact boundaries of regions and layers can be challenging. Therefore, in our research, we attempted to define cortical regions and layers based on clear quantitative criteria.

Methods: We performed immunofluorescent anti-NeuN labelling on five adult human brains in three cortical regions—Brodmann areas (BA) 9, 14r, and 24. We reconstructed the cell bodies of 90,723 NeuN-positive cells and analyzed their morphometric characteristics by cortical region and layer. We used a supervised neural network prediction algorithm to classify the reconstructions into morphological cell types. We used the results of the prediction algorithm to determine the proportions of different cell types in BA9, BA14r and BA24.

Results: Our analysis revealed that the cytoarchitectonic descriptions of BA9, BA14r and BA24 were reflected in the morphometric measures and cell classifications obtained by the prediction algorithm. BA9 was characterized by the abundance of large pyramidal cells in layer III, BA14r was characterized by relatively smaller and more elongated cells compared to BA9, and BA24 was characterized by the presence of extremely elongated cells in layer V as well as relatively higher proportions of irregularly shaped cells.

Discussion: The results of the prediction model agreed well with the qualitative expected cytoarchitectonic descriptions. This suggests that supervised machine learning could aid in defining the morphological characteristics of the cerebral cortex.

KEYWORDS

prefrontal cortex, human, prediction model, neural network, cell classification

1 Introduction

Meaningful research on cortical cytoarchitectonics started in 19th century with the introduction of Nissl staining, which enabled researchers to extensively study the microstructural organization of the cerebral cortex. Despite the widespread use of the Nissl method by many researchers (Meynert, 1867, 1868; Hammarberg, 1895; Flechsig, 1897), initial

works on cytoarchitectonics lacked a truly systematic approach and there was no agreed upon histological division of the cerebral cortex. It was not until Brodmann (1909) developed his cytoarchitectonic map of the cerebral cortex, that research on the morphology and function of different cortical regions began to be more comparable and reproducible. After Brodmann, von Economo and Koskinas made the next great contribution to research on cytoarchitectonics by producing one of the most comprehensive analyses of the human cerebral cortex (von Economo and Koskinas, 1925; von Economo, 1927).

Following these fundamental works, further research was mostly focused on refining Brodmann's map based on new insights. Some of the research was comparative in nature, with the aim of finding both histological and functional homology of cortical regions between different species, usually primates (Ongür and Price, 2000; Ongür et al., 2003). Most of the research was predominantly qualitative (Petrides and Pandya, 1999; Petrides et al., 2012), though some studies attempted to quantify certain types of specialized cells in specific cortical regions (Rivara et al., 2003; Fajardo et al., 2008; González-Acosta et al., 2018). Those studies were somewhat limited because the detection of such specialized cells, and therefore their quantification, was still based on arbitrarily decided qualitative criteria. There were also some attempts to define cortical regions based on quantitative criteria, such as cell density and laminar thickness (Rajkowska and Goldman-Rakic, 1995a,b). However, this research still used exclusively manual quantification. Recently, there have been attempts to use machine learning in delineating cortical layers, with promising results (Štajduhar et al., 2023).

Nowadays, precise localization is extremely important in neuroscience research, and determining the exact cortical regions and layers, in which the morphological and molecular characteristics will be analyzed, is the golden standard in the field. Interestingly, even today, cortical regions and layers are still predominantly delineated by individual experts based on their prior experience and referring to relevant literature. A potential limitation of such an approach could be a less reliable comparability of research conducted by different research groups.

Cortical regions and layers are usually defined by the presence or absence of certain cell types (Nieuwenhuys, 1994). At the same time, the morphometric and molecular characteristics of those cells are often not well defined or agreed upon, though there were some attempts at achieving more objective interneuron classifications (Mihaljević et al., 2014, 2018). Detailed characterization of different cell types is essential due to several reasons. Firstly, many comparative studies showed interspecies differences in morphological and molecular characteristics of certain cortical cell types, especially the different interneuron subpopulations (Džaja et al., 2014; Hladnik et al., 2014; Banovac et al., 2022). Secondly, clinically related studies showed that alterations in cortical neurons found in different neuropsychiatric disorders affect very specific neuron populations, typically in specific cortical regions and layers (Marín, 2012; Prkačin et al., 2023).

The aforementioned shows that spatial localization and precise morphological and molecular definition of different neuron types are essential for understanding the functional organization of the cerebral cortex and its potential alterations in neuropathology. However, since such research heavily relies on the qualitative analysis of experts in the field, it may be prone to interrater bias and thus lack adequate reproducibility. In addition, the training of experts and their analyses are typically time consuming. This means that the applicability of such methodology in clinical practice remains low, which reduces its translational value.

Therefore, in our research, we attempted to define different cell types, as well as cortical regions and layers based on clear quantitative criteria. We also assessed the morphological composition of different cortical regions and layers as well as compared laminar differences between regions. We focused on Brodmann areas (BA) 9, 14r and 24 due to the following: (1) these regions are part of the human prefrontal cortex (PFC), and as such play a key role in integration of information from other cortical regions, as well as being involved in higher cognitive functions in humans (Fuster, 2015); (2) although these three regions are part of the PFC, they are phylogenetically and functionally very different, which should be reflected in their cytoarchitectonics. The aim of our study is to provide a more objective way of defining morphological cell types and delineating specific cortical layers and regions.

2 Materials and methods

2.1 Study design

In order to achieve our aim of developing a more objective way of defining morphological cell types and delineating cortical regions and layers, we structured our research as follows.

We chose PFC tissue blocks containing BA9, BA14r and BA24 from 5 human specimens—for the general localization of these cortical regions we used the cytoarchitectonic maps by Brodmann (1909), von Economo and Koskinas (1925), and Ongür and Price (2000). We confirmed the locations of the cortical regions using Nissl staining (see Supplementary data). We then performed immunofluorescent anti-NeuN labelling on three histological sections in each cortical region (45 sections in total).

After imaging the histological slides, we determined the exact boundaries of the cytoarchitectonic regions and delineated the cortical layers by cross-referencing descriptions and histological depictions in relevant literature (Brodmann, 1909; von Economo and Koskinas, 1925; von Economo, 1927; Braak, 1980; Vogt et al., 1995; Rajkowska and Goldman-Rakic, 1995a; Petrides and Pandya, 1999; Ongür and Price, 2000; Ongür et al., 2003; von Economo and Triarhou, 2009; Petrides et al., 2012) (for a detailed description see Supplementary data).

We then reconstructed the cell bodies of NeuN-positive ($NeuN^+$) cells in all 45 imaged slides and analyzed their morphometric parameters by cortical region and layer. We then additionally classified a representative sample of reconstructions into different morphological cell types using the work of von Economo and Koskinas as our main reference.

Finally, we used a neural network prediction algorithm to classify the rest of the reconstructions into morphological types, based on the input from the manual classification. We used this data to determine the provisionary proportions of various morphological cell types in different cortical regions and layers.

2.2 Brain tissue samples

We analyzed the brain samples of five male human subjects aged from 37 to 51 years with a postmortem delay of 6 to 11 h (Supplementary Table S1). The subjects had no medical history of neurological or psychiatric disorders and no signs of preagonal state at autopsy. The brain tissue is stored in the brain bank as a part of the Zagreb Neuroembryological Collection (Kostovic et al., 1991; Judaš et al., 2011).

The University of Zagreb School of Medicine Ethics Committee approved the tissue collection and research conduction (Approval Nos. 380-59-10106-14-55/152 and 380-59-10106-19-111/210). The information on the subject's identity and history is anonymized, and the brain samples are coded, indicating only the cortical region and the subject's age.

The brain tissue blocks were cut according to Talairach's and Szikla (1980) coordinates. Tissue blocks included parts of the PFC encompassing the superior frontal gyrus (containing BA9), straight gyrus (containing BA14r), and anterior cingulate cortex (containing BA24) (Brodmann, 1909; von Economo and Koskinas, 1925; Ongür and Price, 2000; Banovac et al., 2020). The tissue was fixed by immersion in 4% paraformaldehyde for 24 h, then dehydrated in an ethanol cascade (70, 96, 100%), vitrificated in toluene, and finally embedded in paraffin (Sadeghipour and Babaheidarian, 2019). The tissue was then cut on a microtome into 20 µm-thick coronal slices (Sy and Ang, 2019) and mounted on VitroGnost Plus Ultra adhesive microscope slides (BioGnost, Zagreb, Croatia). The tissue was always cut perpendicular to the dome of the gyrus to avoid distortion of cell body morphology.

2.3 Immunofluorescence labeling

Immunofluorescence was performed according to previously established protocol for paraffin-embedded tissue (Zaqout et al., 2020; Banovac et al., 2022). Histological sections were first photobleached for 48 h using a LED light source (Neumann and Gabel, 2002; Sun et al., 2017) in order to reduce autofluorescence. The sections were deparaffinized and heat antigen retrieval was performed in citrate-based (pH 6.0) unmasking solution (Boenisch, 2005). Protein blocking was done by incubating the sections for 1 h at room temperature (RT) in normal donkey serum (NDS; Chemicon, United States) diluted 1:30 in permeabilization solution (0.3% Triton X-100 in 1X PBS; Sigma-Aldrich, United States). Afterwards, the sections were incubated overnight in an anti-NeuN primary antibody (rabbit polyclonal, Abcam, CN: ab104225, lot: GR3410699-1, RRID: AB_10711153, working dilution: 1:1,000) at 4°C and in an anti-rabbit secondary antibody (donkey conjugated anti-rabbit Alexa 546, Thermo Fisher (Invitrogen), CN: A10040, lot: 2128963, RRID: AB_2534016, working dilution: 1:1,000) for 2 h at RT. The sections were treated with TrueBlack® Lipofuscin Autofluorescence Quencher (Biotium, United States) to further reduce autofluorescence (Banovac et al., 2019) and coverslipped with VectaMount Aqueous Mounting Medium (Vector Laboratories, United States).

Histological sections were imaged by a laser confocal microscope (Olympus FLUOVIEW FV3000RS, Japan) on high-power magnification and using Z-stack, visualizing the entire section thickness.

2.4 Morphometric analysis

The confocal images used in morphometric analysis were maximum Z projections, meaning that the entire section thickness was projected onto a single image.

Neuron cell bodies were included in the morphometric analysis only if they met all of the following criteria: (1) the cell was $NeuN^+$, (2) the cell body was fully visible (i.e., it was not covered by another cell and was not visibly cut on the edge of the section), (3) the outline of the cell body was clearly distinguishable from the background (Supplementary Figure S1).

The neuron cell bodies were reconstructed using Neurolucida 2020 (MBF, Vermont, United States), based on the following principles: (1) the cell body contour was drawn along the very edge of the cell body, i.e., at the border between the cell body signal and the background staining; (2) the cellular processes were not encompassed by the cell body contour; (3) if the transition between the cell body and the cellular process was unclear, the cell body was delineated so that it extended into the cellular process to the point where the extensions of the two adjacent edges of the cell body intersected (Figure 1A).

The reconstructions on each imaged slide were done within a column of cortical tissue. The columns were 2 mm wide at the pial surface and extended towards the border with the white matter, following the vertical orientation of the cells in the tissue. Within the cortical column, each cortical layer (I–VI) was delineated separately. The reconstructions were done by using the *Outline objects* function that automatically detects cell contours in confocal images and produces two-dimensional reconstructions of the cell bodies. The automatically drawn contours were reviewed and corrected by two independent researchers. The cell bodies of a total of 90,723 neurons were reconstructed in this research.

The cell body reconstructions were analyzed using Neurolucida Explorer (MBF, Vermont, USA), which provided the following morphometric parameters for each cell: soma circumference (*Perimeter*), soma surface (*Area*), the largest diameter of the soma contour (*Feret Max*), the smallest diameter of the soma contour (*Feret Min*), ratio between *Feret Max* and *Feret Min* (*Aspect Ratio*), ratio between *Area* and *Feret max* (*Compactness*), degree of indentations of soma circumference (*Convexity*), complexity/irregularity of the soma circumference (*Form Factor*), square of *Compactness* (*Roundness*), and ratio between *Area* and *Convex Area* (*Solidity*) (for a detailed description of each parameter see Supplementary data).

2.5 Classification of morphological cell types

In order to be able to create a prediction algorithm for different morphological cell types, 2,850 of the reconstructed cells were manually classified based on their soma shape and size, using the work of von Economo and Koskinas (1925) as reference. Von Economo and Koskinas refer to three main cell types in the cerebral cortex—granule cells, pyramidal cells and fusiform cells. We introduced the category of polymorphic cells to describe cells with irregular and/or unusual shapes that we could not classify into any of these three main cell types. Von Economo and Koskinas further subdivided pyramidal cells by size (using height and width as the main measures) into small, medium, large, and gigantic. Even though they did not further subdivide fusiform cells, the size range they included for this cell type

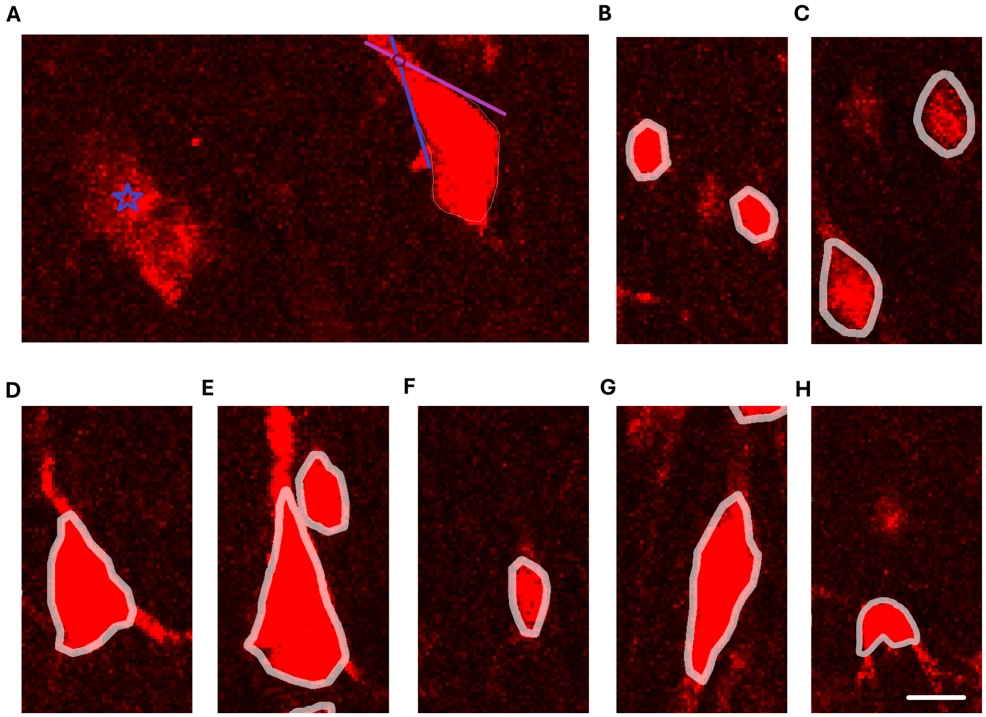

FIGURE 1
Reconstructions of neuron cell bodies on confocal images of NeuN staining. **(A)** Criteria for delineation of cell body contours. The blue star symbol marks NeuN$^+$ staining that is not eligible for reconstruction due to unclear boundaries and poor demarcation between the NeuN$^+$ staining and background staining. The pyramidal cell on the right side shows an example of a cell where the boundary between the apical dendrite is and the cell body is not sharp. The blue and purple lines follow the cell body edges adjacent to the apical dendrite and the red circle marks where the extensions of the edges intersect. The intersection denotes the distal boundary of the reconstructed cell body. **(B)** Reconstructions of typical granule cells. **(C)** Reconstructions of small pyramidal cells. **(D)** Reconstruction of a medium pyramidal cell. **(E)** Reconstruction of a large pyramidal cell. **(F)** Reconstruction of a small fusiform cell. **(G)** Reconstruction of a large fusiform cell. **(H)** Reconstruction of a polymorphic cell. Note that the cell body shape of the polymorphic cell is irregular and has indentations in the cell contour. Scale bar: 10 μm.

was very large (height ranging from 15 to 30 μm), which is why we classified fusiform cells into the small and large subcategories. It should be noted that the classification proposed by von Economo and Koskinas, and adapted in this study, relies exclusively on the neurons' soma shape and size. This classification does not take into account the dendritic and axon morphology of the cells.

Therefore, in this research, the cells were classified into the following categories: granule cells, small pyramidal cells, medium pyramidal cells, large pyramidal cells, gigantic pyramidal cells, small spindle cells, large spindle cells, and polymorphic cells (Table 1 and Figures 1B–H).

In order to get a representative sample, manual classification was performed in all three cortical regions in all of the analyzed brains, and the cells were chosen from all cortical layers. It should be noted that, on the slides we analyzed, we found no cells we could reliably manually classify as gigantic pyramidal cells.

Besides the two-dimensional cell body reconstructions utilized for the morphometric analysis, we provided several representative three-dimensional cell body reconstructions (Supplementary material—3D reconstructions).

2.6 Quantitative analysis

Quantitative analysis was performed in GraphPad Prism version 10.2.2 (GraphPad Software, La Jolla, United States), DATAtab (2024): Online Statistics Calculator (Graz, Austria) and Orange Data Mining version 3.36.2 (Ljubljana, Slovenia) (Demšar et al., 2013).

For each morphometric parameter, the following descriptive statistics were calculated: mean, standard deviation (SD), 95% confidence interval (CI) for mean, median, interquartile range (IQR), mode, minimum and maximum values, and coefficient of variation (CV).

Neuronal morphometric parameters, similarly to neuron densities (Morales-Gregorio et al., 2023), are typically not normally distributed. This was the case in our study as well—we evaluated the distributions graphically and using the D'Agostino-Pearson omnibus K^2 test, with both methods indicating that the data were likely not sampled from a normal distribution. Therefore, non-parametric tests were more appropriate for our analysis.

The differences in morphometric parameters between cortical regions were compared using the Kruskal–Wallis test with Dunn's *post hoc* test.

The association between morphometric parameters was assessed using Spearman's correlation coefficient. The correlation matrix was used to determine which morphometric parameters were most strongly associated with each other (Supplementary Table S2). Since some parameters are mathematically derived from other parameters, we aimed to determine which parameters were most relevant for distinguishing different cell types. We performed factor analysis and assessed the scree plot showing the relationship between the possible factors and the corresponding eigenvalues (Supplementary Figure S2).

TABLE 1 Morphological classification of neurons, modified from von Economo and Koskinas (1925).

Cell type	Cell body shape	Average height (μm)	Average width (μm)
Granular	Circular or polygonal	4–8	4–10
Small pyramidal	Triangular	12	10
Medium pyramidal		25	15
Large pyramidal		30–45	15–20
Gigantic pyramidal		>50	>25
Small fusiform	Spindle-shaped	15	10
Large fusiform		30	15
Polymorphic	Does not fit into any other category (irregular shape)	—	—

Based on the eigenvalue criterion (eigenvalue >1), we determined that for our dataset, the optimal number of factors would be three. We then assessed the factor loadings in the rotated component matrix (Supplementary Table S3) as an aid in informing which parameters were most relevant to describing the morphometric characteristics of different cell types.

Receiver operating characteristic (ROC) analysis was used to assess how effectively different cell types could be classified based on different morphometric parameters at varying threshold values. When determining the desired threshold values, we aimed to achieve a high specificity (preferably above 90%) and a reasonable sensitivity (preferably above 70%).

Based on factor analysis and ROC analysis, we concluded that the parameters *Area*, *Aspect Ratio* and *Form Factor* were most useful for differentiating between different morphological cell types (for a detailed description see Supplementary data).

t-distributed stochastic neighbor embedding (t-SNE) was used to visualize the morphometric data by plotting each datapoint on a two-dimensional map. The t-SNE was run with only the morphometric parameters and two categorical variables (cortical layer and cortical regions) in order to assess whether the grouping of cortical layers would be similar to the results obtained with the neural network prediction algorithm.

The neural network widget in Orange was used to predict which morphological cell type each reconstruction belonged to, based on the cell's morphometric parameters. The neural network widget in Orange uses the multi-layer perceptron supervised learning algorithm developed by scikit-learn (Orange Data Mining, n.d.; scikit-learn, n.d.). The manually classified reconstructions were used as the training data set, while the rest of the reconstructions (87,873 reconstructed cells) constituted the test data set. The predictions from the test data set were used to determine the relative proportions of each morphological cell type. For this analysis, we excluded cells that the prediction algorithm classified into a respective category with less than 50% certainty. The total number of excluded cells was 6026, i.e., 6.86% of the total number of cells in the test data set (Supplementary Table S4).

The chi-square test was used to compare the morphological composition (derived from the predictions of morphological cell types) of cortical regions.

The proportions between the three major morphological cell types (granule, pyramidal and fusiform cells) were visualized using ternary diagrams. The proportions between all seven morphological cell types were visualized using radar diagrams.

For all statistical tests, $p < 0.05$ was considered statistically significant.

3 Results

Our analysis of the cell body reconstructions revealed that the cytoarchitectonic descriptions of BA9, BA14r and BA24 were reflected in the morphometric measures of the cells. Our qualitative observations of the reconstructed cortical columns were also in line with the qualitative descriptions of the analyzed cortical regions (Figure 2; Supplementary Figure S3).

3.1 Average cell size and elongation differed significantly between cortical regions

The average cell size, measured by the parameter *Area*, differed significantly between all three cortical regions ($p < 0.001$ for all comparisons, Kruskal–Wallis test). The cells in BA14r were the smallest on average, with the lowest average *Area* values ($140.53 \pm 80.37\,\mu m^2$). Although the cells in BA24 had the highest average *Area* values ($176.55 \pm 108.83\,\mu m^2$, compared to $164.93 \pm 98.85\,\mu m^2$ in BA9), the largest individual cells were found in BA9 with *Area* values up to $923.41\,\mu m^2$ (Figure 3 and Table 2).

The average elongation of the cells, measured by the parameter *Aspect Ratio*, was significantly lower in BA9 (1.52 ± 0.31) compared to BA14r and BA24 ($p < 0.001$), while the difference between BA14r and BA24 was not significant ($p = 0.111$), though cells in BA24 were slightly more elongated on average (1.59 ± 0.41) than cells in BA14r (1.56 ± 0.33). It is also worth noting that the individual *Aspect Ratio* values were by far the highest in BA24, with maximum values up to 7.60 (compared to 4.19 and 4.52 in BA9 and BA14r respectively). In addition, the CV for *Aspect Ratio* was substantially higher in BA24 (26.09%) than in BA9 (20.36%) and BA14r (20.86%), indicating a higher diversity in cell elongation in this region (Figure 3 and Table 2).

The irregularity and complexity of the cell shape, measured by the parameter *Form Factor*, did not significantly differ between the three cortical regions. Individual cells with the highest cell shape irregularity were found in BA24 with minimum Form Factor values reaching 0.23, compared to 0.31 in BA9 and 0.32 in BA14r (Figure 3 and Table 2).

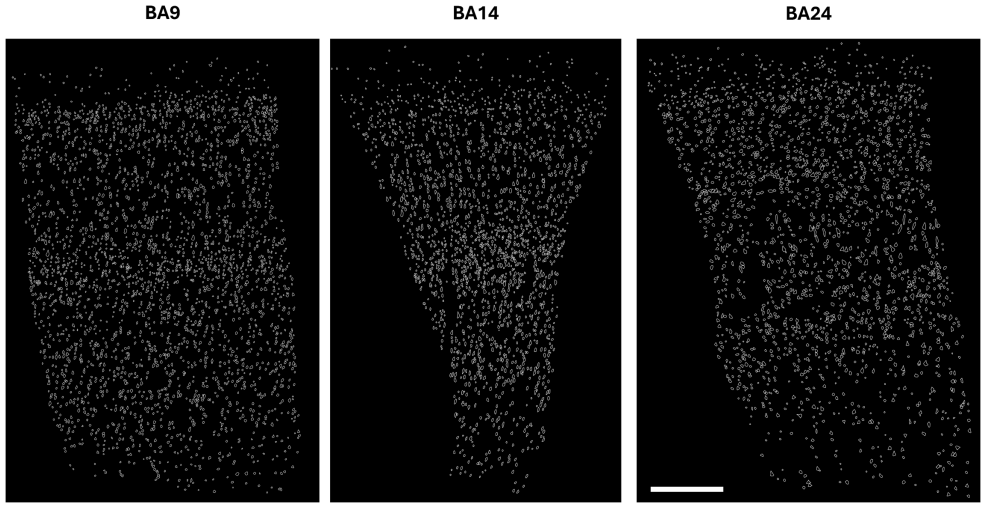

FIGURE 2
Reconstructions of cortical columns of Brodmann area 9, 14r and 24. Scale bar: 500 µm.

3.2 Morphometric parameters differed significantly between cortical layers

The values of *Area*, *Aspect ratio* and *Form Factor* differed significantly between all cortical layers ($p < 0.001$ for all comparisons, Kruskal–Wallis test).

The average cell sizes were substantially lower in layers I, II and IV than in layers III, V and VI in all three of the analyzed cortical regions. The largest individual cells were found in layer III of BA9. The CV for *Area* was highest in layer V in all cortical regions, indicating that layer V had the highest diversity in cell size (Figure 3 and Supplementary Table S5).

On average, cells were far less elongated in layers I, II and IV than in layers III, V and VI in all cortical regions. The most elongated individual cells were found in layer V of BA24, and this layer in BA24 also had by far the highest CV (33.55%) for *Aspect Ratio* (Figure 3 and Supplementary Table S5).

On average, cells had the most irregular shape in layers III, V and VI in all cortical regions (Figure 3 and Supplementary Table S5). These layers also had a higher CV for *Form Factor*, indicating a higher diversity in cell shape complexity compared to layers I, II and IV.

3.3 Neurons can be classified into morphological cell types based on *Area*, *Aspect Ratio* and *Form Factor*

Based on Factor and ROC analysis of the manually classified reconstructions, we determined that the three major morphological cell types—granule cells, pyramidal cells and fusiform cells—could be best distinguished using the parameter *Aspect Ratio* (Figure 4). This is due to the fact that granule cells were the least elongated cell type, while fusiform cells were the most elongated, with pyramidal cells typically falling in between these two categories. ROC analysis revealed that pyramidal and fusiform cells could reliably be distinguished by choosing a threshold for *Aspect Ratio* values of 1.86 (specificity: 90.29%, sensitivity: 82.55%). Distinguishing between pyramidal and granule cells based on *Aspect Ratio* was more challenging, and we determined an acceptable threshold value to be 1.38 (specificity: 80.94%, sensitivity: 69.65%) (Table 3).

The subtypes of pyramidal and fusiform cells could most easily be distinguished using the parameter *Area* (Figure 4). Small and large fusiform cells could be distinguished very reliably with a threshold value of 161.2 µm² for *Area* (specificity: 96.58%, sensitivity: 90.00%). Small and medium pyramidal cells could also be reliably distinguished with a threshold value of 202.2 µm² (specificity: 90.38%, sensitivity: 89.17%). Distinguishing between medium and large pyramidal cells based on *Area* was more challenging, but we determined an acceptable threshold value to be 394.5 µm² (specificity: 89.17%, sensitivity: 70.39%) (Table 3).

Polymorphic cells could be best distinguished using the parameter *Form Factor* (Figure 4), due to such cells having irregular cell body shapes with a high circumference complexity (i.e., lower *Form Factor*). We determined an acceptable threshold value for *Form Factor* to be 0.79 (specificity: 90.20%, sensitivity: 71.32%). A more detailed analysis revealed that distinguishing polymorphic from fusiform cells based only on *Form Factor* values was not sufficiently reliable (the threshold of 0.79 for these two cell types had only 11.05% specificity). Therefore, we analysed other morphometric parameters and determined that polymorphic and fusiform cells could be distinguished by analysing the parameter *Solidity*, since polymorphic cells had more indentations in their cell contours, and thus lower *Solidity* than fusiform cells. An acceptable threshold value for *Solidity* was 0.95 (specificity: 86.00%, sensitivity: 83.87%) (Table 3).

The descriptive statistics for the different cell types are shown in Supplementary Table S6.

3.4 Neural network predictions revealed the morphological composition of cortical regions and layers

After manual classification, the rest of the reconstructions were classified using a neural network prediction algorithm and the

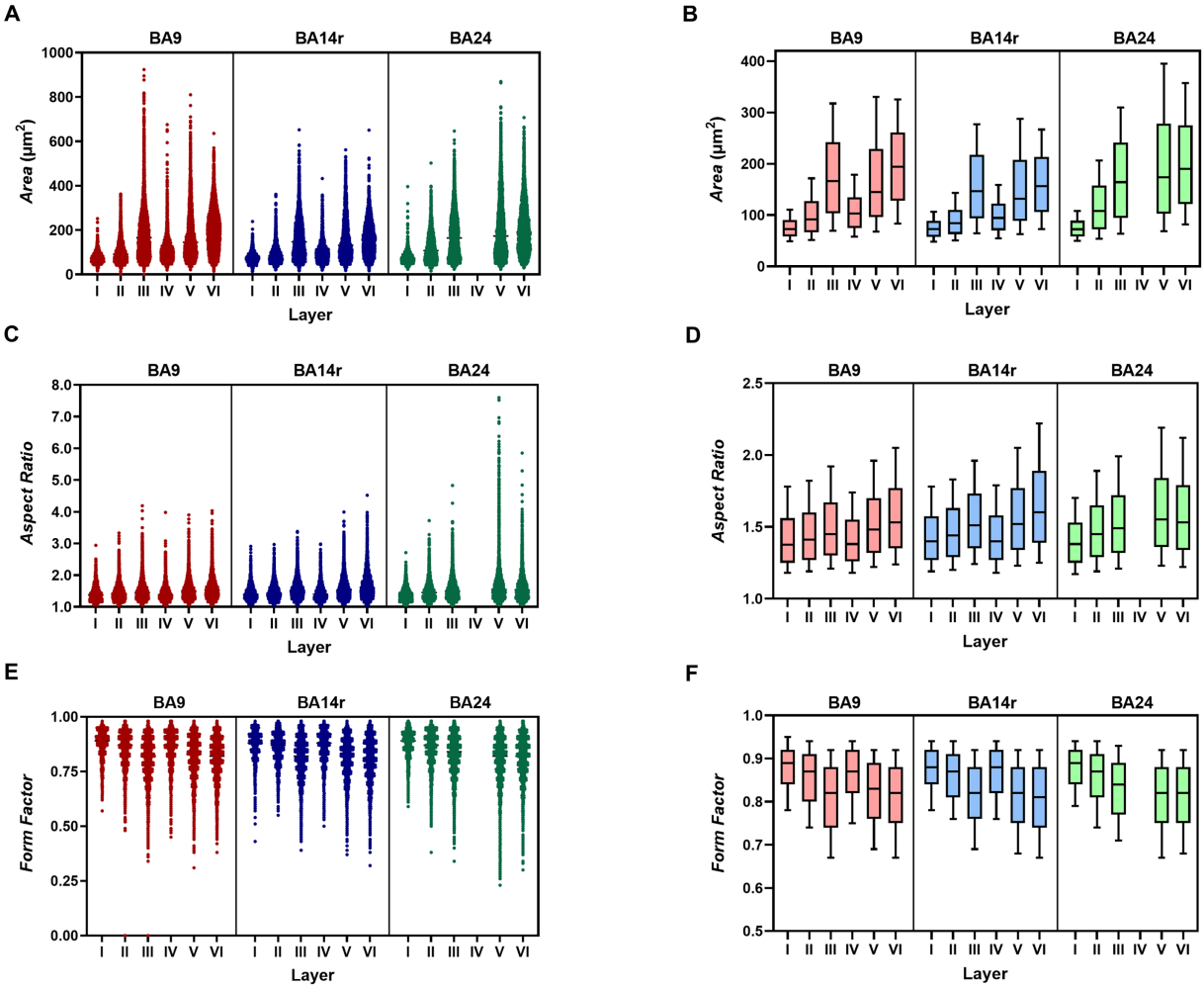

FIGURE 3
Values of morphometric parameters in each layer of each cortical region. **(A)** Scatterplot showing the *Area* values for individual cells. Note the increase in cell size in layer III of BA9 and layer V of BA24. **(B)** Box-plot showing the median *Area* values. The upper and lower borders of the rectangle represent the third and first quartile respectively, while the error bars denote the 90th and 10th percentiles. Note the large median cell sizes in layers III, V and VI, compared to layers I, II and IV. **(C)** Scatterplot showing *Aspect Ratio* values. Note the substantial increase in cell elongation in layer V of BA24. **(D)** Box-plot showing *Aspect Ratio* values. Note the gradual increase in cell elongation from BA9, through BA14r to BA24. **(E)** Scatterplot showing Form Factor values. Note that the lowest individual values are found in BA24. **(F)** Box-plot showing Form Factor values. Note the lower values in layers III, V and VI compared to layers I, II, and IV.

predictions were used to calculate the relative proportions of morphological cell types for each cortical region and layer.

Our analysis determined that granule cells were the predominant cell type in BA14r (47.48% of all cells), while the relative proportions of granule cells were a bit lower in BA9 (41.76%) and BA24 (39.60%). Pyramidal cells were more prevalent in BA9 (46.39%) than in BA14r (43.33%) and BA24 (41.03%). Fusiform and polymorphic cells were most prevalent in BA24 (9.63 and 9.74% respectively), whereas these two cell types combined constituted only around 10% of cells in BA9 and BA14r. The differences in the morphologic composition between cortical regions were statistically significant ($p < 0.001$, chi-squared test).

When analyzing individual cortical layers, it was apparent that layers I, II and IV had very a different morphological structure compared to layers III, V and VI, in all three regions (Figures 5–7).

In layer I, granule cells constituted over 80% of all cell types in all three cortical regions, with the prediction algorithm classifying the rest of the cells as either small pyramidal, small fusiform or polymorphic. No cells in layer I were classified as medium or large pyramidal or as large fusiform.

In layer II, granule cells constituted over 65% of all cell types in BA9 and BA14r, and over 58% in BA24, with most of the other cells (above 20% in each region) being classified as small pyramidal. Less than 1% of cells in this layer were classified as large pyramidal or large fusiform.

In layer III, pyramidal cells were the most prevalent cell type, constituting above 50% of all cells in BA9 and BA14r, and 43.80% in BA24. The prediction algorithm classified only 4.98 and 7.01% of the pyramidal cells as large pyramidal in BA14r and BA24 respectively, while in BA9 23.07% of pyramidal cells were classified as large pyramidal. Granule cells were the second most common cell type in this layer, and were slightly more prevalent in BA14r (38.12%) and BA24 (37.77%) than in BA9 (34.64%). Fusiform and polymorphic cells were relatively rare in BA9 and

TABLE 2 Descriptive statistics for morphometric parameters for the three analyzed cortical regions.

	BA	Mean ± SD	95% CI for mean	CV	Median	IQR	Mode	Minimum	Maximum
Area (μm²)	9	164.93 ± 98.85	163.93–165.93	59.94%	139.66	131.82	51.76	12.19	923.41
	14	140.53 ± 80.37	139.59–141.46	57.19%	117.53	107.33	52.72	13.09	652.10
	24	176.55 ± 108.83	175.20–177.90	61.64%	151.03	148.89	61.32	15.35	869.85
Aspect Ratio	9	1.52 ± 0.31	1.52–1.53	20.36%	1.45	0.37	1.31	1.04	4.19
	14	1.56 ± 0.33	1.56–1.57	20.86%	1.5	0.39	1.34	1.04	4.52
	24	1.59 ± 0.41	1.58–1.59	26.09%	1.5	0.42	1.36	1.05	7.60
Form Factor	9	0.82 ± 0.09	0.82–0.82	11.48%	0.84	0.12	0.88	0.31	0.98
	14	0.82 ± 0.09	0.82–0.83	10.83%	0.84	0.12	0.89	0.32	0.98
	24	0.82 ± 0.10	0.82–0.82	11.56%	0.84	0.13	0.88	0.23	0.98

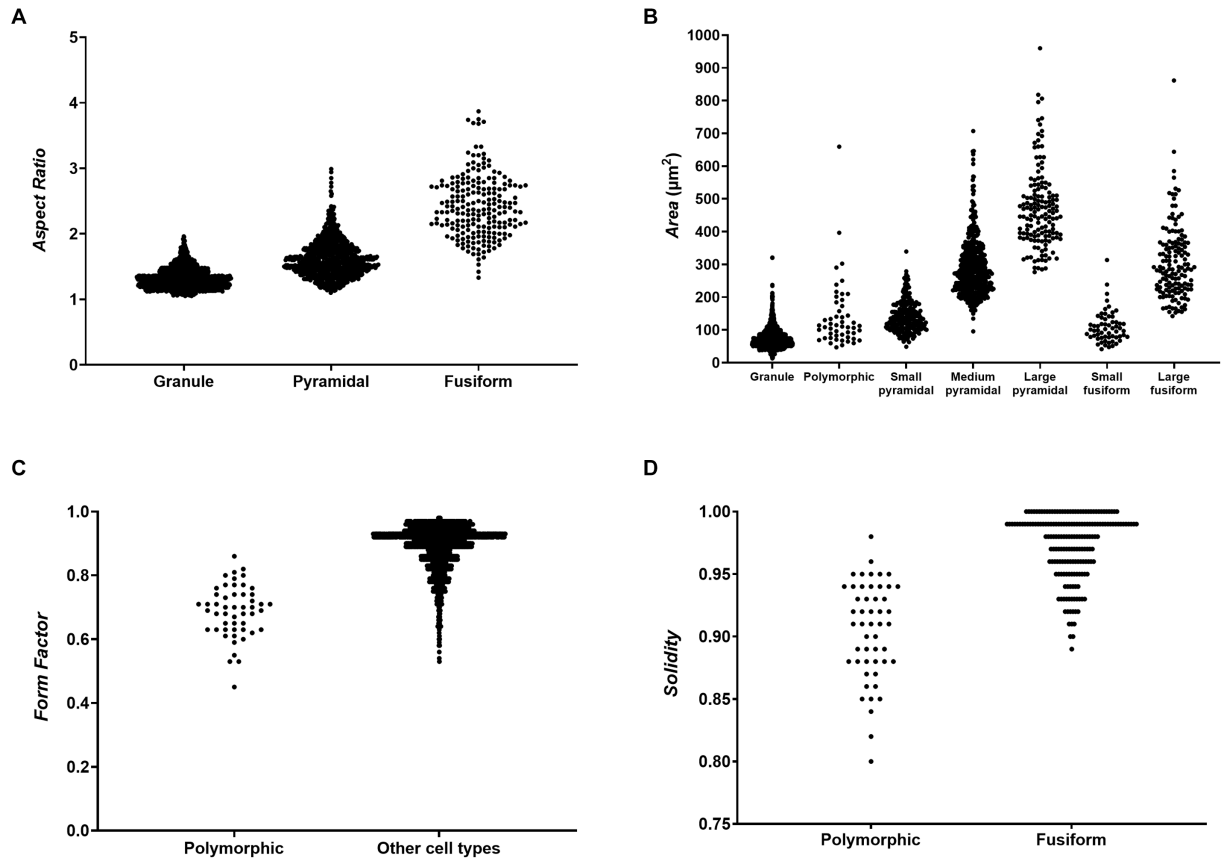

FIGURE 4
Scatter plots showing values of morphometric parameters for different morphological cells types. **(A)** *Aspect Ratio* values for granule, pyramidal and fusiform cells showing that the three main morphological cell types can be distinguished based on cell elongation. **(B)** *Area* values for all cell types showing that subtypes of pyramidal and fusiform cells can be distinguished based on cell size. **(C)** *Form Factor* values for polymorphic cells and all other cell types showing that polymorphic cells have, on average, more complex cell contours. **(D)** *Solidity* values for polymorphic and fusiform cells showing that polymorphic cells have more indentations in their cell contours, which enables them to be distinguished from fusiform cells with similar *Form Factor* values.

BA14r (5% or lower in both regions for both cell types), but were more prevalent in BA24 (fusiform cells—7.68%, polymorphic cells—10.75%).

In layer IV, granule cells were once again the most prevalent cell type and constituted more than 65% of all cell types in BA9 and BA14r, similar to layer II in these regions. Also similar to layer II, the second most prevalent cell type were small pyramidal cells (around 20% in both regions). However, the number of cells classified as medium and large pyramidal in layer IV was slightly larger than in layer II in both cortical regions.

In layer V, pyramidal cells were the most common type (above 45% in all three cortical regions), followed by granule cells (above 35% in all cortical regions). Compared to layer III, almost twice as many cells were classified as fusiform cells in all three cortical regions, with

TABLE 3 Threshold values of morphometric parameters for distinguishing morphological cell types.

Cell type	Proposed threshold values	
Granule	*Aspect Ratio* < 1.38	
Small pyramidal	*Aspect Ratio*: 1.38–1.86	*Area* < 202.2 μm²
Medium pyramidal		*Area*: 202.2–394.5 μm²
Large pyramidal		*Area* > 394.5 μm²
Small fusiform	*Aspect Ratio* > 1.86	*Area* < 161.2 μm²
Large fusiform		*Area* > 161.2 μm²
Polymorphic	*Form Factor* < 0.79 *Solidity* < 0.95	

the proportion of cells classified as fusiform cells in BA24 being especially high (13.74%). In addition, more fusiform cells in layer V were classified as large than as small, which is in contrast to layers I–IV.

In layer VI, pyramidal cells were also the most common cell type (above 45% in all three cortical regions), and granule cells were the second most common, though a bit less prevalent than in layer V (around 30% in all cortical regions). In BA9 and BA14r, almost twice as many cells were classified as fusiform cells than in layer V (above 13% in both regions). This was not the case in BA24, where the proportion of fusiform cells was similar in layers V (13.74%) and VI (11.64%). Out of all the fusiform cells in layer VI, above two thirds were classified as large fusiform in all three cortical regions. In addition, layer VI had the largest proportion of polymorphic cells compared to the other layers in all three cortical regions.

The morphological composition of layers I, II and IV differed only slightly between cortical regions, however, layers III, V and VI revealed relatively region-specific morphological compositions as seen on the radar diagrams (Figures 6, 7).

The results of t-SNE were consistent with the results we obtained by analyzing the neural network predictions (Figure 8). Cells from layers I, II and IV were grouped closer together than cells from layers III, V and VI. No clear separation in the grouping of cells from layers II and IV could be observed, which is reflected in the similar morphological composition of these layers, and the same was true for layers III, V and VI. It should be noted that the groupings of cortical layers by t-SNE were derived independently from the morphological compositions determined by the neural network.

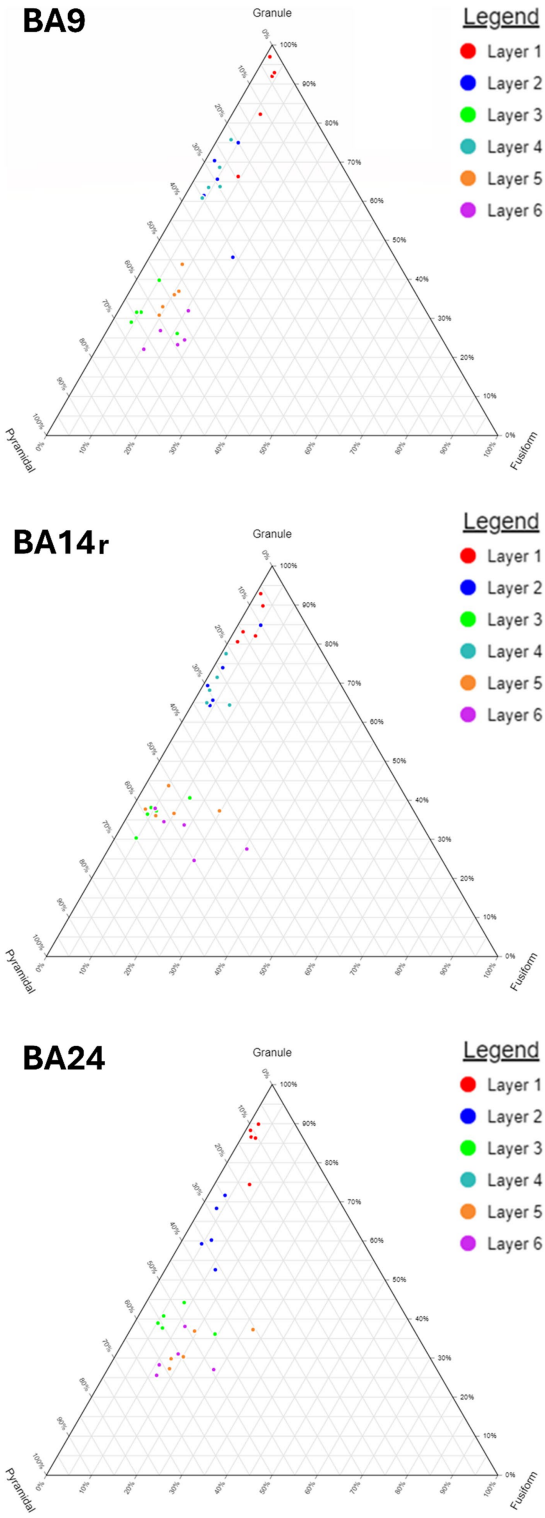

FIGURE 5
Ternary diagrams showing the relative proportions of granule, pyramidal and fusiform cells in Brodmann areas 9, 14r and 24. Note the gradual increase in the proportion of fusiform cells from BA9 through BA14r to BA24. Also note the relatively similar composition of layers II and IV as well as the difference in their composition to layers III, V, and VI.

4 Discussion

In this research we reconstructed the cell bodies of NeuN⁺ cells in three cortical regions of the PFC—BA9, BA14r and BA24. We analyzed the morphometric characteristics of these cell bodies and compared them between these cortical regions and all cortical layers, finding significant differences in the values of *Area*, *Aspect Ratio* and *Form Factor*. We manually classified a portion of the reconstructions into morphological cell types. We used ROC analysis to determine the best thresholds for distinguishing between cell types based on morphometric parameters. We also used the manually classified reconstructions as training data for a neural network prediction algorithm that was then used to classify the rest of the reconstructions. Based on the neural network classification, we established the morphological composition of cortical layers in the three analyzed cortical regions and determined the specificities of each region and layer.

10.3389/fnana.2024.1441645

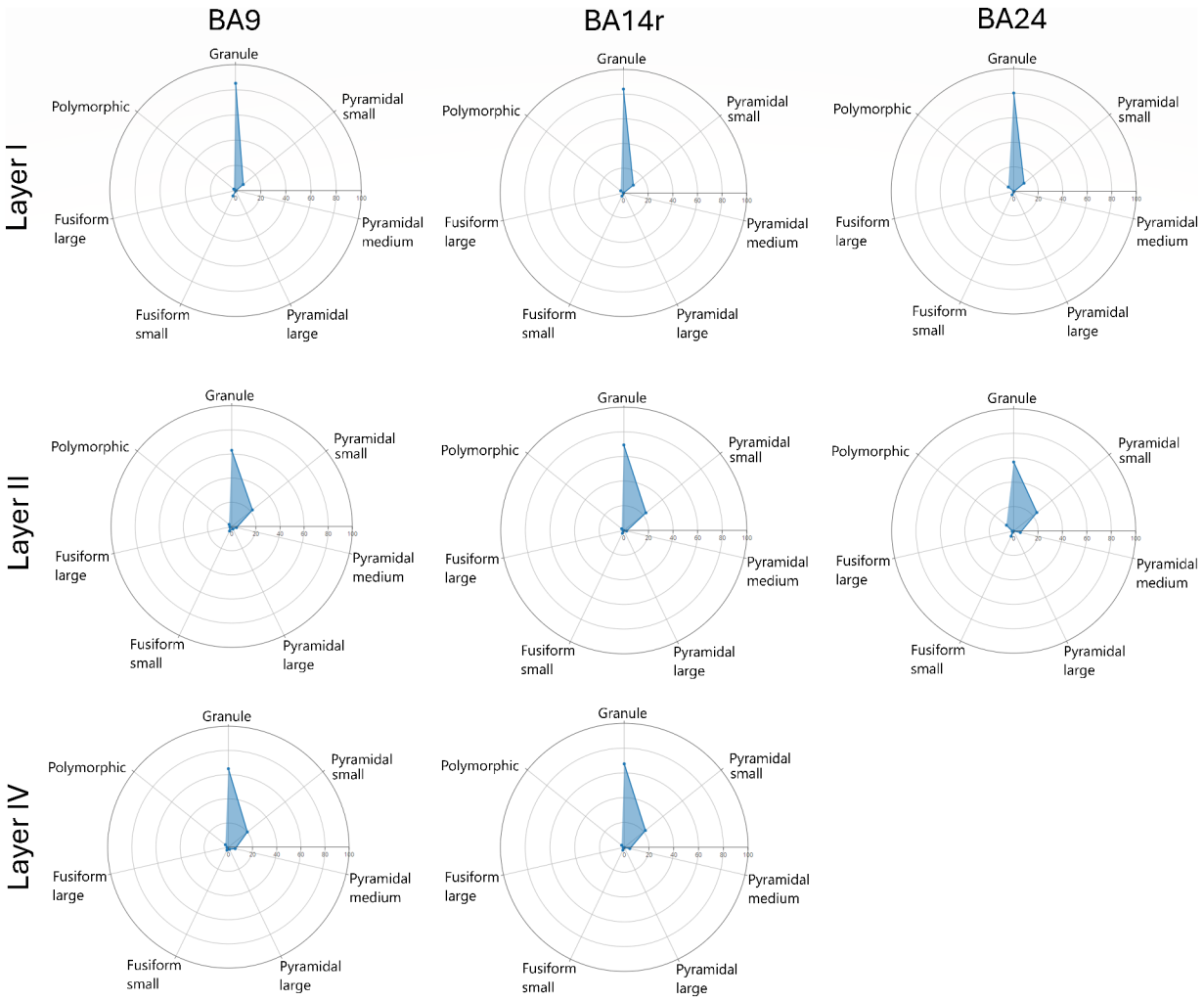

FIGURE 6
Radar diagrams showing the morphological composition of layers I, II and IV in Brodmann areas 9, 14r and 24. Note the similar compositions of layers II and IV as well as the predominance of granule cells in layer I. Also note the slight increase in the proportion of polymorphic cells in BA24.

4.1 BA9 was characterized by an abundance of large pyramidal cells present in layer III

Individual neurons in BA9 were the largest (highest *Area* values) among the three cortical regions, though the average neuron size was somewhat higher in BA24. Laminar analysis showed that such large cells were found almost exclusively in layer III of BA9. This seemed to indicate an abundance of large pyramidal cells in the deep part of layer III, which is characteristic for homotypical isocortical regions in the PFC that have extensive associative projections (Petanjek et al., 2019). This relative abundance of large pyramidal cells in layer III of BA9 was confirmed using the neural network prediction model, with BA9 having over thrice as many large pyramidal cells in layer III than BA14r and BA24.

Neurons in BA9 were less elongated compared to BA14r and BA24. This is in concordance with the cytoarchitectonic descriptions of Brodmann (1909) and von Economo and Koskinas (1925), who described a high proportion of granule and pyramidal cells in this region. This was also in line with the results of our neural network prediction model, which showed the lowest proportion of fusiform cells in this region.

4.2 BA14r was characterized by smaller average cell size and a relative abundance of granule cells in layer III

Neurons in BA14r were, on average, the smallest among the analyzed cortical regions, which was reflected in the relatively low proportions cells classified as large pyramidal and large fusiform by the prediction model. Cytoarchitectonic descriptions of this region mention a significant decrease in the proportion of large pyramidal cells (von Economo and Koskinas, 1925; Ongür et al., 2003), which is consistent with our finding. *Aspect Ratio* values of cells in this region were higher than in BA9, which is in line with the pattern of cell elongation from dorsal to orbital regions of the PFC (von Economo and Koskinas, 1925; Ongür et al., 2003). However, since the overall proportion of fusiform cells did not increase in BA14r compared to BA9, the slightly higher cell elongation in this region cannot be explained by a change in the prevalence of fusiform morphological cell types. It is likely that this increase in cell elongation is a consequence of morphological modifications of pyramidal cells. This process of pyramidal cell transformation into elongated modified

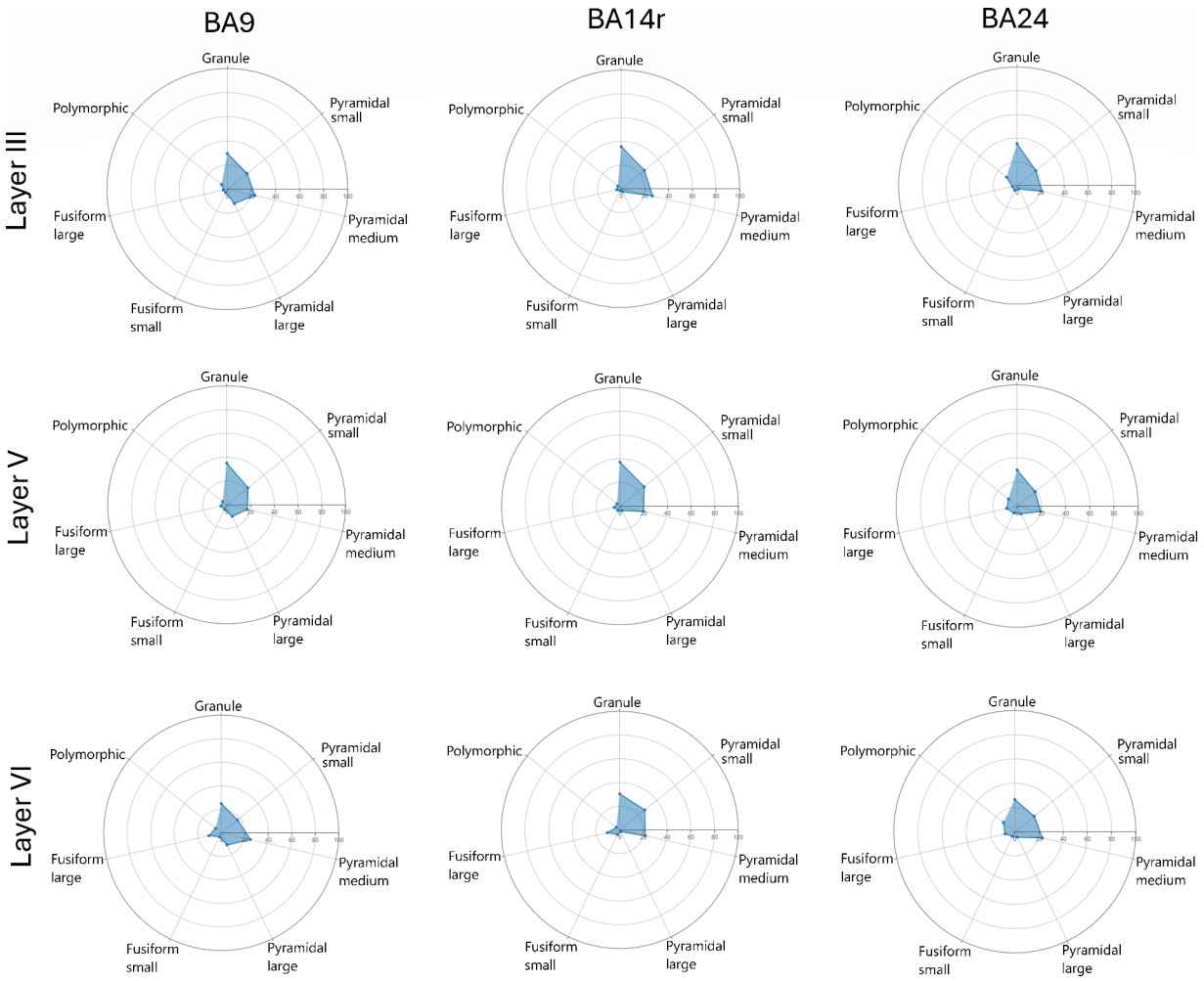

FIGURE 7
Radar diagrams showing the morphological composition of layers III, V and VI in Brodmann areas 9, 14r and 24. Note the increase in the proportion of large pyramidal cells in layer III of BA9 as well as the increase in the proportion of cells classified as large fusiform in layer V of BA24. Also note the slight increase in the proportion of polymorphic cells in BA24.

pyramidal cells was described by von Economo and Koskinas (1925) as spindle transformation (*Verspindelung*), and was described predominantly in layers III and V. These descriptions are consistent with our findings, because we determined the largest increase in cell elongation in layers III, V and VI of BA14r compared to BA9.

Interestingly, even though BA14r is usually described as dysgranular, the proportion of granule cells was generally high in this region. In particular, the proportion of granule cells in layer III of BA14 was slightly higher than in BA9. A likely explanation for this finding is the more difficult delineation between layers III and IV, because of which more granule cells seem to be present in layer III.

4.3 BA24 was characterized by extreme cell elongation in layer V

Neurons in BA24 were the largest on average among the three cortical regions. The average increase in cell size was probably, at least partly, due to the general increase in relative thickness of layers V and VI in BA24, since these layers contained, on average, the largest neurons in general. In addition, the average cell size in layer V of BA24 was exceptionally high with the largest individual cells also being found in layer V of this region. This is in contrast to BA9 and BA14r, where the largest individual cells were found in layer III.

Cell elongation in BA24 was higher on average than in BA9 and BA14r. Further analysis showed that this increase in cell elongation was most prominent in layer V of BA24. This was further confirmed by the neural network prediction model, which showed an increase in the proportion of large fusiform cells in this region, particularly in layer V. This increase is likely due to the presence of specialized cells, called von Economo neurons (VENs) (von Economo and Koskinas, 1925; von Economo, 1927; Banovac et al., 2021; Petanjek et al., 2023). VENs are large, highly elongated rod-shaped cells abundant only in layer V of two cortical regions in humans—the anterior cingulate cortex (which corresponds to BA24) and the fronto-insular cortex.

The increase in cell size, as well as the increase in cell elongation in layer V of BA24 is highly indicative of the presence of VENs. Since in the training data we did not manually classify any specialized cell types, it is most likely that the prediction algorithm classified VENs as large fusiform cells, since that was the cell type they were most similar

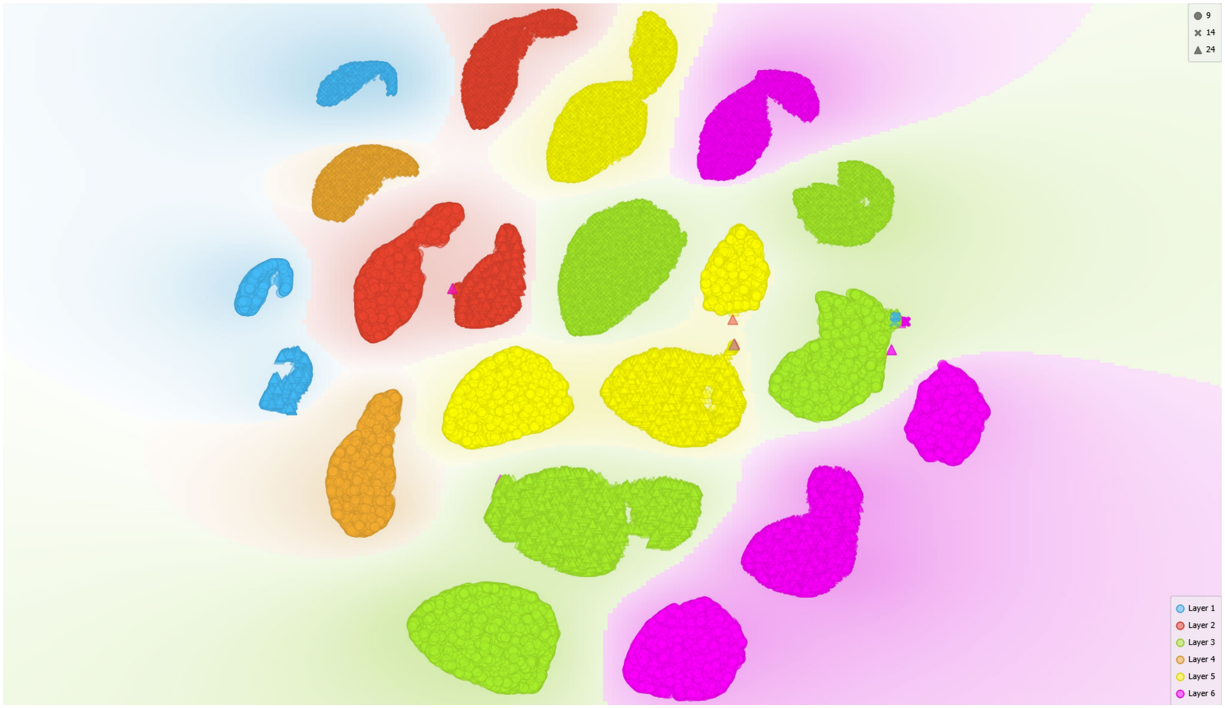

FIGURE 8
Results of t-SNE plotted on a two-dimensional diagram. Note the lack of clear separation in the grouping of layers II and IV as well as layers III, V, and VI.

to. However, it should be noted that VENs are specialized cells and should be distinguished from the typical fusiform cells commonly found in the deep layers of the cerebral cortex.

Interestingly, neurons in BA24 had the lowest individual minimum values of *Form Factor*, indicating that this region contained more cells with highly irregular cell shapes and complex cell contours. This is in concordance with the results of the neural network prediction model, which showed a substantially higher proportion of polymorphic and fusiform cells in this region.

4.4 Objective delineation of cortical regions and layers may have translational potential

Determining the distribution of different neuron types in the cerebral cortex enables the objectivization of morphological and functional organization within specific cortical regions and layers. The results of our research could help develop a standardized way of identifying cortical regions and layers without relying on experts' subjective assessment. This research also has translational potential, with possible applicability in the objective detection of morphological alterations of neural microcircuitry in neuropathological conditions. For example, such an algorithm could be further developed to assist in the evaluation of the histological characteristics of CNS tumors, or in the assessment of progression of various neurodegenerative diseases.

The results of the neural network prediction model were in line with our expectations based on qualitative descriptions of the examined regions' cytoarchitectonics. This supports the notion that the prediction model was relatively successful in classifying cells based on the training data, and suggests that such models could be utilized in aiding morphological analyses in neuroscience research. Future research should focus on cross-validation of the model, as well as on applying such prediction models to other cortical regions, neuropathological conditions, and other species besides humans. When using such an algorithm in other cortical regions, it might be necessary to take into account the presence of additional cell types—e.g., Betz cells in the primary motor cortex or Purkinje cells in the cerebellar cortex.

A conceivable end-goal should be producing a quality model, utilizing machine learning, that could accurately delineate cortical regions and layers, as well as determine their morphological compositions and evaluate possible morphological alterations in neuropathology. In conclusion, we demonstrated that supervised machine learning, if provided with sufficient quality input data, could significantly aid in defining the morphological characteristics of the cerebral cortex.

Data availability statement

The original contributions presented in the study are included in the article/Supplementary material, further inquiries can be directed to the corresponding author.

Ethics statement

The studies involving humans were approved by University of Zagreb School of Medicine Ethics Committee. The studies were

conducted in accordance with the local legislation and institutional requirements. The human samples used in this study were acquired as part of a previous study for which ethical approval was obtained. Written informed consent for participation was not required from the participants or the participants' legal guardians/next of kin in accordance with the national legislation and institutional requirements.

Author contributions

MP: Data curation, Formal analysis, Investigation, Methodology, Resources, Software, Validation, Visualization, Writing – original draft. ZP: Conceptualization, Funding acquisition, Resources, Supervision, Writing – review & editing. IB: Conceptualization, Formal analysis, Funding acquisition, Investigation, Methodology, Project administration, Resources, Software, Supervision, Validation, Visualization, Writing – original draft.

Funding

The author(s) declare that financial support was received for the research, authorship, and/or publication of this article. This research was supported by the Croatian Science Foundation Grant No. IP-2022-10-8493 (Uniqueness in development of interneurons in human prefrontal cortex during fetal life and first postnatal year—implications in pathogenesis of schizophrenia and autism, PI: ZP) and No. IP-2019-04-3182 (Brain extracellular matrix in development and in perinatal hypoxia, PI: Nataša Jovanov Milošević) as well as the University of Zagreb Support Grant No. 10106-23-2407.

Conflict of interest

The authors declare that the research was conducted in the absence of any commercial or financial relationships that could be construed as a potential conflict of interest.

The author(s) declared that they were an editorial board member of Frontiers, at the time of submission. This had no impact on the peer review process and the final decision.

Publisher's note

Supplementary material

The Supplementary material for this article can be found online at: https://www.frontiersin.org/articles/10.3389/fnana.2024.1441645/full#supplementary-material

References

Banovac, I., Sedmak, D., Džaja, D., Jalšovec, D., Jovanov Milošević, N., Rašin, M. R., et al. (2019). Somato-dendritic morphology and axon origin site specify von Economo neurons as a subclass of modified pyramidal neurons in the human anterior cingulate cortex. *J. Anat.* 235, 651–669. doi: 10.1111/joa.13068

Banovac, I., Sedmak, D., Esclapez, M., and Petanjek, Z. (2022). The distinct characteristics of somatostatin neurons in the human brain. *Mol. Neurobiol.* 59, 4953–4965. doi: 10.1007/s12035-022-02892-6

Banovac, I., Sedmak, D., Judaš, M., and Petanjek, Z. (2021). Von Economo neurons—primate-specific or commonplace in the mammalian brain? *Front. Neural Circuits* 15:714611. doi: 10.3389/fncir.2021.714611

Banovac, I., Sedmak, D., Rojnić Kuzman, M., Hladnik, A., and Petanjek, Z. (2020). Axon morphology of rapid Golgi-stained pyramidal neurons in the prefrontal cortex in schizophrenia. *Croat. Med. J.* 61, 354–365. doi: 10.3325/cmj.2020.61.354

Boenisch, T. (2005). Effect of heat-induced antigen retrieval following inconsistent formalin fixation. *Appl. Immunohistochem. Mol. Morphol.* 13, 283–286. doi: 10.1097/01.0000146524.74402.a4

Braak, H. (1980). Architectonics of the human telencephalic cortex. Berlin: Springer.

Brodmann, K. (1909). Vergleichende Lokalisationslehre der Grosshirnrinde in ihren Prinzipien dargestellt auf Grund des Zellenbaues. Leipzig: Barth.

Demšar, J., Curk, T., Erjavec, A., Gorup, C., Hocevar, T., Milutinovic, M., et al. (2013). Orange: data mining toolbox in Python. *J. Mach. Learn. Res.* 14, 2349–2353.

Džaja, D., Hladnik, A., Bičanić, I., Baković, M., and Petanjek, Z. (2014). Neocortical calretinin neurons in primates: increase in proportion and microcircuitry structure. *Front. Neuroanat.* 8:103. doi: 10.3389/fnana.2014.00103

Fajardo, C., Escobar, M. I., Buriticá, E., Arteaga, G., Umbarila, J., Casanova, M. F., et al. (2008). Von Economo neurons are present in the dorsolateral (dysgranular) prefrontal cortex of humans. *Neurosci. Lett.* 435, 215–218. doi: 10.1016/j.neulet.2008.02.048

Flechsig, P. E. (1897). Zur Anatomie des vorderen Sehhügelstiels, des Cingulum und der Acusticusbahn. *Neurol. Cbl* 16, 290–295.

Fuster, J. M. (2015). The prefrontal cortex. Amsterdam: Academic Press.

González-Acosta, C. A., Escobar, M. I., Casanova, M. F., Pimienta, H. J., and Buriticá, E. (2018). Von Economo neurons in the human medial frontopolar cortex. *Front. Neuroanat.* 12:64. doi: 10.3389/fnana.2018.00064

Hammarberg, C. (1895). Studien über Klinik und Pathologie der Idiotie: nebst Untersuchungen über die normale Anatomie der Hirnrinde. Upsala: Berling.

Hladnik, A., Džaja, D., Darmopil, S., Jovanov-Milošević, N., and Petanjek, Z. (2014). Spatio-temporal extension in site of origin for cortical calretinin neurons in primates. *Front. Neuroanat.* 8:50. doi: 10.3389/fnana.2014.00050

Judaš, M., Šimić, G., Petanjek, Z., Jovanov-Milošević, N., Pletikos, M., Vasung, L., et al. (2011). The Zagreb Collection of human brains: a unique, versatile, but underexploited resource for the neuroscience community. *Ann. N. Y. Acad. Sci.* 1225, E105–E130. doi: 10.1111/j.1749-6632.2011.05993.x

Kostovic, I., Judas, M., Kostovic-Knezevic, L., Simic, G., Delalle, I., Chudy, D., et al. (1991). Zagreb research collection of human brains for developmental neurobiologists and clinical neuroscientists. *Int. J. Dev. Biol.* 35, 215–230

Marín, O. (2012). Interneuron dysfunction in psychiatric disorders. *Nat. Rev. Neurosci.* 13, 107–120. doi: 10.1038/nrn3155

Meynert, T. (1867). Der Bau der Gross-Hirnrinde und seine örtlichen Verschiedenheiten, nebst einem pathologisch-anatomischen Corollarium. *Vierteljahresschr. Psychiatr.* 1, 198–217.

Meynert, T. (1868). Neue Untersuchungen über den Bau der Grosshirnrinde und ihre örtlichen Verschiedenheiten. *Allg. Wien. Med. Ztg.* 13, 419–428.

Mihaljević, B., Bielza, C., Benavides-Piccione, R., Defelipe, J., and Larrañaga, P. (2014). Multi-dimensional classification of GABAergic interneurons with Bayesian network-modeled label uncertainty. *Front. Comput. Neurosci.* 8:150. doi: 10.3389/fncom.2014.00150

Mihaljević, B., Larrañaga, P., Benavides-Piccione, R., Hill, S., Defelipe, J., and Bielza, C. (2018). Towards a supervised classification of neocortical interneuron morphologies. *BMC Bioinformatics* 19:511. doi: 10.1186/s12859-018-2470-1

Morales-Gregorio, A., van Meegen, A., and van Albada, S. J. (2023). Ubiquitous lognormal distribution of neuron densities in mammalian cerebral cortex. *Cereb. Cortex* 33, 9439–9449. doi: 10.1093/cercor/bhad160

Neumann, M., and Gabel, D. (2002). Simple method for reduction of autofluorescence in fluorescence microscopy. *J. Histochem. Cytochem.* 50, 437–439. doi: 10.1177/002215540205000315

Nieuwenhuys, R. (1994). The neocortex. An overview of its evolutionary development, structural organization and synaptology. *Anat. Embryol.* 190, 307–337. doi: 10.1007/BF00187291

Ongür, D., Ferry, A. T., and Price, J. L. (2003). Architectonic subdivision of the human orbital and medial prefrontal cortex. *J. Comp. Neurol.* 460, 425–449. doi: 10.1002/cne.10609

Ongür, D., and Price, J. L. (2000). The organization of networks within the orbital and medial prefrontal cortex of rats, monkeys and humans. *Cereb. Cortex* 10, 206–219. doi: 10.1093/cercor/10.3.206

Orange Data Mining. (n.d.) Neural network. Available at: https://orangedatamining.com/widget-catalog/model/neuralnetwork/

Petanjek, Z., Banovac, I., Sedmak, D., Prkačin, M. V., and Hladnik, A. (2023). Von Economo neurons as a specialized neuron class of the human cerebral cortex. *Front. Mamm. Sci.* 2:1242289. doi: 10.3389/fmamm.2023.1242289

Petanjek, Z., Sedmak, D., Džaja, D., Hladnik, A., Rašin, M. R., and Jovanov-Milosevic, N. (2019). The protracted maturation of associative layer IIIC pyramidal neurons in the human prefrontal cortex during childhood: a major role in cognitive development and selective alteration in autism. *Front. Psychiatry* 10:122. doi: 10.3389/fpsyt.2019.00122

Petrides, M., and Pandya, D. N. (1999). Dorsolateral prefrontal cortex: comparative cytoarchitectonic analysis in the human and the macaque brain and corticocortical connection patterns. *Eur. J. Neurosci.* 11, 1011–1036. doi: 10.1046/j.1460-9568.1999.00518.x

Petrides, M., Tomaiuolo, F., Yeterian, E. H., and Pandya, D. N. (2012). The prefrontal cortex: comparative architectonic organization in the human and the macaque monkey brains. *Cortex* 48, 46–57. doi: 10.1016/j.cortex.2011.07.002

Prkačin, M. V., Banovac, I., Petanjek, Z., and Hladnik, A. (2023). Cortical interneurons in schizophrenia—cause or effect? *Croat. Med. J.* 64, 110–122. doi: 10.3325/cmj.2023.64.110

Rajkowska, G., and Goldman-Rakic, P. S. (1995a). Cytoarchitectonic definition of prefrontal areas in the normal human cortex: I. Remapping of areas 9 and 46 using quantitative criteria. *Cereb. Cortex* 5, 307–322. doi: 10.1093/cercor/5.4.307

Rajkowska, G., and Goldman-Rakic, P. S. (1995b). Cytoarchitectonic definition of prefrontal areas in the normal human cortex: II. Variability in locations of areas 9 and 46 and relationship to the Talairach Coordinate System. *Cereb. Cortex* 5, 323–337. doi: 10.1093/cercor/5.4.323

Rivara, C.-B., Sherwood, C. C., Bouras, C., and Hof, P. R. (2003). Stereologic characterization and spatial distribution patterns of Betz cells in the human primary motor cortex. *Anat. Rec. A* 270A, 137–151. doi: 10.1002/ar.a.10015

Sadeghipour, A., and Babaheidarian, P. (2019). Making formalin-fixed, paraffin embedded blocks. *Methods Mol. Biol.* 1897, 253–268. doi: 10.1007/978-1-4939-8935-5_22

scikit-learn. (n.d.) Machine learning in Python. Available at: https://scikit-learn.org/stable/modules/neural_networks_supervised.html

Štajduhar, A., Lipić, T., Lončarić, S., Judaš, M., and Sedmak, G. (2023). Interpretable machine learning approach for neuron-centric analysis of human cortical cytoarchitecture. *Sci. Rep.* 13:5567. doi: 10.1038/s41598-023-32154-x

Sun, Y., Ip, P., and Chakrabartty, A. (2017). Simple elimination of background fluorescence in formalin-fixed human brain tissue for immunofluorescence microscopy. *J. Vis. Exp.* 2017:56188. doi: 10.3791/56188

Sy, J., and Ang, L.-C. (2019). Microtomy: cutting formalin-fixed, paraffin-embedded sections. *Methods Mol. Biol.* 1897, 269–278. doi: 10.1007/978-1-4939-8935-5_23

Talairach, J., and Szikla, G. (1980). Application of stereotactic concepts to the surgery of epilepsy. *Acta Neurochir. Suppl.* 30, 35–54. doi: 10.1007/978-3-7091-8592-6_5

Vogt, B. A., Nimchinsky, E. A., Vogt, L. J., and Hof, P. R. (1995). Human cingulate cortex: surface features, flat maps, and cytoarchitecture. *J. Comp. Neurol.* 359, 490–506. doi: 10.1002/cne.903590310

von Economo, C. (1927). Zellaufbau der Grosshirnrinde des Menschen. Berlin: Springer.

von Economo, C. F., and Koskinas, G. N. (1925). Die Cytoarchitektonik der Hirnrinde des erwachsenen Menschen. Wien: Springer.

von Economo, C., and Triarhou, L. C. (2009). Cellular structure of the human cerebral cortex. Basel: Karger.

Zaqout, S., Becker, L.-L., and Kaindl, A. M. (2020). Immunofluorescence staining of paraffin sections step by step. *Front. Neuroanat.* 14:582218. doi: 10.3389/fnana.2020.582218

frontiers | Frontiers in Molecular Neuroscience

TYPE Original Research
PUBLISHED 15 August 2024
DOI 10.3389/fnmol.2024.1439994

OPEN ACCESS

EDITED BY
Marija Heffer,
Josip Juraj Strossmayer University of Osijek, Croatia

REVIEWED BY
Raquel Campos,
Federal University of Rio de Janeiro, Brazil
Cláudio Roque,
University of Beira Interior, Portugal

*CORRESPONDENCE
Dinko Mitrečić
✉ dinko.mitrecic@mef.hr

RECEIVED 28 May 2024
ACCEPTED 22 July 2024
PUBLISHED 15 August 2024

CITATION
Lisjak D, Alić I, Šimunić I and Mitrečić D (2024) Transplantation of neural stem cells improves recovery of stroke-affected mice and induces cell-specific changes in GSDMD and MLKL expression.
Front. Mol. Neurosci. 17:1439994.
doi: 10.3389/fnmol.2024.1439994

Transplantation of neural stem cells improves recovery of stroke-affected mice and induces cell-specific changes in GSDMD and MLKL expression

Damir Lisjak[1], Ivan Alić[2], Iva Šimunić[1] and Dinko Mitrečić[1]*

[1]Laboratory for Stem Cells, Department for Regenerative Neuroscience, Croatian Institute for Brain Research, School of Medicine, University of Zagreb, Zagreb, Croatia, [2]Department of Anatomy, Histology and Embryology, Faculty of Veterinary Medicine, University of Zagreb, Zagreb, Croatia

Introduction: Stroke, the second leading cause of death and disability in Europe, is primarily caused by interrupted blood supply, leading to ischemia–reperfusion (IR) injury and subsequent neuronal death. Current treatment options are limited, highlighting the need for novel therapies. Neural stem cells (NSCs) have shown promise in treating various neurological disorders, including stroke. However, the underlying mechanisms of NSC-mediated recovery remain unclear.

Methods: Eighty C57Bl/6–Tyrc-Brd mice underwent ischemic stroke induction and were divided into four groups: sham, stroke-affected, stroke-affected with basal cell medium injection, and stroke-affected with NSCs transplantation. NSCs, isolated from mouse embryos, were stereotaxically transplanted into the stroke-affected brains. Magnetic resonance imaging (MRI) and neurological scoring were used to assess recovery. Immunohistochemical analysis and gene expression assays were performed to evaluate pyroptosis and necroptosis markers.

Results: NSC transplantation significantly improved neurological recovery compared to control groups. In addition, although not statistically significant, NSCs reduced stroke volume. Immunohistochemical analysis revealed upregulation of Gasdermin D (GSDMD) expression post-stroke, predominantly in microglia and astrocytes. However, NSC transplantation led to a reduction in GSDMD signal intensity in astrocytes, suggesting an effect of NSCs on GSDMD activity. Furthermore, NSCs downregulated Mixed Lineage Kinase Domain-Like Protein (*Mlkl*) expression, indicating a reduction in necroptosis. Immunohistochemistry demonstrated decreased phosphorylated MLKL (pMLKL) signal intensity in neurons while stayed the same in astrocytes following NSC transplantation, along with increased distribution in microglia.

Discussion: NSC transplantation holds therapeutic potential in stroke recovery by targeting pyroptosis and necroptosis pathways. These findings shed light on the mechanisms underlying NSC-mediated neuroprotection and support their further exploration as a promising therapy for stroke patients.

KEYWORDS

stroke, neural stem cells, cell transplantation, MRI, pyroptosis, necroptosis, neuroinflammation

1 Introduction

Stroke is the second leading cause of death and long-term disability in Europe (Naghavi et al., 2015; Webb et al., 2021). In over 80% of cases, it is caused by a decreased or interrupted blood supply. The pathophysiological elements which make up a complex chain of detrimental effects can be described as an ischemia–reperfusion (IR) injury, which leads to an almost immediate death of some neurons and glia cells, combined with prolonged inflammation. The extent of damage correlates to subsequent neurological dysfunction (Thom et al., 2006). The current treatment options, unfortunately applicable only in 5% of cases are limited to mechanical thrombectomy and intravenous thrombolysis by tissue plasminogen activator (tPA) (Leng and Xiong, 2019; Jang et al., 2021).

Since all described treatment options of ischemic stroke are reperfusion options and are available for only a specific time after the stroke since IR injury later causes more damage than use, it has become a popular field of research. Hypoxia causes significant changes in cellular metabolism because of the limited ATP synthesis due to mitochondrial dysfunction, leading to disruptions in ion concentrations of Na^+, K^+, and Ca^{2+}. Furthermore, it modifies pathways such as xanthine oxidase, hypoxia-inducible factor 1α, NADPH, NAD+, nitric oxide synthase (NOS) that in the end increase production of reactive oxygen species (ROS) (Wu et al., 2018). Hypoxia, HIF1α, ROS, and mitochondrial dysfunction trigger pro-inflammatory cytokines (IL-1, IL-6, TNF), caspases, and activate the NF-κB pathway, leading to apoptosis, necroptosis, pyroptosis, and autophagy. Cell death releases damage-associated molecular patterns (DAMPs), ROS, and NF-κB pathway activation, which are key in activating microglia, astrocytes, and leukocytes, further driving the inflammatory response (Jurcau and Simion, 2021).

Microglia adopt different phenotypes, M1 pro-inflammatory and M2 anti-inflammatory, to respond to the damage. Following transient middle cerebral artery occlusion (MCAO) in mice, microglial infiltration peaks at 48–72 h, where they migrate to the ischemic lesion and cluster near neurons, aiding in the removal of damaged cells (Jayaraj et al., 2019). In the chronic phase, M2 microglia enhance neuroplasticity and promote neurogenesis by secreting neurotrophic factors (Singhal and Baune, 2017).

Neural stem cells (NSCs) represent a natural choice for treatment of brain diseases and, since their first application, measurable beneficial effects keep being reported, including but not limited to Parkinson's disease (Redmond et al., 2007), Lysosomal Storage Diseases (De Filippis and Delia, 1982), Amyotrophic Lateral Sclerosis (Mitrečić et al., 2010), and Multiple Sclerosis (Brown et al., 2021). NSCs display an inherent mechanism for rescuing dysfunctional neurons (Ourednik et al., 2002) which is, at least partly, achieved through the secretion of growth factors, such as brain-derived neurotrophic factor (BDNF), nerve growth factor (NGF) and vascular endothelial growth factor (VEGF) (Nicaise et al., 2011; Červenka et al., 2021). Several studies reported successful transplantation (stereotaxic or intravascular) of NSCs into the animal models of stroke and, a great majority of them, reported improved recovery of the treated animals (Shen et al., 2010; Dai et al., 2013; Mine et al., 2013; Huang et al., 2014; Kondori et al., 2020). However, some of them showed significant improvements to certain elements of pathophysiological processes, while a majority of them reported a reduction in inflammation (Bacigaluppi et al., 2009; Shen et al., 2010; Mine et al., 2013; Huang et al., 2014; Hamblin et al., 2022). Only a few studies reported the reduction of apoptosis, either as a mechanism of improving condition of the host (Shen et al., 2010; Xue et al., 2019), or as a mechanism linked to improved survival of transplant within the tissue affected by ischemia (Kosi et al., 2018). Interestingly, some studies found that the improvements in the health status positively correlated with the decrease in stroke volume (Bacigaluppi et al., 2009; Huang et al., 2014; Kondori et al., 2020), while others found no such effects (Cheng et al., 2015). At the same time, while significant improvements following transplantation of human NSCs to patients have also been reported in clinical trials (Kalladka et al., 2016; Steinberg et al., 2016; Muir et al., 2020), the mechanism by which stem cells achieve these positive effects still remains elusive.

Pyroptosis is a caspase-1 mediated type of cell death characteried by DNA cleavage, actin cytoskeleton destruction and rupture of plasma membrane resulting in the release of proinflammatory cellular content (Bergsbaken et al., 2009). The main effector is Gasdermin D (GSDMD) which, when cleaved, inserts itself into the plasma membrane where it forms oligomeric pores and, subsequently onsets the process of osmotic lysis (Shi et al., 2015). Necroptosis is programmed necrosis mediated by several mediators, including death receptors, members of the tumor necrosis factor receptor superfamily (Dhuriya and Sharma, 2018). Similar to pyroptosis, it also causes the loss of cell membrane integrity and induces the release of cell content causing local inflammation (Liu et al., 2018). The main effector of necroptosis is phosphorylated mixed lineage kinase domain-like protein (pMLKL) which, when translocated to the plasma membrane causes significant membrane permeabilization (Flores-Romero et al., 2020).

The goal of this research is to clarify the role of pyroptosis and necroptosis, through the key factors of these processes, GSDMD and pMLKL, in the pathophysiology of stroke and explore the approach in which NSC transplantation affects these processes. Moreover, the investigation of GSDMD and pMLKL expression and localization following NSC transplantation in stroke-affected mice aims to provide new insights into the mechanisms by which NSCs achieve their neuroprotective advantages and prospective treatment approaches.

2 Materials and methods

2.1 Experimental animals and stroke induction

In total, 82 animals of a C57Bl/6–$Tyr^{c\text{-}Brd}$ mouse strain (The Jackson Laboratory, Bar Harbor, ME, USA) were used, including 80 males equally divided into 4 groups (A - sham, B - stroke affected animals, C - stroke affected animals injected with basal cell medium and D - stroke affected animals injected with NSCs). The remaining two mice were gravid females used for NSCs isolation.

Induction of ischemic brain stroke was performed through an application of an intraluminal filament (Doccol Corporation, Sharon, MA, USA, 6022910PK10Re) and by following modified Koizumi protocol, using 2% Isoflurane (Piramal Critical Care Limited, UK, 66794001725) in pure oxygen as inhalation anesthetic (Shahjouei et al., 2016). A modification in the protocol was made to reduce the number of suture knots. In total just two knots were placed below the bifurcation of the common carotid artery (CCA) into the external carotid artery (ECA) and internal carotid artery (ICA), a distal knot

and a proximal knot. The distal knot was immediately tightened permanently, while the proximal knot was only loosely tightened to allow the intraluminal filament to pass through. An incision in CCA for inserting the filament was made between the distal and proximal knots. The intraluminal filament was inserted through the incision, and the proximal knot was tightened just enough to stop the bleeding. The occlusion lasted for 30 min. After this period, the filament was removed, and the proximal knot was tightened permanently. We found out that in this way, the animals have a higher survival rate, and MRI scans have shown that the strokes were still of proper size.

All experiments were approved by Internal Review Board of the Ethical Committee of the School of Medicine University of Zagreb (380-59-10106-17-100/27) and Ministry of Agriculture-Croatia (525-10/0255-17-6).

2.2 Isolation, cultivation, and transplantation of NSCs

NSCs were isolated from the telencephalic wall of 14.5 days old mice embryos (Alić et al., 2016). The cells were grown in suspension in a proliferation medium and transplanted after the 4th passage. The proliferation medium consisted of DMEM/F-12 (DMEM/F-12 (1:1) (1X) + GlutaMAXTM-I, Gibco by life Technologies, 31331-028) in which was added 2% B-27 (B-27®Supplement (50X), Gibco, 17504-044), 1% N-2 (N-2 Supplement (100X), Gibco, 17502-048), 1% Pen Strep (Penicillin Streptomycin, Gibco, 15070-063), 0.5% HEPES (4-(2-hydroxyethyl)-1-piperazineethanesulfonic acid, Gibco, 15630-056), 0.2% (10 µg/mL) FGFb (Recombinant Mouse Fibroblast Growth Factor-basic, Thermo Fischer Scientific, PMG0035) and 0.2% EGF (20 ng/mL) (Recombinant Mouse Epidermal Growth Factor, Thermo Fischer Scientific, PMG8041). The stereotaxic transplantation of 1 million cells was performed 24 h after stroke induction using Small Animal Stereotaxic Instrument Kopf 900LS (David Kopf Instruments, Tujunga, CA, USA) and Hamilton glass syringe (Hamilton Company, USA, #80100) under inhalation anesthesia targeting border between cortex and striatum, following coordinates determined according to stereotaxic atlas: AP +0.5, ML +2.3, DV -2.5 (Paxinos and Franklin, 2001).

2.3 Magnetic resonance imaging (MRI)

In vivo MR imaging was performed using 7 T BioSpec 70/20 USR MRI system (Bruker BioSpin, Ettlingen, Germany) with Paravison 6.0.1. software in a Tx/Rx configuration. The main scans included a high-resolution T2-weighted and a T2-map Multi-echo Spin-Echo sequence scan (Justić et al., 2022). Each animal was imaged 7 days before MCAO (BL), 24 h after MCAO (D1) and, for half of the animals from each group, 5 days after MCAO (D5).

2.4 Neurological status assessment

In order to quantify the level of impairment and rate of recovery following stroke, a scoring system based on the compilation of the commonly utilized ones was used (Schaar et al., 2010). A score of 0 means that an animal is completely healthy, while the maximum number of negative points was 39. Animals were assessed for appearance and behavior. A score of 0 was given for healthy, clean, and well-groomed fur, 1 for groomed fur with slightly ruffled hairs on the back, and 2 for neglected and dirty fur with ruffled hairs. For ears, a score of 0 was given if both ears were normally upright, 1 if one ear was drooping or pulled back, and 2 if both ears were drooping or pulled back. Eye assessment: 0 if both eyes were normal, 1 or 2 (L/R) if the eyes were slightly closed, and 3 or 4 (L/R) if the eyes were completely closed.

Animal posture was evaluated as follows: 0 points for normal posture, 1 for a slight arch on the back that straightens when walking, 2 for a larger arch that straightens when walking, 3 for a hump that is always present even when walking, and 4 points for the most severe hunch that interferes with walking.

A score of 0 was given for normal motility, 1 for slightly reduced exploratory behavior, 2 for moving limbs without proceeding, 3 for moving only to stimuli, 4 for unresponsiveness to stimuli with normal muscle tone, and 5 for severely reduced muscle tone and premortal signs. For gait disturbances, 0 was given for straight walking, 1 for walking toward the contralateral side, 2 for alternating circling and walking straight, 3 for alternating circling and walking toward the paretic side, 4 for circling and other gait disturbances, and 5 for constant circling toward the paretic side.

Forelimb flexion: 0 if both limbs were extended when held by the tail, 1 if just one limb was extended, and 2 if neither limb was extended. For the degree of body rotation when held by the tail, 0 was given if the animal flexed on both sides, 1 if flexed on just one side, and 2 if there was no flexion and the animal just hung.

For resistance against a lateral push, 0 was given for normal resistance, 1 for weak resistance, and 2 for no resistance. Forelimb placing on the ipsilesional side: 0 for normal placing, 1 for weak placing, and 2 for no placing. For the contralesional side: 0 for normal placing, 1 for weak placing, and 2 for no placing.

The acoustic startle reflex was tested with a clap; 0 was given if there was a response and 1 if there was no response. The whisker reflex was tested with a cotton swab on the left and right sides; 0 was given if there was a response and 1 point if there was no response on each side. The pinna reflex was tested with a cotton swab on the left and right ear; 0 was given if there was a response and 1 point if there was no response on each side. The proprioceptive reflex was tested by touching the legs with a cotton swab; 0 points were given if there was a reflex response of withdrawing the leg, and 1 point if there was no response on each side of the body.

2.5 Isolation and preparation of the brain tissue

To obtain the tissue for immunohistochemical analysis, the animals were anesthetized with an intraperitoneal injection of 2.5% tribromoethanol (2,2,2-Tribromoethanol, SIGMA, T48402-5G), then underwent transcardial perfusion with house made PBS 1X (8 g of NaCl, 1.44 g of Na_2HPO_4, 0.2 g of KCl, and 0.24 g of KH_2PO_4 in 1 L of dH_2O. pH 7.4 adjusted with NaOH) and 4% formaldehyde (BIGNOST Ltd., HR, FNB4-1 L). The isolated brains were submerged in 4% formaldehyde for 24 h, washed in PBS and transferred to 30% sucrose in PBS. The tissue was imbedded in Tissue-Tek O.C.T. Compound, (Sakura Finetek, USA, 4583) and cryotome sectioning of 30 µm frontal sections. To obtain the tissue for qPCR animals were anesthetized with an intraperitoneal injection of 2.5% tribromoethanol, then underwent

transcardial perfusion with PBS, and the brain hemispheres were snap frozen and dry pulverized in liquid nitrogen. Half of the animals from each group were sampled on the 2nd day, and the other half on the 5th day following stroke induction (Alić et al., 2016).

2.6 qPCR

The total RNA was isolated from pulverized tissue by using the commercial QIAshredder (Qiagen, Germantown, MD, USA, 79656) and RNeasy Mini Kit (Qiagen, 74104). The RNA concentration was quantified using NanoDrop ND1000 spectrophotometer (Thermo Fischer Scientific, USA) and based on measured values, it was determined that all samples for transcription would be standardized to contain 25 ng/μL of RNA. The conversion from RNA to cDNA was accomplished utilizing a high-capacity RNA-to-cDNA kit (Applied Biosystems, Bedford, MA, USA, 4387406). The qPCR was performed using TaqMan Gene Expression Assays for two genes of interest: Gasdermin D (*Gsdmd*) (Thermo Fisher Scientific, Mm00509962_g1) and mixed lineage kinase domain-like protein (*Mlkl*) (Thermo Fisher Scientific, Mm01244220_m1). As housekeeping genes Actin-β (*Actb*) (Thermo Fisher Scientific, Mm02619580_g1) and Hypoxanthine phosphoribosyltransferase 1 (*Hprt1*) (Thermo Fisher Scientific, Mm03024075_m1) were used. The relative quantification was performed using the ΔCT method (Hribljan et al., 2018).

2.7 Immunohistochemistry/ immunofluorescence

The brain tissue samples were immunolabeled with specific primary antibodies diluted in PBS with 0.05% Tween 20 (Carl Roth GmbH, Karlsruhe, Germany, 9127.2) and goat serum (Thermo Fisher Scientific, 16210064) at 4°C overnight. Prior to immunostaining, the antigen retrieval was performed in citrate buffer, pH = 6.0 (Thermo Fischer Scientific, 00-4955-58). The primary antibodies were rinsed with PBS and the samples were immunolabeled with fluorescent secondary antibodies diluted in PBS. After rinsing the secondary antibodies with PBS, DAPI (Roche, Basel, Switzerland, 10236276001) was used as a nuclear counterstain. The samples were covered with coverslips with Dako Fluorescent Mounting Medium (Agilent, Santa Clara, CA, USA, S302380-2) and analysed using a confocal microscope OlympusFV3000 (Olympus, Tokyo, Japan) (Alić et al., 2016). Primary antibodies and dilutions used were: anti-GSDMD/1:300 (Abcam, ab219800), anti-phospho MLKL/1:400 (Cell Signaling. #37333), anti-GFAP/1:500 (Abcam, ab4674), anti-IBA1/1:100 (Invitrogen, MA5-27726), anti-MAP2/1:1000 (Abacam, ab5392), anti-NEUN/1:200 (Sigma-Aldrich, MAB377). Secondary antibodies and dilutions used were: Alexa Fluor 488/1:1000 (Life Technologies A11039), Alexa Fluor 488/1:1000 (Life Technologies A11001), Alexa Fluor 546/1:1000 (Life Technologies A11010), Alexa Fluor 647/1:500 (Abcam, ab150171), Alexa Fluor 647/1:500 (Abcam, ab150115).

2.8 Image analyses and statistics

For calculating the volumes of brain hemispheres, T2w MR images were used, while T2map MR images were used to quantify the stroke volume. All the images were processed by manual delineation of hemispheres using the ImageJ software. In total 76 brains were scanned, with 20 of them belonging to the control and 56 to the stroke-affected group. Since repeated measures ANOVA cannot handle missing values that occurred due to decreased number of mice in later time points, some of the obtained raw data has been analysed by fitting a mixed model with a Geisser–Greenhouse correction. While MRI and qPCR data analysis used Tukey Kramer multiple comparisons *post-hoc* test, the *post-hoc* analysis of the neuroscoring data was performed with Šidák's multiple comparisons test to characterize the differences between the groups. This analysis was implemented in GraphPad Prism version 9.3.1.

For performing the analyses of signal intensity, surface covering the visual field and colocalization of two or more signals, the CellProfiler software was used. For this purpose, we used 3 different brains for each gene and scanned 15 images for each brain and for each combination of markers. After manually preparing a pipeline with an acceptable signal-noise ratio, all the images were analysed with an automatic protocol as a single batch. After obtaining the raw data for percentage of slide coverage and mean intensity as well as colocalization through image analysis the parameters were statistically analysed using a two-way ANOVA with Tukey Kramer multiple comparisons *post-hoc* test. The significance levels are as follows: $^{*}p \leq 0.05$, $^{**}p \leq 0.01$, $^{***}p \leq 0.001$ and $^{****}p \leq 0.0001$.

3 Results

3.1 Transplanted NSCs improved recovery of mice affected by stroke

Following ischemic stroke, as visualized by magnetic resonance imaging (MRI) (Figure 1A), the analysis of obtained neurological scores, in all the operated groups on day 1 (D1), revealed a significant worsening in the animal's status compared to sham operated animals (Figure 1B). The comparison of scores between groups on D5 (4 days after NSCs transplantation, cell medium or no treatment) clearly revealed that animals which received NSCs transplantation achieved significantly improved levels of recovery (Group D), when compared with both animals which received basal NSCs medium (Group C) and stroke affected animals (Group B) (Figure 1B).

3.2 Transplanted NSCs reduced the stroke volume in mice

On the day 1, the average stroke volume was approximately 100 mm^3 across all groups with no significant differences. Interestingly, by day 5, variations emerged: the untreated group maintained a volume of around 100 mm^3, the NSCs medium group (Group C) decreased to an average of 91 mm^3, and the NSCs transplanted group (Group D) showed a volume of 80 mm^3 (Figure 1C). Despite noticeable reductions, these differences were not statistically significant (*p* values between groups B-C, B-D, and C-D for D1 and D5 are listed respectively: 0.8582, 0.8372, 0.5349, 0.8918, 0.1381, 0.3211). Exploring additional parameters, we compared stroke volume to the whole brain and ipsilateral hemisphere volumes revealing some distinctions in the NSCs-injected group, although not significant we showed the same trend (*p* values for ratio of stroke

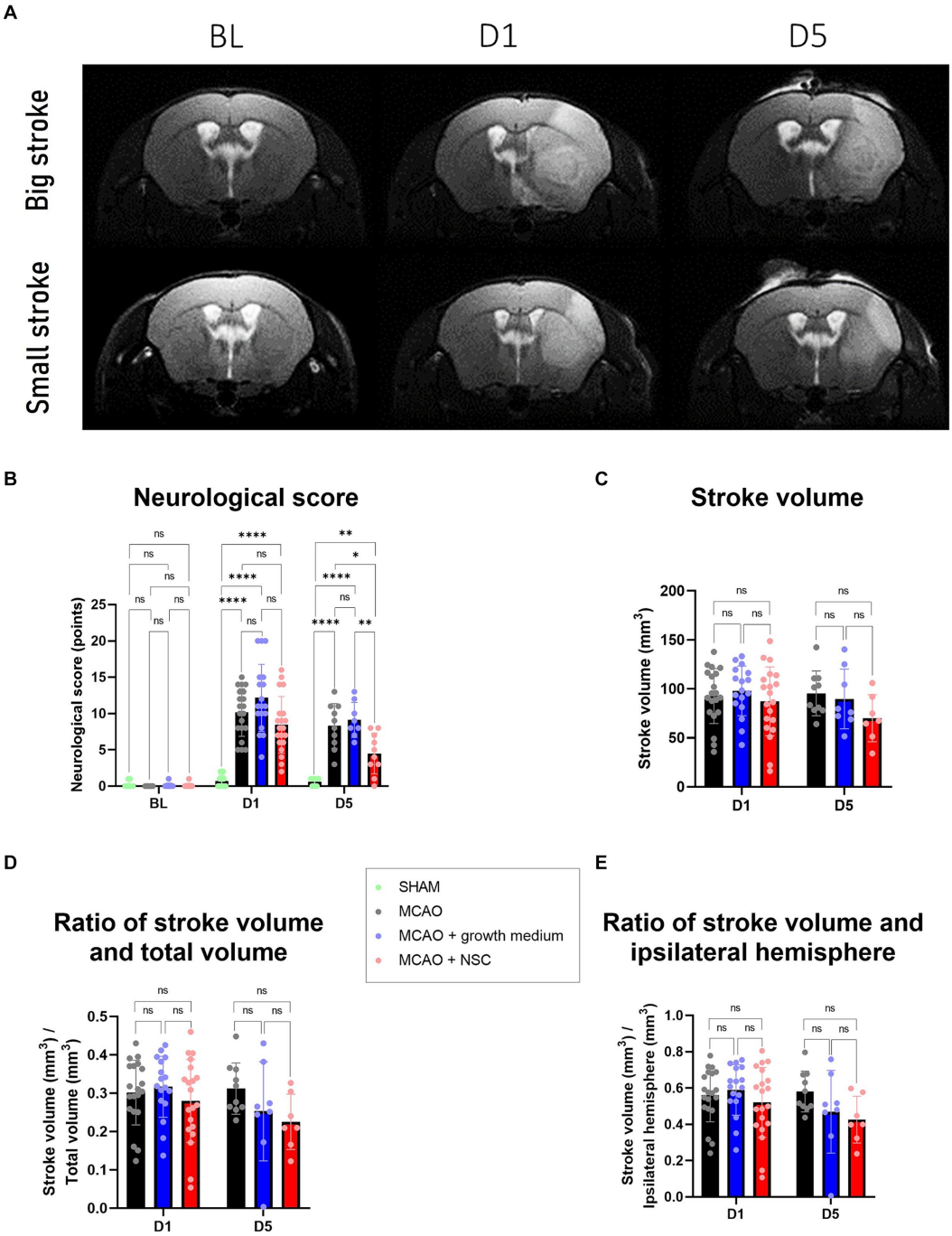

FIGURE 1
(A) MRI scans allowed for measurement of stroke volume on days 1 and 5, as compared to the baseline (BL) image. Upper row represents a big stroke, lower row represents small stroke. **(B)** Neurological score, assessed as described in paragraph 2.4., revealed worsening of the health condition after onset of stroke, which was significantly improved only in the group treated by NSCs (group D), as visible after 5 days. **(C)** Stroke volume, measured by manual delineation in ImageJ from MRI images, was slightly reduced in animals treated by transplantation of medium and more reduced in animals treated by NSCs. D and E: The ratios of stroke vs. the total and ipsilateral brain volume, all measured by manual delineation of MRI images in ImageJ, revealed tendency of improvement in the animals treated by NSCs. The significance levels are as follows: $*p \leq 0.05$, $**p \leq 0.01$, $***p \leq 0.001$ and $****p \leq 0.0001$.

volume and total brain volume between groups B-C, B-D, and C-D for D1 and D5 are listed respectively: 0.8693, 0.7395, 0.4488, 0.3844, 0.1630, 0.8369 and p values for stroke volume and ipsilateral hemisphere volume between groups B-C, B-D, and C-D for D1 and D5 are listed respectively: 0.8441, 0.7292, 0.4104, 0.3314, 0.1517, 0.8660) (Figures 1D,E).

3.3 Transplanted NSCs upregulated the expression of *Gsdmd* while lowering GSDMD signal intensity

Stroke enhanced the expression of *Gsdmd* on RNA level in all groups, and none of the treatments reduced it even after 5 days. Two

days post-stroke and 1 day post-NSCs injection, *Gsdmd* expression showed the greatest increase in the NSCs medium-treated group (Group C), followed by the NSCs-treated group (Group D), while untreated animals showed lower levels. Gene expression analysis 5 days post-stroke (4 days post-transplantation) revealed higher overall values with more uniformity among groups (Figures 2AA,AB). However, there was no statistically significant difference between groups on both days. Comparing same groups in different time points showed statistically significant upregulation for cell treated group and non-treatment group, while results in medium-treated group still showed upregulation but with no statistical differences (Figure 2AC).

Analysis of GSDMD immunohistochemistry signal intensity and coverage revealed increased cell presence 2 days post-stroke. No significant difference appeared 1 day post-cell transplantation. However, by day 5 post-stroke and 4 days post-transplantation, NSCs-transplanted animals (Group D) exhibited statistically significantly reduced slide coverage and overall signal intensity (Figure 2B).

Two days post-stroke with no treatment (Group B), GSDMD-positive cells were prominently present in penumbra region near the hypoxic core, with a majority co-expressing IBA1 or GFAP, indicating expression in both microglia and astrocytes (Figures 2DA–DE). In NSCs transplanted animals (Group D) (Figures 2DF–DJ), 1 day post-procedure, IBA1 and GFAP positive cells persisted (Figure 2, compare B-untreated vs. G-cell treated). A similar pattern was observed 5 days post-stroke (Figures 2EA–EE), with clear GSDMD colocalization with IBA1 and GFAP in brain regions near the hypoxic core. Notably, in transplanted animals (Figures 2EF–EJ), the colocalization of GFAP and GSDMD was less frequent than in untreated animals. Analysis of neuronal markers (MAP2 and NEUN) revealed rare GSDMD-positive neurons in both

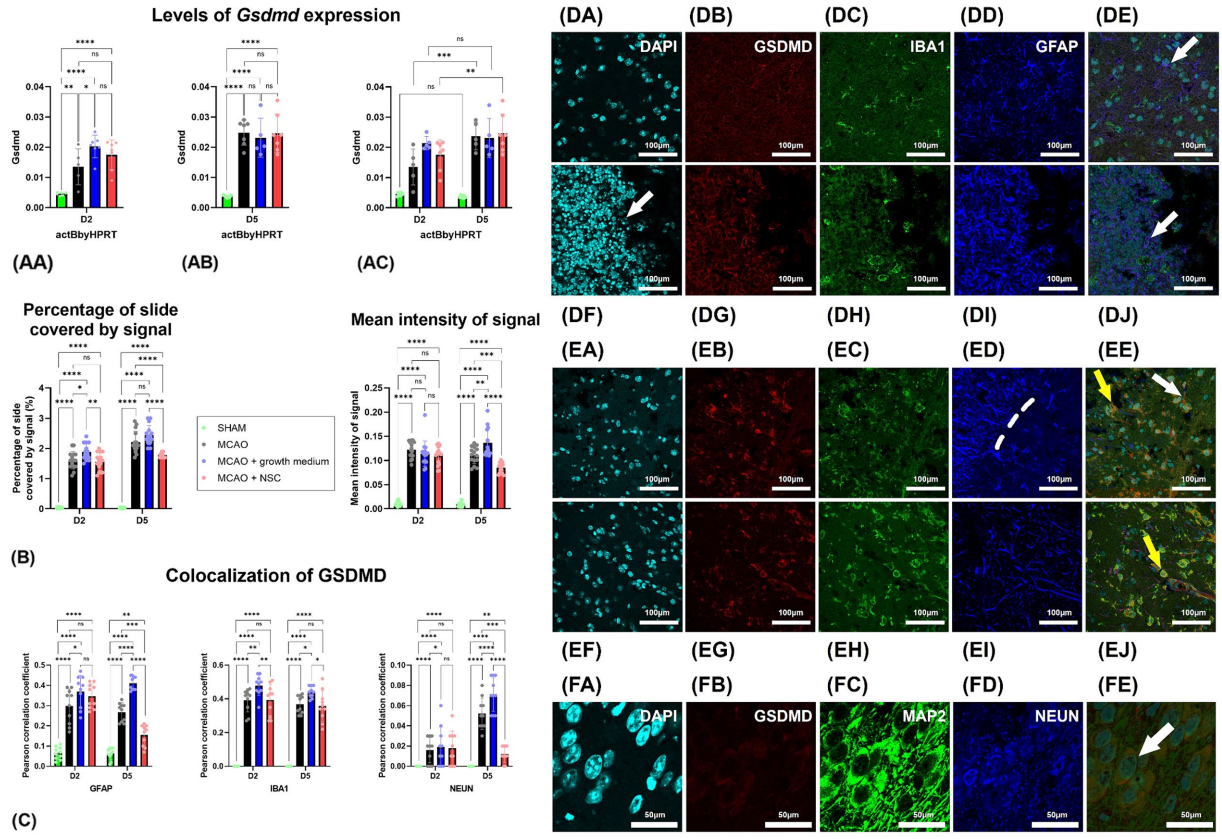

FIGURE 2
Stroke increased *Gsdmd* expression quantified by qPCR in all groups, with no treatment reducing it after 5 days. **(AA)** Two days post-stroke, the highest increase was in the NSCs medium-treated group (Group C), followed by the NSCs-treated group (Group D). **(AB)** Five days post-stroke, expression levels were higher overall but more uniform across groups. **(AC)** Comparing same groups on different timepoints showed that *Gsdmd* expression of the cell-treated (Group D) and non-treated groups (Group B) showed significant upregulation, while the medium-treated group (Group C) showed upregulation without statistical significance. **(B)** Intensity of the total *Gsdmd* signal and percentage of slide coverage, measured on immunofluorescence images in CellProfiler, increased after stroke and was significantly moderated by NSCs 4 days after transplantation. **(C)** Colocalization analyses, measured on immunofluorescence images in CellProfiler, revealed that after stroke GSDMD colocalizes dominantly with GFAP and IBA1 positive cells. Four days after transplantation of NSCs, colocalization of GSDMD and GFAP is strongly reduced. **(DA–DE)** Immunohistochemical analyses on day 2 revealed colocalization of GSDMD with both astrocytes (white arrow) and microglia (yellow arrow). Moreover, GSDMD-positive cells were prominently present in penumbra region near the hypoxic core. There was no visible difference in animals which received NSCs, 1 day after transplantation **(DF–DJ)**. **(EA–EE)** On day 5 colocalization with both astrocytes (white arrow) and microglia (yellow arrow) was found. Transplantation of NSCs significantly reduced presence of GSDMD in astrocytes 5 days after transplantation **(EF–EJ)**. **(FA–FE)** Colocalization of GSDMD and markers of neurons was rather rare finding. Scale bar on images **(DA–EJ)** is 100 μm, while on **(FA–FE)** is 50 μm. The significance levels are as follows: $*p \leq 0.05$, $**p \leq 0.01$, $***p \leq 0.001$ and $****p \leq 0.0001$.

treated and untreated groups at both time points (Figure 2FA–FE). Contralateral hemisphere analysis showed fewer and less intense GSDMD-positive cells compared to the stroke-affected hemisphere (data not shown).

Two days post-stroke, GSDMD predominantly colocalized with IBA1, slightly less with GFAP, and almost none with NEUN. NSCs transplantation showed no significant impact on this pattern. However, by day five post-stroke, in the untreated group, GSDMD was mainly present with IBA1, slightly less in GFAP, and rarely in NEUN positive cells. In contrast, NSCs-transplanted animals exhibited reduced GSDMD presence in GFAP, with no impact on IBA1 colocalization. Furthermore, NSCs transplantation significantly reduced GSDMD presence in neurons, despite their scarcity both two- and five-days post-stroke (Figure 2C).

3.4 Transplanted NSCs downregulated the expression of *Mlkl*, decreased pMLKL in neurons and increased its distribution in microglia

Two days post-stroke and 1 day post-stem cell treatment, *Mlkl* expression increased in both medium-treated and NSCs transplanted groups, while untreated animals showed lower levels of expression (Figure 3AA). Gene expression analysis 5 days post-stroke (4 days post-transplantation) indicated an increase in the untreated group, with lower expression in the medium-treated and NSCs-treated groups (Figure 3AB). Comparing gene expression within the same groups at different timepoints revealed statistically significant downregulation in the medium-treated and NSCs-treated groups, while the non-treated group exhibited a small upregulation, though not statistically significant (Figure 3AC).

Quantification of pMLKL signal intensity through immunohistochemistry showed that 2 days post-stroke, there was a dramatic increase in pMLKL signal intensity and coverage in cells. One day post-NSCs transplantation and 2 days post-stroke showed no significant difference between treated and untreated groups. However, by day 5 post-stroke and 4 days post-transplantation, animals receiving stem cells exhibited significantly lower slide coverage and overall intensity of the pMLKL signal (Figure 3B).

Two days post-stroke, immunohistochemical analysis revealed abundant pMLKL-positive cells near the hypoxic core, predominantly neurons and astrocytes, with rare microglia positive for pMLKL (Figures 3DA–FE). Comparing this to animals receiving cell transplantation showed no obvious difference 1 day post-transplantation (Figures 3DF–DJ). By day 5 post-stroke, pMLKL-positive microglia became more common (Figures 3EA–EJ). Analysis of neuron markers (MAP2 and NEUN) showed widespread pMLKL presence in neurons, a common finding in both treated and untreated animals at both time points (Figures 3FA–FE).

Two days post-stroke, pMLKL primarily colocalized with neurons, with rare colocalization in astrocytes and microglia. By day 5 post-stroke, colocalization with neuronal markers increased, while astrocyte and microglia presence remained unaffected. Notably, NSC transplantation significantly influenced these patterns: astrocyte colocalization remained unaffected, but NSCs increased pMLKL in microglia and decreased it in neurons (Figure 3C).

4 Discussion

Decades of testing stem cell therapy in animal stroke models demonstrate measurable benefits. A meta-analysis of 37 preclinical trials with NSCs reveals consistent improvements in motoric capabilities, with less consistent results in neurological scores and lesion volume (Chen et al., 2016). These promising findings have propelled the therapy into advanced clinical trials, primarily addressing its potential to accelerate human recovery, after early safety assessments (Jaillard et al., 2020; Muir et al., 2020; Lee et al., 2022). However, failure of many clinical trials suggested a need for further improvements of pre-clinical phases. Our group contributed to those endeavors by improving *in vitro* studies, both from methodological points of view (Petrović et al., 2023; Radoszkiewicz et al., 2023), and by focusing on specific molecular elements of events followed by hypoxic injury (Jagečić et al., 2023; Stančin et al., 2023).

In further improvement of understanding the therapeutic mechanisms, the pivotal role of growth factors, released by NSCs, stands out as a central event, contributing to reduced inflammation (Bacigaluppi et al., 2009; Huang et al., 2014; Hamblin et al., 2022). These growth factors, known for their neuroprotective and regenerative effects (Leker et al., 2009), were key players in the observed improvements, with limited studies emphasizing a reduction in apoptosis as a foundational aspect (Shen et al., 2010).

Our focus on pyroptosis and necroptosis stems from the robust neuroinflammatory response triggered after stroke, leading to cytokine release and danger-associated molecules. The activated cells were predominantly in the penumbra rather than the necrotic core. Thus, our morphological analyses concentrated on this region, revealing a significant presence of cells expressing markers for pyroptosis and necroptosis.

After confirming that *Gsdmd* is expressed at very low levels under normal conditions, but strongly upregulated after onset of stroke, we found that a great majority of GSDMD positive cells were microglia and astrocytes but not neurons, and similar results were shown by other authors (Wang et al., 2020). Transplantation of NSCs yielded interesting effects 4 days after the transplantation (5 days after onset of stroke), which were visible in the general increase of expression of *Gsdmd*, but on the other hand dominant overall reduction of this marker's presence, especially in astrocytes, suggesting that transplanted NSCs affect GSDMD activity. Our results can also be compared to some studies in which the authors reported that intravascular transplantation of either olfactory mucosa stem cells or exosomes into a rat stroke model reduces pyroptosis (Liu et al., 2021; Zhuo et al., 2021). However, in both studies, the reduction of pyroptosis was measured on a protein level of a whole brain and analyses of specific cell populations were not performed. We showed that despite gene upregulation in treated groups, transplanted NSCs can reduce activity of GSDMD, predominantly in astrocytes, in stroke affected mouse brain which improved animal recovery. Other studies have also proven that reducing the activity of GSDMD in cells can have significant impact on recovery after ischemic brain stroke, either by pharmacological intervention or by using knockout animals (Wang et al., 2020; Hu et al., 2023). One study proved that stem cells conditioned medium can reduce pyroptosis by inhibiting the NLRP3/caspase-1/interleukin-1β pathway (Liu et al., 2024). It is plausible to hypothesize that at least a part of positive effects can be contributed to the secretion of molecules which decrease levels of inflammatory

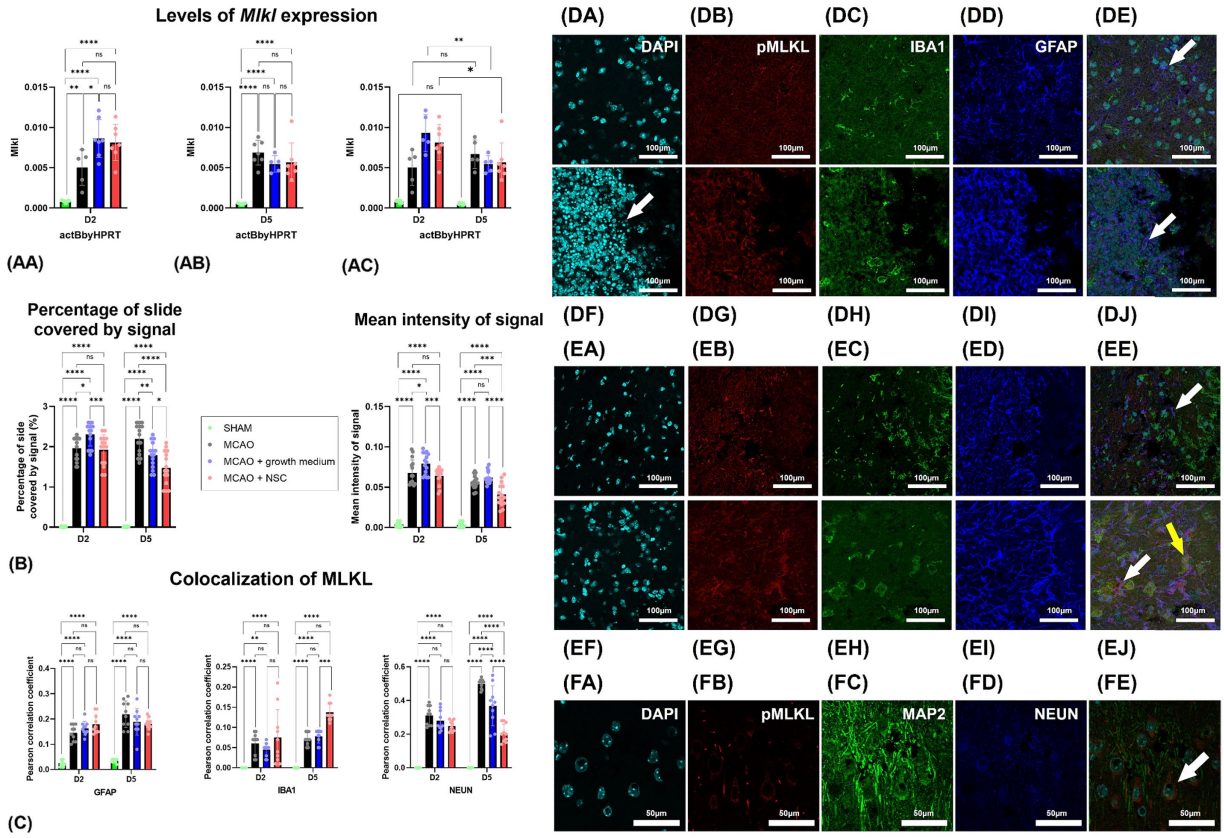

FIGURE 3
(AA) Two days post-stroke, *Mlkl* expression quantified by qPCR increased in both medium-treated and NSCs-transplanted groups, while untreated animals showed lower levels. **(AB)** Five days post-stroke, untreated animals had increased *Mlkl*, while medium-treated and NSCs-treated groups showed lower expression. **(AC)** Comparing gene expression at different timepoints showed significant downregulation of *Mlkl* in medium-treated and NSCs-treated groups, while the non-treated group had a slight, non-significant upregulation. **(B)** Intensity of the total pMLKL signal and percentage of slide coverage, measured on immunofluorescence images in CellProfiler, increased after stroke and was significantly moderated by NSC 4 days after transplantation. **(C)** Colocalization analyses, measured on immunofluorescence images in CellProfiler, revealed that after stroke pMLKL colocalizes dominantly with GFAP and NEUN positive cells. Four days after transplantation of NSCs, colocalization of pMLKL and NEUN was strongly reduced, while colocalization of pMLKL and IBA1 was increased. **(DA–DE)** Immunohistochemical analyses on day 2 revealed abundant pMLKL-positive cells near the hypoxic core and colocalization of pMLKL with astrocytes (white arrow). There was no visible difference in animals which received NSC, 1 day after transplantation **(DF–DJ)**. **(EA–EE)** On day 5 colocalization with astrocytes (white arrow) was found. Transplantation of NSC significantly reduced presence of pMLKL in astrocytes, but increased presence of pMLKL in microglia (yellow arrow) 5 days after transplantation **(EF–EJ)**. **(FA–FE)** Colocalization of pMLKL and neuronal markers. Scale bar on images **(DA–EJ)** is 100 μm, while on **(FA–FE)** is 50 μm. The significance levels are as follows: $*p \leq 0.05$, $**p \leq 0.01$, $***p \leq 0.001$ and $****p \leq 0.0001$.

factors such as caspase-1, NLRP3, GSDMD, IL-1β, and IL-18 (Li et al., 2019; Liang et al., 2021).

The study we conducted revealed dynamic changes in *Mlkl* expression and pMLKL distribution post-stroke, along with findings from other authors (Li et al., 2020). Expression of *Mlkl* went down after cell treatment indicating reduction of necroptosis. Kong et al. reported reduction of necroptosis by addition of MSCs reducing the levels of RIPK1 and RIPK3 in an *in vitro* model of ischemia (Kong et al., 2016). As such, our study is demonstrating the reduction of necroptosis using NSCs on *in vivo* system, rather than on *in vitro* system. Moreover, and different from reports based on RIPKs, we performed our analyses by quantifying the distribution of pMLKL, which is considered the ultimate proof of active necroptosis (Galluzzi et al., 2014). Immunohistochemistry also showed a surge in pMLKL intensity, especially in neurons and astrocytes where NSCs-treated animals displayed significantly reduced intensity by day 5. Colocalization studies demonstrated that initially, pMLKL primarily colocalized with neurons, which was shown by others as well (Han et al., 2019). NSCs treatment influenced this pattern, increasing pMLKL in microglia and decreasing it in neurons. The acknowledged role of inflammation in triggering necroptosis involves key inflammatory markers such as TNF-α, IL-1β, IL-1α, and IL-6 (Zhang et al., 2016; Yang et al., 2017), with NSCs demonstrating the potential to mitigate proinflammatory cytokines (Huang et al., 2014). Since the reduction of necroptosis by its pharmacological inhibitor has also been shown as beneficial in brain ischemia (Northington et al., 2011; Mitroshina et al., 2023), our findings of reduced necroptosis in neurons following NSCs transplantation are in accordance with aforementioned literature and our reports of reduction in stroke volume and accelerated recovery of mice.

In conclusion, we showed the measurable benefits of NSCs therapy targeting pyroptosis and necroptosis in stroke recovery. NSCs, known for releasing growth factors with neuroprotective effects, show promise in reducing inflammation. Our study delves

into pyroptosis and necroptosis post-stroke following NSCs transplantation, revealing *Gsdmd* upregulation, but reducing GSDMD signal intensity in microglia and astrocytes. NSCs transplantation influences necroptosis, leading to its reduction, as indicated by pMLKL intensity reduction in neurons and astrocytes. These findings align with the acknowledged role of inflammation in necroptosis and demonstrate NSCs' potential to mitigate proinflammatory cytokines. The observed reduction in stroke volume and accelerated recovery further underscores the therapeutic potential of NSCs in stroke treatment.

Data availability statement

Publicly available datasets were analyzed in this study. This data can be found here: https://doi.org/10.5281/zenodo.13136667.

Ethics statement

The animal studies were approved by Internal Review Board of the Ethical Committee of the School of Medicine University of Zagreb. The studies were conducted in accordance with the local legislation and institutional requirements. Written informed consent was obtained from the owners for the participation of their animals in this study.

Author contributions

DL: Data curation, Formal analysis, Investigation, Methodology, Resources, Software, Visualization, Writing – original draft, Writing – review & editing. IA: Investigation, Software, Supervision, Validation, Writing – original draft, Writing – review & editing. IŠ: Methodology, Software, Validation, Writing – original draft, Writing – review & editing. DM: Conceptualization, Funding acquisition, Investigation, Methodology, Resources, Supervision, Validation, Writing – original draft, Writing – review & editing.

Funding

The author(s) declare that financial support was received for the research, authorship, and/or publication of this article. Research work of DL was financed by the project ORASTEM granted by Croatian Science Foundation (IP-2016-06-9451), by the project DevDown (IP-2022-10-4656) and by the project *Development of personalized tests for determining the biological age of the brain and early detection of dementia* (BrainClock, NPOO.C3.2.R3-I1.04.0089). Moreover, work of DM and DL were supported by the European Union through the European Regional Development Fund, as the Scientific Centre of Excellence for Basic, Clinical and Translational Neuroscience under Grant Agreement No. KK.01.1.1.01.0007, project "Experimental and clinical research of hypoxic–ischemic damage in perinatal and adult brain".

Conflict of interest

The authors declare that the research was conducted in the absence of any commercial or financial relationships that could be construed as a potential conflict of interest.

Publisher's note

References

Alić, I., Kosi, N., Kapuralin, K., Gorup, D., Gajović, S., Pochet, R., et al. (2016). Neural stem cells from mouse strain Thy1 YFP-16 are a valuable tool to monitor and evaluate neuronal differentiation and morphology. *Neurosci. Lett.* 634, 32–41. doi: 10.1016/j.neulet.2016.10.001

Bacigaluppi, M., Pluchino, S., Jametti, L. P., Kilic, E., Kilic, Ü., Salani, G., et al. (2009). Delayed post-Ischaemic neuroprotection following systemic neural stem cell transplantation involves multiple mechanisms. *Brain J. Neurol.* 132, 2239–2251. doi: 10.1093/BRAIN/AWP174

Bergsbaken, T., Fink, S. L., and Cookson, B. T. (2009). Pyroptosis: host cell death and inflammation. *Nat. Rev. Microbiol.* 7, 99–109. doi: 10.1038/nrmicro2070

Brown, C., McKee, C., Halassy, S., Kojan, S., Feinstein, D. L., and Rasul Chaudhry, G. (2021). Neural stem cells derived from primitive mesenchymal stem cells reversed disease symptoms and promoted neurogenesis in an experimental autoimmune encephalomyelitis mouse model of multiple sclerosis. *Stem Cell Res Ther* 12:499. doi: 10.1186/S13287-021-02563-8

Červenka, J., Tylečková, J., Skalníková, H. K., Kepková, K. V., Poliakh, I., Valeková, I., et al. (2021). Proteomic characterization of human neural stem cells and their Secretome during in vitro differentiation. *Front. Cell. Neurosci.* 14:612560. doi: 10.3389/FNCEL.2020.612560

Chen, L., Zhang, G., Yuchun, G., and Guo, X. (2016). Meta-analysis and systematic review of neural stem cells therapy for experimental ischemia stroke in preclinical studies. *Sci. Rep.* 6:32291. doi: 10.1038/SREP32291

Cheng, Y., Zhang, J., Deng, L., Johnson, N. R., Xichong, Y., Zhang, N., et al. (2015). Intravenously delivered neural stem cells migrate into ischemic brain, differentiate and improve functional recovery after transient ischemic stroke in adult rats. *Int. J. Clin. Exp. Pathol.* 8, 2928–2936

Dai, J., Li, S. Q., Qiu, Y. M., Xiong, W. H., Yin, Y. H., Jia, F., et al. (2013). Migration of neural stem cells to ischemic brain regions in ischemic stroke in rats. *Neurosci. Lett.* 552, 124–128. doi: 10.1016/J.NEULET.2013.07.044

Dhuriya, Y. K., and Sharma, D. (2018). Necroptosis: A regulated inflammatory mode of cell death. *J. Neuroinflammation* 15:199. doi: 10.1186/s12974-018-1235-0

Filippis, LidiaDe, and Delia, Domenico. (1982). "Hypoxia in the regulation of neural stem cells." *Aust. J. Chem.* 68: 2831–2844. doi: 10.1007/s00018-011-0723-5

Flores-Romero, H., Ros, U., Garcia-Saez, A. J., Flores-Romero, H., Ros, U., Garcia-Saez, A. J., et al. (2020). Pore formation in regulated cell death. *EMBO J.* 39:e105753. doi: 10.15252/EMBJ.2020105753

Galluzzi, L., Kepp, O., and Kroemer, G. (2014). MLKL Regulates Necrotic Plasma Membrane Permeabilization. *Cell Res.* 24, 139–140. doi: 10.1038/cr.2014.8

Hamblin, M. H., Murad, R., Yin, J., Vallim, G., and Lee, J. P. (2022). Modulation of gene expression on a transcriptome-wide level following human neural stem cell transplantation in aged mouse stroke brains. *Exp. Neurol.* 347:113913. doi: 10.1016/J.EXPNEUROL.2021.113913

Han, F., Guan, X., Guo, W., and Bai, L. (2019). Therapeutic potential of a TrkB agonistic antibody for ischemic brain injury. *Neurobiol. Dis.* 127, 570–581. doi: 10.1016/j.nbd.2019.04.009

Hribljan, V., Salamon, I., Đemaili, A., Alić, I., and Mitrečić, D. (2018). Transplantation of neural stem cells in the mouse model of ischemic brain stroke and expression of genes

involved in programmed cell death. *Croat. Med. J.* 59, 203–212. doi: 10.3325/cmj.2018.59.203

Hu, R., Liang, J., Ding, L., Zhang, W., Wang, Y., Zhang, Y., et al. (2023). Gasdermin D inhibition ameliorates neutrophil mediated brain damage in acute ischemic stroke. *Cell Death Dis.* 9:50. doi: 10.1038/s41420-023-01349-6

Huang, L., Wong, S., Snyder, E. Y., Hamblin, M. H., and Lee, J. P. (2014). Human neural stem cells rapidly ameliorate symptomatic inflammation in early-stage ischemic-reperfusion cerebral injury. *Stem Cell Res Ther* 5:129. doi: 10.1186/SCRT519

Jagečić, D., Petrović, D. J., Šimunić, I., Isaković, J., and Mitrečić, D. (2023). The oxygen and glucose deprivation of immature cells of the nervous system exerts distinct effects on mitochondria, Mitophagy, and autophagy, depending on the cells' differentiation stage. *Brain Sci.* 13:910. doi: 10.3390/brainsci13060910

Jaillard, A., Hommel, M., Moisan, A., Zeffiro, T. A., Favre-Wiki, I. M., Barbieux-Guillot, M., et al. (2020). Autologous mesenchymal stem cells improve motor recovery in subacute ischemic stroke: a randomized clinical trial. *Transl. Stroke Res.* 11, 910–923. doi: 10.1007/S12975-020-00787-Z

Jang, K. M., Choi, H. H., Jang, M. J., and Cho, Y. D. (2021). Direct endovascular Thrombectomy alone vs. bridging thrombolysis for patients with acute ischemic stroke: a Meta-analysis. *Clin. Neuroradiol.* 32, 603–613. doi: 10.1007/S00062-021-01116-Z

Jayaraj, R. L., Azimullah, S., Beiram, R., Jalal, F. Y., and Rosenberg, G. A. (2019). Neuroinflammation: friend and foe for ischemic stroke. *J. Neuroinflammation* 16:142. doi: 10.1186/s12974-019-1516-2

Jurcau, A., and Simion, A. (2021). Neuroinflammation in cerebral ischemia and ischemia/reperfusion injuries: from pathophysiology to therapeutic strategies. *Int. J. Mol. Sci.* 23:14. doi: 10.3390/ijms23010014

Justić, H., Barić, A., Šimunić, I., Radmilović, M., Ister, R., Škokić, S., et al. (2022). Redefining the Koizumi model of mouse cerebral ischemia: a comparative longitudinal study of cerebral and retinal ischemia in the Koizumi and longa middle cerebral artery occlusion models. *J. Cereb. Blood Flow Metab.* 42, 2080–2094. doi: 10.1177/0271678X221109873

Kalladka, D., Sinden, J., Pollock, K., Haig, C., McLean, J., Smith, W., et al. (2016). Human neural stem cells in patients with chronic Ischaemic stroke (PISCES): a phase 1, first-in-man study. *Lancet* 388, 787–796. doi: 10.1016/S0140-6736(16)30513-X

Kondori, B., Jalali, M. H., Asadi, H., Bahadoran, A. Y., and Raouf Sarshoori, J. (2020). Intra-arterial transplantation of neural stem cells improve functional recovery after transient ischemic stroke in adult rats. *Bratislavske Lekarske Listy* 121, 8–13. doi: 10.4149/BLL_2020_002

Kong, D., Zhu, J., Liu, Q., Jiang, Y., Xu, L., Luo, N., et al. (2016). Mesenchymal stem cells protect neurons against hypoxic-ischemic injury via inhibiting Parthanatos, necroptosis, and apoptosis, but not autophagy. *Cell. Mol. Neurobiol.* 37, 303–313. doi: 10.1007/S10571-016-0370-3

Kosi, N., Alić, I., Salamon, I., and Mitrečić, D. (2018). Stroke promotes survival of nearby transplanted neural stem cells by decreasing their activation of caspase 3 while not affecting their differentiation. *Neurosci. Lett.* 666, 111–119. doi: 10.1016/j.neulet.2017.12.040

Lee, J., Chang, W. H., Chung, J. W., Kim, S. J., Kim, S. K., Lee, J. S., et al. (2022). Efficacy of intravenous mesenchymal stem cells for motor recovery after ischemic stroke: a neuroimaging study. *Stroke* 53, 20–28. doi: 10.1161/STROKEAHA.121.034505

Leker, R. R., Lasri, V., and Chernoguz, D. (2009). Growth factors improve neurogenesis and outcome after focal cerebral ischemia. *J. Neural Transm.* 116, 1397–1402. doi: 10.1007/S00702-009-0329-3

Leng, T., and Xiong, Z.-G. (2019). Treatment for ischemic stroke: from thrombolysis to Thrombectomy and remaining challenges. *Brain Cir.* 5, 8–11. doi: 10.4103/BC.BC_36_18

Li, X., Cheng, S., Hao, H., Zhang, X., Jiehua, X., Wang, R., et al. (2020). Progranulin protects against cerebral ischemia-reperfusion (I/R) injury by inhibiting necroptosis and oxidative stress. *Biochem. Biophys. Res. Commun.* 521, 569–576. doi: 10.1016/J.BBRC.2019.09.111

Li, Z., Liu, F., He, X., Yang, X., Shan, F., and Feng, J. (2019). Exosomes derived from mesenchymal stem cells attenuate inflammation and demyelination of the central nervous system in EAE rats by regulating the polarization of microglia. *Int. Immunopharmacol.* 67, 268–280. doi: 10.1016/J.INTIMP.2018.12.001

Liang, Y., Song, P., Chen, W., Xie, X., Luo, R., Jiehua, S., et al. (2021). Inhibition of Caspase-1 ameliorates ischemia-associated blood-brain barrier dysfunction and integrity by suppressing Pyroptosis activation. *Front. Cell. Neurosci.* 14:540669. doi: 10.3389/fncel.2020.540669

Liu, C., Zhang, K., Shen, H., Yao, X., Sun, Q., and Chen, G. (2018). Necroptosis: a novel manner of cell death, associated with stroke (review). *Int. J. Mol. Med.* 41, 624–630. doi: 10.3892/ijmm.2017.3279

Liu, T., Ma, Z., Liu, L., Pei, Y., Wu, Q., Xu, S., et al. (2024). Conditioned medium from human dental pulp stem cells treats spinal cord injury by inhibiting microglial Pyroptosis. *Neural. Regen. Res.* 19, 1105–1111. doi: 10.4103/1673-5374.385309

Liu, X., Zhang, M., Liu, H., Zhu, R., He, H., Zhou, Y., et al. (2021). Bone marrow mesenchymal stem cell-derived exosomes attenuate cerebral ischemia-reperfusion injury-induced Neuroinflammation and Pyroptosis by modulating microglia M1/M2 phenotypes. *Exp. Neurol.* 341:113700. doi: 10.1016/J.EXPNEUROL.2021.113700

Mine, Y., Tatarishvili, J., Oki, K., Monni, E., Kokaia, Z., and Lindvall, O. (2013). Grafted human neural stem cells enhance several steps of endogenous neurogenesis and improve behavioral recovery after middle cerebral artery occlusion in rats. *Neurobiol. Dis.* 52, 191–203. doi: 10.1016/J.NBD.2012.12.006

Mitrečić, D., Nicaise, C., Gajović, S., and Pochet, R. (2010). Distribution, differentiation, and survival of intravenously administered neural stem cells in a rat model of amyotrophic lateral sclerosis. *Cell Transplant.* 19, 537–548. doi: 10.3727/096368910X498269

Mitroshina, E. V., Saviuk, M., and Vedunova, M. V. (2023). Necroptosis in CNS diseases: focus on astrocytes. *Front. Aging Neurosci.* 14, 1–18. doi: 10.3389/fnagi.2022.1016053

Muir, K. W., Bulters, D., Willmot, M., Sprigg, N., Dixit, A., Ward, N., et al. (2020). Intracerebral implantation of human neural stem cells and motor recovery after stroke: multicentre prospective single-arm study (PISCES-2). *J. Neurol. Neurosurg. Psychiatry* 91, 396–401. doi: 10.1136/JNNP-2019-322515

Naghavi, M., Wang, H., Lozano, R., Davis, A., Liang, X., Zhou, M., et al. (2015). Global, regional, and National age-sex Specific all-Cause and cause-specific mortality for 240 causes of death, 1990-2013: a systematic analysis for the global burden of disease study 2013. *Lancet* 385, 117–171. doi: 10.1016/S0140-6736(14)61682-2

Nicaise, C., Mitrecic, D., and Pochet, R. (2011). Brain and spinal cord affected by amyotrophic lateral sclerosis induce differential growth factors expression in rat mesenchymal and neural stem cells. *Neuropathol. Appl. Neurobiol.* 37, 179–188. doi: 10.1111/J.1365-2990.2010.01124.X

Northington, F. J., Chavez-Valdez, R., Graham, E. M., Razdan, S., Gauda, E. B., and Martin, L. J. (2011). Necrostatin decreases oxidative damage, inflammation, and injury after neonatal HI. *J. Cereb. Blood Flow Metab.* 31, 178–189. doi: 10.1038/JCBFM.2010.72

Ourednik, J., Ourednik, V., Lynch, W. P., Schachner, M., and Snyder, E. Y. (2002). Neural stem cells display an inherent mechanism for rescuing dysfunctional neurons. *Nat. Biotechnol.* 20, 1103–1110. doi: 10.1038/NBT750

Paxinos, G., and Franklin, K. B. J. (2001). The mouse brain in stereotaxic coordinates. *2nd* Edn. San Diego: Academic Press.

Petrović, D. J., Jagečić, D., Krasić, J., Sinčić, N., and Mitrečić, D. (2023). Effect of fetal bovine serum or basic fibroblast growth factor on cell survival and the proliferation of neural stem cells: the influence of homocysteine treatment. *Int. J. Mol. Sci.* 24:14161. doi: 10.3390/ijms241814161

Radoszkiewicz, K., Hribljan, V., Isakovic, J., Mitrecic, D., and Sarnowska, A. (2023). Critical points for optimizing long-term culture and neural differentiation capacity of rodent and human neural stem cells to facilitate translation into clinical settings. *Exp. Neurol.* 363:114353. doi: 10.1016/J.EXPNEUROL.2023.114353

Redmond, D. E., Bjugstad, K. B., Teng, Y. D., Ourednik, V., Ourednik, J., Wakeman, D. R., et al. (2007). Behavioral improvement in a primate Parkinson's model is associated with multiple homeostatic effects of human neural stem cells. *Proc. Natl. Acad. Sci. USA* 104, 12175–12180. doi: 10.1073/PNAS.0704091104

Schaar, K. L., Brenneman, M. M., and Savitz, S. I. (2010). Functional assessments in the rodent stroke model. *Exp. Transl. Stroke Med.* 2, 1–11. doi: 10.1186/2040-7378-2-13/FIGURES/4

Shahjouei, S., Cai, P. Y., Ansari, S., Sharififar, S., Azari, H., Ganji, S., et al. (2016). Middle cerebral artery occlusion model of stroke in rodents: a step-by-step approach. *J. Vasc. Interv. Neurol.* 8, 1–8

Shen, C.-C., Lin, C.-H., Yang, Y.-C., Chiao, M.-T., Cheng, W.-Y., and Ko, J.-L. (2010). Intravenous implanted neural stem cells migrate to injury site, reduce infarct volume, and improve behavior after cerebral ischemia. *Curr. Neurovasc. Res.* 7, 167–179. doi: 10.2174/156720210792231822

Shi, J., Zhao, Y., Wang, K., Shi, X., Wang, Y., Huang, H., et al. (2015). Cleavage of GSDMD by inflammatory caspases determines pyroptotic cell death. *Nat. Cell Biol.* 526, 660–665. doi: 10.1038/nature15514

Singhal, G., and Baune, B. T. (2017). Microglia: An Interface between the loss of neuroplasticity and depression. *Front. Cell. Neurosci.* 11:270. doi: 10.3389/fncel.2017.00270

Stančin, P., Song, M. S., Alajbeg, I., and Mitrečić, D. (2023). Human Oral mucosa stem cells increase survival of neurons affected by in vitro anoxia and improve recovery of mice affected by stroke through time-limited secretion of MiR-514A-3p. *Cell. Mol. Neurobiol.* 43, 1975–1988. doi: 10.1007/s10571-022-01276-7

Steinberg, G. K., Kondziolka, D., Wechsler, L. R., Dade Lunsford, L., Coburn, M. L., Billigen, J. B., et al. (2016). Clinical outcomes of transplanted modified bone marrow-derived mesenchymal stem cells in stroke: a phase 1/2a study. *Stroke* 47, 1817–1824. doi: 10.1161/STROKEAHA.116.012995

Thom, T., Haase, N., Rosamond, W., Howard, V. J., Rumsfeld, J., Manolio, T., et al. (2006). Heart disease and stroke statistics - 2006 update: a report from the American Heart Association statistics committee and stroke statistics subcommittee. *Circulation* 113, e85–e151. doi: 10.1161/CIRCULATIONAHA.105.171600

Wang, K., Sun, Z., Junnan, R., Wang, S., Huang, L., Ruan, L., et al. (2020). Ablation of GSDMD improves outcome of ischemic stroke through blocking canonical and non-canonical Inflammasomes dependent Pyroptosis in microglia. *Front. Neurol.* 11, 1–12. doi: 10.3389/fneur.2020.577927

Webb, A. J. S., Fonseca, A. C., Berge, E., Randall, G., Fazekas, F., Norrving, B., et al. (2021). Value of treatment by comprehensive stroke Services for the Reduction of critical gaps in acute stroke Care in Europe. *Eur. J. Neurol.* 28, 717–725. doi: 10.1111/ENE.14583

Wu, M.-Y., Yiang, G.-T., Liao, W.-T., Tsai, A. P.-Y., Cheng, Y.-L., Cheng, P.-W., et al. (2018). Current mechanistic concepts in ischemia and reperfusion injury. *Cell. Physiol. Biochem.* 46, 1650–1667. doi: 10.1159/000489241

Xue, W. S., Wang, N., Wang, N. Y., Ying, Y. F., and Guo Hui, X. (2019). MiR-145 protects the function of neuronal stem cells through targeting MAPK pathway in the treatment of cerebral ischemic stroke rat. *Brain Res. Bull.* 144, 28–38. doi: 10.1016/J.BRAINRESBULL.2018.08.023

Yang, M., Lv, Y., Tian, X., Lou, J., An, R., Zhang, Q., et al. (2017). Neuroprotective effect of β-Caryophyllene on cerebral ischemia-reperfusion injury via regulation of Necroptotic neuronal death and inflammation: in vivo and in vitro. *Front. Neurosci.* 11, 1–13. doi: 10.3389/fnins.2017.00583

Zhang, S., Wang, Y., Li, D., Junfa, W., Si, W., and Yi, W. (2016). Necrostatin-1 attenuates inflammatory response and improves cognitive function in chronic ischemic stroke mice. *Medicines* 3:16. doi: 10.3390/medicines3030016

Zhuo, Y., Chen, W., Li, W., Huang, Y., Duan, D., Ge, L., et al. (2021). Ischemic-hypoxic preconditioning enhances the mitochondrial function recovery of transplanted olfactory mucosa mesenchymal stem cells via MiR-181a signaling in ischemic stroke. *Aging* 13, 11234–11256. doi: 10.18632/AGING.202807

frontiers | Frontiers in Molecular Neuroscience

TYPE Original Research
PUBLISHED 25 September 2024
DOI 10.3389/fnmol.2024.1456670

OPEN ACCESS

EDITED BY
Marija Heffer,
Josip Juraj Strossmayer University of Osijek, Croatia

REVIEWED BY
Natalie A. Prowse,
Carleton University, Canada
Gamze Guven,
Istanbul University, Türkiye

*CORRESPONDENCE
Mirjana Babić Leko
✉ mbabicleko@gmail.com
Goran Šimić
✉ gsimic@hiim.hr

RECEIVED 01 July 2024
ACCEPTED 28 August 2024
PUBLISHED 25 September 2024

CITATION
Babić Leko M, Španić Popovački E, Willumsen N, Nikolac Perković M, Pleić N, Zubčić K, Langer Horvat L, Vogrinc Ž, Boban M, Borovečki F, Zemunik T, de Silva R and Šimić G (2024) Further validation of the association between *MAPT* haplotype-tagging polymorphisms and Alzheimer's disease: neuropsychological tests, cerebrospinal fluid biomarkers, and *APOE* genotype.
Front. Mol. Neurosci. 17:1456670.
doi: 10.3389/fnmol.2024.1456670

Further validation of the association between *MAPT* haplotype-tagging polymorphisms and Alzheimer's disease: neuropsychological tests, cerebrospinal fluid biomarkers, and *APOE* genotype

Mirjana Babić Leko[1]*, Ena Španić Popovački[1], Nanet Willumsen[2], Matea Nikolac Perković[3], Nikolina Pleić[4], Klara Zubčić[5], Lea Langer Horvat[1], Željka Vogrinc[6], Marina Boban[7,8], Fran Borovečki[7,8,9], Tatijana Zemunik[4,10], Rohan de Silva[2] and Goran Šimić[1]*

[1]Department for Neuroscience, Croatian Institute for Brain Research, University of Zagreb Medical School, Zagreb, Croatia, [2]Reta Lila Weston Institute, Department of Clinical and Movement Neuroscience, UCL Queen Square Institute of Neurology, London, United Kingdom, [3]Division of Molecular Medicine, Ruđer Bošković Institute, Zagreb, Croatia, [4]Department of Biology and Human Genetics, School of Medicine, University of Split, Split, Croatia, [5]Department of Molecular Diagnostics and Genetics, Dubrava University Hospital, Zagreb, Croatia, [6]Laboratory for Neurobiochemistry, Department of Laboratory Diagnostics, University Hospital Centre Zagreb, Zagreb, Croatia, [7]Department of Neurology, University Hospital Centre Zagreb, Kišpatićeva, Zagreb, Croatia, [8]School of Medicine, University of Zagreb, Zagreb, Croatia, [9]Department for Functional Genomics, Centre for Translational and Clinical Research, University of Zagreb Medical School, Zagreb, Croatia, [10]Department of Nuclear Medicine, University Hospital Split, Split, Croatia

Introduction: Genetic studies have shown that variants in the microtubule-associated protein tau (*MAPT*) gene, which encodes tau protein, can increase the risk for Alzheimer's disease (AD). Additionally, two haplotypes of the *MAPT* gene (H1 and H2) are associated with various neurodegenerative disorders, including AD. This study aimed to test the association of *MAPT* haplotypes (H1 and H2) and *MAPT* haplotype-tagging polymorphisms (rs1467967, rs242557, rs3785883, rs2471738, del–In9, rs7521) with AD.

Methods: The study included 964 individuals: 113 with AD, 53 with mild cognitive impairment (MCI), 54 with other dementias, and 744 healthy controls.

Results: The results showed that individuals carrying the A allele in the *MAPT* rs1467967 polymorphism, the GG genotype in the *MAPT* rs7521 polymorphism, and the G allele in the *MAPT* rs242557 polymorphism had worse performance on various neuropsychological tests. Carriers of the C allele in *MAPT* rs2471738 polymorphism and CC homozygotes also showed worse performance on neuropsychological tests and pathological levels of several cerebrospinal fluid (CSF) biomarkers. However, T allele carriers in the *MAPT* rs2471738 polymorphism were more represented among patients with dementia and apolipoprotein E (*APOE*) ε4 carriers. Carriers of the H2 *MAPT* haplotype had worse performance on various neuropsychological tests, consistent with our previous study, which associated the H2 *MAPT* haplotype with pathological levels of CSF AD biomarkers. Regarding the *MAPT* rs3785883 polymorphism, further research is needed since both the AA and GG genotypes were associated with pathological levels of CSF and plasma AD biomarkers.

Discussion: In conclusion, further genetic studies are needed to elucidate the role of *MAPT* haplotypes and *MAPT* haplotype-tagging polymorphisms in the development of AD.

KEYWORDS

Alzheimer's disease, *APOE* gene, biomarkers, cerebrospinal fluid, dementia, *MAPT* gene, *MAPT* haplotypes, *MAPT* polymorphisms

1 Introduction

Alzheimer's disease (AD) is a complex condition influenced by both genetic and environmental factors. Analysis of tau-positron emission tomography (tau-PET) scans from 1,612 individuals identified four different AD subtypes based on the spread of tau pathology: (1) limbic (apolipoprotein E ε4+ [*APOE* ε4+], less tau, amnestic, older onset, 32.7% of cases), (2) lateral temporal (more tau, rapidly progressive, multi-domain impairment, asymmetric, 18.1% of cases), (3) medial temporal lobe-sparing (*APOE* ε4-, younger onset, dysexecutive, 30.2% of cases), and (4) posterior (older onset, slowly-progressing, visuospatial impairment, 19% of cases, also called posterior cortical atrophy or atypical AD) (Vogel et al., 2021). These findings indicate that additional studies are necessary to elucidate AD's complex interplay between genetic and environmental factors. According to AlzGene (Bertram et al., 2007), 1,395 studies identified 695 genes associated with AD. In the sporadic form of AD, which accounts for about 99% of disease cases, the main genetic factor that increases the relative risk of developing AD is the ε4 variant of the *APOE* gene. One ε4 allele increases the risk of developing AD by about three times, while both ε4 alleles increase the relative risk by eight to twelve times (Alzheimer's Association, 2020). Numerous other genes associated with sporadic AD have been discovered, but their influence on the risk of the disease is much smaller than that of the *APOE* gene. These genes include *BIN1*, *CLU*, *ABCA7*, *CR1*, *PICALM*, *MS4A6A*, *CD33*, *MS4A4E*, *CD2AP* (Bertram et al., 2007), *TREM2* (Jonsson et al., 2013), and *PLD3* (Cruchaga et al., 2014), among others. These genes were mostly identified in genome-wide association studies (GWAS) that compared many single nucleotide polymorphisms (SNPs) between AD patients and healthy controls (HC).

The microtubule-associated protein tau (*MAPT*) gene, located on chromosome 17q21.3, encodes the tau protein, which, in addition to amyloid β (Aβ), plays a major role in AD. Although AD is considered a secondary tauopathy (i.e., it is not caused by the mutations in the *MAPT* gene, as is the case in primary tauopathies), certain *MAPT* variants have been shown to increase the risk for AD (Myers et al., 2005; Laws et al., 2007; Chang et al., 2014; Yuan et al., 2017; Zhou and Wang, 2017). Moreover, two *MAPT* haplotypes (H1 and H2), which can be defined by six haplotype-tagging SNPs (rs1467967, rs242557, rs3785883, rs2471738, del–In9, rs7521) (Pittman et al., 2005), have been associated with various neurodegenerative disorders, including AD (Myers et al., 2005; Laws et al., 2007; Kauwe et al., 2008; Di Maria et al., 2010; Pastor et al., 2016; Sánchez-Juan et al., 2019). The *MAPT* H1 haplotype has been shown to increase risk, while *MAPT* H2 haplotype reduces the risk for several neurodegenerative disorders (Strickland et al., 2020). In our previous preliminary study, we observed that the levels of cerebrospinal fluid (CSF) biomarkers differed between patients with different genotypes in *MAPT* SNPs (specifically, rs1467967 and rs2471738) and different *MAPT* haplotypes (Babić Leko et al., 2018). This study aimed to further validate the association of *MAPT* haplotype-tagging polymorphisms with AD. We tested whether there is a difference in the results of neuropsychological tests, levels of CSF and plasma biomarkers, and the frequency of *APOE* genotypes among patients with different genotypes in *MAPT* haplotype-tagging polymorphisms. We also examined whether there is a difference in the distribution of *MAPT* haplotype-tagging polymorphisms and *MAPT* haplotypes between patients with AD and HC. Moreover, we analyzed additional AD biomarkers, such as chitinase 3-like protein 1 (YKL-40), S100 calcium-binding protein B (S100B), neurofilament light chain (NfL), and p-tau$_{181}$/A$\beta_{1\text{-}42}$ ratio.

2 Materials and methods

2.1 Subjects

This study included 964 subjects, of whom 220 were recruited at the University Hospital Centre Zagreb. These 220 participants suffered from various types of primary dementia causes: AD, mild cognitive impairment (MCI), frontotemporal dementia (FTD), vascular cognitive impairment/vascular dementia (VaD), mixed dementia (AD+VaD), non-specific dementia (ND), corticobasal syndrome (CBS), and Parkinson's disease (PD). AD was diagnosed using the criteria of the National Institutes on Aging - Alzheimer's Association (NIA-AA) (McKhann et al., 2011). The following criteria were used for the diagnosis of other dementia types: for MCI, the criteria of Petersen et al. (1999) and Albert et al. (2011); for FTD, the criteria of Neary et al. (1998); and for VaD, the Hachinski Ischemic Score (Hachinski et al., 1975) and the criteria of the National Institute for Neurological Disorders and Stroke – Association Internationale pour la Recherche et l'Enseignement en Neurosciences (NINCDS-AIREN) (Román et al., 1993).

All patients included in this study provided informed consent for lumbar puncture and participation in the study. Patients underwent neurological examinations with complete blood tests, including levels of thyroid hormones, vitamin B12 and B9, and serology for syphilis and Lyme disease. The Ethical Committee of the Clinical Hospital Centre Zagreb (case no. 02/21 AG, class 8.1–18/82–2 from April 24, 2018) and the Central Ethical Committee of the University of Zagreb Medical School (case no. 380–59–10,106-18-111/126, class 641–01/18–02/01 from June 20, 2018) approved all procedures, which were conducted in accordance with the Helsinki Declaration (World Medical Association, 2013).

A larger cohort of 744 HC older than 65 years of age included participants from the "10,001 Dalmatians project," part of the Croatian

Biobank program (Rudan et al., 2009). Participants provided informed consent for participation in the study, and the Ethical Board of the University of Split, School of Medicine (case no. 2181-198-03-04/10-11-0008 and 2181-198-03-04-19-0022) approved all procedures.

Information on demographic data, determined biomarkers, and the number of *APOE* and *MAPT* genotypes and *MAPT* haplotypes in all included cohorts is presented in Table 1.

2.2 Analysis of cerebrospinal fluid and plasma biomarkers

This part of the analysis was done in 220 participants recruited at the University Hospital Centre Zagreb. All biomarkers were analyzed in CSF, while some were also analyzed in plasma. CSF was collected by lumbar puncture between intervertebral spaces L3/L4 or L4/L5, centrifuged at 2,000 g for 10 min, and stored at −80°C in polypropylene tubes. Thrombocyte-free plasma was extracted from venous blood through a series of centrifugations (first at 1,100 g for 3 min, followed by centrifugation at 5,087 g for 15 min) and stored at −20°C.

The following enzyme-linked immunosorbent assays (ELISA) were used for the determination of biomarkers: tau phosphorylated at threonine 181 (p-tau$_{181}$) (Innotest Phospho-Tau [181P], Fujirebio), A$\beta_{1\text{-}42}$ (Innotest β-amyloid1–42, Fujirebio, Gent, Belgium), NfL (Human NF-L/NEFL ELISA Kit, LifeSpan BioSciences, Seattle, WA, USA), S100B (Human S100B, R&D Systems, Minneapolis, MN, USA), and YKL-40 (Chitinase 3-like 1 Quantikine ELISA Kit, R&D Systems). All biomarkers were measured only in CSF, except for S100B and NfL, which were measured in both CSF and plasma.

2.3 Determination of polymorphisms

The salting-out method by Miller et al. (1988) was used for the isolation of DNA from venous blood. In the 220 participants recruited at the University Hospital Centre Zagreb, *MAPT* rs1467967, rs242557, rs3785883, rs2471738, del–In9, rs7521, and *APOE* rs7412 and rs429358 SNPs were determined using TaqMan SNP Genotyping Assays (Applied Biosystems) on an ABI Prism 7,300 Real-Time PCR System apparatus (Applied Biosystems, Foster City, CA). The *MAPT* H1/H2 haplotype is defined by the del-In9 deletion in *MAPT* intron 9.

In 744 participants recruited as part of the "10,001 Dalmatians project," *MAPT* rs3785883, rs2471738, rs7521, rs1800547, and *APOE* rs7412 and rs429358 were determined using Illumina genotyping platforms (CNV370v1, CNV370-Quadv3, and OmniExpressExome-8v1-2_A, Illumina, San Diego, CA). In this cohort, *MAPT* haplotypes were defined by the *MAPT* rs1800547 SNP. *MAPT* rs1467967 and rs242557 polymorphisms were not determined in this cohort of healthy controls. *APOE* ε2, ε3, and ε4 variants were determined by the following combination of *APOE* SNPs: variant ε2 (rs429358 T allele and rs7412 T allele), variant ε3 (rs429358 T allele and rs7412 C allele), and variant ε4 (rs429358 C allele and rs7412 C allele).

2.4 Neuropsychological testing

Participants recruited at the University Hospital Centre Zagreb were tested with various neuropsychological assessments, including the Mini-Mental State Examination (MMSE), the modified MMSE test, the Alzheimer's Disease Assessment Scale-Cognitive subscale (ADAS-Cog), the Picture Pairs Learning and Recall (PPLR) test, the Word Pairs Learning and Recall (WPLR) test, the Visual Association Test (VAT), the Rey–Osterrieth Complex Figure Test (ROCFT), the Clock Drawing Test (CDT), the California Verbal Learning Test (CVLT), the NeuroPsychiatric Inventory (NPI), the Reverse Naming test, the Stroop test, the Visual Reaction Time (VRT) test, and the Boston Naming Test (BNT).

2.5 Statistical analysis

Statistical analysis was performed using SPSS 19.0.1 (SPSS, Chicago, IL, USA) and R statistical software (R Core Team, Vienna, Austria). The level of statistical significance was set at $\alpha = 0.05$.

The frequencies of *APOE* genotypes and different diagnoses among subjects with different *MAPT* genotypes and haplotypes were analyzed using a χ^2-test (Chi-squared test), with Bonferroni correction applied for pairwise comparisons.

Levels of all fluid biomarkers and the majority of variables collected by neuropsychological testing deviated from a normal distribution ($p < 0.05$), except for ADAS-Cog ($p = 0.07$), BNT ($p = 0.153$), PPLR corr ($p = 0.193$), PPLR incorr ($p = 0.126$), PPLR t corr ($p = 0.470$), and PPLR t incorr ($p = 0.288$). Thus, for comparisons of CSF and plasma biomarkers and scores on neuropsychological tests between groups, we used non-parametric tests. First, all variables were compared between groups of patients with different *MAPT* genotypes using the Kruskal-Wallis test (denoted by the letter "H"), followed by *post-hoc* Dunn's test, which corrects *p*-values for multiple comparisons. In addition to statistical analyses between all genotypes (for example, AA vs. AG vs. GG), *MAPT* genotypes were also grouped, and additional analyses were conducted (for example, AA vs. G allele carriers and GG vs. A allele carriers). CSF and plasma biomarkers and scores on neuropsychological tests were compared between two groups (for example, AA vs. G allele carriers) using the Mann–Whitney *U* test. All statistical analyses were conducted in the group of all patients with dementia (1), AD and MCI patients (2), and AD patients (3).

Variables were analyzed using linear regression when the influence of possible covariates had to be considered. Since the distribution of the majority of variables (CSF and plasma biomarkers and scores on neuropsychological tests) deviated from a normal distribution, variables were logarithmically transformed before linear regression. CSF and plasma biomarkers and scores on neuropsychological tests were considered as dependent variables, while *MAPT* genotypes and haplotypes (and covariates) were considered as independent variables.

3 Results

Before analyses, we tested if the variables were associated with sex, age, and *APOE* genotype (ε4+ vs. ε4-). Regarding neuropsychological tests, none of the variables were associated with sex, age, or *APOE* genotype. Thus, there was no need to consider sex, age, or *APOE* genotype as covariates, and analyses were not controlled for the influence of these factors. On the other hand, fluid biomarkers showed an

TABLE 1 Information on demographic data, determined biomarkers, and the number of *APOE* and *MAPT* genotypes in different cohorts.

		AD	MCI	VaD	FTD	DLB	AD/VaD	PD	CBS	ND	All patients with dementia[#,*]	HC[**]	HWE *p*-value[$]
Determined biomarkers	CSF	+	+	+	+	+	+	+	+	+	+	–	
	Plasma	+	+	+	+	+	+	+	+	+	+	–	
	Neuropsychological	+	+	+	+	+	+	+	+	+	+	–	
	Genetic	+	+	+	+	+	+	+	+	+	+	+	
N		113	53	14	23	8	2	2	1	4	220	744	
Age	Median (25–75th Percentile)	73 (67–77)	70 (59–75)	71 (63–78)	61 (57–65)	71 (68–75)	75	68	51	67 (52–68)	71 (62–76)	71 (67–76)	
Sex	F/M	60/53	27/26	6/8	11/12	2/6	0/2	0/2	1/0	3/1	110/110	433/311	
MMSE	Mean ± SD	20 ± 4.5	25.1 ± 3	22.2 ± 5	16.5 ± 5.2	19 ± 3.7	20.5 ± 5.0	15	27	19.3 ± 5.3	21.1 ± 5	–	
APOE	ε2ε2									1	1 (0.5%)	3 (0.4%)	
	ε3ε2	9	1	2	2	1		1	1		17 (7.7%)	71 (9.5%)	
	ε3ε3	58	36	7	15	4	2	1		2	125 (56.8%)	580 (78%)	
	ε4ε3	36	14	4	5	2	1			1	63 (28.6%)	78 (10.5%)	
	ε4ε4	7	2	1	1						11 (5%)	5 (0.7%)	
	ε4ε2	5									5 (2.3%)	7 (0.9%)	
MAPT rs1467967	AA	49	23	6	11	3	1	2	1	4	100 (45.5%)		0.990
	AG	53	21	6	11	4	1				96 (43.6%)		
	GG	11	9	2	1	1					24 (10.9%)		
MAPT rs242557	AA	16	10		5	1				1	33 (15%)		0.788
	AG	48	24	8	11	4		1		2	98 (44.5%)		
	GG	49	19	6	7	3	2	1	1	1	89 (40.5%)		
MAPT rs3785883	AA	10	4	3	1		1				19 (8.6%)	29 (3.9%)	0.768
	AG	34	11	3	10	4		1		1	64 (29.1%)	256 (34.4%)	
	GG	69	38	8	12	4	1	1	1	3	137 (62.3%)	459 (61.7%)	
MAPT rs2471738	TT	7	2								9 (4.1%)	21 (2.8%)	0.768
	TC	37	21	6	7	2		2	1	2	78 (35.5%)	184 (24.7%)	
	CC	69	30	8	16	6	2			2	133 (60.5%)	539 (72.4%)	

(Continued)

10.3389/fnmol.2024.1456670

10.3389/fnmol.2024.1456670

TABLE 1 (Continued)

		AD	MCI	VaD	FTD	DLB	AD/VaD	PD	CBS	ND	All patients with dementia#,*	HC**	HWE *p*-value$
MAPT rs7521	AA	18	13	2	4	3				1	41 (18.6%)	191 (25.7%)	0.876
	AG	65	30	7	17	4	2	1	1	1	128 (58.2%)	362 (48.7%)	
	GG	30	10	5	2	1		1		2	51 (23.2%)	191 (25.7%)	
MAPT haplotypes	H1H1	75	40	8	20	8		1	1	3	156 (70.9%)	491 (66%)	0.281
	H1H2	36	12	6	3		2	1		1	61 (27.7%)	233 (31.3%)	
	H2H2	2	1								3 (1.4%)	20 (2.7%)	

#This group consists of patients with AD, MCI, VaD, FTD, AD/VaD, DLB, ND, PD, and CBS. *Number of participants (percentage of patients with dementia carrying that genotype relative to the total number of patients with dementia). **Number of participants (percentage of healthy controls carrying that genotype relative to the total number of healthy controls). $Testing for Hardy–Weinberg Equilibrium (HWE) was conducted using the Chi-Square test in SPSS. AD, Alzheimer's disease; AD/VaD, mixed dementia; *APOE*, apolipoprotein E; MAPT, Microtubule associated protein tau; CBS, corticobasal syndrome; CSF, cerebrospinal fluid; DLB, dementia with Lewy bodies; F, female; FTD, frontotemporal dementia; HC, healthy controls; HWE, Hardy–Weinberg equilibrium; M, male; MCI, mild cognitive impairment; MMSE, Mini-Mental State Examination; ND, nonspecific dementia; PD, Parkinson's disease; SD, standard deviation; VaD, vascular dementia.

association with sex, age, and *APOE* genotype. More precisely, CSF YKL-40 ($r_S = 0.339$, $p < 0.001$), CSF NfL ($r_S = 0.199$, $p = 0.019$), and plasma NfL ($r_S = 0.413$, $p < 0.001$) were positively correlated with the age of participants. Moreover, NfL plasma levels were significantly increased in males compared to females ($U = 2076$, $Z = -2.392$, $p = 0.017$), while the p-tau$_{181}$/A$\beta_{1\text{-}42}$ ratio was significantly increased in carriers of the ε4 *APOE* genotype ($U = 3{,}875$, $Z = -4.056$, $p < 0.001$).

Additionally, we tested if the interaction between each *MAPT* polymorphism and *APOE* genotype was significantly associated with the tested variables. It was shown that the interaction between rs242557 and *APOE* significantly predicted scores on ADAS-Cog ($\beta = 0.163$, SE = 0.077, $p = 0.037$). The interaction between rs1467967 and *APOE* predicted scores on ROCFTD ($\beta = -0.315$, SE = 0.14, $p = 0.028$). The interaction between rs1467967 and *APOE* ($\beta = 0.201$, SE = 0.081, $p = 0.015$) and rs242557 and *APOE* ($\beta = 0.211$, SE = 0.081, $p = 0.010$) significantly predicted VAT time. Additionally, the interaction between rs2471738 and *APOE* predicted CSF NfL levels ($\beta = 0.168$, SE = 0.070, $p = 0.017$). The interaction between *MAPT* haplotype and *APOE* predicted p-tau$_{181}$/A$\beta_{1\text{-}42}$ ratio ($\beta = -0.419$, SE = 0.115, $p < 0.001$). Thus, for these variables, the aforementioned interactions were considered as covariates.

Scores on neuropsychological tests and levels of CSF and plasma biomarkers in patients with different *MAPT* genotypes and haplotypes are presented in Supplementary Tables S1, S2, respectively.

3.1 *MAPT* rs1467967 genotype

Carriers of the A allele in the *MAPT* rs1467967 polymorphism had significantly lower MMSE scores compared to GG homozygotes. Carriers of the A allele had a significantly lower number of correct answers on the PPLR test, and a higher number of incorrect answers compared to GG homozygotes. Moreover, AA homozygotes had a significantly lower number of correct answers on the WPLR test and a higher number of incorrect answers compared to G allele carriers. AA homozygotes also had poorer performance on ROCFT, with lower scores on ROCFT delayed recall compared to G allele carriers (Figure 1; Table 2).

Plasma and CSF levels of S100B and NfL, as well as CSF p-tau$_{181}$/A$\beta_{1\text{-}42}$ ratio and YKL-40 levels, did not differ significantly between patients with different *MAPT* rs1467967 genotypes.

3.2 *MAPT* rs242557 genotype

G allele carriers in the *MAPT* rs242557 polymorphism had worse performance on the CVLT test compared to AA homozygotes. Specifically, levels of CVLT d and CVLT 1–5 were significantly decreased in G allele carriers compared to AA homozygotes. According to the NPI assessment, GG homozygotes were more depressed than A allele carriers. Moreover, worse performance on VAT (higher levels of VAT, VAT time, and VAT t average) was shown for G allele carriers compared to AA homozygotes (Figure 2; Table 3). PPLR t incorr levels were also higher in carriers of the G allele compared to AA homozygotes.

No significant difference in plasma and CSF levels of S100B and NfL, as well as CSF p-tau$_{181}$/A$\beta_{1\text{-}42}$ ratio and YKL-40 levels, was observed between patients with different *MAPT* rs242557 genotypes.

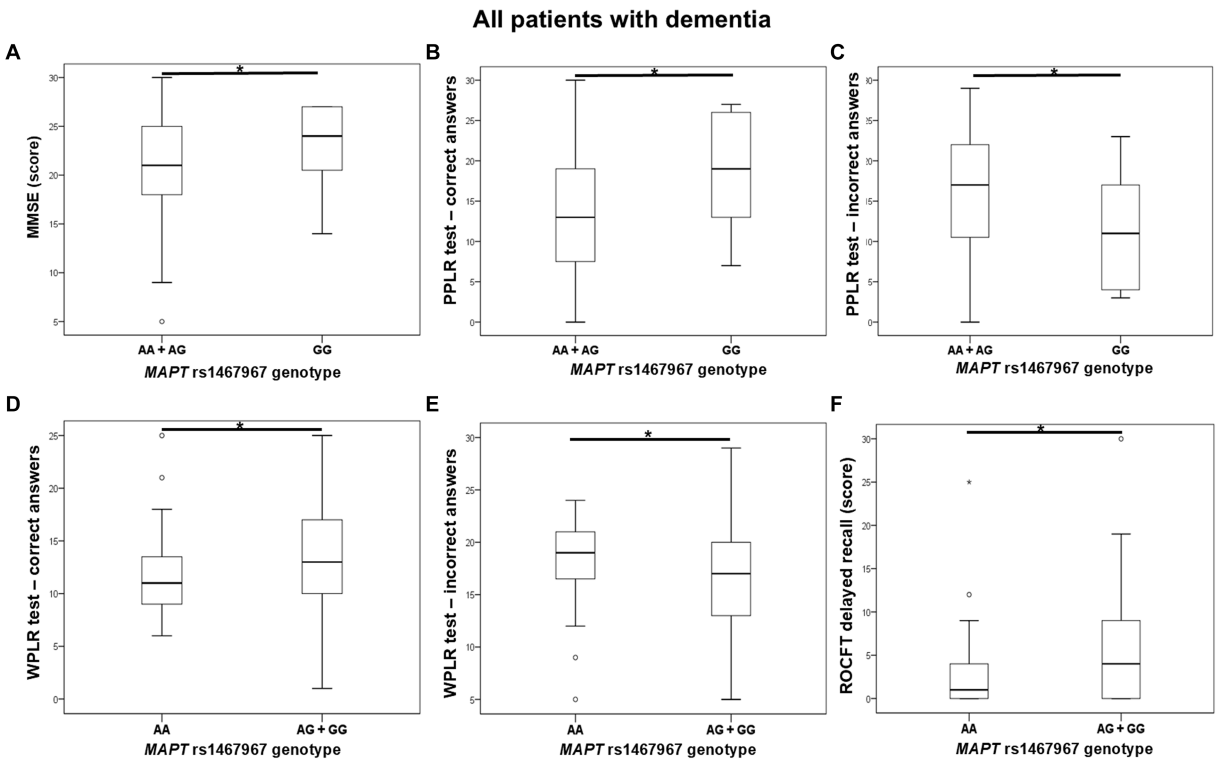

FIGURE 1
AA homozygotes and A allele carriers in the *MAPT* rs1467967 polymorphism showed poorer performance on **(A)** MMSE, **(B,C)** PPLR test, **(D,E)** WPLR test, and **(F)** ROCFT. The group "all patients with dementia" includes patients with AD, MCI, VaD, FTD, AD/VaD, DLB, ND, PD, and CBS. The box represents the interquartile range (between 25th and 75th percentiles), while the whiskers represent the range between the minimum and maximum values.

3.3 *MAPT* rs3785883 genotype

$A\beta_{1\text{-}42}$ levels were significantly decreased in A allele carriers compared to GG *MAPT* rs3785883 homozygotes (Figure 3; Table 4).

There was a significant difference in the distribution of *MAPT* rs3785883 genotypes between HC and patients with dementia ($\chi^2 = 9.2$, df = 1, $p = 0.004$). Specifically, a higher frequency of AA homozygotes was observed among patients with dementia ($p = 0.018$), while G allele carriers were more represented among HC ($p = 0.018$).

Additionally, A allele carriers had significantly increased S100B plasma levels compared to GG homozygotes (Figure 3; Table 4). Moreover, S100B in plasma was increased in carriers of the AG genotype compared to GG homozygotes (Table 4).

S100B in CSF was significantly increased in carriers of the GG genotype compared to A allele carriers (Figure 3; Table 4). In fact, S100B in CSF was increased in carriers of GG homozygotes compared to carriers of the AG genotype (Table 4). In AD patients, an increase in CSF YKL-40 levels was observed in G allele carriers compared to AA homozygotes (Figure 3; Table 4).

No significant difference in scores on neuropsychological tests was observed between patients with different *MAPT* rs3785883 genotypes.

3.4 *MAPT* rs2471738 genotype

TC heterozygotes in the *MAPT* rs2471738 genotype had a lower rate of disinhibition compared to TT homozygotes. C allele carriers had worse performance on the CVLT test (lower CVLT d and CVLT d cue scores). Finally, CC homozygotes made a higher number of errors on the Stroop test compared to T allele carriers (Figure 4; Table 5).

The CSF p-tau_{181}/$A\beta_{1\text{-}42}$ ratio was significantly higher in C allele carriers compared to TT homozygotes (Figure 4; Table 5).

There was a significant difference in the distribution of *MAPT* rs2471738 genotypes between HC and patients with AD ($\chi2 = 11.889$, df = 1, $p = 0.001$), AD and MCI ($\chi2 = 16.631$, df = 1, $p < 0.001$), and patients with dementia ($\chi2 = 16.226$, df = 1, $p < 0.001$). Specifically, a higher frequency of TT homozygotes and T allele carriers was observed among patients with AD ($p < 0.001$, $p = 0.006$, respectively), AD and MCI ($p < 0.001$, $p = 0.001$, respectively), and patients with dementia ($p < 0.001$, $p = 0.002$, respectively). Moreover, among TT homozygotes ($\chi^2 = 6.391$, df = 1, $p = 0.024$), there was a higher number of *APOE* ε4 carriers ($p = 0.046$) (when considering only individuals older than 65 years of age, and after excluding ε4ε2 genotype from analysis) (Figure 4).

3.5 *MAPT* rs7521 genotype

GG homozygotes in the *MAPT* rs7521 genotype exhibited worse performance on the WPLR test. They had a significantly lower number of correct answers on the WPLR test and a higher number of incorrect answers compared to A allele carriers. Furthermore, GG homozygotes had a longer VAT duration on the numbers test compared to AA

TABLE 2 Association of *MAPT* rs1467967 polymorphism with the results of neuropsychological tests.

Variables	*MAPT* rs1467967	
	A allele carriers vs. GG	G allele carriers vs. AA
MMSE	$U = 1{,}662$, $Z = -2.260$, $p = 0.024^{A}$ ($N = 217$, $d_{Cohen} = 0.31$, $\eta^2 = 0.023$)	
	$U = 352$, $Z = -1.960$, $p = 0.050^{C}$ ($N = 111$, $d_{Cohen} = 0.378$, $\eta^2 = 0.034$)	
Correct answers on the PPLR test	$U = 564$, $Z = -2.847$, $p = 0.004^{A}$ ($N = 105$, $d_{Cohen} = 0.408$, $\eta^2 = 0.04$)	
	$U = 387.5$, $Z = -2.050$, $p = 0.040^{B}$ ($N = 133$, $d_{Cohen} = 0.509$, $\eta^2 = 0.061$)	
Incorrect answers on the PPLR test	$U = 582$, $Z = -2.726$, $p = 0.006^{A}$ ($N = 133$, $d_{Cohen} = 0.486$, $\eta^2 = 0.056$)	
Correct answers on the WPLR test		$U = 1852.5$, $Z = -1.958$, $p = 0.050^{A}$ ($N = 136$, $d_{Cohen} = 0.339$, $\eta^2 = 0.028$)
		$U = 1{,}102$, $Z = -2.098$, $p = 0.036^{B}$ ($N = 108$, $d_{Cohen} = 0.411$, $\eta^2 = 0.04$)
Incorrect answers on the WPLR test		$U = 1841.5$, $Z = -2.006$, $p = 0.045^{A}$ ($N = 136$, $d_{Cohen} = 0.348$, $\eta^2 = 0.029$)
		$U = 1{,}099$, $Z = -2.117$, $p = 0.034^{B}$ ($N = 108$, $d_{Cohen} = 0.414$, $\eta^2 = 0.041$)
ROCFT delayed recall		$U = 1008.5$, $Z = -2.138$, $p = 0.033^{A\#}$ ($N = 103$, $d_{Cohen} = 0.418$, $\eta^2 = 0.042$)

Only statistically significant results are presented.
[A]all patients with dementia (patients with AD, MCI, VaD, FTD, AD/VaD, DLB, ND, PD, and CBS), [B]AD and MCI patients, [C]AD patients.
[#]The results remained significant when the analysis was controlled for the influence of the interaction between *MAPT* rs1467967 and *APOE* genotype ($\beta = 0.786$, SE = 0.261, $p = 0.004$). In addition to the results of Mann–Whitney *U* test, we provided information on the number of participants (*N*) and effect size (measured by Cohen's d [d_{Cohen}] or eta² [η^2]). MAPT, Microtubule-associated protein tau; MMSE, Mini-Mental State Examination; PPLR test, Picture Pairs Learning and Recall test; ROCFT, Rey–Osterrieth Complex Figure Test; WPLR test, Word Pairs Learning and Recall test.

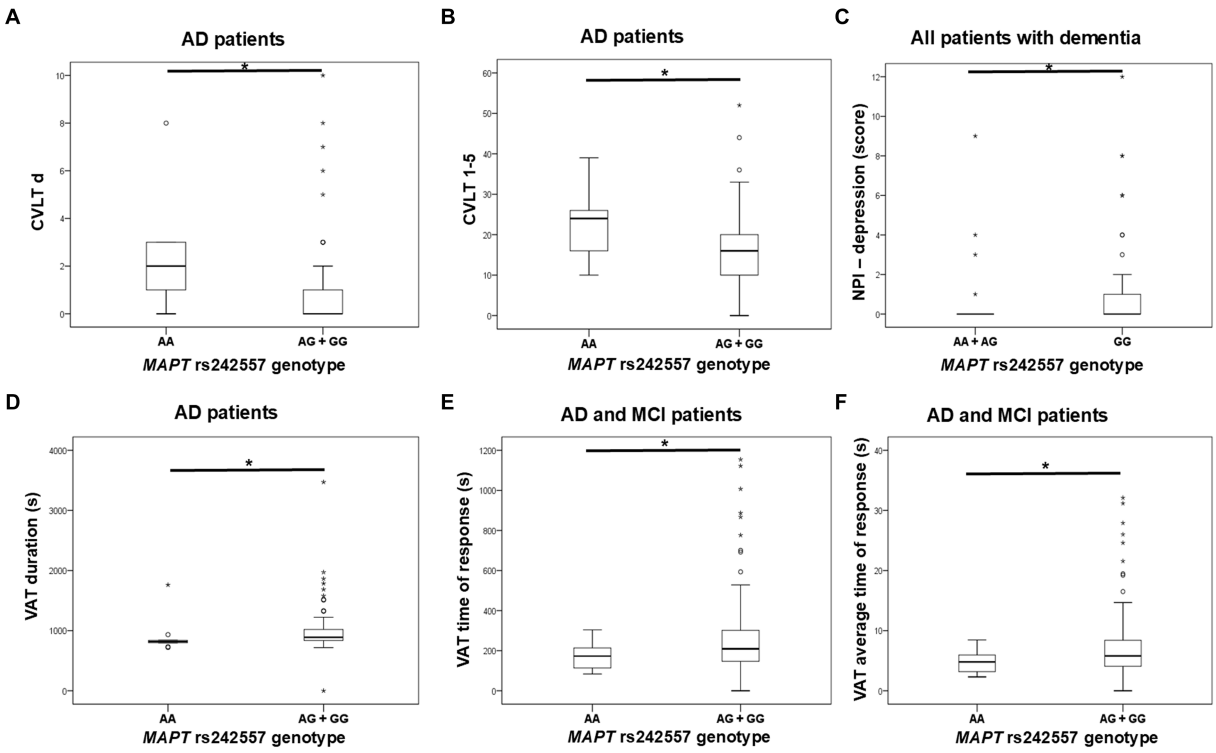

FIGURE 2
GG homozygotes and G allele carriers in the *MAPT* rs242557 polymorphism showed poorer performance on **(A,B)** CVLT, **(C)** NPI assessment, and **(D–F)** VAT test. The group "all patients with dementia" includes patients with AD, MCI, VaD, FTD, AD/VaD, DLB, ND, PD, and CBS. The box represents the interquartile range (between 25th and 75th percentiles), while the whiskers represent the range between the minimum and maximum values.

TABLE 3 Association of *MAPT* rs242557 polymorphism with the results of neuropsychological tests.

Variables	*MAPT* rs242557	
	A allele carriers vs. GG	G allele carriers vs. AA
CVLT d		$U = 124.5, Z = -2.839, p = 0.005^{C}$ ($N = 65$, $d_{Cohen} = 0.63$, $\eta^2 = 0.09$)
CVLT 1–5		$U = 147.5, Z = -1.987, p = 0.047^{C}$ ($N = 65$, $d_{Cohen} = 0.508$, $\eta^2 = 0.061$)
NPI - depression	$U = 950.5, Z = -2.793, p = 0.005^{A}$ ($N = 99$, $d_{Cohen} = 0.366$, $\eta^2 = 0.032$)	
	$U = 556.5, Z = -2.735, p = 0.006^{B}$ ($N = 78$, $d_{Cohen} = 0.436$, $\eta^2 = 0.045$)	
	$U = 284.5, Z = -2.584, p = 0.010^{C}$ ($N = 57$, $d_{Cohen} = 0.52$, $\eta^2 = 0.063$)	
VAT		$U = 138, Z = -2.214, p = 0.027^{C}$ ($N = 66$, $d_{Cohen} = 0.567$, $\eta^2 = 0.074$)
VAT time		$U = 496, Z = -2.027, p = 0.043^{B\#}$ ($N = 108$, $d_{Cohen} = 0.408$, $\eta^2 = 0.04$)
		$U = 122, Z = -2.469, p = 0.014^{C\#}$ ($N = 66$, $d_{Cohen} = 0.651$, $\eta^2 = 0.096$)
VAT t average		$U = 499.5, Z = -2.045, p = 0.041^{B}$ ($N = 108$, $d_{Cohen} = 0.401$, $\eta^2 = 0.039$)
		$U = 130.5, Z = -2.354, p = 0.019^{C}$ ($N = 66$, $d_{Cohen} = 0.606$, $\eta^2 = 0.084$)
PPLR t incorr		$U = 489, Z = -1.988, p = 0.047^{B}$ ($N = 105$, $d_{Cohen} = 0.396$, $\eta^2 = 0.038$)
		$U = 134, Z = -2.141, p = 0.032^{C}$ ($N = 63$, $d_{Cohen} = 0.56$, $\eta^2 = 0.073$)

Only statistically significant results are presented.
[A]all patients with dementia (patients with AD, MCI, VaD, FTD, AD/VaD, DLB, ND, PD, and CBS), [B]AD and MCI patients, [C]AD patients.
[#]Statistical significance lost after considering interaction between rs242557 polymorphism and *APOE* genotype as covariate. In addition to the results of Mann–Whitney *U* test, we provided information on the number of participants (*N*), and effect size (measured by Cohen's d [d_{Cohen}] or eta^2 [η^2]). CVLT, California Verbal Learning Test; MAPT, Microtubule-associated protein tau; NPI, NeuroPsychiatric Inventory; PPLR test, Picture Pairs Learning and Recall test; VAT, Visual Association Test.

homozygotes. G allele carriers and GG homozygotes showed poorer performance on the VRT test. Specifically, VRT discrimination reaction time (DRT) was longer in G allele carriers compared to AA homozygotes. The VRT choice reaction time (CRT) was longer in GG homozygotes compared to A allele carriers. Finally, GG homozygotes had a longer average time for giving correct answers in the Reverse Naming test compared to A allele carriers (RN t avcorr) (Figure 5; Table 6).

There was no significant difference in the distribution of *MAPT* rs7521 genotypes between AD patients (and also all patients with dementia) and HC. Plasma and CSF levels of S100B and NfL, as well as CSF p-tau$_{181}$/A$\beta_{1\text{-}42}$ ratio and YKL-40 levels, did not differ significantly between patients with different *MAPT* rs7521 genotypes.

3.6 *MAPT* haplotypes

Carriers of the H1H1 *MAPT* haplotype exhibited better performance, specifically a higher number of correct answers on the BNT, compared to carriers of the H2 haplotype (H1H2 + H2H2). H1H1 carriers also had fewer incorrect answers on the PPLR test compared to H2 carriers. Finally, H1H1 carriers performed better on the VRT test, with shorter VRT CRT compared to H2 carriers (Figure 6; Table 7). However, H1H1 carriers had higher plasma NfL levels compared to H2 carriers (Figure 6; Table 7).

There was no significant difference in the distribution of *MAPT* haplotypes between AD patients (and also all patients with dementia) and HC. Plasma and CSF levels of S100B, as well as CSF NfL, p-tau$_{181}$/A$\beta_{1\text{-}42}$ ratio, and YKL-40 levels, did not differ significantly between patients with different *MAPT* haplotypes.

4 Discussion

In the current study, we tested the association of *MAPT* haplotype-tagging polymorphisms and *MAPT* haplotypes with AD. We investigated whether there is a difference in the levels of CSF biomarkers, the results of neuropsychological tests, and the frequency of *APOE* genotypes among patients with different *MAPT* genotypes and haplotypes. Multiple GWA studies were conducted using various CSF AD biomarkers as quantitative traits.[1] Additionally, various plasma AD biomarkers were analyzed as quantitative traits in GWAS, including plasma p-tau$_{181}$, NfL, A$\beta_{1\text{-}42}$, A$\beta_{1\text{-}40}$, and t-tau (Stevenson-Hoare et al., 2023). Scores on neuropsychological tests were also used as quantitative traits in AD-associated GWAS (Homann et al., 2022). Due to genetic variability between populations, it is important to replicate studies in different populations. Since GWAS using the aforementioned quantitative traits had not previously been conducted in the Croatian population, we aimed to perform preliminary screening in this study to determine if some of the CSF and plasma biomarkers, as well as scores on neuropsychological tests, are associated with *MAPT* haplotype-tagging polymorphisms and *MAPT* haplotypes.

In this study, we observed that carriers of the A allele and AA genotype in the *MAPT* rs1467967 polymorphism had worse performance on MMSE test, PPLR test, WPLR test, and ROCFT. These results align with our previous study, which showed significantly increased levels of CSF t-tau in AA

1 https://www.ebi.ac.uk/gwas/

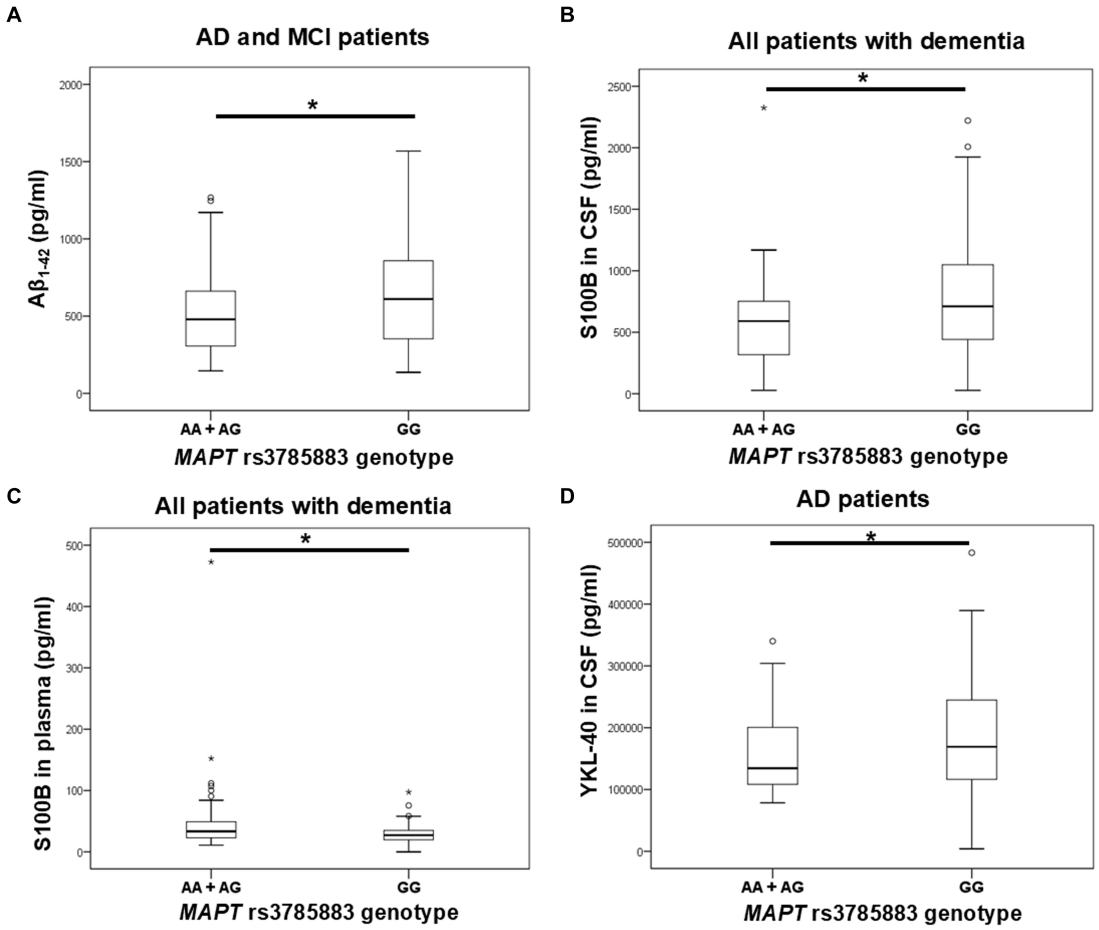

FIGURE 3
A allele carriers in the *MAPT* rs3785883 polymorphism had significantly decreased $A\beta_{1\text{-}42}$ levels **(A)**, and had significantly increased plasma S100B levels **(C)**. Conversely, GG homozygotes in the *MAPT* rs3785883 polymorphism had significantly increased CSF S100B levels **(B)**, and CSF YKL-40 **(D)** levels. The group "all patients with dementia" includes patients with AD, MCI, VaD, FTD, AD/VaD, DLB, ND, PD, and CBS. The box represents the interquartile range (between 25th and 75th percentiles), while the whiskers represent the range between the minimum and maximum values.

homozygotes and increased levels of CSF t-tau and p-tau_{181} in carriers of the AG *MAPT* rs1467967 genotype (Babić Leko et al., 2018). Several studies (Mukherjee et al., 2007; Abraham et al., 2009) and two meta-analyses (Yuan et al., 2017; Zhou and Wang, 2017) failed to show an association of the *MAPT* rs1467967 polymorphism with AD. Similarly, the association of the *MAPT* rs1467967 polymorphism with CSF AD biomarkers was not confirmed in studies of Elias-Sonnenschein et al. (2013) and Kauwe et al. (2008). However, Laws et al. (2007) did show an association between the *MAPT* rs1467967 A allele and AD. Ning et al. also noted that the distribution of rs1467967 genotypes differed between VaD patients and HC, suggesting that the *MAPT* rs1467967 polymorphism could serve as a genetic biomarker for VaD (Ning et al., 2011).

GG homozygotes in the *MAPT* rs242557 polymorphism had worse performance on the CVLT test and exhibited more depression than carriers of the A allele. Additionally, G allele carriers had worse performance on the VAT and PPLR tests. In contrast to our observed results, most previous studies associated the A allele of the *MAPT* rs242557 polymorphism with AD. Compta et al. observed increased CSF t-tau and p-tau_{181} levels in PD patients carrying the A allele in *MAPT* rs242557 polymorphism (Compta et al., 2011), while Laws et al. observed increased CSF t-tau levels in AD patients carrying AA *MAPT* rs242557 genotype (Laws et al., 2007). The A allele in the *MAPT* rs242557 polymorphism has been associated with a higher risk for AD (Myers et al., 2005; Laws et al., 2007; Chang et al., 2014; Yuan et al., 2017; Zhou and Wang, 2017), although some studies failed to observe this association (Mukherjee et al., 2007; Abraham et al., 2009; Feulner et al., 2010; Setó-Salvia et al., 2011; Allen et al., 2014). A recent study involving young healthy adults showed that A allele *MAPT* rs242557 carriers had a thinner cortex in brain regions vulnerable to early tau pathology (Huang et al., 2023). Another study conducted in cognitively healthy elders showed that A allele *MAPT* rs242557 carriers had higher retention of the tau-PET tracer ^{18}F-AV1451 in the hippocampus, making them more likely to develop tau pathology (Shen et al., 2019). However, a study by Tang et al. conducted in 3072 individuals from China showed that plasma tau levels were increased in participants carrying the G allele in the *MAPT* rs242557 SNP, and GG

TABLE 4 Association of *MAPT* rs3785883 polymorphism with the levels of fluid biomarkers.

Variables	*MAPT* rs3785883		
	AA vs. AG vs. GG	A allele carriers vs. GG	G allele carriers vs. AA
$A\beta_{1-42}$		$U = 2{,}510$, $Z = -2.181$, $p = 0.029^{B}$ ($N = 166$, $d_{Cohen} = 0.344$, $\eta^2 = 0.029$)	
Plasma S100B		$U = 1{,}541$, $Z = -2.590$, $p = 0.010^{A}$ ($N = 135$, $d_{Cohen} = 0.457$, $\eta^2 = 0.05$)	
	$H = 7.722$, df = 2, $p = 0.021$; AG vs. GG ($p = 0.047$)^{B} ($N = 133$, $d_{Cohen} = 0.429$, $\eta^2 = 0.044$)	$U = 1{,}449$, $Z = -2.769$, $p = 0.006^{B}$ ($N = 133$, $d_{Cohen} = 0.495$, $\eta^2 = 0.058$)	
CSF S100B	$H = 7.074$, df = 2, $p = 0.029$; AG vs. GG ($p = 0.033$)^{B} ($N = 135$, $d_{Cohen} = 0.4$, $\eta^2 = 0.038$)	$U = 1565.5$, $Z = -2.728$, $p = 0.006^{A}$ ($N = 137$, $d_{Cohen} = 0.479$, $\eta^2 = 0.054$)	
	$H = 9.699$, df = 2, $p = 0.008$; AG vs. GG ($p = 0.011$)^{C} ($N = 94$, $d_{Cohen} = 0.608$, $\eta^2 = 0.085$)	$U = 1531.5$, $Z = -2.636$, $p = 0.008^{B}$ ($N = 135$, $d_{Cohen} = 0.465$, $\eta^2 = 0.051$)	
		$U = 644$, $Z = -3.114$, $p = 0.002^{C}$ ($N = 94$, $d_{Cohen} = 0.678$, $\eta^2 = 0.103$)	
YKL-40			$U = 279.5$, $Z = -2.167$, $p = 0.030^{C\#}$ ($N = 106$, $d_{Cohen} = 0.431$, $\eta^2 = 0.044$)

Only statistically significant results are presented.
[A]all patients with dementia (patients with AD, MCI, VaD, FTD, AD/VaD, DLB, ND, PD, and CBS), [B]AD and MCI patients, [C]AD patients.
[#]Statistical significance lost after considering the age of participants as covariate. In addition to the results of Mann–Whitney *U* test and Kruskal-Wallis test, we included information on the number of participants (*N*) and effect size (measured by Cohen's d [d_{Cohen}] or eta-squared [η^2]). Aβ, amyloid β; MAPT, Microtubule-associated protein tau; S100B, S100 calcium-binding protein B; YKL-40, chitinase 3-like protein 1.

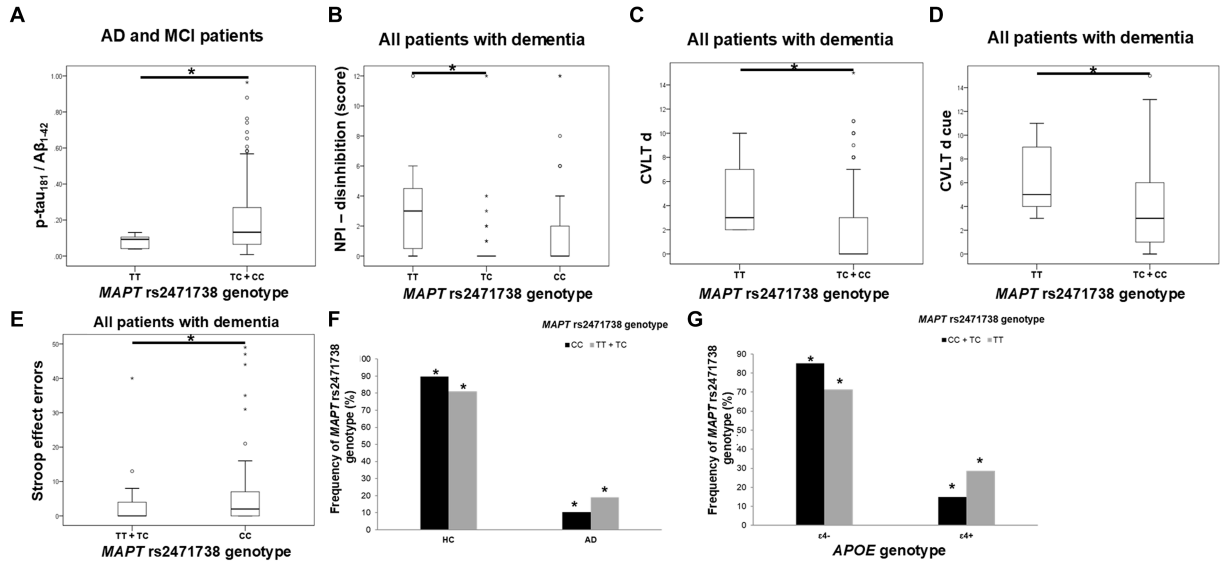

FIGURE 4
C allele carriers in the *MAPT* rs2471738 genotype had higher levels of p-tau_{181}/$A\beta_{1-42}$ ratio **(A)**. TC heterozygotes had a lower rate of disinhibition **(B)** compared to TT homozygotes. C allele carriers and CC homozygotes had worse performance on the CVLT test **(C,D)** and the Stroop test **(E)**. T allele carriers were more frequent among patients with AD **(F)**, and a higher number of *APOE* ε4 carriers was observed among TT homozygotes **(G)**. The group "all patients with dementia" includes patients with AD, MCI, VaD, FTD, AD/VaD, DLB, ND, PD, and CBS. The box represents the interquartile range (between 25th and 75th percentiles), while the whiskers represent the range between the minimum and maximum values.

homozygotes were 1.47 times more likely to develop cognitive impairment compared to AG heterozygotes (Tang et al., 2021).

Carriers of the A allele in the *MAPT* rs3785883 polymorphism had significantly decreased CSF $A\beta_{1-42}$ levels and increased plasma S100B levels. Additionally, a higher frequency of AA homozygotes was observed among patients with dementia. Conversely, GG homozygotes showed a significant increase in CSF S100B and YKL-40 levels. The *MAPT* rs3785883 A allele was associated with an increased risk for AD (Allen et al., 2014), higher levels of CSF p-tau (Kauwe et al., 2008; Cruchaga et al., 2010), earlier age of disease onset (Kauwe et al., 2008), and disease progression (Cruchaga et al., 2010; Peterson et al., 2014). However, some studies reported the association of the *MAPT* rs3785883 G allele with AD (Myers et al., 2005, 2007) or failed to observe any association between *MAPT* rs3785883 and AD

TABLE 5 Association of *MAPT* rs2471738 polymorphism with the results on neuropsychological tests and the levels of fluid biomarkers.

Variables	*MAPT* rs2471738		
	CC vs. TC vs. TT	C allele carriers vs. TT	T allele carriers vs. CC
NPI - disinhibition	H test = 7.375, df = 2, $p = 0.025$; TT vs. TC ($p = 0.023$)[A] ($N = 119$, $d_{Cohen} = 0.441$, $\eta^2 = 0.046$)	$U = 167$, $Z = -2.139$, $p = 0.032$[B] ($N = 90$, $d_{Cohen} = 0.4$, $\eta^2 = 0.038$)	
	$H = 7.765$, df = 2, $p = 0.021$; TT vs. TC ($p = 0.049$)[B] ($N = 90$, $d_{Cohen} = 0.533$, $\eta^2 = 0.066$)		
CVLT d		$U = 150.5$, $Z = -2.555$, $p = 0.011$[A] ($N = 124$, $d_{Cohen} = 0.598$, $\eta^2 = 0.082$)	
		$U = 489$, $Z = -1.988$, $p = 0.047$[B] ($N = 95$, $d_{Cohen} = 0.528$, $\eta^2 = 0.065$)	
CVLT d cue		$U = 174.5$, $Z = -2.106$, $p = 0.035$[A] ($N = 124$, $d_{Cohen} = 0.382$, $\eta^2 = 0.035$)	
		$U = 489$, $Z = -1.988$, $p = 0.047$[B] ($N = 95$, $d_{Cohen} = 0.456$, $\eta^2 = 0.049$)	
Errors on the Stroop test			$U = 1072.5$, $Z = -2.223$, $p = 0.026$[A] ($N = 111$, $d_{Cohen} = 0.414$, $\eta^2 = 0.041$)
CSF p-tau$_{181}$/Aβ_{1-42} ratio		$U = 423$, $Z = -1.962$, $p = 0.050$[B#] ($N = 163$, $d_{Cohen} = 0.311$, $\eta^2 = 0.024$)	
		$U = 196$, $Z = -2.061$, $p = 0.039$[C#] ($N = 112$, $d_{Cohen} = 0.397$, $\eta^2 = 0.038$)	

Only statistically significant results are presented.
[A]all patients with dementia (patients with AD, MCI, VaD, FTD, AD/VaD, DLB, ND, PD, and CBS), [B]AD and MCI patients, [C]AD patients.
[#]Statistical significance lost after considering *APOE* genotype as covariate. In addition to the results of Mann–Whitney *U* test and Kruskal-Wallis test, we included information on the number of participants (*N*) and effect size (measured by Cohen's d [d_{Cohen}] or eta-squared [η^2]). Aβ, amyloid β; CVLT, California Verbal Learning Test; MAPT, Microtubule-associated protein tau; NPI, NeuroPsychiatric Inventory; p-tau$_{181}$, tau phosphorylated at threonine 181.

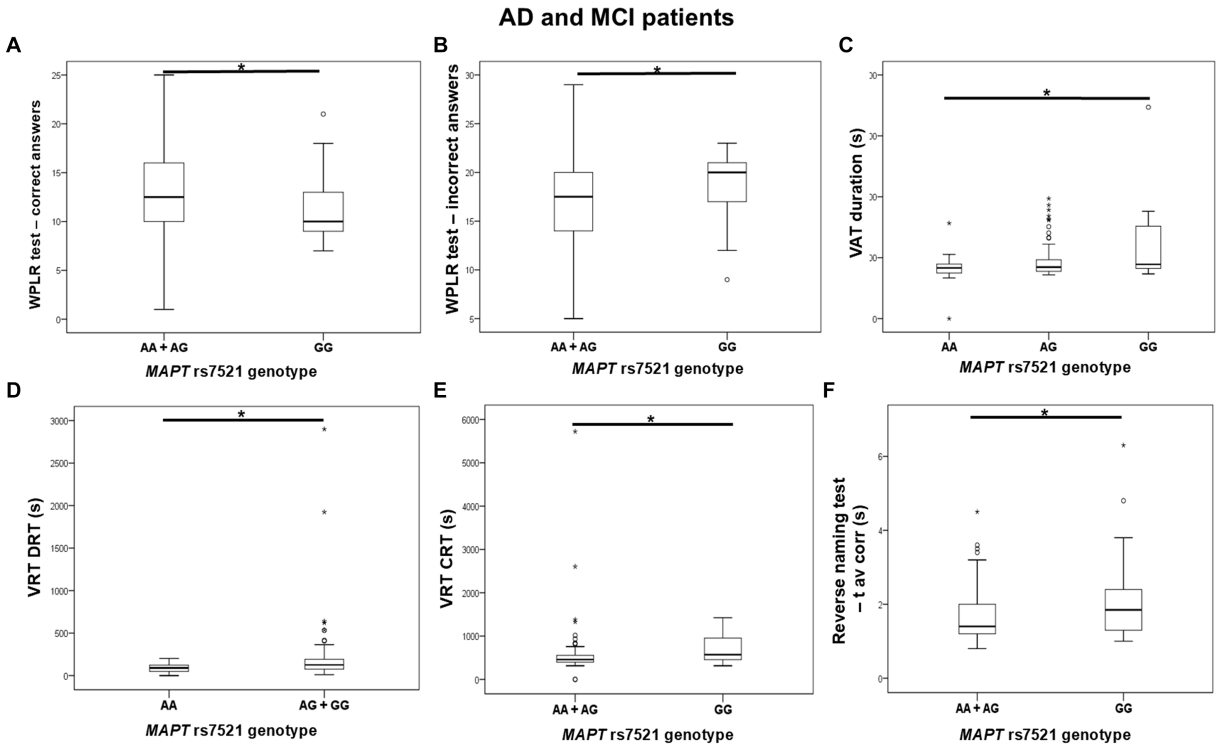

FIGURE 5
GG homozygotes in the *MAPT* rs7521 genotype had worse performance on the WPLR test **(A,B)**, VAT test **(C)**, VRT test **(D,E)**, and Reverse Naming test **(F)** compared to A allele carriers. The box represents the interquartile range (between 25th and 75th percentiles), while the whiskers represent the range between the minimum and maximum values.

TABLE 6 Association of *MAPT* rs7521 polymorphism with the results on neuropsychological tests.

Variables	*MAPT* rs7521		
	AA vs. AG vs. GG	A allele carriers vs. GG	G allele carriers vs. AA
Correct answers on WPLR test		$U = 708$, $Z = -2.583$, $p = 0.010^{B}$ ($N = 108$, $d_{Cohen} = 0.511$, $\eta^2 = 0.061$)	
Incorrect answers on WPLR test		$U = 706$, $Z = -2.597$, $p = 0.009^{B}$ ($N = 108$, $d_{Cohen} = 0.514$, $\eta^2 = 0.062$)	
VAT duration on the numbers test	H test = 7.142, df = 2, $p = 0.028$; AA vs. GG ($p = 0.025$)^{B} ($N = 108$, $d_{Cohen} = 0.454$, $\eta^2 = 0.049$)	$U = 744$, $Z = -2.314$, $p = 0.021^{B}$ ($N = 108$, $d_{Cohen} = 0.457$, $\eta^2 = 0.05$)	
VRT DRT			$U = 419$, $Z = -2.489$, $p = 0.013^{B}$ ($N = 93$, $d_{Cohen} = 0.534$, $\eta^2 = 0.067$)
VRT CRT		$U = 476$, $Z = -2.163$, $p = 0.031^{B}$ ($N = 93$, $d_{Cohen} = 0.46$, $\eta^2 = 0.05$)	
RN t avcorr		$U = 757.5$, $Z = -2.081$, $p = 0.037^{B}$ ($N = 106$, $d_{Cohen} = 0.411$, $\eta^2 = 0.041$)	

Only statistically significant results are presented.
[A]all patients with dementia (patients with AD, MCI, VaD, FTD, AD/VaD, DLB, ND, PD, and CBS), [B]AD and MCI patients, [C]AD patients.
In addition to the results of Mann–Whitney *U* test and Kruskal-Wallis test, we included information on the number of participants (*N*) and effect size (measured by Cohen's d [d_{Cohen}] or eta-squared [η^2]).
MAPT, Microtubule-associated protein tau; RN t avcorr, average time for giving correct answers in the Reverse Naming test; VAT, Visual Association Test; VRT CRT, Visual Reaction Time test choice reaction time; VRT DRT, Visual Reaction Time test discrimination reaction time; WPLR test, Word Pairs Learning and Recall test.

(Mukherjee et al., 2007; Abraham et al., 2009; Setó-Salvia et al., 2011). In this study, we confirmed the association of the *MAPT* rs3785883 A allele with CSF $A\beta_{1\text{-}42}$ levels, as observed by Kauwe et al. (2008). However, given the significant increase in CSF S100B and YKL-40 levels in GG homozygotes, further validation of this SNP's association with AD is necessary using a larger cohort of patients. Despite this, compared to other biomarkers, CSF $A\beta_{1\text{-}42}$ is considered a much more sensitive biomarker of AD. In our opinion, the association of the A allele with this biomarker is more closely related to the pathological changes that occur in AD.

TC heterozygotes in the *MAPT* rs2471738 genotype showed less disinhibition than TT homozygotes. C allele carriers performed worse on the CVLT test and had higher CSF p-tau_{181}/$A\beta_{1\text{-}42}$ ratios, while CC homozygotes made more Stroop test errors. More TT homozygotes and T allele carriers were found in patients with AD, AD and MCI, and dementia, with *APOE* ε4 carriers being more common among TT homozygotes. Our current study also found more TT homozygotes and T allele carriers among dementia patients and *APOE* ε4 carriers, but C allele carriers and CC homozygotes still showed poorer neuropsychological test performance and pathological CSF biomarker levels.

Although *MAPT* rs7521 polymorphism was not previously linked to AD (Mukherjee et al., 2007; Allen et al., 2014; Chang et al., 2014; Yuan et al., 2017; Zhang et al., 2017), we found that GG homozygotes performed worse on the WPLR test, VAT, VRT, and Reverse naming test.

H2 *MAPT* carriers performed worse on the BNT, PPLR, and VRT tests, supporting our previous study results, which showed significantly increased levels of CSF t-tau and p-tau_{231} among carriers of the H2 haplotype (Babić Leko et al., 2018). However, since carriers of H1H1 *MAPT* haplotype showed higher plasma NfL levels, further validation on larger cohorts is needed. Most studies link the H1 *MAPT* haplotype to increased AD risk (Myers et al., 2005; Laws et al., 2007; Kauwe et al., 2008; Di Maria et al., 2010; Pastor et al., 2016; Sánchez-Juan et al., 2019) or suggest the H2 haplotype is protective against AD (Allen et al., 2014; Zhang et al., 2017), though some found no association (Baker et al., 2000; Russ et al., 2001; Mukherjee et al., 2007; Abraham et al., 2009). Interestingly, a recent study involving 338 brain samples of Pick's disease, a relatively rare and predominantly sporadic form of FTD classified as a primary tauopathy, linked the H2 *MAPT* haplotype to an increased risk of Pick's disease (Valentino et al., 2023). Geographical differences in *MAPT* haplotype frequency may also help explain the discrepancies in results. In Europe, the H2 *MAPT* haplotype frequency is the highest in Mediterranean countries (Donnelly et al., 2010). In Croatia, which is part of the Mediterranean Basin, the H2 haplotype frequency is over 30% (around 33%). Thus, although we did not observe a significant difference in the distribution of *MAPT* haplotypes between HC and patients with dementia, carriers of the H2 *MAPT* haplotype showed worse performance on neuropsychological tests and pathological levels of various CSF biomarkers. This suggests that some effects of the H2 *MAPT* haplotype on disease progression might not be observed in other populations due to the smaller frequency of H2 *MAPT* haplotype carriers, which is not the case in the Croatian population.

The main strength of our study is the large number of participants and the inclusion of various biomarkers (such as CSF and plasma biomarkers, neuropsychological test, and *APOE* genotype). The main limitation is the cross-sectional design of the study, which does not allow for longitudinal tracking of participants. Additionally, CSF and plasma biomarkers and neuropsychological tests were determined in only 220 participants out of the total number of 964 participants. CSF biomarkers and neuropsychological tests were also determined only in patients with dementia since our "healthy control" group was recruited within a different project, and they have only genetic data.

In conclusion, our study showed that participants with the A allele in the *MAPT* rs1467967 polymorphism, the G allele in the *MAPT* rs242557 polymorphism, and the GG genotype in the *MAPT* rs7521 polymorphism performed worse on various neuropsychological tests.

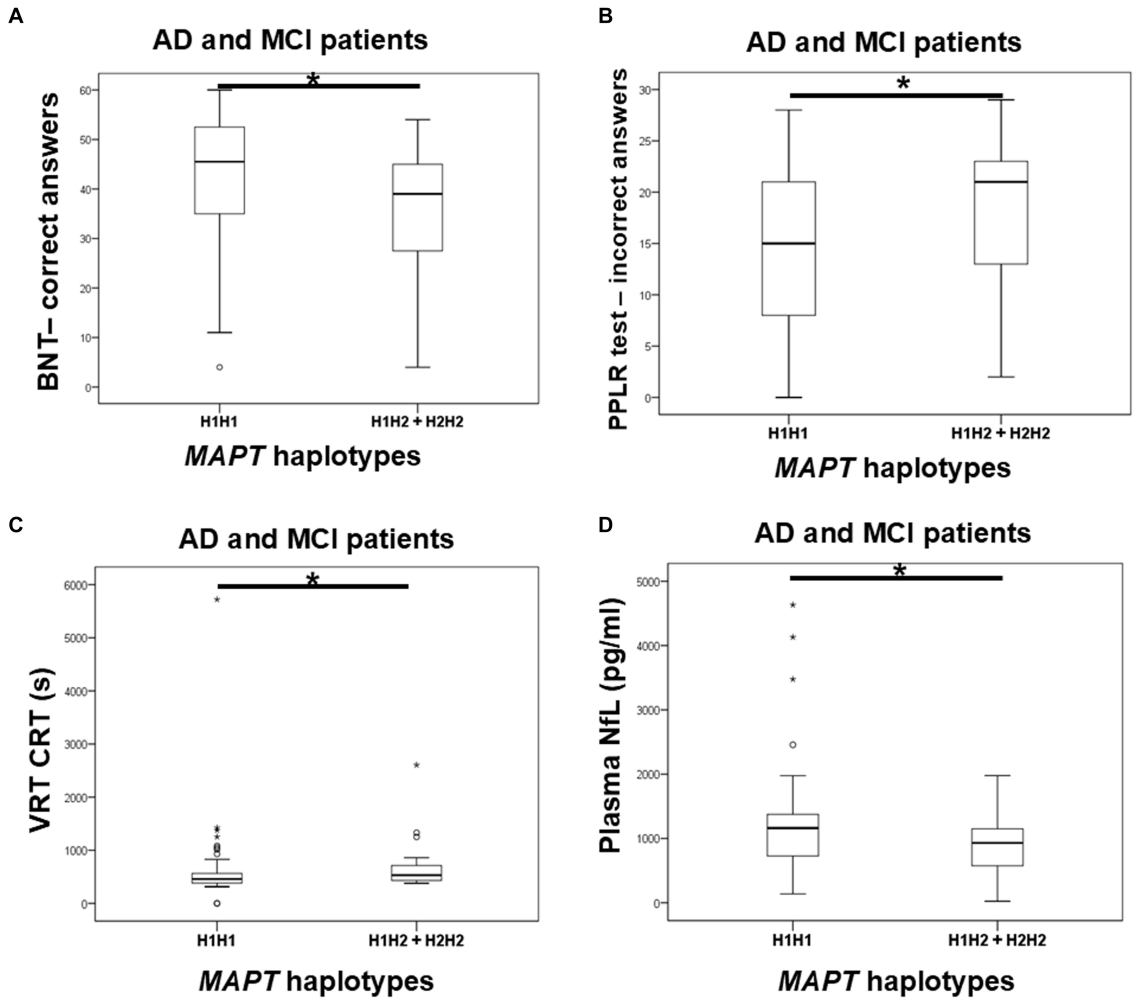

FIGURE 6
Carriers of the H1H1 *MAPT* haplotype had better performance on the BNT **(A)**, PPLR test **(B)**, and VRT test **(C)**. However, carriers of the H1H1 *MAPT* haplotype had higher plasma NfL levels **(D)** compared to carriers of the H2 *MAPT* haplotype. The box represents the interquartile range (between 25th and 75th percentiles), while the whiskers represent the range between the minimum and maximum values.

TABLE 7 Association of *MAPT* haplotypes with the results on neuropsychological tests and the levels of fluid biomarkers.

Variables	*MAPT* haplotypes
	H1H1 vs. H1H2 + H2H2
BNT	$U = 587$, $Z = -2.623$, $p = 0.009^{B}$ ($N = 92$, $d_{Cohen} = 0.568$, $\eta^2 = 0.075$)
Incorrect answers on the PPLR test	$U = 818.5$, $Z = -2.034$, $p = 0.042^{B}$ ($N = 105$, $d_{Cohen} = 0.405$, $\eta^2 = 0.039$)
VRT CRT	$U = 634$, $Z = -2.029$, $p = 0.042^{B}$ ($N = 93$, $d_{Cohen} = 0.43$, $\eta^2 = 0.044$)
Plasma NfL	$U = 1557.5$, $Z = -2.412$, $p = 0.016^{A\#}$ ($N = 139$, $d_{Cohen} = 0.418$, $\eta^2 = 0.042$)
	$U = 1{,}531$, $Z = -2.374$, $p = 0.018^{B\#}$ ($N = 137$, $d_{Cohen} = 0.414$, $\eta^2 = 0.041$)
	$U = 766$, $Z = -2.498$, $p = 0.012^{C}$ ($N = 99$, $d_{Cohen} = 0.519$, $\eta^2 = 0.063$)

Only statistically significant results are presented.
[A]all patients with dementia (patients with AD, MCI, VaD, FTD, AD/VaD, DLB, ND, PD, and CBS), [B]AD and MCI patients, [C]AD patients.
[#]The results remained significant when the analysis was controlled for the influence of sex and age ($\beta = -0.115$, SE = 0.047, $p = 0.015$)[A], ($\beta = -0.111$, SE = 0.047, $p = 0.019$)[B]. In addition to the results of Mann–Whitney *U* test, we provided information on the number of participants (*N*), and effect size (measured by Cohen's d [d_{Cohen}] or eta^2 [η^2]). BNT, Boston naming test; MAPT, Microtubule-associated protein tau; NfL, neurofilament light chain; PPLR test, Picture Pairs Learning and Recall test; VRT CRT, Visual Reaction Time test choice reaction time.

Although T allele carriers in *MAPT* rs2471738 polymorphism were more represented among patients with dementia and *APOE* ε4 carriers, C allele carriers and CC homozygotes still showed worse performance on neuropsychological tests and pathological levels of various CSF biomarkers. Carriers of the H2 *MAPT* haplotype also performed worse on various neuropsychological tests, supporting our previous findings that associated the H2 *MAPT* haplotype with pathological CSF AD biomarkers (Babić Leko et al., 2018). Regarding the *MAPT* rs3785883 polymorphism, further research is needed as both AA genotype and GG genotype showed associations with CSF and plasma AD

biomarkers, although AA homozygotes were more represented among patients with dementia. Our study further confirmed the association of *MAPT* haplotype-tagging polymorphisms and *MAPT* haplotypes with AD. Some of our results align with mainstream findings, such as the association of the A allele in *MAPT* rs1467967 and rs3785883 polymorphisms with worse performance on neuropsychological tests and pathological CSF $A\beta_{1\text{-}42}$ levels, respectively. However, some results differ from most studies, such as the association of the G allele in *MAPT* rs242557 polymorphism and the H2 *MAPT* haplotype with worse performance on neuropsychological tests. Therefore, further research on the association of *MAPT* haplotype-tagging polymorphisms and *MAPT* haplotypes with AD is necessary.

Data availability statement

The data presented in this study are available on request from the corresponding authors.

Ethics statement

The Ethical Committee of the Clinical Hospital Center Zagreb (case no. 02/21 AG, class 8.1-18/82-2, dated April 24, 2018) and the Central Ethical Committee of the University of Zagreb Medical School (case no. 380-59-10,106-18-111/126, class 641-01/18-02/01, dated June 20, 2018) approved all procedures conducted in this research. The studies were conducted in accordance with the local legislation and institutional requirements. Written informed consent for participation in this study was provided by the participants' legal guardians/next of kin.

Author contributions

MBL: Formal analysis, Investigation, Methodology, Project administration, Writing – review & editing, Conceptualization, Data curation, Funding acquisition, Resources, Software, Supervision, Validation, Visualization, Writing – original draft. EŠ: Investigation, Methodology, Writing – review & editing, Formal analysis, Project administration. NW: Investigation, Methodology, Writing – review & editing. MN: Investigation, Methodology, Writing – review & editing. NP: Investigation, Methodology, Software, Writing – review & editing. KZ: Investigation, Methodology, Writing – review & editing. LL: Investigation, Methodology, Writing – review & editing. ŽV: Data curation, Investigation, Methodology, Writing – review & editing. MB: Data curation, Investigation, Methodology, Writing – review & editing. FB: Investigation, Writing – review & editing. TZ: Investigation, Writing – review & editing. RS: Data curation, Investigation, Methodology, Supervision, Validation, Writing – review & editing. GŠ: Conceptualization, Data curation, Formal analysis, Funding acquisition, Investigation, Methodology, Project administration, Resources, Software, Supervision, Validation, Visualization, Writing – original draft, Writing – review & editing.

Funding

The author(s) declare that financial support was received for the research, authorship, and/or publication of this article. This work was funded by the National Recovery and Resilience Plan G.A. NPOO. C3.2.R3-I1.04.0257 to GŠ ("Detection and validation of molecular markers of inflammation in Alzheimer's and Parkinson's disease, multiple sclerosis, and schizophrenia"), University of Zagreb grant no. 10106–24-1526 to GŠ ("Inflammasome, tau protein, and nucleocytoplasmic transport in Alzheimer's disease"), Croatian Science Foundation grant no. IP-2019-04-3584 to GŠ ("Role of the blood–brain barrier, innate immunity, and tau protein oligomerization in the pathogenesis of Alzheimer's disease"), and Croatian Science Foundation grant no. IP-2019-04-2593 to TZ ("Regulation of thyroid and parathyroid function and blood calcium homeostasis").

Conflict of interest

The authors declare that the research was conducted in the absence of any commercial or financial relationships that could be construed as a potential conflict of interest.

The author(s) declared that they were an editorial board member of Frontiers, at the time of submission. This had no impact on the peer review process and the final decision.

Publisher's note

Supplementary material

The Supplementary material for this article can be found online at: https://www.frontiersin.org/articles/10.3389/fnmol.2024.1456670/full#supplementary-material

References

Abraham, R., Sims, R., Carroll, L., Hollingworth, P., O'Donovan, M. C., Williams, J., et al. (2009). An association study of common variation at the *MAPT* locus with late-onset Alzheimer's disease. *Am. J. Med. Genet. Part B Neuropsychiatr. Genet.* 150B, 1152–1155. doi: 10.1002/ajmg.b.30951

Albert, M. S., DeKosky, S. T., Dickson, D., Dubois, B., Feldman, H. H., Fox, N. C., et al. (2011). The diagnosis of mild cognitive impairment due to Alzheimer's disease: recommendations from the National Institute on Aging-Alzheimer's association workgroups on diagnostic guidelines for Alzheimer's disease. *Alzheimers Dement.* 7, 270–279. doi: 10.1016/j.jalz.2011.03.008

Allen, M., Kachadoorian, M., Quicksall, Z., Zou, F., Chai, H., Younkin, C., et al. (2014). Association of *MAPT* haplotypes with Alzheimer's disease risk and *MAPT* brain gene expression levels. *Alzheimers Res. Ther.* 6:39. doi: 10.1186/alzrt268

Alzheimer's Association (2020). 2020 Alzheimer's disease facts and figures. *Alzheimers Dement.* 16, 391–460. doi: 10.1002/ALZ.12068

Babić Leko, M., Willumsen, N., Nikolac Perković, M., Klepac, N., Borovečki, F., Hof, P. R., et al. (2018). Association of *MAPT* haplotype-tagging polymorphisms with cerebrospinal fluid biomarkers of Alzheimer's disease: a preliminary study in a Croatian cohort. *Brain Behav.* 8:e01128. doi: 10.1002/brb3.1128

Baker, M., Graff-Radford, D., Wavrant Devrièze, F., Graff-Radford, N., Petersen, R. C., Kokmen, E., et al. (2000). No association between TAU haplotype and Alzheimer's disease in population or clinic based series or in familial disease. *Neurosci. Lett.* 285, 147–149. doi: 10.1016/S0304-3940(00)01057-0

Bertram, L., McQueen, M. B., Mullin, K., Blacker, D., and Tanzi, R. E. (2007). Systematic meta-analyses of Alzheimer disease genetic association studies: the Alz gene database. *Nat. Genet.* 39, 17–23. doi: 10.1038/NG1934

Chang, C. W., Hsu, W. C., Pittman, A., Wu, Y. R., Hardy, J., and Fung, H. C. (2014). Structural study of the microtubule-associated protein tau locus of Alzheimer's disease in Taiwan. *Biom. J.* 37, 127–132. doi: 10.4103/2319-4170.117891

Compta, Y., Ezquerra, M., Muñoz, E., Tolosa, E., Valldeoriola, F., Rios, J., et al. (2011). High cerebrospinal tau levels are associated with the rs 242557 tau gene variant and low cerebrospinal β-amyloid in Parkinson's disease. *Neurosci. Lett.* 487, 169–173. doi: 10.1016/j.neulet.2010.10.015

Cruchaga, C., Karch, C. M., Jin, S. C., Benitez, B. A., Cai, Y., Guerreiro, R., et al. (2014). Rare coding variants in the phospholipase D3 gene confer risk for Alzheimer's disease. *Nature* 505, 550–554. doi: 10.1038/nature12825

Cruchaga, C., Kauwe, J. S. K., Mayo, K., Spiegel, N., Bertelsen, S., Nowotny, P., et al. (2010). SNPs associated with cerebrospinal fluid phospho-tau levels influence rate of decline in Alzheimer's disease. *PLoS Genet.* 6:e1001101. doi: 10.1371/journal.pgen.1001101

Di Maria, E., Cammarata, S., Parodi, M. I., Borghi, R., Benussi, L., Galli, M., et al. (2010). The H1 haplotype of the tau gene (*MAPT*) is associated with mild cognitive impairment. *J. Alzheimers Dis.* 19, 909–914. doi: 10.3233/JAD-2010-1285

Donnelly, M. P., Paschou, P., Grigorenko, E., Gurwitz, D., Mehdi, S. Q., Kajuna, S. L. B., et al. (2010). The distribution and most recent common ancestor of the 17q21 inversion in humans. *Am. J. Hum. Genet.* 86, 161–171. doi: 10.1016/J.AJHG.2010.01.007

Elias-Sonnenschein, L. S., Helisalmi, S., Natunen, T., Hall, A., Paajanen, T., Herukka, S.-K., et al. (2013). Genetic loci associated with Alzheimer's disease and cerebrospinal fluid biomarkers in a Finnish case-control cohort. *PLoS One* 8:e59676. doi: 10.1371/journal.pone.0059676

Feulner, T. M., Laws, S. M., Friedrich, P., Wagenpfeil, S., Wurst, S. H. R., Riehle, C., et al. (2010). Examination of the current top candidate genes for Alzheimer's disease in a genome-wide association study. *Mol. Psychiatry* 15, 756–766. doi: 10.1038/MP.2008.141

Hachinski, V. C., Iliff, L. D., Zilhka, E., Du Boulay, G. H., McAllister, V. L., Marshall, J., et al. (1975). Cerebral blood flow in dementia. *Arch. Neurol.* 32, 632–637. doi: 10.1001/archneur.1975.00490510088009

Homann, J., Osburg, T., Ohlei, O., Dobricic, V., Deecke, L., Bos, I., et al. (2022). Genome-wide association study of Alzheimer's disease brain imaging biomarkers and neuropsychological phenotypes in the European medical information framework for Alzheimer's disease multimodal biomarker discovery dataset. *Front. Aging Neurosci.* 14:37. doi: 10.3389/FNAGI.2022.840651/FULL

Huang, W., Zeng, J., Jia, L., Zhu, D., O'Brien, J., Ritchie, C., et al. (2023). Genetic risks of Alzheimer's by *APOE* and *MAPT* on cortical morphology in young healthy adults. *Brain Commun.* 5:234. doi: 10.1093/BRAINCOMMS/FCAD234

Jonsson, T., Stefansson, H., Steinberg, S., Jonsdottir, I., Jonsson, P. V., Snaedal, J., et al. (2013). Variant of *TREM2* associated with the risk of Alzheimer's disease. *N. Engl. J. Med.* 368, 107–116. doi: 10.1056/NEJMoa1211103

Kauwe, J. S. K., Cruchaga, C., Mayo, K., Fenoglio, C., Bertelsen, S., Nowotny, P., et al. (2008). Variation in *MAPT* is associated with cerebrospinal fluid tau levels in the presence of amyloid-beta deposition. *Proc. Natl. Acad. Sci.* 105, 8050–8054. doi: 10.1073/pnas.0801227105

Laws, S. M., Friedrich, P., Diehl-Schmid, J., Müller, J., Eisele, T., Bäuml, J., et al. (2007). Fine mapping of the *MAPT* locus using quantitative trait analysis identifies possible causal variants in Alzheimer's disease. *Mol. Psychiatry* 12, 510–517. doi: 10.1038/sj.mp.4001935

McKhann, G. M., Knopman, D. S., Chertkow, H., Hyman, B. T., Jack, C. R., Kawas, C. H., et al. (2011). The diagnosis of dementia due to Alzheimer's disease: recommendations from the National Institute on Aging-Alzheimer's association workgroups on diagnostic guidelines for Alzheimer's disease. *Alzheimers Dement.* 7, 263–269. doi: 10.1016/j.jalz.2011.03.005

Miller, S. A., Dykes, D. D., and Polesky, H. F. (1988). A simple salting out procedure for extracting DNA from human nucleated cells. *Nucleic Acids Res.* 16:1215. doi: 10.1093/nar/16.3.1215

Mukherjee, O., Kauwe, J. S., Mayo, K., Morris, J. C., and Goate, A. M. (2007). Haplotype-based association analysis of the *MAPT* locus in late onset Alzheimer's disease. *BMC Genet.* 8:3. doi: 10.1186/1471-2156-8-3

Myers, A. J., Kaleem, M., Marlowe, L., Pittman, A. M., Lees, A. J., Fung, H. C., et al. (2005). The H1c haplotype at the *MAPT* locus is associated with Alzheimer's disease. *Hum. Mol. Genet.* 14, 2399–2404. doi: 10.1093/hmg/ddi241

Myers, A. J., Pittman, A. M., Zhao, A. S., Rohrer, K., Kaleem, M., Marlowe, L., et al. (2007). The *MAPT* H1c risk haplotype is associated with increased expression of tau and especially of 4 repeat containing transcripts. *Neurobiol. Dis.* 25, 561–570. doi: 10.1016/J.NBD.2006.10.018

Neary, D., Snowden, J. S., Gustafson, L., Passant, U., Stuss, D., Black, S., et al. (1998). Frontotemporal lobar degeneration: a consensus on clinical diagnostic criteria. *Neurology* 51, 1546–1554. doi: 10.1212/wnl.51.6.1546

Ning, M., Zhang, Z., Chen, Z., Zhao, T., Zhang, D., Zhou, D., et al. (2011). Genetic evidence that vascular dementia is related to Alzheimer's disease: genetic association between tau polymorphism and vascular dementia in the Chinese population. *Age Ageing* 40, 125–128. doi: 10.1093/ageing/afq131

Pastor, P., Moreno, F., Clarimón, J., Ruiz, A., Combarros, O., Calero, M., et al. (2016). *MAPT* H1 haplotype is associated with late-onset Alzheimer's disease risk in *APOE*ε4 noncarriers: results from the dementia genetics Spanish consortium. *J. Alzheimers Dis.* 49, 343–352. doi: 10.3233/JAD-150555

Petersen, R. C., Smith, G. E., Waring, S. C., Ivnik, R. J., Tangalos, E. G., and Kokmen, E. (1999). Mild cognitive impairment: clinical characterization and outcome. *Arch. Neurol.* 56, 303–308. doi: 10.1001/archneur.56.3.303

Peterson, D., Munger, C., Crowley, J., Corcoran, C., Cruchaga, C., Goate, A. M., et al. (2014). Variants in *PPP3R1* and *MAPT* are associated with more rapid functional decline in Alzheimer's disease: the Cache County dementia progression study. *Alzheimers Dement.* 10, 366–371. doi: 10.1016/J.JALZ.2013.02.010

Pittman, A. M., Myers, A. J., Abou-Sleiman, P., Fung, H. C., Kaleem, M., Marlowe, L., et al. (2005). Linkage disequilibrium fine mapping and haplotype association analysis of the tau gene in progressive supranuclear palsy and corticobasal degeneration. *J. Med. Genet.* 42, 837–846. doi: 10.1136/jmg.2005.031377

Román, G. C., Tatemichi, T. K., Erkinjuntti, T., Cummings, J. L., Masdeu, J. C., Garcia, J. H., et al. (1993). Vascular dementia: diagnostic criteria for research studies. Report of the NINDS-AIREN international workshop. *Neurology* 43, 250–260. doi: 10.1212/wnl.43.2.250

Rudan, I., Marušić, A., Janković, S., Rotim, K., Boban, M., Lauc, G., et al. (2009). "10 001 Dalmatians:" Croatia launches its national biobank. *Croat. Med. J.* 50, 4–6. doi: 10.3325/cmj.2009.50.4

Russ, C., Powell, J. F., Zhao, J., Baker, M., Hutton, M., Crawford, F., et al. (2001). The microtubule associated protein tau gene and Alzheimer's disease - an association study and meta-analysis. *Neurosci. Lett.* 314, 92–96. doi: 10.1016/s0304-3940(01)02289-3

Sánchez-Juan, P., Moreno, S., de Rojas, I., Hernández, I., Valero, S., Alegret, M., et al. (2019). The *MAPT* H1 haplotype is a risk factor for Alzheimer's disease in *APOE* ε4 non-carriers. *Front. Aging Neurosci.* 11:327. doi: 10.3389/FNAGI.2019.00327

Setó-Salvia, N., Clarimón, J., Pagonabarraga, J., Pascual-Sedano, B., Campolongo, A., Combarros, O., et al. (2011). Dementia risk in Parkinson's disease: disentangling the role of *MAPT* haplotypes. *Arch. Neurol.* 68, 359–364. doi: 10.1001/ARCHNEUROL.2011.17

Shen, X. N., Miao, D., Li, J. Q., Tan, C. C., Cao, X. P., Tan, L., et al. (2019). *MAPT* rs 242557 variant is associated with hippocampus tau uptake on 18F-AV-1451 PET in non-demented elders. *Aging (Albany NY)* 11, 874–884. doi: 10.18632/AGING.101783

Stevenson-Hoare, J., Heslegrave, A., Leonenko, G., Fathalla, D., Bellou, E., Luckcuck, L., et al. (2023). Plasma biomarkers and genetics in the diagnosis and prediction of Alzheimer's disease. *Brain* 146, 690–699. doi: 10.1093/BRAIN/AWAC128

Strickland, S. L., Reddy, J. S., Allen, M., N'songo, A., Burgess, J. D., Corda, M. M., et al. (2020). *MAPT* haplotype-stratified GWAS reveals differential association for AD risk variants. *Alzheimers Dement.* 16, 983–1002. doi: 10.1002/ALZ.12099

Tang, X., Liu, S., Cai, J., Chen, Q., Xu, X., Mo, C. B., et al. (2021). Effects of gene and plasma tau on cognitive impairment in rural Chinese population. *Curr. Alzheimer Res.* 18, 56–66. doi: 10.2174/1567205018666210324122840

Valentino, R. R., Scotton, W. J., Roemer, S. F., Lashley, T., Heckman, M. G., Shoai, M., et al. (2023). Creating the Pick's disease international consortium: association study of *MAPT* H2 haplotype with risk of Pick's disease. *med Rxiv*. doi: 10.1101/2023.04.17.23288471

Vogel, J. W., Young, A. L., Oxtoby, N. P., Smith, R., Ossenkoppele, R., Strandberg, O. T., et al. (2021). Four distinct trajectories of tau deposition identified in Alzheimer's disease. *Nat. Med.* 27, 871–881. doi: 10.1038/s41591-021-01309-6

World Medical Association (2013). World medical association declaration of Helsinki: ethical principles for medical research involving human subjects. *JAMA* 310, 2191–2194. doi: 10.1001/jama.2013.281053

Yuan, H., Du, L., Ge, P., Wang, X., and Xia, Q. (2017). Association of microtubule-associated protein tau gene polymorphisms with the risk of sporadic Alzheimer's disease: a meta-analysis. *Int. J. Neurosci.* 128, 1–22. doi: 10.1080/00207454.2017.1400972

Zhang, C.-C., Zhu, J.-X., Wan, Y., Tan, L., Wang, H.-F., Yu, J.-T., et al. (2017). Meta-analysis of the association between variants in *MAPT* and neurodegenerative diseases. *Oncotarget* 8, 44994–45007. doi: 10.18632/oncotarget.16690

Zhou, F., and Wang, T. (2017). The associations between the *MAPT* polymorphisms and Alzheimer's disease risk: a meta-analysis. *Oncotarget* 8, 43506–43520. doi: 10.18632/oncotarget.16490

frontiers | Frontiers in Molecular Neuroscience

TYPE Perspective
PUBLISHED 22 November 2024
DOI 10.3389/fnmol.2024.1465013

OPEN ACCESS

EDITED BY
Riccardo Ghidoni,
University of Milan, Italy

REVIEWED BY
Francesca Cencetti,
University of Florence, Italy

*CORRESPONDENCE
Senka Blažetić
✉ senka@biologija.unios.hr
Kristina Mlinac-Jerkovic
✉ kristina.mlinac.jerkovic@mef.hr

RECEIVED 15 July 2024
ACCEPTED 04 November 2024
PUBLISHED 22 November 2024

CITATION
Puljko B, Grbavac J, Potočki V, Ilic K, Viljetić B, Kalanj-Bognar S, Heffer M, Debeljak Ž, Blažetić S and Mlinac-Jerkovic K (2024) The good, the bad, and the unknown nature of decreased GD3 synthase expression. *Front. Mol. Neurosci.* 17:1465013. doi: 10.3389/fnmol.2024.1465013

The good, the bad, and the unknown nature of decreased GD3 synthase expression

Borna Puljko[1,2], Josip Grbavac[3], Vinka Potočki[1], Katarina Ilic[4], Barbara Viljetić[3], Svjetlana Kalanj-Bognar[1,2], Marija Heffer[5], Željko Debeljak[6,7], Senka Blažetić[8]* and Kristina Mlinac-Jerkovic[1,2]*

[1]Croatian Institute for Brain Research, School of Medicine, University of Zagreb, Zagreb, Croatia, [2]Department of Chemistry and Biochemistry, School of Medicine, University of Zagreb, Zagreb, Croatia, [3]Department of Medical Chemistry, Biochemistry and Clinical Chemistry, Faculty of Medicine, Josip Juraj Strossmayer University of Osijek, Osijek, Croatia, [4]Department of Neuroimaging, BRAIN Centre, Institute of Psychiatry Psychology and Neuroscience, King's College London, London, United Kingdom, [5]Department of Medical Biology and Genetics, Faculty of Medicine, Josip Juraj Strossmayer University of Osijek, Osijek, Croatia, [6]Department of Pharmacology, Faculty of Medicine, Josip Juraj Strossmayer University of Osijek, Osijek, Croatia, [7]Clinical Institute of Laboratory Diagnostics, Osijek University Hospital, Osijek, Croatia, [8]Department of Biology, Josip Juraj Strossmayer University of Osijek, Osijek, Croatia

This paper explores the physiological consequences of decreased expression of GD3 synthase (GD3S), a biosynthetic enzyme that catalyzes the synthesis of b-series gangliosides. GD3S is a key factor in tumorigenesis, with overexpression enhancing tumor growth, proliferation, and metastasis in various cancers. Hence, inhibiting GD3S activity has potential therapeutic effects due to its role in malignancy-associated pathways across different cancer types. GD3S has also been investigated as a promising therapeutic target in treatment of various neurodegenerative disorders. Drugs targeting GD3 and GD3S have been extensively explored and underwent clinical trials, however decreased GD3S expression in mouse models, human subjects, and *in vitro* studies has demonstrated serious adverse effects. We highlight these negative consequences and show original mass spectrometry imaging (MSI) data indicating that inactivated GD3S can generally negatively affect energy metabolism, regulatory pathways, and mitigation of oxidative stress. The disturbance in several physiological systems induced by GD3S inhibition underscores the vital role of this enzyme in maintaining cellular homeostasis and should be taken into account when GD3S is considered as a therapeutic target.

KEYWORDS

ST8SIA1, gangliosides, glycosphingolipids, lipid metabolism, lipidomics

1 Introduction

Gangliosides, complex glycosphingolipids, challenging to investigate with common molecular biology methods, are highly prevalent in the mammalian nervous system. Specifically, the human brain contains 10–30 times more gangliosides than any other organ (Svennerholm, 1994). Amongst those, GM1, GD1a, GD1b and GT1b represent 97% of all brain gangliosides (Yu et al., 2011). Gangliosides are synthesized by a series of specific glycosyl-and sialyltransferases in a metabolic pathway diverged into four branches (Yu et al., 2011). Hence, we can distinguish between asialo, a-, b-, and c-series of gangliosides according to the number of sialic acids (0, 1, 2, and 3) linked to the inner galactose residue (Schnaar, 2016, 2019). In this paper we are focusing on one of those sialyltransferases: GD3 synthase (GD3S)

(alpha-*N*-acetylneuraminate alpha-2,8-sialyltransferase, EC 2.4. 99.8). GD3S regulates the biosynthesis of GD3 and GD2 from GM3, which are in turn starting points for the synthesis of more complex gangliosides of b-and c-series (Kasprowicz et al., 2022). It is encoded by the (*ST8SIA1, St8sia1*) gene (Kasprowicz et al., 2022) which is not solely expressed in the brain, but the RNA expression of *ST8SIA1* as well as expression of the protein product, GD3S, has been detected in a variety of other tissues, most prominently endocrine tissues, bone marrow, and lymphoid tissues, as illustrated in Supplementary Figure S1. Even though some tissues show a relatively modest RNA expression of the *ST8SIA1* gene, the protein expression is quite strong, e.g., liver and gallbladder, or the skin (Supplementary Figure S1). In this paper we aim to provide insight into the physiological consequences of decreased GD3S expression, accompanied by our own supportive observations and proposed future perspectives.

2 The good

Is achieving a favorable outcome realistic when considering the inhibition of any biosynthetic enzyme involved in ganglioside synthesis? Targeting this enzyme for inhibition has been a compelling research avenue, as elevated GD3S expression is associated with various pathological conditions, from cancer to neurodegenerative diseases.

GD3S has been recognized as one of the key factors in tumorigenesis (Tong et al., 2021). Overexpression of GD3S enhances tumor growth, proliferation, and metastasis in various cancers (Cazet et al., 2010; Schengrund, 2023) including thyroid, lung, colorectal, liver, pancreatic, renal, prostate, breast cancer, and most prominently, glioma and melanoma (Cazet et al., 2010; Yeh et al., 2016; Ma et al., 2017; Lee et al., 2018; Kasprowicz et al., 2022; Seo et al., 2024), illustrated in Supplementary Figure S2. Hence, inhibiting GD3S catalytic activity has raised interest as a potential therapeutic target considering its role in malignancy-associated pathways across different cancer types. Indeed, numerous studies have shown that decrease or abolishment of GD3S expression results in reduced malignancy, inhibition of proliferation, and decreased metastatic potential (Kasprowicz et al., 2022). Specifically, GD3S is highly expressed in GD2-positive breast cancer stem cells, and decreasing its expression results in inhibition of proliferation and self-renewal. This effect has also been demonstrated *in vivo* (Houghton et al., 1985). Promoting proliferation is induced by activating c-Met and the downstream targets MEK/ERK and the PI3K/AKT pathway (Ruan et al., 1999). GD3S was also found to promote metastasis of breast cancer by regulating epithelial-mesenchymal transition (Ruan et al., 1999). Furthermore, the absence of GD3S results in the downregulation of Akt, ERKs, and SFK phosphorylation in GD3S knock-out (GD3SKO) mouse glioma cells (Ohkawa et al., 2021).

Even though GD3S is responsible for the synthesis of b-and c-series gangliosides, ganglioside GD3 (Ohkawa et al., 2021) accounts for over 50% ganglioside content in glioblastoma and is most abundant in hyper-vascularized areas. It is mainly found in cell surface clusters and the cytoplasm of tumor cells (Hedberg et al., 2001). GD3-positive cells were detected in the peritumoral tissue up to 3.5 cm from the tumor edge, suggesting their implication in glioblastoma progression and invasion (Lama et al., 2016). In contrast, ganglioside GD3 is almost absent in the healthy adult human brain, making it a potential therapeutic target (Mennel et al., 2000; Iwasawa et al., 2018). Studies on GD3SKO mice found the animals develop tumors slower and the overall size of tumors was smaller than in wild-type (WT) mice, strengthening the notion that GD3S enhances the malignant properties of gliomas (Zhang et al., 2021). The introduction of GD3S cDNA into a neuroblastoma cell line (SH-SY5Y), which substantially expressed GM2 and GD1a but not GD3 and GD2, increased GD3 and GD2 expression, dispersed cell development and slowed down growth (Ruan et al., 1999).

GD3S has also been investigated as a potential novel therapeutic target in the context of various neurodegenerative disorders (Akkhawattanangkul et al., 2017). Huntington's disease, Parkinson's disease (PD), and Alzheimer's disease (AD) are all characterized by altered ganglioside metabolism (Sipione et al., 2020). GD3S has been recognized as a novel AD treatment objective for cognitive decline, amyloid plaque development, and neurodegeneration (Bernardo et al., 2009). In a study on primary neurons and astrocytes lacking GD3S, Aβ-induced cell death and aggregation were prevented (Bernardo et al., 2009). Furthermore, APP/PSEN1/GD3S$^{-/-}$ triple mutant mice experience improvements in behavioral deficits compared to APP/PSEN1 mice (Bernardo et al., 2009), hence elimination of GD3S improved memory and reduced amyloid-beta plaque loads (Bernardo et al., 2009). In the MPTP-induced (1-methyl-4-phenyl-1,2,3,6-tetrahydropyridine) PD model, suppression of GD3S exhibits neuroprotective qualities and may be a promising target for future research (Akkhawattanangkul et al., 2017). In another study, mice were intrastriatally injected with lentiviral-vector-mediated shRNA targeting GD3S (shGD3S) or scrambled-sequence control (scrRNA) and MPTP was administered. In shGD3S-treated mice, MPTP-induced lesions were smaller. MPTP caused bradykinesia and fine motor skill impairments in scrRNA-treated mice, while these deficiencies were absent in shGD3S-treated mice. These findings show GD3S inhibition prevents MPTP-induced nigrostriatal damage, bradykinesia, and fine motor skill impairments (Dhanushkodi et al., 2019). Furthermore, studies show that GD3 accumulation in plasma membrane lipid microdomains before mitochondrial translocation is crucial for Aβ-induced apoptosis (Kim et al., 2010). GD3S is rapidly activated in different cell types after apoptotic stimuli (Malisan et al., 2002), and GD3S overexpression was shown to cause vascular endothelial ECV304 cell death (Ha et al., 2004). Another research has provided evidence that drug-induced GD3S inhibition reduced CD95-induced apoptosis (De Maria et al., 1997). Additionally, GD3 causes mitochondrial membrane potential ($\Delta\Psi m$) dissipation and swelling in isolated mitochondria, leading to cytochrome c, apoptosis-inducing factor, and caspase 9 release, prevented by enforced Bcl-2 activation (Rippo et al., 2000). In intact cells, suppression of GD3S expression significantly reduced ceramide-induced $\Delta\Psi m$ dissipation, demonstrating endogenous GD3 promotes mitochondrial alterations (Rippo et al., 2000).

The development of therapies targeted against GD3 and GD3S began several decades ago, utilizing various strategies, e.g., direct inhibition with monoclonal antibodies or stimulating the immune response with vaccines. Vaccine strategies have been developed mainly for potential treatment of malignant melanoma or other solid tumors (Yao et al., 1999). However, the clinical activity of some of them remained limited, leading to the cessation of vaccine development (Hein et al., 2024). Monoclonal antibodies, including R24, have been evaluated in clinical trials for melanoma patients. R24, a murine IgG3 anti-GD3 antibody, was tested in 61 patients with metastatic melanoma. Despite mild side effects, R24 confirmed the infiltration of immune cells in the tumor microenvironment following

GD3 inhibition, opening new therapeutic developments (Houghton et al., 1985). Studies have shown GD3S inhibitors, such as Triptolide (TPL) from *Tripterygium wilfordii*, have anti-rheumatic, anti-inflammatory, immunomodulatory, and anti-tumor properties. TPL is a traditional Chinese medicinal herb that inhibits GD3S expression through NF-κB activation (Tong et al., 2021).

Furthermore, GD3SKO mice exhibit less age-related bone loss in skeletal tissue compared to WT mice (Yo et al., 2019). In GD3S KO mice, GD3 is not synthesized instead, other ganglioside species such as GD1a are present in higher amounts, and that increase could be linked to supporting bone maintenance and formation (Sasaki et al., 2022).

3 The bad

After establishing the positive effects of targeted GD3S inhibition, this section is to provide an overview of known negative consequences of decreased GD3S expression *in vitro*, available mouse models and human subject studies across different organ systems including the nervous system, retina, kidneys, and the liver.

GD3SKO mice, genetically engineered mice with nonfunctional *St8sia1* gene are an invaluable tool in the research of physiological and biochemical properties of GD3S and altered ganglioside composition on various cell functions. They are of normal growth and overall nervous tissue morphology, however, they exhibit thermal hyperalgesia and mechanical allodynia, decreased response to formalin-induced prolonged noxious stimulation (Handa et al., 2005), morphological abnormalities in the sciatic nerve, and neuronal disturbances during peripheral nerve regeneration (Ribeiro-Resende et al., 2014). In addition, they exhibit decreased hippocampal neuronal loss following global cerebral ischemia (Wang et al., 2021), impaired olfactory and memory functions due to reduced neurogenesis in the subventricular zone and the dentate gyrus (Fuchigami et al., 2024), impairment in hippocampus-dependent memory function (Tang et al., 2021), depression-like behavior (Wang et al., 2014), a reduction in rod and retinal ganglion cell populations and electrophysiological alterations in retinal ganglion cells, photoreceptors, bipolar and amacrine cells, and reduced contrast sensitivity and visual acuity (Abreu et al., 2021), as well as mild impairment of spontaneous regeneration of neuromuscular junctions in older animals (Rupp et al., 2013). Analysis of neuronal stem cells (NSCs) obtained from GD3SKO mice has shown decreased self-renewal ability compared with those from the WT animals, accompanied by reduced expression and increased degradation rate of EGF receptor (Wang and Yu, 2013).

Ganglioside metabolism has been thoroughly examined in the neuronal retina (Panzetta and Allende, 2000), with substantial GD3S activity shown in the early and late development of rat and chicken retinas (Daniotti et al., 1991, 1992, 1994; Watanabe et al., 1996; Maxzúd and Maccioni, 1997; Panzetta and Allende, 2000). *St8sia1* has been identified as a potential candidate in the acquisition of experience-dependent plasticity in murine visual cortex (Rietman et al., 2012), and polymorphisms in the human *ST8SIA1* have been identified in patients with treatment-resistant ophthalmoplegia (Nel et al., 2017). The visual system of GD3SKO mice exhibits a reduction in retinal ganglion cell (RGC) density, optic nerve fiber number, RGC and photoreceptor electrical activity, visual acuity, and contrast sensitivity, indicating b-series gangliosides are essential for visual system structure and function (Abreu et al., 2021). Furthermore, gangliosides synthesized by GD3S, are present in the inner ear and contribute to the maintenance of the structure and function of auditory cells (Yoshikawa et al., 2009, 2015; Inokuchi et al., 2017; Kurabi et al., 2017).

Other organs are also affected by the lack of GD3S. A study on GD3SKO mice has shown changes in the expression of renal connexins and pannexin1 (Meter et al., 2022). Ganglioside GM3, accumulated in GD3SKO mice, has been documented in podocytes (Savas et al., 2020) and was related to glomerular hypertrophy occurring in diabetic human and rat kidneys (Novak et al., 2013). Furthermore, advanced glycation end products were shown to inhibit bovine retinal pericyte and rat renal mesangial cell proliferation associated with GD3S activity inhibition suggesting its role in the development of diabetic retinopathy and diabetic nephropathy (Masson et al., 2005). Human pancreatic islets of Langerhans contain five distinct endocrine β-4 cell types, which are distinguished by differential expression of *ST8SIA1* and *CD9,* and their distribution is altered in type 2 diabetes (Dorrell et al., 2016). Gene expression analysis suggests *ST8SIA1*$^{-}$ β cells secrete more insulin (Dorrell et al., 2016). Correlation analysis has revealed *ST8SIA1* as one of the genes with integrative changes in RNA expression and DNA methylation in the offspring born to women with pregestational type 1 diabetes (T1DM) (Knorr et al., 2022). Furthermore, in GD3SKO mice liver, a prominent difference in expression of cholesterogenic genes *Srebp1a*, *Insig2a*, and *Ldl* was found, indicating a relationship between gangliosides and regulation of cholesterol metabolism (Mlinac et al., 2012). With everything stated, keeping in mind the high RNA and protein expression of GD3S in multiple organs and tissues (Supplementary Figure S1), the consequences of GD3S inhibition are under-investigated and need to be explored further.

4 The unknown

The complete spectrum of proteins and lipids interacting with GD3S and the functional consequences of these interactions are not well-documented. Identifying them could provide insight into broader cellular processes influenced by GD3S. Additionally, how GD3S activity integrates with other metabolic and signaling pathways under different physiological conditions is still unknown.

To explore the relationship between gangliosides and metabolic pathways, we analyzed nucleus caudatus and putamen (together known as the corpus striatum (CPu), an important part of the basal ganglia) of 4.5 months old GD3SKO and WT mice using mass spectrometry imaging (MSI). The obtained spectra were used for further data processing to observe differences in the lipidome between GD3KO and WT mice. Compared to WTs, CPu region in GD3SKO mice shows significantly reduced (negative t-scores greater than 2 in absolute value) expression of 8 compounds functionally involved in energy metabolism (Table 1). Putatively identified compounds indicate additional not yet identified effects of GD3S and suggest inhibition of GD3S may affect pathways linked to energy production (Table 1).

Putatively identified compounds include propenoyl-CoA and 3-oxopropionyl-CoA which are part of the propanoate metabolism encompassing the metabolism of propionic acid. Propionyl-CoA is a key intermediate in the breakdown of odd-numbered fatty acids as well as some amino acids. Aberrations in this pathway are associated with various diseases, such as primary propionic acidemia and malonyl-CoA decarboxylase deficiency (Pena et al., 2012). In addition,

TABLE 1 Selected putatively identified significant m/z signals and *t*-scores detected by mass spectrometry imaging (MSI)* in the nucleus caudatus and putamen (CPu) region that are reduced in GD3SKO mice compared to WT mice.

KEGG ID	m/z	Name of identified compaund	KO vs WT *p* values	*t*-score	Pathway
C04145	1580.02	All-trans-Nonaprenyl diphosphate	0.03	−3.70880	Ubiquinone biosynthesis
C00894	1641.26	Propenoyl-CoA, Acryloyl-CoA	0.03	−4.06603	Propanoate metabolism
C05989	1673.22	3-Oxopropionyl-CoA, Malonyl semialdehyde-CoA	0.03	−3.98330	Propanoate metabolism
C15670	1703.7	Heme A	0.04	−3.33664	Porphyrin metabolism
C11378	1724.36	Ubiquinone-10, Coenzyme Q10	0.04	−3.43541	Ferroptosis
C05268	1761.34	(S)-Hydroxyhexanoyl-CoA	0.04	−3.51413	Fatty acid elongation and degradation
C05265	1869.46	3-Oxodecanoyl-CoA	0.04	−3.34195	Fatty acid elongation and degradation
C00406	1885.3	Feruloyl-CoA, 4-Hydroxy-3-methoxycinnamoyl-CoA	0.04	−2.94010	Arginine and proline metabolism

KO – GD3SKO mice, WT – wild-type mice, $p < 0.05$. *Imaging mass spectrometry was performed using Shimadzu IMScope TRIO MALDI-IT-TOF (Shimadzu, Kyoto, Japan). Tissue sections were mounted on ITO slides. The matrix (9-aminoacridine) was applied to samples using iMLayer device (Shimadzu, Kyoto, Japan) which included a 15 min sublimation at 180°C, followed by 5 min recrystallization at 37°C with 5% methanol in a vapor chamber. Imaging was performed in negative ion mode within an m/z range of 1,500–1900 Dalton and the following setup: laser diameter 25 µm, laser intensity 46%, 100 laser shots/pixel. Pixel number was 3,000. Data analysis was performed in R software ver. 4.0.1. The expression of a compound is reduced in the CPu region of KO mice when its *t*-score value is negative.

metabolites from fatty acid metabolism can impact other pathways, including lipid and glycosphingolipid synthesis and are decreased in GD3SKO mice (Table 1). Peroxisome proliferator-activated receptors (PPARs), especially PPARα, regulate fatty acid metabolism and influence the expression of lipid metabolism genes (Hu et al., 2023), affecting ganglioside biosynthesis.

Moreover, decreased expression of ubiquinone 10 (coenzyme Q10), a component of the mitochondrial electron transport chain, is related to a range of neurologic, renal, cardiac, and other clinical manifestations (Hargreaves et al., 2020; Mantle et al., 2023). Decreased Q10 synthetic pathway is supported by decreased expression of all-trans-nonaprenyl diphosphate which is important for biosynthesis of ubiquinone and other terpenoid-quinones. Ubiquinone acts as an antioxidant, protecting cells from oxidative damage and reducing stress, vital for maintaining enzyme activities and cellular signaling (Gutierrez-Mariscal et al., 2020). Similarly, heme, which is also identified in our study (Table 1) helps maintain cellular redox balance through the electron transport chain, influencing enzyme expression and function. Heme A is a crucial component of molecular systems required for oxygen transport and cellular respiration. Based on reduced expression of ubiquinone and heme A, GD3S could be related to increased oxidative stress in the cells. In addition, enhanced sulfur metabolism affects the redox state and overall metabolic profile, potentially modulating GD3S-related pathways and influencing ganglioside synthesis involved in tumor growth and metastasis.

When analyzing the consequences of GD3S downregulation or inactivation, other research not directly investigating the mouse or cellular GD3SKO models needs to be considered. It is established that decreased GD3 levels might compromise lipid raft integrity and function, altering cellular communication and signal transduction (Sonnino and Prinetti, 2010). Because the integrity and functionality of cellular membranes are also essential for the correct operation of ion channels and transporters, a decrease in GD3S activity can seriously disturb ion homeostasis. This may result in extensive cellular malfunction, affecting functions like potassium and sodium homeostasis and calcium signaling (Bretscher and Munro, 1993; Ledeen et al., 1998; Simons and Gerl, 2010). For example, in a recent paper exploring ganglioside interactome (Zhang et al., 2024), specific ganglioside-protein interactions were identified, previously anticipated by literature (Ilic et al., 2021; Puljko et al., 2022). They include particular subunits of Na^+/K^+ ATPase and plasma membrane calcium ATPase (Zhang et al., 2024). Since specific gangliosides directly bind these proteins, changed ganglioside composition caused by GD3S inhibition and the consequent lack or accumulation of specific ganglioside species could lead to their disturbed activity and function. In addition, the reshaped ganglioside milieu leads to altered membrane fluidity and consequently dysfunctional ion channels, impacting the cell's ability to maintain proper ion gradients (Puljko et al., 2021) which adds an additional energy-demanding challenge. Furthermore, decreased activity of GD3S has the potential to interfere with calcium signaling pathways and disturb intracellular calcium homeostasis (Ledeen et al., 1998), which has severe implications across multiple signaling pathways since Ca^{2+} is a second messenger. Also, gangliosides play a role in modulating cell–cell/cell-matrix interactions, which are critical for maintaining tissue structure and function, and lower activity of GD3S can impair cell adhesion and migration, potentially affecting tissue integrity and repair mechanisms (Hakomori Si, 2002).

5 Conclusions and perspectives

The known, both good and bad, as well as hypothesized consequences of decreased GD3S expression, are schematically shown in Figure 1. Altered GD3S activity and consequent changed b-series gangliosides synthesis are important contributors to various pathologies, including tumors and neurodegenerative diseases. GD3S overexpression is linked to enhanced tumor proliferation and metastasis in multiple cancers while inhibition of GD3S is a potential therapeutic strategy due to its role in malignancy-associated pathways, evidenced by studies showing reduced malignancy and metastasis upon GD3S suppression (Figure 1). On the other hand, decreased activity of GD3 synthase has significant implications for disturbed cellular homeostasis, including impairing immune responses, cellular adhesion, signal transmission, and membrane integrity. Our own MSI data (Table 1) shows decreased expression of the putatively identified compounds as the consequence of GD3S inactivation in GD3SKO mice which can generally negatively affect energy metabolism, regulatory pathways, and mitigation of oxidative stress.

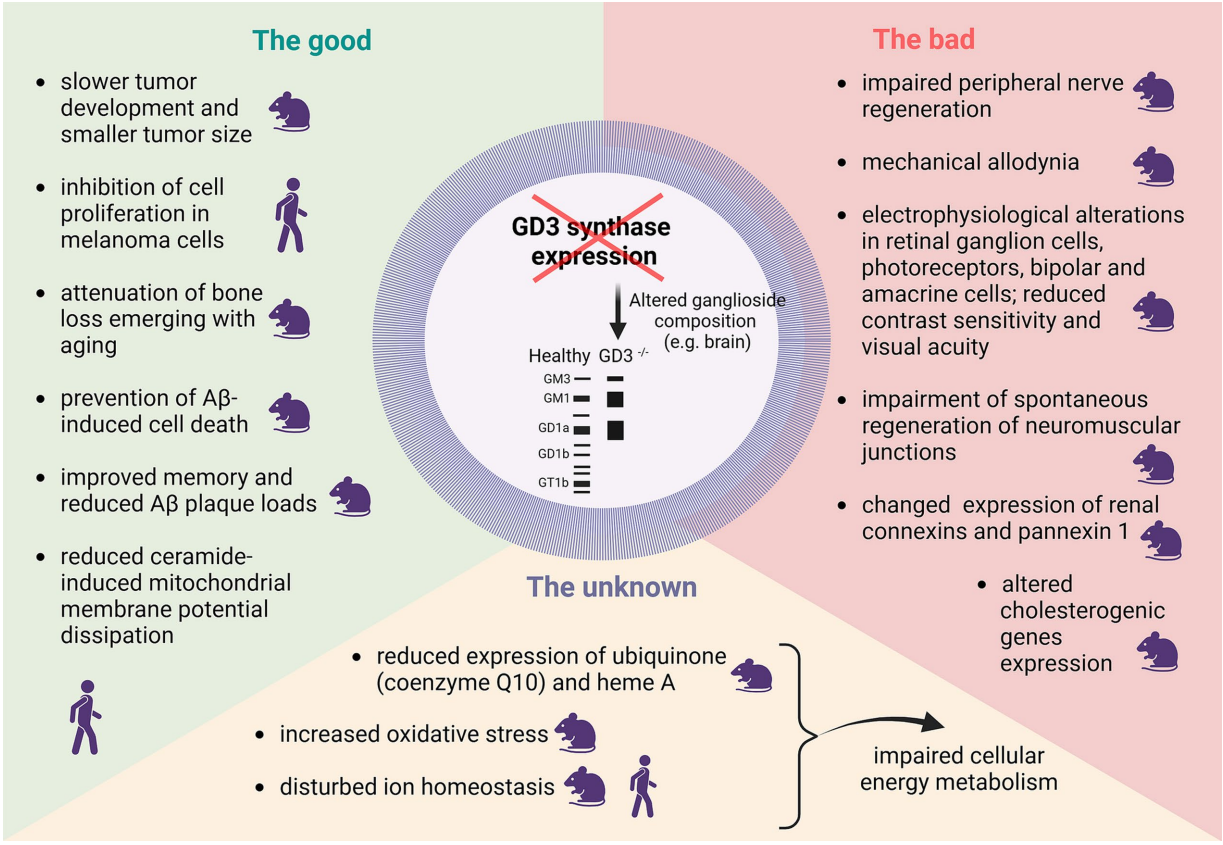

FIGURE 1
Schematic representation of the good, bad and the unknown consequences of decreased GD3 synthase expression. The human or mouse icon highlight whether the research was performed in mouse or human cell lines and/or tissue/ animal models. The figure was created with Biorender.com.

The possible effects of the disturbances on several physiological systems underscore the vital role of GD3S in cellular homeostasis. Further studies should try to elucidate the intricate regulatory pathways governing the expression and activity of GD3S, analyze its diverse functional roles across different tissues, and explore its potential as a therapeutic target in pathological conditions such as cancer, neurodegenerative diseases, and immune disorders. Understanding the molecular underpinnings of GD3S may facilitate the creation of novel strategies for the detection, management, and prevention of a variety of disorders, creating new avenues for targeted therapies and exploiting the role of GD3 synthase in cellular processes for clinical benefit.

Data availability statement

The original contributions presented in the study are included in the article/Supplementary material, further inquiries can be directed to the corresponding authors.

Ethics statement

The animal study was approved by regional ethics committees for scientific experiments and the Croatian Ministry of Agriculture (2158-61-07-14-118). The study was conducted in accordance with the local legislation and institutional requirements.

Author contributions

BP: Conceptualization, Writing – original draft, Writing – review & editing. JG: Investigation, Writing – original draft, Writing – review & editing. VP: Writing – original draft, Writing – review & editing. KI: Writing – original draft, Writing – review & editing. BV: Supervision, Writing – original draft, Writing – review & editing. SK-B: Conceptualization, Funding acquisition, Writing – original draft, Writing – review & editing, Supervision. MH: Writing – original draft, Writing – review & editing, Conceptualization, Funding acquisition. ŽD: Writing – original draft, Writing – review & editing, Formal analysis, Investigation. SB: Conceptualization, Writing – original draft, Writing – review & editing. KM-J: Conceptualization, Funding acquisition, Supervision, Writing – original draft, Writing – review & editing.

Funding

The author(s) declare financial support was received for the research, authorship, and/or publication of this article. This work was supported by research projects funded by the Croatian Science Foundation (grants raft tuning, IP-2014-09-2324 to MH and NeuroReact, IP-2016-06-8636 to SK-B), European Union through the European Regional Development Fund, Operational Programme "Competitiveness and Cohesion 2014–2020", grant agreement no. KK.01.1.1.02.0015, "Research and diagnostics of malignant, infectious

and rare metabolic diseases based on MALDI TOF technology" and University of Zagreb research support grant NEURO-MOD-PUMP, 10106-24-1546 (to KM-J).

Acknowledgments

Figure 1 was created with Biorender.com.

Conflict of interest

The authors declare that the research was conducted in the absence of any commercial or financial relationships that could be construed as a potential conflict of interest.

Publisher's note

Supplementary material

The Supplementary material for this article can be found online at: https://www.frontiersin.org/articles/10.3389/fnmol.2024.1465013/full#supplementary-material

References

Abreu, C. A., Teixeira-Pinheiro, L. C., Lani-Louzada, R., da Silva-Junior, A. J., Vasques, J. F., Gubert, F., et al. (2021). GD3 synthase deletion alters retinal structure and impairs visual function in mice. *J. Neurochem.* 158, 694–709. doi: 10.1111/JNC.15443

Akkhawattanangkul, Y., Maiti, P., Xue, Y., Aryal, D., Wetsel, W. C., Hamilton, D., et al. (2017). Targeted deletion of GD3 synthase protects against MPTP-induced neurodegeneration. *Genes Brain Behav.* 16, 522–536. doi: 10.1111/GBB.12377

Bernardo, A., Harrison, F. E., McCord, M., Zhao, J., Bruchey, A., Davies, S. S., et al. (2009). Elimination of GD3 synthase improves memory and reduces amyloid-β plaque load in transgenic mice. *Neurobiol. Aging* 30, 1777–1791. doi: 10.1016/j.neurobiolaging.2007.12.022

Bretscher, M. S., and Munro, S. (1993). Cholesterol and the Golgi apparatus. *Science* 261, 1280–1281. doi: 10.1126/science.8362242

Cazet, A., Lefebvre, J., Adriaenssens, E., Julien, S., Bobowski, M., Grigoriadis, A., et al. (2010). GD_3 synthase expression enhances proliferation and tumor growth of MDA-MB-231 breast cancer cells through c-met activation. *Mol. Cancer Res.* 8, 1526–1535. doi: 10.1158/1541-7786.MCR-10-0302

Daniotti, J. L., Lancia, C. A., Rösner, H., and Maccioni, H. J. F. (1991). GD3 prevalence in adult rat retina correlates with the maintenance of a high GD3−/GM2-synthase activity ratio throughout development. *J. Neurochem.* 57, 2054–2058. doi: 10.1111/J.1471-4159.1991.TB06421.X

Daniotti, J. L., Landa, C. A., and Maccioni, H. J. F. (1994). Regulation of ganglioside composition and synthesis is different in developing chick retinal pigment epithelium and neural retina. *J. Neurochem.* 62, 1131–1136. doi: 10.1046/J.1471-4159.1994.62031131.X

Daniotti, J. L., Landa, C. A., Rosner, H., and Maccioni, H. J. F. (1992). Adult rat retina interneurons synthesize GD3: GD3 expression by these cells is regulated by cell-cell interactions. *J. Neurochem.* 59, 107–117. doi: 10.1111/J.1471-4159.1992.TB08881.X

De Maria, R., Lenti, L., Malisan, F., D'Agostino, F., Tomassini, B., Zeuner, A., et al. (1997). Requirement for GD3 ganglioside in CD95-and ceramide-induced apoptosis. *Science* 277, 1652–1655. doi: 10.1126/SCIENCE.277.5332.1652

Dhanushkodi, A., Xue, Y., Roguski, E. E., Ding, Y., Matta, S. G., Heck, D., et al. (2019). Lentiviral-mediated knock-down of GD3 synthase protects against MPTP-induced motor deficits and neurodegeneration. *Neurosci. Lett.* 692, 53–63. doi: 10.1016/J.NEULET.2018.10.038

Dorrell, C., Schug, J., Canaday, P. S., Russ, H. A., Tarlow, B. D., Grompe, M. T., et al. (2016). Human islets contain four distinct subtypes of β cells. *Nat. Commun.* 7:11756. doi: 10.1038/ncomms11756

Fuchigami, T., Itokazu, Y., and Yu, R. K. (2024). Ganglioside GD3 regulates neural stem cell quiescence and controls postnatal neurogenesis. *Glia* 72, 167–183. doi: 10.1002/GLIA.24468

Gutierrez-Mariscal, F. M., Arenas-de Larriva, A. P., Limia-Perez, L., Romero-Cabrera, J. L., Yubero-Serrano, E. M., and López-Miranda, J. (2020). Coenzyme Q10 supplementation for the reduction of oxidative stress: clinical implications in the treatment of chronic diseases. *Int. J. Mol. Sci.* 21:7870. doi: 10.3390/ijms21217870

Ha, K. T., Lee, Y. C., and Kim, C. H. (2004). Overexpression of GD3 synthase induces apoptosis of vascular endothelial ECV304 cells through downregulation of Bcl-2. *FEBS Lett.* 568, 183–187. doi: 10.1016/j.febslet.2004.05.020

Hakomori Si, S.-I. (2002). The glycosynapse. *Proc. Natl. Acad. Sci. USA* 99, 225–232. doi: 10.1073/pnas.012540899

Handa, Y., Ozaki, N., Honda, T., Furukawa, K., Tomita, Y., Inoue, M., et al. (2005). GD3 synthase gene knockout mice exhibit thermal hyperalgesia and mechanical allodynia but decreased response to formalin-induced prolonged noxious stimulation. *Pain* 117, 271–279. doi: 10.1016/J.PAIN.2005.06.016

Hargreaves, I., Heaton, R. A., and Mantle, D. (2020). Disorders of human coenzyme Q10 metabolism: an overview. *Int. J. Mol. Sci.* 21:6695. doi: 10.3390/ijms21186695

Hedberg, K. M., Mahesparan, R., Read, T. A., Tysnes, B. B., Thorsen, F., Visted, T., et al. (2001). The glioma-associated gangliosides 3′-isoLM1, GD3 and GM2 show selective area expression in human glioblastoma xenografts in nude rat brains. *Neuropathol. Appl. Neurobiol.* 27, 451–464. doi: 10.1046/J.1365-2990.2001.00353.X

Hein, V., Baeza-Kallee, N., Bertucci, A., Colin, C., Tchoghandjian, A., Figarella-Branger, D., et al. (2024). GD3 ganglioside is a promising therapeutic target for glioma patients. *Neurooncol. Adv.* 6:vdae038. doi: 10.1093/noajnl/vdae038

Houghton, A. N., Mintzer, D., Cordon-Cardo, C., Welt, S., Fliegel, B., Vadhan, S., et al. (1985). Mouse monoclonal IgG3 antibody detecting GD3 ganglioside: a phase I trial in patients with malignant melanoma. *Proc. Natl. Acad. Sci. USA* 82, 1242–1246. doi: 10.1073/PNAS.82.4.1242

Hu, P., Li, K., Peng, X., Kan, Y., Li, H., Zhu, Y., et al. (2023). Nuclear receptor PPARα as a therapeutic target in diseases associated with lipid metabolism disorders. *Nutrients* 15:4772. doi: 10.3390/nu15224772

Ilic, K., Lin, X., Malci, A., Stojanović, M., Puljko, B., Rožman, M., et al. (2021). Plasma membrane calcium ATPase-Neuroplastin complexes are selectively stabilized in GM1-containing lipid rafts. *Int. J. Mol. Sci.* 22:13590. doi: 10.3390/ijms222413590

Inokuchi, J.-I., Go, S., Yoshikawa, M., and Strauss, K. (2017). Gangliosides and hearing. *Biochim. Biophys. Acta Gen. Subj.* 1861, 2485–2493. doi: 10.1016/j.bbagen.2017.05.025

Iwasawa, T., Zhang, P., Ohkawa, Y., Momota, H., Wakabayashi, T., Ohmi, Y., et al. (2018). Enhancement of malignant properties of human glioma cells by ganglioside GD3/GD2. *Int. J. Oncol.* 52, 1255–1266. doi: 10.3892/IJO.2018.4266

Kasprowicz, A., Sophie, G. D., Lagadec, C., and Delannoy, P. (2022, 2022). Role of GD3 synthase ST8Sia I in cancers. *Cancers* 14:1299. doi: 10.3390/CANCERS14051299

Kim, J. K., Kim, S. H., Cho, H. Y., Shin, H. S., Sung, H. R., Jung, J. R., et al. (2010). GD3 accumulation in cell surface lipid rafts prior to mitochondrial targeting contributes to amyloid-β-induced apoptosis. *J. Korean Med. Sci.* 25:1492. doi: 10.3346/JKMS.2010.25.10.1492

Knorr, S., Skakkebæk, A., Just, J., Johannsen, E. B., Trolle, C., Vang, S., et al. (2022). Epigenetic and transcriptomic alterations in offspring born to women with type 1 diabetes (the EPICOM study). *BMC Med.* 20, 1–16. doi: 10.1186/S12916-022-02514-X/TABLES/3

Kurabi, A., Keithley, E. M., Housley, G. D., Ryan, A. F., and Wong, A. C. Y. (2017). Cellular mechanisms of noise-induced hearing loss. *Hear. Res.* 349, 129–137. doi: 10.1016/J.HEARES.2016.11.013

Lama, G., Mangiola, A., Proietti, G., Colabianchi, A., Angelucci, C., D'Alessio, A., et al. (2016). Progenitor/stem cell markers in brain adjacent to glioblastoma: GD3 ganglioside and NG2 proteoglycan expression. *J. Neuropathol. Exp. Neurol.* 75, 134–147. doi: 10.1093/JNEN/NLV012

Ledeen, R. W., Wu, G., Lu, Z. H., Kozireski-Chuback, D., and Fang, Y. (1998). The role of GM1 and other gangliosides in neuronal differentiation. Overview and new finding. *Ann. N. Y. Acad. Sci.* 845, 161–175. doi: 10.1111/j.1749-6632.1998.tb09669.x

Lee, M., Kim, K. S., Fukushi, A., Kim, D. H., Kim, C. H., and Lee, Y. C. (2018). Transcriptional activation of human GD3 synthase (hST8Sia I) gene in curcumin-induced autophagy in A549 human lung carcinoma cells. *Int. J. Mol. Sci.* 19:1943. doi: 10.3390/ijms19071943

Ma, W., Zhao, X., Liang, L., Wang, G., Li, Y., Miao, X., et al. (2017). miR-146a and miR-146b promote proliferation, migration and invasion of follicular thyroid carcinoma via inhibition of ST8SIA4. *Oncotarget* 8, 28028–28041. doi: 10.18632/ONCOTARGET.15885

Malisan, F., Franchi, L., Tomassini, B., Ventura, N., Condò, I., Rippo, M. R., et al. (2002). Acetylation suppresses the proapoptotic activity of GD3 ganglioside. *J. Exp. Med.* 196, 1535–1541. doi: 10.1084/JEM.20020960

Mantle, D., Millichap, L., Castro-Marrero, J., and Hargreaves, I. P. (2023). Primary coenzyme Q10 deficiency: an update. *Antioxidants (Basel)* 12:1652. doi: 10.3390/antiox12081652

Masson, E., Troncy, L., Ruggiero, D., Wiernsperger, N., Lagarde, M., and El Bawab, S. (2005). A-series gangliosides mediate the effects of advanced glycation end products on Pericyte and mesangial cell ProliferationA common mediator for retinal and renal Microangiopathy? *Diabetes* 54, 220–227. doi: 10.2337/DIABETES.54.1.220

Maxzúd, M. K., and Maccioni, H. J. F. (1997). Compartmental organization of the synthesis of GM3, GD3, and GM2 in golgi membranes from neural retina cells. *Neurochem. Res.* 22, 455–461. doi: 10.1023/A:1027311811334

Mennel, H. D., Bosslet, K., Geisseli, H., and Bauer, B. L. (2000). Immunohistochemically visualized localisation of gangliosides Glac2 (GD3) and Gtri2 (GD2) in cells of human intracranial tumors. *Exp. Toxicol. Pathol.* 52, 277–285. doi: 10.1016/S0940-2993(00)80046-9

Meter, D., Racetin, A., Vukojević, K., Balog, M., Ivić, V., Zjalić, M., et al. (2022). A lack of GD3 synthase leads to impaired renal expression of connexins and Pannexin1 in St8sia1 knockout mice. *Int. J. Mol. Sci.* 23:6237. doi: 10.3390/ijms23116237

Mlinac, K., Fon Tacer, K., Heffer, M., Rozman, D., and Kalanj Bognar, S. (2012). Cholesterogenic genes expression in brain and liver of ganglioside-deficient mice. *Mol. Cell. Biochem.* 369, 127–133. doi: 10.1007/S11010-012-1375-Y

Nel, M., Dashti, J. S., Gamieldien, J., and Heckmann, J. M. (2017). Exome sequencing identifies targets in the treatment-resistant ophthalmoplegic subphenotype of myasthenia gravis. *Neuromuscul. Disord.* 27, 816–825. doi: 10.1016/J.NMD.2017.06.009

Novak, A., Režić Mužinić, N., Čikeš Čulić, V., Božić, J., Tičinović Kurir, T., Ferhatović, L., et al. (2013). Renal distribution of ganglioside GM3 in rat models of types 1 and 2 diabetes. *J. Physiol. Biochem.* 69, 727–735. doi: 10.1007/s13105-013-0249-4

Ohkawa, Y., Zhang, P., Momota, H., Kato, A., Hashimoto, N., Ohmi, Y., et al. (2021). Lack of GD3 synthase (St8sia1) attenuates malignant properties of gliomas in genetically engineered mouse model. *Cancer Sci.* 112, 3756–3768. doi: 10.1111/CAS.15032

Panzetta, P., and Allende, M. L. (2000). Ganglioside expression during differentiation of chick retinal cells in vitro. *Neurochem. Res.* 25, 163–169. doi: 10.1023/A:1007560004244

Pena, L., Franks, J., Chapman, K. A., Gropman, A., Ah Mew, N., Chakrapani, A., et al. (2012). Natural history of propionic acidemia. *Mol. Genet. Metab.* 105, 5–9. doi: 10.1016/j.ymgme.2011.09.022

Puljko, B., Stojanović, M., Ilic, K., Kalanj-Bognar, S., and Mlinac-Jerkovic, K. (2022). Start me up: how can surrounding gangliosides affect sodium-potassium ATPase activity and steer towards pathological ion imbalance in neurons? *Biomedicines* 10:1518. doi: 10.3390/biomedicines10071518

Puljko, B., Stojanović, M., Ilic, K., Maček Hrvat, N., Zovko, A., Damjanović, V., et al. (2021). Redistribution of gangliosides accompanies thermally induced Na+, K+-ATPase activity alternation and submembrane localisation in mouse brain. *Biochim Biophys Acta Biomembr* 1863:183475. doi: 10.1016/J.BBAMEM.2020.183475

Ribeiro-Resende, V. T., Araújo Gomes, T., de Lima, S., Nascimento-Lima, M., Bargas-Rega, M., Santiago, M. F., et al. (2014). Mice lacking GD3 synthase display morphological abnormalities in the sciatic nerve and neuronal disturbances during peripheral nerve regeneration. *PLoS One* 9:e108919. doi: 10.1371/journal.pone.0108919

Rietman, M. L., Sommeijer, J.-P., Neuro-Bsik Mouse Phenomics ConsortiumLevelt, C. N., and Heimel, J. A. (2012). Candidate genes in ocular dominance plasticity. *Front. Neurosci.* 6:11. doi: 10.3389/fnins.2012.00011

Rippo, M. R., Malisan, F., Rayagnan, L., Tomassini, B., Condo, I., Costantini, P., et al. (2000). GD3 ganglioside directly targets mitochondria in a bcl-2-controlled fashion. *FASEB J.* 14, 2047–2054. doi: 10.1096/FJ.99-1028COM

Ruan, S., Raj, B. K. M., and Lloyd, K. O. (1999). Relationship of glycosyltransferases and mRNA levels to ganglioside expression in neuroblastoma and melanoma cells. *J. Neurochem.* 72, 514–521. doi: 10.1046/J.1471-4159.1999.0720514.X

Rupp, A., Cunningham, M. E., Yao, D., Furukawa, K., and Willison, H. J. (2013). The effects of age and ganglioside composition on the rate of motor nerve terminal regeneration following antibody-mediated injury in mice. *Synapse* 67, 382–389. doi: 10.1002/SYN.21648

Sasaki, E., Hamamura, K., Mishima, Y., Furukawa, K., Nagao, M., Kato, H., et al. (2022). Attenuation of bone formation through a decrease in osteoblasts in mutant mice lacking the GM2/GD2 synthase gene. *Int. J. Mol. Sci.* 23:9044. doi: 10.3390/ijms23169044

Savas, B., Astarita, G., Aureli, M., Sahali, D., and Ollero, M. (2020). Gangliosides in Podocyte biology and disease. *Int. J. Molec. Sci.* 21:9645. doi: 10.3390/IJMS21249645

Schengrund, C.-L. (2023). The Ying and yang of ganglioside function in cancer. *Cancers (Basel)* 15:5362. doi: 10.3390/cancers15225362

Schnaar, R. L. (2016). Gangliosides of the vertebrate nervous system. *J. Mol. Biol.* 428, 3325–3336. doi: 10.1016/J.JMB.2016.05.020

Schnaar, R. L. (2019). The biology of gangliosides. *Adv. Carbohydr. Chem. Biochem.* 76, 113–148. doi: 10.1016/BS.ACCB.2018.09.002

Seo, S. Y., Ju, W. S., Kim, K., Kim, J., Yu, J. O., Ryu, J.-S., et al. (2024). Quercetin induces mitochondrial apoptosis and downregulates ganglioside GD3 expression in melanoma cells. *Int. J. Mol. Sci.* 25:5146. doi: 10.3390/IJMS25105146

Simons, K., and Gerl, M. J. (2010). Revitalizing membrane rafts: new tools and insights. *Nat. Rev. Mol. Cell Biol.* 11, 688–699. doi: 10.1038/nrm2977

Sipione, S., Monyror, J., Galleguillos, D., Steinberg, N., and Kadam, V. (2020). Gangliosides in the brain: physiology, pathophysiology and therapeutic applications. *Front. Neurosci.* 14:572965. doi: 10.3389/FNINS.2020.572965

Sonnino, S., and Prinetti, A. (2010). Gangliosides as regulators of cell membrane organization and functions. *Adv. Exp. Med. Biol.* 688, 165–184. doi: 10.1007/978-1-4419-6741-1_12

Svennerholm, L. (1994). Designation and schematic structure of gangliosides and allied glycosphingolipids. *Prog. Brain Res.* 101, xi–xiv. doi: 10.1016/S0079-6123(08)61935-4

Tang, F. L., Wang, J., Itokazu, Y., and Yu, R. K. (2021). Ganglioside GD3 regulates dendritic growth in newborn neurons in adult mouse hippocampus via modulation of mitochondrial dynamics. *J. Neurochem.* 156, 819–833. doi: 10.1111/JNC.15137

Tong, L., Zhao, Q., Datan, E., Lin, G. Q., Minn, I., Pomper, M. G., et al. (2021). Triptolide: reflections on two decades of research and prospects for the future. *Nat. Prod. Rep.* 38, 843–860. doi: 10.1039/D0NP00054J

Wang, J., Cheng, A., Wakade, C., and Yu, R. K. (2014). Ganglioside GD3 is required for neurogenesis and long-term maintenance of neural stem cells in the postnatal mouse brain. *J. Neurosci.* 34, 13790–13800. doi: 10.1523/JNEUROSCI.2275-14.2014

Wang, J., and Yu, R. K. (2013). Interaction of ganglioside GD3 with an EGF receptor sustains the self-renewal ability of mouse neural stem cells in vitro. *Proc. Natl. Acad. Sci. USA* 110, 19137–19142. doi: 10.1073/PNAS.1307224110

Wang, J., Zhang, Q., Lu, Y., Dong, Y., Dhandapani, K. M., Brann, D. W., et al. (2021). Ganglioside GD3 is up-regulated in microglia and regulates phagocytosis following global cerebral ischemia. *J. Neurochem.* 158, 737–752. doi: 10.1111/JNC.15455

Watanabe, Y., Nara, K., Takahashi, H., Nagai, Y., and Sanai, Y. (1996). The molecular cloning and expression of α2,8-Sialyltransferase (GD3 synthase) in a rat brain. *J. Biochem.* 120, 1020–1027. doi: 10.1093/OXFORDJOURNALS.JBCHEM.A021494

Yao, T. J., Meyers, M., Livingston, P. O., Houghton, A. N., and Chapman, P. B. (1999). Immunization of melanoma patients with BEC2-keyhole limpet hemocyanin plus BCG intradermally followed by intravenous booster immunizations with BEC2 to induce anti-GD3 ganglioside antibodies. *Clin. Cancer Res.* 5, 77–81.

Yeh, S. C., Wang, P. Y., Lou, Y. W., Khoo, K. H., Hsiao, M., Hsu, T. L., et al. (2016). Glycolipid GD3 and GD3 synthase are key drivers for glioblastoma stem cells and tumorigenicity. *Proc. Natl. Acad. Sci. USA* 113, 5592–5597. doi: 10.1073/pnas.1604721113

Yo, S., Hamamura, K., Mishima, Y., Hamajima, K., Mori, H., Furukawa, K., et al. (2019). Deficiency of GD3 synthase in mice resulting in the attenuation of bone loss with aging. *Int. J. Mol. Sci.* 20:20. doi: 10.3390/ijms20112825

Yoshikawa, M., Go, S., Suzuki, S.-I., Suzuki, A., Katori, Y., Morlet, T., et al. (2015). Ganglioside GM3 is essential for the structural integrity and function of cochlear hair cells. *Hum. Mol. Genet.* 24, 2796–2807. doi: 10.1093/HMG/DDV041

Yoshikawa, M., Go, S., Takasaki, K., Kakazu, Y., Ohashi, M., Nagafuku, M., et al. (2009). Mice lacking ganglioside GM3 synthase exhibit complete hearing loss due to selective degeneration of the organ of Corti. *Proc. Natl. Acad. Sci. USA* 106, 9483–9488. doi: 10.1073/PNAS.0903279106

Yu, R. K., Tsai, Y. T., Ariga, T., and Yanagisawa, M. (2011). Structures, biosynthesis, and functions of gangliosides—an overview. *J. Oleo Sci.* 60, 537–544. doi: 10.5650/JOS.60.537

Zhang, P., Ohkawa, Y., Yamamoto, S., Momota, H., Kato, A., Kaneko, K., et al. (2021). St8sia1-deficiency in mice alters tumor environments of gliomas, leading to reduced disease severity. *Nagoya J. Med. Sci.* 83, 535–549. doi: 10.18999/NAGJMS.83.3.535

Zhang, G.-L., Porter, M. J., Awol, A. K., Orsburn, B. C., Canner, S. W., Gray, J. J., et al. (2024). The human ganglioside Interactome in live cells revealed using clickable Photoaffinity ganglioside probes. *J. Am. Chem. Soc.* 146, 17801–17816. doi: 10.1021/jacs.4c03196

frontiers | Frontiers in Molecular Neuroscience

TYPE Hypothesis and Theory
PUBLISHED 27 November 2024
DOI 10.3389/fnmol.2024.1465023

OPEN ACCESS

EDITED BY
Oliver von Bohlen und Halbach,
Universitätsmedizin Greifswald, Germany

REVIEWED BY
Stephan Maxeiner,
Saarland University, Germany
Alberto Pascual,
Spanish National Research Council (CSIC), Spain

*CORRESPONDENCE
Mario Stojanovic
✉ mario.stojanovic@irb.hr
Svjetlana Kalanj-Bognar
✉ svjetlana.kalanj.bognar@mef.hr

RECEIVED 15 July 2024
ACCEPTED 01 November 2024
PUBLISHED 27 November 2024

CITATION
Stojanovic M and Kalanj-Bognar S (2024) Toll-like receptors as a missing link in Notch signaling cascade during neurodevelopment. *Front. Mol. Neurosci.* 17:1465023. doi: 10.3389/fnmol.2024.1465023

Toll-like receptors as a missing link in Notch signaling cascade during neurodevelopment

Mario Stojanovic[1,2]* and Svjetlana Kalanj-Bognar[1,3]*

[1]Laboratory for Neurochemistry and Molecular Neurobiology, Croatian Institute for Brain Research, School of Medicine, University of Zagreb, Zagreb, Croatia, [2]Laboratory for Cell Biology and Signalling, Department for Molecular Biology, Institute Ruđer Bošković, Zagreb, Croatia, [3]Department for Chemistry and Biochemistry, School of Medicine, University of Zagreb, Zagreb, Croatia

Neurodevelopment encompasses a complex series of molecular events occuring at defined time points distinguishable by the specific genetic readout and active protein machinery. Due to immense intricacy of intertwined molecular pathways, extracting and describing all the components of a single pathway is a demanding task. In other words, there is always a risk of leaving potential transient molecular partners unnoticed while investigating signaling cascades with core functions—and the very neglected ones could be the turning point in understanding the context and regulation of the signaling events. For example, signaling pathways of Notch and Toll-like receptors (TLRs) have been so far unrelated in the vast body of knowledge about neurodevelopment, however evidence from available literature points to their remarkable overlap in influence on identical molecular processes and reveals their potential functional links. Based on data demonstrating Notch and TLR structural engagement and functions during neurodevelopment, along with our description of novel molecular binding models, here we hypothesize that TLR proteins act as likely crucial components in the Notch signaling cascade. We advocate for the hypothesized role of TLRs in Notch signaling by: elaborating components and features of their pathways; reviewing their effects on fates of neural progenitor cells during neurodevelopment; proposing molecular and functional aspects of the hypothesis, along with venues for testing it. Finally, we discuss substantial indications of environmental influence on the proposed Notch-TLR system and its impact on neurodevelopmental outcomes.

KEYWORDS

neurodevelopment, neural progenitor cells, signaling pathways, cell–cell communication, behavior pattern

1 Notch and Toll—structural and signaling features

During neurodevelopment, neural progenitor cells (NPCs) settled in the neuroectodermal zone act as a self-sustainable pool of cells that subsequently differentiate into neurons, oligodendrocytes, and astrocytes. In the decision-making time points, NPCs mobilize crucial developmental pathways, creating the molecular crossroads for diverse cellular fates. Across metazoan clades, the Notch signaling cascade propels developmental mechanisms and represents a fundamental pathway for development of the central nervous system (CNS) (Gaiano and Fishell, 2002; Stasiulewicz et al., 2015; Gozlan and Sprinzak, 2023). Architecture and molecular organization of the developing brain is under the influence of Notch in synergy with multiple pathways, such as Sonic Hedgehog (Shh) and Wnt signaling pathways (Akai et al., 2005; Keilani and Sugaya, 2008; Jacobs and Huang, 2019, 2021; Marczenke et al., 2021).

Being a cell contact-dependent pathway, the Notch signaling hub events occur on the membranes of signal-sending and signal-receiving cells (Fiúza and Arias, 2007; D'Souza et al., 2010; Lovendahl et al., 2018). The principle of the signaling cascade comprises binding of Notch receptors on the signal-receiving cell with the Delta/Serrate/LAG-1(DSL) family of ligands, mostly Jagged and Delta-like (J/D), on the signal-sending cell. The juxtacrine J/D complex association and endocytosis-induced tension generation are vital for exposure of S2 and S3 cleavage sites (Sprinzak and Blacklow, 2021). A series of ADAM and γ-secretase proteolytic cleavages release the membrane-bound Notch intracellular domain (NICD)(Brou et al., 2000; Mumm et al., 2000; Sanchez-Irizarry et al., 2004; Fiúza and Arias, 2007; Lovendahl et al., 2018; Sprinzak and Blacklow, 2021; Wolfe and Miao, 2022), and its nuclear translocation activates Notch-targeted HES and HEY genes (Figure 1) (Kageyama and Ohtsuka, 1999). The selection of receptor and ligand isoforms sets up a large number of binding combinations related to unique (Six et al., 2003; Gordon et al., 2007; D'Souza et al., 2010; Lovendahl et al., 2018; Zeronian et al., 2021; Gozlan and Sprinzak, 2023) molecular and cellular outcomes. Let us first describe Notch and its J/D ligand extracellular engagement mechanism in order to explain in more depth the hypothesis about Toll-like receptors (TLRs) as novel and essential partners in Notch signaling during neurodevelopment.

Notch receptors (Notch1-4) are transmembrane proteins comprised of two non-covalently bound heterodimers (Sanchez-Irizarry et al., 2004; Lovendahl et al., 2018). The extracellular monomer (Notch extracellular domain, NECD) consists of multiple epidermal growth factor (EGF) domains with DSL-interacting EGF domains wrapping the mechanosensory Negative Regulatory Region (NRR) domain (Sanchez-Irizarry et al., 2004; Lovendahl et al., 2018; Sprinzak and Blacklow, 2021). The dimerization complex resembles a mushroom: buried under folds of the LIN-12/Notch repeat (LNR) domain, the heterodimerization (HD) domain protects the intracellular monomer protruding stem with S2 and S3 cleavage sites (Lovendahl et al., 2018; Sprinzak and Blacklow, 2021). In mammals, two Jagged (Jag1-2) and two out of three Delta-like (Dll1, Dll4) ligands bind Notch and pull off the protecting NECD to reveal the cleavage sites, while Dll3 does not bind Notch and is localized in endosome (Nichols et al., 2007; Musse et al., 2012; Lovendahl et al., 2018; Sprinzak and Blacklow, 2021). The JD's extracellular portion also has multiple EGF repeats between the N-terminal C2-like immunoglobulin domain connected to the DSL domain and the cysteine-rich region proximally to the membrane (Lovendahl et al., 2018). Both proteins form rod-like open solenoids as a result of variable EGF repeats (Bork et al., 1996; Wouters et al., 2005; Kelly et al., 2010) and are glycosylated which is a standard structural feature of adhesion molecules (Moloney et al., 2000; Chen et al., 2001; Wouters et al., 2005; Yu et al., 2021). The extracellular portion of the Notch receptor responsible for J/D engagement is between EGF8 and EGF13, while the adhering part of the J/D are C2-like and DSL domains (Cordle et al., 2008a; Musse et al., 2012; Luca et al., 2015; Handford et al., 2018). C2-like domain has lipid-binding properties

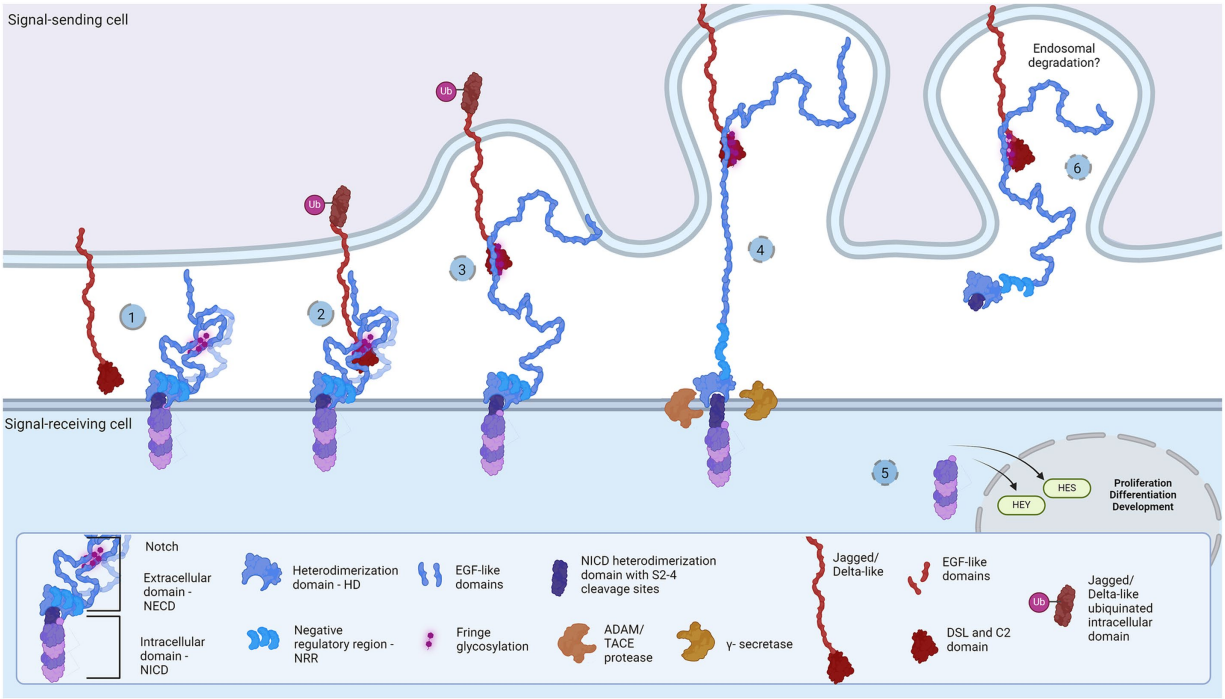

FIGURE 1
Representation of the Notch signaling pathway: The core proteins Notch and DSL ligands, Jagged and Delta-like, bind in *cis* (inhibition) and *trans* (activation) modes. Notch is a dimer of intracellular (Notch intracellular domain, NICD) and extracellular domain (Notch extracellular domain, NECD). (1) The protective dome-like NECD is glycosylated by Fringe glycotransferases. DSL ligand is composed of EGF-like domains with a Notch-interacting DSL/C2 domain. Posttranslational modifications regulate ligand affinity. Upon binding (2), the interaction groove firm binding and tension induction triggers endocytosis of DSL ligand (3) and NECD dissociation from NICD. Exposed NCID is cleaved by ADAM and γ-secretase (4) to release transcription activator NICD domain that regulates HES and HEY gene expression (5). The NECD/DSL complex undergoes endocytosis and is proposed to be degraded in the endosome (6). Created in BioRender. BioRender.com/f38j163.

probably acting as a membrane proximity sensor: the lipids in question are glycosphingolipids (GSLs) in *Drosophila* (Hamel et al., 2010) and phospholipids (PL) in mammals (Ca^{2+}-dependent in Jag) (Chillakuri et al., 2013; Suckling et al., 2017; Handford et al., 2018). Notch EGF10-12 and Jag/Dll C2-DSL interaction groove covers an area of approximately 1,100 $Å^2$ and provides variety and strength of interactions (Cordle et al., 2008a, 2008b; Luca et al., 2015; Handford et al., 2018), i.e., stabilization of glycosylated residues, hydrophobic and H-bond establishment, salt-bridge formation, and Ca^{2+}-dependent structural rigidity induction, enable the conformational change, generate tension which activates endocytosis and NECD dissociation (Nichols et al., 2007; D'Souza et al., 2010; Musse et al., 2012). This action reveals NICD cleavage stem while following proteolytic action leads to subsequent intracellular signaling events (Nichols et al., 2007; Musse et al., 2012; Luca et al., 2017; Sprinzak and Blacklow, 2021). The destiny of the Notch/J/D ligand complex after endocytosis is elusive but is believed to undergo endosomal degradation. In order to bind the Notch receptor, J/D has to be in 'flexed' conformation which exposes the binding groove, and it is supposed that J/D spontaneously transitions between 'flexed' and 'stiff' conformation (Luca et al., 2015, 2017; Handford et al., 2018). The dynamics and steps of conformational transition, how exactly the Jag and Dll achieve their flexed conformation, find and bind Notch, and what happens with the pulled NECD/J/D ligand complex in the signal-sending cell remains unclear. This leaves space for speculations: is there an additional molecule which delivers and presents ligands to Notch receptors; does the signal-sending cell recognizes the final response and if so is there a response-reading machinery in the signal-sending cell? Here we aim to clear up these questions and offer a novel perspective on the Notch signaling cascade, by introducing the TLR family as potential member of the Notch cascade.

The Toll-like receptor (TLR) family of proteins first emerged in Cnidaria (Beutler and Rehli, 2002; Brennan and Gilmore, 2018; Liu et al., 2019) and has since evolved as a patterning tool in development (Barak et al., 2014; Noordstra and Yap, 2021; Umetsu, 2022; Weiss and O'Neill, 2022; Sommariva et al., 2023) and a pattern-recognition tool in immunity (Crack and Bray, 2007; Ma et al., 2007; Park et al., 2009; Scheffel et al., 2012; Anthoney et al., 2018; Chen et al., 2019). The first mention of TLR proteins was the Toll receptor in *Drosophila melanogaster* embryology (Parthier et al., 2014; Al Asafen et al., 2020; Umetsu, 2022), where it serves as a molecular agent for cellular organization in dorsoventral body symmetry formation. Namely, the dosage of ligand Spätzle is measured with the Toll receptor and translated into Dorsal, Snail, and Twist protein gradients, resulting in a cellular patterning of ectoderm, neurogenic ectoderm, and mesoderm (Umetsu, 2022). Later, the same receptor was revealed as a signaling hub in innate immunity upon external pathogen stimuli (Takeda and Akira, 2004; Botos et al., 2011). These two functions are preserved with evolutionary modifications in mammals. For instance, mammalian TLR actions associated with innate immunity differ from *Drosophila*'s due to an additional direct ligand-binding capacity; TLR expression in NPCs and involvement in developmental processes, without apparent endogenous ligand, confirms its role in neurodevelopment. With that said, let us explore the structural and functional features of TLRs that will speak in favor of the hypothesis.

Structurally, the Toll-like receptors form an open solenoid by packing leucine-rich repeats (LRRs) in a horseshoe-shaped extracellular domain with adhesive and binding capacity (Jin et al., 2007; Kang et al., 2009; Park et al., 2009; Botos et al., 2011; Salunke et al., 2012). The function of LRR proteins depends on their structure (specifically, radii and number of LRR modules) (Kobe and Deisenhofer, 1994; Kobe and Kajava, 2001; Enkhbayar et al., 2004) and regarding the LRR composition, TLRs are divided into long and short structures (Figure 2). The intracellular domain of TLRs is a Toll-interleukine-1 receptor (TIR) homology domain that targets TIR-containing proteins, e.g., MyD88 and TRIF, activating TAB2/3/TAK1 and TBK1 relay, TRAF3/6-operated molecular switch. In brief, TLR1,2,4–9, dimers bind TIRAP and MyD88 that scaffold IRAK4/IRAK1/2 and activated TRAF3/6 proteins. Described down-stream effects of signalization upon TLR3 and TLR4 dimerization (Beutler and Rehli, 2002; Ge et al., 2002; Matsumura et al., 2003; Verstak et al., 2009; Smoak et al., 2010; Tukhvatulin et al., 2010) which inlude TRAM and TRIF adaptors, activation of TRAF3 and TRAF6, formation of TAB2/3/TAK1 signalosome and regulation of IKK and MAPK signaling events are presented in Figure 3. TRAF3 activates additional families of IKK-like kinases (TBK1, IKKi). Activated genetic readouts and protein machinery are described in immune answer (Vabulas et al., 2001; Jack et al., 2019; Chen et al., 2021), proliferation and differentiation (Lathia et al., 2008; Ulrich et al., 2015; Song et al., 2019; Mann et al., 2023), mature and apoptotic phenotypes (Cameron et al., 2007; Ma et al., 2007; Stridh et al., 2011; Ishizuka et al., 2013; Li et al., 2013, 2020; Shi et al., 2013; Church et al., 2016; Abdul et al., 2019; Werkman et al., 2020). The library of TLR-activating ligands induces TLR homodimerization in antiparallel orientation, except for versatile TLR2, which builds heterodimers with TLR1, TLR4, or TLR6 in a ligand-dependent fashion (Kang et al., 2009; Schenk et al., 2009; Fernandez-Lizarbe et al., 2013; van Bergenhenegouwen et al., 2013; Koymans et al., 2015; Liu et al., 2019; Ved et al., 2021; Galleguillos et al., 2022). TLR structural features, LRR concave β-sheet, and outer α-helices surface delineate their specificity to ligands, creating a multifaceted recognition hub (Figures 2, 4A) (Werling et al., 2009). Membrane localization of TLR2, TLR4, and TLR5 enables them to recognize and bind di-and triacylated lipoproteins (TLR2/1, TLR2/6) (Jin et al., 2007; Kang et al., 2009), LPS presented by coreceptors (TLR4) (Kim et al., 2007; Park et al., 2009) and flagellin (TLR5) (Smith and Ozinsky, 2002; Yoon et al., 2012). Endosomal TLRs bind viral dsRNA (TLR3), ssRNA (TLR7, TLR8) and ssDNA (TLR9) (Choe et al., 2005; Wang et al., 2006; Botos et al., 2009; Gosu et al., 2019). Mammalian TLRs are designed to fit and bind pathogen-associated molecular pattern molecules (PAMPs), damage-associated molecular pattern molecules (DAMPs), and protein coreceptors (Akashi-Takamura and Miyake, 2008; Park and Lee, 2013; van Bergenhenegouwen et al., 2013). Interestingly, the evolutionary older ligands, particularly in *Drosophila* development, are protein ones, and we could consider that TLRs' protein-binding mode of action makes a conserved *modus operandi* in developmental processes. TLRs, specifically TLR4, recognize and interact with distinct structural features of protein ligands (Vabulas et al., 2001; Kim et al., 2005; Liu et al., 2012; van Bergenhenegouwen et al., 2013; Mehmeti et al., 2019; Ved et al., 2021), particularly protein folds and carbohydrate moieties, opening the possibility that a (glyco) protein could be a potential TLR4 neurodevelopmental ligand. The protein coreceptors that bind to mammalian TLR4 have a distinct C2 globulin fold with a lipid binding pocket; e.g., globulin MD-2 in a complex with LPS is TLR4 binding partner (Gioannini et al., 2004; Kim et al., 2007; Schumann, 2011). TLR4/MD-2 quaternary complex consists of two MD-2 molecules engaged with both TLR4 monomers. Unique structural features of TLR4 allow MD-2 binding at the concave dimerization face of the first and the back of the second TLR4 monomer

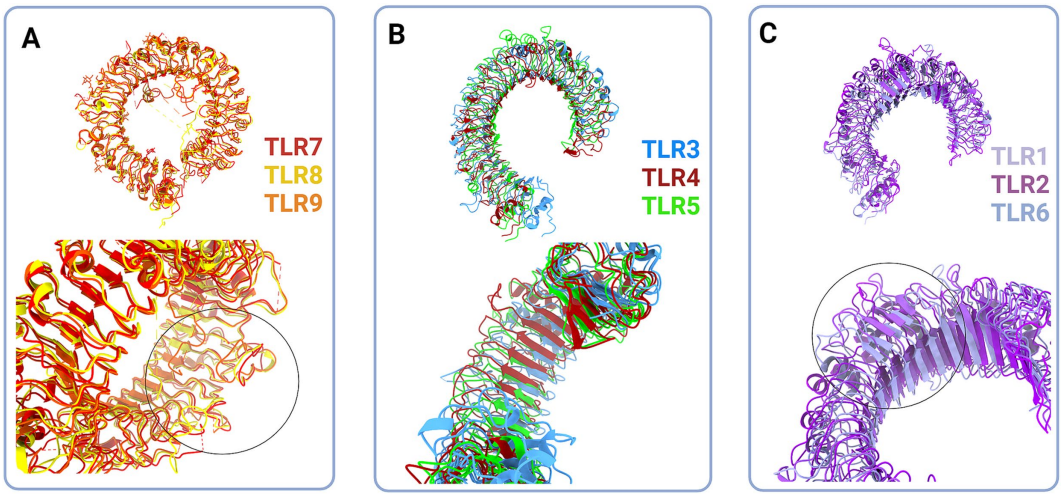

FIGURE 2
Structural classes of Toll-like receptors (TLRs) are long (A and B) and short (C) TLRs. (A) Superimposed structural models of TLR7 (red, hTLR7 PDB:7CYN), TLR8 (yellow, hTLR8 PDB:7R54) and TLR9 (tangerine, mTLR PDB:3WPG) (upper panel). Zooming in on the loops on dimerization side of long TLRs reveals that loops enclose cavity between two dimers (bottom panel, circle). (B) Superimposed structural models of TLR3 (blue, hTLR3 PDB:7C76), TLR 4 (deep red, hTLR4 PBD:3FXI) and TLR5 (green, hTLR5 PDB:3J0A) (upper panel). Zoom in on the LRR types in TLR3, TLR4 and TLR5 (bottom panel). (C) Superimposed structural models of TLR1 (lilac, hTLR1 PDB:6NIH), TLR2 (purple, hTLR2 PDB:6NIG), and TLR6 (light blue, mTLR6 PDB: 3479) (upper panel). Closing up of TLR2, TLR1 and TLR6 β sheets on dimerisation side dictate the ligand cavity depth on top of TLR monomer (bottom panel). Created in BioRender. BioRender.com/o67p300.

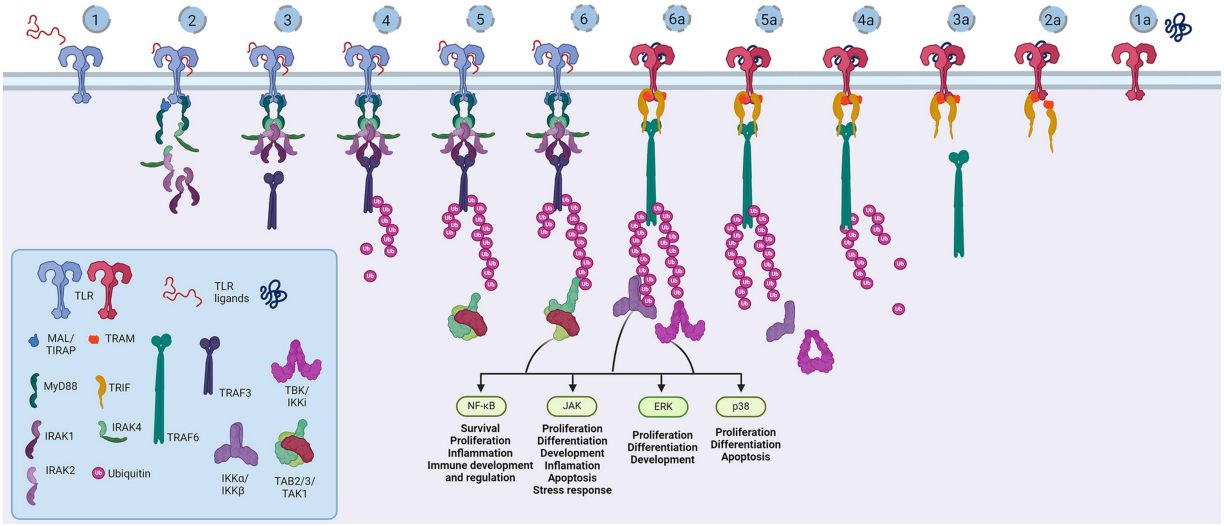

FIGURE 3
Representation of the Toll-like receptor pathway. Toll receptors scaffold signalosomes in membrane proximity, e.g., TLR dimers scaffold Mydosome (TLR2/1, TLR2/6, TLR4, TLR5, TLR7, TLR8 and TLR9) (1–6) and TRIFosome (TLR3 and TLR4) (1a-6a). Ligand binding to TLR (1) primes Mydosome. TLR recruits MAL/TIRAP,MyD88, IRAK1/2 and IRAK4 scaffold in hexameric structures (2) activating TRAF3 and TRAF6 (3) which are able to auto-ubiquinate (4). Poly-ubiquitin chains associate (5) and activate TAB2/3/TAK1 kinases (6). Trifosome is primed with TLR ligand binding (1a). Associated TRAM and TRIF (2a) activate TRAF3 directly (3a) and TRAF6 in a RIP1-dependant fashion. TRAF3 polyubiquitination (4a) recruits (5a) and activates TBK/IKKi kinases (6a). These kinases regulate IKKα/IKKβ kinases and input of NF-κB, JAK, ERK and p38 regulated genes and proceses. Created in BioRender. BioRender.com/a29t370.

(Figure 4A) (Kim et al., 2007). Protein MD-2 and Jag/Dll C2-like domains have evolutionarily conserved folds, showing overall similarity between overlapped models of MD-2 and Jag/Dll C2-like domains (Figure 4A2). This structural similarity between the Notch ligands and the TLR4 coreceptor is the first indication that TLRs possibly act as a binding partners of Notch ligands.

2 Notch and Tolls in neurodevelopment

To investigate the hypothesis on shared Notch and Toll signaling mechanisms with implications for developing nervous system, we demonstrate systematically the striking functional overlaps of

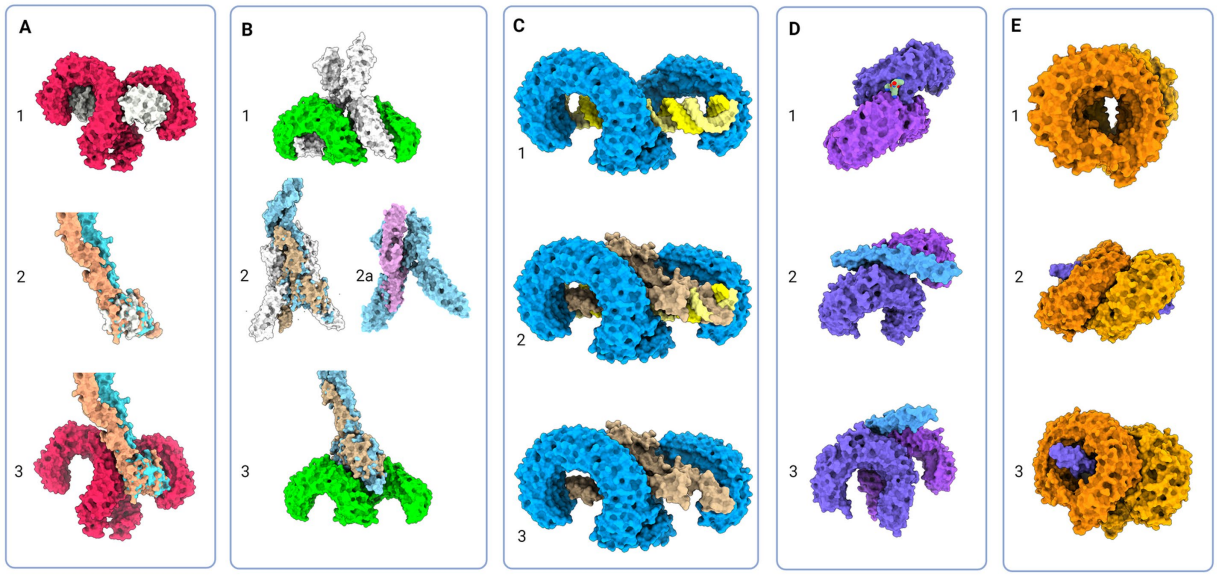

FIGURE 4
Protein models of TLRs with natural ligands and superimposition of TLR and Notch signaling components; (A) 1 - Molecular visualization of TLR4 dimer with coreceptor MD-2 (PDB:3FXI), 2 – Aligned models of MD-2, Jagged (apricot, PDB:5UK5) and Delta-like (tan, PDB:4XL1), 3 – Proposed model of Jagged and Delta-like in complex with TLR4; (B) 1 – TLR5 model in complex with flagellin (PDB:3 V47), 2 – Flagellin model aligned with NECD/Delta-like complex (tan, PDB:4XLW, light blue, PDB:4XL1), 2a – Flagellin model (PDB:3 V47) aligned with APP core domain (lilac, PDB:3NYL), 3 – Proposed model of NECD/Delta-like in complex with TLR5; (C): 1 - TLR3 in complex with dsDNA (PDB:7DAS), 2 – Superimposed NECD/Delta-like complex over dsRNA in complex with TLR3, and 3 – Theoretical binding model of TLR3 and NECD/Delta-like complex; (D) 1 - TLR1/2 in complex with LPS (PDB:2Z7X), 2 and 3 - Theoretical model of TLR2/1 interaction with Notch EGF-like domains (PDB:4D0E) (E) 1 - Model of TLR7 dimers (PDB:5GMF), 2 and 3 – Theoretical model of EGF-like domains (PDB:4D0E) in complex with TLR7. Created in BioRender. BioRender.com/t26j594.

Notch and TLR signaling during neurodevelopment documented in the literature (Table 1).

Described functions of Notch signaling during neurodevelopment encompass NPCs number, identity, spatial organization (Irvin et al., 2001, 2004; Stump et al., 2002; Patten et al., 2006; Keilani and Sugaya, 2008; Kim et al., 2008; Zhou et al., 2010; Rabadán et al., 2012; Blackwood et al., 2020; Marczenke et al., 2021; Mase et al., 2021; Okubo et al., 2021; Li C. et al., 2022; Tran et al., 2023) and connectome formation events (Franklin et al., 1999; Šestan et al., 1999; Breunig et al., 2007; Kuzina et al., 2011; Shi et al., 2011). Notch signaling seems to be crucial for asymmetric NPCs division (Casas Gimeno and Paridaen, 2022) and may be viewed as a switch between NPC differentiation, neurogenesis, and gliogenesis. Also, Notch1 is implicated in radial glia (RG) identity establishment and differentiation to ventral RG (Patten et al., 2003, 2006; Mase et al., 2021). These findings confirm that Notch orchestrates morphology, outgrowth and density ratio of neurons, oligodendrocytes, and astrocytes which eventually has implications on the axonal, dendritic, and synaptic network formation (Šestan et al., 1999; Shi et al., 2011; Kuzina et al., 2011).

Evidenced extensive impact of Notch signaling on critical neurodevelopmental events overlaps with so far known neurodevelopmental functions of TLRs. Firstly, TLR activation affects the immune response during and after (neuro)development, and its effect was observed in cooperation with the Notch pathway and as a Hh and Wnt signaling regulator, respectively (Opitz et al., 2001; Re and Strominger, 2001; Vabulas et al., 2001; Frantz et al., 2001; Matsumura et al., 2003; Leemans et al., 2005; Crack and Bray, 2007; Ziegler et al., 2007; Palaga et al., 2008; Park et al., 2008; Hu et al., 2008; Nichols et al., 2009; Lalancette-Hbert et al., 2009; Cameron and Landreth, 2010; Foldi et al., 2010; Tsao et al., 2011; Liu et al., 2012; Winters et al., 2013; Kim et al., 2013; Okun et al., 2014; Hamidi et al., 2014; Rangasamy et al., 2018; Mehmeti et al., 2019; Martínez-García et al., 2020). Secondly, the expression of TLRs on all cell types across the developing and adult brain unquestionably affirms their impact on neurodevelopment (Barak et al., 2014; Okun et al., 2019).

Clearly, a large body of evidence confirms that certain TLR functions match the scope of Notch functions during embryonic and postnatal brain development (Table 1). Observed functional overlaps indicate that different TLR and Notch proteins govern switches between cellular commitments. For example, the actions of Dll1, TLR2, and TLR4 overlap to some extent: Dll1 induces neurogenesis; loss of Dll1 and TLR4 induces proliferation and gliogenesis; the loss of TLR2 induces proliferation and neurogenesis. From that perspective, TLR2 and Dll are required for proliferation cessation, while TLR4 and Dll1 combinations become inductors of the same cellular fate, suggesting they are a part of the same signaling machinery. It has to be noted that interplay of Notch and TLR signaling has been described in parts, however majority of studies focuses on coordinated responses of the immune system components, based on widely recognized functions of TLRs in innate immunity (Hu et al., 2008; Palaga et al., 2008; Tsao et al., 2011; Shang et al., 2016). The most striking interplay between TLR and Notch in immunity was documented in the study by Hu et al. which confirmed synergistic cooperation between the Notch and TLR pathways mediated by RBP-J. Specifically, the acute TLR induction has been shown to activate HES1 and HEY1 genes, while TLR interleukin genes expression were dependant on NICD nuclear translocation and RBP-J

TABLE 1 Cell-specific expression and functions of Notch and TLR signaling pathways during neurodevelopment.

Cellular type	Notch pathway	TLR pathway
Neural progenitor cells (NPCs)	• Radial glia differentiation is induced by Notch1 (Patten et al., 2003, 2006) • Notch signaling regulates proliferation of NPCs (Kageyama et al., 2009) • Olfactory epithelium stem and progenitor cells utilize Notch (Schwob et al., 2017) • Notch as NPC commitment switch (Zhou et al., 2010) • Overlapping and differential expression of Notch1-3, Jag1-2, Dll1 and Dll3 (Irvin et al., 2001, 2004) • Differential expression of Notch1, Jag1, Jag2, Dll1, Dll3, Hes 1,3,5, Numb and Numblike (Stump et al., 2002); lack of Dll1 leads to impaired neurodevelopment (Arzate et al., 2022) • Brain lipid-binding protein as mediator of Notch signaling in radial glial cells (Anthony et al., 2005)	• NPCs proliferation is regulated by TLR3 (Lathia et al., 2008; Yaddanapudi et al., 2011) • NPCs proliferation is regulated by TLR2 (Okun et al., 2010) • Maternal exposure to TLR3 ligands promotes proliferation of NPCs (Baines et al., 2020) • Maternal exposure to TLR2, TLR4 ligands enhances NPC proliferation and expands neocortex (Mann et al., 2023) • TLR2 and TLR4 differentially regulate spinal cord NPCs (Sanchez-Petidier et al., 2022) • Retinal PC proliferation is under TLR4 control (Shechter et al., 2008) • Differential expression of TLRs in mammalian and *Drosophila* brain (Shmueli et al., 2018) • Expression of TLRs in human CNS (Bsibsi et al., 2002) • Adult hippocampal neurogenesis is under TLR control (Rolls et al., 2007)
Neuron	• Dll1 induces NPC commitment to neuronal phenotype (Kawaguchi et al., 2008) • Dll3 overexpression and translocation to the membrane, as Dll1, promotes and maintains neurogenesis (Ladi et al., 2005) • Jag1 influences neuronal division and periglomerular interneurons (Blackwood et al., 2020) • Dll1 intrecellular domain regulates dorsal root ganglion development (Okubo et al., 2021) • Jag2 in motor neuron generation (Rabadán et al., 2012) • Notch signaling influences dopaminergic neuron number (Trujillo-Paredes et al., 2016). • Notch and Dll guide axon pathfinding (Giniger et al., 1993) • Notch1 and Dll1 regulate mamalian neurite development (Franklin et al., 1999) • Glia and neuron Notch crosstalk in establishment of longitudinal axon connections (Kuzina et al., 2011) • Notch signaling-mediated axon outgrowth (Shi et al., 2011) • Notch regulates neurite outgrowth by contact-inhibition (Šestan et al., 1999) • Notch regulates neuronal cell faith and dendrite morphology (Breunig et al., 2007)	• TLRs regulate differentiation of NSCs into neurons (Ulrich et al., 2015) • After brain injury, TLR2 promotes neurogenesis (Seong et al., 2018) • TLR4 ligands have anti-neurogenic effect (Zaben et al., 2021) • TLR4 has a role in amygdala GABAergic transmission (Varodayan et al., 2018) • TLR3 has potential negative role in axon growth (Cameron et al., 2007) • TLR8 role in developing neurons and axons (Ma et al., 2007) • TLR3 contributes to Wallerian degeneration of white matter (Lee et al., 2017) • TLRs in neuronal morphogenesis (Liu et al., 2014) • TLRs regulate neurogenesis and synaptic physiology (Chen et al., 2019)
Astrocyte	• Jag and Notch mediate retinal gliogenesis (Jin et al., 2023) • Dll1 regulates Bergman glia monolayer formation (Hiraoka et al., 2013) • Neurons induce NPCs astrocyte commitment through Notch signaling (Namihira et al., 2009)	• Adult hippocampal NPCs differentiate into astrocytes at the expense of neurons (Rolls et al., 2007) • Astrocyte populations differently respond to TLR4 and TLR3 ligands in myelination events (Werkman et al., 2020) • TLRs are expressed in astroglia (Li et al., 2021)
Oligodendrocyte	• Radial glia specification into oligodendrocytes is governed by Notch (Kim et al., 2008) • Jag2 regulates spinal cord oligodendrocyte generation (Rabadán et al., 2012) • Notch has dual role in neuron-to-oligodendrocyte switch (Tran et al., 2023) • Notch signaling evidenced in oligodendrocyte genesis and homeostasis (Li C. et al., 2022)	• TLR2 and TLR4 differentially influence oligodendrocyte formation after inflammation (Schonberg et al., 2007) • Inhibition of TLR2 stimulates OPCs and TLR3 inhibition induces apoptosis (Bsibsi et al., 2012) • TLR2 tolerance enhances remyelination in CNS (Wasko et al., 2019) • TLR2/4 ligand, HMBG1, reduces OPC number (Ved et al., 2021) • Transplanted OPCs and inflammation response in myelination (Setzu et al., 2006) • The lack of TLR4 impairs oligodendrocyte formation after injury (Church et al., 2016)

binding. This finding fully supports here presented theory and it would be certainly interesting to confirm the same interplay during neurodevelopment. So far, direct involvement of TLRs in neurodevelopment has been underappreciated, but the herein reviewed findings indicate that TLRs stand at the core program of the nervous system development, and deciphering the role of TLR signaling, particularly as the part of the proposed TLR-Notch complex could be valuable for understanding the spatiotemporal cellular organization of CNS.

3 Hypothesis

We suggest that TLRs are an integral part of the Notch signaling cascade acting as a Notch signaling transductor scaffold and deciphering machinery in both signal-sending and signal-receiving cells. Events that presumably lead to Notch binding and signaling on the signal-receiving cell membrane are organized with TLR1, TLR2, TLR4, and TLR6, while TLR5, TLR3, TLR7, TLR8, and TLR9 are an answer interpreting machinery for the signal-sending cell. The proposed functions for each TLR would occur sequentially as follows: TLR4—ligand bait; TLR1,2,6 heterodimers—Notch sorter and selector; TLR5—answer catcher; TLR3—answer reader; TLR7,8 and 9—answer reader and tuner.

4 Proposed experimental paradigms

To prove the hypothesis, one would need to check for biochemical and physiological evidence of TLR involvement in the Notch pathway and correlate them to the functional and eventually behavior patterns. The biochemistry of the proposed system should first describe chemico-physical interactions, followed by observations using models *in vitro* and *in vivo*, and it could be investigated in several ways:

1) Interactive visualization and analysis of molecular structures utilizing available models from PDB library,[1] bioinformatics tools such as PDBeFold[2] and Chimera program[3];
2) Molecular simulation, the fast-science approach using already existing structural data collected on Notch, Jag, Dll, and TLR which could be uploaded into programs providing us with information on the proposed interaction parameters (orientation, energies, contacts, electrostatic, polar, and non-polar interactions) and enabling understanding and locating target protein interactions;
3) Cross-linking mass spectrometry (XL-MS) analysis of NPCs, *in vitro* and *in vivo*, would provide a series of data regarding the molecular system of interest. Data collected in controlled conditions, the basis for the interaction matrix, would be challenged with the data collected on TLR knock-out (KO) systems and TLR-challenged systems to untangle the communication code of Notch/TLR signaling. The TLR-challenged system could also be a simulation model to investigate the dose-dependent changes introduced by the environmental setup;
4) State-of-the-art cryo-electron microscopy (EM) technology and its further advancements could be implemented for structural and topographical research of the Notch/TLR pathway. *In vitro* models of NPCs, organoids, and *ex vivo* brain imaging would provide starting material for investigation and help describe the exact 3D model and mechanics of Notch/TLR initial signaling events.

The proposed solutions for checking the hypothesis are methodologically feasible and could provide the scientific community with valuable answers. Another way to test the hypothesis would be to use data collected on individuals exposed to TLR agonists *in utero* during critical neurodevelopment stages. Such data may reveal whether TLR challenge acts on neurodevelopment and whether discrete changes in neuronal number, branching and networks strength establishes neurophenotype basis for different neurobehavioral patterns.

However, the limitations of proposed structural analysis approaches should not be overlooked and require to take into account that any posttranslational modification could be responsible for maximal efficiency in binding between Notch/Jag/TLR, thus not fully resolved from available data. Other challenges might arise from the following facts: extracellular proteins are the most lavishly modified proteins; native conformations and molecular dynamics in the cellular environment are entropy-rich and challenging to simulate; glycosylated residues are intrinsic to cellular communication and serve as recognition residues; sugar code enables additional structural recognition means and induces differential affinity towards interaction partners.

5 Supportive evidence for novel interactions within proposed TLR-Notch assembly

Whilst there are currently no *in vivo* supportive data, the interactive visualization and analysis of molecular structures utilizing informatics tools (see footnote 2) and Chimera program (see footnote 3) yields several exciting findings. More specifically, the analyses of molecular structure and potential binding models of TLRs and Notch suggest their novel roles and interactions (also see Figures 4, 5).

The majority representation of the Notch/J/D binding model assumes Notch, Jag, and Dll as stiff sticks protruding perpendicularly to the cellular membrane and interacting similarly, deep within the extracellular matrix and away from a cell membrane. From the above-given information, Notch is a tangled dome-like protein complex that needs ligands to remove protection mechanically and enable message transduction. For this to happen, J/D must be in the precise structural orientation for groove exposure and proximity of potential binding partners (Luca et al., 2015, 2017; Handford et al., 2018). The lipophilic property of J/D C2 domain (Chillakuri et al., 2013; Suckling et al., 2017) could prime the interaction with a signal-receiving cell. It is reasonable to suggest that Jag and Dll span the distance and are loosely tensioned between two cells. Lipid-C2 interactions are an open invitation for anchoring protein that will maximize the conformational flex of the J/D structure and be a docking tool for signal-receiving

1 https://www.rcsb.org/
2 https://www.ebi.ac.uk/msd-srv/ssm/
3 https://www.cgl.ucsf.edu/chimera/

cells. The cross-talk between the C2 domain of J/D and lipids on signal-receiving cells is the point where TLR4 enters the story. By interactive visualization of molecular structures we were able to observe that TLR4 recognizes J/D, binds and locks it in an active conformation, and delivers it to selected Notch (Figure 4A). The described interaction indicates a potential role of TLR4 as a molecular anchorage in signal-receiving cells. We assume that the J/D tethered with a TLR4 would provide an energetically favorable environment and support for flex conformation to ensure its availability for interaction with Notch. The TLR2 with interacting partners TLR1 and TLR6 could be a Notch sorting and 'decision-making' tool. Distinct TLR2 heterodimer complexes would recognize the ligand fetched by TLR4 and choose the appropriately accessorized Notch receptor. The glycosylation status of Notch receptors and J/D ligands may be a motif that allows TLR2 to sort and choose binding combinations (Figure 4D). This mode of action indicates that establishing interaction between TLR4/J/D leads to a Notch-binding tension-generating step in the cascade. We propose that TLR4 and TLR2 act as a fly 'buttoning' Notch and J/D. The J/D/TLR4-tether generates tension between two membranes, and the tension's release might be a cue for the signal-sending cell membrane invagination resulting in Notch dissociation and proteolysis on the signal-receiving cell. We hypothesize that TLR4 and TLR2 support Notch and J/D ligand binding, resulting with promotion of NICD downstream cascade in signal-receiving cells.

The signal-sending cell supposedly integrates the molecular events by gathering stimuli from the pulled NECD/J/D complex. Here, based on analyzed molecular structure, we propose that TLR5 acts as an answer-receiving tool. TLR5 may sense the tension and recognize non-interacting J/D and NECDs EGF domains (Figure 4C). The NECD/J/D complex interface facing the signal-sending cell is bifurcated and shaped like ligands recognized by TLR5. With the help of TLR5, the complex is taken inside the cell, where it would be contextualized. In the endosome, degradation releases strands of Notch EGF repeats, NECD/J/D binding complex, unbound J/D ligands, and J/D ligand intracellular domain. Each degradation product is a piece of valuable information for signaling cells. We propose TLR3 recognizes and gives context to cleaved NECD/J/D binding complex (Figure 4C) while TLR7, TLR8, and TLR9 bind EGF repeats (Figure 4E) giving necessary information about cell-receiving cells responses. One single strand-recognizing TLR could also be sensing the degradation product of the cell's unused ligands and help the signal-sending cell react appropriately to the neighboring population dynamics.

During differentiation, asymmetric inheritance is induced by cellular touch (Casas Gimeno and Paridaen, 2022). TLR links Notch inductors' direct genetic input to TAB/TAK adductors' rearrangements in cytoplasmic and membrane phenotypes to accommodate genetic identity-specific protein output. Notch signaling cascades may form an activated membrane patch that integrates changes in signal-receiving cell. Sequestering and ratio of specific IKK(α/β/γ) and IKK-like (TBK1 and IKKi) pathways are most likely needed for modulation of NF-κB-dependent and independent pathways, creating identity commitment signaling and metabolic landscapes. It is likely that TLR signaling modulates NF-κB signals induced by growth factors and synergistically affects PI3K signaling. TLR also activates IKK complex and its downstream mTORC1 and mTORC2 metabolic programmes that are highly active in neurodevelopment (Switon et al., 2017). The mTORC1 conducts neuronal cytoskeletal organization and mTORC2, which is located in endosomes and orchestrates lipid metabolism, crucial for genesis of membranes—cellular 'skin' and communication platform of all neural cells (Switon et al., 2017). TLRs also induce MAPK cascades, like p38, JNK and ERK which are known to participate in proliferative and differentiative cellular programs in stem cells (Johnson and Lapadat, 2002). MAPK/ERK pathway is IKK-dependant - these pathways could change and dictate daughter cell fate, behavior and metabolism and could be crucial for the timeline of neurodevelopment (Figure 6).

We believe that the hypothesized model introduces the needed complexity and integrative perspective of the mammalian Notch signaling in brain development. Namely, the current model focuses mostly on the signal-receiving cell as the active player, while the role of the signal-sending cell in Notch signaling is not fully understood and is thus overlooked. The current model resembles instruction-giving rather than communication-based decision-making between the cells. We advocate that TLRs untangle the information given by Notch and J/D ligand structure features and provide necessary information and instruction both to signal-sending and signal-receiving cells. Here hypothesized model involving the TLR family in the Notch signaling pathway takes into account two-way intercellular communication in which both cells actively interpret responses in order to efficiently coordinate developmental and homeostatic processes.

6 Relevance of the hypothesized Notch/Toll system for the molecular basis of neurodevelopment

Notch signaling is one of the central cellular homeostatic mechanisms able to exert adaptive responses both during development and in mature cells. In this respect, incorporating TLRs and their putative role as fundamental parts of Notch signaling provides a new perspective for neurodevelopment- and neuroimmune-related studies.

It is reasonable to assume that TLRs play a role in two overlapping pathways in the brain—the TLR Notch-dependent (ND) cellular development/homeostasis pathway and the environment-dependent (ED) cellular (immune) response. Differentiation between the two pathways would add to the understanding of molecular aspects of neurodevelopment at the phylogenetic and ontogenic levels. The TLR-ND pathway would be best studied in the course of development to confirm the exact steps of how specific TLR, Notch, and J/D ligands achieve formation of cellular identity and communication during maturation and adulthood when established identity becomes a matter of innate immunity. The TLR-ED pathway is intertwined with ND-mediated cellular crosstalk, homeostatic neural cell-to-cell communication and its environmental influence surveillance by immune cells. In this context, innate immunity proves that TLR proteins are of utter importance for the brain and its homeostasis. In order to prevent cellular miscommunication, microglia, like all innate immunity cells, express the entire TLR repertoire, functioning as an affinity bead that siphons environmental molecular patterns, PAMPs and DAMPs. The immune component of TLR-ED has been widely studied, and some of the phenomena described involve developmental/homeostatic ND pathway. The way the environmental stimuli influence individual cellular TLR-ND and ED pathways will be further discussed.

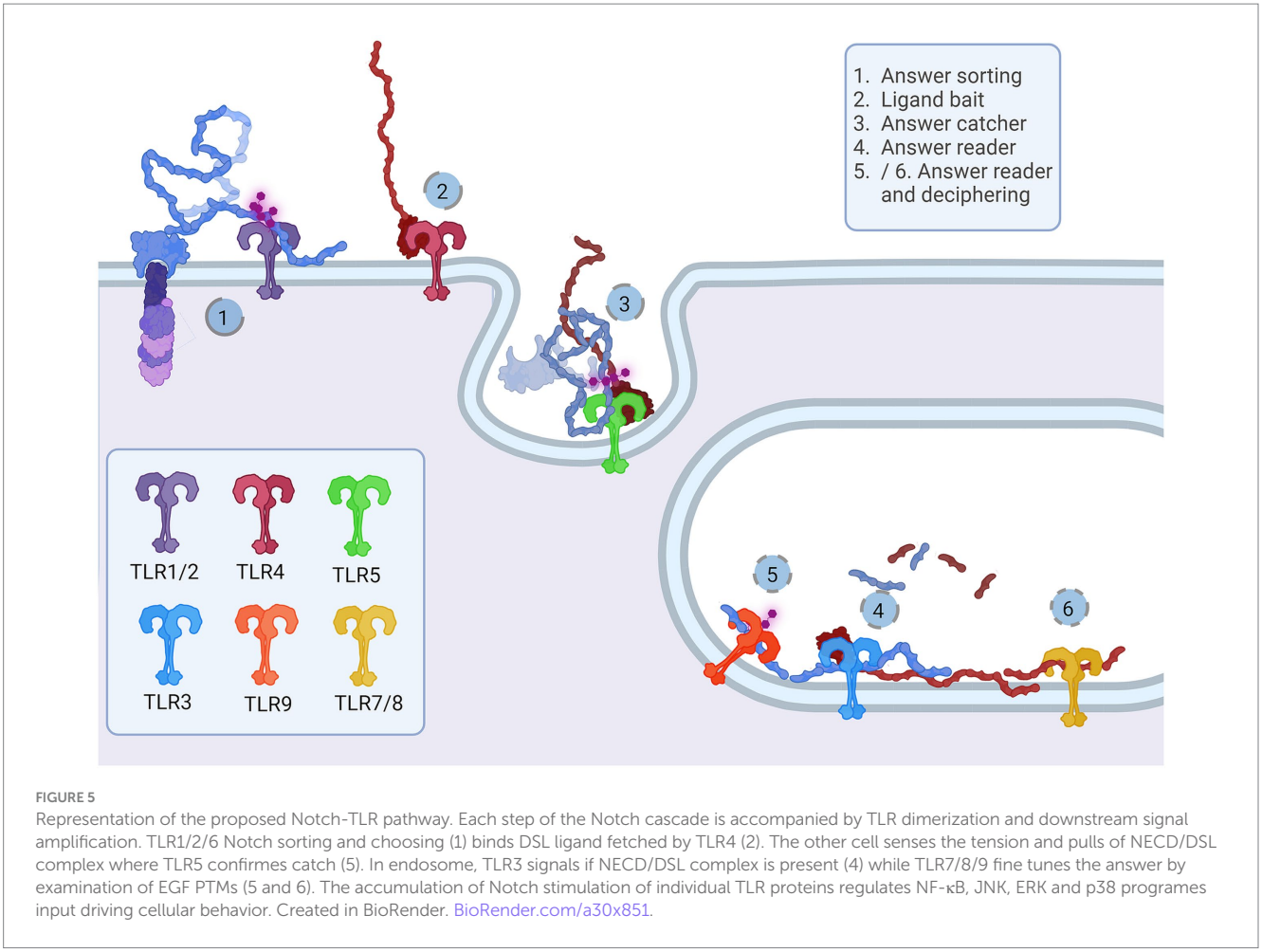

FIGURE 5
Representation of the proposed Notch-TLR pathway. Each step of the Notch cascade is accompanied by TLR dimerization and downstream signal amplification. TLR1/2/6 Notch sorting and choosing (1) binds DSL ligand fetched by TLR4 (2). The other cell senses the tension and pulls of NECD/DSL complex where TLR5 confirmes catch (5). In endosome, TLR3 signals if NECD/DSL complex is present (4) while TLR7/8/9 fine tunes the answer by examination of EGF PTMs (5 and 6). The accumulation of Notch stimulation of individual TLR proteins regulates NF-κB, JNK, ERK and p38 programes input driving cellular behavior. Created in BioRender. BioRender.com/a30x851.

First, we briefly recapitulate the roles of TLRs and their cellular and time-dependent expression patterns during brain development (Table 1) and propose the following sequence of neurodevelopmental events accompanied by TLRs actions. Let us imagine the developing nervous system and the emerging complexity course depending on the cellular ability to communicate with the environment, more precisely, neighboring cells. TLR scaffold, Jag and Dll ligand type on the signal-sending cell, and available Notch receptor on the signal-receiving cell drive the course of proliferation, differentiation, and specialization, e.g., axon, dendrite, and synapse formation.We suggest that NPC TLR-ND system starts as a simple TLR5/TLR3 answer-reading machine for low-specificity Notch binding events. With increasing number of NPCs, the growing density of TLR3-sensing Notch events may allow the emergence of TLR4, TLR7, TLR8, and TLR9. Hipothetically, this quartet slowly silences proliferation and guides NPC asymmetric division and gradual specialization in progenitor subtypes (radial glia, ventral and basal radial glia, retinal progenitor cells, immediate progenitors, oligodendrocyte progenitor cells). The colonization of the brain is now set off.

Waves of climbing young neurons create layers upon layers, as they travel from densely populated, supposedly high-Notch regions, to unpopulated, presumed low-Notch regions.We anticipate that the juxtacrine input of "older" neurons maintains progenitor cell identity on the way to its destination within growing layers. As development proceeds, documented specific changes of TLRs expression paterns (Bsibsi et al., 2002; Shmueli et al., 2018) suggest that TLR3 could be potentially a progenitor and immature phenotype program switch, while TLR4 and TLR9 a differentiative and mature program switches. When situated, TLR7-driven axonal outgrowth (Ma et al., 2007) creates a foundation for establishing the regional-specific neuronal circuitries and networks. The upcoming gliogenesis builds the cell-type diversity; thus, new TLRs emerge (TLR1 and TLR6) which most likely support the novel identity choice. Once positioned glial cells could shed J/D ligands and convey signal to incoming glial progenitors about area population density, creating regions of cell-diverse clusters. When colonization is complete, maturation can take place. Young neurons start to branch, forming inter-regional connections, and oligodendrocytes start myelination in the presumed TLR-ND fashion, where TLR2 and partners support the ongoing Notch events. Astrocytes and already infiltrated microglia mature and continue supporting decades-long network formation and calibration (Schafer et al., 2012, 2013; Miyamoto et al., 2013; Ikegami et al., 2019). Microglial action acquires the brain's environmental experience and plastic potential, e.g., network malleability, progenitor number, and potency, providing necessary adaptation mechanisms for survival and growth. TLR proteins react to the differences in environmental stimuli, creating unique cellular makeup, connection variety, cellular mosaicism, and organism-specific circuitry, resulting in various neurophenotypes, behaviors, conditions, and pathologies. To address

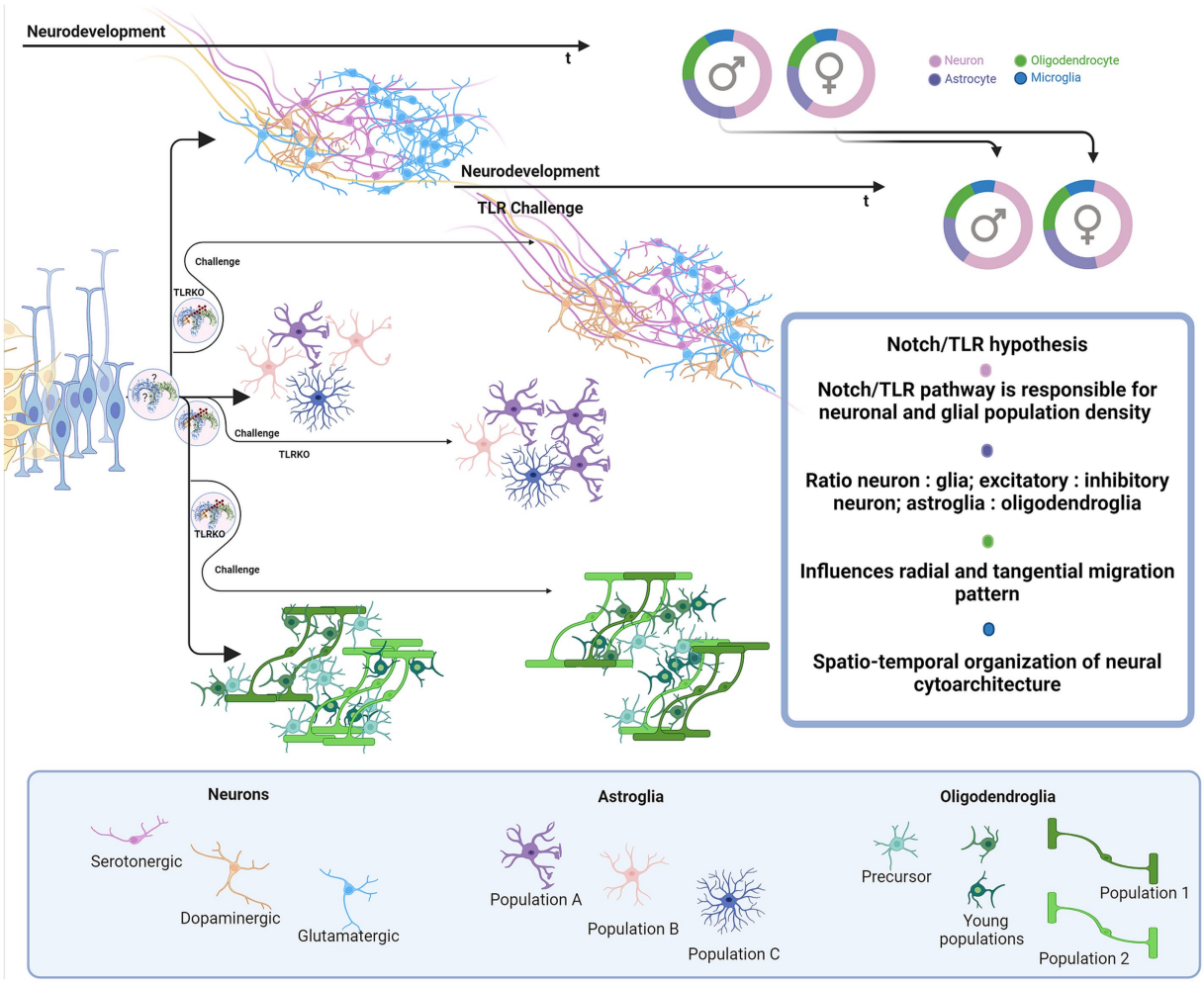

FIGURE 6
Proposed impact of Notch/TLR system on neurodevelopment. Presuming that Notch/TLR system is responsible for cellular adaptation to various stimuli and subsequent formation of cellular identity, challenged TLR system could evolve different environmentally dictated phenotypes in a sex-dependent manner. Male and female neurophenotypes could be challenged to generate variations in density and identity of cellular populations which eventually influences on neural cytoarchitecture, circuitres and behavioral phenotypes. Created in BioRender. BioRender.com/d80v300.

these varieties, one would need to explore the immune response landscape by tracking TLRs involved in ED and address the influence on the ND counterpart pathway.

Multiple neurodivergent phenotypes and conditions are indicated to stem from environmental challenges during pregnancy and neonatal period of neurodevelopment and involve TLRs. For example, autism spectrum disorder (ASD) (Chung et al., 2021; Yu et al., 2023; Vacharasin et al., 2024), attention-deficit/hyperactivity disorder (ADHD) (Ganna et al., 2018; Kim et al., 2020), schizophrenia and neurodevelopmental disorders (NDDs) are associated with maternal immune activation (MIA)(Baghel et al., 2018; Baines et al., 2020; Talukdar et al., 2021; Anderson et al., 2022). In all mentioned NDDs, specific differences in total brain volume or volume of particular regions compared to controls have been documented by neuroimaging studies (Courchesne et al., 2001; Hyakkoku et al., 2010; Lukito et al., 2020; Li T. et al., 2022). Is it possible that these NDDs are associated with MIA disturbance of TLR-ND pathway? If the TLR challenge coincides with neurogenesis, depending on infectious agent and the spatio-temporal neurodevelopmental stage, there is a firm possibility that diversity in neuronal type and number is introduced. The number of neurons residing in specific brain regions (amygdala, hippocampus, cortex, cerebellum) or even sub-structural clusters, can vary, induce mosaicism, and build the potential for alterations of neuronal networks and connections. As described earlier, bacterial LPS induces neuronal overgrowth (Humann et al., 2016; Mann et al., 2023) and dsRNA silences proliferation (Yaddanapudi et al., 2011). Importantly, the essential role of TLR signaling in neurodevelopment is corroborated by a recent finding of the 16p11.2 deletion syndrome which has phenotypic features of ASD (Chung et al., 2021). One of the affected genes in the 16p11.2 deletion syndrome is coding for ERK1 protein (Pucilowska et al., 2015), a downstream element of the TLR cascade. In other words, ASD neurophenotypes may be exacerbated through inhibition of TLR cascade. Viral and bacterial coinfection effects on the TLR2/4 and TLR3 systems probably participate in molecular events underlying an ASD-described increase and decrease in the volume of particular regions. Persistence and duration of

infection could be attributed to the range of ASD phenotypic diversity in individuals.

On the other hand, TLR3 inhibition by viral dsRNA could lower proliferation and neurogenesis capacity which may be associated with decreased number of neurons, atypical cellular density and changed brain volumes in ADHD and schizophrenia. Further, in challenging periods that coincide with neuronal outgrowth and branching involving the TLR7/8/9 system, neurons may shape unusual connections resulting in differential synaptic landscape formation and neural circuitries. The same applies to gliogenesis - if progenitor pool potential is disturbed, the fate of oligodendrocytes and astrocytes can change, and individuals become susceptible to various pathological processes.

When elaborating neuroimmunity in the context of TLRs actions, we should also consider infections caused by the herpes virus family, Epstein–Barr (EBV) and herpes simplex (HSV) virus, and related pathologies, multiple sclerosis (MS) (Hernández-Pedro et al., 2013; Baecher-Allan et al., 2018) and Alzheimer's disease (AD) (Landreth and Reed-Geaghan, 2009; Cameron and Landreth, 2010). Pathogenesis of MS involves innate and adaptive immunity responses related to demyelination, neuronal loss, and lesion formation (Hernández-Pedro et al., 2013). Potential role of TLRs in MS pathogenesis may be related to viral microRNA. Namely, it has been shown that HSV and EBV regulate immune answer and viral life cycle via viral microRNA-filled extracellular vesicles (Forte and Luftig, 2011; Kim et al., 2017; Wang et al., 2018; Cone et al., 2019). EBV infection in adolescence and later life could affect the pool of brain-residing progenitor cells involving the EBV infected cells release of microRNA, exhibiting immune-and viral cycle-regulating properties (Forte and Luftig, 2011; Wang et al., 2018). It is possible that distinct microRNA, circulating via extracellular vesicles, is taken by OPC and NPC. Once in cells, it could be that microRNAs doublestranded harpins bind TLR3 and dysregulate its activity causing the loss of TLR3 information. This drives progenitor cells to premature differentiation (Yaddanapudi et al., 2011; Bsibsi et al., 2012), apoptosis, and lower plastic ability. The myelinating oligodendrocyte has to be in contact with the neuron, astrocyte, progenitor, and immune cell to successfully fullfill its duty to become a new oligodendrocyte and if not, it is non-invasively removed by microglia (Berghoff et al., 2021). If there is a lack of Notch input due to TLR3 inhibition following a viral infection, the dying OPC/oligodendrocyte identity may be obscured and astrocytes and microglia could mistake it for an invading agent. The resulting innate immunity response might instruct adaptive immunity to attack specific subgroups of oligodendrocytes. We suggest that as adaptive immunity attacks myelin, dying cells produce other TLR ligands (particularly ligands of the TLR2 and TLR4, previously shown to affect regulation of oligodendrocyte life-cycle)(Church et al., 2016; Sanchez-Petidier et al., 2022; Brandt et al., 2023) which continue to disrupt homeostasis, leading to loss of neuronal networks integrity and emergence of MS symptoms as an autoimmune condition. Similarly, sporadic AD is frequent in individuals infected with HSV. The reoccurring infection could be detrimental to the hippocampal progenitor cell pool (Walker et al., 2018) and compromise astrocyte-dependent neuron identity and homeostasis by releasing TLR2 and TLR9 ligands (Lima et al., 2010; Zolini et al., 2014). Interestingly, utilizing a molecular visualization tool, we have observed probable processing of amyloid-precursor protein (APP) similarly to Notch: α-secretase cleavage releases the extracellular domain with two distinct structural motifs. APP E2 domain resembles TLR5 ligand flagellin and functions in *cis*- and *trans*-ligation (Rossjohn et al., 1999; Barnham et al., 2003; Wang and Ha, 2004). The extracellular part of APP has many similarities with the Notch/J/D complex, and APP presence is confirmed in dimers with Notch (Di Chen et al., 2006) (Figure 4B2a). Is it possible that APP is one of the natural Notch and TLR ligands, and its ligation and shedding give information about cellular environment and condition of neurons, resulting with growth and repair? Astrocytes seem to be most affected by miscommunication and may play an essential role in bridging the connection between neurons, oligodendrocytes, and microglia (Krasowska-Zoladek et al., 2007; Guerrero-García, 2020; Werkman et al., 2020; Wang et al., 2021). MS and AD-like pathologies have been previously considered in the context of viral infections, however, taking into account TLR signaling may shed light on events which include cellular response to environmental cues leading to disruption in developing and homeostatic pathways.

Brain tissue damage and injuries are cellular environment-changing events that also affect the microglial TLR system and influence the presumed TLR-ND cellular response. TLR is implicated as an essential player in traumatic injuries, tissue damage, and repair, and its many immunity-related roles in responding to tissue damage have been resolved by studies in genetically modified mouse models with TLR deficiency (Zhang et al., 2011; Ishizuka et al., 2013; Winters et al., 2013; Church et al., 2016; Gorup et al., 2019; Wasko et al., 2019; Polsek et al., 2020). The cellular environment in brain injury becomes saturated with DAMPs, and binding events affect the microglial TLR system, influencing TLR-ND cellular communication (Shi et al., 2013). TLR2 and TLR4 influence post-injury cellular recruitment and axonal tissue regeneration potency (Winters et al., 2013; Gorup et al., 2019). Lack of TLR2 is shown to protect the brain from immune invasion and has a poor prognosis in injury repair and tissue regeneration (Gorup et al., 2019). TLR4 activation/inhibition, on the other hand, has regenerative quality, and aids OPC recruitment and axon remyelination (Schonberg et al., 2007). The basic cellular load of mRNA coding for TLR2-engaged downstream scaffold proteins is differential in TLR2KO mice; an increase in load of IRAK1, IRAK4, IKKβ, and IL-6 and a decrease in IRAK3 has been observed (Winters et al., 2013). Since increased neuronal numbers are a phenotypical trait, we can assume that IRAK1, IRAK4, and IKKβ echo neuronal identity metabolism. At the same time, the observed IL-6 increase could be a constant signal for OPC premature maturation and apoptosis, lowering OPC regenerative capacity.

Finally, TLR and Notch signaling pathways may interfere with modeling and functional effects of hormones during sex-dependent differentiation of the brain. Since the presented data suggests that the Notch-TLR pathway is involved in the formation of cellular identity during neurodevelopment, we could make another intriguing assumption as to whether the building up of individual sex-related behavioral (psychological) patterns depends on the same signaling system, activated in response to myriads of environmental stimuli (Figure 6). Certainly, the resolving in more details the interplay of the environment with central cellular homeostatic and adaptive signaling pathways during neurodevelopment and brain maturation may substantially broaden our understanding of sex-related differences of clinical phenotypes reported for several neurodevelopmental, neurological and psychiatric disorders (ASD, ADHD, schizophrenia,

MS, AD) (Krementsov et al., 2014; Carney, 2019; Lins et al., 2019; Hui et al., 2020; Merikangas and Almasy, 2020; Dunstan et al., 2024).

7 Conclusion

We proposed a theoretical framework backed up by preliminary modelling of structural and functional assembly of TLRs and Notch which enables highly coordinated actions of both signaling pathways crucial for intercellular communication and cellular adaptation to environment. We point out so far underappreciated roles of TLRs in neurodevelopment and describe striking functional similarities of TLRs and Notch signaling during embryonic and postnatal brain development. Several possible interactions of TLRs and Notch are introduced and evidenced by preliminary analysis of visualized molecular structures which speaks in favor of the hypothesized intriguing cooperation of Notch and specific TLR isoforms in signal-sending and signal-receiving cellular milieu. We expect that a pilot supportive evidence for here presented hypothesis may provide sound basis for revisiting current viewpoints about interplay of TLR and Notch signaling. Future experimental studies, by including some of our proposed approaches, should better delineate the likely fundamental molecular Notch-TLR interactions which in the nervous system may underlie formation of cellular identity, cytoarchitecture, neural circuitries and diverse neurobehavioral phenotypes.

Data availability statement

The original contributions presented in the study are included in the article/supplementary material, further inquiries can be directed to the corresponding authors.

Author contributions

MS: Conceptualization, Data curation, Investigation, Visualization, Writing – original draft, Writing – review & editing, Methodology, Validation. SK-B: Conceptualization, Funding acquisition, Supervision, Validation, Writing – original draft, Writing – review & editing.

Funding

The author(s) declare that financial support was received for the research, authorship, and/or publication of this article. This work was supported by research project funded by the Croatian Science Foundation grant NeuroReact, IP-2016-06-8636 (to SKB), University of Zagreb support grant, 1123025 (to SKB) and European Union through the European Regional Development Fund, Operational Programme "Competitiveness and Cohesion 2014–2020", grant agreement no. KK.01.1.1.02.0015.

Acknowledgments

Authors express their gratitude to Kristina Mlinac-Jerković and Katarina Ilić, for continuous inspiring discussions, brain-stormings, detail-oriented and playfull scientific imagination which greatly contributed to integration of ideas resulting with this works. Authors also deeply appreciate encouragement, the critical reading and insightful comments by Ivana Rosenzweig and Dinko Mitrečić who made crucial influence on the final version of the manuscript. Figures were created with Biorender.com (CC-BY license issued by BioRender).

Conflict of interest

The authors declare that the research was conducted in the absence of any commercial or financial relationships that could be construed as a potential conflict of interest.

Publisher's note

References

Abdul, Y., Abdelsaid, M., Li, W., Webb, R. C., Sullivan, J. C., Dong, G., et al. (2019). Inhibition of toll-like Receptor-4 (TLR-4) improves neurobehavioral outcomes after acute ischemic stroke in diabetic rats: possible role of vascular endothelial TLR-4. *Mol. Neurobiol.* 56, 1607–1617. doi: 10.1007/s12035-018-1184-8

Akai, J., Halley, P. A., and Storey, K. G. (2005). FGF-dependent notch signaling maintains the spinal cord stem zone. *Genes Dev.* 19, 2877–2887. doi: 10.1101/gad.357705

Akashi-Takamura, S., and Miyake, K. (2008). TLR accessory molecules. *Curr. Opin. Immunol.* 20, 420–425. doi: 10.1016/j.coi.2008.07.001

Asafen, H.Al, Bandodkar, P. U., Carrell-Noel, S., Schloop, A. E., Friedman, J., and Reeves, G. T. (2020). Robustness of the dorsal morphogen gradient with respect to morphogen dosage. *PLoS Comput. Biol.* 16, e1007750–e1007721. doi: 10.1371/journal.pcbi.1007750

Anderson, R. C., O'Keeffe, G. W., and McDermott, K. W. (2022). Characterisation of the consequences of maternal immune activation on distinct cell populations in the developing rat spinal cord. *J. Anat.* 241, 938–950. doi: 10.1111/joa.13726

Anthoney, N., Foldi, I., and Hidalgo, A. (2018). Toll and toll-like receptor signalling in development. *Devleopment* 145, 1–6. doi: 10.1242/dev.156018

Anthony, T. E., Mason, H. A., Gridley, T., Fishell, G., and Heintz, N. (2005). Brain lipid-binding protein is a direct target of notch signaling in radial glial cells. *Genes Dev.* 19, 1028–1033. doi: 10.1101/gad.1302105

Arzate, D. M., Valencia, C., Dimas, M. A., Antonio-Cabrera, E., Domínguez-Salazar, E., Guerrero-Flores, G., et al. (2022). Dll1 haploinsufficiency causes brain abnormalities with functional relevance. *Front. Neurosci.* 16, 1–19. doi: 10.3389/fnins.2022.951418

Baecher-Allan, C., Kaskow, B. J., and Weiner, H. L. (2018). Multiple sclerosis: mechanisms and immunotherapy. *Neuron* 97, 742–768. doi: 10.1016/j.neuron.2018.01.021

Baghel, M. S., Singh, B., Dhuriya, Y. K., Shukla, R. K., Patro, N., Khanna, V. K., et al. (2018). Postnatal exposure to poly (I:C) impairs learning and memory through changes in synaptic plasticity gene expression in developing rat brain. *Neurobiol. Learn. Mem.* 155, 379–389. doi: 10.1016/j.nlm.2018.09.005

Baines, K. J., Hillier, D. M., Haddad, F. L., Rajakumar, N., Schmid, S., and Renaud, S. J. (2020). Maternal immune activation alters fetal brain development and enhances proliferation of neural precursor cells in rats. *Front. Immunol.* 11:1145. doi: 10.3389/fimmu.2020.01145

Barak, B., Feldman, N., and Okun, E. (2014). Toll-like receptors as developmental tools that regulate neurogenesis during development: an update. *Front. Neurosci.* 8, 1–6. doi: 10.3389/fnins.2014.00272

Barnham, K. J., McKinstry, W. J., Multhaup, G., Galatis, D., Morton, C. J., Curtain, C. C., et al. (2003). Structure of the Alzheimer's disease amyloid precursor protein copper binding domain. A regulator of neuronal copper homeostasis. *J. Biol. Chem.* 278, 17401–17407. doi: 10.1074/jbc.M300629200

Berghoff, S. A., Spieth, L., Sun, T., Hosang, L., Schlaphoff, L., Depp, C., et al. (2021). Microglia facilitate repair of demyelinated lesions via post-squalene sterol synthesis. *Nat. Neurosci.* 24, 47–60. doi: 10.1038/s41593-020-00757-6

Beutler, B., and Rehli, M. (2002). Evolution of the TIR, tolls and TLRs: functional inferences from computational biology. *Curr. Top. Microbiol. Immunol.* 270, 1–21. doi: 10.1007/978-3-642-59430-4_1

Blackwood, C. A., Bailetti, A., Nandi, S., Gridley, T., and Hébert, J. M. (2020). Notch dosage: Jagged1 Haploinsufficiency is associated with reduced neuronal division and disruption of Periglomerular interneurons in mice. *Front. Cell Dev. Biol.* 8, 1–14. doi: 10.3389/fcell.2020.00113

Bork, P., Downing, A. K., Kieffer, B., and Campbell, I. D. (1996). Structure and distribution of modules in extracellular proteins. *Q. Rev. Biophys.* 29, 119–167. doi: 10.1017/s0033583500005783

Botos, I., Liu, L., Wang, Y., Segal, D. M., and Davies, D. R. (2009). The toll-like receptor 3:dsRNA signaling complex. *Biochim. Biophys. Acta Gene Regul. Mech.* 1789, 667–674. doi: 10.1016/j.bbagrm.2009.06.005

Botos, I., Segal, D. M., and Davies, D. R. (2011). The structural biology of toll-like receptors. *Structure* 19, 447–459. doi: 10.1016/j.str.2011.02.004

Brandt, A., Kromm, F., Hernández-Arriaga, A., Martínez Sánchez, I., Bozkir, H. Ö., Staltner, R., et al. (2023). Cognitive alterations in old mice are associated with intestinal barrier dysfunction and induced toll-like receptor 2 and 4 signaling in different brain regions. *Cells* 12:2153. doi: 10.3390/cells12172153

Brennan, J. J., and Gilmore, T. D. (2018). Evolutionary origins of toll-like receptor signaling. *Mol. Biol. Evol.* 35, 1576–1587. doi: 10.1093/molbev/msy050

Breunig, J. J., Silbereis, J., Vaccarino, F. M., Šestan, N., and Rakic, P. (2007). Notch regulates cell fate and dendrite morphology of newborn neurons in the postnatal dentate gyrus. *Proc. Natl. Acad. Sci. USA* 104, 20558–20563. doi: 10.1073/pnas.0710156104

Brou, C., Logeat, F., Gupta, N., Bessia, C., LeBail, O., Doedens, J. R., et al. (2000). A novel proteolytic cleavage involved in notch signaling: the role of the disintegrin-metalloprotease TACE. *Mol. Cell* 5, 207–216. doi: 10.1016/S1097-2765(00)80417-7

Bsibsi, M., Nomden, A., van Noort, J. M., and Baron, W. (2012). Toll-like receptors 2 and 3 agonists differentially affect oligodendrocyte survival, differentiation, and myelin membrane formation. *J. Neurosci. Res.* 90, 388–398. doi: 10.1002/jnr.22767

Bsibsi, M., Ravid, R., Gveric, D., and Van Noort, J. M. (2002). Broad expression of toll-like receptors in the human central nervous system. *J. Neuropathol. Exp. Neurol.* 61, 1013–1021. doi: 10.1093/jnen/61.11.1013

Cameron, J. S., Alexopoulou, L., Sloane, J. A., DiBernardo, A. B., Ma, Y., Kosaras, B., et al. (2007). Toll-like receptor 3 is a potent negative regulator of axonal growth in mammals. *J. Neurosci.* 27, 13033–13041. doi: 10.1523/JNEUROSCI.4290-06.2007

Cameron, B., and Landreth, G. E. (2010). Inflammation, microglia, and alzheimer's disease. *Neurobiol. Dis.* 37, 503–509. doi: 10.1016/j.nbd.2009.10.006

Carney, R. S. E. (2019). Does prenatal exposure to maternal inflammation causes sex differences in schizophrenia-related behavioral outcomes in adult rats? *eNeuro* 6:ENEURO.0393–19.2019. doi: 10.1523/ENEURO.0393-19.2019

Casas Gimeno, G., and Paridaen, J. T. M. L. (2022). The symmetry of neural stem cell and progenitor divisions in the vertebrate brain. *Front. Cell Dev. Biol.* 10:885269. doi: 10.3389/fcell.2022.885269

Chen, Y., Lin, J., Zhao, Y., Ma, X., and Yi, H. (2021). Toll-like receptor 3 (TLR3) regulation mechanisms and roles in antiviral innate immune responses. *J. Zhejiang Univ. B* 22, 609–632. doi: 10.1631/jzus.B2000808

Chen, J., Moloney, D. J., and Stanley, P. (2001). Fringe modulation of Jagged1-induced notch signaling requires the action of β4galactosyltransferase-1. *Proc. Natl. Acad. Sci. USA* 98, 13716–13721. doi: 10.1073/pnas.241398098

Chen, C. Y., Shih, Y. C., Hung, Y. F., and Hsueh, Y. P. (2019). Beyond defense: regulation of neuronal morphogenesis and brain functions via toll-like receptors. *J. Biomed. Sci.* 26, 90–13. doi: 10.1186/s12929-019-0584-z

Chillakuri, C. R., Sheppard, D., Ilagan, M. X. G., Holt, L. R., Abbott, F., Liang, S., et al. (2013). Structural analysis uncovers lipid-binding properties of notch ligands. *Cell Rep.* 5, 861–867. doi: 10.1016/j.celrep.2013.10.029

Choe, J., Kelker, M. S., and Wilson, I. A. (2005). Structural biology: crystal structure of human toll-like receptor 3 (TLR3) ectodomain. *Science* 309, 581–585. doi: 10.1126/science.1115253

Chung, W. K., Roberts, T. P., Sherr, E. H., Snyder, L. A. G., and Spiro, J. E. (2021). 16P11.2 Deletion Syndrome. *Curr. Opin. Genet. Dev.* 68, 49–56. doi: 10.1016/j.gde.2021.01.011

Church, J. S., Kigerl, K. A., Lerch, J. K., Popovich, P. G., and McTigue, D. M. (2016). TLR4 deficiency impairs oligodendrocyte formation in the injured spinal cord. *J. Neurosci.* 36, 6352–6364. doi: 10.1523/JNEUROSCI.0353-16.2016

Cone, A. S., York, S. B., and Meckes, D. G. (2019). Extracellular Vesicles in Epstein-Barr Virus Pathogenesis. *Curr. Clin. Microbiol. Rep.* 6, 121–131. doi: 10.1007/s40588-019-00123-6

Cordle, J., Johnson, S., Zi Yan Tay, J., Roversi, P., Wilkin, M. B., de Madrid, B. H., et al. (2008a). A conserved face of the jagged/serrate DSL domain is involved in notch trans-activation and cis-inhibition. *Nat. Struct. Mol. Biol.* 15, 849–857. doi: 10.1038/nsmb.1457

Cordle, J., Redfield, C., Stacey, M., Van Der Merwe, P. A., Willis, A. C., Champion, B. R., et al. (2008b). Localization of the delta-like-1-binding site in human Notch-1 and its modulation by calcium affinity. *J. Biol. Chem.* 283, 11785–11793. doi: 10.1074/jbc.M708424200

Courchesne, E., Karns, C. M., Davis, H. R., Ziccardi, R., Carper, R. A., Tigue, Z. D., et al. (2001). Unusual brain growth patterns in early life in patients with autistic disorder: an MRI study. *Neurology* 57, 245–254. doi: 10.1212/WNL.57.2.245

Crack, P. J., and Bray, P. J. (2007). Toll-like receptors in the brain and their potential roles in neuropathology. *Immunol. Cell Biol.* 85, 476–480. doi: 10.1038/sj.icb.7100103

D'Souza, B., Meloty-Kapella, L., and Weinmaster, G. (2010). Canonical and non-canonical notch ligands. *Curr. Top. Dev. Biol.* 92, 73–129. doi: 10.1016/S0070-2153(10)92003-6

Chen, C.Di, Oh, S. Y., Hinman, J. D., and Abraham, C. R. (2006). Visualization of APP dimerization and APP-Notch2 heterodimerization in living cells using bimolecular fluorescence complementation. *J. Neurochem.* 97, 30–43. doi: 10.1111/j.1471-4159.2006.03705.x

Dunstan, I. K., McLeod, R., Radford-Smith, D. E., Xiong, W., Pate, T., Probert, F., et al. (2024). Unique pathways downstream of TLR-4 and TLR-7 activation: sex-dependent behavioural, cytokine, and metabolic consequences. *Front. Cell. Neurosci.* 18:1345441. doi: 10.3389/fncel.2024.1345441

Enkhbayar, P., Kamiya, M., Osaki, M., Matsumoto, T., and Matsushima, N. (2004). Structural principles of leucine-rich repeat (LRR) proteins. *Proteins Struct. Funct. Genet.* 54, 394–403. doi: 10.1002/prot.10605

Fernandez-Lizarbe, S., Montesinos, J., and Guerri, C. (2013). Ethanol induces TLR4/TLR2 association, triggering an inflammatory response in microglial cells. *J. Neurochem.* 126, 261–273. doi: 10.1111/jnc.12276

Fiúza, U. M., and Arias, A. M. (2007). Cell and molecular biology of notch. *J. Endocrinol.* 194, 459–474. doi: 10.1677/JOE-07-0242

Foldi, J., Chung, A. Y., Xu, H., Zhu, J., Outtz, H. H., Kitajewski, J., et al. (2010). Autoamplification of notch signaling in macrophages by TLR-induced and RBP-J–dependent induction of Jagged1. *J. Immunol.* 185, 5023–5031. doi: 10.4049/jimmunol.1001544

Forte, E., and Luftig, M. A. (2011). The role of microRNAs in Epstein-Barr virus latency and lytic reactivation. *Microbes Infect.* 13, 1156–1167. doi: 10.1016/j.micinf.2011.07.007

Franklin, J. L., Berechid, B. E., Cutting, F. B., Presente, A., Chambers, C. B., Foltz, D. R., et al. (1999). Autonomous and non-autonomous regulation of mammalian neurite development by Notch1 and Delta1. *Curr. Biol.* 9, 1448–1457. doi: 10.1016/S0960-9822(00)80114-1

Frantz, S., Kelly, R. A., and Bourcier, T. (2001). Role of TLR-2 in the activation of nuclear factor κB by oxidative stress in cardiac myocytes. *J. Biol. Chem.* 276, 5197–5203. doi: 10.1074/jbc.M009160200

Gaiano, N., and Fishell, G. (2002). The role of notch in promoting glial and neural stem cell fates. *Annu. Rev. Neurosci.* 25, 471–490. doi: 10.1146/annurev.neuro.25.030702.130823

Galleguillos, D., Wang, Q., Steinberg, N., Zaidi, A., Shrivastava, G., Dhami, K., et al. (2022). Anti-inflammatory role of GM1 and other gangliosides on microglia. *J. Neuroinflammation* 19:9. doi: 10.1186/s12974-021-02374-x

Ganna, A., Satterstrom, F. K., Zekavat, S. M., Das, I., Kurki, M. I., Churchhouse, C., et al. (2018). Quantifying the impact of rare and ultra-rare coding variation across the phenotypic Spectrum. *Am. J. Hum. Genet.* 102, 1204–1211. doi: 10.1016/j.ajhg.2018.05.002

Ge, B., Gram, H., Di Padova, F., Huang, B., New, L., Ulevitch, R. J., et al. (2002). MAPKK-independent activation of p38α mediated by TAB1-dependent autophosphorylation of p38α. *Science* 295, 1291–1294. doi: 10.1126/science.1067289

Giniger, E., Jan, L. Y., and Jan, Y. N. (1993). Specifying the path of the intersegmental nerve of the Drosophila embryo: a role for Delta and notch. *Development* 117, 431–440. doi: 10.1242/dev.117.2.431

Gioannini, T. L., Teghanemt, A., Zhang, D., Coussens, N. P., Dockstader, W., Ramaswamy, S., et al. (2004). Isolation of an endotoxin–MD-2 complex that produces toll-like receptor 4-dependent cell activation at picomolar concentrations. *Proc. Natl. Acad. Sci.* 101, 4186–4191. doi: 10.1073/pnas.0306906101

Gordon, W. R., Vardar-Ulu, D., Histen, G., Sanchez-Irizarry, C., Aster, J. C., and Blacklow, S. C. (2007). Structural basis for autoinhibition of notch. *Nat. Struct. Mol. Biol.* 14, 295–300. doi: 10.1038/nsmb1227

Gorup, D., Škokić, S., Kriz, J., and Gajović, S. (2019). Tlr2 deficiency is associated with enhanced elements of neuronal repair and caspase 3 activation following brain ischemia. *Sci. Rep.* 9, 2821–2810. doi: 10.1038/s41598-019-39541-3

Gosu, V., Son, S., Shin, D., and Song, K. D. (2019). Insights into the dynamic nature of the dsRNA-bound TLR3 complex. *Sci. Rep.* 9, 3652–3614. doi: 10.1038/s41598-019-39984-8

Gozlan, O., and Sprinzak, D. (2023). Notch signaling in development and homeostasis. *Development* 150, 1–4. doi: 10.1242/dev.201138

Guerrero-García, J. J. (2020). The role of astrocytes in multiple sclerosis pathogenesis. *Neurologia* 35, 400–408. doi: 10.1016/j.nrl.2017.07.021

Hamel, S., Fantini, J., and Schweisguth, F. (2010). Notch ligand activity is modulated by glycosphingolipid membrane composition in *Drosophila melanogaster*. *J. Cell Biol.* 188, 581–594. doi: 10.1083/jcb.200907116

Hamidi, S., Schäfer-Korting, M., and Weindl, G. (2014). TLR2/1 and sphingosine 1-phosphate modulate inflammation, myofibroblast differentiation and cell migration in fibroblasts. *Biochim. Biophys. Acta Mol. Cell Biol. Lipids* 1841, 484–494. doi: 10.1016/j.bbalip.2014.01.008

Handford, P. A., Korona, B., Suckling, R., Redfield, C., and Lea, S. M. (2018). Structural insights into notch receptor-ligand interactions. *Adv. Exp. Med. Biol.* 1066, 33–46. doi: 10.1007/978-3-319-89512-3_2

Hernández-Pedro, N. Y., Espinosa-Ramirez, G., De La Cruz, V. P., Pineda, B., and Sotelo, J. (2013). Initial immunopathogenesis of multiple sclerosis: innate immune response. *Clin. Dev. Immunol.* 2013, 1–15. doi: 10.1155/2013/413465

Hiraoka, Y., Komine, O., Nagaoka, M., Bai, N., Hozumi, K., and Tanaka, K. (2013). Delta-like 1 regulates Bergmann glial monolayer formation during cerebellar development. *Mol. Brain* 6:1. doi: 10.1186/1756-6606-6-25

Hu, X., Chung, A. Y., Wu, I., Foldi, J., Chen, J., Ji, J. D., et al. (2008). Integrated regulation of toll-like receptor responses by notch and interferon-γ pathways. *Immunity* 29, 691–703. doi: 10.1016/j.immuni.2008.08.016

Hui, C. W., Vecchiarelli, H. A., Gervais, É., Luo, X., Michaud, F., Scheefhals, L., et al. (2020). Sex differences of microglia and synapses in the hippocampal dentate gyrus of adult mouse offspring exposed to maternal immune activation. *Front. Cell. Neurosci.* 14, 1–12. doi: 10.3389/fncel.2020.558181

Humann, J., Mann, B., Gao, G., Moresco, P., Ramahi, J., Loh, L. N., et al. (2016). Bacterial peptidoglycan traverses the placenta to induce fetal Neuroproliferation and aberrant postnatal behavior. *Cell Host Microbe* 19, 388–399. doi: 10.1016/j.chom.2016.02.009

Hyakkoku, K., Hamanaka, J., Tsuruma, K., Shimazawa, M., Tanaka, H., Uematsu, S., et al. (2010). Toll-like receptor 4 (TLR4), but not TLR3 or TLR9, knock-out mice have neuroprotective effects against focal cerebral ischemia. *Neuroscience* 171, 258–267. doi: 10.1016/j.neuroscience.2010.08.054

Ikegami, A., Haruwaka, K., and Wake, H. (2019). Microglia: lifelong modulator of neural circuits. *Neuropathology* 39, 173–180. doi: 10.1111/neup.12560

Irvin, D. K., Nakano, I., Paucar, A., and Kornblum, H. I. (2004). Patterns of Jagged1, Jagged2, Delta-like 1 and Delta-like 3 expression during late embryonic and postnatal brain development suggest multiple functional roles in progenitors and differentiated cells. *J. Neurosci. Res.* 75, 330–343. doi: 10.1002/jnr.10843

Irvin, D. K., Zurcher, S. D., Nguyen, T., Weinmaster, G., and Kornblum, H. I. (2001). Expression patterns of Notch1, Notch2, and Notch3 suggest multiple functional roles for the notch-DSL signaling system during brain development. *J. Comp. Neurol.* 436, 167–181. doi: 10.1002/cne.1059

Ishizuka, F., Shimazawa, M., Inoue, Y., Nakano, Y., Ogishima, H., Nakamura, S., et al. (2013). Toll-like receptor 4 mediates retinal ischemia/reperfusion injury through nuclear factor-κB and spleen tyrosine kinase activation. *Investig. Ophthalmol. Vis. Sci.* 54, 5807–5816. doi: 10.1167/iovs.13-11932

Jack, C. S., Arbour, N., Manusow, J., Montgrain, V., Blain, M., Mccrea, E., et al. (2019). TLR signaling tailors innate immune responses in human microglia and astrocytes. *J. Immunol.* 175, 4320–4330. doi: 10.4049/jimmunol.175.7.4320

Jacobs, C. T., and Huang, P. (2019). Notch signalling maintains hedgehog responsiveness via a gli-dependent mechanism during spinal cord patterning in zebrafish. *eLife* 8, 1–24. doi: 10.7554/eLife.49252

Jacobs, C. T., and Huang, P. (2021). Complex crosstalk of notch and hedgehog signalling during the development of the central nervous system. *Cell. Mol. Life Sci.* 78, 635–644. doi: 10.1007/s00018-020-03627-3

Jin, M. S., Kim, S. E., Heo, J. Y., Lee, M. E., Kim, H. M., Paik, S. G., et al. (2007). Crystal structure of the TLR1-TLR2 heterodimer induced by binding of a tri-Acylated Lipopeptide. *Cell* 130, 1071–1082. doi: 10.1016/j.cell.2007.09.008

Jin, M., Zhang, H., Xu, B., Li, Y., Qin, H., Yu, S., et al. (2023). Jag2b-Notch3 /1b-mediated neuron-to-glia crosstalk controls retinal gliogenesis. *EMBO Rep.* 24:e57072. doi: 10.15252/embr.202357072

Johnson, G. L., and Lapadat, R. (2002). Mitogen-activated protein kinase pathways mediated by ERK, JNK, and p38 protein kinases. *Science* 298, 1911–1912. doi: 10.1126/science.1072682

Kageyama, R., and Ohtsuka, T. (1999). The notch-Hes pathway in mammalian neural development. *Cell Res.* 9, 179–188. doi: 10.1038/sj.cr.7290016

Kageyama, R., Ohtsuka, T., Shimojo, H., and Imayoshi, I. (2009). Dynamic regulation of notch signaling in neural progenitor cells. *Curr. Opin. Cell Biol.* 21, 733–740. doi: 10.1016/j.ceb.2009.08.009

Kang, J. Y., Nan, X., Jin, M. S., Youn, S. J., Ryu, Y. H., Mah, S., et al. (2009). Recognition of Lipopeptide patterns by toll-like receptor 2-toll-like receptor 6 heterodimer. *Immunity* 31, 873–884. doi: 10.1016/j.immuni.2009.09.018

Kawaguchi, D., Yoshimatsu, T., Hozumi, K., and Gotoh, Y. (2008). Selection of differentiating cells by different levels of delta-like 1 among neural precursor cells in the developing mouse telencephalon. *Development* 135, 3849–3858. doi: 10.1242/dev.024570

Keilani, S., and Sugaya, K. (2008). Reelin induces a radial glial phenotype in human neural progenitor cells by activation of Notch-1. *BMC Dev. Biol.* 8, 1–9. doi: 10.1186/1471-213X-8-69

Kelly, D. F., Lake, R. J., Middelkoop, T. C., Fan, H. Y., Artavanis-Tsakonas, S., and Walz, T. (2010). Molecular structure and dimeric organization of the notch extracellular domain as revealed by electron microscopy. *PLoS One* 5, 1–6. doi: 10.1371/journal.pone.0010532

Kim, J. I., Chang, J. L., Mi, S. J., Lee, C. H., Paik, S. G., Lee, H., et al. (2005). Crystal structure of CD14 and its implications for lipopolysaccharide signaling. *J. Biol. Chem.* 280, 11347–11351. doi: 10.1074/jbc.M414607200

Kim, Y. S., Choi, J., and Yoon, B. E. (2020). Neuron-glia interactions in neurodevelopmental disorders. *Cells* 9:176. doi: 10.3390/cells9102176

Kim, C., Ho, D. H., Suk, J. E., You, S., Michael, S., Kang, J., et al. (2013). Neuron-released oligomeric α-synuclein is an endogenous agonist of TLR2 for paracrine activation of microglia. *Nat. Commun.* 4:1562. doi: 10.1038/ncomms2534

Kim, H., Iizasa, H., Kanehiro, Y., Fekadu, S., and Yoshiyama, H. (2017). Herpesviral microRNAs in cellular metabolism and immune responses. *Front. Microbiol.* 8:1318. doi: 10.3389/fmicb.2017.01318

Kim, H. M., Park, B. S., Kim, J. I., Kim, S. E., Lee, J., Oh, S. C., et al. (2007). Crystal structure of the TLR4-MD-2 complex with bound endotoxin antagonist Eritoran. *Cell* 130, 906–917. doi: 10.1016/j.cell.2007.08.002

Kim, H., Shin, J., Kim, S., Poling, J., Park, H. C., and Appel, B. (2008). Notch-regulated oligodendrocyte specification from radial glia in the spinal cord of zebrafish embryos. *Dev. Dyn.* 237, 2081–2089. doi: 10.1002/dvdy.21620

Kobe, B., and Deisenhofer, J. (1994). The leucine-rich repeat: a versatile binding motif. *Trends Biochem. Sci.* 19, 415–421. doi: 10.1016/0968-0004(94)90090-6

Kobe, B., and Kajava, A. V. (2001). The leucine-rich repeat as a protein recognition motif. *Curr. Opin. Struct. Biol.* 11, 725–732. doi: 10.1016/S0959-440X(01)00266-4

Koymans, K. J., Feitsma, L. J., Brondijk, T. H. C., Aerts, P. C., Lukkien, E., Lössl, P., et al. (2015). Structural basis for inhibition of TLR2 by staphylococcal superantigen-like protein 3 (SSL3). *Proc. Natl. Acad. Sci.* 112, 11018–11023. doi: 10.1073/pnas.1502026112

Krasowska-Zoladek, A., Banaszewska, M., Kraszpulski, M., and Konat, G. W. (2007). Kinetics of inflammatory response of astrocytes induced by TLR 3 and TLR4 ligation. *J. Neurosci. Res.* 85, 205–212. doi: 10.1002/jnr.21088

Krementsov, D. N., Noubade, R., Dragon, J. A., Otsu, K., Rincon, M., and Teuscher, C. (2014). Sex-specific control of central nervous system autoimmunity by p38 mitogen-activated protein kinase signaling in myeloid cells. *Ann. Neurol.* 75, 50–66. doi: 10.1002/ana.24020

Kuzina, I., Song, J. K., and Giniger, E. (2011). How notch establishes longitudinal axon connections between successive segments of the Drosophila CNS. *Development* 138, 1839–1849. doi: 10.1242/dev.062471

Ladi, E., Nichols, J. T., Ge, W., Miyamoto, A., Yao, C., Yang, L. T., et al. (2005). The divergent DSL ligand Dll3 does not activate notch signaling but cell autonomously attenuates signaling induced by other DSL ligands. *J. Cell Biol.* 170, 983–992. doi: 10.1083/jcb.200503113

Lalancette-Hbert, M., Phaneuf, D., Soucy, G., Weng, Y. C., and Kriz, J. (2009). Live imaging of toll-like receptor 2 response in cerebral ischaemia reveals a role of olfactory bulb microglia as modulators of inflammation. *Brain* 132, 940–954. doi: 10.1093/brain/awn345

Landreth, G. E., and Reed-Geaghan, E. G. (2009). Toll-like receptors in Alzheimer's disease. *Curr. Top. Microbiol. Immunol.* 336, 137–153. doi: 10.1007/978-3-642-00549-7_8

Lathia, J. D., Okun, E., Tang, S. C., Griffioen, K., Cheng, A., Mughal, M. R., et al. (2008). Toll-like receptor 3 is a negative regulator of embryonic neural progenitor cell proliferation. *J. Neurosci.* 28, 13978–13984. doi: 10.1523/JNEUROSCI.2140-08.2008

Lee, H., Baek, J., Min, H., Cho, I. H., Yu, S. W., and Lee, S. J. (2017). Toll-like receptor 3 contributes to wallerian degeneration after peripheral nerve injury. *Neuroimmunomodulation* 23, 209–216. doi: 10.1159/000449134

Leemans, J. C., Weening, J. J., Florquin, S., Leemans, J. C., Stokman, G., Claessen, N., et al. (2005). Ischemia / reperfusion injury in the kidney find the latest version: renal-associated TLR2 mediates ischemia / reperfusion injury in the kidney. *J. Clin. Invest.* 115, 2894–2903. doi: 10.1172/JCI22832

Li, L., Acioglu, C., Heary, R. F., and Elkabes, S. (2021). Role of astroglial toll-like receptors (TLRs) in central nervous system infections, injury and neurodegenerative diseases. *Brain Behav. Immun.* 91, 740–755. doi: 10.1016/j.bbi.2020.10.007

Li, G., Forero, M. G., Wentzell, J., Durmus, I., Wolf, R., Anthoney, N., et al. (2020). A toll-receptor map underlies structural brain plasticity. *eLife* 9, 1–32. doi: 10.7554/eLife.52743

Li, T., Hoogman, M., Roth Mota, N., Buitelaar, J. K., Vasquez, A. A., Franke, B., et al. (2022). Dissecting the heterogeneous subcortical brain volume of autism spectrum disorder using community detection. *Autism Res.* 15, 42–55. doi: 10.1002/aur.2627

Li, C., Xie, Z., Xing, Z., Zhu, H., Zhou, W., Xie, S., et al. (2022). The notch signaling pathway regulates differentiation of NG2 cells into oligodendrocytes in demyelinating diseases. *Cell. Mol. Neurobiol.* 42, 1–11. doi: 10.1007/s10571-021-01089-0

Li, X., Yun, Z., Tan, Z., Li, S., Wang, D., Ma, K., et al. (2013). The role of toll-like receptor (TLR) 2 and 9 in renal ischemia and reperfusion injury. *Urology* 81, 1379. e15–1379.e20. doi: 10.1016/j.urology.2013.02.016

Lima, G. K., Zolini, G. P., Mansur, D. S., Lima, B. H. F., Wischhoff, U., Astigarraga, R. G., et al. (2010). Toll-like receptor (TLR) 2 and TLR9 expressed in trigeminal ganglia are critical to viral control during herpes simplex virus 1 infection. *Am. J. Pathol.* 177, 2433–2445. doi: 10.2353/ajpath.2010.100121

Lins, B. R., Marks, W. N., Zabder, N. K., Greba, Q., and Howland, J. G. (2019). Maternal immune activation during pregnancy alters the behavior profile of female offspring of Sprague dawley rats. *eNeuro* 6, ENEURO.0437–ENEU18.2019. doi: 10.1523/ENEURO.0437-18.2019

Liu, H. Y., Chen, C. Y., and Hsueh, Y. P. (2014). Innate immune responses regulate morphogenesis and degeneration: roles of toll-like receptors and Sarm1 in neurons. *Neurosci. Bull.* 30, 645–654. doi: 10.1007/s12264-014-1445-5

Liu, S., Liu, Y., Hao, W., Wolf, L., Kiliaan, A. J., Penke, B., et al. (2012). TLR2 is a primary receptor for Alzheimer's amyloid peptide to trigger Neuroinflammatory activation. *J. Immunol.* 188, 1098–1107. doi: 10.4049/jimmunol.1101121

Liu, G., Zhang, H., Zhao, C., and Zhang, H. (2019). Evolutionary history of the toll-like receptor gene family across vertebrates. *Genome Biol. Evol.* 12, 3615–3634. doi: 10.1093/gbe/evz266

Lovendahl, K. N., Blacklow, S. C., and Gordon, W. R. (2018). The molecular mechanism of notch activation. *Adv. Exp. Med. Biol.* 1066, 47–58. doi: 10.1007/978-3-319-89512-3_3

Luca, V. C., Jude, K. M., Pierce, N. W., Nachury, M. V., Fischer, S., and Garcia, K. C. (2015). Structural basis for Notch1 engagement of Delta-like 4. *Science* 347, 847–853. doi: 10.1126/science.1261093

Luca, V. C., Kim, B. C., Ge, C., Kakuda, S., Wu, D., Roein-Peikar, M., et al. (2017). Notch-jagged complex structure implicates a catch bond in tuning ligand sensitivity. *Science* 355, 1320–1324. doi: 10.1126/science.aaf9739

Lukito, S., Norman, L., Carlisi, C., Radua, J., Hart, H., Simonoff, E., et al. (2020). Comparative meta-analyses of brain structural and functional abnormalities during cognitive control in attention-deficit/hyperactivity disorder and autism spectrum disorder. *Psychol. Med.* 50, 894–919. doi: 10.1017/S0033291720000574

Ma, Y., Haynes, R. L., Sidman, R. L., and Vartanian, T. (2007). An innate immune receptor in brain, neurons and axons. *Cell Cycle* 6, 2859–2868. doi: 10.4161/cc.6.23.5018

Mann, B., Crawford, J. C., Reddy, K., Lott, J., Youn, Y. H., Gao, G., et al. (2023). Bacterial TLR2/6 ligands block Ciliogenesis, Derepress hedgehog signaling, and expand the neocortex. *MBio* 14, e0051023–e0051019. doi: 10.1128/mbio.00510-23

Marczenke, M., Sunaga-Franze, D. Y., Popp, O., Althaus, I. W., Sauer, S., Mertins, P., et al. (2021). GAS1 is required for NOTCH-dependent facilitation of SHH signaling in the ventral forebrain neuroepithelium. *Development* 148, 1–14. doi: 10.1242/dev.200080

Martínez-García, M. Á., Ojeda-Ojeda, M., Rodríguez-Martín, E., Insenser, M., Moncayo, S., Álvarez-Blasco, F., et al. (2020). TLR2 and TLR4 surface and gene expression in White blood cells after fasting and Oral glucose, lipid and protein challenges: influence of obesity and sex hormones. *Biomol. Ther.* 10:111. doi: 10.3390/biom10010111

Mase, S., Shitamukai, A., Wu, Q., Morimoto, M., Gridley, T., and Matsuzaki, F. (2021). Notch1 and Notch2 collaboratively maintain radial glial cells in mouse neurogenesis. *Neurosci. Res.* 170, 122–132. doi: 10.1016/j.neures.2020.11.007

Matsumura, T., Degawa, T., Takii, T., Hayashi, H., Okamoto, T., Inoue, J. I., et al. (2003). TRAF6-NF-κB pathway is essential for interleukin-1-induced TLR2 expression and its functional response to TLR2 ligand in murine hepatocytes. *Immunology* 109, 127–136. doi: 10.1046/j.1365-2567.2003.01627.x

Mehmeti, M., Bergenfelz, C., Källberg, E., Millrud, C. R., Björk, P., Ivars, F., et al. (2019). Wnt5a is a TLR2/4-ligand that induces tolerance in human myeloid cells. *Commun. Biol.* 2, 176–113. doi: 10.1038/s42003-019-0432-4

Merikangas, A. K., and Almasy, L. (2020). Using the tools of genetic epidemiology to understand sex differences in neuropsychiatric disorders. *Genes Brain Behav.* 19, e12660–e12616. doi: 10.1111/gbb.12660

Miyamoto, A., Wake, H., Moorhouse, A. J., and Nabekura, J. (2013). Microglia and synapse interactions: fine tuning neural circuits and candidate molecules. *Front. Cell. Neurosci.* 7, 1–6. doi: 10.3389/fncel.2013.00070

Moloney, D. J., Panin, V. M., Johnston, S. H., Chen, J., Shao, L., Wilson, R., et al. (2000). Fringe is a glycosyltransferase that modifies notch. *Nature* 406, 369–375. doi: 10.1038/35019000

Mumm, J. S., Schroeter, E. H., Saxena, M. T., Griesemer, A., Tian, X., Pan, D. J., et al. (2000). A ligand-induced extracellular cleavage regulates γ-secretase-like proteolytic activation of Notch1. *Mol. Cell* 5, 197–206. doi: 10.1016/S1097-2765(00)80416-5

Musse, A. A., Meloty-Kapella, L., and Weinmaster, G. (2012). Notch ligand endocytosis: mechanistic basis of signaling activity. *Semin. Cell Dev. Biol.* 23, 429–436. doi: 10.1016/j.semcdb.2012.01.011

Namihira, M., Kohyama, J., Semi, K., Sanosaka, T., Deneen, B., Taga, T., et al. (2009). Committed neuronal precursors confer astrocytic potential on residual neural precursor cells. *Dev. Cell* 16, 245–255. doi: 10.1016/j.devcel.2008.12.014

Nichols, J. R., Aldrich, A. L., Mariani, M. M., Vidlak, D., Esen, N., and Kielian, T. (2009). TLR2 deficiency leads to increased Th17 infiltrates in experimental brain abscesses. *J. Immunol.* 182, 7119–7130. doi: 10.4049/jimmunol.0802656

Nichols, J. T., Miyamoto, A., Olsen, S. L., D'Souza, B., Yao, C., and Weinmaster, G. (2007). DSL ligand endocytosis physically dissociates Notch1 heterodimers before activating proteolysis can occur. *J. Cell Biol.* 176, 445–458. doi: 10.1083/jcb.200609014

Noordstra, I., and Yap, A. S. (2021). For whom the cell tolls. *Dev. Cell* 56, 1555–1557. doi: 10.1016/j.devcel.2021.05.013

Okubo, Y., Ohtake, F., Igarashi, K., Yasuhiko, Y., Hirabayashi, Y., Saga, Y., et al. (2021). Cleaved Delta like 1 intracellular domain regulates neural development via notch signal-dependent and-independent pathways. *Development* 148:664. doi: 10.1242/dev.193664

Okun, E., Griffioen, K. J., Gen Son, T., Lee, J. H., Roberts, N. J., Mughal, M. R., et al. (2010). TLR2 activation inhibits embryonic neural progenitor cell proliferation. *J. Neurochem.* 114, 462–474. doi: 10.1111/j.1471-4159.2010.06778.x

Okun, E., Griffioen, K. J., and Mattson, M. P. (2019). Toll-like receptor signaling in neural plasticity and disease. *Trends Neurosci.* 34, 269–281. doi: 10.1016/j.tins.2011.02.005

Okun, E., Griffioen, K. J., Rothman, S., Wan, R., Cong, W. N., De Cabo, R., et al. (2014). Toll-like receptors 2 and 4 modulate autonomic control of heart rate and energy metabolism. *Brain Behav. Immun.* 36, 90–100. doi: 10.1016/j.bbi.2013.10.013

Opitz, B., Schröder, N. W. J., Spreitzer, I., Michelsen, K. S., Kirschning, C. J., Hallatschek, W., et al. (2001). Toll-like Receptor-2 mediates Treponema glycolipid and Lipoteichoic acid-induced NF-κB translocation. *J. Biol. Chem.* 276, 22041–22047. doi: 10.1074/jbc.M010481200

Palaga, T., Buranaruk, C., Rengpipat, S., Fauq, A. H., Golde, T. E., Kaufmann, S. H. E., et al. (2008). Notch signaling is activated by TLR stimulation and regulates macrophage functions. *Eur. J. Immunol.* 38, 174–183. doi: 10.1002/eji.200636999

Park, C., Cho, I., Kim, D., Jo, E., Choi, S., Bae, S., et al. (2008). Toll-like receptor 2 contributes to glial cell activation and heme oxygenase-1 expression in traumatic brain injury. *Neurosci. Lett.* 431, 123–128. doi: 10.1016/j.neulet.2007.11.057

Park, B. S., and Lee, J. O. (2013). Recognition of lipopolysaccharide pattern by TLR4 complexes. *Exp. Mol. Med.* 45:e66. doi: 10.1038/emm.2013.97

Park, B. S., Song, D. H., Kim, H. M., Choi, B. S., Lee, H., and Lee, J. O. (2009). The structural basis of lipopolysaccharide recognition by the TLR4-MD-2 complex. *Nature* 458, 1191–1195. doi: 10.1038/nature07830

Parthier, C., Stelter, M., Ursel, C., Fandrich, U., Lilie, H., Breithaupt, C., et al. (2014). Structure of the toll-Spätzle complex, a molecular hub in Drosophila development and innate immunity. *Proc. Natl. Acad. Sci. USA* 111, 6281–6286. doi: 10.1073/pnas.1320678111

Patten, B. A., Peyrin, J. M., Weinmaster, G., and Corfas, G. (2003). Sequential signaling through Notch1 and erbB receptors mediates radial glia differentiation. *J. Neurosci.* 23, 6132–6140. doi: 10.1523/jneurosci.23-14-06132.2003

Patten, B. A., Sardi, S. P., Koirala, S., Nakafuku, M., and Corfas, G. (2006). Notch1 signaling regulates radial glia differentiation through multiple transcriptional mechanisms. *J. Neurosci.* 26, 3102–3108. doi: 10.1523/JNEUROSCI.4829-05.2006

Polsek, D., Cash, D., Veronese, M., Ilic, K., Wood, T. C., Milosevic, M., et al. (2020). The innate immune toll-like-receptor-2 modulates the depressogenic and anorexiolytic neuroinflammatory response in obstructive sleep apnoea. *Sci. Rep.* 10, 11475–11413. doi: 10.1038/s41598-020-68299-2

Pucilowska, J., Vithayathil, J., Tavares, E. J., Kelly, C., Colleen Karlo, J., and Landreth, G. E. (2015). The 16p11.2 deletion mouse model of autism exhibits altered cortical progenitor proliferation and brain cytoarchitecture linked to the ERK MAPK pathway. *J. Neurosci.* 35, 3190–3200. doi: 10.1523/JNEUROSCI.4864-13.2015

Rabadán, M. A., Cayuso, J., Le Dréau, G., Cruz, C., Barzi, M., Pons, S., et al. (2012). Jagged2 controls the generation of motor neuron and oligodendrocyte progenitors in the ventral spinal cord. *Cell Death Differ.* 19, 209–219. doi: 10.1038/cdd.2011.84

Rangasamy, S. B., Jana, M., Roy, A., Corbett, G. T., Kundu, M., Chandra, S., et al. (2018). Selective disruption of TLR2-MyD88 interaction inhibits inflammation and attenuates Alzheimer's pathology. *J. Clin. Invest.* 128, 4297–4312. doi: 10.1172/JCI96209

Re, F., and Strominger, J. L. (2001). Toll-like receptor 2 (TLR2) and TLR4 differentially activate human dendritic cells. *J. Biol. Chem.* 276, 37692–37699. doi: 10.1074/jbc.M105927200

Rolls, A., Shechter, R., London, A., Ziv, Y., Ronen, A., Levy, R., et al. (2007). Toll-like receptors modulate adult hippocampal neurogenesis. *Nat. Cell Biol.* 9, 1081–1088. doi: 10.1038/ncb1629

Rossjohn, J., Cappai, R., Feil, S. C., Henry, A., McKinstry, W. J., Galatis, D., et al. (1999). Crystal structure of the Nterminal, growth factor-like domain of Alzheimer amyloid precursor protein. *Nat. Struct. Biol.* 6, 327–331. doi: 10.1038/7562

Salunke, D. B., Shukla, N. M., Yoo, E., Crall, B. M., Balakrishna, R., Malladi, S. S., et al. (2012). Structure-activity relationships in human toll-like receptor 2-specific monoacyl lipopeptides. *J. Med. Chem.* 55, 3353–3363. doi: 10.1021/jm3000533

Sanchez-Irizarry, C., Carpenter, A. C., Weng, A. P., Pear, W. S., Aster, J. C., and Blacklow, S. C. (2004). Notch subunit Heterodimerization and prevention of ligand-independent proteolytic activation depend, respectively, on a novel domain and the LNR repeats. *Mol. Cell. Biol.* 24, 9265–9273. doi: 10.1128/mcb.24.21.9265-9273.2004

Sanchez-Petidier, M., Guerri, C., and Moreno-Manzano, V. (2022). Toll-like receptors 2 and 4 differentially regulate the self-renewal and differentiation of spinal cord neural precursor cells. *Stem Cell Res Ther* 13, 1–16. doi: 10.1186/s13287-022-02798-z

Schafer, D. P., Lehrman, E. K., Kautzman, A. G., Koyama, R., Mardinly, A. R., Yamasaki, R., et al. (2012). Microglia sculpt postnatal neural circuits in an activity and complement-dependent manner. *Neuron* 74, 691–705. doi: 10.1016/j.neuron.2012.03.026

Schafer, D. P., Lehrman, E. K., and Stevens, B. (2013). The "quad-partite" synapse: microglia-synapse interactions in the developing and mature CNS. *Glia* 61, 24–36. doi: 10.1002/glia.22389

Scheffel, J., Regen, T., Van Rossum, D., Seifert, S., Ribes, S., Nau, R., et al. (2012). Toll-like receptor activation reveals developmental reorganization and unmasks responder subsets of microglia. *Glia* 60, 1930–1943. doi: 10.1002/glia.22409

Schenk, M., Belisle, J. T., and Modlin, R. L. (2009). TLR2 looks at lipoproteins. *Immunity* 31, 847–849. doi: 10.1016/j.immuni.2009.11.008

Schonberg, D. L., Popovich, P. G., and McTigue, D. M. (2007). Oligodendrocyte generation is differentially influenced by toll-like receptor (TLR) 2 and TLR4-mediated intraspinal macrophage activation. *J. Neuropathol. Exp. Neurol.* 66, 1124–1135. doi: 10.1097/nen.0b013e31815c2530

Schumann, R. R. (2011). Old and new findings on lipopolysaccharide-binding protein: a soluble pattern-recognition molecule. *Biochem. Soc. Trans.* 39, 989–993. doi: 10.1042/BST0390989

Schwob, J. E., Jang, W., Holbrook, E. H., Lin, B., Herrick, D. B., Peterson, J. N., et al. (2017). Stem and progenitor cells of the mammalian olfactory epithelium: taking poietic license. *J. Comp. Neurol.* 525, 1034–1054. doi: 10.1002/cne.24105

Seong, K. J., Kim, H. J., Cai, B., Kook, M. S., Jung, J. Y., and Kim, W. J. (2018). Toll-like receptor 2 promotes neurogenesis from the dentate gyrus after photothrombotic cerebral ischemia in mice. *Korean J. Physiol. Pharmacol.* 22, 145–153. doi: 10.4196/kjpp.2018.22.2.145

Šestan, N., Artavanis-Tsakonas, S., and Rakic, P. (1999). Contact-dependent inhibition of cortical neurite growth mediated by notch signaling. *Science* 286, 741–746. doi: 10.1126/science.286.5440.741

Setzu, A., Lathia, J. D., Zhao, C., Wells, K., Rao, M. S., Ffrench-Constant, C., et al. (2006). Inflammation stimulates myelination by transplanted oligodendrocyte precursor cells. *Glia* 54, 297–303. doi: 10.1002/glia.20371

Shang, Y., Smith, S., and Hu, X. (2016). Role of notch signaling in regulating innate immunity and inflammation in health and disease. *Protein Cell* 7, 159–174. doi: 10.1007/s13238-016-0250-0

Shechter, R., Ronen, A., Rolls, A., London, A., Bakalash, S., Young, M. J., et al. (2008). Toll-like receptor 4 restricts retinal progenitor cell proliferation. *J. Cell Biol.* 183, 393–400. doi: 10.1083/jcb.200804010

Shi, H., Gabarin, N., Hickey, E., and Askalan, R. (2013). TLR-3 receptor activation protects the very immature brain from ischemic injury. *J. Neuroinflammation* 10:1. doi: 10.1186/1742-2094-10-104

Shi, M., Liu, Z., Lv, Y., Zheng, M., Du, F., Zhao, G., et al. (2011). Forced notch signaling inhibits commissural axon outgrowth in the developing chick central nerve system. *PLoS One* 6:e14570. doi: 10.1371/journal.pone.0014570

Shmueli, A., Shalit, T., Okun, E., and Shohat-Ophir, G. (2018). The toll pathway in the central nervous system of flies and mammals. *Neuro Mol. Med.* 20, 419–436. doi: 10.1007/s12017-018-8515-9

Six, E., Ndiaye, D., Laâbi, Y., Brou, C., Gupta-Rossi, N., Israël, A., et al. (2003). The notch ligand Delta1 is sequentially cleaved by an ADAM protease and γ-secretase. *Proc. Natl. Acad. Sci. USA* 100, 7638–7643. doi: 10.1073/pnas.1230693100

Smith, K. D., and Ozinsky, A. (2002). Toll-like receptor-5 and the innate immune response to bacterial flagellin. *Curr. Top. Microbiol. Immunol.* 270, 93–108. doi: 10.1007/978-3-642-59430-4_6

Smoak, K. A., Aloor, J. J., Madenspacher, J., Merrick, B. A., Collins, J. B., Zhu, X., et al. (2010). Myeloid differentiation primary response protein 88 couples reverse cholesterol transport to inflammation. *Cell Metab.* 11, 493–502. doi: 10.1016/j.cmet.2010.04.006

Sommariva, M., Busnelli, M., Menegola, E., Di Renzo, F., Indino, S., Menon, A., et al. (2023). Immunostaining patterns reveal potential morphogenetic role of toll-like receptors 4 and 7 in the development of mouse respiratory system, liver and pancreas. *Anat. Cell Biol.* 56, 228–235. doi: 10.5115/acb.22.221

Song, Y., Shou, L. M., Ai, L. Y., Bei, Y., and Chen, M. T. (2019). Mini-review: the non-immune functions of toll-like receptors. *Crit. Rev. Eukaryot. Gene Expr.* 29, 37–45. doi: 10.1615/CritRevEukaryotGeneExpr.2018027399

Sprinzak, D., and Blacklow, S. C. (2021). Biophysics of notch signaling. *Annu. Rev. Biophys.* 50, 157–189. doi: 10.1146/annurev-biophys-101920-082204

Stasiulewicz, M., Gray, S. D., Mastromina, I., Silva, J. C., Björklund, M., Seymour, P. A., et al. (2015). A conserved role for notch signaling in priming the cellular response to Shh through ciliary localisation of the key Shh transducer Smo. *Development* 142, 2291–2303. doi: 10.1242/dev.125237

Stridh, L., Smith, P. L. P., Naylor, A. S., Wang, X., and Mallard, C. (2011). Regulation of toll-like receptor 1 and-2 in neonatal mice brains after hypoxia-ischemia. *J. Neuroinflammation* 8:45. doi: 10.1186/1742-2094-8-45

Stump, G., Durrer, A., Klein, A. L., Lütolf, S., Suter, U., and Taylor, V. (2002). Notch1 and its ligands Delta-like and jagged are expressed and active in distinct cell populations in the postnatal mouse brain. *Mech. Dev.* 114, 153–159. doi: 10.1016/S0925-4773(02)00043-6

Suckling, R. J., Korona, B., Whiteman, P., Chillakuri, C., Holt, L., Handford, P. A., et al. (2017). Structural and functional dissection of the interplay between lipid and notch binding by human notch ligands. *EMBO J.* 36, 2204–2215. doi: 10.15252/embj.201796632

Switon, K., Kotulska, K., Janusz-Kaminska, A., Zmorzynska, J., and Jaworski, J. (2017). Molecular neurobiology of mTOR. *Neuroscience* 341, 112–153. doi: 10.1016/j.neuroscience.2016.11.017

Takeda, K., and Akira, S. (2004). TLR signaling pathways. *Semin. Immunol.* 16, 3–9. doi: 10.1016/j.smim.2003.10.003

Talukdar, P. M., Abdul, F., Maes, M., Berk, M., Venkatasubramanian, G., Kutty, B. M., et al. (2021). A proof-of-concept study of maternal immune activation mediated induction of toll-like receptor (TLR) and inflammasome pathways leading to neuroprogressive changes and schizophrenia-like behaviours in offspring. *Eur. Neuropsychopharmacol.* 52, 48–61. doi: 10.1016/j.euroneuro.2021.06.009

Tran, L. N., Loew, S. K., and Franco, S. J. (2023). Notch signaling plays a dual role in regulating the neuron-to-oligodendrocyte switch in the developing dorsal forebrain. *J. Neurosci.* 43, 6854–6871. doi: 10.1523/JNEUROSCI.0144-23.2023

Trujillo-Paredes, N., Valencia, C., Guerrero-Flores, G., Arzate, D. M., Baizabal, J. M., Guerra-Crespo, M., et al. (2016). Regulation of differentiation flux by notch signalling influences the number of dopaminergic neurons in the adult brain. *Biol. Open* 5, 336–347. doi: 10.1242/bio.013383

Tsao, P. N., Wei, S. C., Huang, M. T., Lee, M. C., Chou, H. C., Chen, C. Y., et al. (2011). Lipopolysaccharide-induced notch signaling activation through JNK-dependent pathway regulates inflammatory response. *J. Biomed. Sci.* 18, 56–59. doi: 10.1186/1423-0127-18-56

Tukhvatulin, A. I., Logunov, D. Y., Shcherbinin, D. N., Shmarov, M. M., Naroditsky, B. S., Gudkov, A. V., et al. (2010). Toll-like receptors and their adapter molecules. *Biochemist* 75, 1098–1114. doi: 10.1134/S0006297910090038

Ulrich, H., Do Nascimento, I. C., Bocsi, J., and Tárnok, A. (2015). Immunomodulation in stem cell differentiation into neurons and brain repair. *Stem Cell Rev. Rep.* 11, 474–486. doi: 10.1007/s12015-014-9556-6

Umetsu, D. (2022). Cell mechanics and cell-cell recognition controls by toll-like receptors in tissue morphogenesis and homeostasis. *Fly* 16, 233–247. doi: 10.1080/19336934.2022.2074783

Vabulas, R. M., Ahmad-Nejad, P., da Costa, C., Miethke, T., Kirschning, C. J., Häcker, H., et al. (2001). Endocytosed HSP60s use TLR2 and TLR4 to activate the TIR signaling pathway in innate immune cells. *J. Biol. Chem.* 276, 31332–31339. doi: 10.1074/jbc.M103217200

Vacharasin, J. M., Ward, J. A., McCord, M. M., Cox, K., Imitola, J., and Lizarraga, S. B. (2024). Neuroimmune mechanisms in autism etiology - untangling a complex problem using human cellular models. *Oxford Open Neurosci.* 3, 1–17. doi: 10.1093/oons/kvae003

van Bergenhenegouwen, J., Plantinga, T. S., Joosten, L. A. B., Netea, M. G., Folkerts, G., Kraneveld, A. D., et al. (2013). TLR2 & co: a critical analysis of the complex interactions between TLR2 and coreceptors. *J. Leukoc. Biol.* 94, 885–902. doi: 10.1189/jlb.0113003

Varodayan, F. P., Khom, S., Patel, R. R., Steinman, M. Q., Hedges, D. M., Oleata, C. S., et al. (2018). Role of TLR4 in the modulation of central amygdala GABA transmission by CRF following restraint stress. *Alcohol Alcohol.* 53, 642–649. doi: 10.1093/alcalc/agx114

Ved, R., Sharouf, F., Harari, B., Muzaffar, M., Manivannan, S., Ormonde, C., et al. (2021). Disulfide HMGB1 acts via TLR2/4 receptors to reduce the numbers of oligodendrocyte progenitor cells after traumatic injury in vitro. *Sci. Rep.* 11, 6181–6114. doi: 10.1038/s41598-021-84932-0

Verstak, B., Nagpal, K., Bottomley, S. P., Golenbock, D. T., Hertzog, P. J., and Mansell, A. (2009). MyD88 adapter-like (mal)/TIRAP interaction with TRAF6 is critical for TLR2-and TLR4-mediated NF-κB proinflammatory responses. *J. Biol. Chem.* 284, 24192–24203. doi: 10.1074/jbc.M109.023044

Walker, D. G., Tang, T. M., and Lue, L.-F. (2018). Increased expression of toll-like receptor 3, an anti-viral signaling molecule, and related genes in Alzheimer's disease brains. *Exp. Neurol.* 309, 91–106. doi: 10.1016/j.expneurol.2018.07.016

Wang, Y., and Ha, Y. (2004). The X-ray structure of an antiparallel dimer of the human amyloid precursor protein E2 domain. *Mol. Cell* 15, 343–353. doi: 10.1016/j.molcel.2004.06.037

Wang, H., Kulas, J. A., Wang, C., Holtzman, D. M., Ferris, H. A., and Hansen, S. B. (2021). Regulation of beta-amyloid production in neurons by astrocyte-derived cholesterol. *Proc. Natl. Acad. Sci. USA* 118:e2102191118. doi: 10.1073/pnas.2102191118

Wang, J., Shao, Y., Bennett, T. A., Shankar, R. A., Wightman, P. D., and Reddy, L. G. (2006). The functional effects of physical interactions among toll-like receptors 7, 8, and 9. *J. Biol. Chem.* 281, 37427–37434. doi: 10.1074/jbc.M605311200

Wang, M., Yu, F., Wu, W., Wang, Y., Ding, H., and Qian, L. (2018). Epstein-Barr virus-encoded microRNAs as regulators in host immune responses. *Int. J. Biol. Sci.* 14, 565–576. doi: 10.7150/ijbs.24562

Wasko, N. J., Kulak, M. H., Paul, D., Nicaise, A. M., Yeung, S. T., Nichols, F. C., et al. (2019). Systemic TLR2 tolerance enhances central nervous system remyelination. *J. Neuroinflammation* 16, 158–115. doi: 10.1186/s12974-019-1540-2

Weiss, H. J., and O'Neill, L. A. J. (2022). Of flies and men—the discovery of TLRs. *Cells* 11:127. doi: 10.3390/cells11193127

Werkman, I. L., Dubbelaar, M. L., van der Vlies, P., de Boer-Bergsma, J. J., Eggen, B. J. L., and Baron, W. (2020). Transcriptional heterogeneity between primary adult grey and white matter astrocytes underlie differences in modulation of in vitro myelination. *J. Neuroinflammation* 17, 373–318. doi: 10.1186/s12974-020-02045-3

Werling, D., Jann, O. C., Offord, V., Glass, E. J., and Coffey, T. J. (2009). Variation matters: TLR structure and species-specific pathogen recognition. *Trends Immunol.* 30, 124–130. doi: 10.1016/j.it.2008.12.001

Winters, L., Winters, T., Gorup, D., Mitrečić, D., Ćurlin, M., Križ, J., et al. (2013). Expression analysis of genes involved in TLR2-related signaling pathway: inflammation and apoptosis after ischemic brain injury. *Neuroscience* 238, 87–96. doi: 10.1016/j.neuroscience.2013.02.001

Wolfe, M. S., and Miao, Y. (2022). Structure and mechanism of the γ-secretase intramembrane protease complex. *Curr. Opin. Struct. Biol.* 74:102373. doi: 10.1016/j.sbi.2022.102373

Wouters, M. A., Rigoutsos, I., Chu, C. K., Feng, L. L., Sparrow, D. B., and Dunwoodie, S. L. (2005). Evolution of distinct EGF domains with specific functions. *Protein Sci.* 14, 1091–1103. doi: 10.1110/ps.041207005

Yaddanapudi, K., de Miranda, J., Hornig, M., and Lipkin, W. I. (2011). Toll-like receptor 3 regulates neural stem cell proliferation by modulating the sonic hedgehog pathway. *PLoS One* 6:e26766. doi: 10.1371/journal.pone.0026766

Yoon, S., Kurnasov, O., Natarajan, V., Hong, M., Gudkov, A. V., Osterman, A. L., et al. (2012). Structural basis of TLR5-Flagellin recognition and signaling. *Science* 335, 859–864. doi: 10.1126/science.1215584

Yu, X., Mostafijur Rahman, M., Carter, S. A., Lin, J. C., Zhuang, Z., Chow, T., et al. (2023). Prenatal air pollution, maternal immune activation, and autism spectrum disorder. *Environ. Int.* 179:108148. doi: 10.1016/j.envint.2023.108148

Yu, S., Wang, W., Albakri, M., Yu, X., Majihail, G., Lim, S., et al. (2021). O-Fucose and fringe-modified NOTCH1 extracellular domain fragments as decoys to release niche-lodged hematopoietic progenitor cells. *Glycobiology* 31, 582–592. doi: 10.1093/glycob/cwaa113

Zaben, M., Haan, N., Sharouf, F., Ahmed, A., Sundstrom, L. E., and Gray, W. P. (2021). IL-1β and HMGB1 are anti-neurogenic to endogenous neural stem cells in the sclerotic epileptic human hippocampus. *J. Neuroinflammation* 18, 218–215. doi: 10.1186/s12974-021-02265-1

Zeronian, M. R., Klykov, O., Portell i de Montserrat, J., Konijnenberg, M. J., Gaur, A., Scheltema, R. A., et al. (2021). Notch–jagged signaling complex defined by an interaction mosaic. *Proc. Natl. Acad. Sci. USA* 118, 1–12. doi: 10.1073/pnas.2102502118

Zhang, Z., Zhang, Z. Y., Wu, Y., and Schluesener, H. J. (2011). Immunolocalization of toll-like receptors 2 and 4 as well as their endogenous ligand, heat shock protein 70, in rat traumatic brain injury. *Neuroimmunomodulation* 19, 10–19. doi: 10.1159/000326771

Zhou, Z. D., Kumari, U., Xiao, Z. C., and Tan, E. K. (2010). Notch as a molecular switch in neural stem cells. *IUBMB Life* 62, 618–623. doi: 10.1002/iub.362

Ziegler, G., Harhausen, D., Schepers, C., Hoffmann, O., Röhr, C., Prinz, V., et al. (2007). TLR2 has a detrimental role in mouse transient focal cerebral ischemia. *Biochem. Biophys. Res. Commun.* 359, 574–579. doi: 10.1016/j.bbrc.2007.05.157

Zolini, G. P., Lima, G. K., Lucinda, N., Silva, M. A., Dias, M. F., Pessoa, N. L., et al. (2014). Defense against HSV-1 in a murine model is mediated by iNOS and orchestrated by the activation of TLR2 and TLR9 in trigeminal ganglia. *J. Neuroinflammation* 11, 1–12. doi: 10.1186/1742-2094-11-20

frontiers | Frontiers in Cell and Developmental Biology

TYPE Mini Review
PUBLISHED 11 December 2024
DOI 10.3389/fcell.2024.1466141

OPEN ACCESS

EDITED BY
Senka Blažetić,
Josip Juraj Strossmayer University of Osijek, Croatia

REVIEWED BY
Diana Escalante-Alcalde,
National Autonomous University of Mexico, Mexico
Barbara Viljetić,
Josip Juraj Strossmayer University of Osijek, Croatia

*CORRESPONDENCE
Dragana Fabris,
dragana.fabris@mef.hr
Ivana Karmelić,
ivana.karmelic@mef.hr

†These authors have contributed equally to this work and share first authorship

RECEIVED 19 July 2024
ACCEPTED 11 November 2024
PUBLISHED 11 December 2024

CITATION
Karmelić I, Jurilj Sajko M, Sajko T, Rotim K and Fabris D (2024) The role of sphingolipid rheostat in the adult-type diffuse glioma pathogenesis. *Front. Cell Dev. Biol.* 12:1466141. doi: 10.3389/fcell.2024.1466141

The role of sphingolipid rheostat in the adult-type diffuse glioma pathogenesis

Ivana Karmelić[1*†], Mia Jurilj Sajko[2†], Tomislav Sajko[2], Krešimir Rotim[2] and Dragana Fabris[1*]

[1]Department of Medical Chemistry, Biochemistry and Clinical Chemistry, School of Medicine, University of Zagreb, Zagreb, Croatia, [2]Department of Neurosurgery, University Hospital Center "Sestre milosrdnice", Zagreb, Croatia

Gliomas are highly aggressive primary brain tumors, with glioblastoma multiforme being the most severe and the most common one. Aberrations in sphingolipid metabolism are a hallmark of glioma cells. The sphingolipid rheostat represents the balance between the pro-apoptotic ceramide and pro-survival sphingosine-1-phosphate (S1P), and in gliomas it is shifted toward cell survival and proliferation, promoting gliomas' aggressiveness, cellular migration, metastasis, and invasiveness. The sphingolipid rheostat can be altered by targeting enzymes that directly or indirectly affect the ratio of ceramide to S1P, leading to increased ceramide or decreased S1P levels. Targeting the sphingolipid rheostat offers a potential therapeutic pathway for glioma treatment which can be considered through reducing S1P levels or modulating S1P receptors to reduce cell proliferation, as well as through increasing ceramide levels to induce apoptosis in glioma cells. Although the practical translation into clinical therapy is still missing, sphingolipid rheostat targeting in gliomas has been of great research interest in recent years with several interesting achievements in the glioma therapy approach, offering hope for patients suffering from these vicious malignancies.

KEYWORDS

diffuse glioma, glioblastoma, sphingosine-1-phosphate, ceramides, sphingolipid rheostat

1 Introduction

Gliomas, the most prevalent and aggressive form of intracranial cancer, account for over 80% of malignant brain tumors, with glioblastoma multiforme (GBM) as the most common and severe subtype (Ostrom et al., 2014). Despite the significant research interest and certain progress in glioma treatment in recent years, the prognosis for patients with gliomas, especially GBM, remains very poor (Ma et al., 2024). The latest fifth edition of the World Health Organization (WHO) tumor classification of the central nervous system (CNS) introduced significant updates, incorporating molecular and genetic parameters for more precise clinical categorization (Louis et al., 2021). Sphingolipids, especially glycosphingolipids, are abundantly in the brain and integral to cell membrane structure and cellular signaling (Hannun and Obeid, 2018). Abnormalities in sphingolipid metabolism have been implicated in promoting gliomas' aggressiveness, strongly affecting numerous characteristics of tumor phenotype, such as cellular migration, metastasis, and invasiveness (Zaibaq et al., 2022). Their main metabolic enzymes have been actively investigated as new potential targets in glioma therapy development (Wang

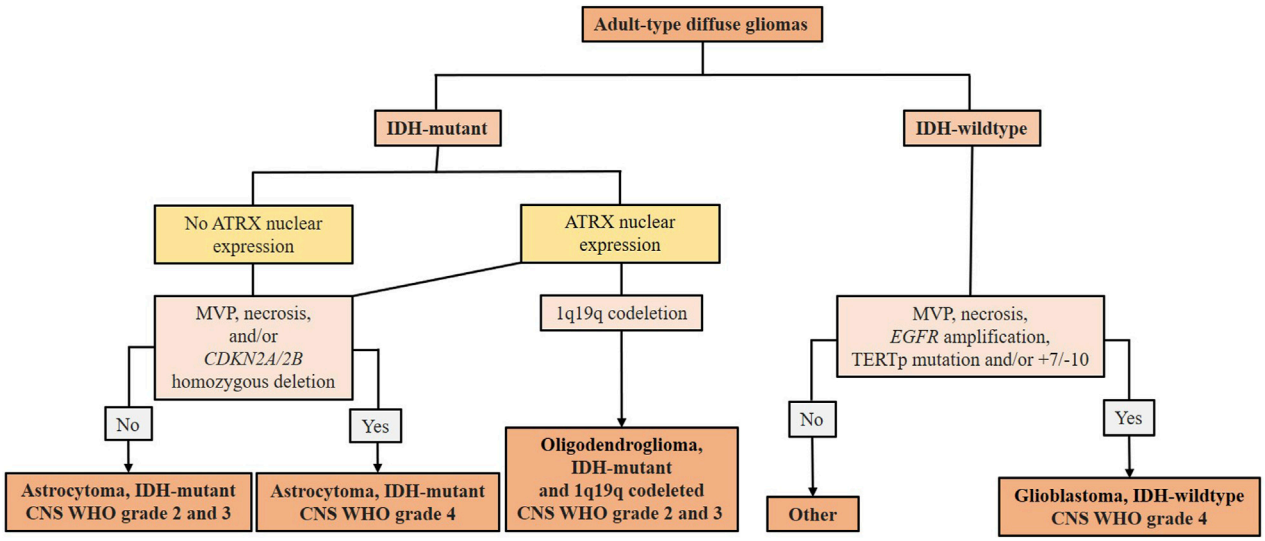

FIGURE 1
Summary scheme of the 2021 WHO classification of adult-type diffuse gliomas (according to Martin et al. (2023)). After the identification of adult-type diffuse glioma, the presence of IDH mutation must be evaluated. In IDH-mutant gliomas, nuclear expression of ATRX is immunohistochemically evaluated. In the absence of ATRX expression, it is classified as astrocytoma, IDH-mutated WHO CNS grade 2 or 3. Astrocytoma, IDH-mutated WHO CNS grade 4 is defined by the presence of MVP, necrosis, and/or *CDKN2A/2B*. If nuclear ATRX expression is conserved and 1p19q codeleted, it is characterized as an oligodendroglioma, IDH-mutated and 1p19q codeleted. Without 1p19q codeletion, it remains astrocytoma, IDH-mutated. IDH-wildtype gliomas are classified as GBMs in the presence of MVP, necrosis, *EGFR* amplification, *TERT* promoter mutation, and/or +7/–10. IDH-wildtype gliomas that do not meet these diagnostic criteria should be investigated for other potential types of glioma tumors. IDH (isocitrate dehydrogenase) - mutations cause the overproduction and accumulation of the 2-hydroxyglutarate, an oncometabolite that promotes DNA methylation leading to changes in the epigenetic status and blocking cellular differentiation (Zaibaq et al., 2022); *ATRX* (α thalassemia/mental retardation syndrome, X-linked gene located in Xq21.1) - loss of function is associated with telomere elongation leading to stronger cellular proliferation (Byun and Park, 2022); MVP (microvascular proliferation); *CDKN2A/2B* - tumor suppressor genes located on chromosome 9p21 involved in cell cycle regulation; their homozygous deletion indicates a higher tumor grade (Louis et al., 2021); 1p19q codeleted - concurrent loss of the short arm of chromosome 1 (1p) and the long arm of chromosome 19 (19q); *EGFR* (epidermal growth factor receptor gene) amplification can lead to overexpression of EGFR protein associated with aggressive behavior of gliomas (Bassi et al., 2021); *TERT* (telomerase reverse transcriptase) promoter mutation can lead to increased activity of telomerase and are associated with enhanced cellular proliferation and tumor progression (Byun and Park, 2022); (+7/–10) - combined whole chromosome 7 gain and whole chromosome 10 loss.

et al., 2022). The "sphingolipid rheostat" concept highlights the opposing roles of ceramide, which induces apoptosis, and sphingosine-1-phosphate (S1P), which promotes proliferation (Cuvillier et al., 1996). This balance between the pro-apoptotic ceramide and pro-survival S1P is crucial in determining the cell's fate, and in glioma it is altered towards the pro-survival S1P signaling, promoting uncontrolled cell proliferation and invasiveness (Zaibaq et al., 2022). This mini-review explores the complex and interconnected metabolic effects of sphingolipids in glioma progression, focusing on new achievements in sphingolipid rheostat targeting as an innovative glioma therapy approach, alone or combined with the established current glioma therapies to improve glioma, particularly GBM patient outcomes.

2 Adult-type diffuse gliomas classification

Diffuse gliomas are the most common type of primary CNS tumors in adults (Lucke-Wold et al., 2024; Martin et al., 2023). The fifth edition of the WHO classification of CNS tumors (CNS5) introduced significant changes by adding molecular and genetic markers to the previously histology based classification, making it more precise and clinically relevant (Louis et al., 2021). According to WHO CNS5, there are three main types of adult-type diffuse gliomas: (I) astrocytoma, isocitrate dehydrogenase (IDH)-mutant; (II) oligodendroglioma, IDH-mutant and 1p/19q codeleted; and (III) glioblastoma, IDH-wildtype (Louis et al., 2021; Gisina et al., 2022) (Figure 1). IDH-mutant diffuse astrocytic tumors are considered as astrocytoma, IDH-mutant CNS WHO grades 2, 3, or 4 (Louis et al., 2021). Oligodendrogliomas, IDH-mutant and 1p/19q codeleted are classified as CNS WHO grade 2 or 3 (Louis et al., 2021). IDH-wildtype diffuse astrocytic tumors are now classified as GBM CNS WHO grade 4 if there is microvascular proliferation (MVP) or necrosis and if they meet 1 or more of 3 specific key molecular criteria (Figure 1), even if they show low-grade histological features (Louis et al., 2021). Further evaluation is necessary to classify other IDH-wildtype gliomas that do not meet these molecular criteria (Louis et al., 2021; Meyer et al., 2021). Astrocytoma, IDH-mutant CNS WHO grade 4 are no longer classified as GBMs due to distinct molecular and epigenetic profiles (Figure 1) and different clinical behaviors (Zaibaq et al., 2022; Rajaratnam et al., 2020). The most malignant and aggressive of the adult-type diffuse gliomas are the astrocytoma, IDH-mutant CNS WHO grade 3 and 4, and GBM, IDH-wildtype CNS WHO grade 4, considered higher-grade gliomas (HGG) (Martin et al., 2023). Glioblastoma accounts for nearly 15% of all brain tumors, with approximately

80% being primary tumors, mainly occurring in older patients, while secondary GBMs develop from lower-grade gliomas primarily in younger patients (Louis et al., 2021). Despite aggressive standard therapy, including radical surgery, radiotherapy and temozolomide (TMZ) chemotherapy, and even with adjuvant chemotherapy, the median overall survival of remains 14–20 months (Ma et al., 2024; Stupp et al., 2005). Other therapies, such as carmustine wafers placed in surgical cavity, anti-VEGF antibodies, PDGF and EGFR inhibitors, and immunotherapy, extend survival for only a few months (Norden and Wen, 2006). Recurrence remains nearly inevitable due to GBM's aggressiveness and therapy resistance, driven by brain tumor-initiating cells (BTICs) (Landis et al., 2018). Lower-grade gliomas, such as astrocytoma, IDH-mutant CNS WHO grade 2 and oligodendroglioma, IDH-mutant and 1q19q codeleted CNS WHO grade 2, have a better prognosis, but their treatment is also challenging as most of them tend to progress to HGG over time (Yu et al., 2020).

3 Sphingolipid metabolism

Sphingolipids are ubiquitous components of eukaryotic cell membranes, especially abundant in human neural tissue, where they contribute (Gault et al., 2010) to membrane structure and serve as signaling molecules in processes like apoptosis, proliferation, angiogenesis, and vesicular trafficking (Ogretmen, 2017). They are commonly divided into simple, sphingoid bases and ceramides, and complex sphingolipids, such as glycosphingolipids, sphingomyelins and sulphatides (Hannun and Obeid, 2018).

Sphingoid bases, long-chain aliphatic amino alcohols, form the structural backbone of sphingolipids and serve as signaling molecules. Their chain length can vary from 12 to 26 carbons, with sphingosine (d18:1) and sphinganine (d18:0) predominating in mammalian tissue; sphingosine arise from sphingolipid degradation, while sphinganine is a precursor in *de novo* sphingolipid biosynthesis (Pruett et al., 2008).

Ceramides, bioactive sphingolipids are synthesized by six ceramide synthase isoforms (CERS1-6) which bind fatty acids of varying chain lengths to a sphingoid base, resulting in ceramides with diverse functions and tissue distributions (Riebeling et al., 2003; Raichur, 2020). In human brain tissue, 18-carbon fatty acid ceramides are the most abundant (Pruett et al., 2008). Ceramides are synthesized either *de novo* or via hydrolysis from complex sphingolipids and are further catabolized by ceramidases to form sphingoid bases, serving as a key intermediates and precursors for all complex sphingolipids (Zheng et al., 2006; Mullen et al., 2012). Bioactive sphingoid bases and ceramides disrupt pro-survival cellular signaling pathways inducing apoptosis by various activating mechanisms (Nganga et al., 2018). Extracellularly oriented ceramides produced by acid sphingomyelinase (sphingomyelin phosphodiesterase 1, SMPD1) in lipid rafts activate membrane receptor clustering with different tumor necrosis factors triggering strong apoptotic signal responses (Dumitru et al., 2009). Intracellularly, ceramides trigger apoptosis by affecting outer mitochondrial membrane permeability and regulating apoptosis-related molecules like phosphatases, kinases, and phospholipase (Gault et al., 2010; Dadsena et al., 2019) During oncogenic transformation, cells often evade apoptosis as ceramidases become more active, hydrolyzing ceramides into sphingosine and fatty acid (Levery, 2005).

Sphingosine kinases 1 and 2 (SPHK1/2) phosphorylate sphingosine to S1P, with SPHK1 being localized in the cytoplasm and SPHK2 in the nucleus, endoplasmic reticulum (ER), mitochondria, and, in cancer cells, in the plasma membrane (Diaz Escarcega et al., 2021). While SPHK1 has mainly pro-survival roles, SPHK2 can promote both pro-apoptotic and pro-survival signals depending on its localization in the cell. SPHK2 can be translocated to the nucleus where the formation of S1P inhibits histone deacetylase 1 and 2 (HDAC1/2) activity, leading to epigenetic changes in gene expression (Diaz Escarcega et al., 2021). Sphingosine-1-phosphate act as a second messenger regulating cell growth, differentiation, migration, and apoptosis by binding to G protein-coupled receptors, S1PR1-5, with variable tissue expression and important roles in development, aging, and pathologies (Merrill, 2011; Sousa et al., 2023; Blaho and Hla, 2014). S1P controls various signaling pathways, including angiogenesis and proliferation, by activating cytosolic effectors, phospholipases, and kinases (Pyne and Pyne, 2000). It is inactivated by ER-enzymes S1P-phosphatases 1 and 2 (SGPP1/2) and phospholipid phosphatases 1–3 (PLPP1-3), or by S1P lyase 1 (SGPL1) localized in the ER and Golgi, but also in plasma membrane, where it directly influences extracellular S1P concentrations (Sousa et al., 2023; Tang and Brindley, 2020) (Figure 2A).

4 Sphingolipid rheostat in gliomas

The sphingolipid rheostat concept refers to the balance between pro-apoptotic ceramides and sphingosine, and pro-survival S1P, where ceramide and sphingosine are directly correlated to the downregulation of S1P and vice versa (Cuvillier et al., 1996) (Figure 2A). Bioactive sphingolipid metabolites may serve as biomarkers for cancer malignancy, progression, and metastasis (Newton et al., 2015) (Figure 2B).

Overexpression of SPHK1 and the resulting production of S1P correlated with malignancy, poor prognosis, and shorter survival time in different types of gliomas, especially GBMs (Young and Van Brocklyn, 2007; Li et al., 2022). Increased SPHK1 and decreased SGPP1/2 expression were a hallmark of cultured GBM cells with upregulation of SPHK1 promoting growth and metastasis of GBM cells (Zaibaq et al., 2022; Abuhusain et al., 2013). Upregulated acid ceramidase (*N*-acyl sphingosine amidohydrolase 1, ASAH1) and SPHK1 were detected in GBM tissues compared to normal brain as well as higher ASAH1 activity in BTICs (Abuhusain et al., 2013). S1P was reported to be, on average, 9-fold higher in GBM tissues compared to normal human brain tissue and correlated with glioma grade, while C18 ceramide was 5-fold lower in GBM tissues (Abuhusain et al., 2013). Fast-proliferating glioblastoma stem cells (GSCs) degrade ceramide and convert sphingosine to S1P more rapidly than slow-proliferating GSCs, and consequently release a significantly higher amount of S1P into the extracellular environment (Marfia et al., 2014). GBM cells and BTICs also release S1P which interacts with S1PRs influencing diverse cellular processes including cell migration,

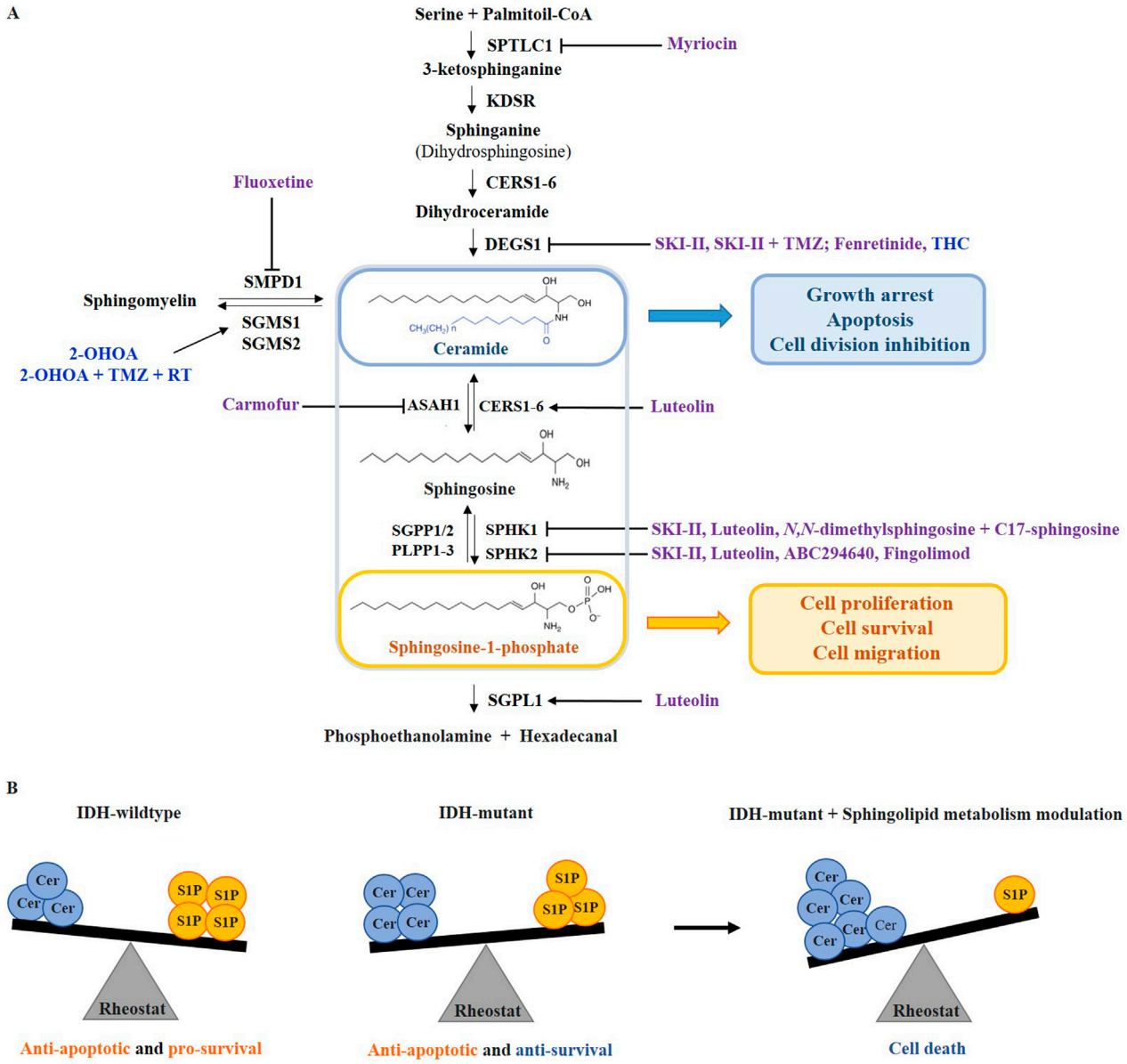

FIGURE 2
The sphingolipid rheostat targeting in adult-type diffuse gliomas. **(A)** The balance between sphingolipids that act as tumor suppressors (ceramide) and those that act as tumor promoters (sphingosine-1-phosphate, S1P) is controlled by targeting the enzymes of sphingolipid metabolic pathway. Drugs that have been involved in clinical trials on glioma patients are colored blue, while pre-clinical drugs are colored purple. **(B)** In IDH-wildtype gliomas, the sphingolipid rheostat is shifted towards high S1P levels, promoting anti-apoptotic and pro-survival signaling. In IDH-mutant gliomas, the sphingolipid rheostat is reversed but with preserved anti-apoptotic signaling. Due to the higher vulnerability of IDH-mutated gliomas, the drugs that induce ceramide accumulation or reduce S1P, can further alter the rheostat inducing cell death. SPTLC1 - serine palmitoyltransferase 1; KDSR - 3-ketosphinganine reductase; CERS1-6 - ceramide synthase 1–6; DEGS1 - dihydroceramide desaturase 1; ASAH1 - acid ceramidase; SGPP1/2 - sphingosine-1-phosphate phosphatases 1 and 2; PLPP1-3 - phospholipid phosphatases 1–3; SPHK1/2 - sphingosine kinase 1 and 2; SGPL1 - sphingosine-1-phosphate lyase 1; SMPD1 - acid sphingomyelinase 1; SGMS1/2 - sphingomyelin synthase 1 and 2; THC - Δ^9-tetrahydrocannabinol; 2-OHOA - 2-hydroxyoleic acid; TMZ - temozolomide; RT - radiotherapy.

differentiation, proliferation, survival against apoptosis and angiogenesis (Zaibaq et al., 2022; Hawkins et al., 2020; Bassi et al., 2021). Moreover, overexpression of S1PR1-3 is observed in glioma cells (Hawkins et al., 2020). S1P also modulates EGFR expression in both cancer and non-cancer cells (Bassi et al., 2021).

Ceramide is considered a tumor suppressor lipid that can induce anti-proliferative and apoptotic responses in various tumor types, including gliomas (Zaibaq et al., 2022; Bassi et al., 2023). Ceramide levels are often reduced in gliomas due to increased degradation or altered synthesis and are significantly lower in HGG, correlating with malignant progression and poor patient survival (Riboni et al., 2002). The expression of various ceramide types and the balance among them are considered critical for different cancer cell progressions, including glioma. Generally, long-chained ceramides (C16, C18, C20) are considered as pro-apoptotic, while

very-long chained ceramides (particularly C24 and C24:1) are associated with proliferative effects (Melero-Fernandez de Mera et al., 2022). In GBM tissue, C18-ceramide levels have been reported to decrease by up to 70%, while reconstitution of C18-ceramide induced cell death in human GBM cells resistant to TMZ (Das et al., 2018).

Recent findings indicate that IDH-wildtype gliomas exhibit a stronger imbalance in sphingolipid rheostat than IDH-mutant gliomas, resulting in elevated ceramide and sphingosine production, which may be the reason why IDH-mutant gliomas are less aggressive than IDH-wildtype (Dowdy et al., 2020). Moreover, several researches have shown that in IDH-mutant gliomas, the sphingolipid balance can be additionally shifted towards increasing pro-apoptotic ceramide production or towards decreasing pro-survival S1P production by targeting enzymes involved in the sphingolipid metabolism like SPHK1/2 and ceramidase, which reduces cancer hallmarks in IDH-mutant gliomas (Zaibaq et al., 2022; Dowdy et al., 2020; Tea et al., 2020) (Figure 2B).

4.1 Current improvements in sphingolipid rheostat targeting in glioma therapy

The sphingolipid rheostat can be altered by targeting enzymes that directly affect the ratio of ceramide to S1P, or by targeting other pathway enzymes that indirectly lead to increased ceramide or decreased S1P levels (Zaibaq et al., 2022; Tea et al., 2020). In gliomas, sphingolipid rheostat is out of balance promoting cell survival, thus providing a rich source of potential therapy targets. Ionizing radiation and TMZ, as current standard therapy for glioma patients, affect the sphingolipid pathway by activating SMPD1 which hydrolyzes sphingomyelin to pro-apoptotic ceramide (Hawkins et al., 2020; Tea et al., 2020).

Preclinical studies have shown that SPHK1 inhibitors can suppress glioma growth by reducing S1P levels. Still, their use in clinical trials is limited due to the conflicting data on the cytotoxic effects on different tumor cell models (Zaibaq et al., 2022; Sousa et al., 2023). Inhibition of SPHK1 selectively blocked angiogenesis, but it did not induce cell death while targeting SPHK1/2 both with dual SPHK inhibitor **SKI-II** proved to be more efficient in decreasing S1P production and promoting anticancer activity (Sousa et al., 2023; French et al., 2006). Additionally, SKI-II acts as a noncompetitive inhibitor of dihydroceramide desaturase 1 (DEGS1), an enzyme that catalyzes the introduction of a double bond into dihydroceramide, converting it into ceramide. The treatment of GBM cells with SKI-II resulted in the accumulation of dihydroceramide and depletion of S1P, which reduced cell proliferation and induced autophagy (Cingolani et al., 2014). SKI-II was found to have a synergistic effect with TMZ and induced cell death in the TMZ-resistant GBM cell lines (Sousa et al., 2023; Cingolani et al., 2014). Both SKI-II alone and combined with TMZ therapy are still in the preclinical testing phase (Sousa et al., 2023).

ABC294640 (Opaganib) as the first-in-class selective competitive inhibitor of SPHK2 has no off-targets on protein kinases and decreases levels of S1P in tissue cultures (Lewis et al., 2018). Dowdy et al. (Dowdy et al., 2020) demonstrated that in IDH-mutant glioma subtypes, the combination of SPHK1 inhibitor ***N,N*-dimethylsphingosine** with **C17 sphingosine** reduced S1P production and enhanced ceramide and sphingosine accumulation. This induced growth arrest and apoptosis, specifically in IDH-mutant gliomas highlighting a metabolic vulnerability characterized by elevated ceramides and decreased SPHK2 expression in IDH-mutant compared to IDH-wildtype gliomas.

Fenretinide, a synthetic retinoid derivative, induces apoptosis in HGG cell lines by indirectly inhibiting DEGS1 (Puduvalli et al., 1999). Although additional testing led to a phase II clinical trial in patients with recurrent glioma and GBM, fenretinide was ineffective at the administered concentrations (Puduvalli et al., 1999; Puduvalli et al., 2004).

Preclinical studies and one pilot study have shown that **THC** (Δ^9-tetrahydrocannabinol) has biostatic effects on recurrent GBM by inhibiting DEGS1 while sparing non-transformed astroglial cells (Velasco et al., 2007; Del Pulgar et al., 2002). The combination of THC and CBD (cannabidiol) in 1:1 ratio (Sativex oral spray) with TMZ is currently in a phase II clinical trial (ARISTOCRAT trial) for GBM therapy (Bhaskaran et al., 2024).

Acid ceramidase (ASAH1) is the key enzyme that reduces ceramide levels by catalyzing its hydrolysis to sphingosine, thus also controlling the pool of sphingosine that can be converted to S1P (Doan et al., 2017a). It has been reported that ASAH1 is upregulated in GBM tissue and correlates with worse patient outcomes and radioresistance (Doan et al., 2017b). *In vitro* inhibition of ASAH1 enzyme with **carmofur**, a fluorouracil derivative, decreased the growth of TMZ-resistant GBM cells and effectively killed GSCs increasing ceramide levels and inducing apoptosis (Hawkins et al., 2023; Dementiev et al., 2019).

The most recent research by Navone et al (Navone et al., 2023) showed that **luteolin**, a natural flavonoid, inhibited the expression of SPHK1/2 while increasing the expression of both SGPL1 and CERS6, which decreased cell viability and survival of TMZ-resistant GSCs.

Myriocin, a competitive inhibitor of serine palmitoyltransferase 1 (SPTLC1), the first enzyme in *de novo* sphingolipid biosynthesis, can inhibit the proliferation of different cancer types by altering the sphingolipid rheostat (Lee et al., 2012; Yaguchi et al., 2017). Treating GBM cells with myriocin led to a 35% decrease in S1P levels (Bernhart et al., 2015). Synthetic sphingolipid analog, **fingolimod** (FTY720) was designed to improve the biostatic properties of myriocin, while also acting as a competitive inhibitor of SPHK2 (Zaibaq et al., 2022; Paugh et al., 2003). Fingolimod-1-phosphate inhibits HDAC1/2 and enhances histone acetylation leading to epigenetic regulation of specific genes that increase sensitivity to chemotherapeutics while also acting as an S1PR1 antagonist in the CNS lymph nodes (Hawkins et al., 2020; Pyne and Pyne, 2020). Carmofur, luteolin, myriocin, and fingolimod are still in the preclinical phase of research (Zaibaq et al., 2022).

Sphingomyelin is a crucial component of membrane lipid rafts essential for signaling. It is synthesized by sphingomyelin synthase 1 and 2 (SGMS1/2) isoenzymes, with SGMS1 being the primary isoform present at significantly lower levels in cancer cell membranes, including GBM, and reduced expression of SGMS1 in gliomas is associated with poorer prognostic outcomes (Fernández-García et al., 2019; Lladó et al., 2014).

Major progress in the therapy of glioma was achieved with synthetic **2-hydroxyoleic acid** (2-OHOA), which proved to be a highly specific activator of the SGMS1 isoform with a significantly higher bioavailability and lower toxicity compared to TMZ when administered in therapeutic doses (Lopez et al., 2023). It has been tested on glioma cell lines, preclinical animal studies, and clinical trials on patients are in phase I-II (Zaibaq et al., 2022; Fernández-García et al., 2019; Lopez et al., 2023). Currently, phase IIB-III trials are testing the combination of 2-OHOA, TMZ, and radiotherapy for GBM (NIHR, 2021), representing the closest a novel sphingolipid modulator has come to potential approval as a glioma therapy.

Recent preclinical research indicates that antidepressant **fluoxetine** (Prozac), a selective serotonin reuptake inhibitor (SSRI), can inhibit SMPD1 and induce cell death in glioma by accumulating sphingomyelin, which results in inhibition of oncogenic EGFR signaling and activating lysosomal stress (Bi et al., 2021). Combining fluoxetine, but not other SSRI inhibitors, with TMZ caused massive GBM cell death and complete tumor regression in mice, and it is now being tested in early phase I clinical trial (UCSD, 2024).

4.2 Future perspectives

Even though many exciting findings have been revealed in recent years regarding sphingolipid rheostat targeting in gliomas, they have still not been translated into viable therapy (Zaibaq et al., 2022). Due to the very complex and interconnected sphingolipid metabolism, it is very challenging to influence the activity of one enzyme or metabolic product and not disrupt the expression or metabolic fate of another. Further obstacles to the clinical application of sphingolipid-targeted therapies include challenges with drug delivery across the blood-brain barrier, lack of target specificity that leads to systemic toxicity, tumor heterogeneity (especially in GBMs), and the absence of reliable biomarkers to identify patients who would benefit most from sphingolipid-based treatments (Rahman and Ali, 2024). To overcome these challenges, research is focused on developing targeted delivery systems, combination therapies, and reliable biomarkers for patient selection (Janneh, 2024). While sphingolipid-targeted therapies represent a promising direction for glioma treatment, their potential can be further enhanced by integrating with existing therapeutic strategies. Combining SPHK inhibitors or ceramide analogs with standard treatments such as TMZ or immunotherapy may produce synergistic effects. Furthermore, the integration of genetic profiling in treatment by identifying specific sphingolipid enzyme profiles in individual tumors could enable a more personalized therapeutic approach (Scorsetti et al., 2022; Zhou et al., 2024). This personalized approach could be particularly valuable in IDH-mutant gliomas, where genetic variations in sphingolipid metabolism may influence treatment outcomes (Kayabolen et al., 2021). A still insufficiently studied field in sphingolipid-based glioma therapy is the role of ceramide variability, as different ceramide chain lengths may have opposing effects, despite the general association of ceramides with pro-apoptotic functions (Melero-Fernandez de Mera et al., 2022; Hartmann et al., 2012). Another interesting potential lies in the less abundant sphingoid base sphinganine (d18:0), although structurally similar to sphingosine, has distinct metabolic origins and lacks sphingosine's apoptotic signaling abilities (Farley et al., 2024). On the other hand, sphinganine-1-phosphate exhibits strong signaling properties and binds to the S1PR1 even stronger than S1P, yet lacks S1P's cytoprotective and proliferative effects (Van Brocklyn et al., 1998). The signaling roles of sphinganine and sphinganine-1-phosphate are yet to be clarified offering an interesting and unexplored field.

5 Conclusion

The sphingolipid rheostat is a critical regulator of cell fate in health and disease. In glioma cells, aberrant expression of enzymes of the sphingolipid metabolism leads the cells to escape apoptosis and promote survival and invasiveness. In recent years, several targeted therapies have been proposed that shift the rheostat towards apoptosis and tumor suppression. Targeting the sphingolipid rheostat for glioma treatment provides not only the first-line therapy options for gliomas but is also responsible for sensitizing particular types of gliomas, such as IDH-mutant glioma, for stronger chemotherapeutic response (Dowdy et al., 2020). Given the high complexity of gliomas, particularly GBM, and the limitations of treatment options available so far, a combination of targeting sphingolipid rheostat with some of the current therapies and with genetic profiling for personalized patient selection offers a promising approach to improve outcomes of patients suffering from these vicious tumors.

Author contributions

IK: Conceptualization, Investigation, Supervision, Visualization, Writing–original draft, Writing–review and editing. MJ: Investigation, Writing–original draft, Writing–review and editing. TS: Writing–review and editing. KR: Writing–review and editing. DF: Conceptualization, Investigation, Supervision, Visualization, Writing–original draft, Writing–review and editing.

Funding

The author(s) declare that financial support was received for the research, authorship, and/or publication of this article. This research was funded by Adris Foundation grant "SphingoMark and Thrombectomy" to DF, grant no. 13127 and by the University of Zagreb Support grant "Sphingolipidomics of stroke thrombi and serum in ischemic stroke" to IK, grant no. 10106-23-2513.

Conflict of interest

The authors declare that the research was conducted without any commercial or financial relationships that could be construed as a potential conflict of interest.

Publisher's note

References

Abuhusain, H. J., Matin, A., Qiao, Q., Shen, H., Kain, N., Day, B. W., et al. (2013). A metabolic shift favoring sphingosine 1-phosphate at the expense of ceramide controls glioblastoma angiogenesis. *J. Biol. Chem.* 288, 37355–37364. doi:10.1074/jbc.M113.494740

Bassi, R., Brambilla, S., Tringali, C., and Giussani, P. (2021). Extracellular sphingosine-1-phosphate downstream of EGFR increases human glioblastoma cell survival. *Int. J. Mol. Sci.* 22 (13), 6824. doi:10.3390/ijms22136824

Bassi, R., Dei Cas, M., Tringali, C., Compostella, F., Paroni, R., and Giussani, P. (2023). Ceramide is involved in temozolomide resistance in human glioblastoma U87MG overexpressing EGFR. *Int. J. Mol. Sci.* 24 (20), 15394. doi:10.3390/ijms242015394

Bernhart, E., Damm, S., Wintersperger, A., Nusshold, C., Brunner, A. M., Plastira, I., et al. (2015). Interference with distinct steps of sphingolipid synthesis and signaling attenuates proliferation of U87MG glioma cells. *Biochem. Pharmacol.* 96 (2), 119–130. doi:10.1016/j.bcp.2015.05.007

Bhaskaran, D., Savage, J., Patel, A., Collinson, F., Mant, R., Boele, F., et al. (2024). A randomised phase II trial of temozolomide with or without cannabinoids in patients with recurrent glioblastoma (ARISTOCRAT): protocol for a multi-centre, double-blind, placebo-controlled trial. *BMC Cancer* 24 (1), 83. doi:10.1186/s12885-023-11792-4

Bi, J., Khan, A., Tang, J., Armando, A. M., Wu, S., Zhang, W., et al. (2021). Targeting glioblastoma signaling and metabolism with a re-purposed brain-penetrant drug. *Cell Rep.* 37 (5), 109957. doi:10.1016/j.celrep.2021.109957

Blaho, V. A., and Hla, T. (2014). Thematic Review Series: lysophospholipids and their Receptors: an update on the biology of sphingosine 1-phosphate receptors. *J. Lipid Res.* 55 (8), 1596–1608. doi:10.1194/jlr.R046300

Byun, Y. H., and Park, C.-K. (2022). Classification and diagnosis of adult glioma: a scoping review. *Brain and NeuroRehabilitation* 15 (3), e23. doi:10.12786/bn.2022.15.e23

Cingolani, F., Casasampere, M., Sanllehí, P., Casas, J., Bujons, J., and Fabrias, G. (2014). Inhibition of dihydroceramide desaturase activity by the sphingosine kinase inhibitor SKI II. *J. Lipid Res.* 55 (8), 1711–1720. doi:10.1194/jlr.M049759

Cuvillier, O., Pirianov, G., Kleuser, B., Vanek, P. G., Cosot, O. A., Gutkind, J. S., et al. (1996). Suppression of ceramide-mediated programmed cell death by sphingosine-1-phosphate. *Nat* 381 (6585), 800–803. doi:10.1038/381800a0

Dadsena, S., Bockelmann, S., Mina, J. G. M., Hassan, D. G., Korneev, S., Razzera, G., et al. (2019). Ceramides bind VDAC2 to trigger mitochondrial apoptosis. *Nat. Commun.* 10 (1), 1832–1912. doi:10.1038/s41467-019-09654-4

Das, A., Zdzislaw, S., Cachia, D., Patel, S. J., and Ogretmen, B. (2018). Exth-51. C18-Ceramide analogue drug overcomes resistance to temozolomide in glioblastoma. *Neuro Oncol.* 20 (Suppl. l_6), vi96. doi:10.1093/neuonc/noy148.399

Del Pulgar, T. G., Velasco, G., Sánchez, C., Haro, A., and Guzmán, M. (2002). *De novo*-synthesized ceramide is involved in cannabinoid-induced apoptosis. *Biochem. J.* 363 (Pt 1), 183–188. doi:10.1042/0264-6021:3630183

Dementiev, A., Joachimiak, A., Nguyen, H., Gorelik, A., Illes, K., Shabani, S., et al. (2019). Molecular mechanism of inhibition of acid ceramidase by carmofur. *J. Med. Chem.* 62 (2), 987–992. doi:10.1021/acs.jmedchem.8b01723

Diaz Escarcega, R., McCullough, L. D., and Tsvetkov, A. S. (2021). The functional role of sphingosine kinase 2. *Front. Mol. Biosci.* 8, 683767. doi:10.3389/fmolb.2021.683767

Doan, N. B., Alhajala, H., Al-Gizawiy, M. M., Mueller, W. M., Rand, S. D., Connelly, J. M., et al. (2017a). Acid ceramidase and its inhibitors: a *de novo* drug target and a new class of drugs for killing glioblastoma cancer stem cells with high efficiency. *Oncotarget* 8 (68), 112662–112674. doi:10.18632/oncotarget.22637

Doan, N. B., Nguyen, H. S., Al-Gizawiy, M. M., Mueller, W. M., Sabbadini, R. A., Rand, S. D., et al. (2017b). Acid ceramidase confers radioresistance to glioblastoma cells. *Oncol. Rep.* 38 (4), 1932–1940. doi:10.3892/or.2017.5855

Dowdy, T., Zhang, L., Celiku, O., Movva, S., Lita, A., Ruiz-Rodado, V., et al. (2020). Sphingolipid pathway as a source of vulnerability in IDH1*mut* glioma. *Cancers (Basel)* 12, 2910. doi:10.3390/cancers12102910

Dumitru, C. A., Weller, M., and Gulbins, E. (2009). Ceramide metabolism determines glioma cell resistance to chemotherapy. *J. Cell Physiol.* 221 (3), 688–695. doi:10.1002/jcp.21907

Farley, S., Stein, F., Haberkant, P., Tafesse, F. G., and Schultz, C. (2024). Trifunctional sphinganine: a new tool to dissect sphingolipid function. *ACS Chem. Biol.* 19 (2), 336–347. doi:10.1021/acschembio.3c00554

Fernández-García, P., Rosselló, C. A., Rodríguez-Lorca, R., Beteta-Göbel, R., Fernández-Díaz, J., Lladó, V., et al. (2019). The opposing contribution of SMS1 and SMS2 to glioma progression and their value in the therapeutic response to 2OHOA. *Cancers* 11 (1), 88. doi:10.3390/cancers11010088

French, K. J., Upson, J. J., Keller, S. N., Zhuang, Y., Yun, J. K., and Smith, C. D. (2006). Antitumor activity of sphingosine kinase inhibitors. *J. Pharmacol. Exp. Ther.* 318 (2), 596 LP–603. doi:10.1124/jpet.106.101345

Gault, C. R., Obeid, L. M., and Hannun, Y. A. (2010). An overview of sphingolipid metabolism: from synthesis to breakdown. *Adv. Exp. Med. Biol.* 688, 1–23. doi:10.1007/978-1-4419-6741-1_1

Gisina, A., Kholodenko, I., Kim, Y., Abakumov, M., Lupatov, A., and Yarygin, K. (2022). Glioma stem cells: novel data obtained by single-cell sequencing. *Int. J. Mol. Sci.* 23 (22), 14224. doi:10.3390/ijms232214224

Hannun, Y. A., and Obeid, L. M. (2018). Sphingolipids and their metabolism in physiology and disease. *Nat. Rev. Mol. Cell Biol.* 19 (3), 175–191. doi:10.1038/nrm.2017.107

Hartmann, D., Lucks, J., Fuchs, S., Schiffmann, S., Schreiber, Y., Ferreirós, N., et al. (2012). Long chain ceramides and very long chain ceramides have opposite effects on human breast and colon cancer cell growth. *Int. J. Biochem. Cell Biol.* 44 (4), 620–628. doi:10.1016/j.biocel.2011.12.019

Hawkins, C. C., Ali, T., Ramanadham, S., and Hjelmeland, A. B. (2020). Sphingolipid metabolism in glioblastoma and metastatic brain tumors: a review of sphingomyelinases and sphingosine-1-phosphate. *Biomolecules* 10 (10), 1357–1423. doi:10.3390/biom10101357

Hawkins, C. C., Jones, A. B., Gordon, E. R., Harsh, Y., Ziebro, J. K., Willey, C. D., et al. (2023). Carmofur prevents cell cycle progression by reducing E2F8 transcription in temozolomide-resistant glioblastoma cells. *Cell Death Discov.* 9 (1), 451. doi:10.1038/s41420-023-01738-x

Janneh, A. H. (2024). Sphingolipid signaling and complement activation in glioblastoma: a promising avenue for therapeutic intervention. *Biochem.* 4 (2), 126–143. doi:10.3390/biochem4020007

Kayabolen, A., Yilmaz, E., and Bagci-Onder, T. (2021). IDH mutations in glioma: double-edged sword in clinical applications? *Biomed* 9 (7), 799. doi:10.3390/biomedicines9070799

Landis, C. J., Tran, A. N., Scott, S. E., Griguer, C., and Hjelmeland, A. B. (2018). The pro-tumorigenic effects of metabolic alterations in glioblastoma including brain tumor initiating cells. *Biochim. Biophys. Acta - Rev. Cancer* 1869 (2), 175–188. doi:10.1016/j.bbcan.2018.01.004

Lee, Y. S., Choi, K. M., Lee, S., Sin, D. M., Yoo, K. S., Lim, Y., et al. (2012). Myriocin, a serine palmitoyltransferase inhibitor, suppresses tumor growth in a murine melanoma model by inhibiting *de novo* sphingolipid synthesis. *Cancer Biol. Ther.* 13 (2), 92–100. doi:10.4161/cbt.13.2.18870

Levery, S. B. (2005). Glycosphingolipid structural analysis and glycosphingolipidomics. *Methods Enzymol.* 405 (1998), 300–369. doi:10.1016/S0076-6879(05)05012-3

Lewis, C. S., Voelkel-johnson, C., and Smith, C. D. (2018). Targeting sphingosine kinases for the treatment of cancer. *Adv. Cancer Res.* 140, 295–325. doi:10.1016/bs.acr.2018.04.015

Li, W., Cai, H., Ren, L., Yang, Y., Yang, H., Liu, J., et al. (2022). Sphingosine kinase 1 promotes growth of glioblastoma by increasing inflammation mediated by the NF-κB/IL-6/STAT3 and JNK/PTX3 pathways. *Acta Pharm. Sin. B* 12 (12), 4390–4406. doi:10.1016/j.apsb.2022.09.012

Lladó, V., López, D. J., Ibarguren, M., Alonso, M., Soriano, J. B., Escribá, P. V., et al. (2014). Regulation of the cancer cell membrane lipid composition by NaCHOleate: effects on cell signaling and therapeutical relevance in glioma. *Biochim. Biophys. Acta - Biomembr.* 1838 (6), 1619–1627. doi:10.1016/j.bbamem.2014.01.027

Lopez, J., Lai-Kwon, J., Molife, R., Welsh, L., Tunariu, N., Roda, D., et al. (2023). A Phase 1/2A trial of idroxioleic acid: first-in-class sphingolipid regulator and glioma cell autophagy inducer with antitumor activity in refractory glioma. *Br. J. Cancer* 129 (5), 811–818. doi:10.1038/s41416-023-02356-1

Louis, D. N., Perry, A., Wesseling, P., Brat, D. J., Cree, I. A., Figarella-Branger, D., et al. (2021). The 2021 WHO classification of tumors of the central nervous system: a summary. *Neuro Oncol.* 23 (8), 1231–1251. doi:10.1093/neuonc/noab106

Lucke-Wold, B., Rangwala, B. S., Shafique, M. A., Siddiq, M. A., Mustafa, M. S., Danish, F., et al. (2024). Focus on current and emerging treatment options for glioma: a

comprehensive review. *World J. Clin. Oncol.* 15 (4), 482–495. doi:10.5306/wjco.v15.i4.482

Ma, S., Pan, X., Gan, J., Guo, X., He, J., Hu, H., et al. (2024). DNA methylation heterogeneity attributable to a complex tumor immune microenvironment prompts prognostic risk in glioma. *Epigenetics* 19 (1), 2318506. doi:10.1080/15592294.2024.2318506

Marfia, G., Campanella, R., Navone, S. E., Di Vito, C., Riccitelli, E., Hadi, L. A., et al. (2014). Autocrine/paracrine sphingosine-1-phosphate fuels proliferative and stemness qualities of glioblastoma stem cells. *Glia* 62 (12), 1968–1981. doi:10.1002/glia.22718

Martin, K. C., Ma, C., and Yip, S. (2023). From theory to practice: implementing the WHO 2021 classification of adult diffuse gliomas in neuropathology diagnosis. *Brain Sci.* 13 (5), 817. doi:10.3390/brainsci13050817

Melero-Fernandez de Mera, R. M., Villaseñor, A., Rojo, D., Carrión-Navarro, J., Gradillas, A., Ayuso-Sacido, A., et al. (2022). Ceramide composition in exosomes for characterization of glioblastoma stem-like cell phenotypes. *Front. Oncol.* 11, 788100. doi:10.3389/fonc.2021.788100

Merrill, A. H. (2011). Sphingolipid and glycosphingolipid metabolic pathways in the era of sphingolipidomics. *Chem. Rev. Am. Chem. Soc.* 111, 6387–6422. doi:10.1021/cr2002917

Meyer, N., Henkel, L., Linder, B., Zielke, S., Tascher, G., Trautmann, S., et al. (2021). Autophagy activation, lipotoxicity and lysosomal membrane permeabilization synergize to promote pimozide- and loperamide-induced glioma cell death. *Autophagy* 17 (11), 3424–3443. doi:10.1080/15548627.2021.1874208

Mullen, T. D., Hannun, Y. A., and Obeid, L. M. (2012). Ceramide synthases at the centre of sphingolipid metabolism and biology. *Biochem. J.* 441 (3), 789–802. doi:10.1042/BJ20111626

Navone, S. E., Guarnaccia, L., Rizzaro, M. D., Begani, L., Barilla, E., Alotta, G., et al. (2023). Role of luteolin as potential new therapeutic option for patients with glioblastoma through regulation of sphingolipid rheostat. *Int. J. Mol. Sci. 2024* 25 (1), 130. doi:10.3390/ijms25010130

Newton, J., Lima, S., Maceyka, M., and Spiegel, S. (2015). Revisiting the sphingolipid rheostat: evolving concepts in cancer therapy. *Exp. Cell Res.* 333 (2), 195–200. doi:10.1016/j.yexcr.2015.02.025

Nganga, R., Oleinik, N., and Ogretmen, B. (2018). Mechanisms of ceramide-dependent cancer cell death. *Adv. Cancer Res.* 140, 1–25. doi:10.1016/bs.acr.2018.04.007

NIHR (2021). LAM-561 in addition to radiation therapy and temozolomide for glioblastoma-adjuvant Licensing and market availability plans Currently in phase II/III clinical trials. Available at: https://io.nihr.ac.uk/tech-briefings/lam-561-in-addition-to-radiation-therapy-and-temozolomide-for-glioblastoma-adjuvant/ (Accessed January 11, 2022).

Norden, A. D., and Wen, P. Y. (2006). Glioma therapy in adults. *Neurologist* 12 (6), 279–292. doi:10.1097/01.nrl.0000250928.26044.47

Ogretmen, B. (2017). Sphingolipid metabolism in cancer signalling and therapy. *Nat. Rev. Cancer* 18 (1), 33–50. doi:10.1038/nrc.2017.96

Ostrom, Q. T., Bauchet, L., Davis, F. G., Deltour, I., Fisher, J. L., Langer, C. E., et al. (2014). The epidemiology of glioma in adults: a "state of the science" review. *Neuro Oncol.* 16 (7), 896–913. doi:10.1093/neuonc/nou087

Paugh, S. W., Payne, S. G., Barbour, S. E., Milstien, S., and Spiegel, S. (2003). The immunosuppressant FTY720 is phosphorylated by sphingosine kinase type 2. *FEBS Lett.* 554 (1–2), 189–193. doi:10.1016/s0014-5793(03)01168-2

Pruett, S. T., Bushnev, A., Hagedorn, K., Adiga, M., Haynes, C. A., Sullards, M. C., et al. (2008). Biodiversity of sphingoid bases ("sphingosines") and related amino alcohols. *J. Lipid Res.* 49, 1621–1639. doi:10.1194/jlr.R800012-JLR200

Puduvalli, V. K., Saito, Y., Xu, R., Kouraklis, G. P., Levin, V. A., and Kyritsis, A. P. (1999). Fenretinide activates caspases and induces apoptosis in gliomas. *Clin. Cancer Res.* 5 (8), 2230–2235.

Puduvalli, V. K., Yung, W. K. A., Hess, K. R., Kuhn, J. G., Groves, M. D., Levin, V. A., et al. (2004). Phase II study of fenretinide (NSC 374551) in adults with recurrent malignant gliomas: a North American brain tumor consortium study. *J. Clin. Oncol.* 22 (21), 4282–4289. doi:10.1200/JCO.2004.09.096

Pyne, N. J., and Pyne, S. (2020). Recent advances in the role of sphingosine 1-phosphate in cancer. *FEBS Lett.* 594 (22), 3583–3601. doi:10.1002/1873-3468.13933

Pyne, S., and Pyne, N. J. (2000). Sphingosine 1-phosphate signalling in mammalian cells. *Biochem. J.* 349 (2), 385–402. doi:10.1042/0264-6021:3490385

Rahman, M. A., and Ali, M. M. (2024). Recent treatment strategies and molecular pathways in resistance mechanisms of antiangiogenic therapies in glioblastoma. *Cancers* 16 (17), 2975. doi:10.3390/cancers16172975

Raichur, S. (2020). Ceramide synthases are attractive drug targets for treating metabolic diseases. *Front. Endocrinol. (Lausanne)* 11, 483. doi:10.3389/fendo.2020.00483

Rajaratnam, V., Islam, M. M., Yang, M., Slaby, R., Ramirez, H. M., and Mirza, S. P. (2020). Glioblastoma: pathogenesis and current status of chemotherapy and other novel treatments. *Cancers* 12 (4), 937. doi:10.3390/cancers12040937

Riboni, L., Campanella, R., Bassi, R., Villani, R., Gaini, S. M., Martinelli-Boneschi, F., et al. (2002). Ceramide levels are inversely associated with malignant progression of human glial tumors. *Glia* 39 (2), 105–113. doi:10.1002/glia.10087

Riebeling, C., Allegood, J. C., Wang, E., Merrill, A. H., and Futerman, A. H. (2003). Two mammalian longevity assurance gene (LAG1) family members, trh1 and trh4, regulate dihydroceramide synthesis using different fatty acyl-CoA donors. *J. Biol. Chem.* 278 (44), 43452–43459. doi:10.1074/jbc.M307104200

Scorsetti, M., Ducray, F., Razis, E. D., Gaca-Tabaszewska, M., Bogusiewicz, J., and Bojko, B. (2022). Metabolomic and lipidomic profiling of gliomas—a new direction in personalized therapies. *Cancers (Basel)* 14 (20), 5041. doi:10.3390/cancers14205041

Sousa, N., Geiß, C., Bindila, L., Lieberwirth, I., Kim, E., and Régnier-Vigouroux, A. (2023). Targeting sphingolipid metabolism with the sphingosine kinase inhibitor SKI-II overcomes hypoxia-induced chemotherapy resistance in glioblastoma cells: effects on cell death, self-renewal, and invasion. *BMC Cancer* 23 (1), 762–823. doi:10.1186/s12885-023-11271-w

Stupp, R., Mason, W. P., van den Bent, M. J., Weller, M., Fisher, B., Taphoorn, M. J. B., et al. (2005). Radiotherapy plus concomitant and adjuvant temozolomide for glioblastoma. *N. Engl. J. Med.* 352 (10), 987–996. doi:10.1056/NEJMoa043330

Tang, X., and Brindley, D. N. (2020). Lipid phosphate phosphatases and cancer. *Biomolecules* 10 (9), 1263. doi:10.3390/biom10091263

Tea, M. N., Poonnoose, S. I., and Pitson, S. M. (2020). Targeting the sphingolipid system as a therapeutic direction for glioblastoma. *Cancers (Basel)* 12 (1), 111. doi:10.3390/cancers12010111

UCSD (2024). Brain tumor trial → fluoxetine and cytotoxic lysosomal stress in glioma (FLIRT). Available at: https://clinicaltrials.ucsd.edu/trial/NCT05634707 (Accessed October 30, 2024).

Van Brocklyn, J. R., Lee, M. J., Menzeleev, R., Olivera, A., Edsall, L., Cuvillier, O., et al. (1998). Dual actions of sphingosine-1-phosphate: extracellular through the gi-coupled receptor edg-1 and intracellular to regulate proliferation and survival. *J. Cell Biol.* 142 (1), 229–240. doi:10.1083/jcb.142.1.229

Velasco, G., Carracedo, A., Blázquez, C., Lorente, M., Aguado, T., Haro, A., et al. (2007). Cannabinoids and gliomas. *Mol. Neurobiol.* 36 (1), 60–67. doi:10.1007/s12035-007-0002-5

Wang, Z., Ge, X., Shi, J., Lu, B., Zhang, X., and Huang, J. (2022). SPTSSA is a prognostic marker for glioblastoma associated with tumor-infiltrating immune cells and oxidative stress. *Oxid. Med. Cell Longev.* 2022 (1), 6711085. doi:10.1155/2022/6711085

Yaguchi, M., Shibata, S., Satomi, Y., Hirayama, M., Adachi, R., Asano, Y., et al. (2017). Antitumor activity of a novel and orally available inhibitor of serine palmitoyltransferase. *Biochem. Biophys. Res. Commun.* 484 (3), 493–500. doi:10.1016/j.bbrc.2017.01.075

Young, N., and Van Brocklyn, J. R. (2007). Roles of sphingosine-1-phosphate (S1P) receptors in malignant behavior of glioma cells. Differential effects of S1P2 on cell migration and invasiveness. *Exp. Cell Res.* 313 (8), 1615–1627. doi:10.1016/j.yexcr.2007.02.009

Yu, D., Xuan, Q., Zhang, C., Hu, C., Li, Y., Zhao, X., et al. (2020). Metabolic alterations related to glioma grading based on metabolomics and lipidomics analyses. *Metabolites* 10 (12), 478–511. doi:10.3390/metabo10120478

Zaibaq, F., Dowdy, T., and Larion, M. (2022). Targeting the sphingolipid rheostat in gliomas. *Int. J. Mol. Sci.* 23 (16), 9255. doi:10.3390/ijms23169255

Zheng, W., Kollmeyer, J., Symolon, H., Momin, A., Munter, E., Wang, E., et al. (2006). Ceramides and other bioactive sphingolipid backbones in health and disease: lipidomic analysis, metabolism and roles in membrane structure, dynamics, signaling and autophagy. *Biochim. Biophys. Acta* 1758 (12), 1864–1884. doi:10.1016/j.bbamem.2006.08.009

Zhou, Y., Tao, L., Qiu, J., Xu, J., Yang, X., Zhang, Y., et al. (2024). Tumor biomarkers for diagnosis, prognosis and targeted therapy. *Signal Transduct. Target Ther.* 9 (1), 132–186. doi:10.1038/s41392-024-01823-2

frontiers | Frontiers in Psychology

TYPE Original Research
PUBLISHED 18 December 2024
DOI 10.3389/fpsyg.2024.1457515

OPEN ACCESS

EDITED BY
Marija Heffer,
Josip Juraj Strossmayer University of Osijek, Croatia

REVIEWED BY
Simone Ciaccioni,
Foro Italico University of Rome, Italy
Marta Sevilla-Sanchez,
University of A Coruña, Spain

*CORRESPONDENCE
Zuzana Križalkovičová
✉ zuzana.krizalkovicova@gmail.com

RECEIVED 18 July 2024
ACCEPTED 21 November 2024
PUBLISHED 18 December 2024

CITATION
Križalkovičová Z, Szabó P, Kumli K, Štefanovský M, Makai A and Szentpéteri J (2024) Neurodevelopmental benefits of judo training in preschool children: a multinational, mixed methods follow-up study.
Front. Psychol. 15:1457515.
doi: 10.3389/fpsyg.2024.1457515

Neurodevelopmental benefits of judo training in preschool children: a multinational, mixed methods follow-up study

Zuzana Križalkovičová[1,2]*, Péter Szabó[2,3,4,5], Kata Kumli[6], Miloš Štefanovský[7], Alexandra Makai[1] and József Szentpéteri[2]

[1]Department of Sports Sciences, Faculty of Health Sciences, Institute of Physiotherapy and Sport Science, University of Pécs, Pécs, Hungary, [2]Medical School, Institute of Transdisciplinary Discoveries, University of Pécs, Pécs, Hungary, [3]Faculty of Humanities, Institute of English Studies, University of Pécs, Pécs, Hungary, [4]Faculty of Sciences, Institute of Sports Science and Physical Education, University of Pécs, Pécs, Hungary, [5]National Virology Laboratory, University of Pécs, Pécs, Hungary, [6]Faculty of Humanities, Institute of Psychology, University of Pécs, Pécs, Hungary, [7]Laboratory of Combat Sports, Department of Gymnastics, Dance, Fitness, and Combat Sports, Faculty of Physical Education and Sports, Comenius University, Bratislava, Slovakia

Introduction: In our quasi-experimental study, we evaluated the neurodevelopmental impact of judo on young children (n = 182) aged 4–7 years, specifically focusing on primitive reflex integration. Participants were divided into judo and non-judo control groups, and assessments were conducted over 6 months across Hungary, Slovakia, and Austria.

Methods: Neurodevelopmental changes were measured using Institute for Neuro-Physiological Psychology (INPP) and Physical and Neurological Examination for Soft Signs (PANESS) for children, while parents completed the Performance Skills Questionnaire (PSQ).

Results: Analysis with Repeated Measures ANOVA (significance set at $p < 0.05$) revealed significant improvements in cognitive and motor performance in judo-practicing children compared to their non-judo counterparts. Furthermore, Spearman correlation analysis revealed that INPP and PANESS were effective in identifying neurodevelopmental changes, PSQ was not suitable as a simplified screening tool for parents, potentially due to its absence of items focused on primitive reflexes.

Conclusion: Despite the limitations of the study, our findings suggest that judo practice could foster central nervous system (CNS) maturation in young children, promoting the potential inclusion of judo in early childhood education programs.

KEYWORDS

neurodevelopment, judo, motor skills, primitive reflexes, cognitive development, CNS, visual perceptual test

1 Introduction

Primarily, our study explored how judo may promote the inhibition and integration of primitive reflexes, potentially leading to improvements in children's physical, mental, and cognitive abilities. The aim of our research was to evaluate the beneficial effects of judo on the maturation of the central nervous system in children aged 4–7 years.

1.1 Primitive reflexes and CNS maturation

The occurrence of mild brain dysfunction, characterized by motor and coordination disorders as well as cognitive and emotional deficiencies, is unfortunately very much present among children (Biotteau et al., 2020). The most measurable and best-discussed part of these dysfunctions in the literature is Developmental coordination disorder (DCD), a neurodevelopmental condition characterized by a marked impairment in the development of motor skills or motor coordination that develops early-on and interferes with an individual's activities of daily living (Blank et al., 2019). Prevalence of DCD is estimated to be 5–6% which is most frequently quoted in the literature (Blank et al., 2019; Hua et al., 2022; Downing and Caravolas, 2020) but ranges in reports between 1.4 and 19%, making it one of the more common childhood disorders (Amador-Ruiz et al., 2018) among others like Attention-Deficit/Hyperactivity Disorder (ADHD) and Specific Learning Disabilities (SLD) (Lino and Chieffo, 2022). Children with DCD often appear clumsy and awkward, struggling to integrate themselves into peer activities. By the coming adolescence, most children with motor skill disorders not only perform poorly in physical education but also have a poor physical self-image, and self-regulation and may underperform academically (Elena Žiaková, 2015).

The basis for the theories that are included in developmental kinesiology (DK) is that the development of human motor function in early childhood is genetically pre-determined and follows predictable patterns or programs, which are formed as the central nervous system (CNS) matures, enabling the infant to control posture, achieve erect posture against gravity, and to move purposefully via muscular activity (Frank et al., 2013). From the 25th to the 40th week of gestation in early development, crucial automatic movement patterns called primitive reflexes are formed. Mostly by the sixth month, possibly up to a year, neonatal reflexes ought to be inhibited, to avoid potential problems in development (Chandradasa and Rathnayake, 2020). One of the most respected methods in Europe that deal with reflex integration is the "Vojta" method based on reflex locomotion, which is a neurophysiologic facilitation system for the CNS. Similar to "Vojta" is Dynamic Neuromuscular Stabilization (DNS) a neuromuscular apparatus that consists of components of locomotion: automatic control of posture, uprighting aimed movements (Bauer et al., 1992) in a reciprocal manner. Given a problem with the inhibition of primitive structures, our brain may utilize its property for neuroplasticity to possibly create new synapses and then implications depending on the stimulus strength and frequency of synaptic activation (Chandradasa and Rathnayake, 2020; Hortobagyi et al., 2022; Gulyaeva, 2017; Rahayu et al., 2020; Chan et al., 2022; Melillo et al., 2020).

Evidently, a sedentary lifestyle and retained primitive reflexes can pose a prevalent problem where additional programs and screening may provide helpful data for future endevors (Melillo et al., 2020; Pecuch et al., 2021). In essence, the lack of inhibition might bottleneck the neurodevelopmental processes and cognitive performance (Stephens-Sarlós et al., 2024). Consequently, there is a search for new methods that, alongside classical rehabilitation (therapy improving fine, gross motor skills, and motor planning) (Offor et al., 2016), can help minimize developmental disadvantages (Geuze et al., 2001). Various therapeutic methods promote CNS maturation for improved outcomes, which align well with the effects of sports, particularly judo (Geuze et al., 2001; Yamasaki, 2023; Perrin et al., 2002; Li et al., 2021).

1.2 CNS maturation and judo

The relationship between physical activity, psychological wellbeing, and cognition has been discussed in sports science over time (Chaddock et al., 2011; Szabo et al., 2024; Moran, 2009). The aspects of sports are frequency, intensity, duration, and mode of physical activity that provide the greatest synergistic benefit for scholastic achievement and neurocognitive health during childhood (Chaddock et al., 2011). Interestingly, sports, particularly judo might be able to facilitate CNS maturation and help assist in education and therapeutic programs (Geuze et al., 2001; Yamasaki, 2023; Perrin et al., 2002; Li et al., 2021). Judo's relationship with neurodevelopment and related benefits in adulthood and among the elderly shows promising data (Descamps et al., 2024; Ciaccioni et al., 2024; Harwood-Gross et al., 2021). Furthermore, judo may influence the self-efficacy of practitioners significantly (Moore et al., 2023) during training, competition, and personality development. Judo encompasses the nurturing of courage and confidence, cognitive skills, disciplined behavior, social and physical contact, coordination skills, fall and throw techniques, monotony tolerance, pain tolerance, conditioning, observation skills, and body control (Galla and Horváth, 1982; Bryman, 2006). Judo's mental training teaches participants how to behave during life's minor and major upheavals, offering some level of protection from not only physical (Miarka et al., 2020) but also potentially psychological injuries. The mind and thinking must be continuously disciplined to be as resilient as the body through the sport (Gutiérrez García and Pérez Gutiérrez, 2012). Judo movements can be both quantitative and qualitative in nature through their well-defined criteria describing movements that are repeated many times, hence affecting the cardiorespiratory system, and utilizing the body's nervous system for alignment and strength that applied to new and different positions (Tomporowski et al., 2015). Motor skill interventions that are open-ended, strategic, and sequential in nature are effective in improving cognition (Shi and Feng, 2022). In essence, the goal of judo is to defeat the given opponent with minimal effort. Timing, softness, and perseverance often triumph over significant resistance and force. By effectively training the center of the body, judo athletes increase their ability to generate and maintain power throughout a fight (Barbado et al., 2016). Trunk stability can positively influence performance in a judo match because it facilitates the transfer of forces generated by the lower body to the upper body (and vice versa) during the application of techniques (Kibler et al., 2006). It also improves balance control similar to gymnastics (van Dieen et al., 2012), which is a key factor in coping with the opponents' disruption of stability (Perrin et al., 2002; Yoshitomi et al., 2006). A stronger core can lead to better coordination of movements and technical skills, resulting in improved overall movement efficiency. It has also been

Abbreviations: INPP, Institute for neuro-physiological psychology; PANESS, Physical and neurological examination for soft signs; PSQ, Performance skills questionnaire; CNS, Central nervous system; DCD, Developmental coordination disorder; ADHD, Attention-deficit/hyperactivity disorder; SLD, Specific learning disabilities; DK, Developmental kinesiology; DNS, Dynamic neuromuscular stabilization; BMI, Body mass index; PSQ, Performance skills questionnaire; ATNR, Asymmetric tonic neck reflex; STNR, Symmetrical tonic neck reflex; TLR, Tonic labyrinth reflex.

shown that rotatory trunk strength is associated with kinetic variables during pulling movements with a change of position, similar to the Morote-seoi-nage throw (Helm et al., 2020). Maintaining balance while disrupting the opponent's is crucial during matches ultimately leading to victory.

From another theoretical perspective considering childhood, judo may even resemble rough and tumble play among mammals which is a crucial part of their developmental process, with usually the playfight continuing until one of the participants is on their back on the ground (Blomqvist and Stylin, 2021; Palagi et al., 2016; Pellis et al., 2022). Despite constant movement and positional changes, which naturally involve bodily proprioception, cross-over motions, twists and turns, level change, and overall coordination, efforts must be made to quickly regain lost balance and maintain equilibrium which connects the movements required for the sport with the process of reflex integration (Galla and Horváth, 1982; Chan et al., 2023; Cid-Calfucura et al., 2023; Lubans et al., 2010; Miarka et al., 2020; Miarka et al., 2016). For these reasons, our study aims to explore the connection between CNS maturation in childhood through judo.

In brief, given the longitudinal nature of our study, we hypothesized that children participating in the judo training program would show significant improvement in the second INPP and PANESS measurement due to the sport. Furthermore, we also hypothesized that participants who perform judo exercises would score better on cognitive (visual perceptual test) tests demonstrating neurodevelopment at the second measurement than their non-judo peers. We hypothesized that those who practice judo would perform better on motor tests (neuromotor test) as well, demonstrating neurodevelopment at the second measurement than their non-judo counterparts. Furthermore, we hypothesized that there is a positive correlation between the two tests. Finally, anticipated a significant positive correlation between INPP and PANESS using the Spearman test, to further validate the robustness of our findings. Additionally, if PSQ had shown a significant negative correlation (due to the scoring), we believed it could be a useful tool for parents to screen their children for the relevant issues.

2 Materials and methods

2.1 Design and sampling

Our quasi-experimental research utilized mixed methods based on quantitative findings from the employed INPP, and PANESS tests integrated (Bryman, 2006) with qualitative results from the PSQ questionnaire. Specifically, INPP and PANESS tests were carried out in person while the questionnaire was distributed using the Google Forms platform to further enhance the data cleaning process where available.

Data collection occurred from January to November 2023 across four countries (Hungary, Slovakia, Croatia, and Austria) in six cities (Pécs, Osijek, Komárno, Gúta, Bratislava, and Vienna). For the Croatian group, we could not carry out repeated measures for our sample, so Croatia was excluded from the statistical analysis. For the map and graphics of study locations and groups (see Supplementary material).

Hungary: Measurements were in Pécs with 101 participants, including two judo groups ($n = 43$) from the "PVSK judo club" and the "Pécsi Sportóvoda" (kindergarten). The control group ($n = 58$) included participants from "Katica Óvoda" (kindergarten) and "Református Óvoda" (kindergarten).

Slovakia: Measurements were with 59 participants in three cities: In Komárno, ($n = 24$) we measured in the "Judo Academy Komárno Judo club" ($n = 8$) and in the Hungarian and Slovak classes in the "Százszorszép Óvoda" (kindergarten) ($n = 16$). In Kollárovo, ($n = 7$) we measured in the "JUDO Klub Gúta." In Bratislava, ($n = 28$), "Judo Centrum" ($n = 11$) we measured participants starting in a preparatory group ($n = 3$) and participants of more advanced preschool age ($n = 8$). The control group ($n = 17$) was "Waldorfská škôlka Hviezdičky" (kindergarten) ($n = 7$) and "Materská Škôlka Novohorská" (kindergarten) ($n = 10$).

Austria: Measurements were in Vienna with 22 participants from the "WAT Stadlau Judo club" ($n = 10$) and a control group from "Waldorfschulen Hietzing" (kindergarten) ($n = 12$).

Participants were assigned to intervention or comparison groups based on whether they practiced Judo or not and for the duration of their time spent in the sport.

Inclusion criteria: 4–7-year-old participants attending kindergarten and/or regularly training in a judo club. For the purposes of our study based on the literature (Witt, 2018; Crane and Temple, 2014; Fraser-Thomas et al., 2008) participants were eligible to be included in the judo groups if they have been training judo for at least a month. Generally, participants train for 10 months annually (aligned with the school year from September 1 to June 30), twice a week for 1 h (either on non-consecutive days or two consecutive hours in 1 day), totaling approximately 80 h annually.

Exclusion criteria: parental and institutional non-consent, severe orthopedic, cardiovascular, neurological, psychiatric, or endocrine disorders, untreated injuries and trauma, Body Mass Index (BMI) >35 kg/m^2, lack of motivation, and muscle pain.

The sampling procedure was a non-invasive, purposive cluster sampling technique which we applied for practicality. Initially, we contacted the University of Pécs for ethical approval. Since our study utilizes non-invasive methods of measurement, involving only observation and standard motor skill assessments, we proceeded accordingly. Practice of judo a traditional Japanese martial art, was not the intervention of the study but an already existing variable. Admittedly, we undertook the rigorous process of seeking consent from both the leaders and the parents. Details about the procedure were put in writing to the institutions, and printable information was given to the parents. All parents were informed about the benefits, procedures, and purpose of the study. Willing institutions, namely kindergartens and judo clubs were contacted through formal agreements, ensuring institutional support and cooperation. The selection procedure complied with the Helsinki Declaration principles (World Medical Association Declaration of Helsinki, 2013), ensured voluntary participation without external influence, and anonymized data processing and reporting. We contacted all the accessible kindergartens within the vicinity, and those who consented proceeded to undergo assessment. Clusters of institutions were selected based on their willingness to participate after a telephone conversation, in the cities of our choice due to distance availability. Parents willing to enroll their children in the study gave their consent by signing a Parental Consent Form. Participants were only involved after their consent had been given according to all the compiled consent forms.

Regarding the follow-up measurements, the data collection was carried out by one person with both the first and follow-up

measurements. The second measurement has been conducted on the participants, with participation rates varying due to reasons such as illness, transition to school, change of kindergarten, and cessation of sports activity. The general characteristic of the first measurement is observed in Supplementary materials. In our article, only 182 of the remaining participants from the initial 262 are present to keep the article clear and transparent, meaning all the included subjects have been assessed and screened twice for the purposes of robust calculations and statistics. The second measurement was carried out after 6 months, at the same location within the institution. The timing of the pre-and post-measurements was from September 2022 to April 2023 in one school year, the six-month interval was followed for every institution.

After written consent from the institutions, parents were informed by the kindergarten teachers and were able to sign the Parental Consent form and contact us for more information using the contact details provided.

Here it is crucial to consider the key factors for judo training in preschool children (4–7 years) which are the acquisition of movement literacy through the development of locomotion, manipulation, and stabilization skills (Lloyd et al., 2015). In terms of long-term sports training, this stage is referred to as the "Active start" (Balyi, 2012). Judo here serves as an ideal form for the child's bio-psycho-social development. The training received by the participants in judo clubs lasted 60 min, at a frequency of 2 times per week, and was dominated by general over specific content. Due to the short concentration time, the children acquired the specific coordination skills of judo in the first part of the training, right after the dynamic warm-up. These included falling techniques, immobilization, and throwing techniques in an adapted form for this age category. The main part of the training consisted of structured play. In particular, chases, relays, obstacle courses, and simple fighting games were used, which primarily develop strength and speed, core stability, cognitive functions, courage, and fair play. The end of the training was directed toward calming the body, through simple stretching exercises, passive lying rest with eyes closed or quizzes oriented to Japanese judo terminology.

However, participants were not trained for the study's measurements, and they were not prepared for the screening exercises. The target group of the research included participants for whom the head of the preschool institution or the judo club agreed to the measurement in the institution's building and allowed the participants to leave the group for the duration of the survey, interrupting the session for about 20 min in the presence of an assistant teacher/coach. If the participant was not outright excluded from the sampling the measurements began. The room used for the study had to be of an appropriate size with adequate lighting, minimal noise, and as little extraneous material as possible to avoid unnecessary physiological stress and potential distractions. Other necessary items were a stopwatch, a chair for the examiner, a chair for the child facing the examiner, and a table. It was crucial to find a place on the floor to guide the participants along the two-meter line, if this was not possible, we had to place a colored 1 cm wide adhesive tape on the floor away from surrounding objects.

The tests were performed with the participants wearing loose clothing and walking barefoot. This neurological examination was designed to help determine the presence of subtle neurological symptoms. The tests did not assess the participant's learning abilities at that time, meaning it was important that the participant fully understood through verbal guidance what was expected from them, with all the tasks to be completed as described.

Consequently, a positive atmosphere was maintained through verbal praise and positive reinforcement. Gentle verbal correction was used when the child did not understand the task. The interaction with each participant had to be done in a few minutes so as not to lose the participants' attention. In order to compensate for the attention problem, the two test's items were woven into each other, resulting in participants not perceiving how long one or the other set of exercises took. Participants always began with simple exercises, with static stances, and then increased difficult exercises.

2.2 Instruments

The INPP test is recognized as a reliable test among practitioners focused on neurodevelopmental issues, educational psychology, and occupational therapy (Blythe, 2005). It is generally practical for assessing certain aspects of neurological and motor development in children. It is based on established theories of neurophysiology and has been used in various studies to examine developmental delays and neurodevelopmental disorders (Blythe, 2005; Blythe, 2014). The INPP test assessed postural reflex actions, crucial for efficient cognitive functioning (Pecuch et al., 2021). In our study the calculated reliability measurement of the INPP test involving Cronbach's alpha and McDonald's omega were (0.793) and (0.812), in the first measurement and in the second (0.797) and (0.826) respectively (see Supplementary material).

INPP includes the Romberg test as well, which is used to assess proprioception and examine static balance (Blythe and Hyland, 1998). The single-leg test is the ability to control static balance and equilibrium by using one side of the body independently of the other. In addition to maintaining balance while standing on one leg, Schrager's test (De Quiros and Schrager, 1979) has shown that observing timing and body position during the test while standing on one leg can provide additional information about the maturity as well as the development of the CNS (Blythe, 2014). Regarding the asymmetric tonic neck reflex (ATNR), turning the head to one side causes the arm and leg to extend on the same side, and on the opposite side, the child retracts the arm and leg (Parmenter, 1983). The symmetrical tonic neck reflex (STNR) in preschool-age participants can be elicited in a quadrupedal position. Considering the STNR the head is extended, the tone of the extensor muscles in the arms increases, and the tone of the flexor muscles decreases (in the hips and knees). When the head is anteflexed, the flexor tone of the arms increases, alongside the tone of the hip and knee muscles (Blythe, 2017a). The tonic labyrinth reflex (TLR) is a primitive response to gravity that regresses with the development of head control, muscle tone, and postural control (Blythe, 2017b). Tansley standard Figures are based on drawing tests originally developed by Gesell to assess fine motor skills and visual-perceptual motor skills (Blythe, 2005).

The test examined balance, proprioception, and coordination, and included static balance and the ability to perform tasks involving crossing the body midline. Balance control not only provides physical stability of movement in space but is also a key reference point for cognitive operations in space, including orientation, direction perception, and understanding of spatial mental operations such as addition and subtraction, multiplication, and division (Blythe, 2005).

Furthermore, the test consists of two subtests, one testing the participant's cognitive abilities (visual perceptual test) and the other their motor skills (neuromotor test). The maximum score for the visual perceptual test was 24 points, the maximum score for the neuromotor test was 60 points and the maximum score for the INPP test was 96 points. The lower the participant's scores on the test, the better their performance. Score ranges regarding INPP were determined as follows: 0 meant No abnormality detected; 1 reflex present to 25 or 25% dysfunction in carrying out the task successfully; 2 reflexes present to 50 or 50% dysfunction in carrying out the task successfully; 3 reflexes present to 75 or 75% dysfunction in carrying out the task successfully; 4 reflexes retained (100%) or unable to carry out the task successfully.

The Physical and Neurological Examination for Soft Signs (PANESS) test was validated and revised by Martha Denckla (Denckla, 1985). It is an internationally accepted valid measurement tool for health professionals and neurologists (Gidley Larson et al., 2007). All the examiner needs are a stopwatch and a score sheet, and it takes only about 30 min. Moderate to excellent inter-rater reliability was identified across PANESS subscores and total scores. The strongest inter-rater reliability was observed for the Timed Motor portion of the PANESS (ICCs >0.90) (Svingos et al., 2023). The PANESS has adequate test–retest and inter-rater reliability (kappa ≥0.5; intraclass coefficient ≥ 0.7), internal consistency (Cronbach's alpha = 0.74), and sensitivity to age-related changes (Cole et al., 2008; Stephens et al., 2018; Vitiello et al., 1989; Crasta et al., 2021). In our study the calculated reliability measurement of the PANESS test involving Cronbach's alpha and McDonald's omega were (0.814) and (0.862), in the first measurement and in the second (0.823) and (0.875) respectively (see Supplementary material). PANESS includes two subscores—Gaits and Stations, and Total Timed—which are summed to produce a Total score (136 points maximum); higher values indicate poorer performance. The Gaits and Stations subscore assesses balance and walking disturbances, as well as excessive motor movements and irregular posture or muscle tone during task execution. The Total Timed score evaluates speed and accuracy deficits in repetitive and patterned motor tasks, along with irregularities in rhythm and overflow of movements (Stephens et al., 2018). The test variables are lateral preference, gait, balance, motor endurance, coordination, and overflow (motor "overflow" refers to the combined movement of body parts not specifically required to perform a task effectively). There are several different forms of motor overflow: associated movement, contralateral motor irradiation and mirror movement (Pitzianti et al., 2017), rhythmic movement disorder, and timed movements (repetitive and patterned) (Dickstein et al., 2005).

The Performance Skills Questionnaire (PSQ) is a validated performance skills questionnaire containing 34 items in three areas: motor skills (10 items), process skills (14 items), and communication skills (10 items). Each item was scored by parents on a Likert scale of 1 to 6, with a higher score indicating better performance skills (maximum score is 204). Parents were asked to rate the extent to which each item characterized their child (very characterized my child - not at all characterized my child). The PSQ yielded three measures, one for each domain, and an overall score (Stephens et al., 2018). Cronbach's coefficient alpha of the whole sample for motor skills, process skills, and communication skills was (0.89, 0.92, and 0.84) respectively in another study (Bart et al., 2010). In our study the calculated reliability measurement of the PSQ test involving Cronbach's alpha and McDonald's omega were (0.954) and (0.959) respectively (see Supplementary material). Data collection occurred after the first measurement. Parents who signed the consent form and were interested in receiving their children's results by email were sent the questionnaire. Questionnaires were distributed using the Google Forms platform from September to November 2022. Parents of 50 Hungarian, 49 Slovak, and 8 Austrian participants completed the Supplementary questions about pregnancy, delivery, and health of participants and the PSQ (Performance Skills Questionnaire) (see Supplementary materials), totaling 107 questionnaires, with a 40.84% response rate. The low response rate was due to the fact that only parents who were interested in receiving their child's test results and willing to complete the questionnaire on the online platform filled it out. The measurement was conducted not only to provide a snapshot of the participants but also to assess how the participants were performing by incorporating a third party, typically a parent who spends daily activities with their children. For statistical purposes, only 80 out of the 107 responses were utilized, due to the fact that some of the children were not measured in the second sampling.

2.3 Statistical analysis

For statistics, descriptive statistics, and the illustration we utilized Jamovi (ŞAhİN and Aybek, 2020) (Version: 2.6.13) and Power BI (Becker and Gould, 2019) (Version: 2.137.1102.0) (see Supplementary materials). Statistical data collection and processing involved descriptive statistics (mean, standard deviation) and normality tests. To test the association between the measurement tools correlation analyses (Spearman variation) were used.

The sample size required was calculated based on a possible loss of 20% for data analysis to detect between-group differences, with an estimated effect size of 0.50, and a significance level adopted as 0.05, statistical power of 0.80, the minimum number of children for each group (judo and kindergarten) was 61. G*Power software (Kang, 2021) (version 3.1.9.7; Heinrich-Heine-Universität Düsseldorf, Düsseldorf, Germany) was used for estimating the minimum number of the individuals participating in the research. To examine the effect of the intervention ANOVA analysis was performed where the first measurement's results were used as covariates.

First, we applied Repeated Measures ANOVA tests to see whether there was a significant difference between the improvement of judo-practicing and non-judo individuals between the first and second time of measurement on the INPP and PANESS tests. For the *post-hoc* analyses, we used Tukey correction. Then, we ran Mann–Whitney *U* tests to observe the potential difference between judo and non-judo participants in the second visual perceptual test and the second neuromotor test. In addition, we used One-way ANOVAs with Games-Howell *post hoc* tests to reveal whether there was a difference between participants having practiced judo for different time periods and participants with no judo experience.

3 Results

The samples comprised 105 non-judo control group participants (57.69%), 44 participants with <1 year of judo practice (24.18%), 27

participants with more than 1 year of judo practice (14.84%), and 6 participants with more than 2 years of practice (3.29%). The sample included 116 males (64.44%) and 66 females (36.67%), with an average age of 4.92 years. Results of the first measurement, the correlation matrix and descriptive statistics are available in the Supplementary material.

First, a Repeated Measures ANOVA revealed a significant difference in the INPP results of both non-judo and judo-practicing participants between the first and second time of measurement, indicating improvement [$F_{(1,\ 180)} = 15.51$, $\eta^2_G = 0.005$, $\eta^2 = 0.003$, $\eta^2_p = 0.079$, $p < 0.001$] (see Figure 1, 2). *Post hoc* analyses with Tukey correction showed that in the case of judo-practicing participants (first measurement: M = 15.56, SE = 1.355; second measurement: M = 7.97, SE = 1.037), the difference between the first and second measurements was bigger [$t(180) = 8.78$, $p < 0.001$] than in the case of non-judo participants (first measurement: M = 18.92, SE = 1.173; second measurement: M = 15.52, SE = 0.898) [$t(180) = 4.55$, $p < 0.001$]. This means that subjects doing judo made more improvement between the two measurements than non-judo participants.

The repeated measures ANOVA also showed a significant difference in the PANESS results of both non-judo and judo-practicing participants between the first and second time of measurement, indicating improvement here as well [$F_{(1,\ 180)} = 15.51$, $\eta^2_G = 0.005$, $\eta^2 = 0.003$, $\eta^2_p = 0.079$, $p < 0.001$] (see Figures 3, 4). Just like in the INPP measurement, *post hoc* analyses with Tukey correction showed that in the case of judo-practicing participants (first measurement: M = 41.32, SE = 2.770; second measurement: M = 27.95, SE = 2.599), the difference between the first and second measurements was bigger [$t(180) = 9.16$, $p < 0.001$] than in the case of non-judo participants (first measurement: M = 59.90, SE = 2.399; second measurement: M = 53.02, SE = 2.250) [$t(180) = -3.28$, $p = 0.027$] (see Figure 5 and Table 1). This indicates that participants practicing judo made more improvement between the two measurements than participants with no judo experience.

Regarding the difference between participants participating in the judo training program and their non-judo peers in the second measurement, the results were the following: Mann–Whitney U tests indicated that a significant difference can be found between

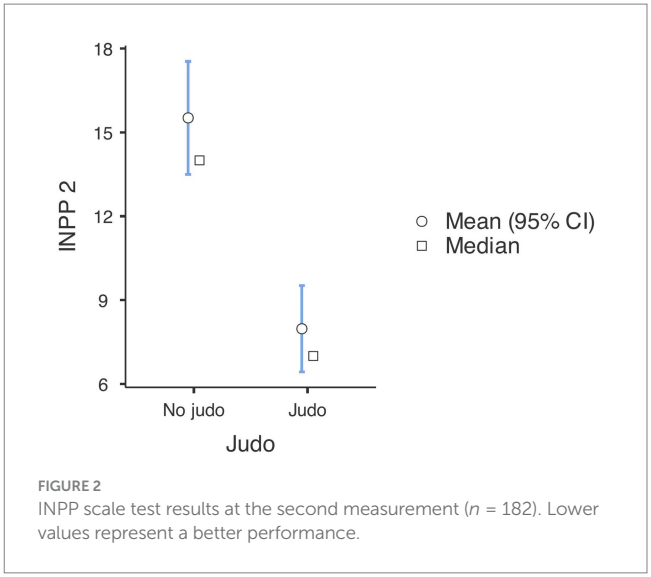

FIGURE 2
INPP scale test results at the second measurement (n = 182). Lower values represent a better performance.

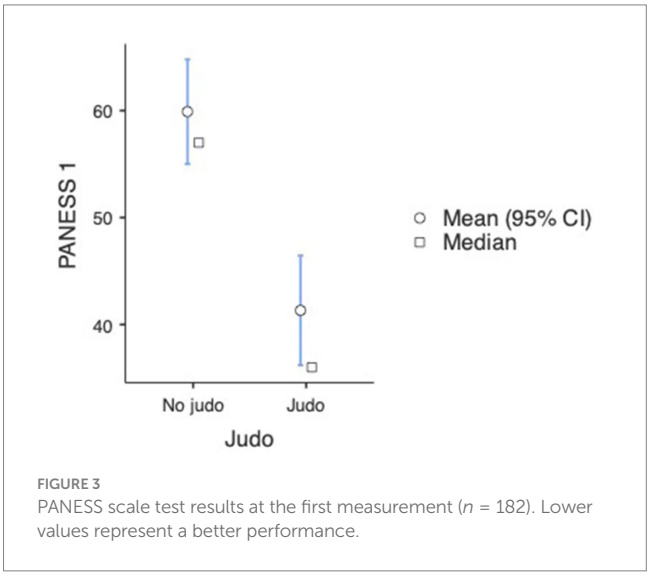

FIGURE 3
PANESS scale test results at the first measurement (n = 182). Lower values represent a better performance.

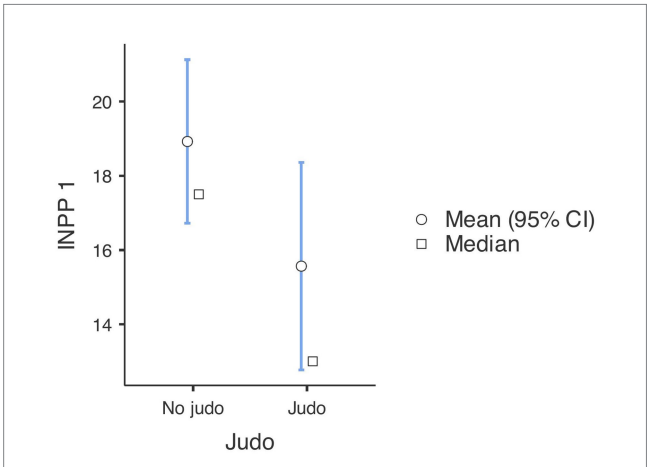

FIGURE 1
INPP scale test results at the first measurement (n = 182). Lower values represent a better performance.

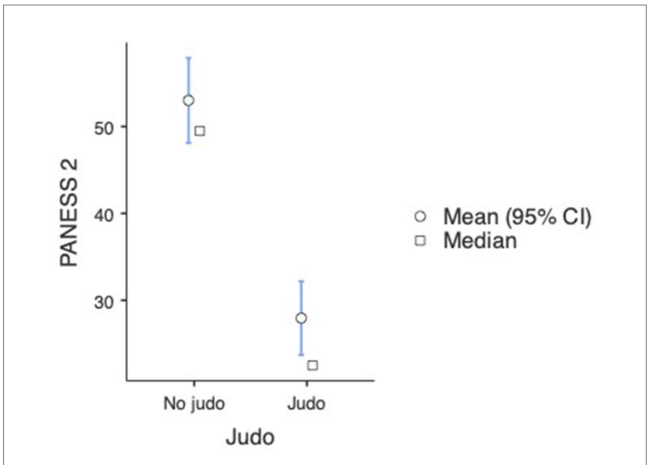

FIGURE 4
PANESS scale test results at the second measurement (n = 182). Lower values represent a better performance.

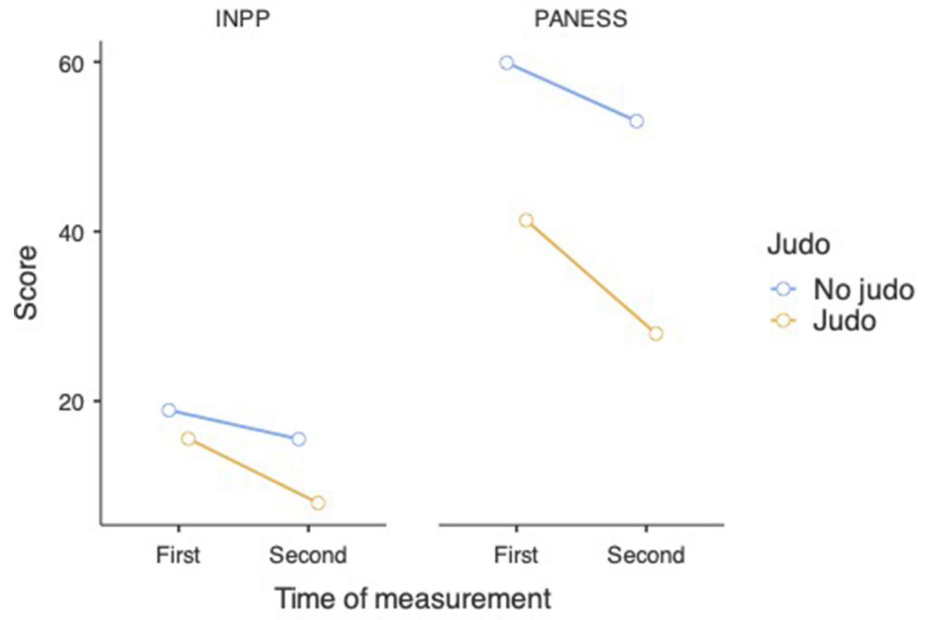

FIGURE 5
Results of tests demonstrating development in the pre-post measurements (n = 182). Lower values represent a better performance.

TABLE 1 Means, standard deviations for outcomes in INPP and PANESS measures (n = 182).

Group descriptives						
	Group	*N*	Mean	Median	SD	SE
INPP 1	No judo	104	18.9	17.5	11.5	1.13
	Judo	78	15.56	13.00	12.60	1.426
INPP 2	No judo	104	15.5	14.0	10.5	1.03
	Judo	78	7.97	7.00	6.94	0.786
PANESS 1	No judo	104	59.9	57.0	25.4	2.49
	Judo	78	41.32	36.00	23.09	2.615
PANESS 2	No judo	104	53.0	49.5	25.4	2.49
	Judo	78	27.95	22.50	19.12	2.165

participants having practiced judo for different time periods and participants with no judo experience in the second visual perceptual test (U = 3,148, p = 0.009). The analysis revealed that the subjects' visual perceptual test score was significantly lower (better) in the case of judo-practicing participants (M = 2.50, SD = 3.74, SE = 0.424) than participants without judo experience (M = 4.60, SD = 5.41, SE = 0.531) (see Figure 6). We used the non-parametric alternative of the independent samples t-test as the assumption of normality was violated (Shapiro–Wilk $p < 0.001$). A One-way ANOVA revealed that a significant difference was found between participants with different amounts of judo training [$F_{(3, 48.3)}$ =14.2, $p < 0.001$]. Games-Howell *post hoc* tests showed that compared to non-judo participants (M = 4.60, SD = 5.41, SE = 0.531), participants with more than 1 year of judo experience (M = 1.70, SD = 2.51, SE = 0.483) [$t(92.6) = 4.03$, $p < 0.001$] and participants with more than 2 years of experience (M = 0.67, SD = 0.82, SE = 0.333) (t(47.6) = 6.27, p < 0.001) got significantly better results on the second visual perceptual test.

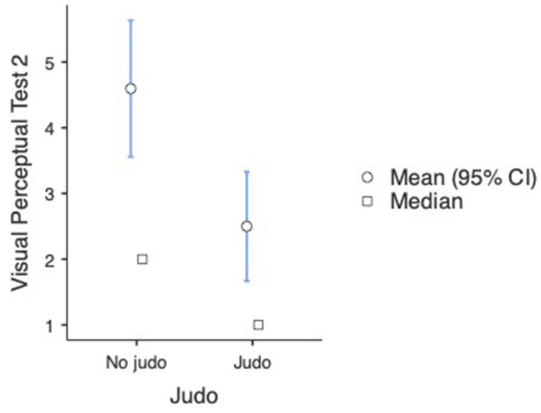

FIGURE 6
Visual perceptual test results at the second measurement (n = 182). Lower values represent a better performance.

Between non-judo participants and participants with <1 year of judo experience (M = 3.22, SD = 4.40, SE = 0.656), there was no significant difference [$t(102) = 1.63$, $p = 0.367$] (see Figure 7).

In the case of the second neuromotor test, we also found a significant difference between judo practitioners and non-judo subjects (U = 1969, $p < 0.001$). The analysis indicated that the judo subjects' neuromotor test scores were significantly lower (better) in the case of participants doing judo (M = 4.78, SD = 3.63, SE = 0.412) than subjects without judo experience (M = 9.38, SD = 6.00, SE = 0.588) (see Figure 8 and Table 2). A One-way ANOVA revealed that a significant difference was found between participants with different amounts of judo training [$F_{(3, 22.6)}$ = 13.3, $p < 0.001$] (see Figure 9 and Table 3). Games-Howell *post hoc* tests showed that compared to non-judo participants (M = 9.38, SD = 5.60, SE = 0.588),

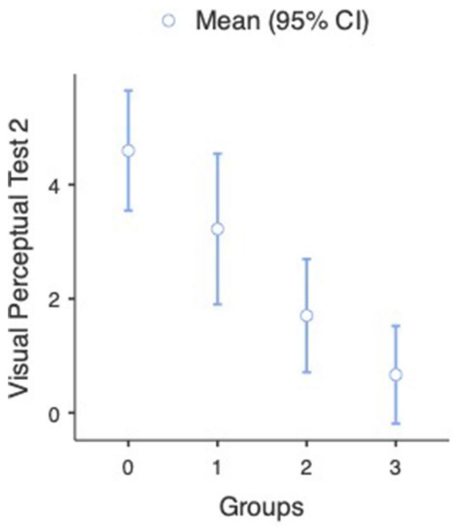

FIGURE 7
Visual perceptual test results at the second measurement (n = 182). 0-non-judo participants, 1-participants with <1 year of judo experience, 2-participants with more than 2 year of judo experience, and 3-participants with more than 2 years of judo experience. Lower values represent a better performance.

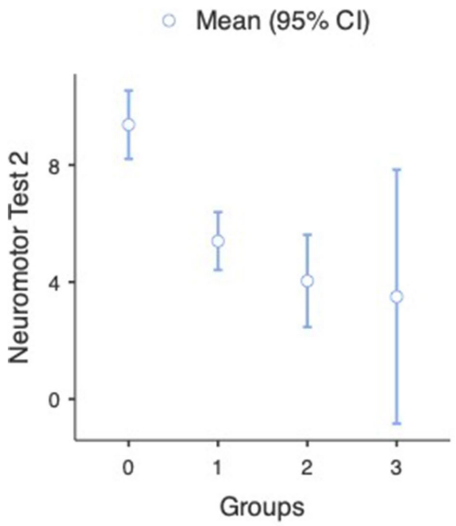

FIGURE 9
Neuromotor test results at the second measurement (n = 182). 0-non-judo participants, 1-participants with <1 year of judo experience, 2-participants with more than 1 year of judo experience, and 3-participants with more than 2 years of judo experience. Lower values represent a better performance.

TABLE 2 **Group descriptives at the second visual perceptual and neuromotor tests measurement (n = 182).**

Group descriptives						
	Group	*N*	Mean	Median	SD	SE
Neuromotor test 2	No judo	104	9.38	8.00	6.00	0.588
	Judo	78	4.78	4.00	3.63	0.412
Visual perceptual test 2	No judo	104	4.60	2.00	5.41	0.531
	Judo	78	2.50	1.00	3.74	0.424

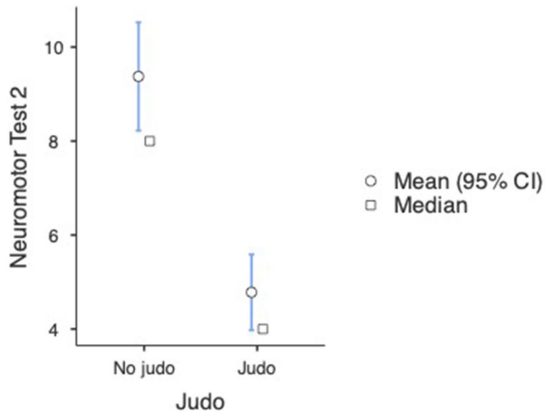

FIGURE 8
Neuromotor test results at the second measurement (n = 182). Lower values represent a better performance.

participants with <1 year of experience (M = 5.40, SD = 3.29, SE = 0.491) [t(139) = 5.19, p < 0.001] and participants with more than 1 year of experience (M = 4.04, SD = 3.99, SE = 0.767) [t(60.3) = 5.52, p < 0.001] got significantly better results on the second neuromotor test. Between non-judo participants and participants with more than 2 years of judo experience (M = 3.50, SD = 4.14, SE = 1.688), there was no significant difference [t(6.28) =3.286, p = 0.058].

Finally, regarding the connection between our measurement tools, we observed a strong positive correlation (Spearman correlation analysis) between the first INPP and first PANESS test results [rho (78) = 0.641, p < 0.001] and also the second INPP and second PANESS test results [rho (78) = 0.777, p < 0.001], further proving the reliability of our testing method. However, neither the first (p = 0.052) nor the second INPP test results (p = 0.055) correlated significantly with the PSQ questionnaire. Moreover, neither the first (p = 0.379) nor the second PANESS test results (p = 0.605) correlated significantly with the PSQ questionnaire (see Supplementary material).

4 Discussion

The aim of our study was to explore how judo training could influence the maturation and inhibition, or integration of primitive reflexes related to improvement in physical, mental, and cognitive abilities among children between 4 and 7 years through the INPP and PANESS tests. Our results are consistent with our hypotheses: participation in judo training increased neurodevelopmental variables compared to non-judo peers.

In mammals the rough and tumble play with parents and among peers reflects similar characteristics to combat sports (Pellis and Pellis, 2007; Blomqvist and Stylin, 2021; Palagi et al., 2016; Fletcher et al., 2011), particularly judo, because the fight lasts until one party is defeated and is on the ground, unable to move. Most likely this is to prepare for the required movements for survival through the practice fight reflecting on the topic at hand.

TABLE 3 Group descriptives at the second visual perceptual and neuromotor tests measurement (n = 182).

Group descriptives					
	Groups	*N*	Mean	SD	SE
Neuromotor test 2	0	104	9.375	5.995	0.588
	1	45	5.400	3.292	0.491
	2	27	4.037	3.985	0.767
	3	6	3.500	4.135	1.688
Visual perceptual test 2	0	104	4.596	5.410	0.531
	1	45	3.222	4.400	0.656
	2	27	1.704	2.509	0.483
	3	6	0.667	0.816	0.333

0-non-judo participants, 1-participants with <1 year of judo experience, 2-participants with more than 1 year of judo experience, and 3-participants with more than 2 years of judo experience.

First, both judo and non-judo groups showed improvements in INPP and PANESS over the 6 months, although, these changes likely reflect the expected developmental progression in this age group (Crasta et al., 2021; Infante-Cañete et al., 2023; Goddard Blythe et al., 2021; Sweeney et al., 2018). However, given the advantages of physical activity in childhood, the judo group showed more improvements from the first to second measurement, which may suggest an acceleration in CNS maturation with judo as a practically suitable physical activity (Pecuch et al., 2021; Infante-Cañete et al., 2023; Goddard Blythe et al., 2021; Gomes da Silva and Arida, 2015; Jing et al., 2024; Liu et al., 2024). Interestingly, participants with more than 1 year of judo experience scored better on cognitive (visual perceptual test) and motor (neuromotor test) measurements compared to non-judo participants.

Meanwhile, a significant positive correlation was identified between INPP total test batteries and PANESS supporting the validity and robustness of both of our measurements and findings. The INPP and PANESS assessments reinforce each other as complementary tools for evaluating neurodevelopmental progress, reinforcing their utility in both clinical and research settings.

Regarding the search for screening methods and potential solutions, the PSQ questionnaire is not a suitable solution for parents to screen their children for specific issues regarding the neurodevelopmental variables that judo can help with. PSQ lacks the sensitivity to capture specific improvements in primitive reflex integration observed by the two other tests. This highlights the need for objective, performance-based measures when assessing neurodevelopmental outcomes in children that are easily accessible to parents.

Consequently, our findings have important implications for early childhood education and intervention programs. Incorporating activities like judo into preschool curricula may enhance neurodevelopmental outcomes, particularly for children at risk of developmental delays. Early intervention is crucial, as the brain is highly plastic during this period, and appropriate stimulation can lead to significant long-term benefits.

Future research could consider randomized controlled trials to strengthen the causal inferences indicated in this study. Investigating the specific elements of judo training that contribute most to neurodevelopmental gains could inform the design of targeted interventions like neuroimaging and detailed analysis of judo movements for primitive reflex integration exercises. Additionally, exploring the long-term effects of sustained judo practice on academic achievement and psychosocial wellbeing would provide valuable insights for educational systems.

Our findings about CNS maturation and judo's role in balance, proprioception, and sensorimotor adaptations align well with other studies in this area, however further investigation is required on the direct impact of martial arts and judo on cognitive development.

4.1 Limitations

Regarding the limitations of our study, we observed the following. Since quasi-experimental designs do not use random assignment, selection bias may occur here, which may affect the internal validity of our results. Our sample may have been influenced by the fact that groups of institutions were selected based on their willingness to participate, but we tried to compensate for this by measuring in more countries and more cities. Second, without randomization, it is challenging to control for external variables that may influence the results, potentially leading to spurious relationships, like parents may not have signed the consent form because they feared their child would do badly on the tests. The kindergartens that contacted us could have been institutions that took better care of their children's development and wanted to prove to themselves and their parents that they were doing well. The results may also have been influenced by the fact that children who have been practicing judo for longer periods were either allowed to train for longer periods because they are exceptionally talented or because they are developmentally delayed and utilize more training to improve their condition. Third, the drop-out rate of children in the second measurement was high. Some of them changed kindergartens and judo clubs or quit the sport. This resulted in a significant drop in the number of items returned, which may limit the generalizability of the results. Fourth, we recorded data at two points in time, limiting the ability to infer causal relationships or changes over time, and in the age group 4–7 years, participants could lose attention and motivation relatively quickly, as behavior and cooperation could not be constant (Pellis and Pellis, 2007; Blomqvist and Stylin, 2021; Palagi et al., 2016; Fletcher et al., 2011).

5 Conclusion

In this study, the neurodevelopment of preschool children who practiced judo was significantly better than that of their non-judo preschool peers. In summary, we found that judo and its preparatory exercises are beneficial, as they encourage natural movement patterns and proper body control, which is crucial for effective motor performance. A further avenue of research shall involve the meticulous biomechanical analysis of judo movements and their effects on the central nervous system using an object-based imaging method for a better understanding of the judo's effect on the CNS while taking the primitive reflexes into account.

Data availability statement

The raw data supporting the conclusions of this article will be made available by the authors, without undue reservation.

Ethics statement

Ethical approval was not required for the study involving human samples in accordance with the local legislation and institutional requirements because ethics approval was not required. Written informed consent for participation in this study was provided by the participants' legal guardians/next of kin.

Author contributions

ZK: Conceptualization, Data curation, Formal analysis, Funding acquisition, Investigation, Methodology, Project administration, Resources, Software, Supervision, Validation, Visualization, Writing – original draft, Writing – review & editing. PS: Formal analysis, Investigation, Supervision, Validation, Writing – original draft, Writing – review & editing. KK: Conceptualization, Formal analysis, Visualization, Writing – original draft, Writing – review & editing. MŠ: Conceptualization, Supervision, Writing – original draft, Writing – review & editing. AM: Data curation, Formal analysis, Software, Writing – original draft, Writing – review & editing. JS: Conceptualization, Methodology, Supervision, Validation, Writing – original draft, Writing – review & editing.

Funding

The author(s) declare that no financial support was received for the research, authorship, and/or publication of this article.

Acknowledgments

The authors express their special thanks to: institutions and parents who participated in the research and who helpfully allowed taking the measurements; Antal Kersics and the PVSK judo Club in Pécs for helping to get to know judo better, oriented toward preschool participants; Elena Žiakova, Ph.D. researcher oriented on the neuro physiotherapy of participants; Erika Jung, Ph.Dr. MBAWU-Director of the Institute of Human Health-helped reach kindergartens in Vienna and Bratislava, Judita Pisárová-IJF- (referee of the International JUDO Federation) who helped professionally. Furthermore, to RoLink Biotechnology Kft., Pécs, Hungary for their consultation on data analysis and illustration.

Conflict of interest

The authors declare that the research was conducted in the absence of any commercial or financial relationships that could be construed as a potential conflict of interest.

Publisher's note

All claims expressed in this article are solely those of the authors and do not necessarily represent those of their affiliated organizations, or those of the publisher, the editors and the reviewers. Any product that may be evaluated in this article, or claim that may be made by its manufacturer, is not guaranteed or endorsed by the publisher.

Supplementary material

The Supplementary material for this article can be found online at: https://www.frontiersin.org/articles/10.3389/fpsyg.2024.1457515/full#supplementary-material

References

Amador-Ruiz, S., Gutierrez, D., Martínez-Vizcaíno, V., Gulías-González, R., Pardo-Guijarro, M. J., and Sánchez-López, M. (2018). Motor competence levels and prevalence of developmental coordination disorder in Spanish children: the MOVI-KIDS study. *J. Sch. Health* 88, 538–546. doi: 10.1111/josh.12639

Balyi, I. (2012). Long-term athlete development. Champaign, IL: Human Kinetics.

Barbado, D., Lopez-Valenciano, A., Juan-Recio, C., Montero-Carretero, C., van Dieën, J. H., and Vera-Garcia, F. J. (2016). Trunk stability, trunk strength and sport performance level in judo. *PLoS One* 11:e0156267. doi: 10.1371/journal.pone.0156267

Bart, O., Rosenberg, L., Ratzon, N. Z., and Jarus, T. (2010). Development and initial validation of the performance skills questionnaire (PSQ). *Res. Dev. Disabil.* 31, 46–56. doi: 10.1016/j.ridd.2009.07.021

Bauer, H., Appaji, G., and Mundt, D. (1992). VOJTA neurophysiologic therapy. *Indian J. Pediatr.* 59, 37–51. doi: 10.1007/BF02760897

Becker, L. T., and Gould, E. M. (2019). Microsoft power BI: extending excel to manipulate, analyze, and visualize diverse data. *Ser. Rev.* 45, 184–188. doi: 10.1080/00987913.2019.1644891

Biotteau, M., Albaret, J. M., and Chaix, Y. (2020). Developmental coordination disorder. *Handb. Clin. Neurol.* 174, 3–20. doi: 10.1016/B978-0-444-64148-9.00001-6

Blank, R., Barnett, A. L., Cairney, J., Green, D., Kirby, A., Polatajko, H., et al. (2019). International clinical practice recommendations on the definition, diagnosis, assessment, intervention, and psychosocial aspects of developmental coordination disorder. *Dev. Med. Child Neurol.* 61, 242–285. doi: 10.1111/dmcn.14132

Blomqvist, T., and Stylin, P. (2021). Integrating rough-and-tumble play in martial arts: a Practitioner's model. *Front. Psychol.* 12:731000. doi: 10.3389/fpsyg.2021.731000

Blythe, S. G. (2005). Releasing educational potential through movement: a summary of individual studies carried out using the INPP test battery and developmental exercise

programme for use in schools with children with special needs. *Child Care Pract.* 11, 415–432. doi: 10.1080/13575270500340234

Blythe, S. G. (2014). Neuromotor immaturity in children and adults: the INPP screening test for clinicians and health practitioners. New York, NY: Wiley Online Library, 32–60.

Blythe, S. G. (2017a). Attention, balance and coordination: The ABC of learning success. New York, NY: John Wiley & Sons, 65–97.

Blythe, S. G. (2017b). Attention, balance and coordination: The ABC of learning success. New York, NY: John Wiley & Sons, 127–148.

Blythe, S. G., and Hyland, D. (1998). Screening for neurological dysfunction in the specific learning difficulty child. *Br. J. Occup. Ther.* 61, 459–464. doi: 10.1177/030802269806101008

Bryman, A. (2006). Integrating quantitative and qualitative research: how is it done? *Qual. Res.* 6, 97–113. doi: 10.1177/1468794106058877

Chaddock, L., Pontifex, M. B., Hillman, C. H., and Kramer, A. F. (2011). A review of the relation of aerobic fitness and physical activity to brain structure and function in children. *J. Int. Neuropsychol. Soc.* 17, 975–985. doi: 10.1017/S1355617711000567

Chan, U., Ayliffe, L., Visvanathan, R., Headland, M., Verma, M., and Jadczak, A. D. (2023). Judo-based exercise programs to improve health outcomes in middle-aged and older adults with no judo experience: a scoping review. *Geriatrics Gerontol. Int.* 23, 163–178. doi: 10.1111/ggi.14553

Chan, Y.-S., Jang, J.-T., and Ho, C.-S. (2022). Effects of physical exercise on children with attention deficit hyperactivity disorder. *Biom. J.* 45, 265–270. doi: 10.1016/j.bj.2021.11.011

Chandradasa, M., and Rathnayake, L. (2020). Retained primitive reflexes in children, clinical implications and targeted home-based interventions. *Nurs. Child. Young People* 32, 37–42. doi: 10.7748/ncyp.2019.e1132

Ciaccioni, S., Castro, O., Bahrami, F., Tomporowski, P. D., Capranica, L., Biddle, S. J. H., et al. (2024). Martial arts, combat sports, and mental health in adults: a systematic review. *Psychol. Sport Exerc.* 70:102556. doi: 10.1016/j.psychsport.2023.102556

Cid-Calfucura, I., Herrera-Valenzuela, T., Franchini, E., Falco, C., Alvial-Moscoso, J., Pardo-Tamayo, C., et al. (2023). Effects of strength training on physical fitness of Olympic combat sports athletes: a systematic review. *Int. J. Environ. Res. Public Health* 20:3516. doi: 10.3390/ijerph20043516

Cole, W. R., Mostofsky, S. H., Larson, J. C., Denckla, M. B., and Mahone, E. M. (2008). Age-related changes in motor subtle signs among girls and boys with ADHD. *Neurology* 71, 1514–1520. doi: 10.1212/01.wnl.0000334275.57734.5f

Crane, J., and Temple, V. (2014). A systematic review of dropout from organized sport among children and youth. *Eur. Phys. Educ. Rev.* 21, 114–131. doi: 10.1177/1356336x14555294

Crasta, J. E., Zhao, Y., Seymour, K. E., Suskauer, S. J., Mostofsky, S. H., and Rosch, K. S. (2021). Developmental trajectory of subtle motor signs in attention-deficit/hyperactivity disorder: a longitudinal study from childhood to adolescence. *Child Neuropsychol.* 27, 317–332. doi: 10.1080/09297049.2020.1847265

De Quiros, J. B., and Schrager, O. L. (1979). Neuropsychological fundamentals in learning disabilities. New York, NY: Academic Therapy Publications.

Denckla, M. B. (1985). Revised neurological examination for subtle signs (1985). *Psychopharmacol. Bull.* 21, 773–800

Descamps, G., Campos, M. J., Rizzo, T., Pecnikar Oblak, V., and Massart, A. G. (2024). Benefits of judo practice for individuals with neurodevelopmental disorders: a systematic literature review. *Sports* 12:182. doi: 10.3390/sports12070182

Dickstein, D. P., Garvey, M., Pradella, A. G., Greenstein, D. K., Sharp, W. S., Castellanos, F. X., et al. (2005). Neurologic examination abnormalities in children with bipolar disorder or attention-deficit/hyperactivity disorder. *Biol. Psychiatry* 58, 517–524. doi: 10.1016/j.biopsych.2004.12.010

Downing, C., and Caravolas, M. (2020). Prevalence and cognitive profiles of children with comorbid literacy and motor disorders. *Front. Psychol.* 11:573580. doi: 10.3389/fpsyg.2020.573580

Elena Žiaková, S. K. (2015). The effect of EEG biofeedback therapy on motor abilities of children with attention deficit hyperactivity disorder. *Eur. J. Med.* 10, 221–234. doi: 10.13187/ejm.2015.10.221

Fletcher, R., May, C., George, J. S., Morgan, P. J., and Lubans, D. R. (2011). Fathers' perceptions of rough-and-tumble play: implications for early childhood services. *Australas. J. Early Childhood* 36, 131–138. doi: 10.1177/183693911103600417

Frank, C., Kobesova, A., and Kolar, P. (2013). Dynamic neuromuscular stabilization & sports rehabilitation. *Int. J. Sports Phys. Ther.* 8, 62–73

Fraser-Thomas, J., Côté, J., and Deakin, J. (2008). Examining adolescent sport dropout and prolonged engagement from a developmental perspective. *J. Appl. Sport Psychol.* 20, 318–333. doi: 10.1080/10413200802163549

Galla, F., and Horváth, I. (1982). Judo övvizsgák (Judo belt exams). Sport, Budapest, 431, 88–102.

Geuze, R. H., Jongmans, M. J., Schoemaker, M. M., and Smits-Engelsman, B. C. M. (2001). Clinical and research diagnostic criteria for developmental coordination disorder: a review and discussion. *Hum. Mov. Sci.* 20, 7–47. doi: 10.1016/S0167-9457(01)00027-6

Gidley Larson, J. C., Mostofsky, S. H., Goldberg, M. C., Cutting, L. E., Denckla, M. B., and Mahone, E. M. (2007). Effects of gender and age on motor exam in typically developing children. *Dev. Neuropsychol.* 32, 543–562. doi: 10.1080/87565640701361013

Goddard Blythe, S., Duncombe, R., Preedy, P., and Gorely, T. (2021). Neuromotor readiness for school: the primitive reflex status of young children at the start and end of their first year at school in the United Kingdom. *Education* 50, 654–667. doi: 10.1080/03004279.2021.1895276

Gomes da Silva, S., and Arida, R. M. (2015). Physical activity and brain development. *Expert. Rev. Neurother.* 15, 1041–1051. doi: 10.1586/14737175.2015.1077115

Gulyaeva, N. V. (2017). Molecular mechanisms of neuroplasticity: an expanding universe. *Biochemistry* 82, 237–242. doi: 10.1134/S0006297917030014

Gutiérrez García, C., and Pérez Gutiérrez, M. (2012). "La contribución del judo a la educación" de Jigoro Kano. Introducción, traducción y notas. *Rev. Artes Marciales Asiáticas* 3, 38–53. doi: 10.18002/rama.v3i3.375

Harwood-Gross, A., Lambez, B., Feldman, R., Zagoory-Sharon, O., and Rassovsky, Y. (2021). The effect of martial arts training on cognitive and psychological functions in at-risk youths. *Front. Pediatr.* 9:707047. doi: 10.3389/fped.2021.707047

Helm, N., Prieske, O., Muehlbauer, T., Krüger, T., Retzlaff, M., and Granacher, U. (2020). Associations between trunk muscle strength and judo-specific pulling performances in judo athletes. *Sportverletz. Sportschaden* 34, 18–27. doi: 10.1055/a-0677-9608

Hortobagyi, T., Vetrovsky, T., Balbim, G. M., Silva, N. C. B. S., Manca, A., et al. (2022). The impact of aerobic and resistance training intensity on markers of neuroplasticity in health and disease. *Ageing Res. Rev.* 80:101698. doi: 10.1016/j.arr.2022.101698

Hua, J., Williams, G. J., Jin, H., Chen, J., Xu, M., Zhou, Y., et al. (2022). Early motor milestones in infancy and later motor impairments: a population-based data linkage study. *Front. Psych.* 13:809181. doi: 10.3389/fpsyt.2022.809181

Infante-Cañete, L., Aguilar-Guerrero, B., and Wallace-Ruiz, A. (2023). Effect of a psychoeducational intervention on motor and perceptual-visual development through the inhibition of primitive reflexes in schoolchildren aged 4 to 7 years old. *Rev. Psicodid.* 28, 182–189. doi: 10.1016/j.psicoe.2023.05.003

Jing, J. Q., Jia, S. J., and Yang, C. J. (2024). Physical activity promotes brain development through serotonin during early childhood. *Neuroscience* 554, 34–42. doi: 10.1016/j.neuroscience.2024.07.015

Kang, H. (2021). Sample size determination and power analysis using the G*power software. *J. Educ. Eval. Health Prof.* 18:17. doi: 10.3352/jeehp.2021.18.17

Kibler, W. B., Press, J., and Sciascia, A. (2006). The role of core stability in athletic function. *Sports Med.* 36, 189–198. doi: 10.2165/00007256-200636030-00001

Li, W., Kong, X., Zhanng, Y., Luo, Y., and Ma, J. (2021). Effects of combat sports on functional network connectivity in adolescents. *Neuroradiology* 63, 1863–1871. doi: 10.1007/s00234-021-02713-y

Lino, F., and Chieffo, D. P. R. (2022). Developmental coordination disorder and Most prevalent comorbidities: a narrative review. *Children* 9:7095. doi: 10.3390/children9071095

Liu, C., Liang, X., and Sit, C. H. P. (2024). Physical activity and mental health in children and adolescents with neurodevelopmental disorders: a systematic review and Meta-analysis. *JAMA Pediatr.* 178, 247–257. doi: 10.1001/jamapediatrics.2023.6251

Lloyd, R. S., Oliver, J. L., Faigenbaum, A. D., Howard, R., de Ste Croix, M. B. A., Williams, C. A., et al. (2015). Long-term athletic development-part 1: a pathway for all youth. *J. Strength Cond. Res.* 29, 1439–1450. doi: 10.1519/JSC.0000000000000756

Lubans, D. R., Morgan, P. J., Cliff, D. P., Barnett, L. M., and Okely, A. D. (2010). Fundamental movement skills in children and adolescents. *Sports Med.* 40, 1019–1035. doi: 10.2165/11536850-000000000-00000

Melillo, R., Leisman, G., Mualem, R., Ornai, A., and Carmeli, E. (2020). Persistent childhood primitive reflex reduction effects on cognitive, sensorimotor, and academic performance in ADHD. *Front. Public Health* 8:431835. doi: 10.3389/fpubh.2020.431835

Miarka, B., Fukuda, H. D., Del Vecchio, F. B., and Franchini, E. (2016). Discriminant analysis of technical-tactical actions in high-level judo athletes. *Int. J. Perform. Anal. Sport* 16, 30–39. doi: 10.1080/24748668.2016.11868868

Miarka, B., Perez, D. I. V., Aedo-Munoz, E., da Costa, L. O. F., and Brito, C. J. (2020). Technical-tactical behaviors analysis of male and female judo Cadets' combats. *Front. Psychol.* 11:1389. doi: 10.3389/fpsyg.2020.01389

Moore, B., Dudley, D., and Woodcock, S. (2023). The effects of a martial arts-based intervention on secondary school students' self-efficacy: a randomised controlled trial. *Philosophies* 8:43. doi: 10.3390/philosophies8030043

Moran, A. (2009). Cognitive psychology in sport: Progress and prospects. *Psychol. Sport Exerc.* 10, 420–426. doi: 10.1016/j.psychsport.2009.02.010

Offor, N., Ossom Williamson, P., and Caçola, P. (2016). Effectiveness of interventions for children with developmental coordination disorder in physical therapy contexts: a systematic literature review and Meta-analysis. *J. Motor Learning Dev.* 4, 169–196. doi: 10.1123/jmld.2015-0018

Palagi, E., Burghardt, G. M., Smuts, B., Cordoni, G., Dall'Olio, S., Fouts, H. N., et al. (2016). Rough-and-tumble play as a window on animal communication. *Biol. Rev. Camb. Philos. Soc.* 91, 311–327. doi: 10.1111/brv.12172

Parmenter, C. L. (1983). An asymmetrical tonic neck reflex rating scale. *Am. J. Occup. Ther.* 37, 462–465. doi: 10.5014/ajot.37.7.462

Pecuch, A., Gieysztor, E., Wolanska, E., Telenga, M., and Paprocka-Borowicz, M. (2021). Primitive reflex activity in relation to motor skills in healthy preschool children. *Brain Sci.* 11:967. doi: 10.3390/brainsci11080967

Pellis, S. M., and Pellis, V. C. (2007). Rough-and-tumble play and the development of the social brain. *Curr. Dir. Psychol. Sci.* 16, 95–98. doi: 10.1111/j.1467-8721.2007.00483.x

Pellis, S. M., Pellis, V. C., Ham, J. R., and Achterberg, E. J. M. (2022). The rough-and-tumble play of rats as a natural behavior suitable for studying the social brain. *Front. Behav. Neurosci.* 16:1033999. doi: 10.3389/fnbeh.2022.1033999

Perrin, P., Deviterne, D., Hugel, F., and Perrot, C. (2002). Judo, better than dance, develops sensorimotor adaptabilities involved in balance control. *Gait Posture* 15, 187–194. doi: 10.1016/S0966-6362(01)00149-7

Pitzianti, M., Grelloni, C., Casarelli, L., D'Agati, E., Spiridigliozzi, S., Curatolo, P., et al. (2017). Neurological soft signs, but not theory of mind and emotion recognition deficit distinguished children with ADHD from healthy control. *Psychiatry Res.* 256, 96–101. doi: 10.1016/j.psychres.2017.06.029

Rahayu, U. B., Wibowo, S., Setyopranoto, I., and Hibatullah Romli, M. (2020). Effectiveness of physiotherapy interventions in brain plasticity, balance and functional ability in stroke survivors: a randomized controlled trial. *NeuroRehabilitation* 47, 463–470. doi: 10.3233/NRE-203210

ŞAhİN, M., and Aybek, E. (2020). Jamovi: an easy to use statistical software for the social scientists. *Int. J. Assessment Tools Educ.* 6, 670–692. doi: 10.21449/ijate.661803

Shi, P., and Feng, X. (2022). Motor skills and cognitive benefits in children and adolescents: relationship, mechanism and perspectives. *Front. Psychol.* 13:1017825. doi: 10.3389/fpsyg.2022.1017825

Stephens, J. A., Denckla, M. B., McCambridge, T., Slomine, B. S., Mahone, E. M., and Suskauer, S. J. (2018). Preliminary use of the physical and neurological examination of subtle signs for detecting subtle motor signs in adolescents with sport-related concussion. *Am. J. Phys. Med. Rehabil.* 97, 456–460. doi: 10.1097/PHM.0000000000000906

Stephens-Sarlós, E., Stephens, P., and Szabo, A. (2024). The efficacy of the sensorimotor training program on sensorimotor development, auditory and visual skills of schoolchildren aged 5–8 years. *Child Youth Care Forum* 6, 1–30. doi: 10.1007/s10566-024-09818-4

Svingos, A. M., Hamner, T., Huntington, K. B., Chen, H. W., Sweeney, K. L., Ellis-Stockley, M., et al. (2023). Inter-rater reliability of the revised physical and neurological examination of subtle signs (PANESS) scored using video review. *Child Neuropsychol.* 29, 922–933. doi: 10.1080/09297049.2022.2140797

Sweeney, K. L., Ryan, M., Schneider, H., Ferenc, L., Denckla, M. B., and Mahone, E. M. (2018). Developmental trajectory of motor deficits in preschool children with ADHD. *Dev. Neuropsychol.* 43, 419–429. doi: 10.1080/87565641.2018.1466888

Szabo, P., Bonet, S., Hetényi, R., Hanna, D., Kovács, Z., and Prisztóka, G. (2024). Systematic review: pain, cognition, and cardioprotection-unpacking oxytocin's contributions in a sport context. *Front. Physiol.* 15:1393497. doi: 10.3389/fphys.2024.1393497

Tomporowski, P. D., McCullick, B., Pendleton, D. M., and Pesce, C. (2015). Exercise and children's cognition: the role of exercise characteristics and a place for metacognition. *J. Sport Health Sci.* 4, 47–55. doi: 10.1016/j.jshs.2014.09.003

van Dieen, J. H., Luger, T., and van der Eb, J. (2012). Effects of fatigue on trunk stability in elite gymnasts. *Eur. J. Appl. Physiol.* 112, 1307–1313. doi: 10.1007/s00421-011-2082-1

Vitiello, B., Ricciuti, A. J., Stoff, D. M., Behar, D., and Denckla, M. B. (1989). Reliability of subtle (soft) neurological signs in children. *J. Am. Acad. Child Adolesc. Psychiatry* 28, 749–753. doi: 10.1097/00004583-198909000-00017

Witt, P. A. (2018). Why children/youth drop out of sports. *J. Park. Recreat. Adm.* 36, 191–199. doi: 10.18666/JPRA-2018-V36-I3-8618

World Medical Association Declaration of Helsinki (2013). Ethical principles for medical research involving human subjects. *JAMA* 310, 2191–2194. doi: 10.1001/jama.2013.281053

Yamasaki, T. (2023). Benefits of judo training for brain functions related to physical and cognitive performance in older adults. *Encyclopedia* 3, 981–995. doi: 10.3390/encyclopedia3030071

Yoshitomi, S. K., Tanaka, C., Duarte, M., Lima, F., Morya, E., and Hazime, F. (2006). Respostas posturais à perturbação externa inesperada em judocas de diferentes níveis de habilidade. *Rev. Bras. Med. Esporte* 12, 159–163. doi: 10.1590/S1517-86922006000300010

frontiers | Frontiers in Human Neuroscience

TYPE Original Research
PUBLISHED 29 January 2025
DOI 10.3389/fnhum.2024.1463740

OPEN ACCESS

EDITED BY
Marija Heffer,
Josip Juraj Strossmayer University of Osijek, Croatia

REVIEWED BY
Toshiaki Taoka,
Nagoya University, Japan
Olivier Baledent,
University of Picardie Jules Verne, France
Kyriaki Astara,
University of Thessaly, Greece

*CORRESPONDENCE
M. Klarica
✉ mklarica@mef.hr

RECEIVED 29 July 2024
ACCEPTED 18 December 2024
PUBLISHED 29 January 2025

CITATION
Strbačko I, Radoš M, Jurjević I, Orešković D and Klarica M (2025) Body position influence on cerebrospinal fluid volume redistribution inside the cranial and spinal CSF compartments.
Front. Hum. Neurosci. 18:1463740.
doi: 10.3389/fnhum.2024.1463740

Body position influence on cerebrospinal fluid volume redistribution inside the cranial and spinal CSF compartments

I. Strbačko[1], M. Radoš[1], I. Jurjević[2], D. Orešković[3] and M. Klarica[1,4]*

[1]Croatian Institute for Brain Research, School of Medicine, University of Zagreb, Zagreb, Croatia, [2]Department of Neurology, University Hospital Centre Zagreb, Zagreb, Croatia, [3]Department of Molecular Biology, Ruđer Bošković Institute, Zagreb, Croatia, [4]Department of Pharmacology, School of Medicine, University of Zagreb, Zagreb, Croatia

Introduction: It is generally accepted that during body position changes from horizontal to vertical there is a short-lasting shift of a certain CSF volume from the cranium into the hydrostatically lower parts of the spinal space, which leads to transitory CSF pressure decrease to negative values.

Methods: In order to test this, we performed MRI volumetry of cranial and spinal part of the CSF space in healthy volunteers of both genders (n = 22) in three different body positions [horizontal (H); elevated head and upper body (H-UP) under an angle about 30° from the base; elevated lower body (B-UP) under an angle about 30° from the base].

Results: Volumes of brain and spinal cord tissue did not change during body position changes. Significant CSF volume (ml) changes occur inside the spinal space in the tested body positions, primarily in the lumbosacral segment (H-UP – 38.1 ± 7.0; H – 34.4 ± 6.5; B-UP – 28.7 ± 6.5), while at the same time no significant CSF volume changes have been observed inside the cranium in two tested positions (H and B-UP) in which it was possible to measure intracranial CSF volume changes or if we sum up cervical and cranial CSF volumes in those positions.

Conclusion: Observed results suggest that during the changes of body position CSF volume redistribution occurs, primarily inside the spinal and not the cranial space. This is in accordance with the new hypothesis by which spinal intradural space can significantly change its volume due to its elasticity, thus adjusting to the influence of gravity and pressure changes.

KEYWORDS

cranial CSF volume, spinal CSF volume, body position, volume redistribution, segmentation, MR volumetry

Introduction

The intracranial space contains certain volumes of cerebrospinal fluid (CSF), cerebral blood and brain parenchyma. According to Monroe – Kellie doctrine, the sum of those volumes is constant. Thus, this doctrine has theoretical implications in the regulation of CSF pressure and volume (Davson et al., 1987). A classical concept of CSF physiology suggests that CSF flows unidirectionally from the site of its secretion to the site of its absorption (Davson

et al., 1987), which implies the existence of pressure gradient inside the CSF system with the highest pressure intracranially at the secretion site and the lowest pressure at the absorption site (Cutler et al., 1968; Pollay, 2010) in order to biophysically enable the supposed unidirectional movement. It is known that during head-up verticalization the intracranial pressure diminishes (Bradley, 1970; Magnæs, 1976a,b; Chapman et al., 1990; Antes et al., 2016), which is considered to be a transitory phenomenon. Namely, the CSF pressure should always stay positive due to continuous secretion, and its temporary decline was explained (according to Monroe-Kellie doctrine) in light of a potential short-term CSF volume redistribution from the cranial into the spinal part of the CSF system under the influence of gravity (Magnaes, 1978; Davson et al., 1987; Magnæs, 1989).

Novel research about the influence of body position on the intracranial pressure values in patients is also interpreted by a classical concept of CSF pressure regulation, according to which CSF pressure depends on the rate of CSF secretion (Vf), the resistance of the CSF circulation pathway (Ro) and the value of venous pressure (Pv) inside the dural sinuses [CSF pressure = (Vf × Ro) + Pv] where CSF absorption hypothetically occurs (Alperin et al., 2005a,b, 2016; Qvarlander et al., 2013; Holmlund et al., 2018; Linden et al., 2018). It is believed that a decrease of venous pressure inside the cranium during body verticalization diminishes CSF circulation resistance and facilitates CSF absorption into the dural sinuses (Qvarlander et al., 2013; Holmlund et al., 2018; Linden et al., 2018), suggesting that in this position a transitory decrease of intracranial CSF volume occurs.

About 15 years ago a novel concept regarding the physiology and pathophysiology of fluids inside the craniospinal space was created, according to which CSF, interstitial fluid and blood are interconnected, and the net water turnover between those three compartments depends on the gradients of hydrostatic and osmotic forces that are present between the central nervous system tissue capillaries, interstitial fluid and CSF (Bulat – Klarica –Orešković hypothesis) (Orešković and Klarica, 2010, 2011; Bulat and Klarica, 2011; Naidich et al., 2013; Thomale, 2021; Atchley et al., 2022; Theologou et al., 2022; Bajda et al., 2023). Thus, according to this concept, the CSF pressure is not dependent on the velocity of secretion inside the ventricles, the resistance to unidirectional CSF circulation from the ventricles to the cortical subarachnoid space or the pressure inside the venous sinuses (the dominant site of absorption) and that clearance of brain metabolites takes place locally (near to the site of their production) through various transport systems of the capillary network.

The role of respiration and blood vessels pulsation in CSF dynamics is being extensively researched (Balendet et al., 2004; Yamada, 2014; Orešković and Klarica, 2014), and it was observed that pulsatile CSF to-and-fro movements significantly change in various pathophysiological conditions. During the last 12 years, a glymphatic pathway concept has been developed and described in the literature (Iliff et al., 2012, 2013; Nedergaard and Goldman, 2020; Bohr et al., 2022; Smets et al., 2023). It's believed that movement of different marker substances via perivascular space into and out of the brain tissue following their application into the CSF system can help the clearance of brain metabolic waste (probably important for some neurodegenerative diseases) (Iliff et al., 2012; Nedergaard and Goldman, 2020).

Examinations done on larger experimental animals about 10 years ago (Klarica et al., 2014) implied that the intracranial CSF pressure is continuously negative during the vertical head-up position and that this is not a transitory phenomenon but a physiological CSF state inside the cranium. If the intracranial CSF pressure is continuously negative and stable in the upright position and if this is not a transitory observation, a question arises as to what is happening with the CSF volume? Is the CSF volume really redistributed between the cranial and the spinal CSF space under the influence of gravity and does this potential volume change also affect the CSF pressure value and compliance alteration in individual CSF compartments? In order to answer these questions and to improve the understanding of CSF physiology as well as CSF volume and pressure regulation in individual segments of the CSF system, we analyzed CSF volumes inside the cranial and spinal CSF space in three different body positions in healthy volunteers.

Materials and methods

Research participants

This research was done on 22 healthy volunteers, of which 11 were male and 11 were female. Subjects were 20 to 34 years old, 25.5 years on average. Their height varied from 158 to 187 cm, while they weighed between 50 and 110 kg (see Supplementary Table S1). Before the MRI imaging, all subjects filled out a standardized questionnaire where they stated their brief medical history, if they had any severe diseases or surgical procedures. We, as medical doctors, reviewed each form to ensure that our subjects were healthy (no significant health problems) and had not had surgery that could affect the cerebrospinal system. Additional analysis was done based on performed MRI imaging, and any pathological condition inside the craniospinal system was excluded.

This research gained a positive opinion of the Ethics Committee of the University of Zagreb School of Medicine (Reg. number: 380-59-10106-15-168/39, Class: 641-01/15-02/01). All subjects were thoroughly acquainted with the method of magnetic resonance imaging in writing and orally, and filled out a questionnaire with their basic and medical data in order to determine whether there were any contraindications to the safety of MRI imaging. All data obtained and used during this research are protected, anonymized and stored in the appropriate database.

MRI volumetry

MRI imaging was done in Polyclinic „Neuron" situated in Croatian Institute for Brain Research, on the MRI device with a 3 T magnetic field (Magnetom Prisma^{FIT}, Siemens, Germany). The width of the MRI device tunnel is standard and measures 60 cm. For cranial imaging, high-resolution sagittal MPRAGE T1 sequences were used, and spinal imaging was performed using high—resolution sagittal T2 sequences. Subjects were recorded in three different body positions: (1) horizontal position (H); (2) elevated lower body position (B-UP) under a certain angle α (about 30°) from the base; and (3) elevated head and upper body position (H-UP) under a certain angle β (about 30°) from the base (Figure 1).

For cranial imaging we used a 64-canal head and neck coil which is fixed to the MRI device bed and cannot be moved, so each

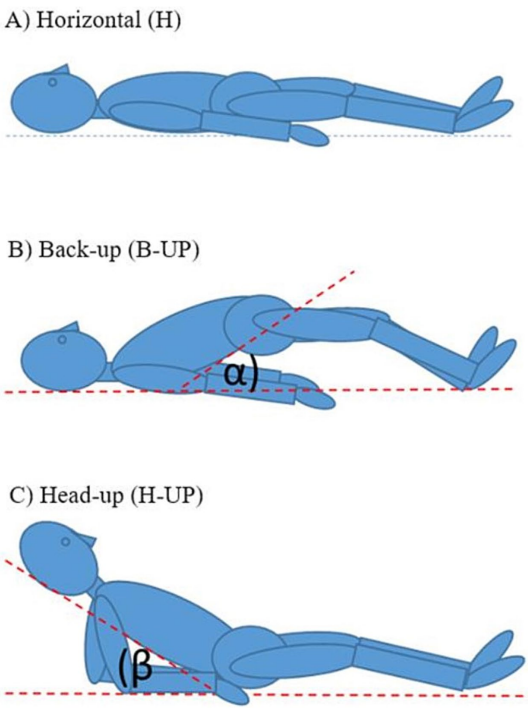

FIGURE 1
Schematic representation of the body position during MRI imaging: **(A)** horizontal position (H), **(B)** elevated lower body position (B-UP) under the certain angle α (about 30°) in relation to the base, **(C)** elevated head and the upper body position (H-UP) under the certain angle β (about 30°) in relation to the base.

participant underwent cranial imaging in two positions H and B-UP. The spinal part of the system was recorded in all three positions in each subject – for spinal imaging we used the coil fixed in the MRI device bed and a large flexible coil (Big Flexi) for spinal imaging in the B-UP position. The duration of MRI imaging per subject in all three positions was from 46 min to a maximum of 1 h and 18 min, with the average duration of 59 min and 57 s. Imaging of the cranial and spinal parts in the horizontal position (H) lasted from 17 to 36 min, an average of 23 min. Imaging of the cranial and spinal part in the elevated lower body position (B-UP) lasted from 16 to 41 min, about 24 min and 3 s on average. Imaging in the elevated head and upper body position (H-UP) was the shortest since only the spinal part was recorded, and lasted from 9 to a maximum of 20 min, an average of 12 min and 55 s.

High-resolution sagittal T1 sequences (TR/TE = 2300/3 ms, FOV = 250 × 250, voxel dimensions: 0.97 × 0.97 × 1 mm) were used for the cranial part, which are suitable for precise morphometric analysis and for automatic segmentation of the cranium. For the spinal part, high-resolution sagittal T2 sequences were used (for the horizontal position TR/TE = 1700/221 ms, FOV = 340 × 340 mm, voxel dimensions = 1.08 × 1.06 × 1.06 mm; for the position with the head and upper body raised for cervical and thoracic part TR/TE = 1700/224 ms, FOV = 390 × 390 mm, voxel dimensions 1.24 × 1.21 × 1.22 mm; for the position with the head and upper body raised for lumbosacral part TR/TE = 1980/224 ms, FOV = 380 × 380 mm, voxel dimensions: 1.21 × 1.18 × 1.25 mm; for the position with the lower body raised for cervical and thoracic part TR/TE = 1700/224 ms, FOV = 390 × 390 mm, voxel size: 1.24 × 1.21 × 1.22 mm; for position with the lower body raised for lumbosacral part TR = 1980/224 ms, FOV = 380 × 380 mm, voxel size: 1.21 × 1.18 × 1.25 mm) which provide a good contrast between the cerebrospinal fluid and the surrounding tissue, i.e., enable clear detection of the edges of the cerebrospinal fluid space, which is necessary for high-quality volumetric analysis and segmentation.

Volumetric analysis

For the interpretation of intracranial MRI imaging, we used a verified *online* programme for brain imaging analysis volBrain (Manjón and Coupé, 2016) (Figure 2). This programme was used for a quantitative analysis of the MRI signal intensity, and an automated segmentation was used to determine the total brain volume, as well as specific volumes of grey and white matter, the total CSF volume intracranially and the volume of lateral ventricles.

Due to the atypical positions of the subjects during the recording, we could not use automatic segmentation for the spinal part. For the spinal part analysis, we used a semi-automated segmentation method with the ITK SNAP programme (Yushkevich et al., 2006) (Figure 2) which, even though it is time-consuming and requires manual volume tracing, enables obtaining precise dana which was very significant considering atypical positions of the participants inside the MRI device. We analyzed the volumes of the total spinal compartment, as well as cervical, thoracic and lumbosacral parts separately, including the volumes of the spinal medulla and the cerebrospinal fluid in all three body positions.

Statistical analysis

We used Kolmogorov–Smirnov test to analyze the distribution of all continuous values, and the differences between the groups were analyzed by one-way variance analysis (engl. One Way ANOVA) with an additional *post-hoc* Bonferroni test in the case of significant differences. Graphic displays of the differences in continuous values showed the arithmetic mean with concomitant 95% confidence intervals. All p values under 0.05 were considered statistically significant. A licensed programme support MedCalc® Statistical Software version 20.106 (MedCalc Software Ltd., Ostend, Belgium; https://www.medcalc.org; 2022) was used for the analysis.

Results

Volumetric analysis of the brain and spinal medulla MRI images in different body positions

Since it is normally expected that brain and spinal medulla volumes do not change during the changes of body position, a comparation of these volumes is significant as a kind of control method for both automated brain segmentation and semiautomated medulla segmentation. By analyzing brain volumes and volumes of medulla spinalis in total as well as each (cervical, thoracic and lumbosacral) segment individually, it was determined that there was

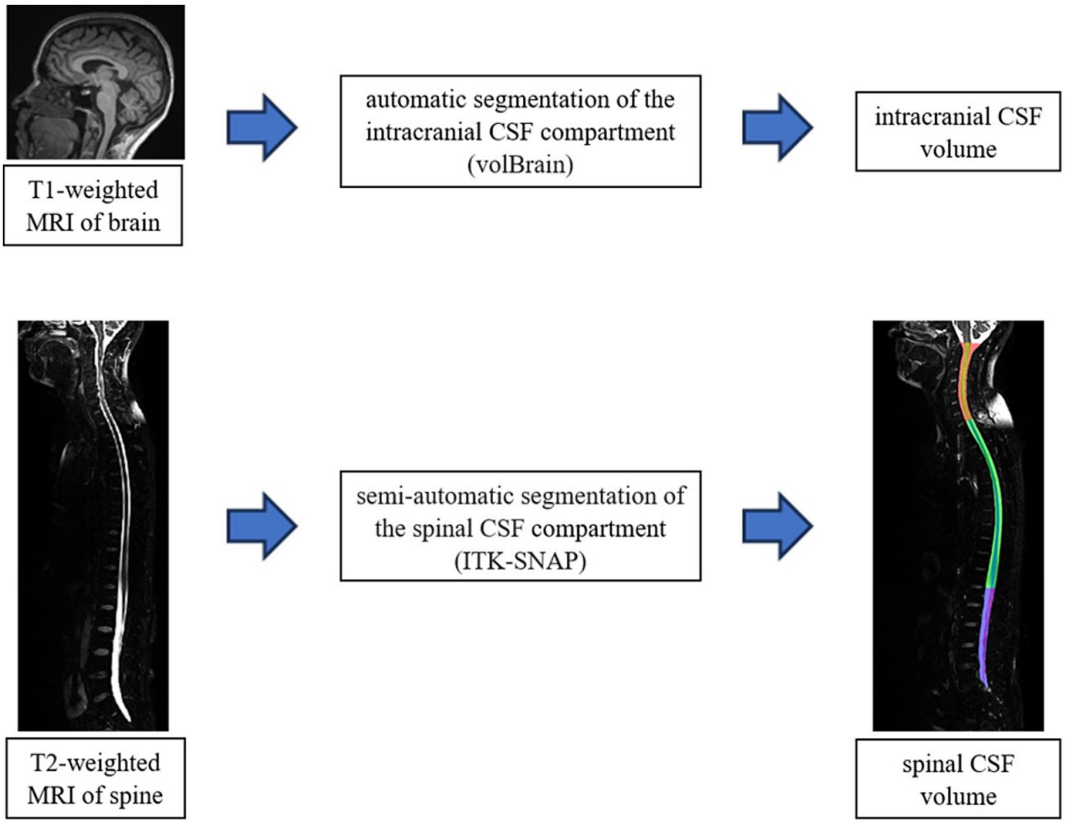

FIGURE 2
Schematic representation of the volumetric analysis process of MRI images of the brain (volBrain) and spine (ITK-SNAP). The final result of the segmentation of the spinal part (cervical-red, thoracic-green and lumbosacral-blue part) in the ITK-SNAP programme is shown in the down part of scheme.

no statistically significant difference between those volumes in different body positions, which implies that our measuring methods were reliable and our results plausible. The average brain volume in the H position was 1330.4 ± 112.1 mL; of which white mater volume was averagely 556.7 ± 66.7 mL; while the average grey matter volume was 773.8 ± 62.9 mL. In the B-UP position, the average brain volume amounted to 1333.3 ± 107.4 mL; the average white matter volume was 553.6 ± 63.5 mL; while the average grey matter volume was 779.8 ± 58.9 mL. The average measured value of the total spinal medulla volume was 29.8 ± 3.5 mL in the H position, 29.4 ± 3.1 mL in the B-UP position and 30.5 ± 3.2 mL in the H-UP position.

Intracranial CSF volume

Using automated segmentation in the volBrain programme, volumes of total intracranial CSF and of lateral ventricles CSF were measured in two positions: H position and B-UP position. By subtraction of the lateral ventricles CSF volume from the total intracranial CSF volume, the approximate value of subarachnoid CSF volume was obtained (taking into account that this volume also contains the volumes of the third and the fourth ventricle which were not individually analyzed in the volBrain programme).

By analyzing the obtained results, it was determined that there is no statistically significant difference in the volumes of the total intracranial CSF, lateral ventricles CSF or subarachnoid CSF between two studied body positions in which there were no changes of the head position (H and B-UP) (Figure 3). The average intracranial CSF volume value in H position amounts to 183.5 ± 44.9 mL, the average volume of lateral ventricles CSF was 13.2 ± 6.6 mL, and the average subarachnoid CSF volume was 170.2 ± 40.7 mL. In the B-UP position, the average intracranial CSF volume value was 184.0 ± 43.2 mL, average CSF volume of lateral ventricles was 13.4 ± 6.8 mL, and the average subarachnoid CSF volume was 170.6 ± 38.6 mL.

Influence of body position on the spinal CSF volume distribution

Analyzing the values of the total spinal CSF volume in 22 subjects and in three different body positions (H, B-UP and H-UP), it was determined that there was no statistically significant difference (Figure 4). The average value of the spinal CSF volume was 108.8 ± 19.2 mL in the H position, 102.8 ± 17.3 mL in the B-UP position and 115.9 ± 18.5 mL in the H-UP position. However, it is our observation that there is a tendency to volume change, especially during head lift. In addition, we analyzed individual values of the CSF volumes in the cervical and thoracic vertebral segments in 22 subjects in three different body positions, and it was also determined that there

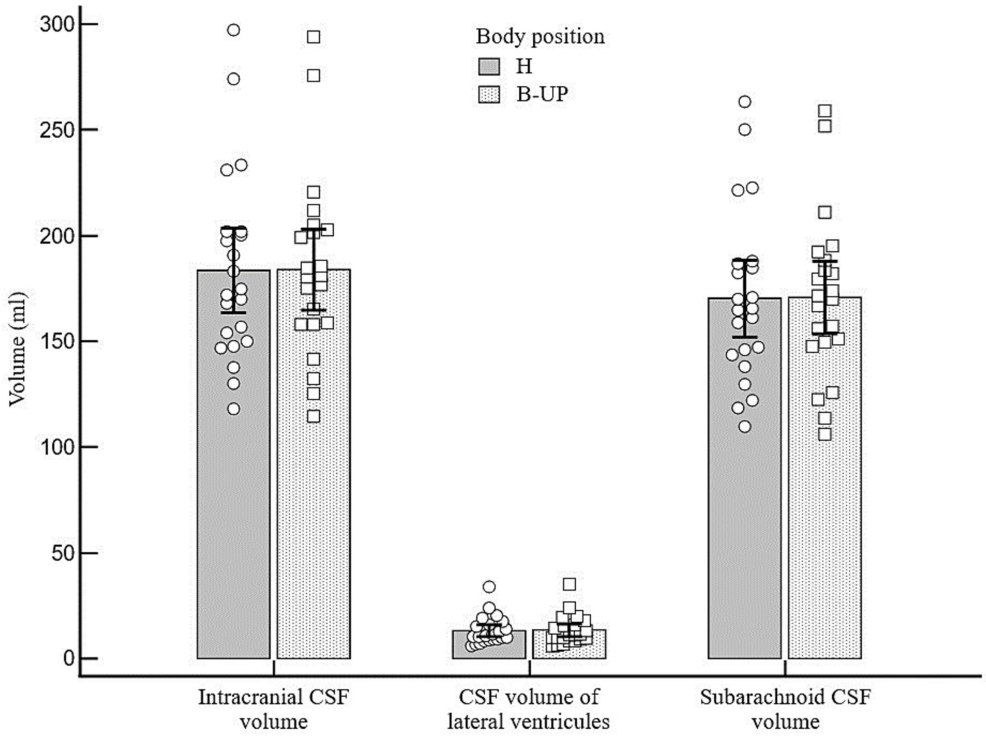

FIGURE 3
Differences between the measured values of intracranial, ventricular and subarachnoid CSF volumes (ml) related to different body positions during MRI imaging. Columns represent the values of arithmetic means of intracranial, lateral ventricles and subarachnoid CSF volumes with their 95% confidence intervals in the horizontal position (H) and in the position with the elevated lower body (B-UP), while white circles and squares represent individual values of those volumes in 22 subjects. There were no statistically significant differences in intracranial, ventricular and cranial subarachnoid CSF volumes in different body positions.

was no statistically significant difference, even when we summed up the cervical and thoracic segment and compared them that way.

Influence of body position on the lumbosacral CSF volume distribution

As for individual data, if we look at the results regarding CSF volumes in the lumbosacral part, 19 out of 22 subjects had lower CSF volume in the B-UP position compared to the horizontal position, while 21 out of 22 subjects had higher CSF volume in the H-UP position compared to the horizontal position. The analysis of variance was used to study CSF volume values in the lumbosacral segment in 22 subjects and in three different body positions, and a statistically significant difference was obtained between different body positions on MRI imaging ($p < 0.001$) (Figure 5). An additional *post-hoc* Bonferroni analysis showed significant differences primarily between H position and B-UP position ($p = 0.016$), and between the H-UP and B-UP positions ($p < 0.001$). The highest average values were in the H-UP position (38.1 ± 7.0 mL), followed by the H position (34.4 ± 6.5 mL), while the lowest values were in the B-UP position (28.7 ± 6.5 mL). We also analyzed volumes of the total CSF in the thoracic and lumbosacral parts of the spine in 22 subjects and in three different body positions (Figure 6). The analysis of variance was performed and a significant difference was detected between three different body positions ($p = 0.011$) regarding the total thoracic and lumbosacral CSF volume. An additional *post-hoc* Bonferroni analysis showed a significant difference primarily between the H-UP and B-UP positions ($p = 0.009$). The highest average CSF volume values in the thoracic and lumbosacral parts were in the H-UP position (88.1 ± 14.5 mL), while they were lowest in the B-UP position (74.6 ± 14.1 mL). The average total thoracic and lumbosacral CSF volume in the H position measured 80.8 ± 15.1 mL.

Influence of body position on the total craniospinal CSF volume distribution

The average total intracranial and spinal CSF volume measured 292.2 ± 55.4 mL in the H position and 286.8 ± 53.9 mL in the B-UP position, while average total intracranial and cervical CSF volume measured 211.4 ± 46.7 mL in the H position and 212.2 ± 45.2 mL in the B-UP position. A one-way analysis of variance showed no statistically significant difference between the mentioned volumes, which implies that body position changes had no significant influence on the CSF volume.

Discussion

Our study shows that the amount of total craniospinal CSF volume in healthy volunteers is much higher than stated in the current

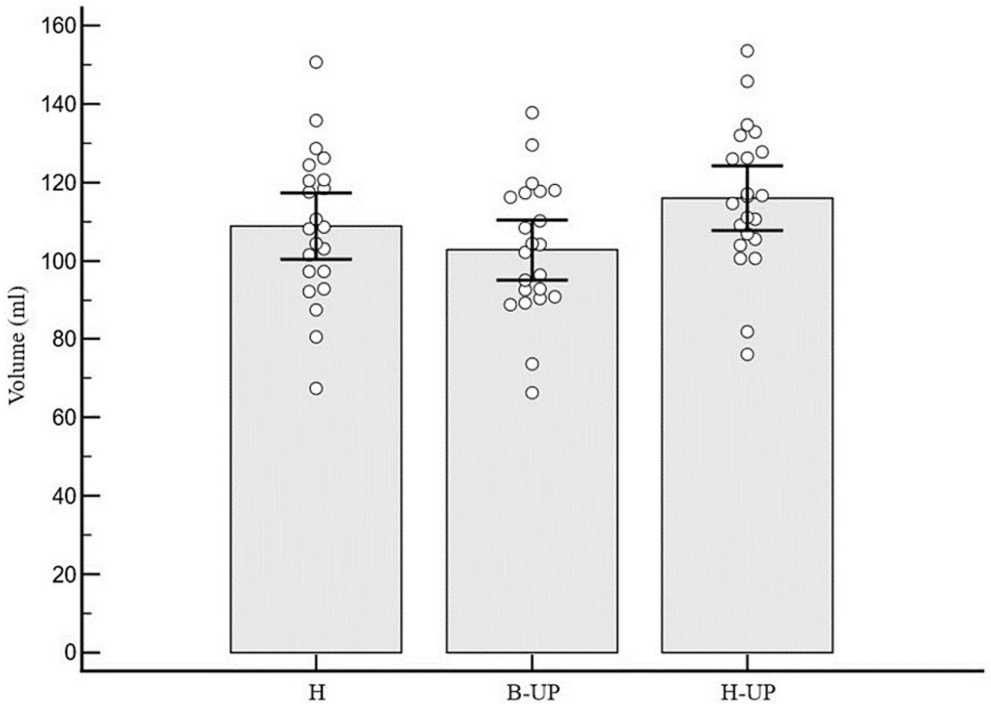

FIGURE 4
Differences between measured values of the total spinal CSF volume (ml) related to body position during MRI imaging. Columns represent the values of arithmetic means of total spinal CSF volume with their 95% confidence intervals in horizontal position (H), in the position with elevated lower body (B-UP) and in the position with elevated head and upper body (H-UP), while white circles represent individual values of those volumes in 22 subjects. There were no statistically significant differences between the measured total spinal CSF volume in different body positions.

textbooks, and that changes in body position lead to CSF volume alterations in line with the new hypothesis according to which spinal intradural space, due to its elasticity, can significantly change its volume, thus adjusting to the influence of gravity and other pathophysiological changes of neurofluid volume and pressure. Namely, significant CSF volume changes occur inside the spinal space in the tested body positions, primarily in the lumbosacral segment (Figures 5, 6), while at the same time no significant CSF volume changes have been observed inside the cranium in two tested positions in which it was possible to measure intracranial CSF volume changes (Figure 3), or if we added up cervical and cranial CSF volumes in those positions (see Results).

Correlation between participant age/ height and CSF volume

Most previously published studies showed that the total intracranial CSF volume is about 150 mL with 25 mL inside the lateral ventricles (Sakka et al., 2011; Naidich et al., 2013; Brinker et al., 2014; Miyajima and Arai, 2015). More recent studies reveal that intracranial volumes change linearly, depending on the participants' age (Beheshti et al., 2019; Statsenko et al., 2021; Yamada et al., 2023). In the study done on 133 healthy volunteers between 21 and 92 years of age, an increase of intracranial CSF volume of about 30 mL per decade, starting from 265 mL in the twenties and up to 488 mL above 80 years was observed (Yamada et al., 2023). It was detected that CSF volume inside the lateral ventricles changes very little up to 60 years (average volume around 20 mL), however, it significantly increases after 60 years of age. The average age of our subjects of both genders was 25.5 years (20–34 years), and the total cranial CSF volume was about 184 mL with 13 mL inside the lateral ventricles, which fits well with the mentioned study results.

The total spinal CSF volume was about 81 mL (range 52–103 mL) in 22 healthy elderly volunteers, of which the cervical CSF volume was about 19 mL, the thoracic CSF volume was about 38 mL and the lumbosacral CSF volume was about 25 mL (Edsbagge et al., 2011). Spinal CSF volume in that age group did not significantly correlate with the subject gender or height. Contrary to that, a study done on pediatric population (Jang et al., 2019) showed linear correlations with the subject height and weight. The mean thoracolumbosacral CSF volume per weight (ml/kg) was 1.95 in neonates and infants, 1.82 mL in toddlers and preschoolers, 1.38 in schoolers and 0.99 in adolescents (Jang et al., 2019). In our study on younger healthy volunteers, the average value of the total spinal CSF volume was 108.8 mL, and it was observed that there is a correlation between their height and CSF volume in the spinal subarachnoid space (Table 1).

Thus, by analyzing the existing results from the literature as well as our results, it can be concluded that a significant correlation exists between the participants' age and the intracranial CSF volume, as well as between their age and the total craniospinal CSF volume, which

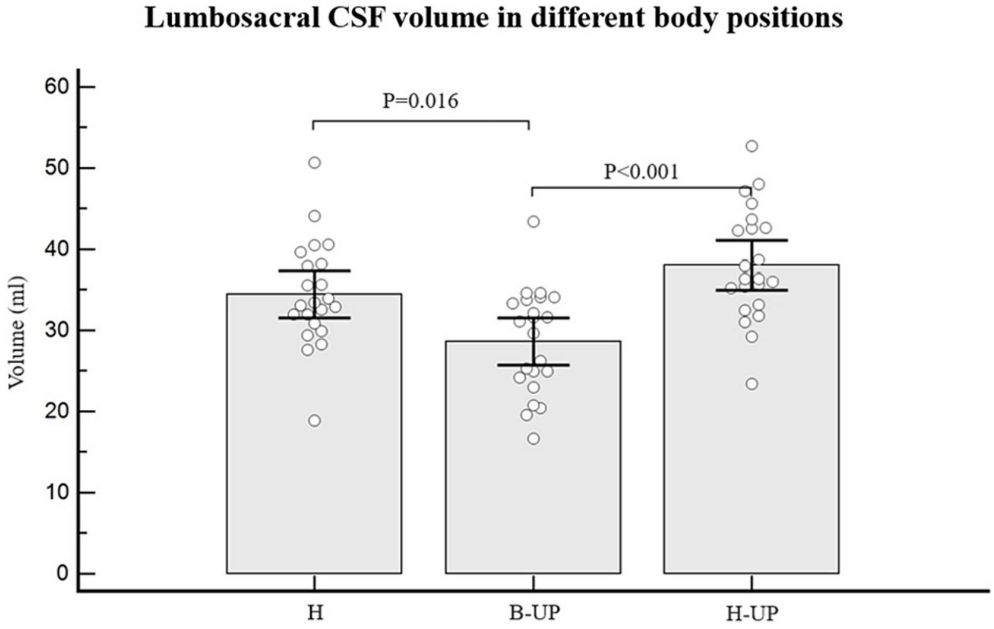

FIGURE 5
Differences between measured values of lumbosacral CSF volume (ml) related to the changes of body position during MRI imaging. Columns represent the values of arithmetic means of lumbosacral CSF volumes with their 95% confidence intervals in the horizontal position (H), in the position with the elevated lower body (B-UP) and in the position with the elevated head and upper body (H-UP), while white circles represent individual values of those volumes in 22 subjects. The analysis of variance determined significant difference between the three MRI measuring positions ($p < 0.001$). An additional post-hoc Bonferroni analysis showed significant differences primarily between the horizontal (H) position and the elevated lower body position (B-UP) ($p = 0.016$), as well as between the elevated head and upper body position (H-UP) and the elevated lower body position (B-UP) ($p < 0.001$).

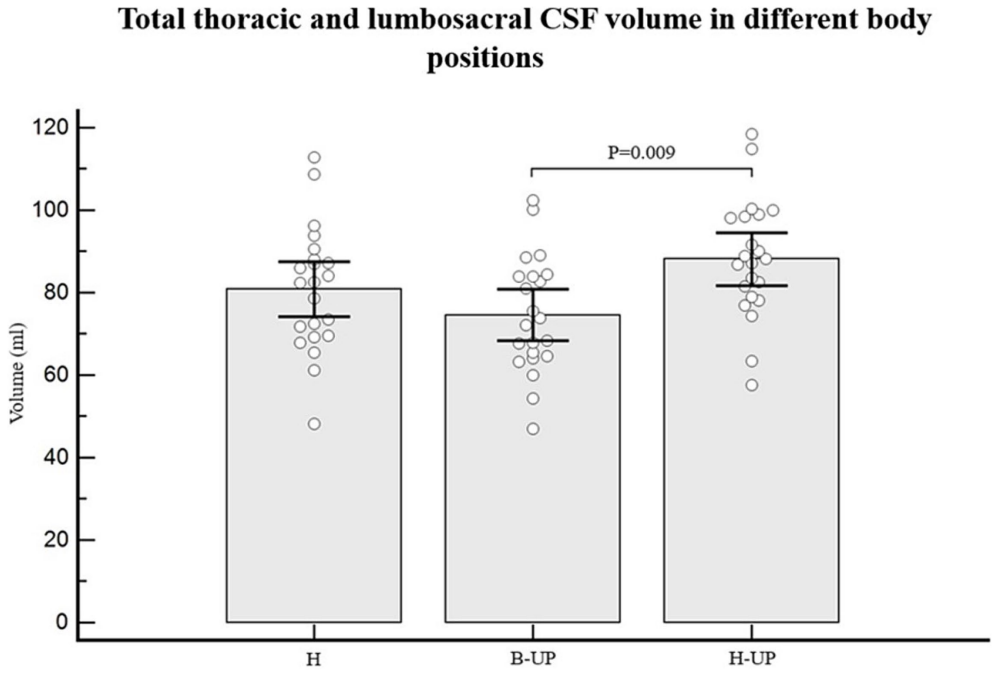

FIGURE 6
Differences between measured values of total thoracic and lumbosacral CSF volume (ml) related to the changes of body position during MRI imaging. Columns represent the values of arithmetic means of the total thoracic and lumbosacral CSF volumes with their 95% confidence intervals in horizontal position (H), in the position with elevated lower body (B-UP) and in the position with elevated head and upper body (H-UP), while white circles represent individual values of those volumes in 22 subjects. A post-hoc Bonferroni analysis showed significant differences primarily between the elevated head and upper body position (H-UP) and the elevated lower body position (B-UP) ($p = 0.009$).

TABLE 1 Correlations between the subjects age and height, and their spinal, cranial and total spinal + cranial CSF volumes (volume values from the horizontal position) shows a significant positive correlation between the age and the cranial CSF volume (correlation coefficient = 0.432), as well as between the age and the total spinal + cranial CSF volume (correlation coefficient = 0.336).

Correlations					
			CSF spinal horizontal (ml)	CSF intracranial horizontal (ml)	Total CSF intracranial + spinal horizontal (ml)
Kendall tau_b coefficient	Age	Correlation coefficient	0.038	0.432**	0.336*
		p	0.815	0.009	0.041
		N	22	22	22
	Height (cm)	Correlation coefficient	0.329*	0.039	0.110
		p	0.034	0.799	0.480
		N	22	22	22

* Correlation is significant at the 0.05 level (2-tailed). ** Correlation is significant at the 0.01 level (2-tailed). The spinal CSF volume is significantly positively correlated to height (correlation coefficient = 0.329).

means that older age is related to a larger CSF volume both inside the cranium, and inside the cranial and spinal space combined. The spinal CSF volume in healthy young volunteers was also positively correlated to their height, which implies that higher participants have larger spinal CSF volumes. However, our previous study on NPH patients older than 65 did not show that the spinal CSF volume correlates significantly with the patients' height (Kudelić et al., 2023) which is similar to results from another study on healthy elderly volunteers (Edsbagge et al., 2011). Thus, it seems that age and height differences between subjects can only partly explain the variations in results obtained by a volumetric analysis of the total intracranial CSF in mentioned studies.

Both in this study on healthy young volunteers as well as in our previous study on NPH patients in which total, cranial and spinal CSF volumes were determined, it can be easily observed that the total CSF volumes in certain individuals were significantly larger than it was previously published. Namely, in the NPH patients' study, the total CSF volumes varied from 254.8 mL to 594.1 mL (mean 422.8 ± 108.4 mL) (Kudelić et al., 2023). Even when 70 mL (an average increase of the ventricular volume due to hydrocephalus) was subtracted, the total volume was still significantly larger (around 350 mL) than it was previously believed (around 150 mL). In this study on healthy volunteers, the total CSF volume varied from an average of 292.2 ± 55.4 mL in the horizontal position to 286.8 ± 53.9 mL in the B-UP position (see Results). It can be concluded from our two craniospinal volumetry studies that both total and cranial CSF volumes notably depend on the subject age and that they increase as one is getting older.

Influence of body position changes on the intracranial CSF volume

Despite the fact that the craniospinal CSF system makes a sole functional unit, most investigations are limited to the analysis of the cranial CSF space, completely disregarding the spinal part of the CSF system. Our previous experimental observations on cats and on a model show that changes of body position can significantly expand or narrow the spinal dura in the lumbosacral and vertebral segments (Klarica et al., 2014, 2019), which is why our earlier publications (Klarica et al., 2009; Bulat and Klarica, 2011; Jurjević et al., 2011) described the spinal dural space as the dominant site for the compensation of acute volume changes inside the craniospinal CSF space. Volume changes in the lumbosacral segment have been noticed even before (Martins et al., 1972) during various physiological processes such as changes of breathing depth, Valsalva test, etc. Keeping in mind the biophysical characteristics of the dura (Tunturi, 1978), we assumed that body position changes, due to the influence of hydrostatic forces, will lead to the widening of certain parts of the CSF system (most prominently at the site with the highest hydrostatic force, i.e., the lumbosacral part) and to CSF redistribution predominantly inside the spinal CSF system which can alter its volume, while the intracranial CSF volume would remain within the normal range, without statistically significant variations.

In two described body positions (H and B-UP) there was no significant change of the intracranial CSF volume. Moreover, with further detailed analyses no significant CSF volume changes were observed in the subarachnoid space or in the ventricular system (Figure 3). A classical hypothesis assumes that during the head-up verticalization a significant CSF shift occurs into the spinal part of the CSF system under the influence of gravity (Magnæs, 1976a,b, 1989; Magnaes, 1978; Davson et al., 1987). It was observed with MRI and ultrasound that during body verticalization there is a simultaneous CSF shift in the cervical segment together with cervical vein expansion (Alperin et al., 2005a,b), which indirectly suggests that CSF moves from the cranial into the spinal compartment. Furthermore, it is believed that this CSF displacement is the cause of a short-term pressure decrease during the head-up verticalization. Namely, numerous studies have noted that during the changes of body position from the horizontal to sitting or standing positions there is a drop of intracranial pressure which often reaches subatmospheric values (Masserman, 1934; Loman, 1935; Von Storch, 1937; Bradley, 1970; Fox et al., 1973; Portnoy et al., 1973; McCullough and Fox, 1974; Chapman et al., 1990; Antes et al., 2016). According to the classical concept, this pressure change is short-lasting considering the constant CSF secretion, thus compensating the displaced volume. However, it was described on MRI imaging done with the changes of body position from the horizontal to head-up that the cervical section of CSF space becomes narrower (Alperin et al., 2005a,b). This data suggests that CSF is more significantly displaced from the cervical segment into the

hydrostatically lower parts than it is shifted from the cranial into the spinal part, as the latter would lead to the widening of the cervical segment, or it should at least stay the same as before the changes of body position.

Our results cannot be explained by the classical hypothesis, however, they fit into the new concept of CSF physiology created by our research group, with one of the basic postulates being the preservation of neurofluid volumes (blood, CSF, interstitial fluid) inside the intracranial space (Orešković et al., 2002, 2017a,b; Orešković and Klarica, 2010, 2011, 2014; Bulat and Klarica, 2011; Klarica et al., 2014; Radoš et al., 2014; Klarica et al., 2019). Namely, that concept interprets the mentioned CSF pressure decrease by the physical laws that can be applied to the fluids enclosed inside the spaces with hard walls (spaces with low elasticity) which cannot significantly alter their volumes (Klarica et al., 2014). Our hypothesis presumes that the CSF volume inside the intracranial space is only modestly changeable, and that it is not significantly dependent on the body position. Thus, during the changes of body position, the CSF pressure inside the cranial space changes significantly, however, without significant CSF volume changes (Klarica et al., 2014).

It appears that the cranial space preserves volume, since it was also noticed that there is no significant intracranial CSF volume change during the changes of its volume throughout the entire craniospinal space due to the lumbar CSF extraction (Alperin et al., 2016; Nikić et al., 2016). Thus, the CSF volume decrease in the spinal part caused by lumbar drainage did not lead to significant CSF volume changes inside the cranium, i.e., there was no extraction or redistribution of CSF from the cranial into the spinal part, even though the CSF pressure certainly changed significantly.

Distribution of the spinal CSF volume during the changes of body position

The total spinal CSF volume was without any significant change (Figure 4), which implies that there was no notable CSF displacement from the cranial into the spinal part during body position changes (H to B-UP) as it was previously assumed, but there was primarily a redistribution of CSF volume within the spinal part of the system. The spinal CSF redistribution is best displayed in Figure 5, which shows the results of a lumbosacral segment volumetric analysis, thus confirming our expectation that CSF redistribution will be most pronounced in the most caudal part of the spinal system, in which epidural space is the widest and where hydrostatic pressure is predominantly changed.

During the change of body position from H to B-UP there is a statistically significant CSF volume reduction in the lumbosacral segment ($p < 0.016$). An additional volumetric analysis shows that the lumbosacral CSF volume is significantly larger in the H-UP position compared to the previous B-UP position ($p < 0.001$). Results imply that the dural sac in the lumbosacral segment can significantly alter its volume (the smallest average CSF volume in the lumbosacral segment was 28.7 mL in the B-UP position, while the largest volume was 38.1 mL in the H-UP position), depending on the fullness of the CSF system. Thus, it seems that lifting the head and upper body leads to CSF redistribution from the cervical and thoracic segment into the more caudal lumbosacral segment under the influence of gravity. This redistribution is biophysically possible due to the fact that spinal dura can be significantly narrowed and distended since it is not firmly attached to the bone as it is in the cranium, but it hangs freely inside the spinal canal (Martins et al., 1972).

With lifting the lower part of the body, our results show a decrease of CSF volume inside the lumbosacral segment, probably due to the CSF redistribution to the more cranial parts of the spinal CSF system. In this position we also measured the intracranial CSF volume which did not differ significantly compared to the horizontal position, so we can conclude that the CSF shift is predominantly restricted to the spinal part of the CSF system.

From a biophysical standpoint, a slight additional volume shift is possible from the cranium into the perioptic space (in the B-UP position), as well as from the perioptic space into the cranium and from the cranium into the spinal space (in the H-UP position). Since the CSF volume surrounding the optical nerve is very small, that shift should not lead to any significant change of the spinal volume (as can be seen in Figure 4). As a limitation of this study, it should certainly be pointed out that we observed CSF volume changes during the changes of the body position mostly 30 degrees from the position of the head. It is possible that more pronounced changes in the vertical head-up body position (90 degrees) or vertical head-down position (270 degrees) would also lead to more significant CSF volume redistribution inside the spinal canal.

Clinical implications of our results

The results obtained in this research cannot be explained by a classical concept of CSF physiology, but they fit into the new concept designed by our research group, according to which biophysical characteristics of the craniospinal system are of utmost importance for the understanding of the changes of CSF pressure and volume during the changes of body position.

It is our belief that the negative intracranial pressure during the head-up verticalization is not a consequence of significant CSF shift, however, it can be explained by the Law of fluid mechanics which describe how fluid (CSF) acts inside the rigid (cranial) space opened at the bottom (foramen magnum), while the spinal part is pivotal for the compensation of volume changes throughout the entire craniospinal CSF system due to its unique biophysical characteristics (Klarica et al., 2014). The cranium plays an important role in the prevention of significant changes in the volumes of blood, CSF and brain parenchyma, and it does not allow any sudden changes of those volumes during normal daily activities, enabling an adequate brain perfusion in the vertical head-up position. This can be corroborated by numerous clinical issues that patients often have after craniectomy (Ashayeri et al., 2016; Tarr et al., 2020; Mustroph et al., 2022).

The mentioned redistribution of CSF inside the spinal canal due to the changes of body position could provide a reason for faster redistribution of the substances applied into the cisterna magna within the spinal subarachnoid space compared to their distribution into the cranial space if the human subjects or experimental animals move freely post application (Vladić et al., 2000, 2009; Klarica et al., 2019). Namely, CSF volume movement, which during inactivity mostly occurs due to pulsations (Orešković and Klarica, 2014), is additionally enhanced during body position changes due to gravitational redistribution inside the spinal canal (Klarica et al., 2019). This

phenomenon significantly affects the distribution of both metabolites and drugs applied intrathecally for various indications (Kouzehgarani et al., 2021).

Conclusion

Changes of body position from horizontal to those with head above or below level of the remaining body caused significant CSF volume redistribution inside the spinal subarachnoid space of healthy volunteers, while CSF volume inside the cranium did not significantly change, nor did the volumes of brain tissue and spinal cord.

Limitations

In this research, we had a relatively small number of subjects, although sufficient for statistical analysis, with whom we changed the body position by only 30 degrees. Body position changes are significantly limited by the width of the tunnel (60 cm) in which the patient is located during MR imaging. Another important limitation concerns the coils, which must be placed directly next to the part of the body being recorded. Due to the mentioned technical limitations, intracranial CSF volumes can only be recorded in the horizontal position (H) and in the position with raised lower part of the trunk (B-UP). It would be very meaningful to record intracranial and spinal volumes in the head-up (H-UP) position, as we would expect even more significant changes in terms of cervico-lumbar redistribution of the CSF volume.

Data availability statement

The raw data supporting the conclusions of this article will be made available by the authors, without undue reservation.

Ethics statement

The studies involving humans were approved by Ethics Committee of the University of Zagreb School of Medicine. The studies were conducted in accordance with the local legislation and institutional requirements. The participants provided their written informed consent to participate in this study.

Author contributions

IS: Data curation, Formal analysis, Investigation, Methodology, Writing – original draft. MR: Conceptualization, Data curation, Formal analysis, Investigation, Methodology, Supervision, Validation, Writing – original draft, Writing – review & editing. IJ: Formal analysis, Investigation, Methodology, Validation, Writing – original draft, Writing – review & editing. DO: Formal analysis, Methodology, Supervision, Writing – original draft. MK: Conceptualization, Formal analysis, Funding acquisition, Methodology, Project administration, Supervision, Writing – original draft, Writing – review & editing.

Funding

The author(s) declare that financial support was received for the research, authorship, and/or publication of this article. This work has been supported by the Croatian Science Foundation and the Ministry of Science and Education of the Republic of Croatia (Project: Pathophysiology of cerebrospinal fluid and intracranial pressure. No. 108-1080231-0023). The research was co-financed by the Scientific Centre of Excellence for Basic, Clinical and Translational Neuroscience (project "Experimental and clinical research of hypoxic–ischemic damage in perinatal and adult brain"; GA KK01.1.1.01.0007 funded by the European Union through Europe).

Acknowledgments

We would like to thank MRI technologist Tomislav Brateljenović for technical assistance in performing the study.

Conflict of interest

The authors declare that the research was conducted in the absence of any commercial or financial relationships that could be construed as a potential conflict of interest.

Publisher's note

Supplementary material

The Supplementary material for this article can be found online at: https://www.frontiersin.org/articles/10.3389/fnhum.2024.1463740/full#supplementary-material

References

Alperin, N., Bagci, A. M., Lee, S. H., and Lam, B. L. (2016). Automated quantitation of spinal CSF volume and measurement of Craniospinal CSF redistribution following lumbar withdrawal in idiopathic intracranial hypertension. *AJNR Am. J. Neuroradiol.* 37, 1957–1963. doi: 10.3174/AJNR.A4837

Alperin, N., Hushek, S. G., Lee, S. H., Sivaramakrishnan, A., and Lichtor, T. (2005a). MRI study of cerebral blood flow and CSF flow dynamics in an upright posture: the effect of posture on the intracranial compliance and pressure. *Acta Neurochir. Suppl.* 95, 177–181. doi: 10.1007/3-211-32318-X_38

Alperin, N., Lee, S. H., Sivaramakrishnan, A., and Hushek, S. G. (2005b). Quantifying the effect of posture on intracranial physiology in humans by MRI flow studies. *J. Magn. Reson. Imaging* 22, 591–596. doi: 10.1002/jmri.20427

Antes, S., Tschan, C. A., Heckelmann, M., Breuskin, D., and Oertel, J. (2016). Telemetric intracranial pressure monitoring with the Raumedic Neurovent P-tel. *World Neurosurg.* 91, 133–148. doi: 10.1016/j.wneu.2016.03.096

Ashayeri, K., Jackson, E., Huang, J., Brem, H., and Gordon, C. R. (2016). Syndrome of the trephined: a systematic review. *Neurosurgery* 79, 525–534. doi: 10.1227/NEU.0000000000001366

Atchley, T. J., Vukic, B., Vukic, M., and Walters, B. C. (2022). Review of cerebrospinal fluid physiology and dynamics: a call for medical education reform. *Neurosurgery* 91, 1–7. doi: 10.1227/neu.0000000000002000

Bajda, J., Pitla, N., and Gorantla, V. R. (2023). Bulat-Klarica-Oreskovic hypothesis: a comprehensive review. *Cureus* 15:e45821. doi: 10.7759/cureus.45821

Balendet, O., Gondry-Jouet, C., Meyer, M.-E., DeMarco, G., Le Gars, D., Henry-Feugeas, M.-C., et al. (2004). Relationship between cerebrospinal fluid and blood dynamics in healthy volunteers and patients with communicating hydrocephalus. *Invest. Radiol.* 39, 45–55. doi: 10.1097/01.rli.0000100892.87214.49

Beheshti, I, Nugent, S, Potvin, O, and Duchesne, S. (2019). Bias-adjustment in neuroimaging-based brain age frameworks: A robust scheme. *Neuroimage Clin.* 24:102063. doi: 10.1016/j.nicl.2019.102063

Bohr, T., Hjorth, P. G., Holst, S. C., Hrabetová, S., Kiviniemi, V., Lilius, T., et al. (2022). The glymphatic system: current understanding and modeling. *iScience* 25:104987. doi: 10.1016/j.isci.2022.104987

Bradley, K. C. (1970). Cerebrospinal fluid pressure. *J. Neurol. Neurosurg. Psychiatry* 33, 387–397. doi: 10.1136/jnnp.33.3.387

Brinker, T, Stopa, E, Morrison, J, and Klinge, P. (2014). A new look at cerebrospinal fluid circulation. *Fluids Barriers CNS.* 11:10. doi: 10.1186/2045-8118-11-10

Bulat, M., and Klarica, M. (2011). Recent insights into a new hydrodynamics of the cerebrospinal fluid. *Brain Res. Rev.* 65, 99–112. doi: 10.1016/j.brainresrev.2010.08.002

Chapman, P. H., Cosman, E. R., and Arnold, M. A. (1990). The relationship between ventricular fluid pressure and body position in Normal subjects and subjects with shunts: a telemetric study. *Neurosurgery* 26, 181–189. doi: 10.1227/00006123-199002000-00001

Cutler, R. W. P., Page, L., Galicich, J., and Watters, G. V. (1968). Formation and absorption of cerebrospinal fluid in man. *Brain* 91, 707–720. doi: 10.1093/brain/91.4.707

Davson, H., Welch, K., and Segal, M. B. (1987). The physiology and pathophysiology of the cerebrospinal fluid. Edinburgh: Churchill Livingstone.

Edsbagge, M., Starck, G., Zetterberg, H., Ziegelitz, D., and Wikkelso, C. (2011). Spinal cerebrospinal fluid volume in healthy elderly individuals. *Clin. Anat.* 24, 733–740. doi: 10.1002/ca.21153

Fox, J. L., McCullough, D. C., and Green, R. C. (1973). Effect of cerebrospinal fluid shunts on intracranial pressure and on cerebrospinal fluid dynamics: 2. A new technique of pressure measurements: results and concepts 3. A concept of hydrocephalus. *J. Neurol. Neurosurg. Psychiatry* 36, 302–312. doi: 10.1136/jnnp.36.2.302

Holmlund, P., Eklund, A., Koskinen, L. O. D., Johansson, E., Sundstrom, N., Malm, J., et al. (2018). Venous collapse regulates intracranial pressure in upright body positions. *Am. J. Physiol. Regul. Integr. Comp. Physiol.* 314, R377–R385. doi: 10.1152/ajpregu.00291.2017

Iliff, J. J., Wang, M., Liao, Y., Plogg, B. A., Peng, W., Gundersen, G. A., et al. (2012). A paravascular pathway facilitates CSF flow through the brain parenchyma and the clearance of interstitial solutes, including amyloid β. *Sci. Transl. Med.* 4:147ra111. doi: 10.1126/SCITRANSLMED.3003748

Iliff, J. J., Wang, M., Zeppenfeld, D. M., Venkataraman, A., Plog, B. A., Liao, Y., et al. (2013). Cerebral arterial pulsation drives paravascular CSF—interstitial fluid exchange in the murine brain. *J. Neurosci.* 33, 18190–18199. doi: 10.1523/JNEUROSCI.1592-13.2013

Jang, Y. E., Lee, J. H., Seo, Y. S., Yoon, H. C., Lee, H. S., Lee, H. J., et al. (2019). Lumbosacral and thoracolumbosacral cerebrospinal fluid volume changes in neonates, infants, children, and adolescents: a retrospective magnetic resonance imaging study. *Paediatr. Anaesth.* 29, 92–97. doi: 10.1111/pan.13530

Jurjević, I., Radoš, M., Orešković, J., Prijić, R., Tvrdeić, A., and Klarica, M. (2011). Physical characteristics in the new model of the cerebrospinal fluid system. *Coll. Antropol.* 35, 51–56.

Klarica, M., Orešković, D., Božić, B., Vukić, M., Butković, V., and Bulat, M. (2009). New experimental model of acute aqueductal blockage in cats: effects on cerebrospinal fluid pressure and the size of brain ventricles. *Neuroscience* 158, 1397–1405. doi: 10.1016/j.neuroscience.2008.11.041

Klarica, M., Radoš, M., Erceg, G., Petošić, A., Jurjević, I., and Orešković, D. (2014). The influence of body position on cerebrospinal fluid pressure gradient and movement in cats with Normal and impaired Craniospinal communication. *PLoS One* 9:e95229. doi: 10.1371/journal.pone.0095229

Klarica, M., Radoš, M., and Orešković, D. (2019). The movement of cerebrospinal fluid and its relationship with substances behavior in cerebrospinal and interstitial fluid. *Neuroscience* 414, 28–48. doi: 10.1016/j.neuroscience.2019.06.032

Kouzehgarani, G. N., Feldsien, T., Engelhard, H. H., Mirakhur, K. K., Phipps, C., Volker Nimmrich, V., et al. (2021). Harnessing cerebrospinal fluid circulation for drug delivery to brain tissues. *Adv. Drug Deliv. Rev.* 173, 20–59. doi: 10.1016/j.addr.2021.03.002

Kudelić, N, Koprek, I, Radoš, M, Orešković, D, Jurjević, I, Klarica, M, et al. (2023). Predictive value of spinal CSF volume in the preoperative assessment of patients with idiopathic normal-pressure hydrocephalus. *Front Neurol.* 14:1234396. doi: 10.3389/fneur.2023.1234396

Linden, C., Qvarlander, S., Johannesson, G., Johansson, E., Ostlund, F., Malm, J., et al. (2018). Normal-tension glaucoma has normal intracranial pressure: a prospective study of intracranial pressure and intraocular pressure in different body positions. *Ophtalmology* 125, 361–368. doi: 10.1016/j.ophtha.2017.09.022

Loman, J. (1935). Effects of alterations in posture on the cerebrospinal fluid pressure. *Arch. Neurol. Psychiatr.* 33, 1279–1295. doi: 10.1001/archneurpsyc.1935.02250180138007

Magnæs, B. (1976a). Body position and cerebrospinal fluid pressure. Part 1: clinical studies on the effect of rapid postural changes. *J. Neurosurg.* 44, 687–697. doi: 10.3171/jns.1976.44.6.0687

Magnaes, B. (1976b). Body position and cerebrospinal fluid pressure. Part 2: clinical studies on orthostatic pressure and the hydrostatic indifferent point. *J. Neurosurg.* 44, 698–705. doi: 10.3171/jns.1976.44.6.0698

Magnaes, B. (1978). Movement of cerebrospinal fluid within the craniospinal space when sitting up and lying down. *Surg. Neurol.* 10, 45–49. PMID: 684606

Magnæs, B. (1989). Clinical studies of cranial and spinal compliance and the Craniospinal flow of cerebrospinal fluid. *Br. J. Neurosurg.* 3, 659–668. doi: 10.3109/02688698908992689

Manjón, J. V., and Coupé, P. (2016). volBrain: an online MRI brain Volumetry system. *Front. Neuroinform.* 10:30. doi: 10.3389/fninf.2016.00030

Martins, A. N., Wiley, J. K., and Myers, P. W. (1972). Dynamics of the cerebrospinal fluid and the spinal dura mater. *J. Neurol. Neurosurg. Psychiatry* 35, 468–473. doi: 10.1136/jnnp.35.4.468

Masserman, J. H. (1934). Cerebrospinal hydrodinamics. *Arch. Neurol. Psychiatr.* 32, 523–533. doi: 10.1001/archneurpsyc.1934.02250090060006

McCullough, D. C., and Fox, J. L. (1974). Negative intracranial pressure hydrocephalus in adults with shunts and its relationship to the production of subdural hematoma. *J. Neurosurg.* 40, 372–375. doi: 10.3171/jns.1974.40.3.0372

Miyajima, M, and Arai, H. (2015). Evaluation of the Production and Absorption of Cerebrospinal Fluid. *Neurol Med Chir (Tokyo).* 55, 647–56. doi: 10.2176/nmc.ra.2015-0003

Mustroph, C. M., Stewart, C. M., Mann, L. M., Saberian, S., Deibert, C. P., and Thompson, P. W. (2022). Systematic review of syndrome of the trephined and reconstructive implications. *J. Craniofac. Surg.* 33, e647–e652. doi: 10.1097/SCS.0000000000008724

Naidich, T. P., Castillo, M., Cha, S., and Smirniotopoulos, J. G. (2013). Imaging of the brain. Philadelphia: Elsevier Saunders.

Nedergaard, M., and Goldman, S. A. (2020). Glymphatic failure as a final common pathway to dementia. *Science* 370, 50–56. doi: 10.1126/science.abb8739

Nikić, I., Radoš, M., Frobe, A., Vukić, M., Orešković, D., and Klarica, M. (2016). The effects of lumboperitoneal and ventriculoperitoneal shunts on the cranial and spinal cerebrospinal fluid volume in a patient with idiopathic intracranial hypertension. *Croat. Med. J.* 57, 293–297. doi: 10.3325/cmj.2016.57.293

Orešković, D., and Klarica, M. (2010). The formation of cerebrospinal fluid: nearly a hundred years of interpretations and misinterpretations. *Brain Res. Rev.* 64, 241–262. doi: 10.1016/j.brainresrev.2010.04.006

Orešković, D., and Klarica, M. (2011). Development of hydrocephalus and classical hypothesis of cerebrospinal fluid hydrodynamics: facts and illusions. *Prog. Neurobiol.* 94, 238–258. doi: 10.1016/j.pneurobio.2011.05.005

Orešković, D., and Klarica, M. (2014). A new look at cerebrospinal fluid movement. *Fluids Barriers CNS* 11:16. doi: 10.1186/2045-8118-11-16

Orešković, D., Klarica, M., and Vukić, M. (2002). The formation and circulation of cerebrospinal fluid inside the cat brain ventricles: a fact or an illusion? *Neurosci. Lett.* 327, 103–106. doi: 10.1016/S0304-3940(02)00395-6

Orešković, D., Radoš, M., and Klarica, M. (2017a). New concepts of cerebrospinal fluid physiology and development of hydrocephalus. *Pediatr. Neurosurg.* 52, 417–425. doi: 10.1159/000452169

Orešković, D., Radoš, M., and Klarica, M. (2017b). The recent state of a hundred years old classic hypothesis of the cerebrospinal fluid physiology. *Croat. Med. J.* 58, 381–383. doi: 10.3325/cmj.2017.58.381

Pollay, M. (2010). The function and structure of the cerebrospinal fluid outflow system. *Cerebrospinal Fluid Res.* 7:9. doi: 10.1186/1743-8454-7-9

Portnoy, H. D., Schulte, R. R., Fox, J. L., Croissant, P. D., and Tripp, L. (1973). Anti-siphon and reversible occlusion valves for shunting in hydrocephalus and preventing post-shunt subdural hematomas. *J. Neurosurg.* 38, 729–738. doi: 10.3171/jns.1973.38.6.0729

Qvarlander, S., Sundstrom, N., Malm, J., and Eklund, A. (2013). Postural effects on intracranial pressure: modeling and clinical evaluation. *J. Appl. Physiol.* 115, 1474–1480. doi: 10.1152/japplphysiol.00711.2013

Radoš, M., Klarica, M., Mučić-Pucić, B., Nikić, I., Raguž, M., Galkowski, V., et al. (2014). Volumetric analysis of cerebrospinal fluid and brain parenchyma in a patient with hydranencephaly and macrocephaly – case report. *Croat. Med. J.* 55, 388–393. doi: 10.3325/cmj.2014.55.388

Sakka, L, Coll, G, and Chazal, J. (2011). Anatomy and physiology of cerebrospinal fluid. *Eur Ann Otorhinolaryngol Head Neck Dis.* 128, 309–16. doi: 10.1016/j.anorl.2011.03.002

Smets, N. G., Strijkers, G. J., Vinje, V., and Bakker, E. N. T. (2023). Cerebrospinal fluid turnover as a driver of brain clearance. *NMR Biomed.* 37:e5029. doi: 10.1002/nbm.5029

Statsenko, Y, Habuza, T, Charykova, I, Gorkom, KN, Zaki, N, Almansoori, TM, et al. (2021). Predicting Age From Behavioral Test Performance for Screening Early Onset of Cognitive Decline. *Front Aging Neurosci.* 13:661514. doi: 10.3389/fnagi.2021.661514

Tarr, J. T., Hagan, M., Zhang, B., Tanna, N., Andrews, B. T., Lee, J. C., et al. (2020). Syndrome of the trephined: quantitative functional improvement after large cranial vault reconstruction. *Plast. Reconstr. Surg.* 145, 1486–1494. doi: 10.1097/PRS.0000000000006836

Theologou, M., Natsis, K., Kouskouras, K., Chatzinikolaou, F., Varoutis, P., Skoulios, N., et al. (2022). Cerebrospinal fluid homeostasis and hydrodynamics: a review of facts and theories. *Eur. Neurol.* 85, 313–325. doi: 10.1159/000523709

Thomale, U. W. (2021). Integrated understanding of hydrocephalus-a practical approach for a complex disease. *Childs Nerv. Syst.* 37, 3313–3324. doi: 10.1007/s00381-021-05243-3

Tunturi, A. R. (1978). Elasticity of the spinal cord, pia, and denticulate ligament in the dog. *J. Neurosurg.* 48, 975–979. doi: 10.3171/jns.1978.48.6.0975

Vladić, A., Klarica, M., and Bulat, M. (2009). Dynamics of distribution of ^{3}H-inulin between the cerebrospinal fluid compartments. *Brain Res.* 1248, 127–135. doi: 10.1016/j.brainres.2008.10.044

Vladić, A., Strikić, N., Jurčić, D., Zmajević, M., Klarica, M., and Bulat, M. (2000). Homeostatic role of the active transport in elimination of [^{3}H] benzylpenicillin out of the cerebrospinal fluid system. *Life Sci.* 67, 2375–2385. doi: 10.1016/s0024-3205(00)00823-7

Von Storch, T. J. C. (1937). Factors producing lumbar cerebrospinal fluid pressure in man in the erect posture. *Arch. Neurol. Psychiatr.* 38, 1158–1175. doi: 10.1001/archneurpsyc.1937.02260240038003

Yamada, S. (2014). Cerebrospinal physiology: visualization of cerebrospinal fluid dynamics using the magnetic resonance imaging time-spatial inversion pulse method. *Croat. Med. J.* 55, 337–346. doi: 10.3325/cmj.2014.55.337

Yamada, S, and Mase, M. (2023). Cerebrospinal Fluid Production and Absorption and Ventricular Enlargement Mechanisms in Hydrocephalus. *Neurol Med Chir (Tokyo).* 63, 141–151. doi: 10.2176/jns-nmc.2022-0331

Yushkevich, P. A., Piven, J., Hazlett, H. C., Smith, R. G., Ho, S., Gee, J. C., et al. (2006). User-guided 3D active contour segmentation of anatomical structures: significantly improved efficiency and reliability. *NeuroImage* 31, 1116–1128. doi: 10.1016/j.neuroimage.2006.01.015

Frontiers in
Molecular Neuroscience

Leading research into the brain's molecular structure, design and function

Part of the most cited neuroscience series, this journal explores and identifies key molecules underlying the structure, design and function of the brain across all levels.

Discover the latest Research Topics

See more →

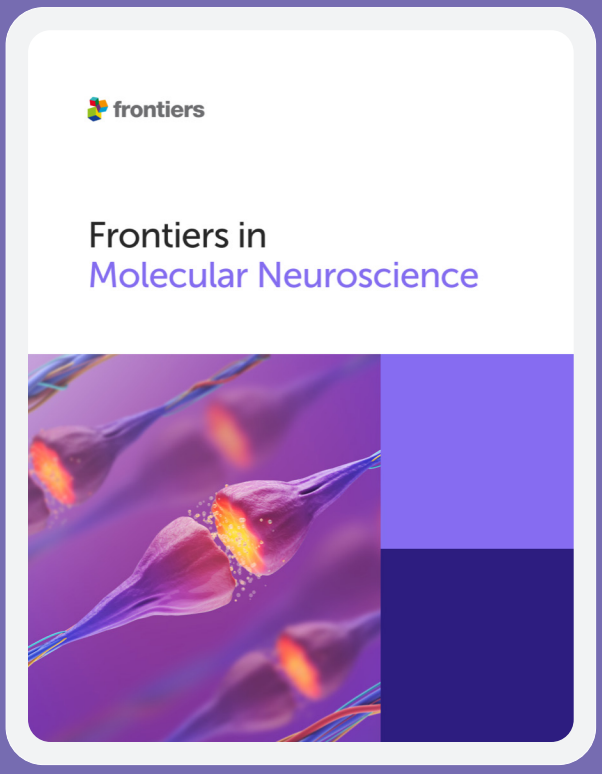

Frontiers

Avenue du Tribunal-Fédéral 34
1005 Lausanne, Switzerland
frontiersin.org

Contact us

+41 (0)21 510 17 00
frontiersin.org/about/contact